U.S. Department
of Commerce

Volume 99
Number 1
January 2001

Fishery Bulletin

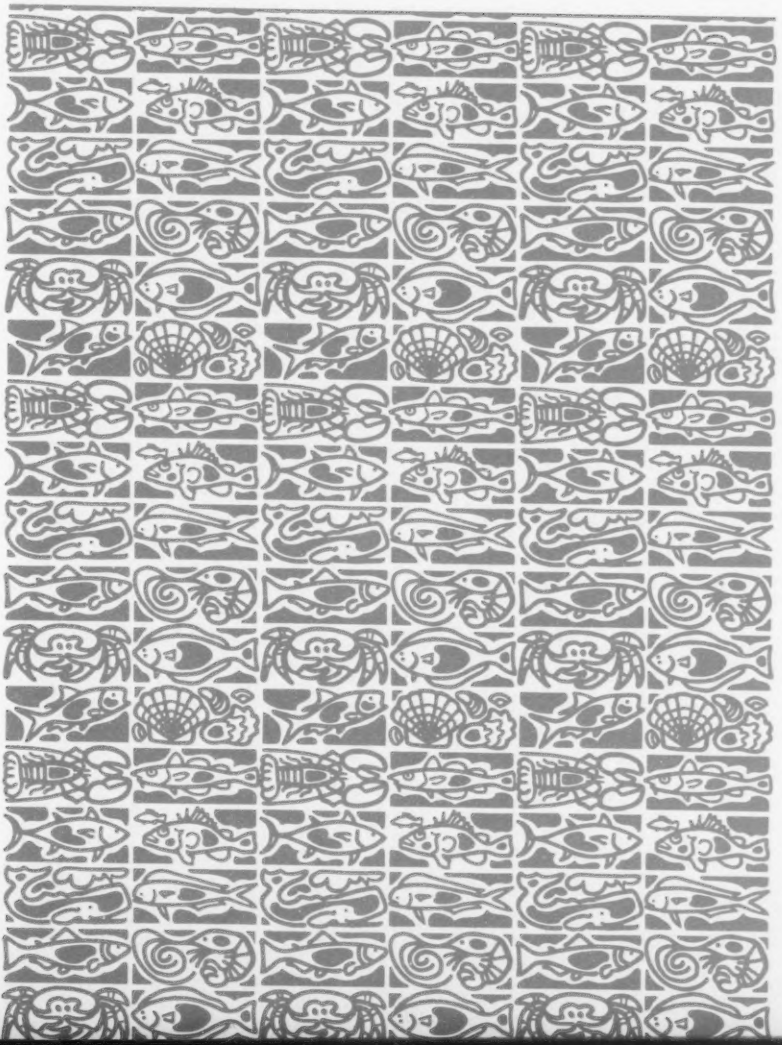

U.S. Department of Commerce

Norman Y. Mineta
Secretary

National Oceanic and Atmospheric Administration

D. James Baker
Under Secretary for Oceans and Atmosphere

National Marine Fisheries Service

Penelope D. Dalton
Assistant Administrator for Fisheries

Fishery Bulletin

Scientific Editor
Dr. John V. Merriner

Editorial Assistant
Sarah Shoffler

Southeast Fisheries Science Center
National Marine Fisheries Service, NOAA
101 Pivers Island Road
Beaufort, NC 28516

Managing Editor
Sharyn Matriotti

National Marine Fisheries Service
Scientific Publications Office
7600 Sand Point Way NE, BIN C15700
Seattle, Washington 98115-0070

Editorial Committee

Dr. Andrew E. Dizon	National Marine Fisheries Service
Dr. Harlyn O. Halvorson	University of Massachusetts, Boston
Dr. Ronald W. Hardy	University of Idaho, Hagerman
Dr. Richard D. Methot	National Marine Fisheries Service
Dr. Theodore W. Pietsch	University of Washington, Seattle
Dr. Joseph E. Powers	National Marine Fisheries Service
Dr. Harald Rosenthal	Universität Kiel, Germany
Dr. Fredric M. Serchuk	National Marine Fisheries Service

***Fishery Bulletin* web site: fishbull.noaa.gov**

The *Fishery Bulletin* (ISSN 0090-0656) is published quarterly by the Scientific Publications Office, National Marine Fisheries Service, NOAA, 7600 Sand Point Way NE, BIN C15700, Seattle, WA 98115-0070. Periodicals postage is paid at Seattle, WA, and at additional mailing offices. POSTMASTER: Send address changes for subscriptions to Fishery Bulletin, Superintendent of Documents, Attn.: Chief, Mail List Branch, Mail Stop SSOM, Washington, DC 20402-9373.

Although the contents of this publication have not been copyrighted and may be reprinted entirely, reference to source is appreciated.

The Secretary of Commerce has determined that the publication of this periodical is necessary according to law for the transaction of public business of this Department. Use of funds for printing of this periodical has been approved by the Director of the Office of Management and Budget.

For sale by the Superintendent of Documents, U.S. Government Printing Office, Washington, DC 20402. Subscription price per year: $55.00 domestic and $68.75 foreign. Cost per single issue: $34.00 domestic and $42.50 foreign. **See back for order form.**

The *Fishery Bulletin* carries original research reports and technical notes on investigations in fishery science, engineering, and economics. It began as the Bulletin of the United States Fish Commission in 1881; it became the Bulletin of the Bureau of Fisheries in 1904 and the *Fishery Bulletin* of the Fish and Wildlife Service in 1941. Separates were issued as documents through volume 46; the last document was No. 1103. Beginning with volume 47 in 1931 and continuing through volume 62 in 1963, each separate appeared as a numbered bulletin. A new system began in 1963 with volume 63 in which papers are bound together in a single issue of the bulletin. Beginning with volume 70, number 1, January 1972, the *Fishery Bulletin* became a periodical, issued quarterly. In this form, it is available by subscription from the Superintendent of Documents, U.S. Government Printing Office, Washington, DC 20402. It is also available free in limited numbers to libraries, research institutions, State and Federal agencies, and in exchange for other scientific publications.

U.S. Department of Commerce
Seattle, Washington

Volume 99
Number 1
January 2001

Fishery Bulletin

Contents

Articles

1-14 **Begg, Gavin A., William J. Overholtz, and Nancy J. Munroe**
The use of internal otolith morphometrics for identification of haddock (*Melanogrammus aeglefinus*) stocks on Georges Bank

15–28 **Brown-Peterson, Nancy J., Robin M. Overstreet, Jeffrey M. Lotz, James S. Franks, and Karen M. Burns**
Reproductive biology of cobia, *Rachycentron canadum*, from coastal waters of the southern United States

29–39 **Caretta, James V., Barbara L. Taylor, and Susan J. Chivers**
Abundance and depth distribution of harbor porpoise (*Phocoena phocoena*) in northern California determined from a 1995 ship survey

40–48 **Dagorn, Laurent, Erwan Josse, and Pascal Bach**
Association of yellowfin tuna (*Thunnus albacares*) with tracking vessels during ultrasonic telemetry experiments

49–62 **Gharrett, Anthony J., Andrew K. Gray, and Jonathan Heifetz**
Identification of rockfish (*Sebastes* spp.) by restriction site analysis of the mitochondrial ND-3/ND-4 and 12S/16S rRNA gene regions

Companion articles

63–71 **Harvey, Euan, David Fletcher, and Mark Shortis**
A comparison of the precision and accuracy of estimates of reef-fish lengths determined visually by divers with estimates produced by a stereo-video system

72–80 **Harvey, Euan, David Fletcher, and Mark Shortis**
Improving the statistical power of length estimates of reef fish: a comparison of estimates determined visually by divers with estimates produced by a stereo-video system

The conclusions and opinions expressed in *Fishery Bulletin* are solely those of the authors and do not represent the official position of the National Marine Fisheries Service (NOAA) or any other agency or institution.

The National Marine Fisheries Service (NMFS) does not approve, recommend, or endorse any proprietary product or proprietary material mentioned in this publication. No reference shall be made to NMFS, or to this publication furnished by NMFS, in any advertising or sales promotion which would indicate or imply that NMFS approves, recommends, or endorses any proprietary product or proprietary material mentioned herein, or which has as its purpose an intent to cause directly or indirectly the advertised product to be used or purchased because of this NMFS publication.

81–93 **Lazzari, Mark A.**
Dynamics of larval fish abundance in Penobscot Bay, Maine

94–107 **Nelson, R. John, Maureen P. Small, Terry D. Beacham, and K. Janine Supernault**
Population structure of Fraser River chinook salmon (*Oncorhynchus tshawytscha*): an analysis using microsatellite DNA markers

108–122 **Nichol, Daniel G. , and Erika I. Acuna**
Annual and batch fecundities of yellowfin sole, *Limanda aspera,* in the eastern Bering Sea

123–138 **Noll, Claire, Natalia V. Varnavskaya, Evgeny A. Matzak, Sharon L. Hawkins, Victoria V. Midanaya, Oleg N. Katugin, Charles Russell, Natalya M. Kinas, Charles M. Guthrie III, Hiroshi Mayama, Fumio Yamazaki, Bruce P. Finney, and Anthony J. Gharrett**
Analysis of contemporary genetic structure of even-broodyear populations of Asian and western Alaskan pink salmon, *Oncorhynchus gorbuscha*

139–150 **Panfili, Jacques, and Javier Tomás**
Validation of age estimation and back-calculation of fish length based on otolith microstructures in tilapias (Pisces, Cichlidae)

151–167 **Pella, Jerome, and Michele Masuda**
Bayesian methods for analysis of stock mixtures from genetic characters

168–179 **Soh, SungKwon, Donald R. Gunderson, and Daniel H. Ito**
The potential role of marine reserves in the management of shortraker rockfish (*Sebastes borealis*) and rougheye rockfish (*S. aleutianus*) in the Gulf of Alaska

180–192 **St John, Jill, Garry R. Russ, Ian W. Brown, and Lyle C. Squire**
The diet of the large coral reef serranid *Plectropomus leopardus* in two fishing zones on the Great Barrier Reef, Australia

Notes

193–196 **Adam, M. Shiham, and Geoffrey P. Kirkwood**
Estimating tag-shedding rates for skipjack tuna, *Katsuwonus pelamis,* off the Maldives

197–201 **DeMaster, Douglas P., Lloyd F. Lowry, Kathryn J. Frost, and Rebecca A. Bengston**
The effect of sea state on estimates of abundance for beluga whales (*Delphinapterus leucas*) in Norton Sound, Alaska

202–209 **Pierce, Daryl J., Behzad Mahmoudi, and Raymond R. Wilson Jr.**
Age and growth of the scaled herring, *Harengula jaguana,* from Florida waters, as indicated by microstructure of the sagittae

210–216 **Stone, Heath H., and Langille K. Dixon**
A comparison of catches of swordfish, *Xiphias gladius,* and other pelagic species from Canadian longline gear configured with alternating monofilament and multifilament nylon gangions

217 *Subscription form*

The use of internal otolith morphometrics for identification of haddock (*Melanogrammus aeglefinus*) stocks on Georges Bank

Gavin A. Begg
William J. Overholtz
Nancy J. Munroe

Northeast Fisheries Science Center
National Marine Fisheries Service, NOAA
166 Water Street
Woods Hole, Massachusetts 02543
Present address (for G. A. Begg): Marine Research Institute
P.O. Box 1390
121 Reykjavik, Iceland
E-mail address (for G. A Begg): gavin@hafro.is

Abstract—Internal otolith morphometrics, coupled with image analysis procedures and multivariate statistical analyses, were examined to investigate stock structure of haddock (*Melanogrammus aeglefinus*) on Georges Bank in the northwest Atlantic. Samples were collected during spring 1995–97 from the Northeast Peak (eastern Georges Bank) and the Great South Channel (western Georges Bank) spawning components. The structure of transverse sagittal otolith sections were described for individual haddock samples from each spawning component by using a combination of linear morphometrics, shape characteristics, and growth increments. Analyses were structured to account for the effects of size, sex, age, and year class. Significant differences in internal otolith structure were found between eastern and western Georges Bank haddock, providing phenotypic evidence of stock separation between the two spawning components. Eastern Georges Bank haddock tended to have smaller internal otolith dimensions than western Georges Bank haddock; these differences appeared to be related to growth rates. Total classification success for each spawning component varied from 61% to 83% for the different age and year-class combinations. Results from this study may be helpful in forming consistent stock definitions that can be used by both U.S. and Canadian fishery management agencies for rebuilding stocks of haddock on Georges Bank.

Manuscript accepted 29 June 2000.
Fish. Bull. 99:1–14 (2001).

Otoliths are crystalline structures composed of calcium carbonate and are ideal structures for use in fish stock identification, containing a range of measurable characteristics including linear and shape morphometrics, optical density, and microstructural zonation and growth patterns, and elemental constituents (Ihssen et al., 1981; Campana and Neilson, 1985; Pawson and Jennings, 1996). Otoliths grow throughout the life of fish, are metabolically inert, and are typically available as a historical time series because of routine age and growth assessments (Campana and Neilson, 1985; Campana and Casselman, 1993).

Linear and shape morphometrics of otoliths have been widely used for fish stock identification (e.g. Messieh et al., 1989; Dawson, 1991; Smith, 1992; Campana and Casselman, 1993; Friedland and Reddin, 1994), although their use has been questioned because of within-stock differences in sex, age, and year-class variation (Castonguay et al., 1991; Begg and Brown, 2000). Moreover, otolith morphometrics have been found to be strongly correlated with growth, which influences development of otolith crystalline microstructure (Smith, 1992; Campana and Casselman, 1993). Stock definitions based on differences in otolith structure, therefore, depend not only on differential growth rates, but on the consistency of the environment integrated over the life history of fish in each stock (Campana and Casselman, 1993). Although otolith morphometrics cannot be used to differentiate stocks on a genetic basis, they can provide a phenotypic basis for stock separation that is useful for fisheries management (Casselman et al., 1981; Begg and Waldman, 1999).

Fisheries management is moving towards a precautionary approach to ensure sustainable utilization of our marine resources (FAO, 1995; ICES[1]). One requirement of the precautionary approach is to consider the full impact of management actions, including explicit consideration of stock complexity (Garcia and Grainger, 1997). For this reason, there is a growing interest in the importance and recognition of individual spawning components within historically established management units (FAO, 1995; Stephenson, 1999).

The importance of individual spawning components has been acknowledged in the management of haddock, *Melanogrammus aeglefinus*, a commercially important groundfish of the northwest Atlantic. The interest in haddock stock complexity is exemplified on Georges Bank (Fig. 1), where this species forms an important transboundary resource among U.S. and Canadian fishermen (Halliday and Pinhorn, 1990; Begg,

[1] ICES (International Council for the Exploration of the Sea). 1997. Report of the study group on the precautionary approach to fisheries management. ICES council meeting (CM) 1997/assess 7, 41 p.

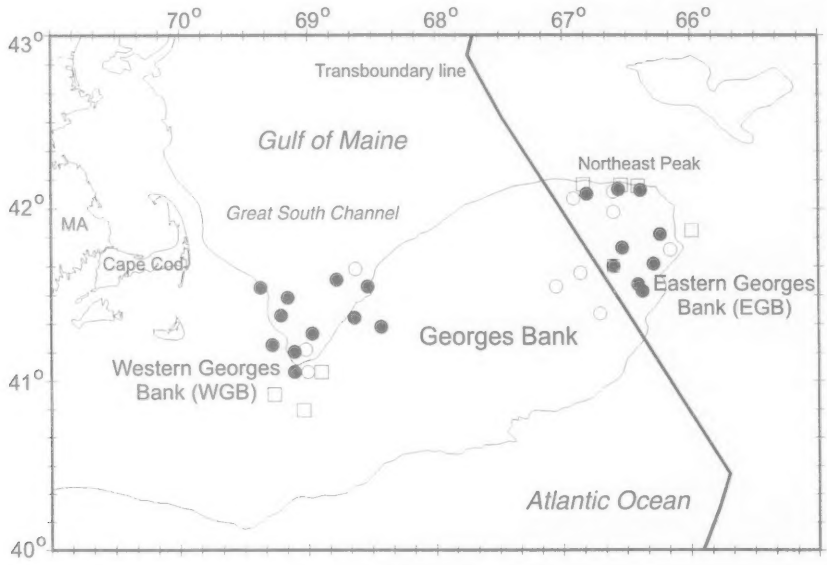

Figure 1

Northeast Fisheries Science Center stratified random survey stations from where eastern and western Georges Bank haddock samples were collected in 1995 (open squares), 1996 (open circles), and 1997 (closed circles) for stock identification based on internal otolith morphometrics.

1998). During 1935 to 1960, annual landings of haddock on Georges Bank averaged 46,000 metric tons (t), before increasing to 150,000 t in 1965 owing to exceptional recruitment from the 1962 and 1963 year classes and intense fishing resulting from the entrance of distant water fleets (Clark et al., 1982). However, following these record landings the resource collapsed, and annual landings declined to less than 5,000 t during the mid-1970s. The resource temporarily increased during the late 1970s and early 1980s when annual landings increased to 27,000 t owing to the large 1975 and 1978 year classes, before declining to a record low level of 2,300 t in 1995 (Brown, 1998).

Currently, the haddock resource on Georges Bank is in a depleted condition and is the focus of rebuilding plans by both the U.S. and Canadian fishery management agencies (Brown, 1998; Gavaris and Van Eeckhaute, 1998). The fact that each nation conducts separate analytical assessments, using different stock definitions for the resource, is problematic. The United States assesses Georges Bank haddock as a single stock, encompassing historical spawning components on the Northeast Peak (eastern Georges Bank) and the Great South Channel (western Georges Bank); whereas Canada assesses only the spawning component on the Northeast Peak (Brown, 1998; Gavaris and Van Eeckhaute, 1998) (Fig. 1). Since the mid-1980s, the majority of the haddock resource has been concentrated over eastern Georges Bank, where the majority of landings have been taken by the Canadian fishery (Brown, 1998). The changing resource status of haddock on Georges Bank has probably been due to greater depletion of the western Georges Bank spawning component, which may now be contributing at a much lower level to the overall productivity of the resource (Van Eeckhaute et al., 1999). Stock rebuilding plans of both nations need to examine the identity versus the separateness, of spawning components on Georges Bank and develop uniform stock definitions for the resource.

Haddock stocks on Georges Bank have been examined by using a variety of techniques, although the results in terms of identification have been far from conclusive. Differences in distribution, life history, and otolith shape characteristics have indicated the existence of separate eastern and western Georges Bank spawning components (Smith and Morse, 1985; Gavaris and Van Eeckhaute, 1998; Begg et al., 1999; Begg and Brown, 2000). In contrast, tag-recapture, ichthyoplankton surveys, and genetic analyses have indicated some interchange of haddock across the Bank that may reflect a single spawning component (Needler, 1930; Schroeder, 1942; Morse et al., 1987; Purcell et al., 1996). Hence, there remains considerable uncertainty regarding the stock structure of haddock on Georges Bank.

The limitations associated with traditional stock identification techniques have been a major factor responsible for the remaining uncertainty regarding haddock stock structure on Georges Bank (Begg, 1998). Consequently, we used a new stock identification technique based on internal otolith morphometrics. We considered internal otolith morphometrics as a generic term describing the otolith microstructure of individual growth zones as well as the linear and shape dimensions of transverse otolith sec-

Table 1

Details of haddock samples used in analysis of internal otolith morphometrics for stock identification.

Region	Date captured	Age group (years)	Length range (cm)	*n*
Eastern Georges Bank (EGB)	10–11 Apr 1995	1	21–28	7
		2	31–37	10
	21–23 Apr 1996	1	21–32	6
		3	41–53	9
		4	45–54	9
	6–8 Apr 1997	2	38–45	18
		3	40–47	10
		4	41–58	16
		5	49–62	10
Western Georges Bank (WGB)	13 Apr 1995	1	24–31	11
	16–20 Apr 1996	2	31–47	9
		3	40–55	9
	25 Mar–23 Apr 1997	2	36–44	17
		3	39–60	44
		4	47–67	37
		5	50–73	10

tions. Although, linear morphometrics and shape analysis of "external" or whole otoliths have been used for fish stock identification, there has been little use of "internal" otolith morphometrics, probably because of the time, expense, and potential difficulties in obtaining consistent otolith sections. However, most fisheries agencies now use a standardized procedure for sectioning otoliths. These standardized procedures enable consistent and comparable otolith sections to be obtained, providing a consistent, rapid, and readily accessible structure that can be examined for stock identification.

We investigated the feasibility of using internal otolith morphometrics for fish stock identification, by considering Georges Bank haddock as a representative case study. For the purposes of our study, we considered a stock, or spawning component, as a semidiscrete, self-reproducing group of fish with definable morphometric characteristics that are assumed to be homogeneous for management purposes (Begg and Waldman, 1999). Variation in these characteristics is assumed to be evidence that distinct geographic regions are partially occupied throughout the life history of the fish, thereby providing a phenotypic basis for stock identification (Ihssen et al., 1981).

Materials and methods

Sample collection

Haddock samples were collected in 1995, 1996, and 1997 during spring Northeast Fisheries Science Center (NEFSC) stratified random bottom trawl surveys, when the fish were assumed to be on or near their spawning grounds. Most of the adults (ages 2+) sampled were in spawning condition. Samples were collected from survey stations throughout eastern (EGB) and western Georges Bank (WGB) (Fig. 1; Table 1). At sea, haddock samples were measured (fork length [FL], to the nearest cm), sex and maturity were determined by macroscopic examination of the gonads, and sagittal otolith pairs were removed from each sample. In the laboratory, one otolith from each pair was sectioned and assigned an age by following standard methods for northwest Atlantic species (Pentilla and Dery, 1988). Standardized sectioning procedures ensured consistent and comparable otolith sections for morphometric measurements and subsequent statistical analyses.

Internal otolith morphometrics

Internal otolith morphometrics were obtained from each otolith section by using the OPTIMAS™ (version 6.2) image analysis system (Media Cybernetics, 1996). All measurements were taken at a magnification of 15×. The perimeter of each otolith section was traced in a counterclockwise direction to allow morphometrics to be calculated for each structure (shape). Six linear morphometrics (length, width, $A1$, $H1$, $A2$, and $H2$) were measured for each sample, where $A1$ is the growth increment to the first annulus, $H1$ is the width of the hyaline band of the first annulus, $A2$ is the growth increment to the second annulus, and $H2$ is the width of the hyaline band of the second annulus (Fig. 2). In addition, four shape variables (area, perimeter, circularity, and rectangularity) were measured for each sample. Circularity was defined as the perimeter of the otolith section squared divided by its area, and rectangularity was defined as the otolith section area divided

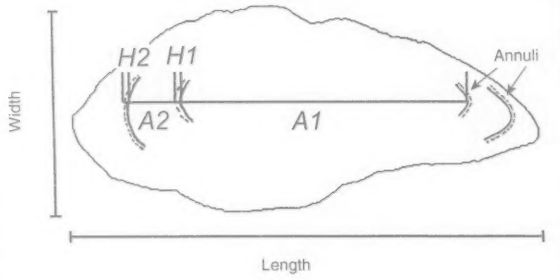

Figure 2
Internal otolith morphometric variables that were measured for stock identification of haddock on Georges Bank.

by the area of its enclosing rectangle oriented along the length of the section (Media Cybernetics, 1996).

Data analysis

Internal otolith morphometrics were compared between eastern and western Georges Bank haddock for stock identification. All variables were first examined for assumptions of normality and homoscedasticity and were subsequently $\log_e$-transformed prior to statistical analysis if these assumptions were not satisfied. Following transformation, all variables conformed to statistical assumptions. Analysis of covariance (ANCOVA) was then used to determine the effect of fish length on the magnitude of each variable. Those variables found to have significant interactions ($P<0.05$) between sampling region and fish length (i.e. samples with unequal slopes) were excluded from further statistical analyses. In contrast, those variables found to have samples with equal slopes, but that significantly correlated with fish length, were corrected for fish length by using their respective common within-group slope (b) to standardize the samples.

Potential confounding sources of variation among samples, such as sex, age, and year-class differences, were examined and accounted for in the analyses before interpreting stock differences. Such confounding variables need to be examined to ensure interpretations of stock differences are real and not simply the result of sample variation (Castonguay et al., 1991; Begg and Brown, 2000). Consequently, multivariate analysis of variance (MANOVA) was used to examine differences between the sexes in their internal otolith structure, for samples from the same region and year class, and of the same age, by using the appropriate length-corrected internal otolith morphometric variables. One-way, fixed effects, unbalanced analysis of variance (ANOVA) was then used to examine individual variables to interpret any significant differences detected by the MANOVAs. Significance levels were corrected for multiple testing by using the Bonferroni adjustment factor (Sokal and Rohlf, 1995). The same tests were then used to examine the internal otolith structure of different-age fish (sampled from the same region and year), and fish originating from different year classes (same region and age). Tukey's honestly significant difference (HSD) tests were used for *a posteriori* comparisons for each significant variable. The same multi- and univariate tests were then used to examine the internal otolith structure of haddock sampled from eastern and western Georges Bank. These analyses were used to determine if there was any evidence for stock separation of haddock across the Bank.

Principal component (PC) analysis of the length-corrected internal otolith morphometric variables was conducted for samples of the same age and year class to provide an unbiased indication of separation between eastern and western Georges Bank haddock (i.e. there were no *a priori* assumptions of group membership). ANOVA was used on the significant principal components to examine differences in the PC scores between the proposed groups. Forward stepwise canonical discriminant analysis was then used to detect differences in the internal otolith structure of eastern and western Georges Bank haddock samples. The significant ($P<0.05$) canonical variate (CV) derived by each analysis represented the optimal combination of morphometric variables that provided the best overall discrimination between the samples. ANOVA was used to examine differences in the CV scores. Jack-knifed cross-validation procedures were used to give unbiased estimates of classification success (SPSS, Inc., 1997).

Results

All the internal otolith morphometric variables, except for $A1$ and rectangularity, were $\log_e$-transformed prior to statistical analysis to correct for nonnormality and inequality of variances. ANCOVA indicated a significant correlation between fish length and region for otolith width (homogeneity of slopes test, $P<0.0222$) (Table 2). Significant region-specific differences in the correlation between fish length and otolith width (i.e. regional differences in growth rate) made it necessary to remove otolith width as an analysis

Table 2

Internal otolith morphometric variables significantly correlated with fish length, and the corresponding regression coefficients (b) required to standardize the variables for fish length.

Otolith morphometric variable	Length × region			Length			
	F	df	P	F	df	P	b
$A1$	0.85	15,200	0.6195	1.70	1,215	0.1936	—
$H1$	1.27	13,183	0.2333	1.22	1,196	0.2713	—
$A2$	0.92	12,181	0.5274	2.36	1,193	0.1261	—
$H2$	1.19	12,155	0.2918	11.62	1,167	0.0008	0.01810
Length	1.16	15,200	0.3082	103.65	1, 215	0.0001	0.00922
Width	1.93	15,200	0.0222	—	—	—	—
Area	1.53	15,200	0.0971	91.91	1, 215	0.0001	0.01514
Perimeter	1.48	15,200	0.1165	88.05	1, 215	0.0001	0.00837
Circularity	1.06	15,200	0.4007	2.92	1, 215	0.0889	—
Rectangularity	1.63	15,200	0.0695	8.50	1, 215	0.0039	–0.00092

Table 3

Results of MANOVA and ANOVA showing significant differences in the length-corrected internal otolith morphometric variables between age groups for eastern (EGB) and western Georges Bank (WGB) haddock.

Region	Year	Age group comparison (years)	MANOVA			Significant variable	ANOVA		
			F	df	P		F	df	P
EGB	1995	1 vs. 2	15.51	6,10	0.0002	length	19.16	1,15	0.0005
						area	28.70	1,15	0.0001
						perimeter	12.39	1,15	0.0031
	1996	1,3 vs. 4	3.98	12,34	0.0007	length	32.79	2,21	0.0001
						area	127.78	2,21	0.0001
						perimeter	23.13	2,21	0.0001
						circularity	6.93	2,21	0.0049
	1997	2,3,4 vs. 5	4.05	24,135	0.0001	$A1$	6.87	3,50	0.0006
						$H1$	4.75	3,50	0.0054
						length	4.90	3,50	0.0046
						area	7.71	3,50	0.0002
WGB	1996	2 vs. 3	4.71	8,9	0.0163	length	11.99	1,16	0.0032
						perimeter	9.19	1,16	0.0079
	1997	2,3,4 vs. 5	5.46	24,297	0.0001	area	10.81	3,104	0.0001
						circularity	7.46	3,104	0.0001
						rectangularity	4.96	3,104	0.0029

variable. The same ANCOVAs also indicated that $H2$ and otolith length, area, perimeter, and rectangularity were correlated with fish length ($P<0.004$), resulting in those variables being corrected for fish length by using their respective within-group regression coefficient (Table 2).

Internal otolith morphometrics were not significantly different between the sexes (MANOVA, $P>0.05$), resulting in the sexes being pooled within each region, year and age strata to increase the statistical power used in subsequent analyses. In contrast, significant differences were found between the different age groups of haddock (Table 3). Not unexpectedly, haddock that were 1 and 2 years of age tended to have significantly smaller otoliths than haddock that were 3, 4, and 5 years of age (HSD, $P<0.05$). Likewise, there were significant differences indicative of annual growth differences found in the internal otolith morphometrics of haddock sampled from different year classes (Table 4). Hence, the remaining

Table 4

Results of MANOVA and ANOVA showing significant differences in the length-corrected internal otolith morphometric variables between year classes for eastern (EGB) and western Georges Bank (WGB) haddock.

Region	Age (yr)	Year-class comparison (yr)	MANOVA			Significant variable	ANOVA		
			F	df	*P*		*F*	df	*P*
EGB	1	1994 vs. 1995	1.23	6, 6	0.4034	—	—	—	—
	2	1993 vs. 1995	7.82	8, 18	0.0002	—	—	—	—
	3	1993 vs. 1994	2.22	9, 9	0.1255	*H*2	11.83	1, 17	0.0031
	4	1992 vs. 1993	1.90	9, 15	0.1309	perimeter	11.57	1, 23	0.0025
						circularity	9.14	1, 23	0.0060
WGB	2	1994 vs. 1995	1.76	8, 17	0.1549	—	—	—	—
	3	1993 vs. 1994	3.55	9, 43	0.0023	*H*1	15.59	1, 51	0.0002

Table 5

Results of MANOVA and ANOVA showing significant differences in the length-corrected internal otolith morphometric variables between haddock from eastern and western Georges Bank.

Year	Age (yr)	MANOVA			Significant variable	ANOVA		
		F	df	*P*		*F*	df	*P*
1995	1	1.60	6, 11	0.2357	rectangularity	5.76	1, 16	0.0289
1996	3	1.18	9, 8	0.4109	—	—	—	—
1997	2	2.10	8, 26	0.0726	circularity	10.37	1, 33	0.0029
	3	4.30	9, 44	0.0005	*A*1	22.76	1, 52	0.0001
					*A*2	7.84	1, 52	0.0072
					*H*2	7.41	1, 52	0.0088
	4	3.22	9, 43	0.0045	*A*2	3.97	1, 51	0.0518
	5	5.53	9, 10	0.0067	*A*1	9.70	1, 18	0.0060
					*H*2	9.90	1, 18	0.0056

analyses were conducted for samples of individual ages and year classes in order to minimize the effects of these confounding variables.

Significant differences in the internal otolith morphometrics between haddock sampled on eastern and western Georges Bank were found in three out of six comparisons (Table 5). Eastern Georges Bank haddock tended to have smaller otoliths (i.e. length, area, perimeter, circularity and rectangularity) than western Georges Bank haddock; this finding was derived mainly from the first growth increment (*A*1) which also tended to be smaller (Fig. 3). For the three significant comparisons, scatter plots of the most significant individual internal otolith morphometrics for samples from each age group typically showed separation patterns between eastern and western Georges Bank haddock, albeit with some overlap (Figs. 4–6).

Principal component analysis provided further support that haddock from eastern and western Georges Bank separated into two groups (Fig. 7). Eastern and western Georges Bank haddock samples, 1 and 3 (1994 year class) years of age were mainly separated on the first principal component (PC I) (ANOVA, $P<0.06$), whereas samples that were 2, 3 (1993 year class), and 5 years of age were mainly separated on the second and third principal components (PC II and PC III) (ANOVA, $P<0.05$). Principal components I, II, and III accounted on average for 38.7 ±5.3% SD, 22.6 ±5.9%, and 15.6 ±0.7% of the total variation in the data. Differences in length, area, and perimeter were mainly responsible for the observed separations along the first principal component, whereas *A*1, *H*1 and *A*2 were the main variables responsible for separation along the second and third principal components.

Discriminant analysis also indicated that haddock comprise two groups on Georges Bank (Fig. 8). Significant differences in the discriminant (CV I) scores between eastern and western Georges Bank haddock were found for all age groups (ANOVA, $P<0.05$), except age group 4. Total classification success varied from 61% to 83% for the different age and year-class combinations (Table 6).

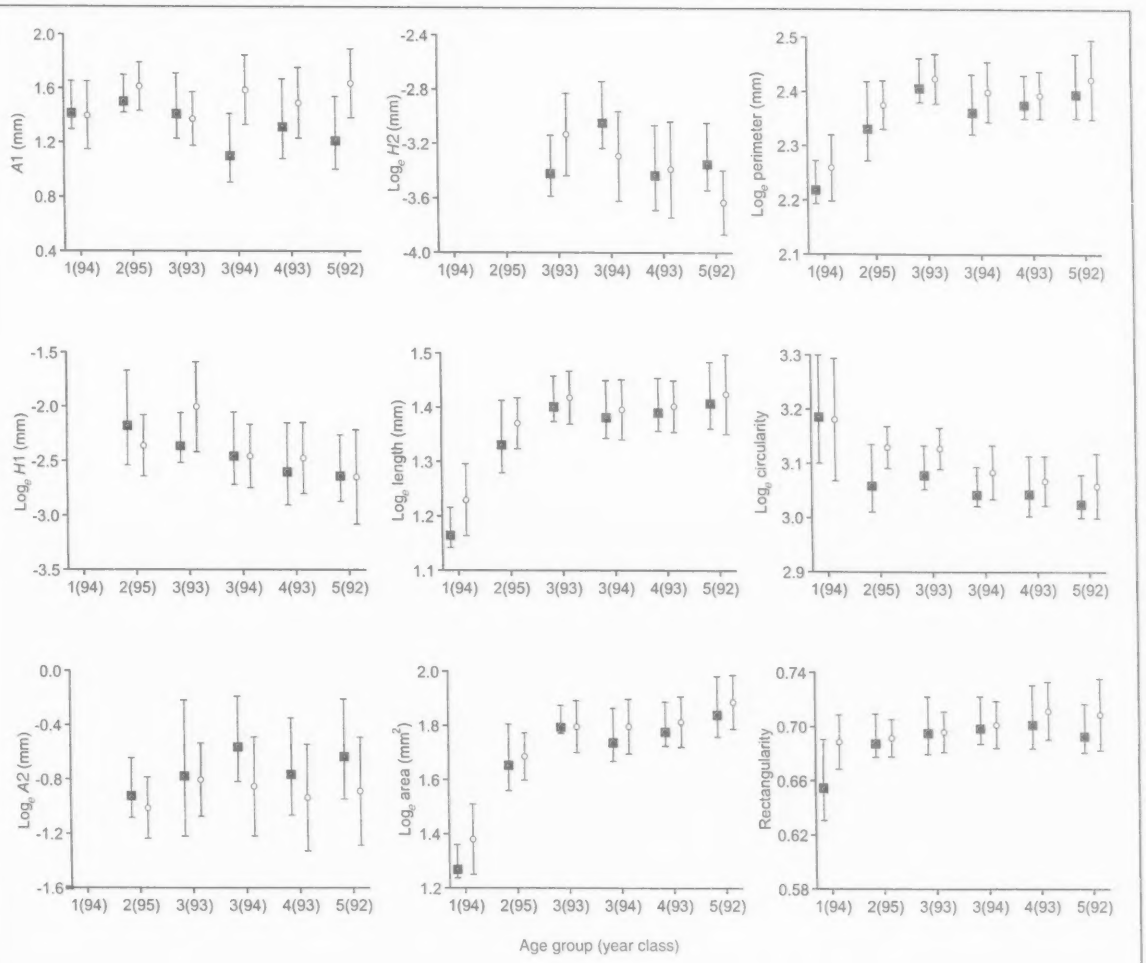

Figure 3

Mean ± standard deviation of age-specific internal otolith growth morphometrics (*A*1, *H*1, *A*2, *H*2, and otolith length, area, perimeter, circularity, and rectangularity) for eastern Georges Bank (squares) and western Georges Bank (circles) haddock.

Discussion

We found significant differences in the internal otolith structure between eastern and western Georges Bank haddock in three out of six comparisons; providing a phenotypic basis for stock separation across the Bank. Of the three nonsignificant comparisons, two were influenced by low sample sizes (n=18), whereas the third was marginally nonsignificant (P>0.07) (Table 6). Eastern Georges Bank haddock tended to have smaller internal otolith morphometrics than western Georges Bank haddock, particularly during the first year of life when growth differences between progeny from the two spawning components may be most apparent.

Differences in the internal otolith structure of eastern and western Georges Bank haddock corresponded with apparent differences in their growth rates. Commercial landings data indicated smaller mean lengths and weights at age for eastern than for western Georges Bank haddock, indicative of slower growth rates (and resultant smaller otoliths) for eastern Georges Bank haddock (Brown[2]). Likewise, other studies have found significant relationships between linear and shape otolith morphometrics and fish growth (e.g., Mosegaard et al., 1988; Reznick et al., 1989; Secor and Dean, 1989; Smith and Kostlan, 1991; Fowler and Short, 1996). Consequently, regional differences in growth rate may be a principal determinant in

[2] Brown, R. W. 2000. Annual assessment data (unpubl. data). Food Web Dynamics Program, Population Dynamics Branch, Northeast Fisheries Science Center, 166 Water St., Woods Hole, MA 02543.

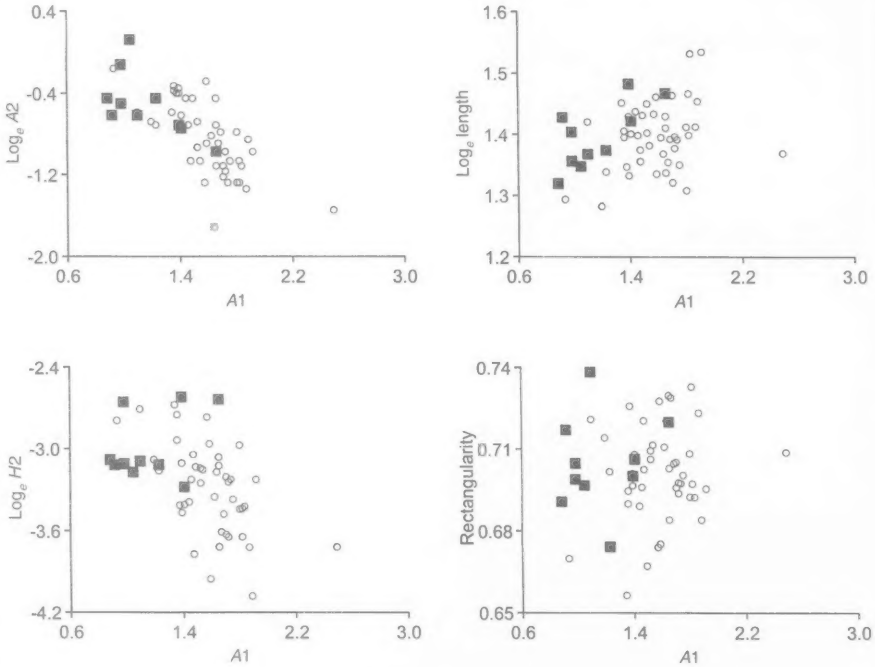

Figure 4

Scatter plots of internal otolith morphometric variables for 3-year-old haddock (1994 year class) showing grouping patterns of eastern Georges Bank (squares) and western Georges Bank (circles).

Table 6

Age- and year-class–specific jack-knifed cross-validation classification matrices of the frequency of assigned haddock samples from eastern (EGB) and western Georges Bank (WGB).

	Correct classification (%) of haddock samples by age group (year class)					
	Age 1 (1994)	Age 2 (1995)	Age 3 (1993)	Age 3 (1994)	Age 4 (1993)	Age 5 (1992)
n	18	35	18	54	53	20
EGB	71	72	67	80	75	80
WGB	64	88	56	84	59	70
Total	67	80	61	83	64	75

the development of regional differences in otolith morphometrics (Smith, 1992; Campana and Casselman, 1993). Growth (i.e. metabolic activity) alters the rate of otolith crystalline growth, which determines the size and shape of individual crystals, and ultimately the size and shape of individual otoliths (Gauldie, 1990). Differences in otolith shape may be mediated through differences in orientation and packing of otolith crystals that are influenced by rate of crystalline growth (Smith, 1992). Fast growth tends to form long thin crystals, in contrast to slow growth which forms short compacted crystals (Gauldie and Nelson, 1990).

Differences in growth rates (and hence, otolith structure) of eastern and western Georges Bank haddock appear to derive mainly from differences in water temperature and diet. Eastern Georges Bank haddock are affected more by colder Scotian Shelf waters than western Georges Bank haddock, which are affected more by warmer Gulf of Maine waters (Drinkwater and Mountain, 1997). Furthermore, eastern Georges Bank haddock appear to have less available food and have a diet that is less rich in protein (Garrison[3]). Hence, the colder waters and poorer diets experienced by eastern Georges Bank haddock correspond to slower growth rates. Moreover, this correspondence suggests that environmental factors are major determinants of otolith growth as has been inferred in other

[3] Garrison, L. P. 2000. Unpubl. data. Food Web Dynamics Program, Population Biology Branch, Northeast Fisheries Science Center, 166 Water St., Woods Hole, MA 02543.

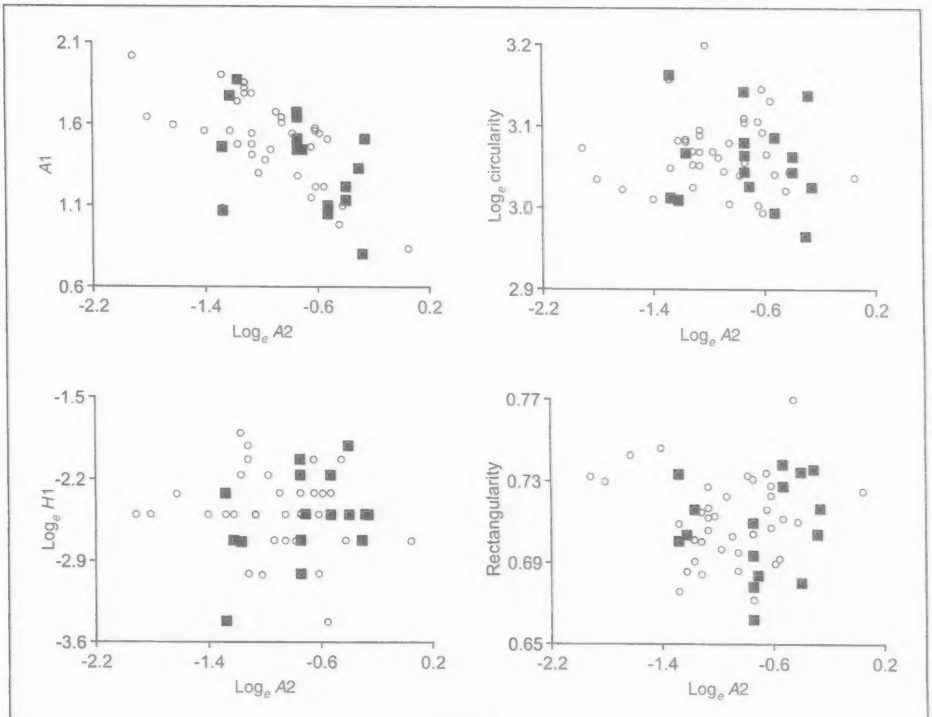

Figure 5

Scatter plots of internal otolith morphometric variables for 4-year-old haddock (1993 year class) showing grouping patterns of eastern Georges Bank (squares) and western Georges Bank (circles).

studies (Campana and Neilson, 1985; Mosegaard et al., 1988; Campana and Casselman, 1993), although there may also be a genetic contribution (Gauldie and Nelson, 1990; Friedland and Reddin, 1994).

The eastern and western Georges Bank spawning components, therefore, probably comprise phenotypically separate individuals that reflect differences in otolith structure due to environmental variation. These types of morphological differences indicate growth rate differences linked to the environment, rather than any genetic differences. Our results concur with previous studies that indicate separate spawning components on Georges Bank (Smith and Morse, 1985; Begg et al., 1999; Begg and Brown, 2000), although the degree of connectivity between the two components is not known. Larvae spawned on the Northeast Peak recruit to the central part of the Bank as they develop and are advected from there along its southern flank (Lough and Bolz 1989), whereas some larvae spawned throughout the Great South Channel are advected along the northern flank, with the result that there is some mixing between progeny. Further studies need to examine mixing rates and spawning-site fidelity of individual fish originating from the eastern and western Georges Bank spawning components in order to determine if there is an underlying genetic basis for stock separation.

Analysis of internal otolith morphometrics may provide a more detailed description of individual fish stocks than morphometric analysis of whole otoliths because the use of internal otolith morphometrics specifically incorporates individual growth zones, as well as characteristic shape qualifiers. Measurement of the first growth zone in whole otoliths has commonly been used in stock identification studies, although the results have been far from conclusive (e.g. Dawson, 1991; Hopkins[4]; Marecos[5]). Likewise, mixed results have been found for microstructure analysis of otolith nuclear dimensions and growth incremental widths (e.g. Rybock et al., 1975; Neilson et al., 1985; Mosegaard and Madsen[6]). Certainly, the use of more than one growth or shape dimension improved our ability to identify groups, but the utility or cost-effectiveness of internal otolith morphometrics may be questioned when compared to shape analysis of whole otoliths.

[4] Hopkins, P. J. 1986. Mackerel stock discrimination using otolith morphometrics. ICES CM 1986/H 7, 16 p.

[5] Marecos, M. L. 1986. Preliminary analysis of horse mackerel (*Trachurus trachurus* L.) otolith (L1) measurements. ICES CM 1986/H 72, 8 p.

[6] Mosegaard, H., and K. P. Madsen. 1996. Discrimination of mixed herring stocks in the North Sea using vertebral counts and otolith microstructure. ICES CM 1996/H 17, 8 p.

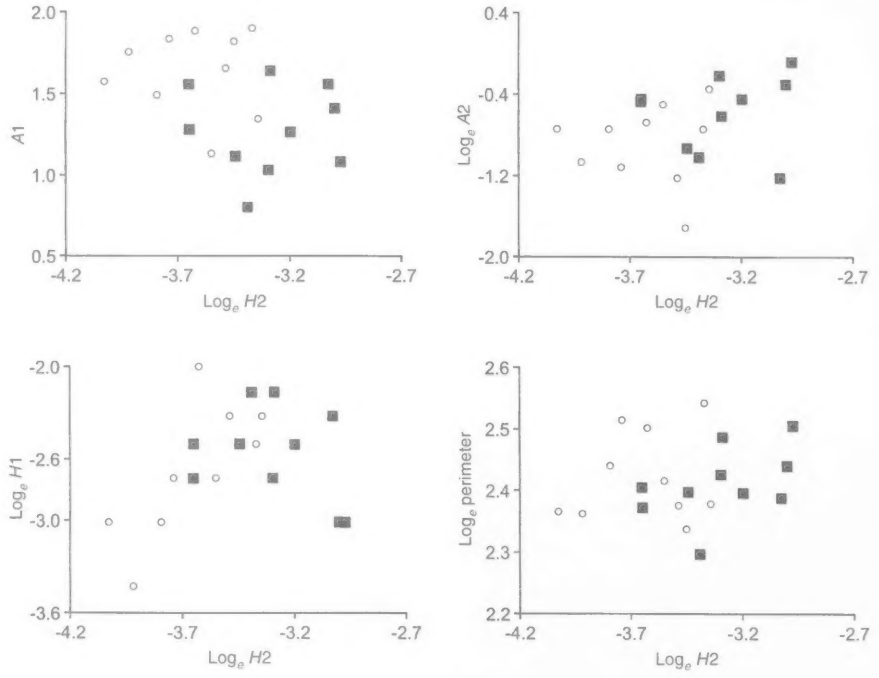

Figure 6

Scatter plots of internal otolith morphometric variables for 5-year-old haddock (1992 year class) showing grouping patterns of eastern Georges Bank (squares) and western Georges Bank (circles).

Classification success similar to our present study was found between eastern and western Georges Bank haddock in a comparable study where whole-otolith shape analysis was used (Begg and Brown, 2000). However, the use of internal otolith morphometrics entailed a few more caveats than that of whole-otolith shape analysis; therefore internal otolith morphometrics was questioned as a preferred tool for stock identification. Although our approach was semi-automated, with an aim to increasing objectivity and decreasing processing time, the use of internal otolith morphometrics still required some interpretation by the person taking the measurements. This was particularly true for growth zones, where interpretation partly compromised our goals of increasing objectivity and speed. Difficulties in interpreting measurements when growth zones are poorly defined can also be a source of uncertainty (Hopkins[4]). These sources of uncertainty should be minimized, provided the person taking the measurements is also an experienced reader of otolith growth increments.

Internal otolith morphometrics are useful for stock *identification*, but significant overlap among variables may preclude their use for stock *discrimination*, that is to say for classifying unknown fish according to origin of spawning component. Although mean values may differ between stocks, measurements from individual fish may not allow them to be classified to a particular stock because of individual within-stock growth differences (Pawson and Jennings, 1996). For example, slow-growing fish from a fast-growing stock may be incorrectly classified with a slow-growing stock (Campana and Casselman, 1993). However, provided growth differences exist and analyses are conducted to account for samples of mixed ages and year classes to minimize the effects of these confounding variables, internal otolith morphometrics can be a useful phenotype-based stock identification tool.

Results from this analysis on internal otolith morphometric differences have added to the evidence indicating separation between the eastern and western Georges Bank haddock spawning components. Although these differences do not provide a genetic basis for separation between the two spawning components, they do reflect the phenotypic characteristics of each spawning component, indicative of stock separation during life history. Studies such as this one, are needed to provide evidence of stock structure if historically established management units are to be changed in response to changing exploitation and resource patterns. Evidence of stock separation within the Georges Bank haddock resource may be useful in forming stock definitions that can be used by both the U.S. and Canada in defining

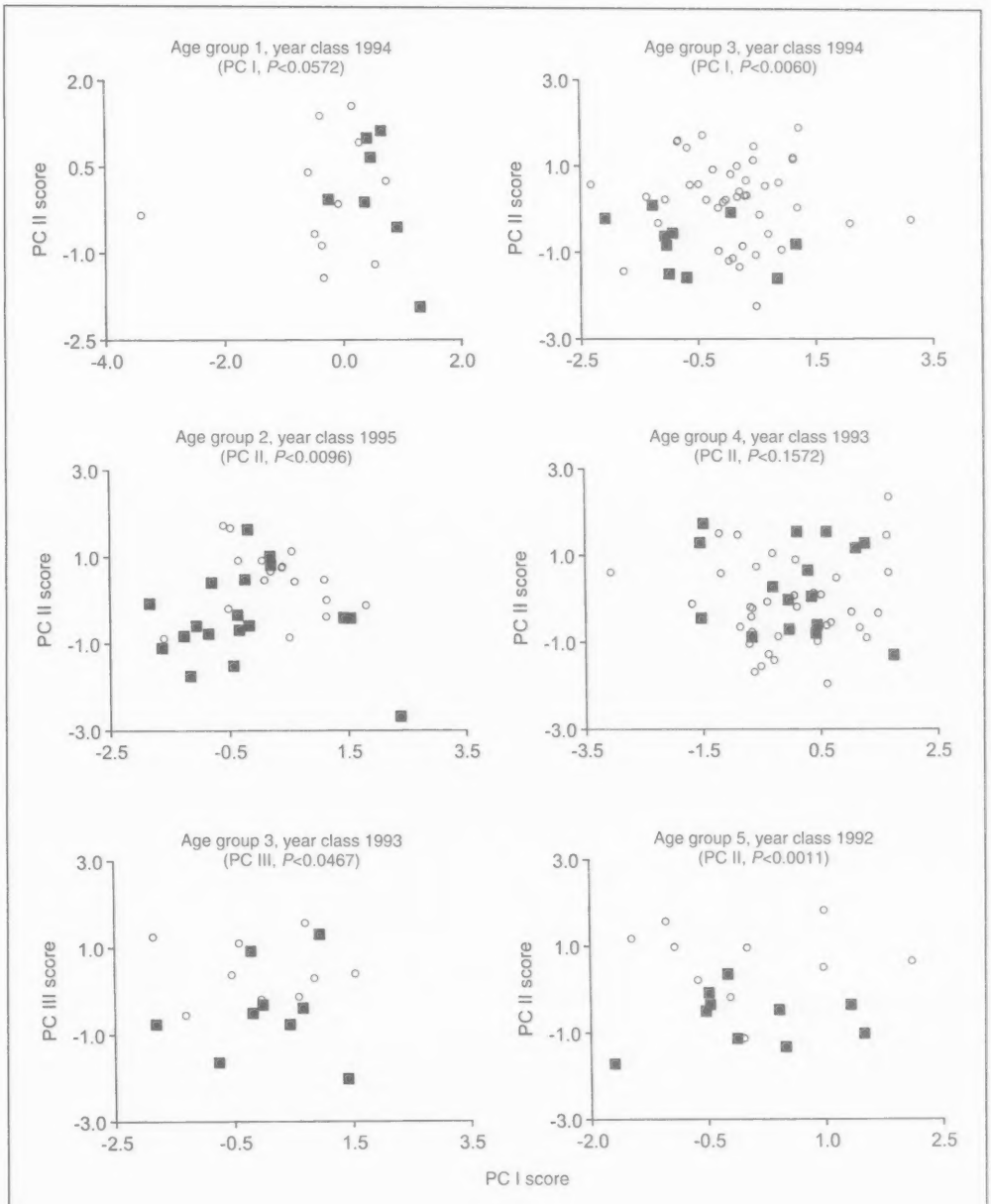

Figure 7

Principal component (PC) analysis of internal otolith morphometric variables and ANOVA results showing grouping patterns of eastern Georges Bank (squares) and western Georges Bank (circles) haddock.

management units that are consistent and account for the underlying stock structure of the resource. An incorrect decision could lead to significant shifts in resource distribution, changes in stock productivity, or declines in recruitment across stock unit boundaries. Although the precautionary approach would imply that we accept the two stock hypothesis as the default scenario until proven otherwise, this has not been the case. It would be desirable to ensure the conservation and stock rebuilding potential of both spawning components, particularly because we do not know at present the relative contribution of each to the overall status of haddock on Georges Bank.

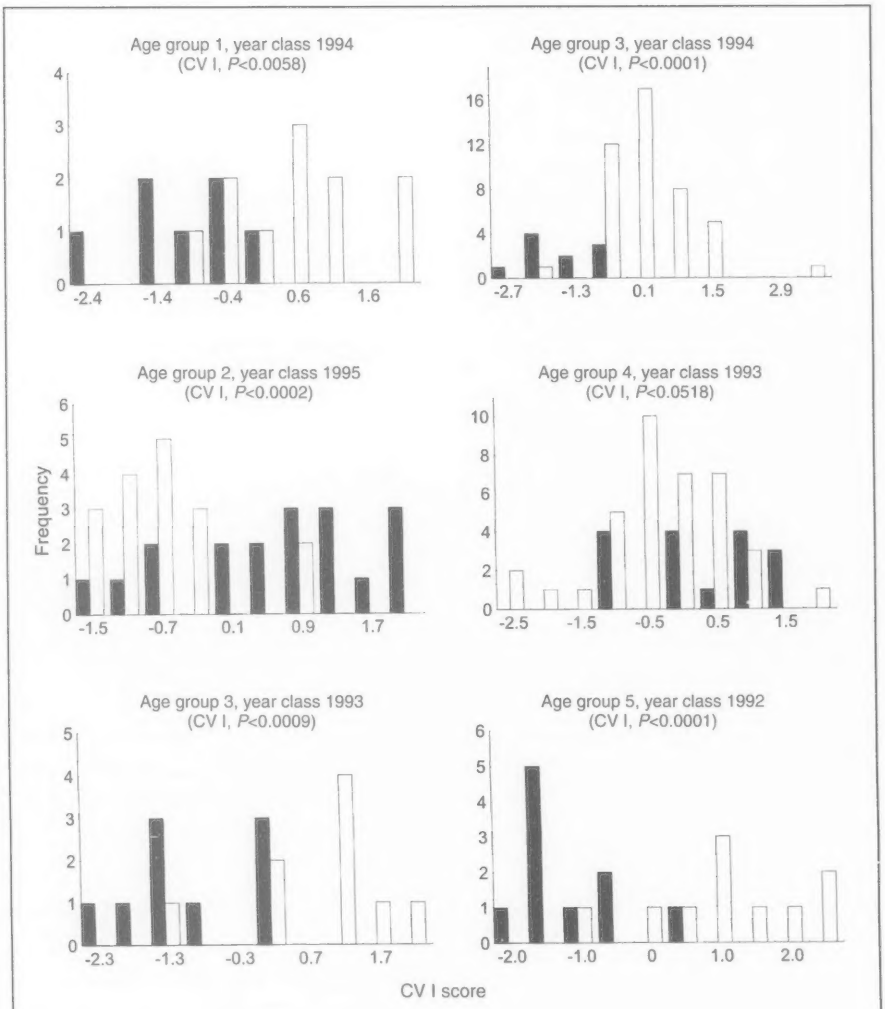
Age group 1, year class 1994
(CV I, P<0.0058)
Age group 3, year class 1994
(CV I, P<0.0001)
Age group 2, year class 1995
(CV I, P<0.0002)
Age group 4, year class 1993
(CV I, P<0.0518)
Age group 3, year class 1993
(CV I, P<0.0009)
Age group 5, year class 1992
(CV I, P<0.0001)
Frequency
CV I score

Figure 8

Discriminant (CV I) scores of internal otolith morphometric variables and corresponding ANOVA results showing grouping patterns of eastern Georges Bank (squares) and western Georges Bank (circles) haddock.

Acknowledgments

We would like to thank Russell Brown, Steve Murawski, Kevin Friedland, and two anonymous reviewers for their comments; Ruth Haas-Castro for assistance with OPTIMAS; and Frank Almeida, George Bolz, Jay Burnett, and Christine Esteves for their suggestions and assistance with ageing and collection of samples. This work was performed while G.A.B. held a National Research Council (NOAA/NMFS/NEFSC) Research Associateship.

Literature cited

Begg, G. A.
1998. A review of stock identification of haddock, *Melanogrammus aeglefinus*, in the northwest Atlantic Ocean. Mar. Fish. Rev. 60(4):1–15.

Begg, G. A., and R. W. Brown.
2000. Stock identification of haddock *Melanogrammus aeglefinus* on Georges Bank based on otolith shape analysis. Trans. Am. Fish. Soc. 129:935–945.

Begg, G. A., J. A. Hare, and D. D. Sheehan.
1999. The role of life history parameters as indicators of stock structure. Fish. Res. 43:141–163.
Begg, G. A., and J. R. Waldman.
1999. An holistic approach to fish stock identification. Fish. Res. 43:35–44.
Brown, R. W.
1998. Haddock. *In* Status of the fishery resources off the northeastern United States for 1998, p. 53–56. U.S. Dep. Commer., NOAA Tech. Memo. NMFS-NE-115.
Campana, S. E., and J. M. Casselman.
1993. Stock discrimination using otolith shape analysis. Can. J. Fish. Aquat. Sci. 50: 1062–1083.
Campana, S. E., and J. D. Neilson.
1985. Microstructure of fish otoliths. Can. J. Fish. Aquat. Sci. 42:1014–1032.
Casselman, J. M., J. J. Collins, E. J. Crossman, P. E. Ihssen, and G. R. Spangler.
1981. Lake whitefish (*Coregonus clupeaformis*) in the Great Lakes region. Can. J. Fish. Aquat. Sci. 38:1772–1789.
Castonguay, M., P. Simard, and P. Gagnon.
1991. Usefulness of fourier analysis of otolith shape for Atlantic mackerel (*Scomber scombrus*) stock discrimination. Can. J. Fish. Aquat. Sci. 48:296–302.
Clark, S. H., W. J. Overholtz, and R. C. Hennemuth.
1982. Review and assessment of the Georges Bank and Gulf of Maine haddock fishery. J. Northwest Atl. Fish. Sci. 3:1–27.
Dawson, W. A.
1991. Otolith measurement as a method of identifying factors affecting first-year growth and stock separation of mackerel (*Scomber scombrus* L.). J. Cons. Int. Explor. Mer 47:303–317.
Drinkwater, K. F., and D. G. Mountain.
1997. Climate and oceanography. *In* Northwest Atlantic groundfish: perspectives on a fishery collapse (J. Boreman, B. S. Nakashima, J. A. Wilson and R. L. Kendall, eds.), p. 3–25. Am. Fish. Soc., Bethesda, MD.
FAO (Food and Agriculture Organization of the United Nations).
1995. Code of conduct for responsible fisheries. FAO, Rome, 41 p.
Fowler, A. J., and D. A. Short.
1996. Temporal variation in the early life-history characteristics of the king george whiting (*Sillaginodes punctata*) from analysis of otolith microstructure. Mar. Freshwater Res. 47:809–18.
Friedland, K. D., and D. G. Reddin.
1994. Use of otolith morphology in stock discriminations of Atlantic salmon (*Salmo salar*). Can. J. Fish. Aquat. Sci. 51:91–98.
Garcia, S. M., and R. Grainger.
1997. Fisheries management and sustainability: a new perspective of an old problem? *In* Developing and sustaining world fisheries resources: the state of science and management: second world fisheries congress proceedings (D. A. Hancock, D. C. Smith, A. Grant, and J. P. Beumer, eds.), p. 631–654. CSIRO Publishing, Collingwood, Australia.
Gauldie, R. W.
1990. A measure of metabolism in fish otoliths. Comp. Biochem. Physiol. 97A:475–480.
Gauldie, R. W., and D. G. A. Nelson.
1990. Otolith growth in fishes. Comp. Biochem. Physiol. 97A:119–135.
Gavaris, S., and L. Van Eeckhaute.
1998. Assessment of haddock on eastern Georges Bank. Can. Dep. Fish. Oceans, DFO Atl. Fish. Res. Doc. 98/66, 75 p.
Halliday, R. G., and A. T. Pinhorn.
1990. The delimitation of fishing areas in the northwest Atlantic. J. Northwest Atl. Fish. Sci. 10:1–51.
Ihssen, P. E., H. E. Booke, J. M. Casselman, J. M., McGlade, N. R. Payne, and F. M. Utter.
1981. Stock identification: materials and methods. Can. J. Fish. Aquat. Sci. 38:1838–1855.
Lough, R. G., and G. R. Bolz.
1989. The movement of cod and haddock larvae onto the shoals of Georges Bank. J. Fish Biol. 35 (suppl. A):71–79.
Media Cybernetics
1996. OPTIMAS, version 6.2, eighth ed. Media Cybernetics, Silver Spring, Maryland, vol. I: xiii + 474 p., vol. II: viii + 630 p.
Messieh, S. N., C. MacDougall, and R. Claytor.
1989. Separation of Atlantic herring (*Clupea harengus*) stocks in the Gulf of St. Lawrence using digitized otolith morphometrics and discriminant function analysis. Can. Tech. Rep. Fish. Aquat. Sci. 1647, 22 p.
Morse, W. W., M. P. Fahay, and W. G. Smith.
1987. MARMAP surveys of the continental shelf from Cape Hatteras, North Carolina, to Cape Sable, Nova Scotia (1977–1984). Atlas 2: annual distribution patterns of fish larvae. U.S. Dep. Commer., NOAA Tech. Memo. NMFS-S/NEC 47, 215 p.
Mosegaard, H., H. Svedang, and K. Taberman.
1988. Uncoupling of somatic and otolith growth rates in Arctic char (*Salvelinus alpinus*) as an effect of differences in temperature response. Can. J. Fish. Aquat. Sci. 45:1514–1524.
Needler, A. W. H.
1930. The migrations of haddock and the interrelationships of haddock populations in North American waters. Contrib. Can. Biol. 6:241–313.
Neilson, J. D., G. H. Green, and B. Chan.
1985. Variability in dimensions of salmonid otolith nuclei: implications for stock identification and microstructure interpretation. Fish. Bull. 83:81–89.
Pawson, M. G., and S. Jennings.
1996. A critique of methods for stock identification in marine capture fisheries. Fish. Res. 25:203–217.
Pentilla, J., and L. M. Dery.
1988. Age determination methods for Northwest Atlantic species. U.S. Dep. Commer., NOAA Tech. Rep. NMFS 72:37–40.
Purcell, M. K., I. Kornfield, M. Fogarty, and A. Parker.
1996. Interdecadal heterogeneity in mitochondrial DNA of Atlantic haddock (*Melanogrammus aeglefinus*) from Georges Bank. Molecular Mar. Biol. Biotech. 5:185–192.
Reznick, D., E. Lindbeck, and H. Bryga.
1989. Slower growth results in larger otoliths: an experimental test with guppies (*Poecilia reticulata*). Can. J. Fish. Aquat. Sci. 46:108–12.
Rybock, J. T., H. F. Horton, and J. L. Fessler.
1975. Use of otoliths to separate juvenile steelhead trout from juvenile rainbow trout. Fish. Bull. 73:654–659.
Schroeder, W. C.
1942. Results of haddock tagging in the Gulf of Maine from 1923 to 1932. J. Mar. Res. 5:1–19.
Secor, D. H., and J. M. Dean.
1989. Somatic growth effects on the otolith-fish size relationship in young pond-reared striped bass, *Morone saxatilis*. Can. J. Fish. Aquat. Sci. 46:113–121.
Smith, M. K.
1992. Regional differences in otolith morphology of the deep

slope red snapper *Etelis carbunculus*. Can. J. Fish. Aquat. Sci. 49:795–804.

Smith, M. K., and E. Kostlan.
1991. Estimates of age and growth of ehu *Etelis carbunculus* in four regions of the Pacific from density of daily increments in otoliths. Fish. Bull. 89:461–472.

Smith, W. G., and W. W. Morse.
1985. Retention of larval haddock *Melanogrammus aeglefinus* in the Georges Bank region, a gyre-influenced spawning area. Mar. Ecol. Prog. Ser. 24:1–13.

Sokal, R. R., and F. J. Rohlf.
1995. Biometry, third ed. Freeman and Company, New York, NY, 887 p.

SPSS, Inc.
1997. SYSTAT 7.0 statistics. SPSS Incorporated, Chicago, IL, 751 p.

Stephenson, R. L.
1999. Stock complexity in fisheries management: a perspective of emerging issues related to population sub-units. Fish. Res. 43:247–249.

Van Eeckhaute, L. A. M., S. Gavaris, and E. A. Trippel.
1999. Movements of haddock, *Melanogrammus aeglefinus*, on eastern Georges Bank determined from a population model incorporating temporal and spatial detail. Fish. Bull. 97:661–679.

Reproductive biology of cobia, *Rachycentron canadum*, from coastal waters of the southern United States

Nancy J. Brown-Peterson
Robin M. Overstreet
Jeffrey M. Lotz

Department of Coastal Sciences
Institute of Marine Sciences
The University of Southern Mississippi
703 East Beach Drive
Ocean Springs, Mississippi 39564
E-mail address (for N. J. Brown-Peterson): Nancy.Brown-peterson@usm.edu

James S. Franks

Center for Fisheries Research and Development
Institute of Marine Sciences
The University of Southern Mississippi
703 East Beach Drive
Ocean Springs, Mississippi 39564

Karen M. Burns

Center for Fisheries Enhancement
Mote Marine Laboratory
1600 Thompson Parkway
Sarasota, Flordia 34236

Abstract—Reproductive biology of the cobia, *Rachycentron canadum*, is described from four coastal areas in the southern United States. Samples were obtained from recreational fishermen between December 1995 and November 1997 from the southeastern United States (Moreheau City, NC, to Cape Canaveral, FL), the eastern Gulf of Mexico (Ft. Myers to Crystal River, FL), the north-central Gulf of Mexico (Destin, FL, to Chandeleur Islands, LA) and the western Gulf of Mexico (Port Aransas, TX). Histological evidence of spawning occurred from April through September in all areas. Some female cobia (17–32%) throughout the Gulf of Mexico had spent or regressed ovaries by July. Gonadosomatic index peaked between May and July throughout the region. Ovaries of females from all areas contained both postovulatory follicles (POF) and oocytes in final oocyte maturation (FOM) during all months of the reproductive season. Batch fecundity was calculated by using three different methods: oocytes >700 µm were fixed in 1) Gilson's fixative or 2) 10% neutral buffered formalin (NBF), and 3) oocytes undergoing FOM were sectioned for histological examination. Mean batch fecundity ranged from 377,000 ±64,500 to 1,980,500 ±1,598,500 eggs; there was no significant difference among methods. Batch fecundity calculated with the NBF method showed a positive relationship with fork length (P=0.021, r^2=0.132) and ovary-free body weight (OFBW; P=0.016, r^2=0.143). Relative batch fecundity was not significantly different among months during the spawning season and averaged 53.1 ±9.4 eggs/g OFBW for the NBF method and 29.1 ±4.8 eggs/g OFBW for the FOM method. Although spawning frequencies were not significantly different among areas (P=0.07), cobia from the southeastern United States and north-central Gulf of Mexico were estimated to spawn once every 5 days, whereas cobia from the western Gulf of Mexico were estimated to spawn once every 9 to 12 days.

Manuscript accepted 22 August 2000.
Fish. Bull. 99:15–28 (2001).

The cobia, *Rachycentron canadum* (Goode, 1884), is a large coastal pelagic fish found worldwide in tropical and subtropical waters with the exception of the eastern Pacific (Shaffer and Nakamura, 1989). The cobia is a highly prized recreational species and record size fish have been caught in coastal waters off the southern United States, as well as off Western Australia, Nigeria, and Kenya (International Game Fish Association, 1998). Most specimens captured in the southern United States are landed by recreational anglers along the southeastern U.S. coast and in the Gulf of Mexico; however, some are caught incidentally by U.S. commercial fisheries, particularly in Florida waters (Shaffer and Nakamura, 1989).

Cobia are specifically targeted by a growing number of anglers in the southern United States, as evidenced by the increase in fishing tournaments for cobia. Information on age, growth, and seasonal movement is being collected through tagging programs in Virginia, Florida, Mississippi, and Louisiana (International Game Fish Association, 1998), and the age and growth of cobia from the north-central Gulf of Mexico was recently described by Franks et al. (1999). Limited information on the reproductive biology of cobia from the southern United States includes descriptions of the eggs, larvae, and juveniles from Chesapeake Bay (Joseph et al., 1964), North Carolina (Hassler and Rainville, 1975), and the northern Gulf of Mexico (Ditty and Shaw, 1992). Summer spawning of cobia has been reported from Chesapeake Bay (Richards, 1967), North Carolina (Smith, 1995), the northern Gulf of Mexico (Dawson, 1971; Burns et al.[1]), Louisiana (Thomp-

[1] Burns, K. M., C. Neidig, J. Lotz, and R. Overstreet. 1998. Cobia (*Rachycentron canadum*) stock assessment study in the Gulf of Mexico and in the South Atlantic. Final Rep., MARFIN Coop. Agreement NA57FF0294 to NMFS (NOAA), 108 p. Mote Marine Laboratory, 1600 Thompson Parkway, Sarasota, FL 34236.

son et al.[2]) and Texas (Finucane et al.[3]). Biesiot et al. (1994) described the biochemical changes in developing ovaries of cobia from the northern Gulf of Mexico and reported that spawning occurred during spring and summer. The most comprehensive information on cobia reproduction to date provides a detailed description of the gonadal maturation and spawning season for cobia from the north-central Gulf of Mexico (Lotz et al., 1996) and furnishes evidence that cobia are multiple, or batch spawners. Lotz et al. (1996) estimated batch fecundity on the basis of the largest mode of oocytes, but they did not estimate spawning frequency.

Our study was undertaken to document more thoroughly the reproductive biology of cobia from the southern region of the United States. Specifically, we describe and compare the spawning seasons and gonadal development from four coastal areas: the southeastern United States, the eastern Gulf of Mexico, the north-central Gulf of Mexico, and the western Gulf of Mexico. Additionally, batch fecundity and spawning frequency are estimated for cobia from the region. The results are discussed in light of the migratory nature of cobia throughout coastal waters of the southern United States.

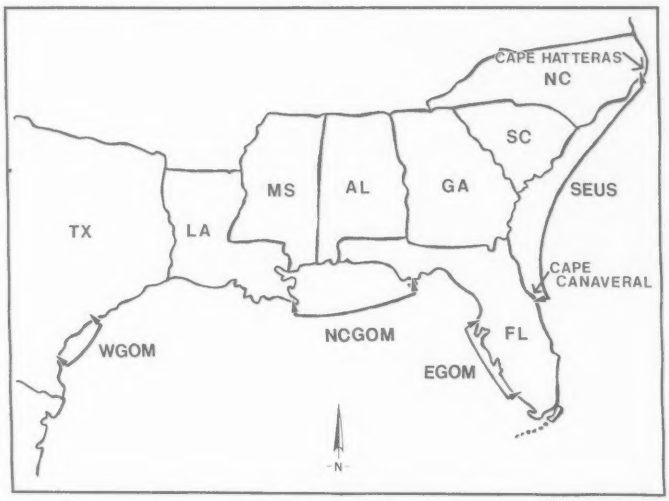

Figure 1

Areas sampled for cobia within the southern United States. SEUS = southeastern United States; EGOM = eastern Gulf of Mexico; NCGOM = northcentral Gulf of Mexico; WGOM = western Gulf of Mexico.

Materials and methods

Sample collection

Cobia were sampled from the coastal waters of four general regions in the southern United States (Fig. 1). The regions were defined as the southeastern United States (SEUS; Morehead City, North Carolina, to Cape Canaveral, Florida), the eastern Gulf of Mexico (EGOM; Ft. Myers to Crystal River, Florida), the north-central Gulf of Mexico (NCGOM; Destin, Florida to the Chandeleur Islands, Louisiana), and the western Gulf of Mexico (WGOM; Port Aransas area, Texas). In our study, coastal waters are defined as those extending over the continental shelf for 20 km in the Atlantic Ocean and for 80 km in the Gulf of Mexico.

We sampled cobia opportunistically from the recreational and charter boat fisheries from December 1995 to December 1997. Additional samples were taken in the north-central Gulf of Mexico during February and March 1999. Sampling teams were present at major cobia fishing tournaments throughout the study area; most samples from the SEUS and the NCGOM came from fishing tournaments. The majority of the cobia sampled from the EGOM were captured by nontournament recreational anglers. All fish from Texas were obtained from one charter boat captain during regular fishing trips. Anglers were interviewed to determine the location of capture of each fish. Fork length (FL, cm) and total weight (TW, g) were recorded at the dock and gonads were excised and placed on ice for transport to the laboratory. In the laboratory, gonads were weighed to the nearest 0.1 g (gonadal weight [GW]) and the gonadosomatic index (GSI) was calculated by using the formula

$$GSI = [GW/(TW - GW) \times 100].$$

Fish weights were unavailable from the WGOM; hence GSIs were not calculated for this region. Sections were removed from both left and right gonads and preserved in 10% neutral buffered formalin (NBF) for histological analysis. Cobia have been shown previously to have homogeneous oocyte development within the ovary (Lotz et al., 1996); thus, multiple sections of the same ovary were not removed for analysis. For fecundity analysis, two portions (approximately 5 g each) of the ovary were removed, weighed to the nearest 0.1 g, and preserved in Gilson's fixative (GF) and 10% NBF, respectively.

Histological analysis

Tissues were placed into individually labeled cassettes and rinsed with running tap water overnight prior to de-

[2] Thompson, B. A., C. A. Wilson, J. H. Render, M. Beasley, and C. Cauthron. 1992. Age, growth and reproductive biology of greater amberjack and cobia from Louisiana waters. Final Rep., MARFIN Coop. Agreement NA90AA-H-MF722 to NMFS (NOAA), 77 p. Coastal Fisheries Institute, LSU Center for Coastal, Energy and Environmental Resources, Baton Rouge, LA 70803.

[3] Finucane, J. H., L. A. Collins and L. E. Barger. 1978. Ichthyoplankton/mackerel eggs and larvae. Environmental studies of the south Texas outer continental shelf, 1977. Final rep. to Bur. Land Manage. Natl. Mar. Fish. Serv., NOAA, Galveston, TX 77550.

hydration and embedment in paraffin, following standard histological techniques. The paraffin blocks were sectioned at 4 µm by using a rotary microtome. Duplicate slides were prepared for each tissue, resulting in a total of four slides for each cobia specimen (two from each gonad). The slides were stained with Gill's I hematoxylin and eosin phloxine (Polyscientific Corporation) following standard histological procedures.

Three separate views from each side of the gonad of each fish were examined to determine maturity stages. Ovarian maturity classes were based on those previously described for cobia by Lotz et al. (1996). The entire ovarian section was examined for the presence of postovulatory follicles (POF) and oocytes undergoing final oocyte maturation (FOM). POF stages were classified following the methods of Hunter et al. (1986), although age estimates for POF stages in cobia are unverified. FOM stages were classified following Brown-Peterson et al. (1988). Following inspection of the entire ovarian section, three areas were arbitrarily selected from each slide for quantification of oocytes. Oocytes in all stages of development (including atretic oocytes) and POFs were counted at 100× and the percentage of each oocyte stage in the field of view was estimated. Oocyte atresia stages were classified by following the methods of Hunter and Macewicz (1985a).

The entire testicular section from each cobia was examined to determine the maturity classification for male fish. Three arbitrarily selected portions of each section were examined at 100× and 400× to classify all stages of spermatogenesis observed. Testicular maturity stages were based on those described for cobia by Lotz et al. (1996). Particular attention was given to the presence and amount of spermatogenesis in the testis.

Estimates of batch fecundity

Batch fecundity was estimated from the counts of oocytes in samples of ovarian tissue. Oocyte counts were obtained after teasing oocytes from tissues fixed in either GF or NBF for three to four months or from histological evaluation of tissue sections. The volumetric method was used to estimate fecundity for tissues fixed in GF or NBF (Bagenal and Braum, 1971). All oocytes freed from each GF or NBF sample were placed in 50 mL of water, stirred to homogeneity, and ten 1-mL samples were removed, combined, and the total volume brought to 50–70 mL with water. The diluted sample was stirred to homogeneity and 1-mL subsamples were removed, counted and replaced three to six times for each ovarian sample. All oocytes >700 µm from each subsample were counted and measured by using a stereo dissecting microscope and a computerized image analysis system. Oocytes of this size were used because Lotz et al. (1996) previously showed that cobia have a distinct mode of large oocytes prior to spawning. Typically, 25–100 oocytes were measured and counted in each subsample.

Estimates of batch fecundity based on histological evaluation were obtained by counting the number of oocytes undergoing FOM in six fields under a compound microscope at 100× magnification. The area of a single field of view was determined to be 0.0249 cm^2 by using a stage micrometer. The number of oocytes in final maturation observed in a field of view was converted to the number per mL by the formula

$$N \times 0.0249^{3/2} = N \times 0.003939.$$

FOMs were counted as 1 if ≥50% of the oocyte was in the field of view and were uncounted if <50% of the oocyte was in the field of view. The total number of FOMs in a fish was then determined by multiplying the estimated number per mL by the total volume of the ovaries. In all cases, fecundity was expressed as both batch fecundity (mean number of eggs/batch) and relative fecundity (number of eggs/gram of ovary-free body weight).

Ovarian volume was determined by volumetric displacement. The observed relationship between ovarian weight and ovarian volume was determined and that relationship was used to estimate ovarian volumes of fish for which direct volume measurements were unavailable. The analysis was restricted to fish with ovarian weights >500g.

Estimates of spawning frequency

Two methods based on histological observations were used to estimate spawning frequency of cobia: 1) the percentage of females in the late developing ovarian class with 0- to 24-h POF in the ovary and 2) the percentage of females in the late developing ovarian class undergoing FOM. Only fish in the late developing ovarian class were included in these analyses, because this is the only class in which cobia have the potential to spawn. For both methods, estimates of spawning frequency were determined according to the procedure of Hunter and Macewicz (1985b). The percentage of fish in the late developing maturity stage with ovaries containing either FOMs or POFs was calculated for each month in each region. This value represents the percentage of the fish in the population that are about to spawn (FOMs) or have just spawned (POFs). Spawning frequency (the number of days between spawnings) was determined by dividing 100 (representing the total population of fish) by the percentage of fish with FOMs or POFs in the ovaries.

Statistical analysis

Student's *t*-test was used to test for differences in GSI values between years. Batch fecundity data were tested for normality and homogeneity of variance. Simple linear regression was used to test the relationship between batch fecundity as the dependent variable and FL or ovary-free body weight as the independent variable. One way analysis of variance was determined for relative batch fecundity. A Mann-Whitney *U* test was used to compare fecundity estimates for the various methods used to determine fecundity. A chi-square test was used to test for differences in spawning frequency among areas. All statistics were computed by using SPSS-PC version 7.5 (SPSS, Inc., 1997) or Systat 8.0 (SPSS, Inc., 1998). Results were considered significant if $P < 0.05$.

Table 1

Numbers of cobia examined histologically from each sampling area.

Area	Males *n*	Months of capture	Females *n*	Months of capture
Southeastern United States (SEUS)	33	February–May	60	February–June
Eastern Gulf of Mexico (EGOM)	43	February–December	60	March–December
North-central Gulf of Mexico (NCGOM)	48	March–October	204	February–September
Western Gulf of Mexico (WGOM)	23	May–August	59	May–August
Totals	147		383	

Results

Fish collections

A total of 530 cobia (147 males, 383 females) from the southern United States were collected for histological analysis. The months and numbers of samples collected varied by region, but in all regions fish were collected primarily during the reproductive season (Table 1). Specimens ranged from 35.5 to 138.5 cm FL for females and 36.5 to 127.0 cm FL for males. Weights ranged from 0.64 to 34.93 kg for females and 0.91 to 40.82 kg for males.

Accurate estimates of the size and age at sexual maturity of cobia from the southern United States could not be determined in this study. Small, immature specimens were rare in recreational catches owing to a minimum retention size of 84 cm FL for cobia in state territorial waters and the EEZ. We collected only six sexually immature specimens (all females from the EGOM) during this study. The smallest reproductively active female encountered was 70 cm FL.

Spawning season and gonadal development

Cobia have a protracted spawning season (April through September) throughout the southern United States as determined from GSI values and histological assessments. There was no significant difference (P>0.05) in GSI values between corresponding months in 1996 and 1997 for either males or females in any region, with the exception of males in September from the NCGOM (P=0.049). Therefore, monthly data for 1996 and 1997 by region were combined (Fig. 2). GSI values for both sexes in SEUS increased sharply from April to May (Fig. 2A), indicating the onset of the reproductive season. GSI values for both sexes of cobia from EGOM began to increase in March, peaked in July, and declined and leveled off thereafter (Fig. 2B). GSI values for females from NCGOM increased in March, peaked in May, and then declined through September (Fig. 2C). In contrast, GSI values of males from NCGOM steadily increased through July, then fell precipitously in August (Fig. 2C). GSI values for males reached similar mean maxima in the SEUS and the NCGOM regions but were lower in the EGOM. However, mean GSI values of females were higher in both May and June for cobia from the SEUS than during any month from the Gulf of Mexico (Fig. 2).

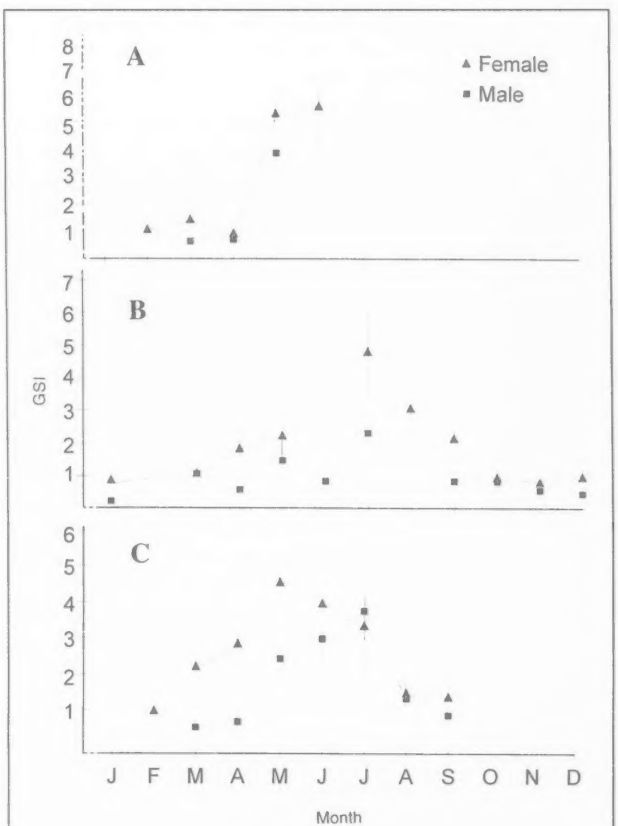

Figure 2

Monthly (1996 and 1997 combined) gonadosomatic index (GSI) values for cobia from the southern United States. Values represent mean ±1SE. (solid triangles=female, solid squares=male) (**A**) Southeastern United States. (**B**) Eastern Gulf of Mexico. (**C**) North-central Gulf of Mexico.

Table 2

Percentage of cobia in each ovarian maturity class for SEUS (Morehead City, NC, to Cape Canaveral, FL). Monthly data from 1996 and 1997 were combined. Percentage atresia was calculated for each development stage for ovaries with alpha- or beta-stage atresia only.

	Month of capture				
Class	February (n=3)	March (n=31)	April (n=10)	May (n=10)	June (n=6)
Early developing	66	41.9	20	0	0
% atresia	100	92	0	—	—
Mid-developing	34	16	10	0	0
% atresia	100	80	100	—	—
Late developing	0	41.9	70	100	100
% atresia	—	85	66	60	0
Spent	0	0	0	0	0
% atresia	—	—	—	—	—
Regressed	0	3.2	0	0	0
% atresia	—	0	—	—	—

Table 3

Percentage of cobia in each ovarian maturity class for EGOM (Crystal River to Ft. Meyers, FL). Monthly data from 1996 and 1997 combined. Percentage atresia was calculated for each development stage for ovaries with alpha- or beta-stage atresia only.

	Month of capture									
Class	March (n=2)	April (n=7)	May (n=3)	June (n=2)	July (n=6)	August (n=6)	September (n=3)	October (n=11)	November (n=13)	December (n=7)
Immature	100	0	0	50	0	16	0	18	7	0
Early developing	0	29	0	0	0	0	0	0	0	0
% atresia	—	50	—	—	—	—	—	—	—	—
Mid-developing	0	14	66	0	0	0	0	0	0	0
% atresia	—	0	50	—	—	—	—	—	—	—
Late developing	0	57	33	50	83	67	33	0	0	0
% atresia	—	50	0	0	0	50	0	—	—	—
Spent	0	0	0	0	17	0	0	18	8	14
% atresia	—	—	—	—	0	—	—	100	100	100
Regressed	0	0	0	0	0	17	66	64	85	86
% atresia	—	—	—	—	—	100	100	86	45	83

Histological analysis showed that all males from all areas were ripe during all months. Spermatogenic activity varied over the reproductive season, but males captured during February–May exhibited active spermatogenesis throughout the testis. No spermatogenesis occurred during August and September, but the testis contained spermatozoa. Males from EGOM during October through December had spermatozoa in the testis, although 50% or more of the males in November and December had the testis classified as spent.

Histological examination of ovaries revealed all classes of maturity, from early developing through regressed. Differences in monthly ovarian maturity between corresponding months in 1996 and 1997 were minimal; thus, monthly data were combined (Tables 2–5). A majority of ovaries from female cobia were in the late developing class by March in the NCGOM (Table 4) and by April in SEUS (Table 2) and EGOM (Table 3). Data from the WGOM (Table 5) were limited to only a portion of the reproductive season. Ovarian recrudescence began in February in the

Table 4

Percentage of cobia in each ovarian maturity class for NCGOM (Destin, FL, to Chandelier Islands, LA). Monthly data from 1996 and 1997 were combined. Percentage atresia was calculated for each developmental stage for ovaries with alpha- or beta-stage atresia only.

	Month of capture							
Class	February (n=10)	March (n=6)	April (n=20)	May (n=112)	June (n=1)	July (n=25)	August (n=8)	September (n=22)
Early developing	60	0	0	4.5	0	0	0	0
% atresia	60	—	—	20	—	—	—	—
Mid developing	0	33	10	7	0	4	0	0
% atresia	—	100	100	62	—	0	—	—
Late developing	0	67	90	88.5	100	64	37.5	18
% atresia	—	75	44	38	0	31	33	25
Spent	10	0	0	0	0	28	50	23
% atresia	100	—	—	—	—	86	100	80
Regressed	30	0	0	0	0	4	12.5	59
% atresia	0	—	—	—	—	0	0	100

Table 5

Percentage of cobia in each ovarian maturity class for WGOM (Port Aransas, TX) in 1996. Percentage atresia was calculated for each developmental stage for ovaries with alpha- or beta-stage atresia only.

	Month of capture			
Class	May (n=1)	June (n=8)	July (n=48)	August (n=2)
Mid developing	0	0	4	50
% atresia	—	—	50	0
Late developing	100	100	73	50
% atresia	0	0	5.7	0
Spent	0	0	21	0
% atresia	—	—	100	—
Regressed	0	0	2	0
% atresia	—	—	100	—

SEUS and the NCGOM, and females in the late developing class occurred in both areas by March (Tables 2 and 4). Spent females were initially observed in July in the Gulf of Mexico (Tables 3–5), although some females remained in the late developing class through September (Tables 3 and 4). Some females in the regressed class occurred in July throughout the Gulf of Mexico (Tables 3–5). In July, lengths of spent and regressed fish ranged from 88.0 to 93.0 cm FL in the EGOM, from 85.5 to 102.1 cm FL in the NCGOM, and from 86.4 to 128.3 cm FL in the WGOM.

Ovarian tissue in all classes of maturity showed atresia throughout the reproductive season. Alpha- and beta-stage atresia of yolked oocytes (Fig. 3A) was most prevalent in spent fish, but also occurred in females in the early, mid and late developing ovarian classes (Tables 2–5). Atresia of hydrated oocytes (Fig. 3B) occurred in ovaries in the late developing and spent classes only (5–10%). Atresia of nonyolked oocytes was difficult to recognize but was common (50–90%) in early developing ovaries. The later stages of atresia (gamma and delta, Fig. 3C) occurred in ovaries in all maturity classes. Many late developing females (60–85%) from the SEUS exhibited alpha- or beta-stage atresia during March through May (Table 2). Similarly, females from NCGOM exhibited high levels of atresia (75%) in ovaries in the late developing class during March (Table 4). Less atresia (38–50%) occurred during April and May in the ovaries of cobia from the Gulf of Mexico (Tables 3 and 4) as compared with cobia from the SEUS (Table 2).

Female cobia underwent final oocyte maturation (FOM) in all four areas sampled during April through September. The early stages of FOM were characterized by early lipid coalescence (Fig. 4A), followed by complete lipid coalescence and migration of the nucleus to the periphery of the oocyte (Fig. 4B). The final stages of FOM, characterized by breakdown of the nuclear membrane, yolk coalescence and hydration, were not observed in any sample. Final oocyte maturation was a synchronous process and most oocytes within an ovary were in the same stage of FOM (Fig. 4C). The percentage of mature oocytes (≥600 μm) undergoing FOM varied from 5% to 84% of the oocytes within a 100× microscopic field of view for all ovaries examined. Females from the EGOM had the highest mean percentage of mature oocytes undergoing FOM (49%). The mean percentage of mature oocytes undergoing FOM was lower, but similar, among the other regions (NCGOM, 19%; SEUS, 16%; WGOM, 15%). The mean percentage of females in the late-developing ovarian class undergoing

FOM ranged from 11% in the WGOM to 59% in the EGOM. On average, 19% of the females from SEUS and NCGOM were undergoing FOM.

The presence of POFs in cobia ovaries indicated spawning had commenced, although POFs were uncommonly observed; the greatest density of POF recorded was five per 100× microscopic field of view. Postovulatory follicles occurred in cobia ovaries in the late-developing class from all regions during April through September, suggesting that although cobia were in the late-developing class by March, spawning commenced in April. The 0-to12-h POF stage (Fig. 5A) was infrequently observed (16%) and was absent in females from the WGOM. The 24-h POF stage (Fig. 5B) was the most frequently observed (51%) and was most common in cobia from EGOM and NCGOM. The 48-h POF stage (33%, Fig. 5C) was difficult to distinguish from gamma- and delta-stage atresia, and most commonly occurred in cobia from theWGOM.

Spawning frequency

Estimates of monthly spawning frequency for the POF and FOM methods (Table 6) were consistent throughout the spawning season in all regions. Both methods showed good agreement for fish from SEUS and NCGOM. The POF method indicated a more frequent estimate of spawning rate in the NCGOM. On the other hand, the FOM method resulted in a more frequent spawning rate for cobia from the WGOM. Cobia from SEUS and NCGOM were estimated to spawn every 4 to 5 days, whereas those from WGOM spawned every 9 to 12 days. Chi-square analysis showed no significant difference in spawning frequency estimates for the three regions for either the POF (P=0.08) or the FOM (P=0.409) method. Months where fewer than five specimens had late developing ovaries were eliminated from the analysis because spawning frequency estimates would probably be inaccurate. No estimate was made for cobia from the EGOM, and spawning frequencies for the WGOM were based on fish captured in July. Spawning frequency estimates for SEUS were based on data from April, May, and June, whereas estimates for NCGOM were based on data from April, May, and July.

Relationship of ovary weight and volume

Direct volume measurements were performed for 86 females with ovarian weights

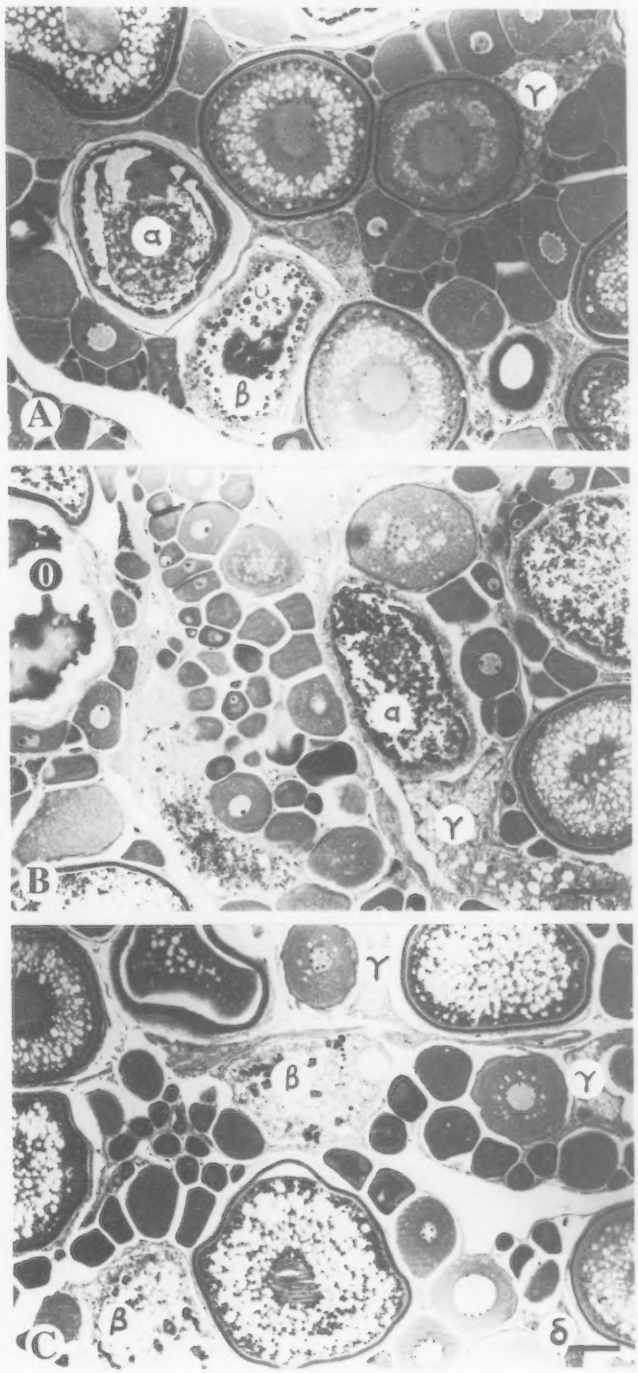

Figure 3

Stages of atresia in cobia ovaries. (**A**) Alpha (α), beta (β), and gamma (γ) stage atresia in a late-developing or spent ovary. Scale bar = 0.1 mm. (**B**) Alpha-stage atresia of a hydrated oocyte (0). Scale bar = 0.1 mm. (**C**) Beta (β), gamma (γ) and delta (δ) stages of atresia in a spent ovary. Scale bar = 0.1 mm.

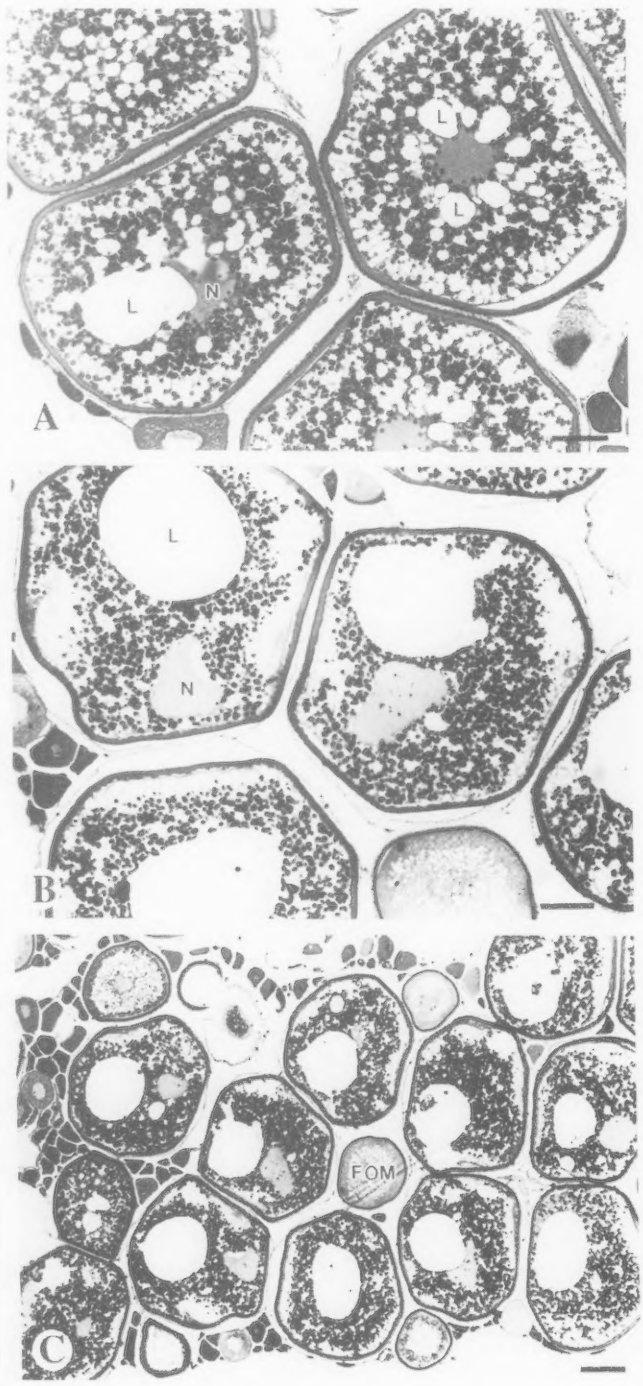

Figure 4

Final oocyte maturation (FOM) in late-developing cobia ovaries. (**A**) Early stage of FOM showing initial lipid coalescence (L). Scale bar = 0.1 mm. (**B**) More advanced stage of FOM. Lipids have coalesced to form a single large droplet (L) and the nucleus (N) is beginning to migrate to the periphery of the oocyte. Scale bar = 0.1 mm. (**C**) Oocytes undergoing synchronous FOM. Scale bar = 0.2 mm.

>500 g. The observed relationship was linear, and the best fit equation as judged by the least squares criterion was mL = –8.54 + 0.96g (r^2=0.978). The relationship indicated that cobia ovaries from 500 to 1600 g were less dense than seawater and that ovary density remained constant over that range.

Batch fecundity

Batch fecundity estimates were compared for samples from 11 females with ovaries fixed in GF, for 40 females with ovaries fixed in NBF, and for 26 ovarian samples examined by the histological method and where oocytes were undergoing FOM from April through September. Samples of this type were limited; therefore we combined observations from SEUS, EGOM, and NCGOM. Fecundity estimates for individual fish varied widely; however, there was no significant difference in mean estimates among the three methods (Mann-Whitney *U*-test, P>0.05; Table 7). Mean batch fecundity ranged from 377,000 ±64,500 eggs (CV=2.677) with the histological method to 1,980,500 ±1,598,500 eggs (CV=0.875) with the GF method.

Batch fecundity estimates for all three methods showed substantial variation. A Kolmogorov-Smirnov test of normality showed that batch fecundity was normally distributed for NBF samples (40 df, P>0.05) and FOM samples (26 df, P>0.05) and could be analyzed by using parametric statistics. Batch fecundity determined with the GF method was not used for further analyses owing to the small sample size. Regression analysis showed a significant, positive relationship between batch fecundity (BF) and FL (P=0.021, r^2=0.132) and BF and ovary-free body weight (OFBW; P=0.016, r^2=0.143) for NBF samples. The relationship between BF and OFBW for NBF samples (Fig. 6A) was described by

$$BF = OFBW^{1.717} - 36.813.$$

There was no significant relationship between BF and FL (P=0.105) or OFBW (P=0.097) for FOM samples. The relationship between BF and OFBW for FOM samples (Fig. 6B) was described by

$$BF = 19.29 \times \text{OFBW} + 1{,}113{,}713 \quad [r^2=0.11, P=0.097].$$

Mean batch fecundity, as determined from the NBF method, averaged 854,100 ±166,200 eggs and ranged from 247,100 ±204,400 eggs in August (n=2) to 923,000 ±237,700 eggs in May (n=26). Mean batch fecundity, as

determined with the FOM method, averaged 377,000 ±64,500 eggs and ranged from 212,500 ±122,700 eggs in August (n=5) to 637,000 ±376,600 eggs in September (n=3).

Relative batch fecundity (Table 8) did not vary significantly from April through September as determined by the NBF method (F=0.636, df=37, P=0.639) and the FOM method (F=0.468, df=24, P=0.759). Relative batch fecundity for the NBF method averaged 53.1 ±9.4 eggs/g ovary-free body weight throughout the reproductive season (n=39, Table 8) and it was lowest in August and highest in June. Relative fecundity values determined with the FOM method were lower than those with the NBF method, averaging 29.1 ±4.8 eggs/g ovary-free weight (n=25, Table 8), and were lowest in June and highest in July.

Potential annual fecundity for cobia was estimated from batch fecundity and spawning frequency estimates. A female cobia weighing 20 kg from SEUS or NCGOM may potentially spawn 20,952,000 (FOM method) to 38,232,000 (NBF method) eggs between April and September. In contrast, the same size female from WGOM would potentially spawn 8,730,000 (FOM method) to 21,240,000 eggs (NBF method) between April and September, with the data provided here.

Discussion

Our data show that the reproductive biology of cobia is similar throughout the coastal waters of the southern United States. Although sample sizes from some regions and months were small due to reliance on recreational catches for samples, we feel the data adequately represent the reproductive population from the four regions. Spawning commences in April throughout the region, as evidenced by the presence of oocytes undergoing FOM as well as 24-h POFs. These findings are in agreement with previous studies of cobia reproduction in the southeastern U.S. Atlantic Ocean (Smith, 1995) and the north-central Gulf of Mexico (Biesiot et al., 1994; Lotz et al., 1996; Thompson et al.[2]). Collections of larval cobia from the Gulf of Mexico during May through September (Ditty and Shaw, 1992) also confirm the spawning season. Reproductive activity of female cobia probably ceases during September in the Gulf of Mexico and extends at least through June in the SEUS. Smith (1995) reported that cobia from North Carolina spawned through July. Eggs and larvae

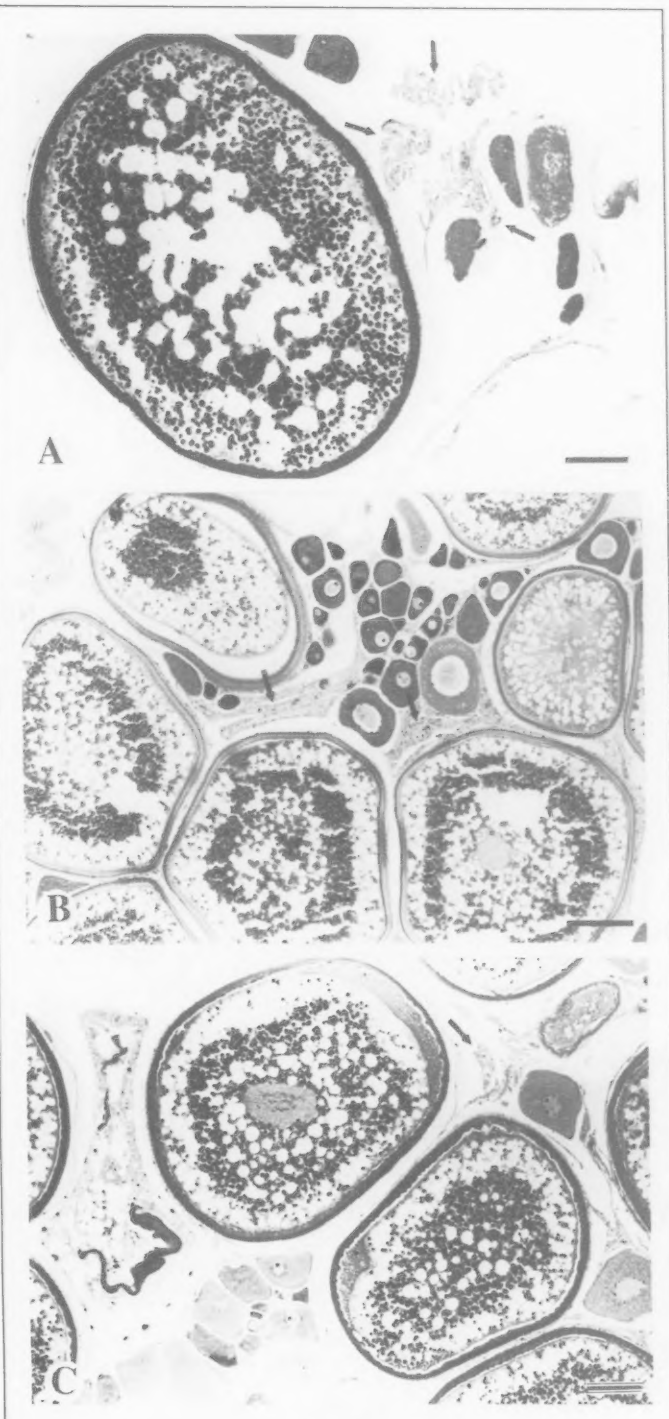

Figure 5

Postovulatory follicles (POF) in late-developing cobia ovaries. (**A**) 0- to 12-h POF (arrows). Scale bar = 0.1 mm. (**B**) 24-h POF (arrows). Scale bar = 0.2 mm. (**C**) 48-h POF (arrow). Scale bar = 0.1 mm.

Table 6

Mean estimated spawning frequencies of cobia from three regions in the southern United States. Spawning frequencies are estimated from the percentage of ovaries in the late developing ovarian class containing either postovulatory follicles (POF) or undergoing final oocyte maturation (FOM). Spawning frequency estimates were based on data from April to June in SEUS, from April, May, and July in NCGOM, and during July in WGOM.

	Region		
Spawning frequency	Southeastern United States (SEUS) (n=23)	Northcentral Gulf of Mexico (NCGOM) (n=135)	Western Gulf of Mexico (WGOM) (n=35)
% POFs	19.4	24.8	8.1
Frequency (POFs)	5.2 days	4.0 days	12.3 days
% FOM	19.4	19.8	10.8
Frequency (FOM)	5.2 days	5.0 days	9.2 days

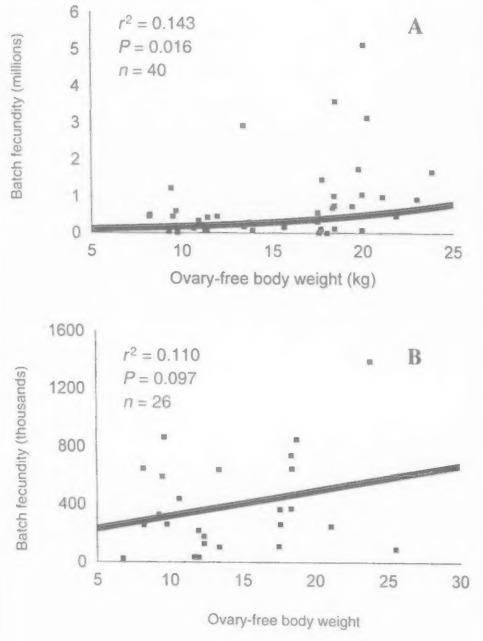

Figure 6

Relationship between batch fecundity (BF) and ovary-free body weight (OFBW) for cobia from the southern United States. Cobia were captured from April through September of 1996 and 1997 from the southeastern United States, the eastern Gulf of Mexico, and the north-central Gulf of Mexico. (**A**) Batch fecundity determined from formalin-fixed oocytes >700 µm. $BF = OFBW^{1.717} - 36.813$. (**B**) Batch fecundity determined from histological sections of oocytes undergoing final oocyte maturation. $BF = 19.29O \times OFBW + 1{,}113{,}713$.

Table 7

Batch fecundity estimates (no. of eggs) of cobia from the southern United States determined with three different methods. All means were not statistically different (Mann-Whitney U-test, P>0.05). NBF = neutral buffered formalin. FOM = final oocyte maturation.

	Fecundity method		
Measurement	Gilson's fixative (n=11)	10% NBF (n=40)	Histology (FOM) (n=26)
Percentage of ovary counted	0.02	0.02	0.005
Mean number of eggs	1,980,500	854,000	377,000
Standard error	1,598,500	166,200	64,500
Coefficient of variation	2.677	1.246	0.873
Minimum number of eggs	2,700	8,000	22,900
Maximum number of eggs	17,848,800	5,132,000	1,390,000

of cobia were collected from the Chesapeake Bay from mid-June through mid-August (Joseph et al., 1964), whereas cobia eggs from North and South Carolina were collected from mid-May through the end of August (Hassler and Rainville, 1975; Shaffer and Nakamura, 1989).

Gonadosomatic index values are indicators of the duration of the reproductive season for cobia, and they correlated well with our histological findings. However, Jons and Miranda (1997) advised caution in their use because of regional and temporal variations in GSI values. Therefore, GSI values should not be used for comparing or indexing

Table 8

Monthly mean relative batch fecundity expressed as number of eggs/g ovary-free body weight for cobia in the southern United States. Batch fecundity was determined from oocytes >700 µm in neutral buffered formalin (NBF) and from histological sections of oocytes undergoing final oocyte maturation (FOM). All means were not statistically different (ANOVA, $P>0.05$).

	NBF		FOM	
Month	*n*	Relative fecundity ±1SE	*n*	Relative fecundity ±1SE
April	1	46.6	0	—
May	25	51.2 ±12.2	8	24.6 ±4.9
June	2	115.7 ±102.2	3	21.9 ±12.9
July	5	44.0 ±9.2	6	40.2 ±12.9
August	2	29.8 ±25.2	5	24.6 ±14.9
September	4	57.7 ±27.5	3	33.2 ±13.0
Overall	39	53.1 ±9.4	25	29.1 ±4.8

maturity stages, particularly in multiple spawning fish. The GSI profile for both male and female cobia from the SEUS is similar to that described by Smith (1995) for cobia from North Carolina. On the other hand, GSI peaks for cobia from the northern Gulf of Mexico vary among studies. Biesiot et al. (1994) reported that female GSI values peaked in April, Lotz et al. (1996) found peak female GSI values in May, and Thompson et al.[2] reported peak female GSI values in June. Our data for females mirror those presented by Lotz et al. (1996); however, we suspect annual differences.

Our study was not designed to determine the size or age at first maturity for cobia. However, our limited data suggest that both sexes of cobia may achieve sexual maturity at a smaller size than that reported by Lotz et al. (1996) for the north-central Gulf of Mexico. This apparent difference in the size at sexual maturity could be partially explained by regional differences; most small female cobia in the present study (<85 cm FL) were captured in EGOM, whereas Lotz et al. (1996) sampled in NCGOM.

Male cobia are probably capable of spawning throughout the year because of the presence of sperm in the testis. A more detailed analysis of the histological pattern and spermatogenesis of male cobia will be discussed separately (Brown-Peterson et al.[4]). A similar longer reproductive season for male fish has been reported for other species with protracted spawning seasons including common snook (*Centropomus undecimalis,* Grier and Taylor, 1998; Taylor et al., 1998), spotted seatrout (*Cynoscion nebulosus,* Brown-Peterson et al., 1988), red drum (*Sciaenops ocellatus,* Grier et al., 1987), and blue tilapia (*Oreochromis aureus,* Grier and Abraham, 1983).

Cobia have a protracted spawning season, yet a portion of the females in the population may spawn during April–June only. Other females remain in spawning condition throughout September in the Gulf of Mexico. Lotz et al. (1996) and Biesiot et al. (1994) reported a similar occurrence in cobia from the NCGOM, and a high percentage of female cobia off Louisiana are spent and regressed by July (Thompson[5]). A comparable phenomenon, i.e. asynchronous cessation of spawning, was reported in the weakfish (*C. regalis*) in Chesapeake Bay (Lowerre-Barbieri et al., 1996). It is difficult to explain early cessation of spawning by some female cobia. Spent and regressed fish in July and August had a broad length distribution (85 to128 cm FL), suggesting that multiple age classes in the fishery have an abbreviated reproductive season. Perhaps some females delay ovarian maturation and spawn between July and September; this theory would account for the small percentage of females in the early- and mid-developing classes in May and June.

Differences in the amount of oocyte atresia during the spawning season between cobia from the SEUS and the Gulf of Mexico suggest differential spawning success during the early portion of the reproductive season. High percentages of alpha and beta atresia in cobia in the late-developing class from SEUS during March, April, and May suggest that many oocytes do not reach final maturation and that the atresia may be related to variable or unfavorable environmental conditions during spring (March–May) in the region. Hay and Brett (1988) showed a similar occurrence for Pacific herring (*Clupea harengus pallasi*) of increased atresia at the beginning of the reproductive season—condition they attributed to environmental factors rather than the female's physiological ability. Lowerre-Barbieri et al. (1996) used similar reasoning to explain the increased percentage of alpha and beta atresia present in the ovaries of weakfish captured during the beginning of the spawning season in Chesapeake Bay. Cobia from NCGOM also showed high percentages of atresia during March, the beginning of the reproductive season but prior to the initiation of spawning in that area. The lower percentage of females in the late-developing class with atretic oocytes in the Gulf of Mexico during April and May suggests a relatively high spawning success during the early portion of the spawning season in the Gulf of Mexico, and it also may suggest more stable environmental conditions in this region during late spring.

In the absence of hydrated oocytes in any cobia that we or Lotz et al. (1996) examined, we used three different methods to estimate fecundity of cobia containing large (>700 µm) oocytes. The wide range of results found among methods highlights the variations to be expected when estimating batch fecundity of a multiple spawning species.

[4] Brown-Peterson, N. J., H. J. Grier and R. M. Overstreet. 2000. Manuscript in preparation. Reproductive classes in male cobia (*Rachycentron canadum*) defined by changes in the germinal epithelium. Abstract and presentation at the 80th annual meeting of the American Society of Ichthyologists and Herpetologists, June 2000, La Paz, B.C.S., Mexico.

[5] Thompson, B. A. 1999. Personal commun. Coastal Fisheries Institute, LSU Center for Coastal, Energy and Environmental Resources, Baton Rouge, LA 70803.

It is reasonable to assume that a female will not always spawn the same number of oocytes during each spawning event and that this variation in batch size may not be related to body size, as indicated for fecundity estimates with the FOM method. Furthermore, although only large oocytes were counted with the GF and NBF methods, not all females with oocytes >700 µm underwent FOM, as determined by histological inspection. Because histological inspection is not always practical when fecundity estimates are taken, we feel our estimates should include all fish with oocytes >700 µm. Both the GF and NBF methods resulted in higher, but not significantly different, fecundity estimates than those yielded by the histological method, suggesting that the wide variation among individual fish obscures any meaningful difference among methods.

We believe our most accurate fecundity estimates are based on the actual histological counts of oocytes undergoing FOM. Our approach is supported by Hunter and Macewicz's (1985b) finding that oocytes undergoing FOM can be used for fecundity estimates in fish with rapid FOM when hydrated oocytes are unavailable. Although the exact time frame of FOM is unknown for cobia, we presume it is relatively rapid. For example, fish in the early stages of FOM were captured in the morning. Cobia are presumed to spawn during the day, probably the late afternoon, on the basis of collections of fertilized eggs (Ditty and Shaw, 1992). Other multiple spawning fish from similar latitudes (e.g. *C. nebulosus* [see Brown-Peterson et al., 1988], black drum, *Pogonias cromis* [see Fitzhugh et al., 1993], and *C. undecimalis* [see Taylor et al., 1998]) undergo FOM within 12 h. Several large scombrids also have rapid FOM (McPherson, 1993; Schaefer, 1996; Farley and Davis, 1998). From this evidence, we conclude that accurate batch fecundity estimates can be made for cobia by using oocytes from fish undergoing FOM.

The estimated mean batch fecundity values from the present study (1.9×10^6 eggs with the GF method, 8.5×10^5 with the NBF method, and 3.8×10^5 with the histologic method) are lower than previous mean estimates by Lotz et al. (1996) of 4.8×10^7 and Richards (1967) of 2–5 $\times 10^6$ eggs. Differences in methods no doubt explain the wide range in estimates. We used only oocytes >700 µm for fecundity estimates rather than all oocytes >550 µm used by Lotz et al. (1996) and Richards (1967). Our methods ensured that only oocytes likely to undergo hydration within the following 24 h were included in fecundity estimates. Lotz et al. (1996) suggested that their batch fecundity values may have been an overestimate because all the oocytes counted may not have been released during spawning. Richards (1967) probably also overestimated the batch fecundity of cobia, although his estimates are close to ours obtained by using the GF method.

Batch fecundity was not estimated for any species by using direct histological counts of oocytes undergoing FOM; thus, it is difficult to compare our results with other published results. Even though the estimates appear low when compared with more traditional methods of estimating fecundity, there is less variation in the counts. The relatively small sample size (n=26) used in our study for the FOM method may have resulted in an underestimation of batch fecundity. Increasing the sample size from <30 to 298 fish resulted in an increase as great as 33% in batch fecundity estimates for Atlantic mackerel (*Scomber scombrus*, see Watson et al., 1992). Although our batch fecundity estimates for cobia are realistic first approximations, additional samples are necessary to produce a more accurate mean estimate of batch fecundity, a crucial value for accurate spawning stock biomass assessments. In addition, the large variations in batch fecundity among individual fish are probably a biologically accurate representation of variations in batch size in this multiple spawning species. Thus, assigning a single value to the batch fecundity of cobia does not give a biologically accurate portrayal of spawning stock biomass.

The mean relative fecundity of 29.1 ±4.8 to 53.1 ±9.4 eggs/g ovary-free body weight calculated for cobia is low when compared with co-occurring inshore and estuarine fish in the region (Brown-Peterson et al., 1988; Fitzhugh et al., 1993). Cobia, like the co-occurring tripletail (*Lobotes surinamensis*), wahoo (*Acanthocybium solandri*), common dolphinfish (*Coryphaena hippurus*), king mackerel (*Scomberomorus cavalla*), and greater amberjack (*Seriola dumerili*), is a large, subtropical pelagic fish and exhibits a very different life history than smaller nearshore and estuarine species. Fecundity data are available only for two of these co-occurring species: wahoo, with an estimated relative fecundity of 57.7 eggs/g (Brown-Peterson et al., 2000) and tripletail, with an estimated relative fecundity of 47.6 eggs/g (Brown-Peterson and Franks, in press). Values from both species compare favorably with our estimates for cobia. Other pelagic species for which relative batch fecundity values are available include Atlantic mackerel (55.5 eggs/g; Watson et al., 1992), southern bluefin tuna (*Thunnus maccoyii*, 57 eggs/g; Farley and Davis, 1998) and yellowfin tuna (*Thunnus albacares*, 68 eggs/g; Schaefer, 1996). When the relative fecundity of the cobia is compared with that of other species with similar habitats and life histories, our estimate appears within the range of reported values for other pelagic species.

Our study represents the first report of spawning frequency for cobia. The FOM and the POF methods produced estimates of spawning at five-day intervals for cobia in the SEUS and NCGOM. However, these estimates are based on three months of data for a potential six-month spawning season and thus may not represent the spawning frequency throughout the entire reproductive period for each region. Regardless, this spawning frequency is lower than that reported for other large pelagic species, such as narrow barred Spanish mackerel (*S. commerson*, 2–3 d, McPherson, 1993), southern bluefin tuna (daily spawners, Farley and Davis, 1998), yellowfin tuna (1–2 d, Schaefer, 1996) and wahoo (2–6 d, Brown-Peterson et al., 2000), as well as for the smaller pelagic carangids (3 d, Clarke and Privitera, 1995), spotted seatrout (2–7 d, Brown-Peterson et al., 1988), common snook (1.1–2.5 d, Taylor et al., 1998), and red drum (2–4 d, Wilson and Neiland, 1994). Perhaps, the longer intervals between spawnings for cobia may be due to the longer distances that cobia need to travel between feeding and spawning grounds in comparison with the distances traveled by the

species just mentioned. The exact location of cobia spawning is unknown; early surveys have suggested spawning immediately outside the mouth of Chesapeake Bay (Joseph et al., 1964), whereas later data from the southeastern United States have indicated that cobia spawn offshore of North Carolina (Hassler and Rainville, 1975) and South Carolina (Shaffer and Nakamura, 1989). Egg collections in Crystal Bay, FL (Ditty and Shaw, 1992), imply that spawning occurs nearshore in the Gulf of Mexico, although other egg and larval evidence (Shaffer and Nakamura, 1989; Ditty and Shaw, 1992) suggest spawning occurs in the Gulf of Mexico on the shelf 50–90 km from shore. Further evidence for offshore spawning was the collection of small larvae (3.8–6.8 mm) 50–90 km off the coast of Texas (Finucane et al.[3]). Because most of our samples were captured no more than 40 km from shore, cobia in immediate pre- or postspawning condition may not occur in those locations. In addition, our hook-and-line method of capture may be biased against cobia in immediate pre- or postspawning condition owing to changes in feeding behavior at these stages.

Although spawning frequencies of cobia from the three study areas were not significantly different, the apparent lower spawning frequency of cobia in the WGOM may be biologically relevant. Cobia from SEUS and NCGOM were estimated to be capable of spawning up to 36 times during the six-month spawning season, whereas fish from WGOM were estimated as capable of spawning 15 to 20 times during the spawning season. Hydrologic features of the areas may explain the differences. The southeastern United States and the north-central Gulf of Mexico have substantial inputs of freshwater from major river systems which may result in high productivity in those areas (Livingston et al., 1997) and hence abundant food sources. In contrast, there is little freshwater input along the western Gulf of Mexico.

Another possible explanation for the differences in spawning frequencies may be that many cobia in the Gulf of Mexico spawn in a single location that is closer to the north-central region than to the western region. The lack of 12-h POFs and the predominance of 48-h POFs seen in the ovaries of cobia from the western Gulf of Mexico may be due to the longer distance that western cobia must travel from the spawning grounds. This hypothesis assumes that cobia in the Gulf of Mexico do not have distinct breeding areas or subpopulations—a hypothesis supported by Hrincevich's (1993) work on the molecular genetics of cobia. Although Hrincevich (1993) did find a high degree of heterogeneity in cobia mtDNA, this heterogeneity did not support the hypothesis that discrete stocks of cobia exist in the northern Gulf of Mexico. The genetic data, in combination with data from tagging studies in the northern Gulf of Mexico (Franks et al.[6]), suggest that cobia intermix not only within the Gulf of Mexico but also along the southeastern Atlantic coast of the United States. Thus, the overall similarities in the reproductive biology of cobia throughout the southern United States are not surprising. The information provided in our study on batch fecundity and spawning frequency of cobia should aid effective management of cobia stocks, as well as underscore areas where additional research is needed.

[6] Franks, J. S., J. T. McBee, and M. T. Allen. 1992. Studies on the seasonal movements and migratory patterns of the cobia, *Rachycentron canadum*, in Mississippi marine waters and adjacent Gulf waters. Interim Contract Rep. to Miss. Dep. Wildl., Fish, and Parks/Bur. Mar. Res, and U.S. Fish and Wildl. Serv, Atlanta, GA 30303. [Available from Gulf Coast Res. Lab., Ocean Springs, MS 36566-7000.]

Acknowledgments

We thank the Mote Marine Laboratory (MML) sampling team (Teresa DeBruler, Carole Neidig, Marion Hersey, Diana Skapura, Roger DeBruler, and Sasha Koulish [MML staff] and Jonnie Walker, Rob Roberts and Don and Toma Marshall [MML volunteers]), the Gulf Coast Research Laboratory (GCRL) sampling team (Don Barnes, Casey Nicholson, Nate Jordan, Jody Peterson, Jason Steckler, Nicola Garber, and Melanie Griggs), Scott Holt (The University of Texas Marine Science Institute), and Hal Osborne (Texas Department of Parks and Wildlife) for assistance with collecting cobia samples. We also thank the many anglers, charter boat captains, tournament directors, and student interns who assisted our sampling efforts. Histological support for this project was provided by Marie Wright, Kim Lamey, Mary Tussey, and Tershara Matthews (GCRL); Leslie Christmas (GCRL) furnished the fecundity counts. We thank Susan Carranza (GCRL) for photographic development and drawing of Figure 1. Mark Peterson (GCRL) assisted with statistical analysis and reviewed the manuscript. Joseph W. Smith (National Marine Fisheries Service, Beaufort, NC) was the technical monitor for this project. This project was funded by the National Oceanic and Atmospheric Administration, National Marine Fisheries Service (grant numbers NA57FF0294, NA86FL476, and NA96FL0358).

Literature cited

Bagenal, T. B., and E. Braum.
1971. Eggs and early life history. *In* Methods for assessment of fish production in fresh waters, (W. E. Ricker, ed.), p. 159–181. IBP (Int. Biol. Prgramme), Handbook 3, 2nd ed., Blackwell Sci. Publ., Oxford, England.

Biesiot, P. M., R. M. Caylor, and J. S. Franks.
1994. Biochemical and histological changes during ovarian development of cobia, *Rachycentron canadum*, from the northern Gulf of Mexico. Fish. Bull. 92:686–696.

Brown-Peterson, N. J.. and J. S. Franks.
In press. Aspects of the reproductive biology of tripletail, *Lobotes surinamensis*, in the northern Gulf of Mexico. Proc. Gulf Caribb. Fish. Inst. 52.

Brown-Peterson, N. J., J. S. Franks, and A. M. Burke.
2000. Preliminary observations on the reproductive biology of wahoo, *Acanthocybium solandri*, from the northern Gulf of Mexico and Bimini, Bahamas. Proc. Gulf Caribb. Fish. Inst. 51:414–427.

Brown-Peterson, N., P. Thomas, and C. R. Arnold.
1988. Reproductive biology of the spotted seatrout, *Cynoscion nebulosus*, in south Texas. Fish. Bull. 86:373–388.

Clarke, T. A., and L. A. Privitera.
1995. Reproductive biology of two Hawaiian pelagic carangid fishes, the bigeye scad, *Selar crumenophthalmus*, and the round scad, *Decapturus macarellus*. Bull. Mar. Sci. 56:33–47.

Dawson, C. E.
1971. Occurrence and description of prejuvenile and early juvenile Gulf of Mexico cobia, *Rachycentron canadum*. Copeia 1971:65–71.

Ditty, J. G., and R. F. Shaw.
1992. Larval development, distribution, and ecology of cobia, *Rachycentron canadum*, (Family: Rachycentridae) in the northern Gulf of Mexico. Fish. Bull. 90:668–677.

Farley, J. H. and T. L. O. Davis.
1998. Reproductive dynamics of southern bluefin tuna, *Thunnus maccoyii*. Fish. Bull. 96:223–236.

Fitzhugh, G. R., B. A. Thompson, and T. G. Snider III.
1993. Ovarian development, fecundity and spawning frequency of black drum *Pogonias cromis* in Louisiana. Fish. Bull. 91:244–253.

Franks, J. S., J. R. Warren, and M. V. Buchanan.
1999. Age and growth of cobia, *Rachycentron canadum*, from the northeastern Gulf of Mexico. Fish. Bull. 97:459–471.

Grier, H. J., and M. Abraham.
1983. A model for testicular recrudescence in *Oreochromis aureus*. *In* International symposium on tilapia in aquaculture (L. Fishelson and Z. Yaron, eds.), p. 200–209. Tel Aviv Univ. Press, Tel Aviv.

Grier, H. J.. and R. G. Taylor.
1998. Testicular maturation and regression in the common snook. J. Fish Biol. 53:521–542.

Grier, H. J., R. G. Taylor, and R. O. Reese.
1987. The mechanism of tubule elongation during testicular recrudescence in the redfish, *Sciaenops ocellatus* (Perciformes). *In* Proceedings of the V congress of European ichthyologists (S. O. Kullander and B. Fernholm, eds.), p. 285–291. Swedish Museum of Natural History, Stockholm.

Hassler, W. W., and R. P. Rainville.
1975. Techniques for hatching and rearing cobia, *Rachycentron canadum*, through larval and juvenile stages. Publ. UNC-SC-75-30, Univ. N.C. Sea Grant Coll. Prog., Raleigh, NC, 26 p.

Hay, D. E., and J. R. Brett.
1988. Maturation and fecundity of Pacific herring (*Clupea harengus pallasi*): an experimental study with comparisons to natural populations. Can. J. Fish. Aquat. Sci. 45:399–406.

Hrincevich, A. W.
1993. Mitochondrial DNA analysis of cobia *Rachycentron canadum* population structure using restriction fragment length polymorphisms and cytochrome B sequence variation. M.S. thesis, Univ. Southern Mississippi, Hattiesburg, MS, 91 p.

Hunter, J. R., and B. J. Macewicz.
1985a. Rates of atresia in the ovary of captive and wild northern anchovy, *Engraulis mordax*. Fish. Bull. 83:119–136.
1985b. Measurement of spawning frequency in multiple spawning fishes. *In* An egg production method for estimating spawning biomass of pelagic fish: application to the northern anchovy, *Engraulis mordax* (R. Lasker, ed.), p. 79–94. U.S. Dep. Commer., NOAA Tech. Rep. NMFS 36.

Hunter, J. R., B. J. Macewicz, and H. R. Sibert.
1986. The spawning frequency of skipjack tuna, *Katsuwonus pelamis*, from the south Pacific. Fish. Bull. 84:895–903.

International Game Fish Association.
1998. World record game fishes. International Game Fish Association, Pompano Beach, FL, 352 p.

Jons, G. D., and L. E. Miranda.
1997. Ovarian weight as an index of fecundity, maturity and spawning periodicity. J. Fish Biol. 50:150–156.

Joseph, E. B., J. J. Norcross, and W. H. Massman.
1964. Spawning of the cobia, *Rachycentron canadum*, in the Chesapeake Bay area, with observations of juvenile specimens. Chesapeake Sci. 5:67–71.

Livingston, R.J., X. Niu, F.G. Lewis III, and G.C. Woodsum.
1997. Freshwater input to gulf estuaries: long-term control of trophic organization. Ecol. Appl. 7:277–299.

Lotz, J. M., R. M. Overstreet, and J. S. Franks.
1996. Gonadal maturation in the cobia, *Rachycentron canadum*, from the northcentral Gulf of Mexico. Gulf Res. Reports 9:147–159.

Lowerre-Barbieri, S. K., M. E. Chittenden Jr., and L. R. Barbieri.
1996. The multiple spawning pattern of weakfish in the Chesapeake Bay and Middle Atlantic Bight. J. Fish. Biol 48:1139–1163.

McPherson, G. R.
1993. Reproductive biology of the narrow barred Spanish mackerel (*Scomberomorus commerson* Lacepede, 1800) in Queensland waters. Asian Fish. Sci. 6:169–182.

Richards, C. E.
1967. Age, growth and fecundity of the cobia, *Rachycentron canadum*, from the Chesapeake Bay and adjacent mid-Atlantic waters. Trans. Am. Fish. Soc. 96:343–350.

Schaefer, K. M.
1996. Spawning time, frequency, and batch fecundity of yellowfin tuna, *Thunnus albacares*, near Clipperton Atoll in the eastern Pacific Ocean. Fish. Bull. 94:66–76.

Shaffer, R. V., and E. L. Nakamura.
1989. Synopsis of biological data on the cobia, *Rachycentron canadum*, (Pisces: Rachycentridae). U.S. Dep. Commer., NOAA Tech. Rep. NMFS 82 [FAO Fish Synop. 153], 21 p.

Smith, J. W.
1996. Life history of cobia, *Rachycentron canadum* (Osteichthyes: Rachycentridae), in North Carolina waters. Brimleyana 23:1–23.

SPSS, Inc.
1997. SPSS PC version 7.5. SPSS, Inc., Chicago, IL, 628 p.

SPSS, Inc.
1998. SYSTAT 8.0: statistics. SPSS, Inc, Chicago, IL, 1086 p.

Taylor, R. G., H. J. Grier, and J. A. Whittington.
1998. Spawning rhythms of common snook in Florida. J. Fish Biol. 53:502–520.

Watson, J. J, I. G. Priede, P. R. Witthames, and A. Owari-Wadunde.
1992. Batch fecundity of Atlantic mackerel, *Scomber scombrus* L. J. Fish Biol. 40:591–598.

Wilson, C. A., and D. L. Nieland.
1994. Reproductive biology of red drum, *Sciaenops ocellatus*, from the neritic waters of the northern Gulf of Mexico. Fish. Bull. 92:841–850.

Abundance and depth distribution of harbor porpoise (*Phocoena phocoena*) in northern California determined from a 1995 ship survey

James V. Carretta
Barbara L. Taylor
Susan J. Chivers

Southwest Fisheries Science Center
National Marine Fisheries Service, NOAA
P.O. Box 271
La Jolla, California 92038
E-mail address (for J. V. Caretta): Jim.Caretta@noaa.gov

Abstract—We estimate abundance and describe the depth distribution of harbor porpoise (*Phocoena phocoena*) in northern California from a November 1995 ship survey. This was the first ship survey designed to systematically survey different depth strata out to 91 m (50 fathoms) in this region. Harbor porpoise abundance in northern California is estimated at 5686 (CV=0.29, log-normal 95% CI=3498–9242), based on 377 km of transect effort and 153 porpoise sightings. Using a confidence interval of differences approach, we determined that our abundance estimate was significantly different (P=0.08; α=0.10) from an aerial survey estimate obtained 1 to 2 months earlier in the same region, where abundance was estimated at 13,145 (CV=0.39, log-normal 95% CI=6316–27,357). Possible explanations for differences in estimates include seasonal movement of porpoise to other areas or depths, insufficient transect effort during the ship survey, or underestimates of the fraction of porpoise groups missed on the trackline due to large swells. Porpoise distribution in northern California was not random with respect to water depth; significantly more porpoise than expected occurred at depths of 20 to 60 m and fewer porpoise than expected occurred at depths >60 m.

Manuscript accepted 21 July 2000.
Fish. Bull. 99:29–39 (2001).

The abundance and distribution of harbor porpoise (*Phocoena phocoena*) in California waters has recently been described from a series of aerial surveys conducted by the U.S. National Marine Fisheries Service (NMFS) (Forney et al., 1991; Barlow and Forney, 1994; Forney 1995; Forney, 1999). The most recent abundance estimate was 5732 (CV=0.28) for central California and 11,066 (CV=0.39) for northern California, based on aerial surveys conducted from 1993 to 1997.[1] Declining trends in porpoise abundance have recently been described in central California based on aerial surveys conducted from 1986 to 1995 (Forney, 1995, 1999). This perceived decline is unexpected because the central California population was expected to recover following a substantial reduction in fishery-related mortality beginning in the late 1980s (Barlow and Forney, 1994; Barlow and Hanan, 1995; Julian and Beeson, 1998). Forney (1999) noted that harbor porpoise abundance was negatively correlated with positive sea surface temperature anomalies off central California and suggested that perceived declines in porpoise abundance may be due to interannual movement of animals in and out of the study area in response to changing oceanographic conditions, rather than an actual population decline. Because the aerial survey study area was limited to nearshore waters ≤91 m (50 fathoms) in depth, one possible explanation was that porpoise might move into deeper waters in response to anomalous periods of warm water (Forney, 1999). Another explanation is that harbor porpoise moved north into northern California in response to warm-water episodes (Forney's trend data showed an increase in porpoise abundance in northern California during the same period of decline in central California, although sample sizes from northern California were too small to make unequivocal statements about trends in population size). Forney (1995, 1999) recommended that directed vessel surveys examine the influence of oceanographic and environmental variables on the distribution and abundance of harbor porpoise and focus on possible changes in the depth distribution of porpoise and the distribution of prey species (Forney 1995, 1999). Current knowledge of harbor porpoise stock structure off California suggests that porpoise do not make long-distance movements; thus it is possible that a perceived population decline in central California is the result of small-scale changes in porpoise distribution, given that aerial survey transects have remained unchanged since 1986 (Forney 1995, 1999).

Today, NMFS recognizes (and manages separately) four stocks of harbor porpoise along the U.S. west coast; 1)

[1] Forney, K. A. 1999. The abundance of California harbor porpoise estimated from 1993–97 aerial line-transect surveys. Administrative report LJ-99-02. National Marine Fisheries Service, Southwest Fisheries Science Center, 16 p. [Available from Southwest Fisheries Science Center, P.O. Box 271, La Jolla, CA 92038.]

central California; 2) northern California; 3) Oregon-Washington outer coast; and 4) inland Washington waters (Barlow et al., 1997, 1998, Forney et al., 1999). Evidence for geographic subdivision of harbor porpoise populations along the U.S. west coast is apparent from pollutant studies (Calambokidis and Barlow, 1991), which reveal latitudinal gradients in chlorinated hydrocarbon levels in waters off Washington, Oregon, and California. Molecular genetic studies have also demonstrated larger-scale geographic population subdivisions within the northeast Pacific, where four putative populations (Alaska, British Columbia, Washington, and California) are recognized (Rosel et al., 1995). More recent genetic analyses, based on more sampling locations and different genetic markers, have provided evidence to support recognition of these four populations. Smaller-scale geographic subdivision within California remains unresolved.[2]

We present the results of a 13–30 November 1995 line-transect ship survey in waters off California, which was designed to estimate abundance and describe the depth distribution of harbor porpoise. This was the first ship survey to cover this region in late autumn and to survey systematicallly different depth strata out to 91 m (50 fathoms). The 1995 ship survey contrasts with previous NMFS ship surveys that were conducted earlier in the year along the 18-m isobath and that relied on models of porpoise density at different depths to calculate abundance (Barlow, 1988). We estimate porpoise abundance for two regions within California (Fig. 1): Bodega Bay to the California-Oregon border, hereafter referred to as "northern California," and Point Sur to San Francisco Bay in central California, hereafter referred to as "region 2," as delineated by Barlow (1988). We emphasize results from northern California because relatively little survey effort was conducted in central California. We compare statistically aerial and ship survey abundance estimates in 1995 with those from recent aerial surveys in northern California and region 2 in central California, using a confidence interval of differences (CI_d) method proposed by Lo (1994). We also describe the depth distribution of harbor porpoise in northern California from the 1995 ship survey sighting data.

Methods

Observers searched for marine mammals during daylight hours from the 53-m NOAA research vessel *McArthur*. Nine observers rotated through five duty stations on the flying bridge 10 m above sea level, spending 30 minutes at each station. Two observers at the periphery of the flying bridge scanned from the trackline to the ship's beam (0 to 90 degrees) with 7× binoculars and two inner observers scanned from the trackline to 45 degrees on each side. The middle observer recorded data into a laptop computer and searched for porpoise groups by naked eye. A sixth independent observer opportunistically searched from the ship's bridge level (~7.5 m above sea level) to estimate the fraction of porpoise groups missed by the primary team of five observers.

A series of predetermined saw-tooth transect lines began at Point Conception, California (34°27′N) and ended at the California-Oregon border (42°00′N). Transect lines extended from approximately the 20-m isobath to the 91-m (50 fathom) isobath. Some depths greater than 91 m were surveyed, especially where the axes of submarine canyons intersected our transects. The ship could not routinely operate in water depths shallower than 20 m. The ship proceeded along the transect lines in passing mode, i.e. it did not deviate from course even when porpoise groups were sighted. The study area was divided into several *a priori* analysis regions (Fig. 1), the same as those used by Barlow (1988) and Barlow and Forney (1994). The region referred to as "northern California" incorporates region 4 and that part of region 5 that is south of the California-Oregon border (Fig. 1). Areas of each region were previously calculated by Forney.[3]

An event-driven data acquisition program (PPCRUISE) was used to record all sighting and effort data. The program was run on a laptop computer linked to the ship's GPS system to obtain geographic position data. For each harbor porpoise group sighted, bearing and distance from the ship were recorded. Observers obtained the bearing to harbor porpoise groups using mounted protractors on the flying bridge. Distance to harbor porpoise groups was read from calibrated reticle marks imprinted on the eyepiece of 7× binoculars (Barlow and Lee, 1994) or estimated by eye for some close groups. Depth soundings were recorded systematically every two minutes while the ship was underway. The position of each porpoise sighting was calculated to correct for differences between the position of the ship and porpoise groups. Depths at which porpoise were sighted were determined from National Ocean Service (NOS) hydrographic survey data[4] by using a triangulated irregular surface model in Arc Info GIS.

To estimate abundance, we used transect data collected only during calm sea states, defined as Beaufort 0 through 2 (wind speeds up to 6 knots, no whitecaps present). Porpoise abundance was estimated out to the 91-m isobath. Effort segments in deeper water were excluded from line-transect analysis to allow direct spatial comparison with recent aerial survey results (Barlow and Forney, 1994; Forney[1]). Porpoise abundance in region i was estimated

[2] Chivers, S. J. 1999. Personal commun. NMFS, Southwest Fisheries Science Center, P.O. Box 271, La Jolla, CA. 92038.

[3] Forney, K. 1988. Contour mapping and the calculation of areas between 10m depth contours along the coasts of California, Oregon and Washington. Administrative report LJ-88-23, National Marine Fisheries Service, Southwest Fisheries Center, 18 p. [Available from Southwest Fisheries Science Center, P.O. Box 271, La Jolla, CA 92038.]

[4] National Oceanic and Atmospheric Administration (NOAA), National Geophysical Data Center (NGDC). 1999. National Ocean Service (NOS) hydrographic survey data, U.S. coastal waters, version 4.0, available on CD-ROM. Website: *http://www.ngdc.noaa.gov/ngdc.html*

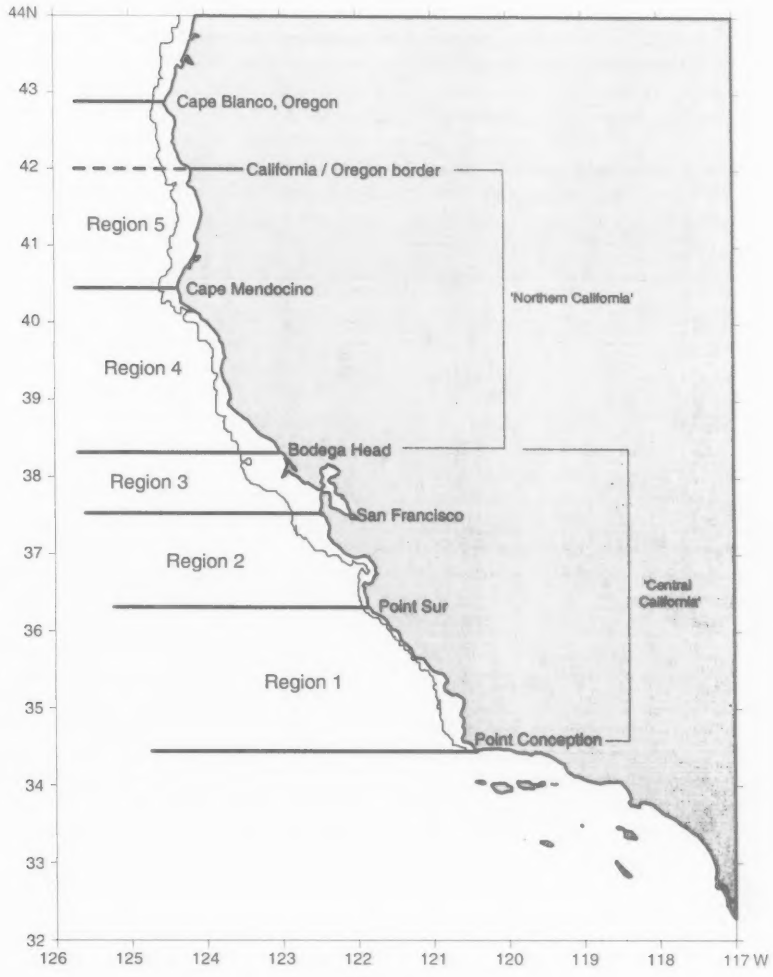

Figure 1

Study regions referred to in text. "Northern California" is defined as region 4 as well as part of region 5 south of the California-Oregon border. Central California includes regions 1–3. The thin line just offshore from Point Conception to Cape Blanco, Oregon, delineates the 91-m (50-fathom) depth contour.

by using standard line-transect methods (Buckland et al., 1993):

$$\hat{N} = \frac{A_i n_i S_i f(0)}{2L_i g(0)},$$

where A_i = size of the study area (km^2) in region i;
n_i = number of sightings in region i;
S_i = mean group size in region i;
$f(0)$ = sighting probability density (/km) at zero perpendicular distance
L_i = length of transect line (in km) surveyed in region i, and
$g(0)$ = probability of seeing a porpoise group directly on the trackline.

The histogram of radial sighting distances revealed spikes at distances corresponding to whole and half-reticle binocular readings, which suggests that observers tended to round-off radial sighting distances. In the absence of rounding error, the distance interval between any two adjacent radial sighting distances should have been relatively equal for both near and distant sightings, but these intervals usually increase with distance because of reduced precision in reading reticles at greater distances. Theoretically, a linear regression of dis-

tance from the observer against the interval between adjacent radial sighting distances should have a slope of zero in the absence of rounding error. Following Barlow,[5] we modeled the rounding error in radial sighting distances with this regression method, where the slope of the regression represents the percentage of rounding error. As a result, we smeared radial sighting distances by a random factor between ±4%. Observers also showed a tendency to round bearing angles to the nearest 5 degrees; therefore we smeared angles by a random number between ±5 degrees to further reduce the effects of rounding (Buckland et al., 1993).

We noted a problem in the recording of radial sighting distances when the ship was closer than 5.6 km (3 nmi) to shore. In these cases, the shoreline was closer than the true horizon and radial sighting distances were sometimes recorded by using the shoreline as the horizon (documented from database comments and inferred in other cases). The use of the shoreline as a false horizon introduces errors because resulting radial (and perpendicular) sighting distances are positively biased. Thirty sightings were identified for which shoreline bias probably resulted in positively biased distance readings. Frequency distributions of "shoreline-biased" and "unbiased" perpendicular sighting distances were significantly different (Kolmogorov-Smirnov test, $P<0.001$) and the "shoreline-biased" distribution revealed a higher proportion of sightings beyond 400 m. To reduce this bias, we excluded the "shoreline-biased" sightings prior to data truncation and to fitting the detection function to the perpendicular distance data. Buckland et al. (1993) recommend truncation of 5% to 10% of the largest perpendicular distances prior to model fitting. We truncated all sightings beyond 1 km, which eliminated 10% of all sightings. Three models (hazard rate, half-normal, and uniform) were fitted to the perpendicular distance data by using the program DISTANCE (Laake et al.[6]) and the most parsimonious model was selected by DISTANCE based on minimizing Akaike's Information Criterion (AIC: Akaike, 1973; Buckland et al., 1993). We also fitted the above models by using other truncation distances and bin intervals to examine the sensitivity of abundance estimates to these values.

Because large porpoise groups are more likely to be detected at greater distances than single animals or pairs, it is possible to introduce bias into abundance estimates by overestimating mean group size. Truncation of distance data will reduce potential overestimation of group size because the largest groups are eliminated, thus minimizing this bias. An additional step to reduce overestimation is to test for dependence between group size and detection distance by regressing the log of the observed group size against the detection probability at distance x [$\log(s_i)$ versus $\hat{g}(x)$], as recommended by Buckland et al. (1993). If the regression is significant at $\alpha = 0.15$, the mean group size is replaced with the regression-based estimate of mean group size at zero distance, where theoretically, group size bias should not occur. We used this regression method in the program DISTANCE to determine which group sizes to use for estimating abundance.

We tested the null hypothesis that harbor porpoise are randomly distributed with respect to depth by comparing the proportion of porpoise sightings to the proportion of survey effort within 20-m depth intervals. We used depth soundings as a measure of survey effort because soundings were taken at regular 2-minute intervals while the ship was underway. If harbor porpoise are randomly distributed by depth, then the proportion of porpoise sightings to depth soundings should be relatively equal for a given depth interval. Distributions were compared by using a nonparametric Kolmogorov-Smirnov goodness-of-fit test.

Precision of the abundance estimates was estimated with two methods. Log-normal confidence intervals were calculated analytically with formulae presented in Buckland et al. (1993). Bootstrap confidence intervals and coefficients of variation (CV) were calculated as follows. Effort and sighting data from region i were divided into 5-km effort segments (for Beaufort 0–2 sea states only). A TRUEBASIC computer program (BOOTPORP) was written to randomly draw (with replacement) effort segments within each region until the number of kilometers drawn equaled the number of kilometers actually surveyed. A pseudo-abundance estimate was then calculated from this bootstrap sample and the process was repeated 2000 times. The CV of the point estimates were calculated as the standard error of the 2000 bootstrap estimates divided by the original point estimate. Bootstrap 95% confidence intervals were determined by identifying the 2.5th and 97.5th percentiles of the 2000 bootstrap estimates. For each bootstrap sample, the effective half-strip width [ESW or $1/f(0)$], was treated as a random variable drawn from a normal distribution with a mean and standard error equal to that obtained from the detection model fitted to the truncated perpendicular distances. The probability of detecting a trackline group of porpoise, $g(0)$, was estimated for each bootstrap as a random variable drawn from a binomial distribution with mean = 0.769 (SE=0.117). This $g(0)$ value was calculated by Barlow[5] with independent observer methods, using a nearly identical vessel and the same observer configuration that we used. Owing to an insufficient number of sightings by the independent observers during our survey, we could not independently estimate a value for $g(0)$.

We statistically compared abundance estimates obtained from the 1995 ship survey with estimates from aerial surveys conducted 1 to 2 months earlier (Forney, 1999), using the "confidence interval of differences" approach proposed by Lo (1994) and adopted by Forney and Barlow (1998) for bootstrap confidence intervals. Commonly used comparative methods, such as those based on whether confidence intervals overlap or whether one population mean is in-

[5] Barlow, J. 1987. Abundance estimation for harbor porpoise (*Phocoena phocoena*) based on ship surveys along the coasts of California, Oregon, and Washington. Administrative report LJ-87-05, National Marine Fisheries Service, Southwest Fisheries Center, 36 p. [Available from Southwest Fisheries Science Center, P.O. Box 271, La Jolla, CA 92038.]

[6] Laake, J. L., S. T. Buckland, D. R. Anderson, and K. P. Burnham. 1996. DISTANCE user's guide, 82 p. Colorado Cooperative Fish and Wildlife Research Unit, Colorado State University, Fort Collins, CO 80523.

cluded within the confidence interval of a second mean, have been shown to be biased, because α levels do not approach the intended value of 0.05 (Lo, 1994). Therefore, we used a third method proposed by Lo (1994), based on the confidence interval of the difference (CI_d), between two population means. Through computer simulation, we generated 5000 log-normal pseudo-abundance estimates for the aerial and ship surveys (N^*), using the mean estimate and CV from each respective survey. The difference between ship and aerial pseudo-estimates was calculated as

$$d^* = N^*_{ship} - N^*_{air}$$

and a 95% confidence interval of the differences (CI_d) was calculated from the 5000 d^* values with the percentile method. Aerial and ship survey estimates were considered significantly different if the resulting CI_d did not include zero. Under the alternative hypothesis that abundance estimates were significantly different, we estimated the statistical power of this test by constructing one thousand 95% CI_d intervals through simulation, using the observed effect size and variance from the ship and aerial surveys in 1995. The probability of committing a type-II error β was calculated as the fraction of 1000 intervals that included zero (indicating no significant difference at α=0.05). An initial power analysis at $\alpha = 0.05$ revealed that the power to detect a difference as large as the one observed between aerial and ship estimates was low (=0.13). We therefore generated a power curve in order to objectively reselect an α level for the CI_d test that would provide an approximate power of 0.80 (Cohen, 1988). This resulted in an α level = 0.10; therefore, all statistical comparisons between aerial and ship estimates were considered statistically significantly different if the 90% CI_d did not include zero. Following Forney and Barlow (1998), we estimated the significance level for this comparison by iteratively constructing a range of confidence intervals from the simulated data (i.e. 80%, 90%, 95%, 96%, 97%...) and we identified the threshold α level (two-tailed) where the CI_d just included zero.

Results

We surveyed a total of 594 km of transect in California during calm sea states (Beaufort 0–2) and detected 170 harbor porpoise groups within the truncation distance of 1 km (Figs. 2 and 3, Table 1). Most survey effort (377 km) occurred in northern California, where 153 groups of harbor porpoise were seen, mostly in the vicinity of Cape Mendocino. No harbor porpoise were seen within regions 1 and 3 in central California, but the amount of survey effort in these regions (60 and 91 km, respectively) was low. Owing to persistent coastal fog, transect coverage within region 3 was limited to the offshore area near the Farallon Islands. In region 2, only 17 porpoise groups were detected within the 1-km truncation distance, but only 91 km of trackline was surveyed.

The perpendicular distance data were best fitted with the half-normal model without adjustment terms and had

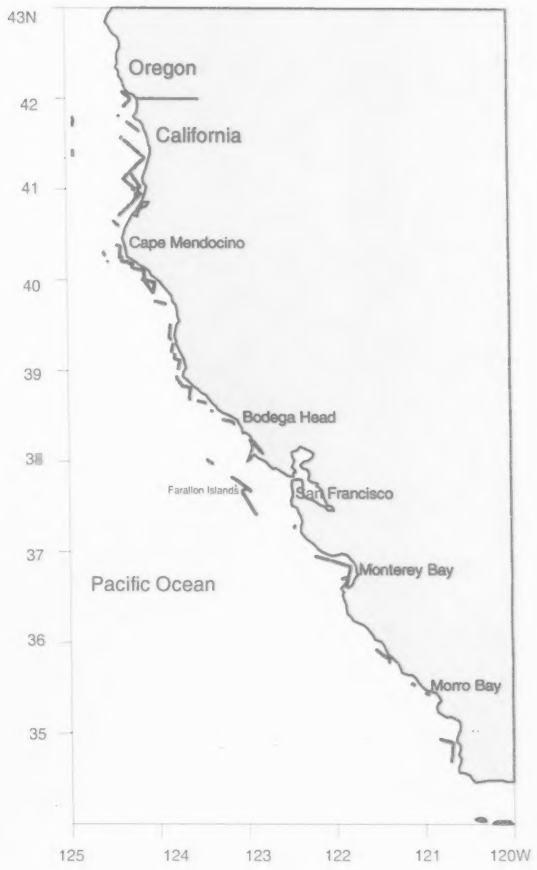

Figure 2

On-effort transect effort (594 km) shown as thick gray lines in central and northern California during calm (Beaufort 0–2) sea states.

the lowest AIC value of all competing models (χ^2 goodness-of-fit test, P=0.84, Fig. 4). Several truncation distances and interval groupings were explored when fitting a detection function to the distance data, and all fits resulted in estimates of abundance within 9% of each other. In general, the lowest abundances were obtained with hazard-rate models. Here, we report only the results obtained with the half-normal model with a truncation distance of 1 km. We used the observed mean group size of 2.45 for region 2 and 2.65 for northern California to estimate porpoise abundance because the regression of the log of observed group size versus $\hat{g}(x)$ was not significant (r^2=0.11, P<0.89), suggesting no school size bias within the truncation distance of 1 km.

Abundance of harbor porpoise in northern California was estimated at 5686 (log-normal 95% CI=3498–9242; bootstrap CV=0.29, bootstrap 95% CI=2760–8394) out to the 91 m isobath, based on 377 km of transect effort and 153 porpoise sightings in calm sea states (Beaufort 0–2). A statistical comparison of our estimate with the aerial

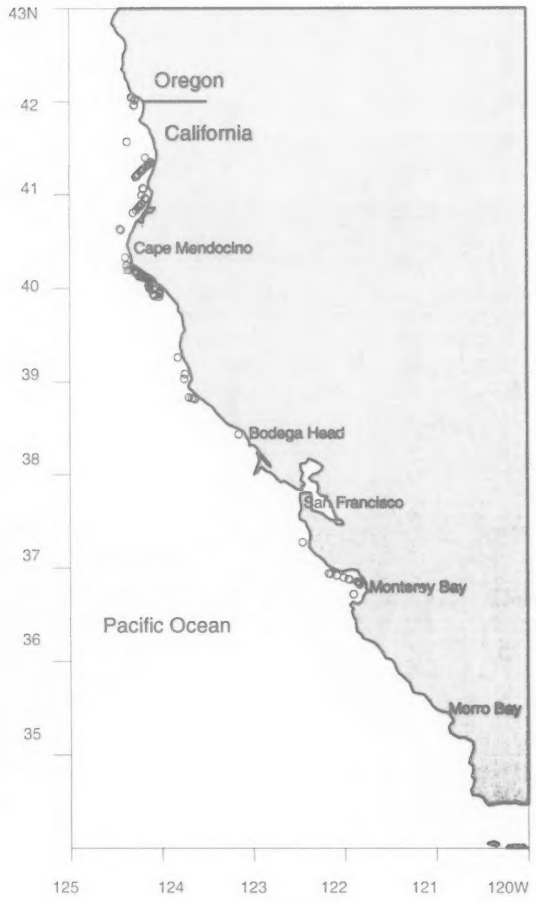

Figure 3

On-effort sightings of harbor porpoise recorded in central and northern California during calm (Beaufort 0–2) sea states.

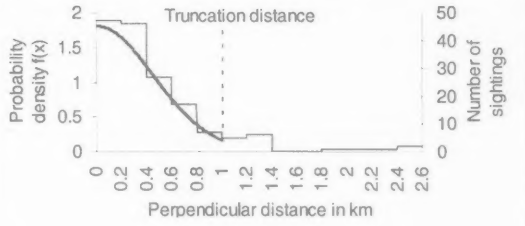

Figure 4

Half-normal model fit to the perpendicular distance data. Data were truncated at 1 km, which eliminated 10% of all observations. The model fitted the data well, as determined by a chi-square goodness-of-fit test (P=0.84).

survey estimate obtained 1–2 months earlier (N=13,145 CV=0.39)1 revealed that the 90% confidence interval of differences (CI_d) did not include zero, indicating that aerial and ship abundance estimates were significantly different at $\alpha = 0.10$ (90% CI_d =–17,275 to –257, P=0.08, Fig. 5, A and B). Porpoise abundance for region 2 was estimated at 1041 (log-normal 95% CI=559–1941; bootstrap CV=0.44, bootstrap 95% CI=587–4138), based on 91 km of survey effort and 17 porpoise sightings. Our estimate for region 2 was significantly different (90% CI_d=–4084 to –162, P=0.07, α=0.10) from an estimate obtained with aerial surveys 1 to 2 months earlier in the year (N=2861 CV=0.39).1

In northern California, harbor porpoise were not distributed randomly with respect to water depth (Kolmogorov-Smirnov test, P<0.001; Fig. 6A). High proportions of porpoise sightings with respect to survey effort were found between 20 to 60 m, and fewer porpoise than expected were found in waters deeper than 60 m. Because calm sighting conditions often occur in nearshore shallow waters where porpoise densities are relatively high (Barlow, 1988), we also examined relative abundance at depth for rough sea states (Beaufort 3–4) to see if the overall depth patterns held. The depth distribution of porpoise was similar in rough sea states: more porpoise than expected occurred between 20 to 40 m and fewer porpoise than expected were seen at depths of 40 to 120 m (Kolmogorov-Smirnov test, P<0.002, Fig. 6B). During our survey, the area from shore to the 20-m isobath went largely unsurveyed because of the ship's draft and the presence of local navigational hazards. Owing to an insufficient number of sightings within region 2 (n=25, depth range=20 to 93 m), we did not attempt to statistically describe the depth distribution of harbor porpoise for that region.

Discussion

Abundance of harbor porpoise off northern California

Our estimate of porpoise abundance for northern California (5686, log-normal 95% CI=3498–9242) is considerably lower than estimates for the same area from 1988 to 1993 aerial surveys (9250, 95% CI=5943–14,397; Barlow and Forney, 1994). Barlow and Forney (1994) estimated 2.05 porpoise/km^2 in northern California from aerial surveys (corrected for missed groups), whereas we estimated 1.26 porpoise/km^2 (also corrected for missed groups). From 1984–85 ship surveys conducted in September, Barlow (1988) estimated 12,700 porpoise (2.09 porpoise/km^2) from Bodega Head, California to Cape Blanco, Oregon, an area approximately 23% larger than our our study area in northern California. From aerial survey data collected 1 to 2 months prior to our ship survey, Forney[1] reported a preliminary estimate of 13,145 porpoise (CV=0.39, log-normal 95% CI=6316–27,357; 2.92 porpoise/km^2) for northern California. This aerial estimate is significantly different from our ship survey estimate, as determined by the confidence interval of differences test (90% CI_d=–17,275 to –257, P=0.08, α=0.10). Had we used the traditional α level

of 0.05, these two estimates would not have been significantly different, but the power to detect such a difference was low (0.13). This result highlights recent criticisms of statistical significance testing (Johnson, 1999) and underscores the importance of estimating statistical power to aid in decision-making. Regardless, real differences exist between aerial and ship estimates obtained in 1995, as evidenced in Figure 5, A and B, which may be due to a number of factors.

Animals may have moved out of the study area between the time of the two studies. Seasonal movements of harbor porpoise are known to occur on the Atlantic coast (Polacheck et al., 1995), and in Glacier Bay, Alaska (Taylor and Dawson, 1984). In California, the situation is less clear because polluntant evidence suggests limited latitudinal movement along the coast (Calambokidis and Barlow, 1991) and genetic stock structure remains unresolved (Chivers[2]). Several researchers have reported highest porpoise densities during late summer and autumn throughout California (Barlow, 1988, Monterey Bay; Calambokidis et al.[7], central California; Dohl et al.[8], California-wide; Goetz, 1983, northern California; Sekiguchi, 1995, Monterey Bay). Barlow (1988) and Sekiguchi (1995) observed the lowest harbor porpoise densities in Monterey Bay during winter. Forney (1995, 1999) reported harbor porpoise abundance was negatively correlated with positive sea-surface temperature anomalies in the Monterey Bay region in autumn, a finding that suggests that animals move in response to changing oceanographic conditions. Pyle and Gilbert (1996) reported harbor porpoise sightings near Southeast Farallon Island in central California only from March to November, even though observers searched year-round over a ten-year period (1982–92). Collectively, the data suggest small-scale seasonal movement of harbor porpoise along the California coast. Most cetacean species in California show seasonal trends in distribution and abundance (Forney and Barlow, 1998) and despite the restriction of harbor porpoise to neritic habitat

Table 1

Estimates of harbor porpoise abundance, precision, and effort from the most recent ship and aerial surveys in California waters. Sizes of study areas and transect lengths are given in kilometers. Effective half-strip widths (ESWs) are given in meters. Regions are shown in Figure 1. Bold rows indicate regions under comparison between the two studies.

Study	No. of groups *n*	Mean group size	Area (km^2)	Transect length (km)	ESW (meters)	*g*(0)	Porpoise density (no. of porpoise/m^2)	Abundance (no. of individuals)	CV	Lower 95% CI	Upper 95% CI
1995 ship (our study)											
Central California	17	2.45	6951	217	554	**0.769**	—	—	—	—	—
Region 1	**0**	**—**	**1985**	**60**	**554**	**0.769**	—	—	—	—	—
Region 2	17	2.45	1917	91	554	0.769	0.54	1041	**0.44**	**559**	**1941**
Region 3	**0**	**—**	**3049**	**66**	**554**	**0.769**	—	—	—	—	—
Northern CA	153	2.65	4504	377	554	0.769	1.26	5686	0.29	3498	9242
1995 aerial[1]											
Central California	101		6951	2035	197	0.292	0.86	6007	0.27	3584	10,067
Region 1	13	2.08	1985	858	197	0.292	0.27	542	**0.48**	**222**	**1326**
Region 2	**62**	**2.00**	**1917**	**720**	**197**	**0.292**	**1.49**	**2861**	**0.40**	1353	6048
Region 3	26	1.73	3049	457	197	0.292	0.85	2604	0.43	**1166**	**5814**
Northern California	**85**	**1.62**	**4504**	**374**	**197**	**0.292**	**2.92**	**13,145**	**0.39**	**6316**	**27,357**

[1] Forney, K. A. 1999. The abundance of California harbor porpoise estimated from 1993–97 aerial line-transect surveys. Administrative report LJ-99- 02, National Marine Fisheries Service, Southwest Fisheries Science Center, 16 p. [Available from Southwest Fisheries Science Center, P.O. Box 271, La Jolla, CA 92038.]

[7] Calambokidis, J., C. Ewald, G. H. Steiger, S. M. Cooper, I. D. Szczepaniak, and M. A. Webber. 1990. Harbor porpoise studies in the Gulf of the Farallones. Final contract report CX 8000-8-0001 to the Gulf of the Farallones National Marine Sanctuary, 57 p. Fort Mason Center, Bldg. 201, San Francisco, CA 94123.

[8] Dohl, T. P., R. C. Guess, M. L. Duman, and R. C. Helm. 1983. Cetaceans of central and northern California, 1980–1983: status, abundance, and distribution. Contract rep. 14-12-0001-29090, p. 135–152. Pacific OCS Region, Minerals Management Service, U.S. Department of the Interior, Washington D.C.

along the California coast, they probably respond to seasonal or interannual oceanographic changes.

Large swells (3 m) during our ship survey may have caused observers to miss more porpoise groups on the trackline than is accounted for by our $g(0)$ correction factor. The independent observer recorded an insufficient number of sightings during our survey; therefore we could not independently estimate $g(0)$. Instead, we adopted the $g(0)$ value of 0.769 (SE=0.117) estimated by Barlow[5] who used the same searching method and vessel type as we did. During our survey, the largest swells (3 m) occurred in northern California, where porpoise densities are highest. Further, swell height increased with latitude in California and the slope of the regression was significant (Zar, 1984; ANOVA, $P<<0.005$). Even in calm sea states, porpoise groups may be easily missed because animals surface behind large swells and thus are not observed. Our transect lines frequently were oriented directly into the prevailing northwest swell or directly down-swell as a consequence of our sampling design, possibly contributing to more groups being missed on the transect line than expected. If swells were considerably larger during 1995 survey than during the 1980s surveys, then Barlow's $g(0)$ value may not reflect the fraction of trackline groups missed and our estimate of abundance would be negatively biased by an unknown, but nontrivial, amount. Larger winter swells may also help explain why porpoise densities from winter vessel surveys are generally lower than those from summer and autumn surveys (Goetz, 1983; Barlow, 1988; Sekiguchi, 1995; Calambokidis et al.[7]).

Abundance in northern California may be underestimated because the area inshore of the 20-m isobath, known to have relatively high porpoise densities, was not routinely surveyed. Only 2% of all survey effort and 4% of all sightings occurred at depths shallower than 20 m. Shallow water effort is included in our abundance estimate, thus we implicitly assume that porpoise density from shore to 20 m is equal to that in the remainder of our study area. Depth data from aerial surveys conducted from 1988 to 1997 support this assumption. Porpoise encounter rates (weighted by effort for each depth stratum) are nearly equal for the area from shore to 90 m (0.33 porpoise/km) and from 20 to 90 m (0.32 porpoise/km) (NMFS[9]). However, these data were collected primarily during September and October and may not reflect the depth distribution of harbor porpoise in November. During our survey, if porpoise densities were significantly higher from shore to 20 m than from 20 to 90 m, our estimate of porpoise abundance would be negatively biased by an unknown amount. The same bias might result if significant numbers of harbor porpoise moved into waters deeper than 90 m between the time of the aerial and ship surveys.

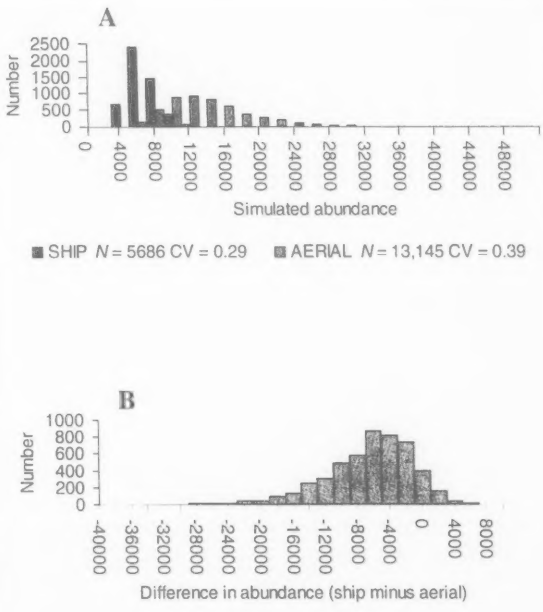

Figure 5

Distribution of simulated log-normal abundance estimates for 1995 ship and aerial surveys in northern California (**A**). Difference between 5000 simulated abundance estimates for 1995 ship and aerial survey in northern California (**B**).

The distribution of harbor porpoise in northern California is highly clustered, especially near Cape Mendocino, where densities are highest, and our level of survey effort may not have fully captured the spatial heterogeneity in porpoise densities in northern California. The bootstrap CV of ship abundance estimate was not extremely precise (0.29) and reflects the spatial variability in porpoise encounter rates in northern California on small (5-km bootstrap unit) scales. The estimated number of transect effort in kilometers needed to attain higher levels of precision for the northern California estimate, following the method described in Buckland et al. (1993, p. 303–304) were approximately 800 and 3200 km, respectively, to obtain CVs of 0.20 and 0.10 (we surveyed 377 km). These effort estimates assume a Poisson distribution of porpoise, and are probably conservative. Repeated sampling of our transect lines over a longer period may have yielded an estimate of abundance more similar to recent aerial surveys. An adaptive sampling method, as used by Palka and Pollard (1999), would be useful on future surveys to increase sampling effort in known high-density regions.

Abundance of harbor porpoise off central California

Region 1 has the lowest densities of harbor porpoise in California (Barlow, 1988; Forney et al., 1991; Dohl et al.[3]) and we did not detect any porpoise during 60 km of survey

[9] NMFS (National Marine Fisheries Service). 1999. Unpubl. data. Protected Resources Div., Southwest Fisheries Science Center, P.O. Box 271, La Jolla, CA. 92038.

effort. The most recent estimate of porpoise abundance for region 1 is 627 (CV=0.452) from a 1997 aerial survey (Forney[1]).

Our estimate of porpoise abundance for region 2 is 1041 (log-normal 95% CI 559–1941, CV=0.44). This is less than the 1778 porpoise (95% log-normal CI=1096–2885, CV=0.25) estimated by Barlow and Forney (1994) from 1988–93 aerial surveys, and 1459 porpoise (CV=0.61) estimated from 197 km of ship survey effort in 1984–85 (Barlow, 1988). Our estimate is statistically significantly different (90% CI_d=–4084 to –162, P=0.07, α=0.10) from an aerial survey estimate made 1–2 months earlier (2861, 95% CI=1353–6048, CV=0.39).[1] To obtain abundance CVs of 0.30, 0.20, and 0.10 for the 1995 ship survey in region 2 would have required approximately 175, 400, and 1600 km of transect effort respectively (we surveyed 91 km).

We surveyed 66 km in region 3 in the Gulf of the Farallones during calm sea states and did not detect any harbor porpoise. Harbor porpoise are known to be abundant in this area, where a total of 552 sightings were recorded during small-vessel studies conducted between 1977 and 1985 (Szczepaniak and Webber[10]). However, a majority of these sightings were 10–20 km west of the mouth of San Francisco Bay and only a small number of sightings were recorded within 10 km of the Farallon Islands, where nearly all of our survey effort in region 3 occurred (Fig. 2). Calambokidis et al.[7] conducted year-round surveys in the Gulf of the Farallones and found high porpoise densities within 10–20 km of San Francisco Bay but sighted no porpoise offshore near the Farallon Islands. Szczepaniak[11] found the same pattern during autumn surveys. No specimens were reported from the Farallon Islands in the 208 stranding records of harbor porpoise from 1915 to 1985 summarized by Szczepaniak.[11] Further evidence of low porpoise densities in this area comes from studies at Southeast Farallon Island, where over the ten-year period 1982–92, observers stationed year-round at the island detected only 68 groups of harbor porpoise (Pyle and Gilbert, 1996). The collective evidence suggests that harbor porpoise are uncommon in the immediate vicinity of the Farallon Islands, where water depths generally range from 55 to 75 m. In California, this depth range is characterized by relatively low porpoise densities, as discussed in the next section.

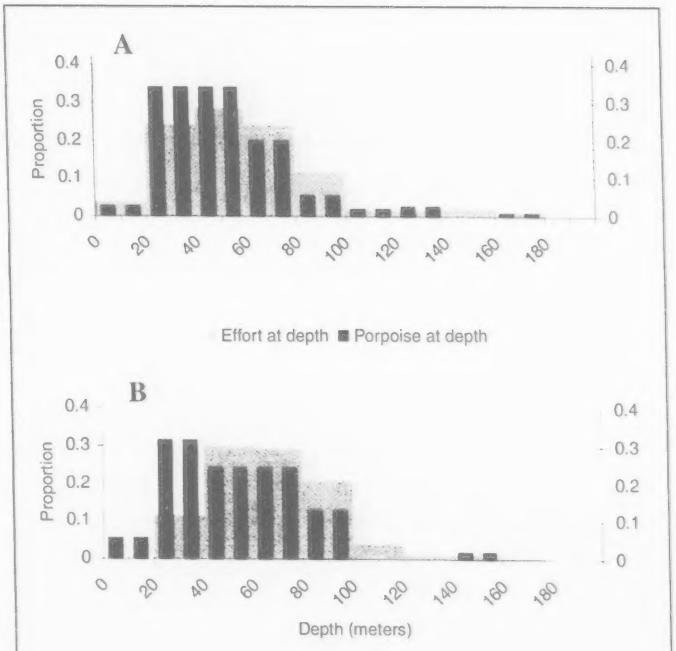

Figure 6

Relative proportions of survey effort and porpoise sightings at depth for (**A**) calm sea states and (**B**) rough sea states. Proportions were compared by using a Kolmogorov-Smirnov goodness-of-fit test. The proportion of porpoise at depth was significantly different from effort proportions for both calm (P<0.005) and rough (P<0.002) sea states. More porpoise than expected occurred at depths of 20–60 m in calm sea states and at depths of 0–40 m in rough sea states.

Depth distribution of harbor porpoise

In northern California, we found that higher numbers of harbor porpoise than expected occurred at depths of 20 to 60 m and fewer porpoise than expected in waters deeper than 60 m (Fig. 6, A and B). Barlow (1988) found the abundance of harbor porpoise along the California, Oregon, and Washington coasts to be roughly constant from shore to 55 m, declining linearly with depth, and he found that no harbor porpoises were detected in waters deeper than 110 m. We encountered 19 porpoise groups in waters deeper than 91 m (range 101 to 215 m) over submarine canyons near Cape Mendocino, where deep canyons intersect shallow water habitat characterized by higher porpoise densities. Our observed depth distribution of harbor porpoise is similar to that of Calambokidis et al.,[7] who found porpoise only at depths <70 m, but who surveyed to depths of 120 m. In contrast, near the Northern San Juan Islands, Washington, porpoise occur more often than expected at depths >100 m and fewer than expected occur at depths <75 m (Raum-Suryan, 1995; Raum-Suryan and Harvey,

[10] Szczepaniak, I. D., and M. A. Webber. 1985. Status of the harbor porpoise (*Phocoena phocoena*) in the eastern north Pacific, with an emphasis on California. Final report to Center for Environmental Education, 52 p. Washington, D.C. 20004.

[11] Szczepaniak, I. D. 1987. Abundance and distribution of harbor porpoise (*Phocoena phocoena*) in the Gulf of the Farallones National Marine Sanctuary. Final report to National Park Service, 48 p. Point Reyes National Seashore, Point Reyes, CA 94956.

1998). We attribute these differences in depth distribution between California and the San Juan Islands to habitat: porpoises near the San Juan Islands occupy an inland waterway characterized by numerous islands with steep bathymetry, wheras the open coastline of California has relatively gentler bathymetry. In both areas harbor porpoise do not occur far from land. Along the outer coasts of Oregon and Washington, Green et al.[12] reported approximately 25% of all harbor porpoise at depths of 100 to 200 m; further, the depth distribution of harbor porpoise changed seasonally, in summer, 56% of porpoise were inshore of the 100-m isobath and during winter, this proportion increased to 86%.

Much of what we know about harbor porpoise abundance and depth distribution in California comes from aerial and ship data collected in late summer and early autumn, largely because weather conditions are more favorable at this time of year. For northern California, in particular, there is a bias towards collection of autumn data: the depth distribution model of Barlow (1988) contained only September data and past abundance surveys have relied on summer and autumn data (Barlow, 1988; Forney, 1995; 1999). The exception to this seasonal collection of data are year-round aerial surveys conducted by Dohl et al.[8] off central and northern California. However, Dohl's surveys were not ideally suited to estimate porpoise abundance because their transect lines were oriented perpendicular to the shoreline and most survey effort occurred far offshore of known porpoise habitat. Additional winter and spring aerial surveys are needed in California to investigate seasonal differences in harbor porpoise distribution and abundance. To permit direct seasonal comparisons, we suggest that winter-spring surveys use existing transect lines from past summer-autumn aerial surveys. We recommend aerial surveys over ship surveys because they permit coverage of shallow water areas where larger research vessels cannot operate; are more cost-effective for surveying large areas, thus maximizing data collection during brief fair-weather periods; and reduce the influence of large ocean swells that compromise the effectiveness of a ship line-transect survey.

Acknowledgments

We thank the marine mammal observers who spent many hours collecting the sightings and effort data: W. Armstrong, M. Donahue, B. Hanson, B. Odom, D. Outram, K. Raum-Suryan, R. Rowlett, (and S.J.C. and B.L.T.). We also thank the officers and crew of the NOAA ship *McArthur* for all their support. Charles Stinchcomb assisted in identifying shoreline-biased sightings. Karin Forney provided unpublished data on harbor porpoise encounter rates at depth from previous aerial surveys and patiently reviewed the CI_d method. Tim Gerrodette provided a FORTRAN subroutine used to correct sighting positions in relation to vessel positions. Rich Cosgrove provided NOS bathymetric data used to determine the depth distribution of porpoise. This survey was funded by the NMFS Office of Protected Resources. Lastly we thank Jay Barlow, Debbie Palka, Kim Raum-Suryan, and two anonymous reviewers for their critiques of the manuscript. An earlier draft of this manuscript served as working paper 98-PSRG-5 at the November 1998 Pacific Scientific Review Group meeting in Seattle, WA.

[12] Green, G. A., J. J. Brueggeman, R. A. Grotefendt, C. E. Bowlby, M. L. Bonnell, and K. C. Balcomb III. 1992. Cetacean distribution and abundance off Oregon and Washington, 1989–1990. Chapter 1 *in* Oregon and Washington marine mammal and seabird surveys (J. J. Brueggeman, ed.), p. 1–140. Final report to OCS (Offshore Continental Shelf) Study MMS 91-0093. [Available from Ebasco Environmental, 10900 NE 8th St., Bellevue, WA 98004.]

Literature cited

Akaike, H.
1973. Information theory and an extension of the maximum likelihood principle. *In* International symposium on information theory, 2nd ed., (B. N. Petran and F. Csàaki, eds.), p. 267–281. Akadèemiai Kiadi, Budapest, Hungary.

Barlow, J.
1988. Harbor porpoise (*Phocoena phocoena*) abundance estimation in California, Oregon, and Washington: I. Ship Surveys. Fish. Bull. 86:417–432.

Barlow, J., and K. A. Forney.
1994. An assessment of the 1994 status of harbor porpoise in California. U.S. Dep. Commer., NOAA Technical Memo., NOAA-TM-NMFS-SWFSC-205, 17 p. [Available from Southwest Fisheries Science Center, P.O. Box 271, La Jolla, CA 92038.]

Barlow, J., K. A. Forney, P. S. Hill, R. L. Brownell Jr., J. V. Carretta, D. P. DeMaster, F. Julian, M. S. Lowry, T. Ragen, and R. R. Reeves.
1997. U.S. Pacific marine mammal stock assessments: 1996. U.S. Dep. Commer., NOAA Technical Memo., NOAA-TM-NMFS-SWFSC-248, 223 p. [Available from Southwest Fisheries Science Center, P.O. Box 271, La Jolla, CA 92038.]

Barlow, J., and D. Hanan.
1995. An assessment of the status of harbour porpoise in central California. Rep. Int. Whal. Comm. (special issue) 16:123–140).

Barlow, J., and T. Lee.
1994. The estimation of perpendicular sighting distance on SWFSC research vessel surveys for cetaceans: 1974 to 1991. U.S. Dep. Commer., NOAA Tech. Memo., NOAA-TM-NMFS-SWFSC-207, 46 p. [Available from Southwest Fisheries Science Center, P.O. Box 271, La Jolla, CA 92038.]

Barlow, J., P. S. Hill, K. A. Forney, and D. P. DeMaster.
1998. U.S. Pacific marine mammal stock assessments: 1998. U.S. Dep. Commer, NOAA Technical Memo., NOAA-TM-NMFS-SWFSC-258, 40 p. [Available from Southwest Fisheries Science Center, P.O. Box 271, La Jolla, CA 92038.]

Buckland, S. T., D. R. Anderson, K. P. Burnham, and J. L. Laake.
1993. Distance sampling: estimating abundance of biological populations. Chapman and Hall, London, 446 p.

Calambokidis, J., and J. Barlow.
1991. Chlorinated hydrocarbon concentrations and their use in describing population discreteness in harbor porpoises from Washington, Oregon, and California. *In* Marine Mammal Strandings in the United States (J.E. Reynolds

and D.K. Odell, eds.), p. 101–110. U.S. Dep. Commer., NOAA Technical Report NMFS 98.

Cohen, J.
1988. Statistical power analysis for the behavioral sciences. Lawrence Erlbaum Assoc. Publ., Hillsdale, NJ, 567 p.

Forney, K. A.
1995. A decline in the abundance of harbor porpoise, *Phocoena phocoena,* in nearshore waters off California, 1986–93. Fish. Bull. 93(4):741–748.

Forney, K. A.
1999. Trends in harbor porpoise abundance off central California, 1986–95: evidence for interannual changes in distribution? J. Cetacean Res. and Manage. 1:73–80.

Forney, K. A., and J. Barlow.
1998. Seasonal patterns in the abundance and distribution of California cetaceans, 1991–1992. Mar. Mamm. Sci. 14(3): 460–489.

Forney, K. A., D. A. Hanan, and J. Barlow.
1991. Detecting trends in harbor porpoise abundance from aerial surveys using analysis of covariance. Fish. Bull. 89:367–377.

Forney, K. A., M. M. Muto, and J. Baker.
1999. U.S. Pacific marine mammal stock assessments: 1999. U.S. Dep. Commer., NOAA Technical Memo., NOAA-TM-NMFS-SWFSC-282, 62 p. [Available from Southwest Fisheries Science Center, P.O. Box 271, La Jolla, CA 92038.]

Goetz, B. J.
1983. Harbor porpoise (*Phocoena phocoena*) movements in Humboldt Bay, California and adjacent waters. M.A. thesis, Humboldt State Univ., Arcata, CA, 118 p.

Johnson, D. H.
1999. The insignificance of statistical significance testing. J. Wildl. Manage. 63(3):763–772.

Julian, F., and M. Beeson.
1998. Estimates for marine mammal, turtle, and seabird mortality for two California gillnet fisheries: 1990–95. Fish. Bull. 96:271–284.

Lo, N. C. H.
1994. Level of significance and power of two commonly used procedures for comparing mean values based on confidence intervals. Calif. Coop. Oceanic Fish. Invest. Rep. 35:246–253.

Palka, D., and J. Pollard.
1999. Adaptive line transect survey for harbor porpoises. *In* Proceedings of the symposium on surveys, status and trends of marine mammal populations, Seattle, Washington, USA, February 25–27 1998, (G. W. Garner, S. C. Amstup, J. L. Laake, B. F .J. Manly, L. L. McDonald, and D. G. Robertson, eds.), p 3–11. A.A. Balkema Publishers, Rotterdam, Netherlands.

Polacheck, T., F.W. Wenzel, and G. Early.
1995. What do stranding data say about harbor porpoises? Int. Whal. Comm. (special issue) 16:169–179.

Pyle, P., and L. Gilbert.
1996. Occurrence patterns and trends of cetaceans recorded from Southeast Farallon Island, California, 1973 to 1994. Northwestern Naturalist 77:1–8.

Raum-Suryan, K. L.
1995. Distribution, abundance, habitat use, and respiration patterns of harbor porpoise (*Phocoena phocoena*) off the Northern San Juan Islands, Washington. M.S. thesis, Moss Landing Marine Laboratory, San Jose State University, San Jose, CA, 77 p.

Raum-Suryan, K .L. and J. T. Harvey.
1998. Distribution and abundance of and habitat use by harbor porpoise, *Phocoena phocoena,* off the northern San Juan Islands, Washington. Fish. Bull. 96:808–822.

Rosel, P. E., A. E. Dizon, and M. G. Haygood.
1995. Variability of the mitochondrial control region in populations of the harbour porpoise, *Phocoena phocoena*, on interoceanic and regional scales. Can. J. Fish. Aquat. Sci. 52:1210–1219.

Sekiguchi, K.
1995. Occurrence, behavior and feeding habits of harbor porpoises (*Phocoena phocoena*) at Pajaro Dunes, Monterey Bay, California. Aquat. Mamm. 21(2):91–103.

Taylor, B.L. and P.K. Dawson.
1984. Seasonal changes in density and behavior of harbor porpoise (*Phocoena phocoena*) affecting census methodology in Glacier Bay National Park, Alaska. Rep. Int. Whal Comm. 34:479–483.

Zar, J.H.
1984. Biostatistical analysis, 2nd ed. Prentice Hall. Englewood Cliffs, NJ, 718 p.

Abstract—Three yellowfin tuna (*Thunnus albacares*) carrying ultrasonic depth-sensitive transmitters developed a strong association with the tracking vessel, following it at speeds up to 5 knots (2.6 m/s). Two fish associated with the tracking vessel during daytime, and the other fish during day and night periods. Swimming behavior appeared to depend on the speed of the vessel. The tuna remained within a few meters of the surface when the vessel was traveling at high speeds but moved deeper when the vessel drifted. The behavior of these fish is compared to those of other yellowfin tuna tracked in other situations (associated with fish-aggregating devices or unassociated with devices). The reasons for these associations are not known but some hypotheses are advanced.

Association of yellowfin tuna (*Thunnus albacares*) with tracking vessels during ultrasonic telemetry experiments

Laurent Dagorn
Institut de Recherche pour le Développement (IRD)
BP 5045
34032 Montpellier
Cedex 1, France
E-mail address: dagorn@ird.fr

Erwan Josse
Institut de Recherche pour le Développement (IRD)
BP 70
29280 Plouzané, France

Pascal Bach
Institut de Recherche pour le Développement (IRD)
BP 5045
34032 Montpellier
Cedex 1, France

Tunas associate with floating objects, such as logs, anchored man-made fish-aggregating-devices (FADs) (see Fréon and Misund, 1999, for a review), and fishing boats (Fonteneau and Diouf, 1994). Numerous ultrasonic telemetry experiments have been conducted (Cayré and Chabanne, 1986; Holland et al., 1990; Cayré, 1991; Cayré and Marsac, 1993; Marsac et al., 1996; Bach et al., 1998; Josse et al., 1998; Marsac and Cayré, 1998; Brill et al., 1999) to determine the behaviors of tunas associated with anchored FADs, but no published studies have examined fish associated with drifting objects. Moreover, during ultrasonic telemetry experiments, the assumption is that neither the transmitter nor the tracking operation alters the behavior of the fish. Some yellowfin tuna, however, have developed associations with the tracking vessel—a rare behavior previously observed on two occasions (Cayré et al., 1996; Brill et al., 1999). In other words, in these situations, the vessel is not following the fish but the fish is following the vessel.

In our study, we examined the movements of three yellowfin tuna, which clearly followed the tracking vessel during ultrasonic telemetry experiments. Our objective was to characterize these associations and to compare them with other types of association behavior. We discuss these observations in relation to some hypotheses on the nature of tuna associations with floating objects and propose ideas for future studies.

Materials and methods

Fish movements were monitored with acoustic telemetry techniques from the research vessel RV *Alis*. Tracking operations were conducted between October 1995 and April 1996 in French Polynesia. The depth-sensitive acoustic transmitters carried by the fish and the ultrasonic receiving equipment were built by VEMCO (Shad Bay, Nova Scotia, Canada), and are described in detail in Dagorn et al. (2000).

Fish were caught on vertical longline gear and transmitters were attached externally with either nylon tie-wraps (as described by Holland et al., 1990) or a stainless steel dart (as described by Brill et al., 1993).

During tracking operations, simultaneous acoustic data were collected be-

Manuscript accepted 10 July 2000.
Fish. Bull. 99:40–48 (2001).

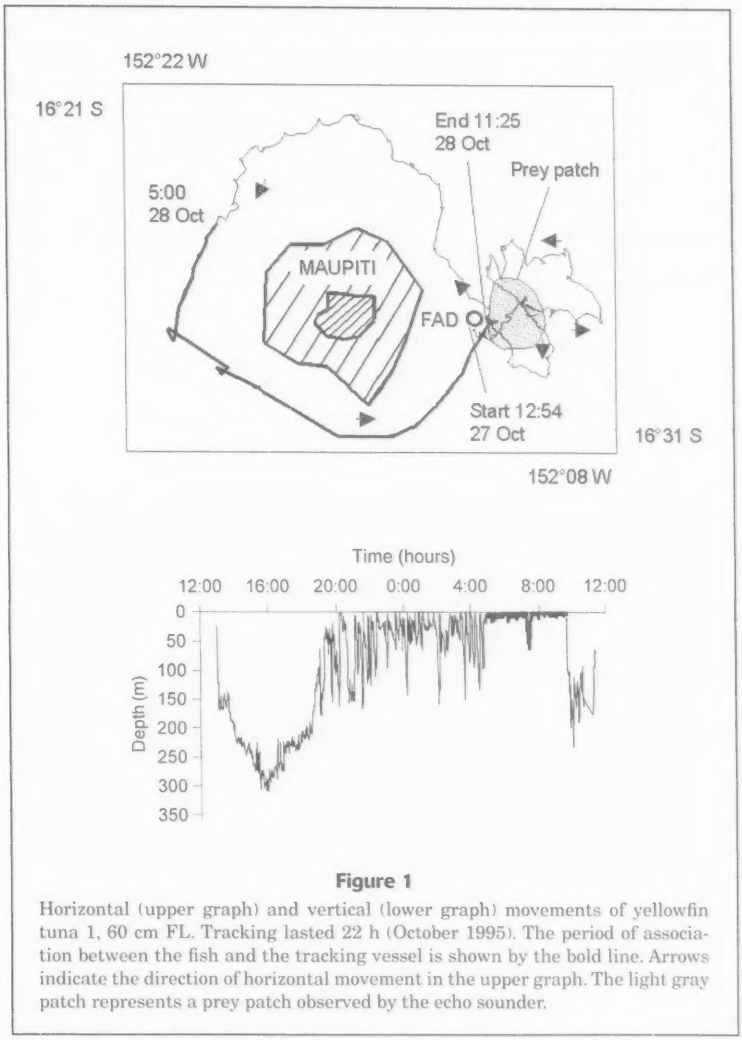

Figure 1

Horizontal (upper graph) and vertical (lower graph) movements of yellowfin tuna 1, 60 cm FL. Tracking lasted 22 h (October 1995). The period of association between the fish and the tracking vessel is shown by the bold line. Arrows indicate the direction of horizontal movement in the upper graph. The light gray patch represents a prey patch observed by the echo sounder.

tween 10 and 500 m depth with a SIMRAD (SIMRAD, Horten, Norway) EK500 scientific sounder connected to a hull-mounted SIMRAD ES38B split-beam transducer (frequency 38 kHz, beam angle 6.9°). Acoustic data, along with vessel position, were simultaneously logged on a personal computer running SIMRAD EP 500 software (Simrad, 1994). Vessel speeds were estimated from straight-line calculations by using positions of the tracking vessel based on data from the Global Positioning System for the first two fish. Speeds were taken directly from the knot meter of the vessel for fish 3, which provided a greater volume of data on real-time movements of the tracking vessel.

When the crew suspected the fish had become associated with the tracking vessel, experiments were developed to test the association (complete turns, changes in vessel speed and direction, etc.). Fish that clearly followed the vessel during such tests were considered to be associated.

Results

Of the fourteen yellowfin tuna that were tagged and tracked in French Polynesia from 1985 to 1997, three individuals clearly exhibited strong and lengthy associations with the research vessel.

Tuna 1 (60 cm FL) was caught at a depth of 120 m at midday close to a FAD anchored near Maupiti Island, located within the Leeward Islands of the Society Archipelago. The fish was tracked for 22 h as indicated in Figure 1. This fish associated with the FAD immediately after release but shifted to a free-swimming (unassociated) phase directed offshore (eastward movement) until 17:14 h, crossing for the first time a patch of mid-water prey observed on the echo-sounder. After crossing the patch for the second time (beginning of the night), the tuna returned to the FAD but did not re-associate; rather it began a cir-

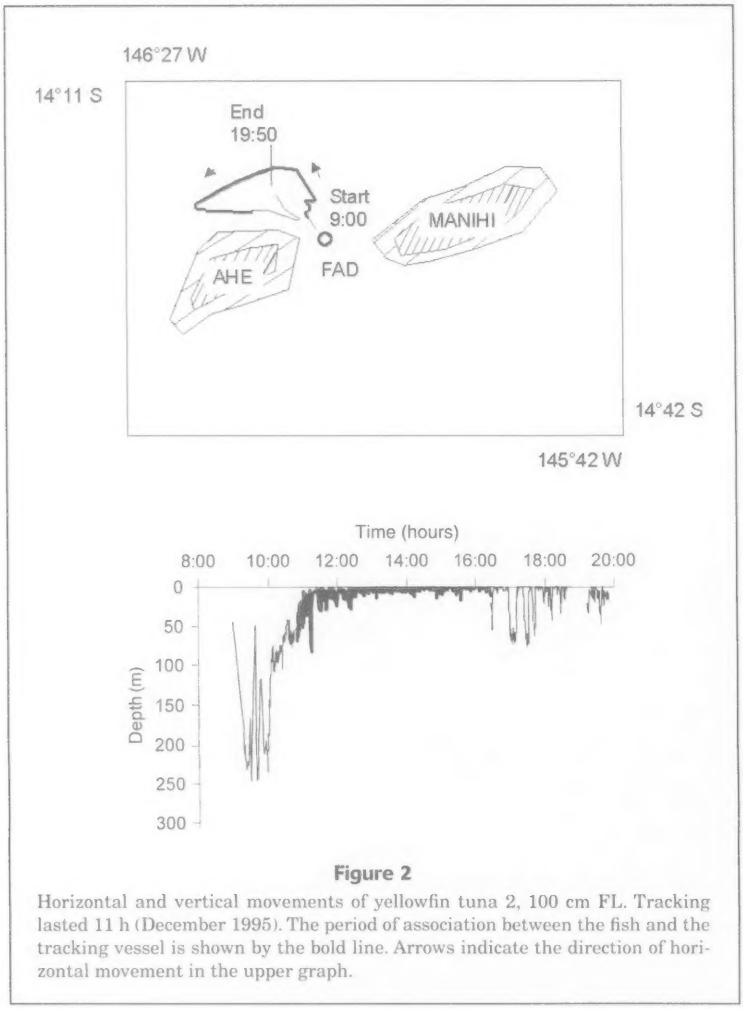

Figure 2

Horizontal and vertical movements of yellowfin tuna 2, 100 cm FL. Tracking lasted 11 h (December 1995). The period of association between the fish and the tracking vessel is shown by the bold line. Arrows indicate the direction of horizontal movement in the upper graph.

cular movement around the island. The fish became associated with the tracking vessel after traveling half-way around the island. The association occurred simultaneously with a change in its vertical movement pattern, shifting from a movement pattern between the surface and 150 m to a surface oriented behavior that kept the fish within a few meters of the surface (Fig. 1). As the boat continued to move around the island, the fish maintained the association and swam within 10 m of the surface, except for an excursion to 50 m around 07:30. However, this dive occurred simultaneously with a XBT (expendable bathythemograph) launch and the fish may have followed the instrument as it went down, a behavior also observed by Block et al. (1997). When the tracking vessel reached the FAD where the fish had been caught the day before, the fish broke its association with the ship and dove, likely to join a small tuna school observed on the echo-sounder under the FAD at around 150 m depth.

Yellowfin tuna 2 (100 cm FL) was captured at 9:00 while it was associated with a FAD off Ahe Island (Tuamotu Archipelago) and after being followed for 11 h. Immediately after its release, the fish returned to the depth at which it was caught (between 200 and 250 m) and left the FAD heading northwest (Fig. 2). Before 11:00, the fish rose to the surface and became associated with the boat; the main engine was then shut down and the vessel drifted. Around 11:15, the boat began to move and the fish followed. The fish remained strongly associated with the moving vessel, swimming within the first 10 m below the surface until 16:25, when it began to break off the association, making some rapid dives to 70 m. Contact was lost at 18:38, after a sudden departure of the fish during a heavy rain squall. The fish was briefly relocated at 19:14.

Yellowfin tuna 3 (108 cm FL) was caught at 07:38, close to a FAD located off the island of Tahiti (Fig. 3). After release, the yellowfin tuna returned to the depth where

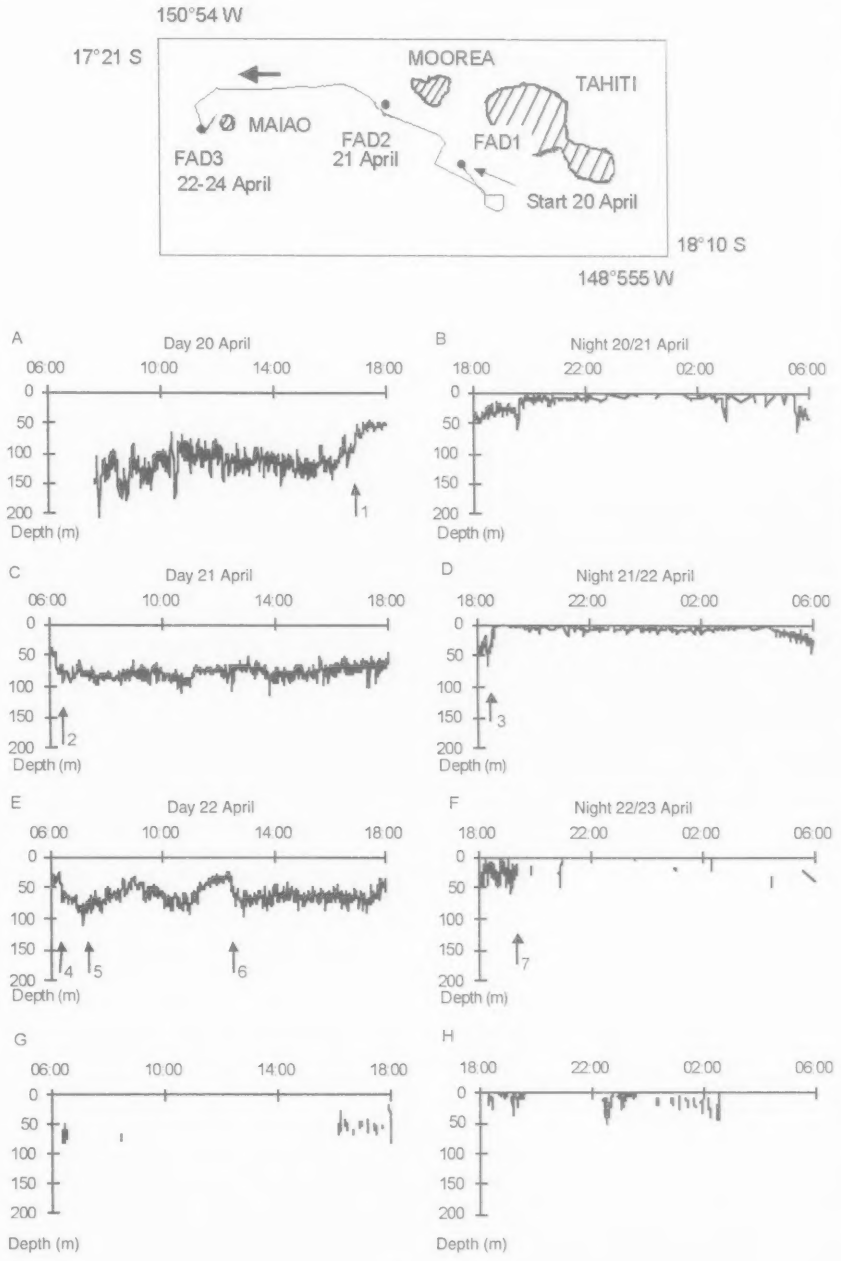

Figure 3

Horizontal and vertical movements of yellowfin tuna 3, 108 cm FL. Tracking lasted 91 h (April 1996). This fish was always associated with the tracking vessel. Arrows indicate the direction of horizontal movement in the upper graph. Changes in the movements of the tracking vessel are represented by vertical arrows on the graphs representing the vertical movements of the fish. 1 = the vessel left FAD1 to move to FAD2 during the night; 2 = the vessel arrived at FAD2; 3 = the vessel left FAD2 to go to FAD3; 4 = the vessel arrived at FAD3. 5 = the vessel left the FAD to go close to the Maiao island; 6 = the vessel came back to FAD3 and start drifting; 7 = the vessel moved away from FAD to conduct trawl and acoustic survey operations.

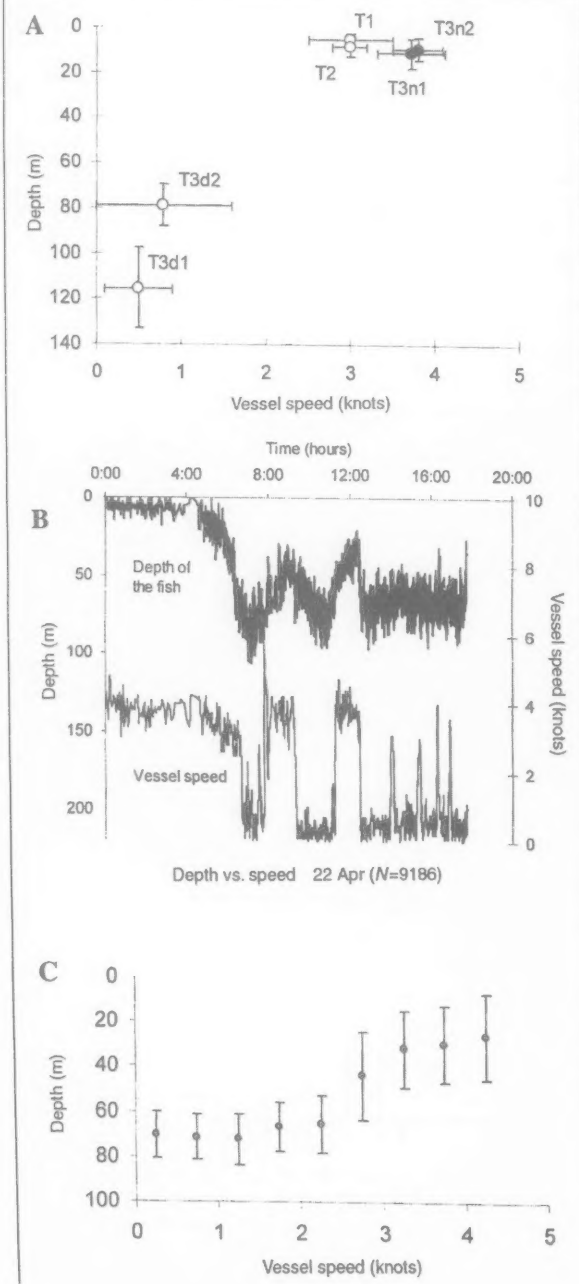

Figure 4

Relationships between swimming depths of the fish and the speed of the tracking vessel during associations. (**A**) Mean values (±SD) corresponding to each association: T1, T2, T3 for tunas 1, 2, 3; d1, d2, representing day times (white dots) and n1, n2 representing night times (black dots) of the first two 24-h cycles of the track of tuna 3. The two other graphs represent details of the association between tuna 3 and the tracking vessel during the third day (22 April 1996) where many changes in the vessel speeds occurred: (**B**) vertical movements and vessel speeds in relation to time; and (**C**) depth versus vessel speed (mean value ±SD).

it was captured (approximately 150 m) and immediately became associated with the tracking vessel. It remained at a depth between 80 m and 150 m while the vessel drifted close to the FAD. When the ship left the FAD (FAD1) at 16:20 to go to an other FAD (FAD2 South of Moorea Island), the fish moved closer to the surface and followed in a similar manner to that exhibited by yellowfin tuna 1 and 2. It remained within a school of other yellowfin tuna (individual size ranging from 20 to 50 kg) that could be seen from the ship, swimming just below the surface. During the second day (21 April), the fish remained associated with the ship as it drifted close to FAD2. Mean swimming depth was 75 m. During the second night (21–22 April), the vessel moved from FAD2 to FAD3, southwest of Maiao Island, and the fish followed, swimming close to the surface as during the first night. When the vessel and the fish arrived at FAD3 in the morning of 22 April, the fish left the surface and came under the ship. Around 07:45, the vessel left the FAD to shelter close to Maiao Island to find better sea conditions, with the tagged yellowfin tuna and the school following closely. The fish remained associated when the vessel returned to the FAD at 12:30. In the afternoon, the vessel drifted close to the FAD until 19:00, after which it made rapid accelerations away from the FAD to break off the association. The strategy was successful, and the fish remained associated with the FAD. During the fourth day (23 April), trawl and acoustic survey operations were conducted away from the FAD. The fish did not associate with the vessel during this period, but its presence at the FAD was regularly observed. Attempts to reassociate the fish with the tracking vessel were not successful because the fish returned to the FAD when the ship moved 0.5 nmi from the FAD. The fish remained associated with the FAD until operations terminated.

Figure 4 shows the relationships between swimming depths and the speed of the vessel during all observed associations. Shallower swimming depths were observed when the vessel was moving at higher speeds, both during daytime (tuna 1 and 2) and nighttime (tuna 3) associations. Figure 4 also shows in detail the response of tuna 3 to rapid changes in vessel speed during the third day (22 April), when the vessel was moving between FAD3 and the Maiao Island, or drifting close to the FAD or to the island. This day represents an example of frequent changes in vessel speed and corresponding changes in swimming depths of the fish.

Discussion

Individual yellowfin tuna have been documented associating with tracking vessels in the Indian Ocean (a 108-cm yellowfin tuna, Cayré et al., 1996) and near the main Hawaiian Islands (a 167-cm yellowfin tuna, Brill et al., 1999). However, these authors merely noted the occurrence of the associations without providing further analyses or comments on this striking behavior. It is noteworthy that all these fish were yellowfin tuna. It

seems, however, that this behavior is not size dependent (sizes ranged from 60 to 167 cm FL) nor is it related to the size of the tracking vessel: 12-m vessel for Cayré et al. (1996), 20-m and 53-m vessels for Brill et al. (1999), and 28-m vessel in our study.

Horizontal movements

The horizontal movements of fish associated with tracking vessels duplicated the horizontal movements of the tracking vessel. Therefore, the observed paths are not comparable with horizontal movements of tagged fish that were not associated with tracking vessels. Our results, however, give information on the duration of associations and possible "competition" between FADs and tracking vessel to attract the tagged fish.

Considering the different patterns of movements of tunas observed at anchored FADs, Holland (1996) proposed three horizontal patterns: 1) fish that leave the FAD and show no tendency to return to it over the duration of the track; 2) fish that spend the entire duration of the track (day and night) within a few hundred meters of the FAD, and 3) fish that spend daylight hours at the FAD site, leave at night and return to the same or an adjacent FAD the next day. Fish 1 and 2, as well as the 167-cm yellowfin tuna tracked by Brill et al. (1999) near the main Hawaiian Islands, associated with the tracking vessel during daytime, which corresponds to the third class defined by Holland (1996). Conversely, Cayré et al. (1996) reported a nighttime association between a 108-cm yellowfin tuna and the tracking vessel. Moreover, fish 3 remained associated with the tracking vessel for more than two 24 h (continuous day and night cycles) which corresponds to the second pattern defined by Holland (1996). Although our sample size was small, the three fish of our study, and the two other yellowfin tuna that exhibited such association (Cayré et al., 1996; Brill et al., 1999), exhibited different lengths of associations, at different periods of the diurnal cycle, all of which also correspond to the variety of patterns observed for fish associated with anchored FADs. These features, however, cannot be used to determine if tuna treat drifting and anchored floating objects differently, as first proposed by Holland et al. (1990).

The possible competition between FADs and the tracking vessel to aggregate tuna is an interesting feature of our results. The three tuna were caught close to and were considered associated with a FAD. Yellowfin tuna 1 and 2 left their FADs after release and did not associate immediately with the tracking vessel, whereas yellowfin tuna 3 associated with the tracking vessel after release. In the last part of their track, yellowfin tuna 1 and 3 clearly abandoned the vessel to associate with FADs. The presence of yellowfin tuna 2 was also noticed close to the FAD a few hours after the end of the tracking. Attempts to reaggregate yellowfin tuna 3 while associated with the third visited FAD were not successful. However, it is noteworthy that this tuna chose to associate with the tracking vessel rather than to FADs 1 or 2 on the previous days, showing a different motivation than those exhibited toward FAD3. Cayré et al. (1996) attempted to abandon the associated 108-cm yellowfin tuna by rapid vessel accelerations, trying to make the fish associate with a FAD, but without success. We cannot determine the reason for a possible preference of fish toward vessels or FADs. We can only propose that tuna regard the vessel and FADs in a similar manner, or that the choice in aggregating between these two structures depend on factors (external or internal stimuli) that we could not record during our experiments.

Vertical movements

It is known that the swimming depth of yellowfin tuna is controlled by the diurnal cycle: surface swimming at night and deep swimming at daytime (Carey and Olson, 1982; Cayré and Chabanne, 1986; Holland et al., 1990; Cayré, 1991). However, besides this diurnal behavior, it seems that fish travel closer to the surface when associated with a moving vessel: yellowfin tuna 1 and 2 swam very close to the surface (mean swimming depth=5.3 m ±2.9 for tuna 1 and 8.4 m ±4.5 for tuna 2) when they were associated with the moving vessel during daytime. Yellowfin tuna 3 also exhibited very shallow swimming depths when associated with the tracking vessel, but during nighttime (mean swimming depth=11.3 ±6.6 and 9.3 ±4.8 for the first two nights). Cayré et al. (1996) and Brill et al. (1999) did not report any relationship between the swimming depth of the fish and the speed of the tracking vessel. Figure 4 indicates definite relationships between fish swimming depths and the speed of the vessel during the associations. However, while this vertical reaction of the associated fish to the different vessel speeds have been observed during daytime, we should mention that no observations were made to examine the response of the fish to low vessel speeds during nighttime, which should have been deeper than the depths exhibited by yellowfin tuna 3 during the first two nights. This association behavior is similar to that observed by Holland et al. (1990), in that fish tend to be closer to the surface when associated with FADs. We propose that floating objects generally induce the fish to swim closer to the surface and that this tendency increases when floating objects are moving fast.

In addition to the shallower swimming of yellowfin tuna when associated with moving vessels, the amplitude of vertical oscillations are drastically reduced. We suggest that when fish are associated with a vessel, they reduce the amplitudes of their vertical oscillations, and that the mean swimming depth is partly controlled by the speed of the vessel (i.e. the distance from the fish to the tracking vessel decreases when the vessel speed increases). The reasons for this change are not known. More data are clearly needed to examine the exact effects of a floating object (including its speed) on the vertical pattern of associated fish and to distinguish these effects from those due to the diurnal cycle, thermoregulation, or foraging behavior.

Hypotheses to explain why tunas associate or disassociate with tracking vessels

The reasons why pelagic fish associate with floating objects are still not known conclusively (Fréon and Misund, 1999).

Tagging operations certainly represent a stress for the fish, especially when performed after a traumatic capture and removal from the water to attach the tag. If we assume that a fish considers this particularly large floating object (the tracking vessel) to be a shelter against the stress or possible injury caused by tagging procedures, the association with the vessel could then be interpreted as an antipredator behavior (shelter from predator hypothesis, Suyehiro, 1952, cited in Fréon and Misund, 1999). In fact, Block et al. (1992) and Brill et al. (1993) did observe badly injured fish swimming within a few meters of the surface (one Indo-Pacific blue marlin and one striped marlin, respectively), which corresponds to the swimming pattern exhibited by our fish when following the moving tracking vessel. If an injury or significant stress occurred during the capture or tagging operations, one could expect to see post-tagging antipredator behavior. The time delay between release and the onset of association behavior differs from one fish to another and ranges up to 16 hours after release (tuna 1), which argues against a stress-related association caused by the tagging operation. Moreover, observations of a school of yellowfin tuna exhibiting the same association as yellowfin tuna 3 prove that nontagged and apparently noninjured and nonstressed tuna develop the same association. Our observations thus do not support the "shelter from predator" hypothesis as an explanation for the attraction of tuna to the tracking vessel.

The role of social behavior to explain the association of fish with floating objects has been expressed in the "meeting point" hypothesis (Dagorn, 1994; Dagorn and Fréon, 1999; Fréon and Misund, 1999). This hypothesis proposes the enhancement of fish aggregation by floating objects through improving the encounter rate between small schools or between isolated individuals, or both. According to this hypothesis, tuna associate with various floating objects (drifting logs, anchored FADs, boats) to increase their chances of encountering conspecifics. Yellowfin tuna 1 and 2 seemed to be isolated during the tracking, whereas yellowfin tuna 3 was a member of a school. Yellowfin tuna 1 broke its association with the tracking vessel, joining individuals (observed by the echo-sounder) located under a FAD. It is not possible to know if the fish left the tracking vessel because of the FAD or because of the conspecifics. This observation, however, appears to support the "meeting point" hypothesis: this tuna and those of the aggregation benefited from their respective associations to find more conspecifics. Yellowfin tuna 3 was visually observed to be with a school during nights when the school swam close to the boat, and acoustically observed when it was associated with FAD3. The school was estimated to be composed of 80 individuals while associated with FAD3. Our observations were not precise enough to determine if new individuals joined the school during the 4-day experiment, nor if the school broke its association with the boat to join a group already aggregated to FAD3, in a manner similar to that shown by yellowfin tuna 1. However, we believe that the present observations do not reject the meeting point hypothesis.

Yellowfin tuna 1 and 3 left the tracking vessel to stay close to anchored FADs. It is difficult to know, however, if they broke the vessel association to associate with FADs or to join conspecifics located close to the FADs, or both. Contact with yellowfin tuna 2 was lost owing to a heavy rain. We do not know if the fish voluntarily broke off the association with the vessel or if it simply lost contact with the vessel. For instance, if the fish used the sound of the vessel to stay close, it is possible that the sound of the vessel was masked by the rain.

Because it is very important to know why tuna associate with floating objects (or vessels in the present case), it is also essential to understand why tuna leave floating objects. Although the sample size of our study was very small, it seems that the presence of other floating objects, conspecifics, or bad sea conditions can be responsible. Understanding the reasons why tuna form and break off aggregations is of major importance when studying the consequences of aggregation on tuna movements and distribution (Dagorn and Fréon, 1999).

Future studies

The objective of a sonic tagging experiment is to observe movements of a fish in its natural environment. The variety of experiments conducted throughout all the tropical oceans (Cayré and Chabanne, 1986; Holland et al., 1990; Cayré, 1991; Cayré and Marsac, 1993; Marsac et al. 1996; Bach et al., 1998; Josse et al., 1998; Marsac and Cayré, 1998; Brill et al., 1999; Dagorn et al., 2000) have contributed to a considerable increase in knowledge on the behavioral ecology of tropical tunas. Nevertheless, when a fish associates with a tracking vessel, although a very rare event, this objective has been violated. Among the tracking experiments on 14 yellowfin tuna in French Polynesia, the distinction between vessel-associated and unassociated individuals was very obvious. Moreover, this striking behavior has never been observed on other tuna species during tracking experiments (i.e. bigeye tuna, *Thunnus obesus*, and skipjack tuna, *Katsuwonus pelamis*). We consider that there is no possible doubt on the nature of the movements exhibited by a tagged individual (free movements or patterns associated with the vessel), which insures the validity of the interpretations of sonic tagging results. However, these rare events can be used to study the associations of fish with floating objects in a general sense. Rather than interrupting the tracking operation, we propose to develop particular experiments to improve our knowledge on tuna behavior. During the associations with vessels described in this paper, fish sometimes followed the vessel at speeds of up to 5 knots (2.6 m/s). It could be useful to use this behavior to study *in situ* the relationship between endurance time and velocity. Moreover, it is important to collect data on the duration of associations. Observations of the biological environment of the associated fish would also be very useful to test the validity of certain concepts, such as the "meeting point" hypothesis. During our experiments, we observed the biological environment (i.e. both prey and conspecifics) using an echo-sounder. The sounder assisted us to observe patches of prey (for yellowfin tuna 1) and the tuna aggregation

joined by yellowfin tuna 1, and also helped to determine the size of the school that yellowfin tuna 3 was drawn away from. However, the use of a multibeam sonar that can observe the few meters below the surface could provide complementary information, especially for such close observations. Similar sonar units have been successfully used to observe the structure and the behavior of small pelagic fish schools (Gerlotto et al., 1999) and would be particularly appropriate for the observation of both tuna schools and prey in the vicinity of a tracking vessel. A long-range multibeam omnidirectional sonar could also provide useful information on the horizontal distribution and spatial dynamics of tuna schools around the vessel.

Rather than disregarding tuna aggregations around tracking vessels, we propose to continue collecting information on such events. The tracking vessel represents a useful and fully instrumented, mobile floating object adapted to conduct detailed ethological observations to improve our knowledge of the behavior of tuna aggregated around floating objects.

Acknowledgments

This work was done within the frame of the ECOTAP Program (studies of tuna behavior using acoustic and fishing experiments), which is a joint program between SRM (Service des Ressources Marines de Polynésie Française), IFREMER (Institut français de recherche pour l'exploitation de la mer), IRD (Institut de Recherche pour le Développement). The authors wish to thank all the scientists who participated in the cruises, as well as the officers and crew of the IRD RV *Alis* for providing valuable help during all the cruises. We are also very grateful to David Itano and Dave McConaghay, who kindly improved the English text, and the three referees who made many constructive suggestions.

Literature cited

Bach, P., L. Dagorn, E. Josse, F.-X. Bard, R. Abbes, A. Bertrand, and C. Misselis.
1998. Experimental research and fish aggregating devices (FADs) in French Polynesia. SPC FAD (Fish Aggregating Device) Inf. Bull. 3:3–19

Block, B. A., D. T., Boothand, and F. G. Carey.
1992. Depth and temperature of the blue marlin, *Makaira nigricans*, observed by acoustic telemetry. Mar. Biol. 114:175–183

Block, B. A., J. E. Keen, B. Castillo, H. Dewar, E. V. Freund, D. J. Marcinek, R. W. Brill, and C. Farwell.
1997. Environmental preferences of yellowfin tuna (*Thunnus albacares*) at the northern extent of its range. Mar. Biol. 130:119–32.

Brill, R. W., B. A. Block, C. H. Boggs, K. A. Bigelow, E. V. Fruend, and D. J. Marcinek.
1999. Horizontal movements and depth distribution of large adult yellowfin tuna (*Thunnus albacares*) near the Hawaiian Islands, recorded using ultrasonic telemetry: implications for the physiological ecology of pelagic fishes. Mar. Biol. 133:395–408.

Brill, R. W., D. B. Holts, R. K. C. Chang, S. Sullivan, H. Dewar, and F. G. Carey.
1993. Vertical and horizontal movements of striped marlin (*Tetrapturus audax*) near the Hawaiian Islands, determined by ultrasonic telemetry, with simultaneous measurement of oceanic currents. Mar. Biol. 117:567–574.

Carey, F. G., and R. J. Olson.
1982. Sonic tracking experiments with tunas. Collect. Vol. Sci. Pap. ICCAT 17:458–466.

Cayré, P.
1991. Behaviour of yellowfin tuna (*Thunnus albacares*) and skipjack tuna (*Katsuwonus pelamis*) around fish aggregating devices (FADs) in the Comoros Islands as determined by ultrasonic tagging. Aquat. Living Resour. 4:1–12

Cayré, P., and J. Chabanne.
1986. Marquage acoustique et comportement de thons tropicaux (albacore: *Thunnus albacares*, et listao: *Katsuwonus pelamis*) au voisinage d'un dispositif concentrateur de poissons. Océanogr. Trop. 21(2):167–83

Cayré, P., and F. Marsac.
1993. Modeling the yellowfin tuna (*Thunnus albacares*) vertical distribution using sonic tagging results and local environmental parameters. Aquat. Living Resour. 6:1–14

Cayré, C., D. Norungee, F. Marsac, and F. Conand.
1996. Rapport de la campagne ACMAR06 (Marquage acoustique de thonidés) à l'Ile Maurice, du 11 au 16 février 1996. Doc. Sci. AT/COI/PTR2, 29 (4), 13 p. [Available from the Indian Ocean Commission (IOC), Avenue Sir Guy Forget, Quatre Bornes, Ile Maurice.]

Dagorn, L.
1994. Le comportement des thons tropicaux modélisé selon les principes de la vie artificielle. Ph.D. diss., ENSA de Rennes, France, 250 p.

Dagorn, L., P. Bach, and E. Josse.
2000. Movement patterns of large bigeye tuna (*Thunnus obesus*) in the open ocean, determined using ultrasonic telemetry. Mar. Biol. 136: 361–371.

Dagorn, L., and P. Fréon.
1999. Tropical tuna associated with floating objects: a simulation study of the meeting point hypothesis. Can. J. Fish. Aq. Sci. 56(6):984–993

Fonteneau, A., and T. Diouf.
1994. An efficient way of bait-fishing for tunas recently developed in Senegal. Aquat. Living Resour. 7:139–51

Fréon, P., and O.A. Misund.
1999. Dynamics of pelagic fish distribution and behaviour: effects on fisheries and stock assessment. Fishing News Books, Blackwell's, Oxford, 348 p.

Gerlotto, F., M. Soria, and P. Fréon.
1999. From 2D to 3D: the use of multibeam sonar for a new approach in fisheries acoustics. Can. J. Fish. Aquat. Sci. 56(1):6–12

Holland, K. N.
1996. Biological aspects of the association of tunas with FADs. SPC FAD (Fish Aggregating Device) Inf. Bull. 2: 2–7

Holland, K. N., R. W. Brill, and R. K. C. Chang.
1990. Horizontal and vertical movements of yellowfin tuna and bigeye tuna associated with fish aggregating devices. Fish. Bull. 88:493–507

Josse, E., P. Bach, and L. Dagorn.
1998. Simultaneous observations of tuna movements and their prey by sonic tracking and acoustic surveys. *In* Advances in invertebrates and fish telemetry (J. P. Lagardère M.-L. Bégout-Anras, and G. Claireaux, eds.), p. 61–69. Hydrobiologia 371/372.

Marsac, F., and P. Cayré.
1998. Telemetry applied to behaviour analysis of yellowfin tuna (*Thunnus albacares*, Bonnaterre, 1788) movements in a network of fish aggregating devices. *In* Advances in invertebrates and fish telemetry (J. P. Lagardère, M.-L. Bégout-Anras, and G. Claireaux, eds.), p. 155–171. Hydrobiologia 371/372.

Marsac, F., P. Cayré, and F. Conand.
1996. Analysis of small scale movements of yellowfin tuna around fish aggregating devices (FADs) using sonic tagging. *In* Proceedings of the expert consultation on Indian Ocean tunas, 6th session, Colombo, Sri Lanka, 25–29 September 1995 (A. A. Anganuzzi, K. A. Stobberup, and N. J. Webb, eds.), p. 151–159. IPTP (Indo-Pacific Tuna Project) Coll. 9.

Simard.
1994. Simrad EP500: echo processing system. Simrad Subsea A/S, Horten, Norway.

Identification of rockfish (*Sebastes* spp.) by restriction site analysis of the mitochondrial ND-3/ND-4 and 12S/16S rRNA gene regions

Anthony J. Gharrett

Andrew K. Gray

Fisheries Division, School of Fisheries and Ocean Sciences
University of Alaska Fairbanks
11120 Glacier Highway
Juneau, Alaska 99801
E-mail address (for A. J. Gharrett): ffajg@uaf.edu

Jonathan Heifetz

Auke Bay Laboratory
Alaska Fisheries Science Center
National Marine Fisheries Service, NOAA
11305 Glacier Highway
Juneau, Alaska 99801-8626

Abstract—Species-specific restriction site variation in the 12S/16S rRNA and ND-3/ND-4 mtDNA regions was used to distinguish among 15 rockfish species of the genus *Sebastes* common to the waters of Alaska. Intraspecific variation exhibited by eight of the species (based on five individuals of each species) did not obscure the interspecific variation, except possibly between *S. zacentrus* and *S. variegatus*. Intraspecific nucleotide diversity averaged 0.0024 substitutions per nucleotide, whereas interspecific nucleotide divergence averaged 0.0249. In contrast, the average nucleotide divergences between *Sebastes* and two other scorpaenid species, *Helicolenus hilgendorfi* and *Sebastolobus alascanus*, were 0.0805 and 0.1073, respectively. Cladistic and phenetic analyses supported some, but not all, of the subgenera assignments of *Sebastes*. A scheme for distinguishing among the species studied was presented. Restriction sites of 10 restriction endonucleases were mapped in the two PCR-amplified mtDNA regions by using double digests. In all, we detected 153 sites corresponding to 640 (13.5%) of the 4815 nucleotides in the two regions combined. The ND-3/ND-4 region exhibited substantially more intraspecific, interspecific, and intergeneric variation than the 12S/16S rRNA region.

Manuscript accepted 22 August 2000.
Fish. Bull. 99:49–62 (2001).

The species-rich genus of *Sebastes* rockfish has challenged both fisheries scientists and ichthyologists since they were first described from Alaskan waters by Tilesius (*S. ciliatus*; 1813, cited in Eschmeyer, 1998) and Richardson (*S. caurinus*; 1845). Both the large number of species, about 100 worldwide (Ishida, 1984; Kendall, 1991), and the metamorphoses that occur in larval and juvenile fish produce a confusing number of forms. The diversity of species and forms combine to limit our knowledge of the biology, including life histories, of rockfishes. To date, identification to species is not possible for many larvae and juveniles (e.g. Kendall, 1991; Moser, 1996), and distinguishing between some adult species may be difficult. For example, adult *S. variegatus* is similar to *S. zacentrus* and adult *S. mystinus*, *S. melanops*, and *S. ciliatus* are often misidentified (Love[1]). The inability to identify species constrains surveys of larval abundance and, consequently, ecological studies that are important for conservation and management of rockfish and other species. In addition, the questions facing biologists and fishery managers require tools that can resolve intraspecific population (stock) structure, as well as methods for identifying species.

The size of the genus and the paucity of information about some of the species have also contributed to a chaotic history of their systematics and many aspects of the phylogeny have not been resolved (Kendall[2] and reviewed in Cramer [1895] and Phillips [1957]. Cuvier (1829, cited in Eschmeyer,1998) first described the genus *Sebastes* for northern Atlantic specimens. The number of genera recognized for the species presently placed in *Sebastes* has expanded and contracted repeatedly, reaching a maximum of 15 (Jordan et al., 1930) and now these genera are generally considered subgenera. When combined with five northwestern Pacific Ocean (Matsubara, 1943) and one northern Atlantic Ocean subgenus, *Sebastes* comprises about 22 subgenera (Kendall, 1991).

Identification and systematics of fish depend largely on morphological characters; morphology alone, however, does not always provide sufficient criteria, especially for identification of larval and juvenile forms. Genetic information, obtained by using biochemical or molecular methods, has been used to address systematic problems. In some

[1] Love, M. 2000. Personal commun. Marine Sciences Institute, University of California, Santa Barbara, CA. 93106.

[2] Kendall, A.W. 2000. Personal commun. NMFS Alaska Fisheries Center, 7600 Sandpoint Way NE, Seattle, WA 98115.

instances, genetic differences can be used to differentiate between species that have overlapping morphologies. For example, cryptic species of southern Atlantic Ocean *Sebastes* species were recognized from mtDNA analysis (Rocha-Olivares et al., 1999a). Genera and many species of rockfish can be distinguished from protein electrophoresis differences (e.g. Tsuyuki et al., 1968; Johnson et al., 1972). More recently, allozyme data (Seeb, 1986) and mtDNA variation (Johns and Avise, 1998; Rocha-Olivares, 1998a; Seeb, 1998; Rocha-Olivares et al. 1999b, 1999c) have been used to address questions about the evolution and systematics of *Sebastes*. Genetic differences may provide the means for identifying rockfish larvae and juveniles that cannot be identified from their morphology (Seeb and Kendall, 1991). Recently, Rocha-Olivares (1998b) devised a PCR-based approach for identification of *Sebastes* species. The advantage of his approach is that it is fast. The disadvantage is that failed PCR reactions are part of the identification scheme. However, failed reactions can also result from poor quality DNA or intraspecific variation and lead to misidentification of the specimens. Intraspecific genetic variation can also provide information about population structure (e.g. Wishard et al., 1980; Seeb et al., 1988; Rocha-Olivares and Vetter, 1999).

Vertebrate mitochondrial DNA (mtDNA) is compact (about 16,500 base pairs) and has been completely sequenced in a variety of organisms including carp (*Cyprinus carpio*; Chang et al., 1994) and rainbow trout (*Oncorhynchus mykiss*; Zardoya et al., 1995). Because mitochondria are transmitted primarily through maternal genes (Gyllensten et al., 1991), mtDNA is haploid and clonally inherited (Meyer, 1993). Restriction fragment analyses of PCR-amplified regions of mtDNA provide a rapid and practical method for detecting nucleotide sequence variation in mtDNA between individuals or species. Sequence variation detected by restriction enzymes produces binary character-state data that can be used in phylogenetic analyses (e.g. Dowling et al., 1992). An advantage of restriction site surveys over sequencing is that they are practical for detecting variation in large sequence spans. The number of nucleotides screened in restriction site surveys depends on the number of restriction enzymes used and their match with the DNA sequence.

We have developed primers that can be used to PCR amplify regions of *Sebastes* mtDNA. The amplified regions provide material for addressing species identification and stock identification questions about rockfish. In addition, the haplotypes observed provide information for addressing systematic relationships among *Sebastes*.

Our objective in this study was to examine the potential that restriction fragment analyses of PCR-amplified mtDNA regions have for the study of rockfish biology. We asked the following specific questions: 1) Is there interspecific haplotype variation? 2) Is there intraspecific haplotype variation? 3) Does intraspecific variability compromise the use of mtDNA restriction fragments in species identification? 4) Can a simple strategy for identifying species be devised? 5) If there is interspecies variation, how do similarities between species correlate with (presumed) systematic relationships? To answer these questions, we conducted restriction site analyses on five individuals from each of 15 different *Sebastes* species common in Alaskan waters and mapped the sites using double digests to determine individual-based haplotypes. From these data, we examined intra- and inter-specific divergences and used both phenetic and cladistic procedures to examine relationships among the haplotypes. We also mapped the sites for shortspine thornyhead (*Sebastolobus alascanus*) and *Helicolenus hilfendorfi* to facilitate analysis. Finally, we developed a mtDNA restriction fragment-based strategy for identifying *Sebastes* species.

Materials and methods

Adult specimens of 15 different species of *Sebastes* rockfish and *Sebastolobus alascanus* were collected from the eastern Gulf of Alaska (Table 1). These species are the most abundant of the approximately 25 species reported in the region. In the field, species identification was confirmed by using the pictoral guide of Kramer and O'Connell (1988) and the key and descriptions in Hart (1973). H. Ida (Kitasato University, Sanriku, Japan) provided samples of *Helicolenus hilgendorfi* from Japanese coastal waters. Samples of heart tissue from each specimen were preserved in 95% ethanol or a solution of 20% dimethyl sulfoxide (DMSO), 0.25M ethylenediaminetetraacetic acid (EDTA) at pH 8 and saturated with NaCl (Seutin et al., 1991).

Total cellular DNA was isolated by phenol-chloroform extraction (Wallace, 1987) or with Puregene DNA™ isolation kits (Gentra Systems, Inc., Minneapolis, MN). Two target regions were PCR-amplified from total cellular DNA with primers that we developed for coho salmon (*Oncorhynchus kisutch*) mtDNA studies. The ND3/ND4 region begins in the glycyl tRNA gene and spans the NADH-dehydrogenase subunit-3, arginyl tRNA, NADH-dehydrogenase subunit-4L, and NADH-dehydrogenase subunit-4 genes, ending in the histidyl tRNA gene. The 12S/16S region extends from near the phenylalanyl tRNA end of the 12S rRNA gene through the valyl tRNA gene to near the leucyl tRNA end of the 16S rRNA gene (Table 2). From restriction digests, we estimated that the ND3/ND4 and 12S/16S regions comprised 2385 and 2430 base pairs (bp), respectively, as compared with 2331 and 2402, respectively, for *O. mykiss*. Target sequences were amplified by heating to 94°C for 5 min, followed by 30 cycles for 1 min at 94°C, 1 min at 55°C, and 3 min at 72°C using Taq polymerase from Perkin Elmer (Norwalk, CT) according to manufacturer's directions. ND3/ND4 amplification required 3mM $MgCl_2$, whereas amplification of 12S/16S required 2mM $MgCl_2$.

Single digests of subsamples of the PCR-amplified mtDNA regions were made by using 10 restriction endonucleases. *Bst*U I, *Cfo* I, *Dde* I, *Hin*f I, *Mbo* I, *Msp* I, and *Rsa* I have 4-nucleotide recognition sites; *Bst*N I recognizes an ambiguous 5-nucleotide site; and *Hin*d II and *Sty* I recognize ambiguous 6-nucleotide sites. Digestions were carried out under conditions recommended by the manufacturers. Fragments were separated by electrophoresis through 1.5% agarose (a mixture composed of one part

Table 1

Rockfish and related species and subgenera of *Sebastes* spp. used in mitochondrial DNA haplotype comparisons. The number designates the species and the letter indicates the particular composite haplotype observed.

Designation	Common name	Species	Subgenus
1, a and b	Pacific ocean perch	*Sebastes alutus*	*Acutomentum*
2, a and b	rosethorn rockfish	*Sebastes helvomaculatus*	*Sebastomus*
3	quillback rockfish	*Sebastes maliger*	*Pteropodus*
4, a and b	redbanded rockfish	*Sebastes babcocki*	*Rosicola*
5, a and b	black rockfish	*Sebastes melanops*	*Sebastosomus*
6	yellowtail rockfish	*Sebastes flavidus*	*Sebastosomus*
7, a–d	sharpchin rockfish	*Sebastes zacentrus*	*Allosebastes*
8	harlequin rockfish	*Sebastes variegatus*	*Allosebastes*
9	redstripe rockfish	*Sebastes proriger*	*Allosebastes*
10, a and b	rougheye rockfish	*Sebastes aleutianus*	*Zalopyr*
11, a and b	yelloweye rockfish	*Sebastes ruberrimus*	*Sebastopyr*
12	shortraker rockfish	*Sebastes borealis*	*Zalopyr*
13	light dusky rockfish	*Sebastes ciliatus*	*Sebastosomus*
14	silvergray rockfish	*Sebastes brevispinis*	*Acutomentum*
15, a and b	copper rockfish	*Sebastes caurinus*	*Pteropodus*
16	helicolenus	*Helicolenus hilgendorfi*	
17, a–d	shortspine thornyhead	*Sebastolobus alascanus*	

Table 2

Primers used for polymerase chain reaction amplification of rockfish (*Sebastes*, *Helicolenus*, and *Sebastolobus* spp.) mtDNA regions. a = Thomas and Beckenbach (1989); b = Cronin et al. (1993); c = Gharrett[1]; d = Anderson et al. (1981); e = Anderson et al. (1982); f = Roe et al. (1985); g = Chang et al., 1994; h = Zardoya et al. (1995).

Region amplified	Sequence	Location in *O. mykiss*[h]	Source
ND3/ND4	5′ TAACGCGTATAAGTGACTTCCAA 3′	bp 10574–10596	from a (similar to b)
	5′ TTTTGGTTCCTAAGACCAATGGAT 3′	bp 12881–12904	from a and c (similar to b)
12S/16S	5′ AATTCAGCAGTGATAAACATT 3′	bp 1234–1254	consensus: d, e, f, g
	5′ AGATAGAAACTGACCTGGATT 3′	bp 3615–3635	consensus: d, e, f, g

[1] Gharrett, A. J. 2000. Unpubl. *Oncorhynchus kisutch* sequences. Fisheries Division, Univ. Alaska, Fairbanks, 11120 Glacier Hwy., Juneau, AK 99801.

Ultra Pure™ agarose [BRL Gibco, Grand Island, NY] and two parts Synergel™ [Diversified Biotech Inc., Boston, MA]) in 0.5×TBE buffer (TBE is 90 mM tris-boric acid, and 2 mM EDTA, pH 7.5). DNA in the gel was stained with ethidium bromide and photographed on an ultraviolet light transilluminator. Digests that produced small unresolvable fragments on agarose gels were subjected to electrophoresis on 8% polyacrylamide gels (29:1 acrylamide:bisacrylamide) in 2×TAE (TAE is 40 mM tris-acetic acid and 1 mM EDTA, pH 8.0). DNA in polyacrylamide was stained with SYBR Green 1 Nucleic Acid Stain™ (Molecular Probes, Eugene, OR). Molecular weight markers used to estimate restriction fragment sizes were 100 base pair (bp) or 25-bp ladders (BRL Gibco, Grand Island, NY). Restriction sites were mapped by using double digests. Double digests were examined both in agarose and polyacrylamide by using 100- and 25-bp ladders. Composite haplotypes for all 10 restriction enzymes and both mtDNA regions were determined for each individual.

Generalized (relaxed Dollo) parsimony trees (Swofford et al., 1996) were computed from shared restriction sites by a heuristic search with PAUP* 4.0 (Swofford, 1998), which assumed unordered states. Because the likelihood of the loss of a site is higher than the restoration of a lost site, we conducted analyses that assumed 1) no added cost, 2) twice the cost, and 3) four-times the cost for restoring a site. Multiple maximum parsimony trees from each analysis were combined to produce a majority consensus tree using PAUP* 4.0 (Swofford, 1998). A maximum-likelihood tree was estimated with the program RESTML in

PHYLIP 3.57c (Felsenstein[3]), assuming that all restriction sites were 4 bp long (PHYLIP, Felsenstein[3]). Nucleotide divergences (proportion of nucleotide substitutions) and their standard errors were estimated according to Nei and Tajima (1983), Nei (1987), and Nei and Miller (1990) by using REAP (McElroy et al., 1990).

Results

Restriction fragment patterns from double digests were used to construct restriction site maps for comparisons of species and detection of intraspecies variation (Appendix 1). The map includes 153 restriction sites, 36 of which were common in all haplotypes and 28 of which were cladistically uninformative because the presence or absence occurs only in a single haplotype. Many of the cladistically uninformative sites, however, were useful in species delineation. These data represent 153 restriction sites (79.3 on average) corresponding to 640 nucleotides (332.05 on average) per haplotype.

Among the 85 fish examined were 30 different composite haplotypes (Table 3); each species had haplotypes that were distinct from those of other species, although *S. variegatus* composite haplotype 8 differed at a single site from *S. zacentrus* composite haplotype 7c (Table 4). All other pairs of species differed by 5 or more sites. Intraspecific variation was observed in nine of the seventeen species even when only five specimens of each species were analyzed. The most variable species were *S. zacentrus* and *Sebastolobus alascanus,* each of which had four haplotypes. In the study, differences between haplotypes ranged from a single site difference or 0.0014 nucleotide substitutions per site to 65 restriction site differences and 0.120 nucleotide substitutions per site (Table 4). Nucleotide divergence within variable species averaged 0.0024 subsitutions (1.56 site changes), whereas divergences between *Sebastes* species averaged ten-fold higher, 0.0249 (15.4 site changes), ranging from 0.0015 (1 site change) to 0.0384 (25 site changes). Nucleotide divergences between *Sebastes* species and *Sebastolobus alascanus* averaged 0.1073 (59.2 site changes) and divergences between *Sebastes* species and *H. hilgendorfi* averaged 0.0805 (43.5 site changes).

Distribution of the variation between the two different mtDNA regions (ND3/ND4 and 12S/16S) reflects their rates of evolution. In the 12S/16S region, which is more conservative, 27 of 58 restriction sites were shared by all haplotypes. Nucleotide diversities between *Sebastes* species averaged 0.0094 nucleotide changes per nucleotide (a total of 3.29 sites differences in the region), divergences between *Sebastes* and *H. hilgendorfi* averaged 0.0641 (12.67 site differences), and divergences between *Sebastes* and *Sebastolobus alascanus* averaged 0.0561 (18.03 site differences). In contrast, in the ND3/ND4 region only 9 of 95 sites were common to all haplotypes; and nucleotide divergences between *Sebastes* species averaged 0.0471 (12.11 site differences) and divergences between *Sebastes* and *H. hilgendorfi* and between *Sebastes* and *Sebastolobus alascanus* averaged 0.1373 (31.75 site differences) and 0.1929 (40.93 site differences), respectively. The maximum likelihood and majority consensus tree for the 60 maximum parsimony trees that imposed a cost of two for regained restriction sites had identical topologies (Fig. 1). The topologies of parsimony trees, which had either no additional cost or a cost of four, were somewhat different. Several groups of species were present in all three parsimony topologies. The *S. zacentrus-S. variegatus* pair, mentioned above, and each of four species pairs—*S. melanops-S. flavidus*, *S. babcocki-S. helvomaculatus*, *S. proriger-S. brevispinis,* and *S. maliger-S. caurinus*—clustered tightly at subterminal nodes. A more interior cluster of species included *S. melanops*, *S. flavidus*, *S. babcocki*, and *S. helvomaculatus*. In addition, *S. maliger* and *S. caurinus* clustered separately from all other *Sebastes* species and the *Sebastes* species were distinct from *H. hilgendorfi* and *Sebastolobus alascanus*.

The mtDNA variation we observed among *Sebastes* species provides a tool for identifying species. From our data, numerous schemes could be devised that distinguish among the *Sebastes* species examined. We propose a simple scheme that minimizes the number of digests required and involves separation of restriction fragments from the ND3/ND4 PCR product on an agarose-Synergel™ gel using only four restriction enzymes. *Mbo* I digests produce 11 different haplotypes (haplotypes A–K; Figure 2A; Table 3); *S. alutus* (B), *S. melanops* (E), *S. babcocki* (G and H), *S. ruberrimus* (I), and *S. caurinus* (J) are species specific. If *Mbo* I haplotypes A (*S. helvomaculatus* or *S. flavidus*) or C (*S. maliger* or *S. caurinus*) are observed, digest the ND3/ND4 PCR product with *Hin*d II; *Hin*d II haplotype B is specific for *S. helvomaculatus* and *Hin*d II haplotype C is specific for *S. maliger* (Fig. 2B; Table 3). If *Mbo* I haplotypes F (*S. ciliatus* or *S. borealis*) or K (*S. aleutianus*, *S. proriger*, or *S. brevispinis*) are observed, digest the ND3/ND4 PCR product with *Bst*N I; *Bst*N I haplotype A is specific for *S. ciliatus* and *Bst*N I haplotype G is specific for *S. brevispinis* (Fig. 2C; Table 3). *Mbo* I and *Bst*N I haplotypes do not distinguish between *S. aleutianus* and *S. proriger*, but *Cfo* I haplotype B is specific for *S. aleutianus* (Fig. 2D, Table 3). The combined haplotype of *Mbo* I, *Hin*d II, *Bst*N I, and *Cfo* I can be used to identify *S. borealis* (KAFD) and *S. proriger* (FAFD) (Fig. 2). The single difference between *S. zacentrus* and *S. variegatus* is the presence of a 123-bp fragment in *Rsa* I digests of *S. zacentrus* (Table 2; Appendix 1).

This simple scheme takes advantage of unique single-site differences for several of the species. Although a neighbor-joining tree (Saitoh and Nei, 1987) appeared stable to intraspecific variation for increased sample sizes of three species (data not shown), a single site change that produces apparent convergence between taxa in our scheme is conceivable. Increased certainty can be achieved by conducting digests with all four enzymes. With this strategy there will be at least two site differences between every pair of species, except *S. proriger* and *S. brevispinis*, which

[3] Felsenstein, J. 1993. PHYLIP (Phylogeny Inference Package) version 3.57c. Distributed by the author. Department of Genetics, Box 357360, Univ. Washington, Seattle, WA 98195-7360.

Table 3

Composite haplotypes for *Sebastes* spp., *Helicolenus hilgendorfi*, and *Sebastolobus alascanus* in the 12S/16S and ND3/ND4 mtDNA regions. The species codes are listed in Table 2. The haplotype codes refer to haplotypes in Table 4. Five individuals were analyzed for each species. Where intraspecific variation was observed, alternative haplotypes are presented.

	12S/16S haplotypes									
Species	*Bst*N I	*Bst*U I	*Cfo* I	*Dde* I	*Hin*d II	*Hin*f I	*Mbo* I	*Msp* I	*Rsa* I	*Sty* I
1a	A	A	A	D	A	B	C	B	A	A
1b	A	A	A	D	A	A	C	B	A	A
2a	A	A	A	C	A	B	B	A	D	A
2b	A	A	A	C	A	B	C	A	D	A
3	A	A	A	D	A	B	A	A	B	A
4a	A	A	A	C	A	B	C	B	B	A
4b	A	A	A	C	A	B	C	B	B	A
5a	A	A	A	D	A	B	C	B	D	A
5B	A	A	A	D	A	B	C	B	D	A
6	A	A	A	A	A	B	C	B	D	A
7a	A	A	A	B	A	B	C	A	C	A
7b	A	A	A	B	A	B	C	A	C	A
7c	A	A	A	B	A	B	C	A	C	A
7d	A	A	A	B	A	B	C	A	C	A
8	A	A	A	B	A	B	C	A	C	A
9	A	A	A	D	A	B	C	A	C	A
10a	A	A	A	D	A	B	C	B	A	A
10b	A	A	A	D	A	B	C	B	A	A
11a	A	A	A	D	A	C	C	A	A	A
11b	A	A	A	D	A	C	C	A	A	A
12	B	A	A	A	A	B	C	A	C	A
13	A	A	A	D	A	B	C	A	A	A
14	A	A	A	D	A	A	C	A	C	A
15a	A	A	A	D	A	B	A	A	A	A
15b	A	A	A	D	A	B	A	A	A	A
16	D	B	B	F	B	B	F	B	A	A
17a	C	B	B	E	A	D	E	B	E	B
17b	C	B	B	E	A	D	E	B	E	B
17c	C	B	B	E	A	D	E	B	E	B
17d	C	B	B	E	A	D	E	B	E	B

	ND3/ND4 haplotypes									
Species	*Bst*N I	*Bst*U I	*Cfo* I	*Dde* I	*Hin*d II	*Hin*f I	*Mbo* I	*Msp* I	*Rsa* I	*Sty* I
1a	B	C	A	J	A	A	B	B	C	C
1b	B	C	A	J	A	A	B	B	C	C
2a	F	C	D	K	B	A	A	B	C	C
2b	F	C	D	K	B	A	A	B	E	C
3	F	B	D	L	C	D	C	C	B	A
4a	F	C	D	G	A	A	G	B	B	C
4b	F	C	D	F	A	A	H	B	B	C
5a	D	C	D	F	A	B	E	A	A	C
5B	D	C	D	F	A	B	E	B	A	C
6	E	C	D	H	A	C	A	B	A	C
7a	F	A	D	E	A	A	D	B	C	C
7b	F	A	D	A	A	A	D	B	C	C
7c	F	C	D	E	A	A	D	B	C	C

continued

Table 3 (continued)

	ND3/ND4 haplotypes									
Species	*Bst*N I	*Bst*U I	*Cfo* I	*Dde* I	*Hin*d II	*Hin*f I	*Mbo* I	*Msp* I	*Rsa* I	*Sty* I
7d	F	A	D	E	A	A	D	B	C	B
8	F	C	D	E	A	A	D	B	B	C
9	F	C	D	E	A	A	K	E	B	C
10a	F	C	B	N	A	E	K	D	D	C
10b	F	C	B	N	A	F	K	D	D	C
11a	C	C	A	B	A	D	I	B	D	C
11b	C	C	D	B	A	D	I	B	D	C
12	F	C	D	D	A	A	F	B	B	C
13	A	D	A	M	A	A	F	B	F	C
14	G	C	D	C	A	A	K	D	B	D
15a	F	B	C	L	A	G	C	C	B	A
15b	F	B	C	L	A	G	J	C	B	A
16	J	G	F	Q	A	A	N	G	H	A
17a	H	E	E	O	A	H	M	F	G	F
17b	I	E	E	O	A	H	M	F	G	F
17c	H	F	E	O	A	H	M	F	G	E
17d	H	E	E	P	A	H	M	F	G	F

can be resolved by using *Msp* I, and *S. zacentrus* and *S. variegatus* (see above). We do not recommend using *Dde* I because it has many sites, often produces small fragments requiring both agarose and polyacrylamide gels for resolution, and is, therefore, time consuming to analyze. However, the restriction patterns of *Dde* I are nearly species specific.

Discussion

Sufficient interspecies restriction site variation occurred in the ND3/ND4 and 12S/16S mtDNA regions in *Sebastolobus alascanus*, *Helicolenus hilgendorfi*, and 15 *Sebastes* species to distinguish among them. Intraspecific variation was observed in nine of the seventeen species, but it did not interfere with our ability to distinguish between species. We used the interspecific variation to devise a strategy to identify the species we studied. Intraspecific variability can serve as a basis for stock identification.

A broader survey, particularly for *S. zacentrus* and *S. variegatus*, might reveal overlaps in haplotype compositions that compromise the ability to distinguish between some species pairs. This would be most likely if there were gene flow between the species or if the species had recently diverged. Otherwise, extending the analysis to other mtDNA regions and additional restriction endonucleases should increase resolution. Of course, additional intraspecific variation has the potential to obscure the topology of trees. To test this possibility, we examined trees that included the additional haplotypes observed in samples of 40 to 126 individuals each from *S. caurinus* (n=79), *S. aleutianus* (n=126), and *S. borealis* (n=40) (data not shown). The additional haplotypes (5, 13, and 5, respectively) increased the number of branches at the tip of the species limbs but did not influence or obscure relationships with other species. We are currently investigating the population structure of *S. aleutianus*, *S. borealis*, S. *alutus*, *S. caurinus*, and *Sebastolobus alascanus* by using mtDNA restriction site variation.

Because of the similarity of many *Sebastes* species, there is a chance that very similar species can be misidentified. In fact, a young dusky rockfish (*S. ciliatus*) and a young yellowtail rockfish (*S. flavidus*) were misidentified in the field as black rockfish (*S. melanops*) prior to our mtDNA analysis. Also, it is possible that closely related species may hybridize (e.g. Seeb, 1998). Because hybrids carry only the maternal lineage and because only the maternal contributor can be identified, mtDNA analysis is a poor tool for identifying hybrids.

In addition to providing a tool that can distinguish among a variety of rockfish species, the data appear to provide criteria that may prove useful in unraveling some questions about rockfish systematics. Both outgroups are distinct from *Sebastes*; *H. hilgendorfi* is more closely related than *Sebastolobus alascanus*. The 15 *Sebastes* species studied include eight subgenera, five of which were represented by two or more species. Despite the uncertainty in some of the subgenus assignments,[2] our analyses of mtDNA restriction sites show some concordance with subgeneric assignments. Unfortunately, the only recently reviewed subgenus is *Sebastomus* (Chen, 1971), for which we have only a single representative (*S. helvomaculatus*). A phylogeny of subgenera is unavailable.

Several species pairs were persistent in the analyses. Within *Sebastes*, *S. maliger* and *S. caurinus* (subgenus *Pteropodus*) were distinct from the other *Sebastes* species.

Table 4

Differences between haplotypes (see Table 3 and Appendix 1) of rockfish (*Sebastes, Helicolenus,* and *Sebastolobus* spp.). Above the diagonal are the number of restriction site differences. Below the diagonal are estimates of evolutionary differences (nucleotide substitutions per site; Nei and Tajima 1981; Nei and Miller 1990). An average of 79.3 sites and 332.05 bases were examined for each haplotype (McElroy et al.1990).

Species	1a	1b	2a	2b	3	4a	4b	5a	5b	6
1a		1	14	14	21	13	13	16	15	16
1b	0.0015		15	15	22	14	14	17	16	17
2a	0.0224	0.0243		2	19	9	9	14	13	14
2b	0.0222	0.0240	0.0031		19	9	9	14	13	14
3	0.0335	0.0354	0.0306	0.0302		16	18	21	20	21
4a	0.0208	0.0226	0.0143	0.0141	0.0253		2	11	10	13
4b	0.0210	0.0229	0.0145	0.0143	0.0290	0.0031		11	10	13
5a	0.0260	0.0279	0.0225	0.0222	0.0334	0.0175	0.0177		1	6
5b	0.0242	0.0260	0.0207	0.0204	0.0315	0.0158	0.0160	0.0015		5
6	0.0267	0.0286	0.0230	0.0227	0.0340	0.0213	0.0216	0.0094	0.0078	
7a	0.0192	0.0210	0.0194	0.0191	0.0306	0.0246	0.0249	0.0260	0.0242	0.0265
7b	0.0210	0.0229	0.0212	0.0210	0.0325	0.0265	0.0269	0.0280	0.0260	0.0285
7c	0.0174	0.0192	0.0176	0.0174	0.0287	0.0227	0.0230	0.0242	0.0223	0.0246
7d	0.0210	0.0228	0.0213	0.0210	0.0327	0.0264	0.0268	0.0279	0.0260	0.0284
8	0.0192	0.0210	0.0194	0.0191	0.0272	0.0211	0.0214	0.0226	0.0208	0.0231
9	0.0205	0.0223	0.0207	0.0204	0.0283	0.0190	0.0193	0.0206	0.0188	0.0243
10a	0.0223	0.0242	0.0295	0.0256	0.0336	0.0208	0.0211	0.0223	0.0239	0.0296
10b	0.0238	0.0257	0.0310	0.0272	0.0351	0.0224	0.0227	0.0206	0.0221	0.0312
11a	0.0261	0.0281	0.0333	0.0293	0.0339	0.0280	0.0283	0.0333	0.0313	0.0376
11b	0.0277	0.0296	0.0313	0.0274	0.0320	0.0260	0.0264	0.0313	0.0294	0.0356
12	0.0208	0.0226	0.0209	0.0206	0.0285	0.0192	0.0194	0.0210	0.0192	0.0216
13	0.0190	0.0208	0.0329	0.0325	0.0302	0.0277	0.0281	0.0336	0.0317	0.0381
14	0.0339	0.0324	0.0342	0.0337	0.0383	0.0324	0.0328	0.0270	0.0285	0.0308
15a	0.0321	0.0340	0.0325	0.0321	0.0075	0.0272	0.0311	0.0355	0.0336	0.0361
15b	0.0351	0.0371	0.0356	0.0351	0.0104	0.0303	0.0342	0.0385	0.0366	0.0391
16	0.0740	0.0767	0.0835	0.0779	0.0745	0.0724	0.0735	0.0827	0.0843	0.0885
17a	0.1043	0.1028	0.1148	0.1084	0.1043	0.0981	0.1041	0.0996	0.1011	0.1055
17b	0.1055	0.1041	0.1161	0.1097	0.1057	0.0995	0.1055	0.1010	0.1025	0.1070
17c	0.1031	0.1016	0.1136	0.1071	0.1029	0.0968	0.1029	0.0983	0.0998	0.1043
17d	0.1028	0.1013	0.1133	0.1069	0.1029	0.0966	0.1026	0.0981	0.0996	0.1040

Species	7a	7b	7c	7d	8	9	10a	10b	11a	11b
1a	12	13	11	13	12	13	14	15	16	17
1b	13	14	12	14	13	14	15	16	17	18
2a	12	13	11	13	12	13	18	19	20	19
2b	12	13	11	13	12	13	16	17	18	17
3	19	20	18	20	17	18	21	22	21	20
4a	15	16	14	16	13	12	13	14	17	16
4b	15	16	14	16	13	12	13	14	17	16
5a	16	17	15	17	14	13	14	13	20	19
5b	15	16	14	16	13	12	15	14	19	18
6	16	17	15	17	14	15	18	19	22	21
7a		1	1	1	2	7	14	15	14	13
7b	0.0016		2	2	3	8	15	16	15	14
7c	0.0015	0.0031		2	1	6	13	14	13	12
7d	0.0016	0.0032	0.0032		3	8	15	16	15	14
8	0.0031	0.0047	0.0015	0.0048		5	12	13	12	11
9	0.0109	0.0126	0.0093	0.0126	0.0078		9	10	11	10

continued

None of the other subgenera were as coherent. The haplotypes of *S. zacentrus* and *S. variegatus* (subgenus *Allosebastes*) were very similar and the haplotype of a third member, *S. proriger*, generally clustered nearby. Similarly, the haplotypes of *S. maliger* and *S. flavidus* (subgenus *Sebastosomus)* were tightly clustered, but the branch for the haplotype of the third member, *S. ciliatus*, was distal; and different tree construction methods inconsistently placed

Table 4 (continued)

Species	7a	7b	7c	7d	8	9	10a	10b	11a	11b
10a	0.0227	0.0246	0.0208	0.0245	0.0193	0.0140		1	14	13
10b	0.0243	0.0262	0.0224	0.0260	0.0208	0.0155	0.0015		15	14
11a	0.0229	0.0248	0.0210	0.0247	0.0195	0.0174	0.0226	0.0242		1
11b	0.0210	0.0229	0.0192	0.0228	0.0177	0.0157	0.0208	0.0223	0.0015	
12	0.0143	0.0161	0.0126	0.0160	0.0111	0.0093	0.0174	0.0189	0.0211	0.0193
13	0.0227	0.0246	0.0243	0.0245	0.0227	0.0207	0.0292	0.0308	0.0266	0.0282
14	0.0239	0.0258	0.0221	0.0258	0.0206	0.0122	0.0236	0.0252	0.0274	0.0255
15a	0.0292	0.0311	0.0272	0.0311	0.0257	0.0269	0.0322	0.0338	0.0361	0.0340
15b	0.0322	0.0342	0.0303	0.0342	0.0288	0.0299	0.0353	0.0368	0.0391	0.0371
16	0.0795	0.0823	0.0811	0.0821	0.0839	0.0843	0.0740	0.0756	0.0801	0.0817
17a	0.1151	0.1136	0.1166	0.1186	0.1151	0.1101	0.0996	0.1011	0.1014	0.1029
17b	0.1164	0.1149	0.1179	0.1199	0.1164	0.1115	0.1010	0.1025	0.1031	0.1046
17c	0.1140	0.1124	0.1155	0.1173	0.1140	0.1090	0.0983	0.0998	0.1002	0.1017
17d	0.1136	0.1120	0.1151	0.1170	0.1136	0.1086	0.0981	0.0996	0.0999	0.1014

Species	12	13	14	15a	15b	16	17a	17b	17c	17d
1a	13	12	21	20	22	41	58	59	57	57
1b	14	13	20	21	23	42	57	58	56	56
2a	13	20	21	20	22	45	62	63	61	61
2b	13	20	21	20	22	43	60	61	59	59
3	18	19	24	5	7	42	59	60	58	58
4a	12	17	20	17	19	40	55	56	54	54
4b	12	17	20	19	21	40	57	58	56	56
5a	13	20	17	22	24	45	56	57	55	55
5b	12	19	18	21	23	46	57	58	56	56
6	13	22	19	22	24	47	58	59	57	57
7a	9	14	15	18	20	43	62	63	61	61
7b	10	15	16	19	21	44	61	62	60	60
7c	8	15	14	17	19	44	63	64	62	62
7d	10	15	16	19	21	44	63	64	62	62
8	7	14	13	16	18	45	62	63	61	61
9	6	13	8	17	19	46	61	62	60	60
10a	11	18	15	20	22	41	56	57	55	55
10b	12	19	16	21	23	42	57	58	56	56
11a	13	16	17	22	24	43	56	57	55	55
11b	12	17	16	21	23	44	57	58	56	56
12		13	14	17	19	44	61	62	60	60
13	0.0212		19	18	20	43	62	63	61	61
14	0.0221	0.0307		23	25	50	59	60	58	58
15a	0.0271	0.0288	0.0369		2	41	62	63	61	61
15b	0.0301	0.0317	0.0399	0.0030		43	64	65	63	63
16	0.0811	0.0786	0.0928	0.0734	0.0765		61	62	60	60
17a	0.1117	0.1135	0.1055	0.1118	0.1147	0.1145		1	3	1
17b	0.1131	0.1150	0.1070	0.1131	0.1160	0.1158	0.0014		4	2
17c	0.1105	0.1124	0.1045	0.1105	0.1135	0.1129	0.0043	0.0057		4
17d	0.1102	0.1120	0.1040	0.1104	0.1133	0.1130	0.0014	0.0029	0.0058	

S. ciliatus on the tree (not shown). Haplotypes of *S. aleutianus* and *S. borealis* (subgenus *Zalopyr*) were found in the same general region of the tree, but are not sister taxa. Likewise, the two representatives of *Acutomentum*, *S. alutus* and *S. brevispinis*, were not monophyletic sister taxa. Disparities, such as we observed between relationships of haplotype and assignments of subgenera, have also been reported for allozyme comparisons (Seeb, 1986) and mtDNA cytochrome *b* sequences (Johns and Avise, 1998; Rocha-Olivares, 1998a; Rocha-Olivares et al., 1999a, 1999b). The members of subgenera *Acutomentum* and *Allosebastes*, in particular, seem discordant with trees. It is important to recall that the systematics is not unequivocal and controversies date back more than a century (e.g. Cramer, 1895). Therefore, discrepancies between the molecular-based comparisons and current systematic place-

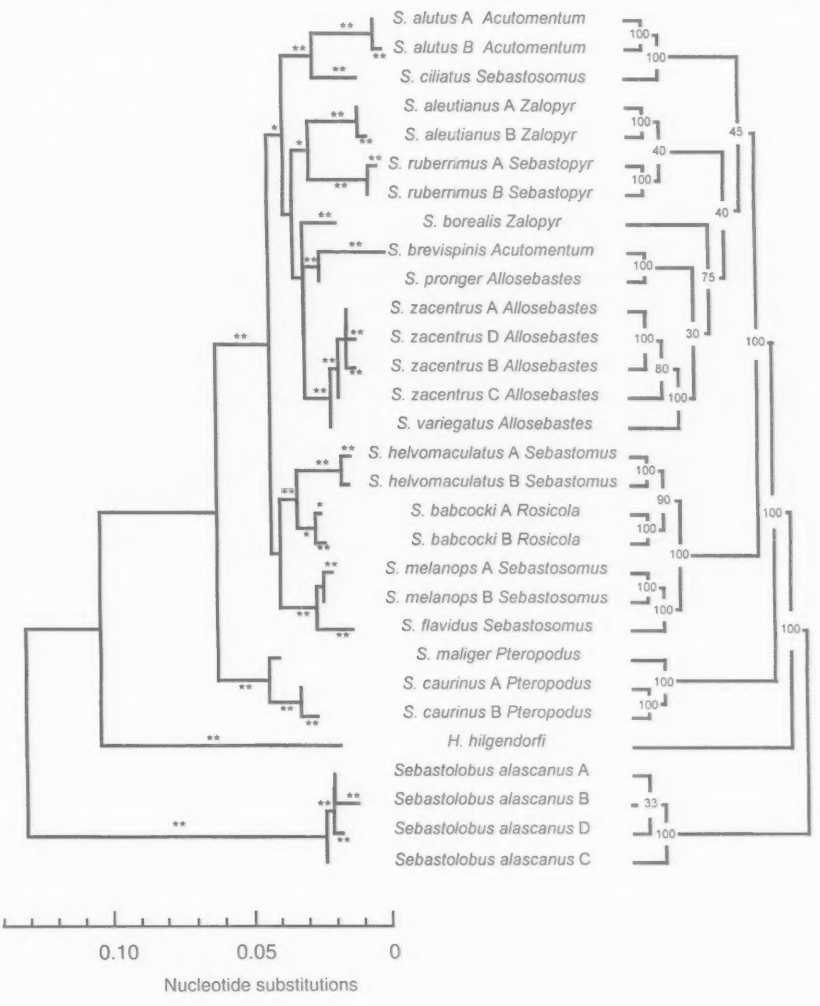

Figure 1

Maximum likelihood (PHYLIP; Felsenstein[3]) and maximum parsimony consensus trees (PAUP*; Swofford, 1998) trees estimated from restriction site data for haplotypes of 15 *Sebastes* spp., *Helicolenus hilgendorfi*, and *Sebastolobus alascanus*. Haplotype and restriction site data are provided in Appendix 1 and Table 3, respectively. On the maximum likelihood tree, * and ** indicate distances that are significantly positive ($P<0.05$ and $P<0.01$, respectively). On the maximum parsimony consensus tree, the numbers at nodes indicate the percentage of trees that included those branches.

ments do not necessarily discredit the validity of the molecular comparisons.

Use of restriction site data in mtDNA holds promise for the identification and systematics of *Sebastes* and suggests the possibility of applications for stock identification. Larval and juvenile rockfish carry mtDNA that is adequate for PCR amplification (e.g. see Seeb and Kendall, 1991; Rocha-Olivares 1998b). Combining molecular identification with morphometry may solve many of the problems of identification that accompany rockfish studies. The apparent coherence of closely related rockfish species that we observed in both cladistic and phenetic analyses suggests that we should focus our applications on groups of species that are presumed to be close relatives. The consensus tree depicting relationships among interior clades within the *Sebastes* parsimony tree did not unequivocally position those clades either in this study or analyses of the cytochrome *b* region (Johns and Avise, 1998; Rocha-Olivares, 2000). Consequently, determination of higher level relationships among *Sebastes* requires analysis of additional mtDNA regions. Moreover, because the divergence of mtDNA sequences provides only one perspective of the evolution of *Sebastes* divergence, the relationships inferred by mtDNA analyses must be corroborated by analysis of the interspecific divergence of nuclear genes.

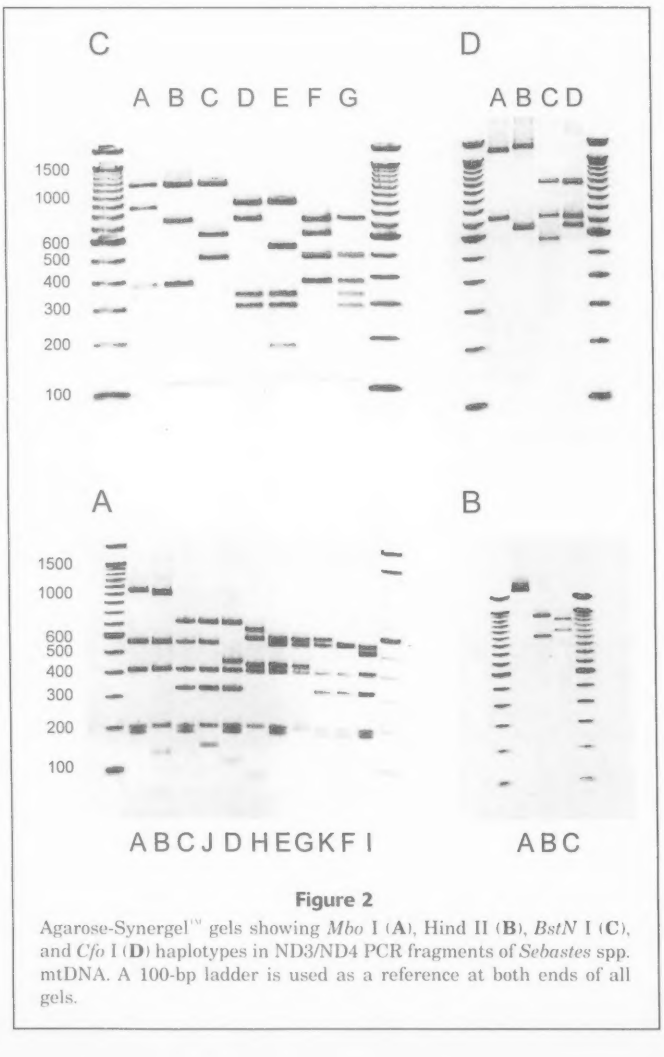

Figure 2

Agarose-Synergel™ gels showing *Mbo* I (**A**), Hind II (**B**), *BstN* I (**C**), and *Cfo* I (**D**) haplotypes in ND3/ND4 PCR fragments of *Sebastes* spp. mtDNA. A 100-bp ladder is used as a reference at both ends of all gels.

Acknowledgments

We gratefully acknowledge the many crew members and scientists aboard the research vessels *John N. Cobb* and *Miller Freeman* who participated in collecting specimens for our study. L. Densmore and T. Dowling provided constructive comments on early drafts of this manuscript. Three anonymous reviewers provided constructive comments. A.W. Kendall Jr. and M. S. Love contributed advice and insight that helped us develop this paper. J. A. Gharrett and D. Churikov reviewed drafts of this paper. This work was supported by the National Marine Fisheries Service Auke Bay Laboratory and the U.S. Geological Services (Biological Resources Division) Western Regional Office in Seattle, WA (R.W.O. 32).

Literature cited

Anderson, S., A. T. Bankier, G. T. Barrell, M. H. L. DeBruijn, and A. R. Coulson.
1981. Sequence and organization of the human mitochondrial genome. Nature 290:457–465.

Anderson, S., M. H. L. DeBruijn, A. R. Coulson, I. C. Eperon, and F. Sanger.
1982. Complete sequence of bovine mitochondrial DNA. J. Mol. Biol. 56:683–717.

Chang, Y-S., F-L. Huang, and T-B. Lo.
1994. The complete nucleotide sequence and gene organization of carp (*Cyprinus carpio*) mitochondrial genome. J. Mol. Evol. 38:138–155.

Chen, L.-C.
1971. Systematics, variation, distribution, and biology of rockfishes of the subgenus *Sebastomus* (Pices, Scorpaenidae, *Sebastes*). Bull. Scripps Inst. Ocean. Univ. Cal., Univ. Cal. Press, Berkeley and Los Angeles, CA, 115 p.

Cramer, F.
1895. On the cranial characters of the genus *Sebastodes* (rock-fish). Contributions to biology from the Hopkins Seaside Laboratory, Leland Stanford Junior University Publications. Reprinted from Proc. Cal. Acad. Sci., series 2, vol. V, 54 p.

Cronin, M. A., W. J. Spearman, R. L. Wilmot, J. C. Patton, and J. W. Bickham.
1993. Mitochondrial DNA variation in chinook (*Oncorhynchus tshawytscha*) and chum (*O. keta*) detected by restriction enzyme analysis of polymerase chain reaction (PCR) products. Can. J. Fish. Aquat. Sci. 30:708–715.

Dowling, T. E., W. R. Hoeh, G. R. Smith, and W. M. Brown.
1992. Evolutionary relationship of shiners in the

genus *Luxilus* (Cyprinidae) as determined by analysis of mitochondrial DNA. Copeia 1992:306–322.

Eschmeyer, W. N. (ed.).
1998. Catalog of fishes. California Academy of Sciences, San Francisco, CA, 2905 p.

Gyllensten, U., D. Wharton, A. Josefsson, and A. C. Wilson.
1991. Paternal inheritance of mitochondrial DNA in mice. Nature 352:255–257.

Hart, J. L.
1973. Pacific fishes of Canada. Bulletin 189, Fisheries Research Board of Canada, Ottawa, 740 p.

Ishida, M.
1984. Taxonomic study of the sebastine fishes in Japan and its adjacent waters. Master's thesis, Hokkaido Univ., Hakodate, Hokkaido, Japan, 267 p.

Johns, G. C., and J. C. Avise.
1998. Tests for ancient species flocks based on molecular phylogenetic appraisals of *Sebastes* rockfishes and other marine fishes. Evolution 52(4):1135–1146.

Johnson, A. G., F. M. Utter, and H. O. Hodgins.
1972. Electrophoretic investigation of the family Scorpaenidae. Fish. Bull. 70:403–413.

Jordan, D. S., B. W. Evermann, and H. W. Clark.
1930. Check-list of the fishes and fish-like vertebrates of North and Middle America north of the northern boundary of Venezuela and Columbia. U. S. Com. Fish., Rep. 1928, part 2, 670 p.

Kendall, A. W., Jr.
1991. Systematics and identification of larvae and juveniles of the genus *Sebastes*. Environ. Biol. Fish. 30:173–190.

Kramer, D. E., and V. M. O'Connell.
1988. Guide to Northeast Pacific rockfishes genera *Sebastes* and *Sebastolobus*. Alaska Sea Grant Advisory Bulletin 25, Alaska Sea Grant College Program, Univ. Alaska, Fairbanks, 78 p.

Matsubara, K.
1943. Studies on the scorpaenoid fishes of Japan: anatomy, phylogeny, and taxonomy. Trans. Sigenkagaku Kenkyusyo 1, 490 p.

McElroy, D. M., P. Moran, E. Bermingham, and I. Kornfield.
1990. REAP: an integrated environment for the manipulation and phylogenetic analysis of restriction data. J. Hered. 83:157–158.

Meyer, A.
1993. Evolution of mitochondrial DNA in fishes. *In* Biochemistry and molecular biology in fishes, vol. 2: Molecular biology frontier (P. W. Hochachka and T. P. Mommsen, eds.), p. 1–38. Elsevier, Amsterdam.

Moser, H. G.
1996. Scorpaenidae: scorpionfishes and rockfishes. *In* California Cooperative Oceanic Investigations, Atlas 33: the early stages of the fishes in the California Current region (H. G. Moser, ed.), p. 733–795. Allen Press, Lawrence, KS.

Nei, M.
1987. Molecular Evolutionary Genetics. Columbia Univ. Press, New York, NY, 512 p.

Nei, M., and J. C. Miller.
1990. A simple method for estimating average number of nucleotide substitutions within and between populations from restriction data. Genetics 97:145–163.

Nei, M. and F. Tajima.
1983. Maximum likelihood estimation of the number of nucleotide substitutions from restriction sites data. Genetics 105: 207–217.

Phillips, J. B.
1957. A review of the rockfishes of California (Family Scorpaenidae). State of California, Department of Fish and Game, Marine Fisheries Branch, Fish Bull. 104, 158 p.

Richardson, J.
1845. Ichthyology, part 2. *In* The zoology of the voyage of H.M.S. Sulphur, under the command of Captain Sir Edward Belcher, during the years 1836–1842, no. 9 (R. B. Hinds, ed.), p. 71–98, pls. 55–64. Smith, Elder & Co., London. [Cited in Eschmeyer (1998).]

Rocha-Olivares, A.
1998a. Molecular evolution, systematics, zoogeography, and levels of intraspecific genetic differentiation in the species of the antitropical subgenus *Sebastomus*, *Sebastes* (Scorpaeniformes, Teleostei) using mitochondrial DNA sequence data. Ph.D. diss., Univ. Cal., San Diego, CA, 240 p.
1998b. Multiplex haplotype-specific PCR: a new approach for species identification of the early life stages of rockfishes of the species-rich genus *Sebastes* Cuvier. J. Exper. Mar. Biol. Ecol. 231:279–290.

Rocha-Olivares, A., H. G. Moser, and J. Stannard.
2000. Molecular identification and description of pelagic young of rockfishes *Sebastes constellatus* and *Sebastes ensifer*. Fish. Bull. 98:353–363.

Rocha-Olivares, A., R. H. Rosenblatt, and R. D. Vetter.
1999a. Cryptic species of rockfishes (*Sebastes*:Scorpaenidae) in the southern hemisphere inferred from mitochondrial lineages. J. Hered. 90: 404–411.
1999b. Evolution of a mitochondrial cytochrome *b* gene sequence in the species-rich genus *Sebastes* (Teleostei, Scoraenidae) and its utility in testing monophyly of the subgenus *Sebastomus*. Mol. Phylogenet. Evol. 11: 426–440.
1999c. Molecular evolution, systematics, and zoogeography of the rockfish subgenus *Sebastomus* (*Sebastes*, Scorpaenidae) based on mitochondrial cytochrome *b* and control region sequences. Mol. Phylogenet. Evol. 11: 441–458.

Rocha-Olivares, A., and R. D. Vetter.
1999. Effects of oceanic circulation on the gene flow, genetic structure, and phylogeography of the rosethorn rockfish (*Sebastes helvomaculatus*). Can. J. Fish. Aquat. Sci. 56:803–813.

Roe, B. A., D-P. Ma, R. K. Wilson, and J. F-H. Wong.
1985. The complete nucleotide sequence of the *Xenopus laevis* mitochondrial genome. J. Biol. Chem. 260:9759–9774.

Saitoh, N., and M. Nei.
1987. The neighbor-joining method: a new method for reconstructing phylogenetic trees. Mol. Biol. Evol. 4:406–425.

Seeb, L. W.
1986. Biochemical systematics and evolution of the scorpaenid genus *Sebastes*. Ph.D. diss., Univ. Washington, Seattle, WA, 176 p.
1998. Gene flow and introgression within and among three species of rockfishes, *Sebastes auriculatus*, *S. caurinus*, and *S. maliger*. J. Hered. 89:393–404.

Seeb, L. W., and A. W. Kendall Jr.
1991. Allozyme polymorphisms permit the identification of larval and juvenile rockfishes of the genus *Sebastes*. Environ. Biol. Fish. 30:191–201.

Seeb, L. W., F. M. Utter, and D. R. Gunderson.
1988. Genetic variation and population structure of Pacific ocean perch (*Sebastes alutus*). Can. J. Fish. Aquat. Sci. 45:78–88.

Seutin, G., B. N. White, and P. T. Boag.
1991. Preservation of avian blood and tissue samples for DNA analysis. Can. J. Zool. 69:82–90.

Swofford, D. L.
1998. PAUP . Phylogenetic analysis using parsimony (and other methods), version 4. Sinauer Associates, Sunderland, MA.

Swofford, D. L., G. J. Olsen, P. J. Waddell, and D. M. Hillis.
1996. Phylogenetic inference *In* Molecular systematics, 2nd ed. (D. M. Hillis, C. Moritz, and B. K. Mable, eds.), p. 407–514. Sinauer Assoc., Sunderland, MA.

Thomas, W. K., and A. T. Beckenbach.
1989. Variation in salmonid mitochondrial DNA: evolutionary constraints and mechanisms of substitution. J. Mol. Evol. 29:233–245.

Tsuyuki, H., E. Roberts, R. H. Lowes, W. Hadaway, and S. J. Westrheim.
1968. Contribution of protein electrophoresis to rockfish (Scorpaenidae) systematics. J. Fish. Res. Board Can. 25:2477–2501.

Wallace, D. W.
1987. Large- and small-scale phenol extractions. *In* Methods in enzymology, vol. 12: Guide to molecular cloning techniques (S. L. Berger and A. R. Kimmel, eds.), p. 33–41. Academic Press, San Diego, CA.

Wishard, L. N., F. M. Utter, and D. R. Gunderson.
1980. Stock separation of five rockfish species using naturally occurring biochemical genetic markers. Mar. Fish. Rev. 42:64–73.

Zardoya, R., A. Garrido-Pertierra, and J. M. Bautista.
1995. The complete nucleotide sequence of the mitochondrial DNA genome of the rainbow trout, *Oncorhynchus mykiss*. Mol. Evol. 41:942–951.

Appendix 1

Restriction site locations for *Sebastes* spp., *Helicolenus hilgendorfi*, and *Sebastolobus alascanus* in the 12S/16S and ND3/ND4 mtDNA regions. The *Sebastes* species are listed in Table 2; five individuals of each species are represented. Sites were mapped by double digests. Haplotypes for each restriction endonuclease are presented for each mtDNA region. X's denote presence and O's denote absence of a site. (X)'s are sites that occur in the primers and were present in all PCR products. They were not used in the analysis.

12S/16S

Rsa I hapotypes						*Mbo* I haplotypes							*Msp* I haplotypes			*Dde* I haplotypes							*Cfo* I haplotypes		
sites	A	B	C	D	E	sites	A	B	C	D	E	F	sites	A	B	sites	A	B	C	D	E	F	sites	A	B
293	O	O	O	O	X	201	O	X	X	O	O	O	65	X	X	44	X	X	X	X	X	X	537	X	X
507	O	O	X	X	O	849	X	X	X	X	O	X	766	X	X	55	X	X	X	X	X	X	602[1]	X	O
588	O	O	O	O	X	1015	X	X	X	X	X	O	1259	O	X	976	X	X	X	X	X	O	665[1]	X	X
761	X	X	X	X	X	1403	X	X	X	X	X	X	1390	X	X	1043	X	X	O	X	X	O	1898	X	X
950	O	O	O	O	X	1507	X	O	X	X	X	X	1535	X	X	1056	X	X	O	X	O	O	2268	X	X
1000	X	X	X	X	O	1746	O	O	O	X	O	O	2226	X	X	1304	X	X	X	X	X	O			
1071	X	X	X	X	O	1984	X	X	X	X	X	X	2403	X	X	1735	O	X	X	X	X	O			
1263	O	O	O	O	X	2059	X	X	X	X	X	X				2181	X	O	X	X	X	O			
1308	O	X	O	X	X	2228	X	X	X	X	X	X				2393	X	X	X	X	X	X			
1358	X	X	X	X	X	2318	X	X	X	X	X	X													
2164	O	O	O	O	X	2388	X	X	X	X	X	X													

Hinf I haplotypes					*Hind* II haplotypes			*Sty* I haplotypes			*Bst*N I haplotypes					*Bst*U I haplotypes		
sites	A	B	C	D	sites	A	B	sites	A	B	sites	A	B	C	D	sites	A	B
982	O	O	X	O	1717	X	O	295	X	O	326	X	X	X	X	87	X	X
1291	X	X	X	O				2053	O	X	988	O	O	O	X	600[1]	X	O
2094	O	X	X	O				2254	X	X	1687	O	O	X	O	664[1]	X	X
											1741	O	X	O	O	729	X	X
											2416	(X)	(X)	(X)	(X)	1872	X	X
																2128	X	X

ND3/ND4

Cfo I haplotypes							*Bst*U I haplotypes								*Hinf* I haplotypes								
sites	A	B	C	D	E	F	sites	A	B	C	D	E	F	G	sites	A	B	C	D	E	F	G	H
709	X	O	X	X	X	X	4	(X)	(X)	(X)	(X)	(X)	(X)	(X)	130	O	X	O	O	O	X	O	O
1221	O	O	O	O	X	X	344	O	O	O	O	O	X	O	389	O	X	X	O	O	O	O	X
1436	O	O	O	O	X	O	1499	O	O	O	O	X	O	O	494	X	X	X	X	X	X	X	X
1741	O	X	X	X	O	O	1854	O	O	O	X	O	O	O	853	O	O	O	O	O	O	O	X
1813	O	O	X	O	O	O	2025	O	X	X	O	O	O	O	1448	O	O	O	O	O	O	O	X
							2306	O	X	O	O	X	X	X	1537	O	O	O	O	O	O	X	O
															1755	O	O	O	O	X	X	O	O
															1888	O	O	O	X	O	O	O	X
															2232	X	X	X	X	X	X	X	X

Sty I haplotypes							*Msp* I haplotypes								*Rsa* I haplotypes								
sites	A	B	C	D	E	F	sites	A	B	C	D	E	F	G	sites	A	B	C	D	E	F	G	H
49	X	X	X	X	X	X	30	X	X	X	X	X	X	X	346	O	O	O	X	X	O	X	X
194	O	O	O	X	X	X	933	O	O	O	O	O	X	O	742	O	O	O	O	O	O	O	X
365	X	X	X	X	O	O	1199	O	O	O	O	O	X	O	1077	O	O	O	O	O	X	O	O
391	O	O	O	O	X	X	1261	O	O	O	O	O	O	X	1231	O	O	O	O	O	O	X	O
534	X	O	X	X	X	X	1738	X	X	X	X	X	X	X	1492	O	O	O	O	O	O	O	X
1258	O	O	O	O	O	X	1826	X	X	O	X	X	O	O	1863	O	O	X	O	X	O	O	X
1570	O	X	X	X	X	X	1844	O	O	O	X	X	O	O	1985	O	X	X	X	X	X	X	X
2311	X	X	X	X	X	X	2073	O	O	O	O	O	X	O									
							2110	O	X	X	O	X	O	O									

continued

Appendix 1 (continued)

	Dde I haplotypes																
sites	A	B	C	D	E	F	G	H	I	J	K	L	M	N	O	P	Q
65	O	O	O	O	O	O	O	O	O	O	O	O	O	O	O	O	X
195	X	O	O	X	X	X	X	X	X	X	X	X	X	X	O	O	O
266	O	O	O	O	O	O	X	O	X	O	O	X	O	O	X	X	X
298	X	X	O	X	X	X	X	O	X	X	X	X	X	X	O	O	X
336	X	X	X	X	X	X	X	X	X	X	X	X	X	X	X	X	X
374	X	X	X	O	X	O	O	O	O	X	O	O	X	O	O	O	O
590	O	X	X	X	X	X	X	X	X	X	X	X	X	X	O	O	X
624	O	O	X	O	O	O	O	O	O	O	O	O	O	O	O	O	O
663	O	O	O	O	O	O	O	O	O	O	O	O	O	O	O	O	X
695	O	O	O	O	O	O	O	O	X	O	O	X	O	O	O	O	O
754	O	O	O	O	O	O	O	O	X	O	O	X	X	O	O	O	X
1257	O	O	O	O	O	O	O	O	O	O	O	O	O	O	O	O	X
1409	O	O	O	O	O	O	O	O	O	O	X	O	O	O	O	O	O
1560	O	O	O	O	O	O	O	O	X	O	O	X	O	O	O	O	O
1577	O	O	O	O	O	O	O	O	O	O	O	O	O	O	X	X	X
1601	X	O	X	X	X	X	X	X	X	X	X	X	X	X	O	O	O
1696	O	O	O	O	O	O	O	O	O	O	O	O	O	O	O	O	X
1722	O	O	O	O	O	O	O	O	O	X	O	O	O	X	X	X	X
1779	O	O	X	O	O	O	O	O	X	O	O	X	X	O	O	O	O
1795	O	O	O	O	O	X	X	X	X	X	X	X	X	O	O	O	X
1912	X	X	X	X	X	X	X	X	O	X	X	X	X	X	O	O	X
2089	O	O	O	O	O	O	O	O	O	O	O	O	O	O	X	O	O
2188	O	O	O	O	O	O	O	O	O	O	O	O	O	O	X	X	O
2374	(X)	(X)	(X)	(X)	(X)	(X)	(X)	(X)	(X)	(X)	(X)	(X)	(X)	(X)	(X)	(X)	(X)

	Mbo I haplotypes													
sites	A	B	C	D	E	F	G	H	I	J	K	L	M	N
198	X	X	X	X	X	X	X	X	X	X	X	X	O	O
272	O	O	O	O	O	O	O	O	O	O	O	O	X	O
302	O	O	O	O	O	O	O	O	O	O	O	O	O	X
648	O	O	O	X	O	O	O	O	O	O	O	O	O	O
746/														
210	O	O	O	O	O	O	O	O	O	O	O	X	O	O
758	X	X	X	X	X	X	X	O	X	X	X	X	X	O
797	O	O	O	O	O	O	O	O	O	O	O	O	X	O
861	O	O	O	O	O	O	X	X	O	O	O	O	O	O
886	O	X	O	O	O	O	O	O	O	O	O	O	O	O
900	O	O	O	O	O	O	O	O	O	X	O	O	O	O
940	X	X	X	X	X	X	X	X	X	X	X	X	X	X
971	O	X	O	O	O	X	O	O	O	O	O	O	O	O
1029	O	O	O	O	O	O	O	O	X	O	O	O	X	O
1534	O	O	O	O	X	X	X	X	X	O	X	X	X	X
1647	O	O	X	X	O	X	O	O	X	X	X	X	O	X
1979	X	X	X	X	X	X	X	X	X	X	X	X	O	X
2016	O	O	O	O	O	O	O	O	O	O	O	O	O	X

	*Bst*N I haplotypes									
sites	A	B	C	D	E	F	G	H	I	J
112	O	X	X	X	X	X	X	X	X	X
291	O	O	O	O	X	O	O	O	O	O
551	O	O	O	O	O	O	O	X	X	O
829	X	X	O	X	X	X	X	X	X	X
1035	O	O	O	O	O	O	O	O	O	X
1214	X	X	X	O	O	X	X	O	O	O
1261	O	O	O	O	O	O	O	O	X	O
1694	O	O	X	X	X	X	X	O	O	O
1982	O	O	O	X	X	O	X	O	O	O
2325	X	X	X	X	X	X	X	X	X	X

	*Hin*d II haplotypes	
sites	A	B
1007	O	X
1103	O	O

[1] Two *Cfo* I and *Bst*U I sites are the same.

A comparison of the precision and accuracy of estimates of reef-fish lengths determined visually by divers with estimates produced by a stereo-video system

Euan Harvey

Department of Marine Science
University of Otago
304 Castle Street
Dunedin, New Zealand
Present address: Department of Botany
University of Western Australia
Western Australia 6907, Australia
E-mail address: euanh@cyllene.uwa.edu.au

David Fletcher

Department of Mathematics and Statistics
University of Otago
539 Castle Street
Dunedin, New Zealand

Mark Shortis

Department of Geomatics
University of Melbourne
Parkville, Melbourne
Victoria 3052, Australia

Abstract–Visual estimates of reef-fish length are a nondestructive and useful way of determining the biomass, mean length, or length frequency of reef fish. Consequently, visual estimates of reef-fish length are often an important component of reef-fish monitoring programs, many of which increasingly use volunteers. We compared estimates of the length of plastic fish silhouettes determined visually by experienced scientific and novice SCUBA divers. Novice divers showed a similar level of accuracy (mean error: 2.3 cm) to that of experienced scientific divers (mean error: 2.1 cm). Significant improvements in accuracy and precision were provided by a stereo-video system (mean error: 0.6 cm). After minimal training in the use of hardware and software, volunteers can obtain a high degree of measurement accuracy and precision with a stereo-video system, allowing them to assist with monitoring reef-fish lengths.

Manuscript accepted 14 July 2000.
Fish. Bull. 99:63–71 (2001).

The marine environment is affected by many anthropogenic activities (e.g. the exploitation of marine resources for food, medicine, and curios) with the result that many environments are compromised by siltation and pollution. Reef fish, an important commercial, recreational, and cultural resource, are likewise being exploited at an increasing rate. Consequently, it is important that environmental managers and scientists have objective evidence of the magnitude and effect of these impacts. Data on the community structure of reef-fish assemblages, including precise and repeatable estimates of the length frequency and abundance of individual species, provide this information. Information on the length frequency of a fish population when linked with even a rudimentary knowledge of the biology of the species may allow estimates of recruitment to the adult population, fishing intensity, and rates of recovery from fishing (McCormick and Choat, 1987) or other impacts.

Accurate and precise length and abundance data are difficult to obtain because fish occupy different habitats and display varying behavior over a range of spatial and temporal scales. Environmental surveys are commonly used to determine the abundance and length frequency of reef-fish assemblages with SCUBA divers who count and visually estimate the length of individual reef fish (Jones and Chase, 1975; Harmelin-Vivien and Bouchon-Navaro, 1981; Russ, 1985; Bellwood, 1988; Bellwood and Alcala, 1988; Kulibicki, 1989; Samoilys, 1989; Francour, 1991, 1994). Visual census techniques have many advantages, compared with other sampling techniques, in that they are quantitative, quick, nondestructive, and repeatable (English et al., 1994). The disadvantages of visual census techniques is that the observers undertaking the sampling need to be trained and must have experience to identify, count, and estimate the length of reef fish accurately (English et al., 1994). In addition, visual census techniques involving SCUBA divers are restricted to shallow depths owing to the constraints of decompression diving.

Two important sources of error affect the accuracy and precision of visual length estimates:

1 The estimation of the length of reef fish underwater is complicated by the air-water interface in the diver's mask which causes objects to be magnified in size by a factor of 1.3 and to appear to be closer to the observer than they actually are;
2 Researchers using SCUBA have been shown to be inefficient when performance underwater is compared with similar activities in air (Hollien and Rothman, 1975). The accuracy and precision of diver's estimates of reef-fish length is probably affected by the detrimental physiological effects related to SCUBA diving (Baddeley, 1965; Baddeley et al., 1968; Baddeley, 1971).

The level of precision and accuracy associated with visual length estimates influences comparisons of data over different temporal or spatial scales in two distinct ways. First, bias in the estimates can make the results of the analysis less reliable. Second, any lack of precision in the estimates arising from both sampling error and measurement error tends to reduce the power of the statistical analysis. The Great Barrier Reef Marine Park Authority (GBRMPA, 1979), Bell et al. (1985), and Polunin and Roberts (1993) have performed calibration studies in order to quantify measurement error and have concluded that such error is relatively small and can be ignored. However, they did not directly assess the extent to which such error reduces the precision of a statistical analysis. Harvey and Shortis (1996) demonstrated that subjectivity in visual length estimates can be overcome, and the accuracy and precision of length estimates enhanced, by using a simple and relatively inexpensive underwater stereo-video system.

The objectives of our study were 1) to compare the accuracy and precision of stereo-video measurements of reef-fish length with visual estimates made by novice and experienced scientific SCUBA divers; 2) to evaluate the effect of operator training and experience on the precision and accuracy of length measurements made with a stereo-video system; and 3) to assess the effect of water clarity on the accuracy and precision of stereo-video measurements.

Methods of optimizing the accuracy and precision of stereo-video length estimates are discussed and the accuracy and precision of experienced divers' estimates are compared to one other study.

Materials and methods

Comparison of length estimates made by novice and experienced scientific divers with estimates generated by a stereo-video system

The accuracy and precision of length estimates were tested by a simple procedure that is used routinely for calibrating diver estimates of the lengths of reef fish (GBRMPA, 1979; Bell et al., 1985; English et al., 1994). Typically, polyvinyl chloride (PVC) sticks or silhouettes of fish are placed in the water and their lengths estimated. The accuracy of the diver estimate is then assessed from the difference between the real size and the estimate. In this study, 16 plastic silhouettes of fish, ranging from 10 to 49 cm in length, were placed at distances of between 3.0 and 6.6 meters from a transect rope. Each diver moved along the transect rope estimating the length of each of the sixteen silhouettes when they were opposite them. Each diver repeated this process five times, i.e. five transects each with estimates of the lengths of the sixteen silhouettes. Five transects were completed with the stereo-video system in the same manner. The distances from the transect rope and the order of the individual silhouettes were kept constant throughout the trial. All silhouettes were weighted in a way that their length orientation remained perpendicular to the transect. Therefore, the error measures presented here do not take into consideration that in the field the divers may have to make length estimates where orientation of the live fish in relation to the diver changes.

Novice divers Novice divers were defined as experienced SCUBA divers who had made few, if any, estimates of the lengths of reef fish underwater. Eight novice divers made length estimates in a saltwater pool at the Portobello Marine Laboratory (PML) between May 1994 and January 1995. No more than two transects were completed on any one day, except one diver who completed four consecutive transects in one day. Between transects and dives, data were not available to divers in order to avoid memorization of previous estimates or of silhouette lengths. The novice divers made only 594 of a possible 640 length estimates because 46 silhouettes (7%) were not recorded. The majority of the missing estimates were from the smaller silhouettes (approximately 10 cm long) or from a silhouette placed farthest from the transect (6.6 meters).

Experienced scientific divers Experienced scientific divers were considered active marine scientists who had been, or who were currently involved in research that required them to make estimates of reef fish length. Six experienced scientific divers estimated the length of the plastic silhouettes between October 1994 and June 1996. Three of the divers made their estimates in a saltwater pool at PML, whereas the other three made their estimates in freshwater swimming pools elsewhere. A total of 480 length estimates were made, and all silhouettes were recorded. Owing to time constraints, all of the length estimates were made on consecutive transects during one dive.

Stereo-video measurements For interested readers a comprehensive description of the design and calibration of the stereo-video can be found in Harvey and Shortis (1996, 1998) and will not be described here.

Stereo-video length estimates were made in the same way as those made by the divers; the stereo-video system recorded the silhouette as it was moved along the transect line by a diver. Measurements were made in the University of Melbourne swimming pool in July 1994. 80 silhouettes were recorded (16 silhouettes×5 transects). Four sets of images were rejected because the orientation of the

silhouette to the stereo-video rig was greater than 50 degrees, resulting in a deterioration of the accuracy and precision of measurements (Harvey and Shortis, 1996). Thus, 76 pairs of images were retained for analysis, from each of which ten measurements were made.

To test whether measurements made by an inexperienced volunteer using the stereo-video software would differ from those made by an experienced operator, two volunteers were given brief instructions on how to operate the stereo-video software and were asked to make measurements of the silhouettes. Measurements made by the inexperienced operators were then compared with those made from the same images by an experienced operator.

To determine whether changes in the water clarity affect the accuracy and precision of length estimates made by the stereo-video system, a further three transects were sampled in a saltwater swimming pool at the PML during August 1994. Water clarity was measured with a tape measure to record the distance to the farthest, clearly visible silhouette. A silhouette was clearly visible at up to 25 meters in the swimming pool at the University of Melbourne and up to 5.5 meters in the saltwater pool at PML.

We expected that the accuracy of measurements obtained with the stereo-video system would improve with operator experience. To evaluate the effect of experience, the same operator remeasured the images recorded in the swimming pool in Melbourne, approximately one year after the initial analysis. In the intervening period the operator routinely used the stereo-video system for analysis of fish lengths and was by far the most experienced person using the system.

Analysis of data

Four measures of error were used to summarize the accuracy of each length estimate. If the observed fish length is O and the true length is T, these four measures are

Error: $E = O - T$;
Relative error: $RE = (O - T)/T = E/T$;
Absolute error: $AE = |O - T| = |E|$;
Relative absolute error: $RAE = |O - T|/T = |E|/T = |RE|$.

The four measures provide different types of information. The error E will be positive or negative according to whether the observed length is an overestimate or an underestimate. If the mean of E is close to zero, the reason might be that all the estimates are accurate or that some are overestimates and others are underestimates to approximately the same degree. The absolute error AE ignores the direction of the error, and thus would provide different mean values for these two scenarios. The relative errors RE and RAE are of interest because it might be expected that these would be consistent across a range of fish lengths. The measure of accuracy used by St John et al. (1990) was simply $RE + 1$.

The results for the novice and experienced scientific divers were summarized prior to further analysis by calculating, for each silhouette and each observer, the mean length estimate over all transects. The repeat transects were therefore used solely to provide a reliable estimate of the error made by each observer on each silhouette. If the transects were truly independent, use of the mean would tend to provide a conservative estimate of the error a diver would make on one transect. Because the transects were swum in quick succession, they were not independent and therefore the degree to which their error was underestimated should be small. Each mean length estimate was then used to derive the four summaries of error, for each silhouette and each observer. For each measure of error, a two-factor analysis of variance was performed, the factors being type of observer and silhouette length. The individual observers provided the replication needed for this analysis.

To summarize the estimates made by using the stereo-video, the mean length estimate over all ten measurements was calculated (for each silhouette, transect, and operator). The mean of these over all five transects was then calculated for each silhouette and operator and converted to the four summary measures of error. For each measure of error, a one-factor analysis of variance was performed, with silhouette length being the factor. The individual operators (one experienced and two inexperienced) provided the replication needed for this analysis.

The two types of diver data and all video data were analyzed separately, rather than in a single analysis of variance because for each silhouette the variation between video operators was found to be much lower than that between experienced scientific divers and novice divers, making the usual assumption of equal variance invalid (Underwood, 1981). Comparison of the video technique with that of the experienced scientific divers and novice divers was therefore made by comparing 95% confidence intervals. The purpose of the analysis of variance for the video data was to provide an estimate of the standard error associated with the mean (for each measure of error) over all silhouettes.

To compare the data of experienced and inexperienced stereo-video operators, the mean estimated length over the ten repeat measurements obtained per image was calculated. These means were then converted to the four measures of error. Each measure of error was then analyzed by using a two-factor analysis of variance, with operator and silhouette as the factors. In this analysis, therefore, unlike those for comparing estimates from divers with those produced with the stereo-video system, the transects provided replication against which to compare operators. This analysis is reasonable, because in comparing the operators, the transects can be regarded as independent.

To compare the use of a stereo-video system under the two water-clarity conditions, a three-factor analysis of variance was performed on the individual errors. In this analysis, the factors were water clarity, silhouette, and transect (nested within each combination of water clarity and silhouette). Prior to this analysis, the estimates for one of the silhouettes in 5.5-m water clarity were removed because this silhouette was 6.6 meters from the transect and could not be seen clearly.

For the 1994 and 1995 stereo-video data used to assess operator experience, a three-factor analysis of variance

was performed on the individual errors, the factors being year, silhouette, and transect (nested within each combination of year and silhouette).

With the stereo-video system, the mean of ten measurements should result in greater accuracy and precision than use of a single measurement. In order to assess the extent of this improvement, the above analysis was performed a further five times by using the first 1, 2, 4, 6, and 8 measurements.

One of the most commonly cited papers on the training of divers to estimate fish lengths with accuracy and precision is that of Bell et al. (1985). The data for this paper originated from a report published by the Great Barrier Reef Marine Park Authority (GBRMPA, 1979). Tables 7, 10, 12, and 15 in that report contain underwater length estimates of pieces of orange PVC conduit (cut into 50 lengths ranging from 6 to 94 cm) determined by experienced scientific divers. Three experienced divers undertook four transects estimating the lengths of the conduit seen. The estimates of a fourth diver are also included in Tables 10, 12, and 15 of the report. We have chosen to disregard this diver's data because he was considered inexperienced at the time. We have summarized these results by first calculating the mean length estimate over all four transects for each silhouette and diver. Each of these means was then expressed by using the four summary measures of error described: error, absolute error, relative error, and relative absolute error. For each measure of error, a one-factor analysis of variance was performed, with silhouette being the factor. The individual divers provided the replication needed for this analysis.

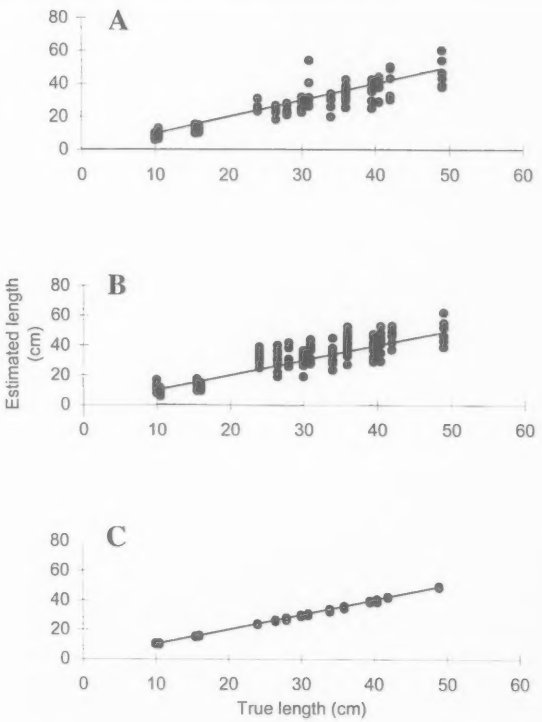

Figure 1

Comparison of the length estimates made by (**A**) experienced scientific divers, (**B**) novice divers and (**C**) a stereo-video system. Each point shows the mean estimate made over five repeat transects by one diver or operator. The line in each plot indicates the true length for each silhouette.

Results

Comparison of length estimates made by novice and experienced scientific divers with estimates generated by a stereo-video system

Figure 1 shows the range of length estimate means over five transects for the novice and experienced scientific divers and for the stereo-video system. The variability of the estimates was greatest for the novice divers and slightly less for the experienced scientific divers. By comparison, the length estimates made by the stereo-video system showed little variability around the true lengths.

The coefficient of variation (CV=standard deviation/mean) was significantly lower for the stereo-video than it was for either the experienced scientific or the novice divers (Fig. 2).

For all four measures of error (E, RE, AE, and RAE), there was no significant interaction between type of diver and silhouette size, suggesting that any differences between experienced scientific and novice divers were consistent across the silhouettes. For this reason, the results are presented as means across all silhouettes (Fig. 3). For both E and RE, the difference between the experienced scientific and novice divers was highly significant ($P<0.0001$); for AE and RAE, the difference was close to significant at the 5% level ($P=0.08$ and $P=0.05$ respectively; $F_{1,91}=5.96$ [E], =1.75 [AE], =6.28 [RE], =1.94 [RAE]).

For both the diver and stereo-video data, there were significant differences (at the 5% level) between silhouettes, for all measures of error except RAE on the diver data. Inspection of the silhouette means showed no clear pattern for these differences. Any pattern would be difficult to interpret because the silhouettes were placed at different distances from the transect line in order to provide a range of sizes at a range of distances from the transect line and thus make the comparison of means in Figure 3 widely applicable.

The GBRMPA divers had a mean measurement error of –2.4 cm (SE=0.2 cm) which is similar to the –2.1 cm (SE=0.6 cm) mean error recorded by the experienced scientific divers used in our study (Fig. 3). Because 26 of the silhouettes used in the GBRMPA study were larger than any of those used in our study, it might be argued that the relative errors are more directly comparable. The mean RE for the GBRMPA divers was –4.6% (SE=0.5%), compared with a mean of –8.6% (SE=1.9%) for the experienced scientific divers used in our study. These results suggest that the experienced divers in the two studies had comparable skills.

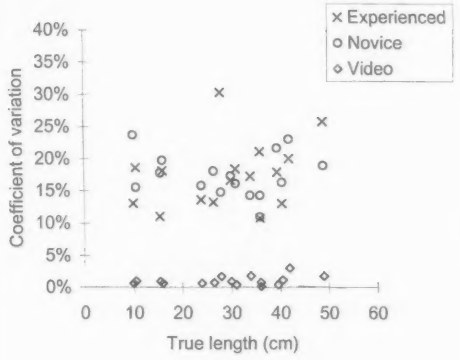

Figure 2

Coefficients of variation between divers or operators of length estimates for experienced scientific divers, novice divers, and a stereo-video system.

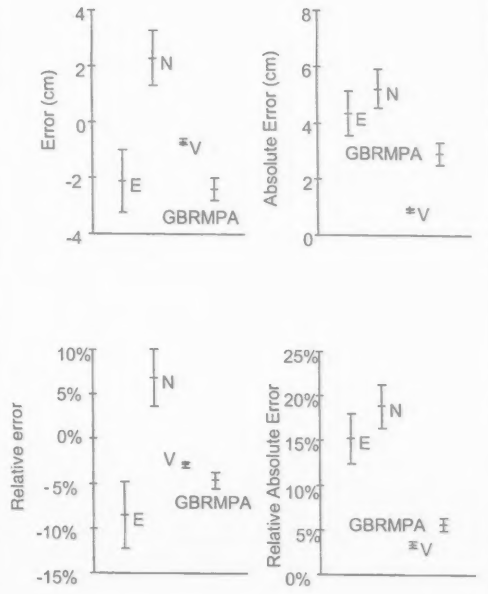

Figure 3

Means and 95% confidence intervals for each measure of error, for each method of estimating fish length. E = experienced divers; N = novice divers; V = stereo-video system, GBPRMA= Great Barrier Reef Marine Park Authority data.

For all four measures of error, there was no significant interaction between software operators and silhouette, but there was a significant operator effect (Fig. 4). This finding suggests that the differences between operators were consistent across silhouettes. Although the differences between the operators were statistically significant, they were small compared with the differences between divers and the stereo-video system (cf. Figs. 3 and 4). ($F_{2,180}$=6.0, P=0.003 [E]; $F_{2,180}$ =14.6, P<0.001 [AE]; $F_{2,180}$= 3.6, P=0.029 [RE]; $F_{2,180}$=10.2, P<0.001 [RAE]).

There is little difference in the accuracy of measurements made under poor water clarity (mean E=–0.99 cm) compared with those made under good water clarity (mean E=–0.6 cm). The RAE is more consistent across silhouettes for good water clarity than it is for poor clarity. For the larger silhouettes, the RAE is lower under poor water clarity than under good water clarity (Fig. 5). This is probably a result of lower contrast, permitting more accurate pointing to the tail and snout of each silhouette (discussed further in the next section).

For all four measures of error, there was no significant interaction between years and silhouette, but highly significant differences (P<0.001 in all cases, $F_{1,121}$=15.0 [E]; $F_{2,180}$=27.1 [AE]; $F_{2,180}$ =14.6 [RE]; $F_{2,180}$=25.8 [RAE]) between years (Fig. 6). These results suggest that with increasing operator experience the measurement error can improve. This is probably a consequence of the operator learning to distinguish and select the edges of objects of interest accurately.

One of the advantages of stereo-video measurements over diver visual estimates is that the image is stored and it is possible to make numerous repeat measurements of the same object in the laboratory. Taking the mean of this set of measurements would result in greater accuracy and precision than using a single measurement. Improvement of the accuracy of estimates can be seen by comparing the mean error, for each of the three operators, as the number of repeat measurements is increased from 1 to 10 (Fig. 7). There is improvement in the error for both inexperienced operators and the experienced operator, even after ten repeat measurements (Fig. 7).

Discussion

Our results highlight the differences in the accuracy and precision of length estimates of silhouettes of reef fish made by novice and experienced scientific divers in comparison with those produced by a stereo-video system. Our length estimates were made under ideal conditions where the plastic models were fixed in position. Under real field conditions fish move, occur at different distances from the divers and have behavioral and morphological differences that can influence length estimates. Consequently, the measures of error presented in our study can most likely be considered a best case scenario. As with Darwall and Dulvy (1996), the results obtained by novice divers were similar to, but slightly less accurate than, those obtained by experienced scientific divers (mean errors of 2.3 cm and –2.1 cm respectively). Our results also demonstrate that significant improvements in accuracy can be obtained by using a stereo-video system (mean error –0.6 cm). Similar improvements in precision were also recorded: mean CVs

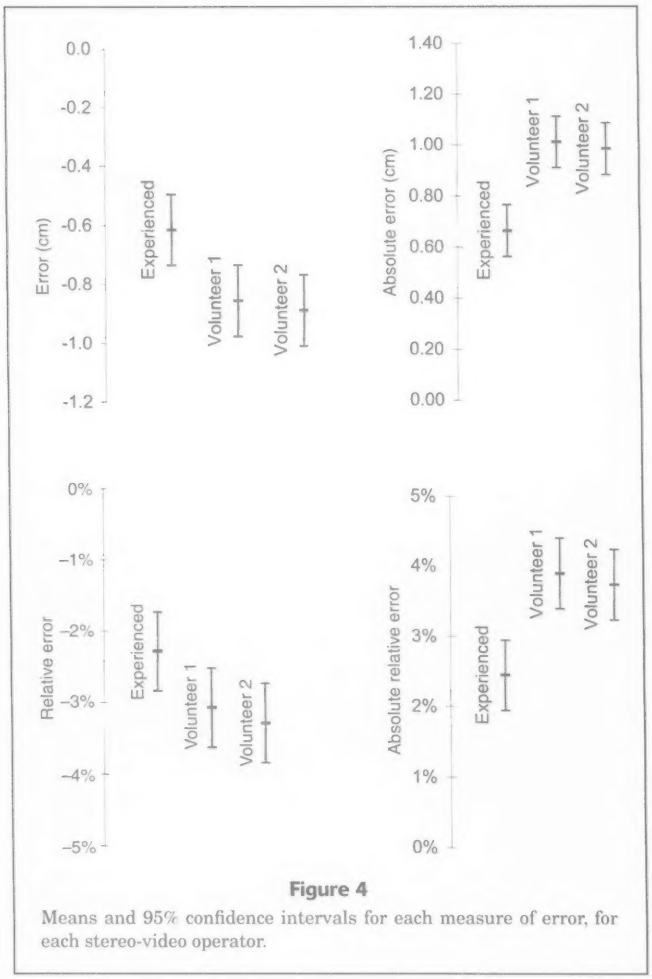

Figure 4

Means and 95% confidence intervals for each measure of error, for each stereo-video operator.

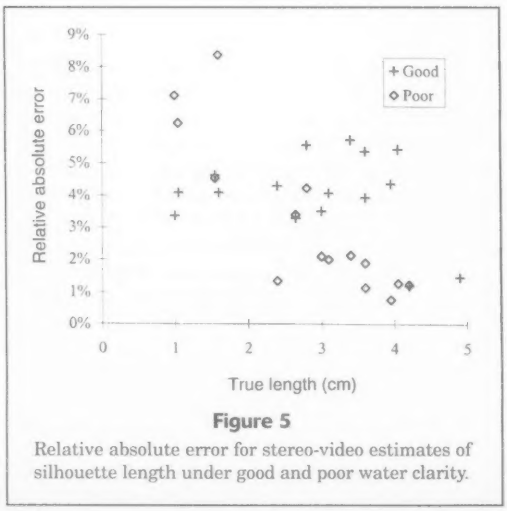

Figure 5

Relative absolute error for stereo-video estimates of silhouette length under good and poor water clarity.

were 18.2%, 18.6%, and 1.6% for novice scientific divers, experienced scientific divers, and the stereo-video system, respectively. The results of the experienced divers' estimates are similar to those obtained in other published research studies (Bell et al., 1985).

In general, water clarity does not appear to affect the accuracy or precision of the measurements made from the stereo-video system. The accuracy of the of the stereo-video system is limited to the ability of the operator to accurately point out image locations of interest that are then recorded to subpixel resolution. Discrete sampling of the CCD (charged coupled device) sensors, combined with noise artifacts from the video tape recording and frame grabbing, tends to smear the edges of the images and blur details (Shortis et al., 1993). This result is particularly noticeable under recording conditions with good water clarity and high contrast where there is a problem with the detection of the edge of the silhouette. The edges or outline of the points of interest (in this instance, the snout and fork of the tail of each silhouette) become significantly blurred within the computer image owing to sampling and noise effects on each pixel. There is a tendency for the observer to select a location inside the true edge of the point of interest because the location most nearly matches the local appearance of the body of the object of interest. This results in the underestimation of silhouette length, as demonstrated in Figure 1. Under poor water clarity, the edges of the silhouettes have less contrast with the dark background. This lack of contrast permits more accurate pointing to the edges of the object of interest because the sampling and noise effects generate a smaller disparity between the real and apparent edges (Fig. 8). Less accurate measurements will be made when the contrast becomes so low that the operator cannot discriminate between the object of interest and the background. Hence, where there is sufficient contrast to discriminate the object from the background, lower contrast will realize more accurate values that ameliorate the underestimation of length.

Advantages of stereo-video census techniques

The use of a stereo-video system for the measurement of reef-fish length has many advantages. It significantly decreases measurement error and is relatively insensitive to operator experience. The data suggest that the stereo-video system provides far greater accuracy and precision than even experienced scientific divers, and potentially allows inexperienced volunteers to participate in monitoring programs without compromising the accuracy or precision of the data collected. This degree of accuracy and precision may be important in research where the objective is to detect small (5–30%) changes in the mean length of a population or assemblage of reef fish, with a high level

of statistical power (Harvey et al., 2000). With minimal training, volunteers can assist with the analysis of images. In addition, a remote stereo-video system can be used to record length-frequency data without harm to the fish from far greater depths and over longer periods of time than is possible by employing SCUBA divers. These advantages will likely have applications in fisheries management and deep sea biological surveys.

Unlike a diver who often has to make an immediate decision on the identity and length of a fish, a stereo-video system observer can review the images later and repeatedly. Multiple images of the same fish are recorded, enabling the selection of paired images with the best angle of orientation to the cameras. Moreover, where images of fish are at an acute angle to the cameras, the system is still able to make accurate measurements provided that the head and tail of the fish can be seen in both images (Harvey and Shortis, 1996). In addition, once an image is on screen, multiple measurements of one fish can be made over a short period of time (example 10 measurements in 30 seconds), further reducing measurement error. Our results suggest that at least five such measurements yield the most accurate results.

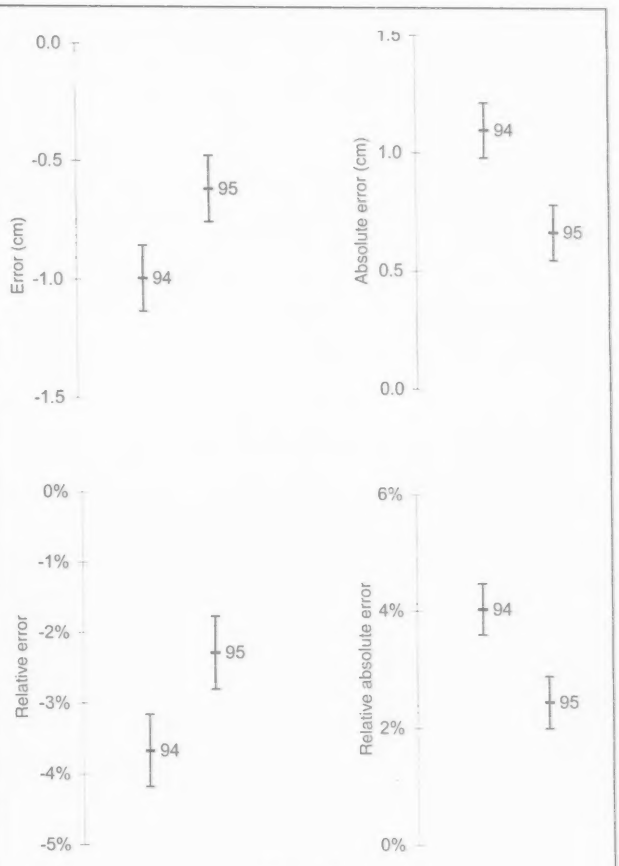

Figure 6

Means and 95% confidence intervals, for each measure of error, for 1994 and 1995.

Disadvantages of an stereo-video system

One of the disadvantages of a stereo-video system is the financial cost of the equipment: two video cameras with underwater housings; a PC computer; and a suitable frame grabber required to convert video sequences to the readable format of digital images. Time constraints also need to be considered. Although approximately 3 minutes are required to complete a calibration in the water, approximately one hour is required in the laboratory to capture the 32 images and process them into a calibration file (Harvey and Shortis, 1998). The major time constraint occurs in the selection and synchronization of the paired video images from the left and right videotapes. Once the calibration and synchronization processes are complete, recording of image locations with the measurement observation system is reasonably efficient. The observer visually locates object features of interest, positions a cursor on the feature and clicks the mouse. Some physical constraints also need to be considered with a design like ours. A bar 1.5 m wide is used to separate the video cameras and may become entangled if used in large algal beds such as those of *Macrocystis pyrifera*. In addition, the underwater video housings create water resistance and the system can be difficult to maneuver into a strong current. This system is unsuitable for censusing cryptic species, because its base separation is too large to maneuver into small crevices. The system is best deployed off a boat, i.e. a boat large enough to safely carry the stereo-rig, a calibration cube (see Harvey and Shortis, 1996),

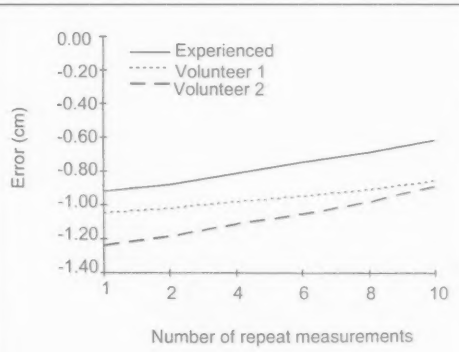

Figure 7

Improvements in the accuracy of stereo-video measurements due to increasing the number of repeat measurements.

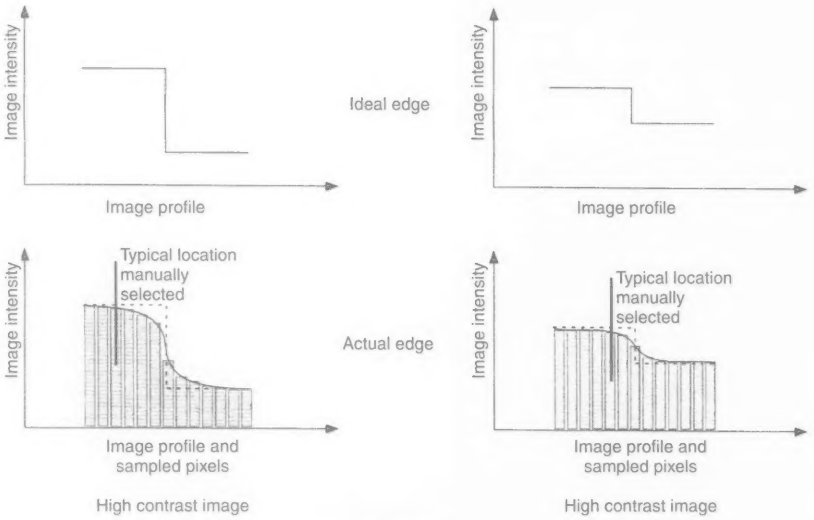

Figure 8

The effects of different contrast in images for location of the edges of objects.

divers, and diving equipment. Shore-based diving would be extremely difficult.

Before a stereo-video system is used to collect and measure field data, operators should practice taking measurements in the laboratory with a set of test objects of known size, so that they may learn to distinguish the edge of the object accurately within a range of water clarity.

Conclusions

Many of the problems outlined in our study can be overcome in the near future. The development of digital video cameras and frame grabbing boards have improved image quality and the ease of image acquisition and synchronization. These developments will also facilitate the analysis of streams of video images rather than single images, thereby greatly increasing the speed of image processing. In the future, the combination of stereo-videography with neural networks and fuzzy logic could facilitate automated pattern recognition, classification, and measurement of reef fish from video images.

Worldwide, temperate and tropical reefs are being threatened by anthropogenic disturbances. There is a need to describe the ecological structure and function of reef-fish assemblages and to monitor the effects of disturbance on these populations. This type of research has traditionally been carried out by government agencies and academic institutions. However, limitations in funding and resources are forcing these agencies to use supplementary sources of data. Consequently, the use of volunteers in monitoring programs is increasing (Halusky et al., 1994; Mumby et al., 1995; Darwall and Dulvy, 1996). Hunter and Maragos (1992) suggested that new technology in computing and underwater video systems may allow recreational and volunteer SCUBA divers to assist with surveys of coral reefs without compromising the data quality. We have demonstrated that volunteers can in fact carry out surveys of the length of reef fish using a stereo-video without compromising data quality. Although the differences in the accuracy of stereo-video measurements made by an experienced operator and volunteers is statistically significant, these are negligible in comparison to errors in visual estimates by divers. Our study specifically addresses length estimates and does not address estimation of abundance. However, if someone is estimating all the lengths of a fish observed within a sample unit they are also effectively recording relative abundance. The accuracy and precision of abundance estimates is an important issue. Factors that need addressing include the accuracy of estimates made by a diver at a distance from the fish and the behavioral differences of fish at various spatial and temporal scales. These are complex issues that are beyond the scope of the present study.

Quantitative sampling of reef-fish length frequency or biomass for monitoring programs requires reliable identification skills and the ability to make precise and accurate estimates of reef-fish length. It is suggested that volunteer SCUBA divers could be trained to use a stereo-video system both in the water and in the laboratory for making measurements. Volunteers, under the guidance of professional scientists, could assist with monitoring programs of reef-fish length frequency and abundance without having any effect on the quality of data recorded. The data collected and analyzed from stereo-video images are proven to be considerably more precise and accurate than visual estimates undertaken by experienced scientific divers.

Acknowledgments

We acknowledge financial aid from the New Zealand Department of Conservation (research grant 1822), the University of Otago Research Committee, the Southland Regional Council (New Zealand) and the Division of Sciences at the University of Otago, Dunedin, New Zealand, and support from Sony New Zealand Ltd, THC Milford Sound, Fiordland Lobster Company, and Mobil and Gore Services Ltd. The authors are also grateful to James Seager, of the Department of Geomatics at the University of Melbourne, for assistance with software development, and to June Hill, Callum Duncan, Lisa Kelleher, and Andrea Brown for assisting with field trials. Additionally we thank all the divers who willingly gave their time to assist with our research. We would also like to acknowledge the Great Barrier Reef Marine Park Authority for allowing us access to data. This manuscript was greatly improved by comments from Howard Choat, June Hill, Philip Mladenov, Keith Probert, and four anonymous reviewers.

Literature cited

Baddeley, A. D.
1965. The influence of depth on manual dexterity of free divers : a comparison between open sea and pressure chamber testing. J. Appl. Psych. 50:81–85.
1971. Diver performance. *In* Underwater science (J. D. Woods and J. N. Lythgoe (eds.), p. 33–67. Oxford Univ. Press, London.

Baddeley, A. D., J. W. De Figueredo, J. W. Hawkswell Curtis, and A. N. Williams.
1968. Nitrogen narcosis and underwater performance. Ergonomics 11(2):157–164.

Bell, J. D., G. J. S. Craik, D. A. Pollard, and B. C. Russell.
1985. Estimating length frequency distributions of large reef fish underwater. Corals Reefs 4:41–4.

Bellwood, D. R.
1988. On the use of visual survey methods for estimating reef fish standing stocks. Fishbyte (April):14–16.

Bellwood, D. R., and A. C. Alcala.
1988. The effect of minimum length specification on visual census estimates of density and biomass of coral reef fishes. Coral Reefs 7:23–27.

Darwall, W. R. T., and N. K. Dulvy.
1996. An evaluation of the suitability of non-specialist volunteer researchers for coral reef fish surveys. Mafia Island, Tanzania—a case study. Biol. Conserv. 78:223–231.

English, S., C. Wilkinson, and V. Baker (eds.).
1994. Survey manual for tropical marine resources, 368 p. [Available from the Australian Institute of Marine Science. P.M.B. No. 3, Townsville Mail Centre, Australia 4810.]

Francour, P.
1991. The effect of protection level on a coastal fish community at Scandola, Corsica. Rev. Ecol. Terre Vie 46:65–81.
1994. Pluriannual analysis of the reserve effect on ichthyofauna in the Scandola natural reserve (Corsica, Northwestern Mediterranean). Oceanol. Acta 17(3):309–317.

GBRMPA (Great Barrier Reef Marine Park Authority).
1979. Workshop on coral trout assessment techniques: workshop series 3. G.B.R.M.P.A., Queensland, Australia, 64 p.

Halusky, J. G., W. J. Seaman, and E. W. Strawbridge.
1994. Effectiveness of trained volunteer divers in scientific documentation of artificial aquatic habitats. Bull. Mar. Sci. 55(2–3):939–959.

Harmelin-Vivien, M. L., and Y. Bouchon-Navaro.
1981. Trophic relationships among chaetodontid fishes in the Gulf of Aquaba (Red Sea). *In* Proc. 4th int. coral reef symp. 2:537–544.

Harvey, E., and M. Shortis.
1996. A system for stereo-video measurement of subtidal organisms. Mar. Tech. Soc. J. 29(4)10–22.
1998. Calibration stability of an underwater stereo-video system: implications for measurement accuracy and precision. Mar. Tech. Soc. J. 32(2):3–17.

Harvey, E., D. Fletcher, and M. R. Shortis.
2000. Improving the statistical power of length estimates of reef fish: a comparison of estimates determined visually by divers with estimates produced by a stereo-video system. Fish. Bull. 99(1)72–80.

Hollien, H., and H. B. Rothman.
1975. The effectiveness of diver's work with and without the aid of communication systems. Mar. Tech. Soc. J. 9(8):3–10.

Hunter, C., and J. Maragos.
1992. Methodology for involving recreational divers in long-term monitoring of coral reefs. Pac. Sci. 46(3)381–382.

Jones, R. S., and J. A.Chase.
1975. Community structure and distribution of fishes in an enclosed high island lagoon in Guam. Micronesia 11:127–148.

Kulbicki, M.
1989. Correlation between catch data from bottom longlines and fish censuses in the SW lagoon of New Caledonia. *In* Proc. 6th int. coral reef symp. 2, p. 305–312. Townsville, Australia.

McCormick, M. I., and J. H. Choat.
1987. Estimating total abundance of a large temperate-reef fish using visual strip-transects. Mar. Biol., 96(4): 469–478.

Mumby, P. J., A. R. Harborne, P. S. Raines, and J. M. Ridley.
1995. A critical assessment of data derived from Coral Cay Conservation volunteers. Bull. Mar. Sci. 56(3):737–751.

Polunin, N. V. C., and C. M. Roberts.
1993. Greater biomass and value of target coral reef fishes in two small Caribbean marine reserves. Mar. Ecol. Prog. Ser. 100:167–176.

Russ, G. R.
1985. Effects of protective management on coral reef fishes in the central Phillipines. *In* Proc. 5th int. coral reef symp. 4, p. 219–224. Tahiti.

Samoilys, M. A.
1989. Abundance and species richness of the coral reef fish on the Kenyan Coast: the effects of protective management and fishing. *In* Proc. 6th int. coral reef symp. 2:261–266. Townsville, Australia.

Shortis, M. R., W. L. Snow, B. A.Childers, and W. K. Goad,.
1993. The influence of storage media on the accuracy and repeability of photogrammetric measurements using CCD cameras. *In* Videometrics II, p. 80–92. SPIE (International Society for Optical Engineering) 2067.

St. John, J., Russ, G. R., and W. Gladstone.
1990. Accuracy and bias of visual estimates of numbers, size structure and biomass of coral reef fish. Mar. Ecol. Prog. Ser. 64:253–262.

Underwood, A. J.
1981. Techniques of analysis of variance in experimental marine biology and ecology. Oceanogr. Mar. Biol. Ann. Rev. 19(513–605):513–605.

Abstract—We calculated the power of visual length estimates by novice and experienced scientific SCUBA divers and estimates generated by a stereo-video system to detect changes in the mean length of three common species of reef fish from New Zealand. Length estimates from a stereo-video system had much greater power for blue cod (mean length=33.1 cm., range 19.5–50.1 cm.) and snapper (mean length=31.7 cm., range 23–71 cm.). For a third species, red cod (mean length=42.5 cm., range 13–74 cm.), the statistical power of diver and stereo-video estimates was much less for an equivalent number of samples owing to the greater variation in the true mean length of red cod recorded at different sites. At 90% power, a stereo-video system detected a 15% (~5-cm) change in the mean length of blue cod with 63% less samples (10) than those required by the experienced scientific divers (27). Novice scientific divers required 28 samples.

Improving the statistical power of length estimates of reef fish: a comparison of estimates determined visually by divers with estimates produced by a stereo-video system

Euan Harvey

Department of Marine Science
University of Otago
304 Castle Street
Dunedin, New Zealand
Present address: Department of Botany
University of Western Australia
Western Australia 6907, Australia
E-mail address: euanh@cyllene.uwa.edu.au

David Fletcher

Department of Mathematics and Statistics
University of Otago
539 Castle Street
Dunedin, New Zealand

Mark Shortis

Department of Geomatics
University of Melbourne
Parkville, Melbourne
Victoria 3052, Australia

Visual censuses of reef fish have been used to monitor fish communities as indicators of environmental degradation (Hourigan et al., 1988; Fausch et al., 1990) and as a fisheries management tool for assessing the condition of reef fish stocks (Ault et al., 1998). Ault et al. (1998) used data on the average length of a fish stock as an index of fishing effects. Information on the length frequency or mean length of a fish population when linked with even a rudimentary knowledge of the biology of the species may allow estimates of recruitment to the adult population, fishing intensity, and rates of recovery from fishing (McCormick and Choat, 1987).

Environmental surveys commonly use SCUBA divers to count and visually estimate the length of individual reef fish (Jones and Chase, 1975; Harmelin-Vivien and Bouchon-Navaro, 1981; Bellwood and Alcala, 1988; Samoilys, 1989; English et al., 1994). These visual censuses have many advantages in comparison with other sampling techniques: they are quantitative, quick, nondestructive and repeatable (English et al., 1994). Visual census techniques have been widely adopted and are used to monitor changes in the relative abundance or mean length of reef fish within marine protected areas (Bell, 1983; McCormick and Choat, 1987; Alcala, 1988; Cole et al., 1990; Francour, 1991, 1994; Russ and Acala, 1996) and as a tool for assessing the standing stock or biomass of individual species of reef fish (Craik, 1981; Russ, 1985; Medley et al., 1993; Polunin and Roberts, 1993; Hart et al., 1996). Biomass is estimated from the relationship between length and the weight of an individual fish of a certain species (Kulbicki, 1989; Kulbicki et al.,1993). However, the question not yet addressed is how useful are data from visual length estimates for detecting changes in the mean length or length frequency of a population of reef fish?

The advantages of assessing the statistical power of environmental monitoring programs has been discussed by

Manuscript accepted 14 July 2000.
Fish. Bull. 99:72–80 (2001).

a number of authors (Green, 1979; Andrew and Mapstone, 1987; Gerrodette, 1987; Hayes, 1987; Peterman, 1990a, 1990b; Fairweather, 1991). Statistical power is defined as the probability of correctly rejecting a null hypothesis and is $1-\beta$, where β is the probability of a type-II error (Andrew and Mapstone, 1987; Gerrodette, 1987; Fairweather, 1991). An example of a type-II error in environmental monitoring would be to conclude that no impact has occurred when one has. Therefore, low statistical power can be disastrous for environmental monitoring because adverse environmental impacts go undetected (Fairweather, 1991). Despite this problem, few marine ecologists and biologists make use of power analysis (Fairweather, 1991). Power analysis has been used to determine the optimum size of sample units and levels of replication needed to detect an effect of a particular size with a desired level of probability (Andrew and Mapstone, 1987; Gerrodette, 1987; Fairweather, 1991). Power is a function of sample size, the probability of a type-I error (α) and the effect size (Gerrodette, 1987). Fairweather (1991) discussed the issues associated with deciding upon an appropriate level of power. Low power can be attributed not only to the sample design, but also to biases and errors inherent in the sampling method (Andrew and Mapstone, 1987) and power analysis must account for the uncertainty of measurement error (Gerrodette, 1987).

Historically, reef-fish ecologists have failed to calculate and publish the power of their sampling programs. Furthermore, it is frequently assumed by many researchers that their visual estimates of reef-fish length are both accurate and precise. In the published literature on reef fish studies containing data on visual length estimates, we found only three examples out of forty-three papers in which the authors stated the accuracy of their *in situ* visual length estimates (Sweatman, 1985; Polunin and Roberts, 1993; Green, 1996).

The aims of our study were 1) to examine the accuracy and precision of length estimates made by a number of experienced and novice scientific SCUBA divers, and so determine their power to detect changes in the mean length of populations of three common species of reef fish from around New Zealand coastal waters and 2) to demonstrate that the power to detect changes in mean length can be greatly improved for two of the three species by using an underwater stereo-video system instead of divers' visual estimates.

The three fish species that we consider are blue cod (*Parapercis colias*), red cod (*Pseudophycis bachus*), and snapper (*Pagrus auratus*). All three species support commercial trawl (red cod and snapper), long line (snapper), and trap (blue cod) fisheries. Blue cod and snapper are also the focus of popular recreational fisheries and thus are important species in New Zealand.

Methods and materials

To assess the extent to which measurement error will affect the power of visual estimates to detect changes in mean length of a population of fish, we considered the following simple scenario. Suppose we are interested in comparing the mean lengths of two fish populations and we collect length estimates by randomly selecting dive locations within each site. At each location, the dive involves the visual collection of data from a strip-transect or point-count method to measure the length of each of a number of fish of the species concerned. Later, we will assume that the same numbers of fish are encountered on each dive. This is clearly unrealistic because the numbers encountered will obviously differ: it merely helps to simplify the discussion of power analysis. The analysis we consider here involves first transforming the estimated lengths by using natural logarithms, calculating the mean log-length at each location in each site, and then comparing sites by a standard t-test, with the locations acting as replicates. The reason for considering log-length rather than length is twofold. First, it may be more prudent to perform such an analysis on the log-scale, for the usual reason of wanting to satisfy the assumptions of the t-test. Second, the power analysis can then be framed in terms of our ability to detect a percentage change in mean length. As a consequence, the standard allometric relationship between log-length and log-weight (Kulbicki, 1989) implies that the results given here for the power to detect a percentage change in mean length will also apply to an equivalent proportional change in mean weight.

The estimated length of fish j at dive location i can be written as

$$y_{ij} = x_{ij} e_{ij},$$

where x_{ij} = the true length of the fish; and
e_{ij} = the relative accuracy of the estimate (see St John et al., 1990).

This equation shows that variation in estimated length will arise from two sources: first, from the natural variation, both between and within dive locations, of the true lengths of the fish; second, from the variation, between and within dives, in the relative accuracy of the estimate. It is this second component of variation that will be influenced by using stereo-video system as opposed to experienced or novice scientific divers. The relative magnitudes of the two sources of variation will determine the benefits to be expected from improving the measurement of length. Thus, if the natural variation in true length is large in relation to the measurement error, there will be little statistical benefit in reducing the latter.

On a log-scale this equation can be written as

$$\log y_{ij} = \log x_{ij} + \log e_{ij}.$$

The variation in $\log x_{ij}$ between and within dive locations can be expressed in a one-way random effects model as

$$\log x_{ij} = a_i + b_{ij},$$

with $\mathrm{Var}(a_i) = \sigma_a^2$ and $\mathrm{Var}(b_{ij}) = \sigma_b^2$ (Sokal and Rolf, 1995). Thus σ_a^2 and σ_b^2 are the between-dive and within-dive variance components, respectively.

Now consider the variation in $\log e_{ij}$. We can write

$$e_{ij} = d_i \varepsilon_{ij},$$

where d_i = an effect applying to all estimates made during dive i; and
ε_{ij} = an effect applying solely to the estimate for fish j during that dive.

The value of d_i will be influenced by the conditions at location i, as well as by the diver used at that location. The value of ε_{ij} will be influenced by the activity of the fish and its orientation to the diver.

We can now write

$$\text{Log} e_{ij} = \log d_i + \log \varepsilon_{ij},$$

with $\text{Var}(\log d_i) = \sigma_d^2$ and, $\text{Var}(\log \varepsilon_{ij}) = \sigma_\varepsilon^2$, analogous to the equation for $\log x_{ij}$. Again, σ_d^2 and σ_e^2 are the between-dive and within-dive variance components.

The power analysis that follows involves predicting the variation we would expect in $\log y_{ij}$ for a given number of dive locations (n) and a fixed number of fish at each location (m). The equations above can be combined to show that this variation has four components. Because

$$\log y_{ij} = a_i + b_{ij} + \log d_i + \log \varepsilon_{ij},$$

we have

$$V(\log y_{ij}) = \sigma_a^2 + \sigma_b^2 + \sigma_d^2 + \sigma_\varepsilon^2.$$

Going one step further, the predicted variance of the mean of $\log y_{ij}$ over all fish (j) and all dives (i) at that site can be written as

$$V = \frac{\sigma_a^2 + \frac{\sigma_b^2}{m}}{n} + \frac{\sigma_d^2 + \frac{\sigma_\varepsilon^2}{m}}{n}.$$

Assuming the number of dives and fish recorded per dive is the same at the second site, the predicted power to detect a difference D in the mean log-lengths at the two sites is given by

$$F_t\left[\frac{D}{SED} - t_{\alpha/2}\right],$$

where $F_t[.]$ = cumulative distribution function;
$t_{\alpha/2}$ = the upper $\alpha/2\%$ point for the t-distribution with $2(n-1)$ degrees of freedom, and SED = $\sqrt{2V}$, which is the standard error of the difference in the two mean log-lengths (see Sokal and Rohlf, 1995, p. 263). Note that if the analysis involved the comparison of $s>2$ sites, the degrees of freedom for the t-distribution would be $s(n-1)$. Because the analysis is on a log-scale, the difference D is calculated as $D=\log(R+1)$, where R is the percentage change of interest.

In order to evaluate the power, we needed estimates of the four variance components. The first two, σ_a^2 and σ_b^2, were estimated by using catch data on true length for populations of red cod, blue cod, and snapper from around New Zealand from trawl and trap surveys by the Fisheries Division of the National Institute of Water and Atmospheric Research. The length data for red cod and snapper came from a number of locations around New Zealand (Fig. 1). The depths at which these fish were collected ranged between 20 and 40 m. The locations at which they were collected were grouped into sites, such that two locations that were within approximately 30 km of each other were considered to be at the same site. For red cod, there were 12 sites, each with between two and four locations: at each location, lengths were recorded for between 12 and 20 fish. For snapper, there were six sites, two of which contained 14 locations, and the other four had just two locations each. At each location, lengths were recorded for between 10 and 91 fish. The log-lengths were then analyzed by using nested analysis of variance. Site and location were specified to be random factors, and location was nested within the site. The location and residual variance components were used as estimates of σ_a^2 and σ_b^2, respectively. The data for blue cod came from one site, at five locations off Stewart Island. There were between 47 and 51 fish lengths recorded per location. The log-lengths were analyzed by using analysis of variance, with location being specified as a random factor. The location and residual variance components were used as estimates of σ_a^2 and σ_b^2, respectively. The remaining two variance components, σ_d^2 and σ_ε^2 were estimated by using data on the measurement error of novice scientific divers, experienced scientific divers, and a stereo-video system. These errors were determined by using a simple testing procedure for calibrating diver estimates of the lengths of reef fish. Silhouettes of fish were placed in the water and their lengths estimated by following the methods of the GBRMPA (1979), Bell et al. (1985), and English et al. (1994). There were eight novice divers and six experienced divers, each of who swam five repeat transects. On each transect they estimated the length of sixteen silhouettes. The same procedure was used for the stereo-video estimates: for each image the estimate used was the mean of ten measurements. The novice divers and three of the experienced divers made their length estimates in a saltwater pool. For the stereo-video system and the other three experienced divers, measurements were made in a swimming pool. Definitions of novice and experienced scientific divers are the same as those given in Harvey et al. (2000), which contains a full presentation of the data and detailed description of the method used. A full description of the design and calibration of the system can be found in Harvey and Shortis (1996, 1998).

The novice and experienced diver estimates were both analyzed by using nested analysis of variance of the logarithm of the relative accuracy (estimated length divided by true length). Diver and silhouette were specified to be random factors, and silhouette was nested within diver. The diver and silhouette variance components were used as estimates of σ_d^2 and σ_ε^2, respectively. The stereo-video estimates were analyzed by using analysis of variance of the logarithm of the relative accuracy, and silhouette

was specified as a random factor. The silhouette variance component was used as an estimate of σ^2_ε. Note that for the stereo-video estimates, we took σ^2_d. This is because there should be no variation in the accuracy and precision of measurement made with a stereo-video system operated by different divers over different dives. Operators either swim the system along a transect or locate it in one area to record point counts. The operator has no control over the configuration of the camera system and cannot change any of the parameters; both these features of the system would preserve measurement accuracy and precision. Over the duration of one dive, and between several dives, the small variations in calibration stability that occur have minimal effect on the accuracy and precision of measurements (Harvey and Shortis, 1998). Harvey et al. (2000) have shown that very small variations in measurement accuracy (mean error –0.25 cm) may occur depending on the level of experience of the operators with the software used for making measurements from the images in the laboratory. To minimize this error, measurements where made where the orientation of a fish was less than 50 degrees perpendicular to the camera rig (Harvey and Shortis, 1996).

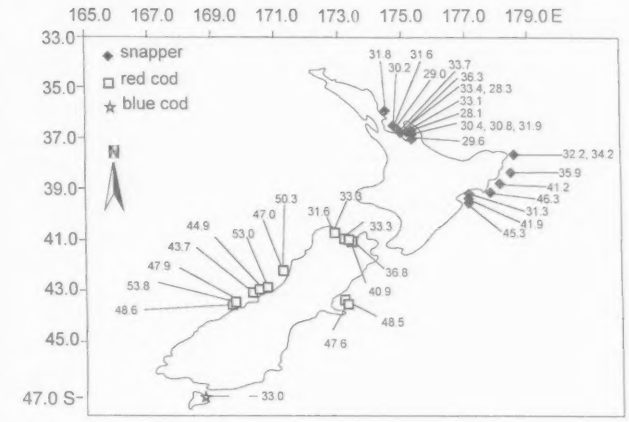

Figure 1

Map of the distribution of sites where fish were collected. The mean lengths shown for each site are in cm.

Results

The estimates of the variance components used in the power analysis are shown in Tables 1 and 2, together with their 90% confidence limits. Figure 2 shows the predicted power of visual estimates made by novice and experienced scientific divers and the predicted power of estimates made by a stereo-video system to detect a 15% change in the mean length of populations of blue cod, snapper, and red cod based on recording 30 fish per sample. Fifteen percent has been selected as an effect size because it represents a 5-cm change in the mean length of the population of blue cod used for our study. The results show that for each of the three species, the experienced scientific divers had greater power to detect changes than did novice scientific divers. However, for blue cod and snapper (Fig. 2), the stereo-video system had much greater power to detect changes in the mean length than either novice or experienced scientific divers. For example, we could achieve 90% power to detect a 15% change in the mean length of blue cod by recording 10 samples per site with the stereo-video system, with 27 samples per site for experienced scientific divers, and with 28 samples per site for novice divers. Similar conclusions apply to snapper with 11, 23, and 29 samples being required, respectively, under the same conditions. The advantage of the stereo-video system was not as good for red cod (30, 43, and 50 samples, respectively) as a result of the greater variability in their true mean length between locations than that recorded for the other two species (Fig. 2).

Table 1

Estimates of the variance components σ^2_a (between dive locations) and σ^2_b (within dive locations) of the natural logarithm of true fish length, for each of three species (90% confidence limits shown in parentheses).

Species	Between dive locations	Within-dive locations
Red cod	0.025 (0.015,0.060)	0.076 (0.068,0.084)
Snapper	0.008 (0.005,0.014)	0.027 (0.025,0.029)
Blue cod	0.008 (0.004,0.060)	0.019 (0.016,0.022)

Influence of effect size

Around the southern coastal waters of New Zealand, blue cod may reach a maximum size of 50 cm, averaging 20–30 cm. (Ayling and Cox, 1982). The sample of blue cod on which our power analysis was based had a mean length of 33 cm. A 15% change in mean length would represent a change of 5 cm. Figure 3 shows how the advantages of stereo-video measurements over diver estimates diminish as the size of the change to be detected increases. For example, to detect a 30% change in the mean length of blue cod with 90% power 4 samples were needed per site with the stereo-video system, 9 samples were needed with experienced scientific divers, and nine samples with novice scientific divers. A 50% change would be detected with 90% power with three samples per site with the stereo-video system, five samples with experienced scientific divers, and five samples with novice scientific divers.

The influence of numbers of fish per sample

As the numbers of fish recorded per sample decreases (for example from 30 to 10 to 1), the number of samples that need to be recorded to maintain an equivalent level of power increases. For example, to detect an effect size

Table 2

Estimates of the variance components σ^2_d (between divers) and σ^2_e (within divers) of the natural logarithm of relative accuracy (estimated length/true length), for experienced scientific divers, novice divers, and the stereo-video system (90% confidence limits shown in parentheses). The value of σ^2_d is taken to be zero for the stereo-video system.

	Between divers		Within divers	
Experienced divers	0.015	(0.006,0.067)	0.022	(0.017,0.030)
Novice divers	0.016	(0.008,0.063)	0.023	(0.017,0.031)
Stereo-video system			0.00020	(0.0001,0.0005)

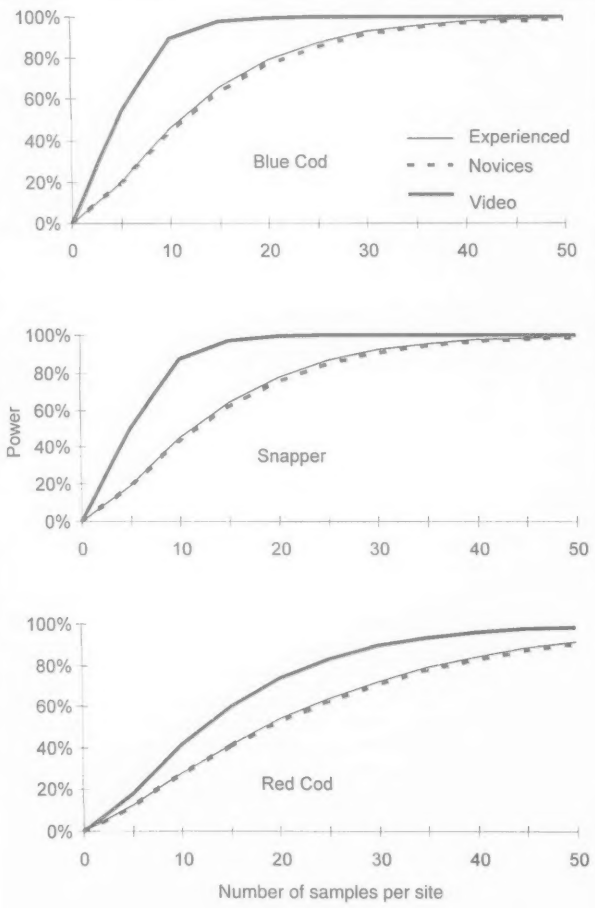

Figure 2

The power of novice scientific divers, experienced scientific divers and a stereo-video system to detect a 15% change in the mean length of a population of blue cod, snapper, and red cod. n = 30 fish; α = 5%.

of 15% with 90% power for blue cod when only one fish is being recorded per sample, 30 samples per site need to be recorded with the stereo-video system, 70 with experienced scientific divers, and 71 with novice scientific divers. When 30 fish are recorded per sample only 10, 27, and 28 samples are required, respectively (Fig. 4).

Influence of α

With stereo-video measurements, an increase in the value of α has little effect on the number of samples required to achieve a high level of power. When α is set at 5%, 10%, and 20%, we required 10, 9, and 7 samples per site, respectively, to detect a 15% change in the mean length of our population of blue cod with 90% power (Fig. 5). To achieve a similar level of power with experienced scientific divers 27, 22, and 17 samples needed to be recorded per site, whereas 28, 23, and 18 samples were required for novice scientific divers.

Discussion

Our research suggests that the power to detect changes in the mean length of three common species of fish from coastal waters of New Zealand will be higher when length estimates are made by a stereo-video system rather than by experienced or novice scientific divers. In addition, the level of power to detect these changes will differ between species, depending on the natural variability in mean length between different sites and locations. Managers and environmental researchers need to be aware of this issue when selecting suitable species of fish to be included in monitoring programs. For some species of fish (e.g. red cod), the variability in mean length between sites may be so great that even with a stereo-video system, unrealistically large numbers of samples need to be taken per site to detect changes in the order of 30% with high statistical power.

A stereo-video system may have many advantages in monitoring programs, particularly where few fish are recorded per sample. Fewer samples need to be taken per site with a stereo-video system to obtain an equivalent level of power compared with the number of samples needed with experienced scientific divers (Fig. 2), thus both time and money are saved in the field.

Even though calibration procedures are recommended and used by some researchers (GBRMPA, 1979; Bell et al., 1985; Polunin and Roberts, 1993; Darwall and Dulvy, 1996), interdiver variability and diver measurement error may still invalidate comparisons of the changes in the mean length between sites and over time. Consequently, it is important that the level of precision and accuracy of length estimates is stated in reports and

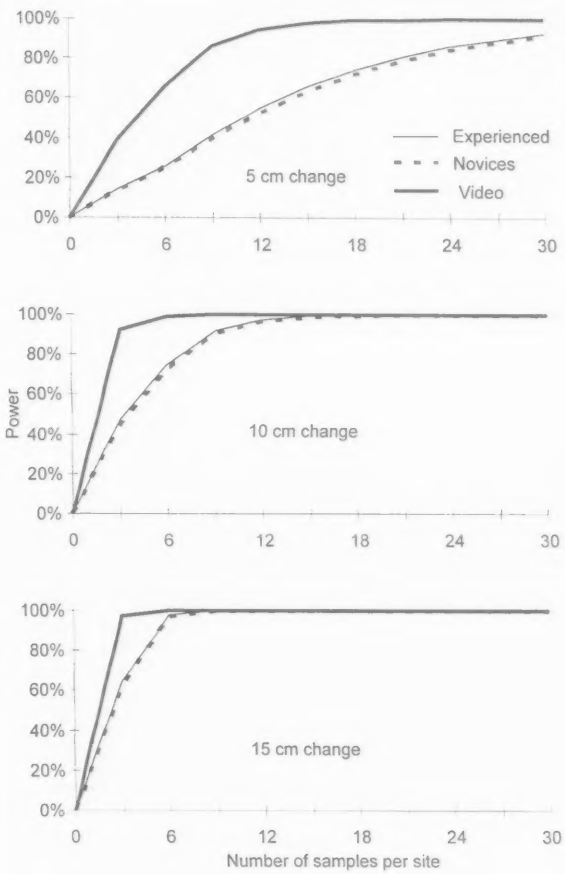

Figure 3

The influence of 5 cm, 10 cm, and 15 cm effect sizes on the power of novice scientific divers, experienced scientific divers, and a stereo-video system to detect changes in the mean length of a population of blue cod. $n = 30$ fish; $\alpha = 5\%$.

publications and that measurement error is minimized to allow realistic interpretation of the data and comparisons of assemblages or individual species. Because of these errors and biases, it is likely that many studies lack the statistical power to detect small, but biologically important, changes in fish length within reef-fish communities.

Increasing numbers of volunteers are assisting with sampling for monitoring programs, particularly in third world countries (Halusky et al., 1994; Mumby et al., 1995; Darwall and Dulvy, 1996). Darwall and Dulvy (1996) noted that the advantages of using volunteers in surveys include not only greater manpower, enabling large spatial surveys, but also financial savings and increased public awareness of environmental issues through participation.

To overcome the problem of subjectivity in visual estimates and to enhance the accuracy and precision of length estimates, and ultimately the power of a monitoring program, an underwater stereo-video system could be used. The use of an underwater stereo-video system provides an opportunity for volunteers to be involved in monitoring programs without compromising the quality of the data.

In assessing the statistical precision of visual length estimates, we have focused solely on the extra variability in the estimates introduced by measurement error. This error can also introduce a bias in the estimates. For example, the experienced scientific divers used by Harvey et al. (2000) had a mean relative error of –8.6% (SE=1.9%), suggesting that they would on average underestimate the true length by between 5% and 12%. In the type of study for which we have predicted the power to detect a difference in mean length, this bias will make little, if any, contribution to the loss of precision because the true lengths

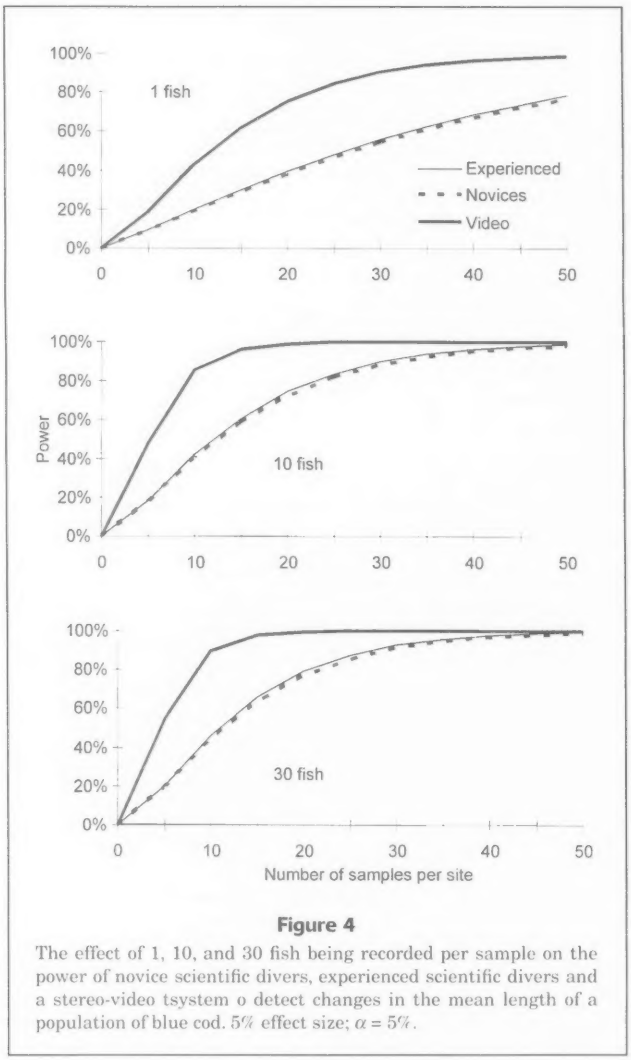

Figure 4

The effect of 1, 10, and 30 fish being recorded per sample on the power of novice scientific divers, experienced scientific divers and a stereo-video tsystem o detect changes in the mean length of a population of blue cod. 5% effect size; $\alpha = 5\%$.

will be tend to be underestimated by the same amount at the two sites.

For clarity of exposition, we have considered only the simplest possible study in which mean lengths of size-frequency distributions might be compared. We would expect that, at least qualitatively, the power comparisons made in our study would apply equally to other, more complex, sampling designs. Likewise, the focus of our study has been on mean length (and thereby biomass), but we conjecture that the benefits of using a stereo-video system will apply equally well for the comparison of size-frequency distributions.

Our calculations are based on length estimates made by divers and a stereo-video system in a controlled environment with plastic silhouettes. Under field conditions with moving fish, variable light conditions, and with other objects such as corals or kelps in the field of view providing a scale, diver and stereo-video estimates may be more or less accurate and precise, and thus change the power analysis.

Conclusion

A stereo-video system provides a new and alternative method for collecting length data on reef fish through nondestructive visual sampling. The use of a stereo-video system reduces measurement error substantially, thus increasing the statistical power of a monitoring program to detect changes in the mean length of a population of fish. When environmental managers set program goals of detecting small effect sizes (30% or less of the mean length of the target fish population) with a high statistical power (example 90%), the use of stereo-video technology

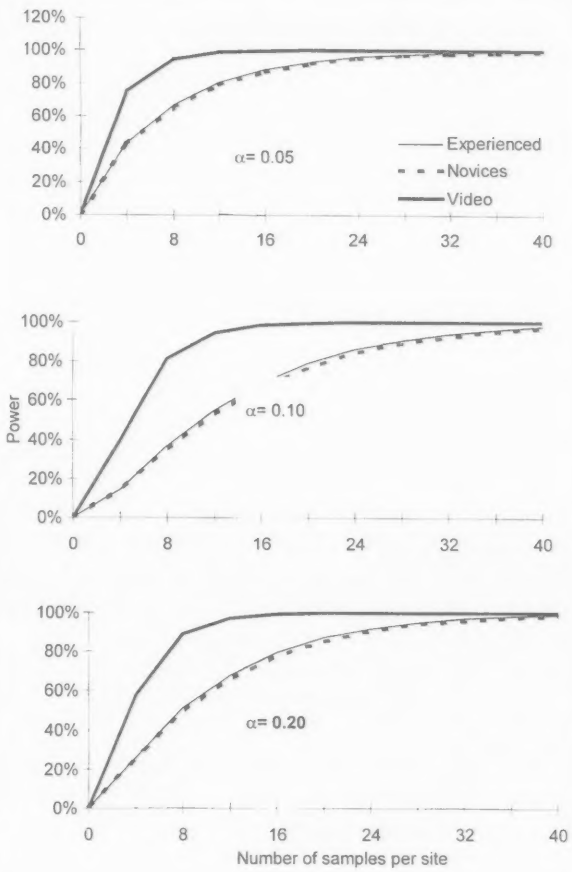

Figure 5

The effect of decreasing alpha values on the power of novice scientific divers, experienced scientific divers, and a stereo-video to detect changes in the mean length of a population of blue cod. 15% effect size; recording size = 30 fish.

in visual surveys of reef-fish length can potentially save both time and money on field costs. However, when the goal of the program is to detect larger changes, the advantages of a stereo-video system are not so great owing to the time needed to calibrate the system and analyze stereo images after the data are recorded (Harvey and Shortis, 1998).

Acknowledgments

We acknowledge financial aid from the New Zealand Department of Conservation (research grant 1822), the University of Otago Research Committee, the Southland Regional Council (New Zealand) and the Division of Sciences at the University of Otago, Dunedin, New Zealand, and from Sony New Zealand Ltd, THC Milford Sound, Fiordland Lobster Company, and Mobil and Gore Services Ltd. We are grateful to James Seager, of the Department of Geomatics at the University of Melbourne, for assistance with software development, and to June Hill, Callum Duncan, Lisa Kelleher, and Andrea Brown for assisting with field trials and to all the divers who willingly gave their time to assist with this research. We would also like to acknowledge Glenn Carbines and the Fisheries Division, National Institute of Water and Atmospheric Research, for allowing us access to data. This manuscript was greatly improved by comments from Howard Choat, June Hill, Philip Mladenov, Keith Probert, and four anonymous reviewers.

Literature cited

Alcala, A. C.
1988. Effects of marine reserves on coral reef fish abundances and yields of Phillipine coral reefs. Ambio 17:194–199.

Andrew, N. L., and B. D. Mapstone.
1987. Sampling and the description of spatial pattern in marine ecology. Oceanogr. Mar. Biol. Ann. Rev. 25:39–90.

Ault, J. S., J. A. Bohnsack, and G. A. Meester.
1998. A retrospective (1979–1996) multispecies assessment of coral reef fish stocks in the Florida Keys. Fish. Bull. 96:395–414.

Ayling, T., and G. Cox.
1982. Collins guide to the sea fishes of New Zealand. Collins, Auckland, 343 p.

Bell, J. D.
1983. Effects of depth and marine reserve fishing restrictions on the structure of a rocky reef fish assemblage in the northwestern Mediterranean Sea. J. Appl. Ecol. 20:40–47.

Bell, J. D., G. J. S. Craik, D,. A. Pollard, and B. C. Russell.
1985. Estimating length frequency distributions of large reef fish underwater. Coral Reefs 4:41–44.

Bellwood, D. R., and A. C. Alcala.
1988. The effect of minimum length specification on visual census estimates of density and biomass of coral reef fishes. Coral Reefs 7:23–27.

Cole, R. G., T. M. Ayling, and R. G. Creese.
1990. Effects of marine reserve protection at Goat Island, northern New Zealand. N.Z. J. Mar. Freshwater Res., 24:197–210.

Craik, G. J. S.
1981. Underwater survey of coral trout *Plectropomus leopardus* (Serranidae) populations in the Capricornia section of the Great Barrier Reef Park. *In* Proc 4th int coral reef symp (Manila) 1:53–58.

Darwall, W. R. T., and N. K. Dulvy.
1996. An evaluation of the suitability of non-specialist volunteer researchers for coral reef fish surveys. Mafia Island, Tanzania—a case study. Biol. Conserv. 78:223–231.

English, S., C. Wilkinson, and V. Baker (eds.).
1994. Survey manual for tropical marine resources. Australian Institute of Marine Science, P.M.B. No. 3, Townsville Mail Centre, Australia 4810, 368 p.

Fairweather, P. G.
1991. Statistical power and design requirements for environmental monitoring. Aust. J. Mar. Freshwater Res. 42: 555–567.
Fausch, K.D., J. Lyons, J. R. Karr, and P. L. Angermeier.
1990. Fish communities as indicators of environmental degradation. Am. Fish. Soc. Symp. 8:123–144.
Francour, P.
1991. The effect of protection level on a coastal fish community at Scandola, Corsica. Rev. Ecol. Terre Vie 46:65–81.
1994. Pluriannual analysis of the reserve effect on ichthyofauna in the Scandola natural reserve (Corsica, Northwestern Mediterranean). Oceanol. Acta 17(3):309–317.
Gerrodette, T.
1987. A power analysis for detecting trends. Ecology 68(5): 1364–1372.
GBRMPA (Great Barrier Reef Marine Park Authority).
1979. Workshop on coral trout assessment techniques. Workshop series 3. GBRMPA, Queensland, Australia, 64 p.
Green, A. L.
1996. Spatial, temporal and ontogenetic patterns of habitat use by coral reef fishes (Family Labridae). Mar. Ecol. Prog. Ser. 133:1–11.
Green, R. H.
1979. Sampling design and statistical methods for environmental biologists. Wiley Interscience, New York, NY, 257 p.
Halusky, J. G., W. J. Seaman, and E. W. Strawbridge.
1994. Effectiveness of trained volunteer divers in scientific documentation of artificial aquatic habitats. Bull. Mar. Sci., 55(2–3):939–959.
Harmelin-Vivien, M. L., and Y. Bouchon-Navaro.
1981. Trophic relationships among chaetodontid fishes in the Gulf of Aquaba (Red Sea). *In* Proc 4th int coral reef symp (Manila) 2:537–544.
Hart, A. M., D. W. Klumpp, and G. R. Russ.
1996. Response of herbivorous fishes to crown-of-thorns starfish *Acanthaster planci* outbreaks. II. Density and biomass of selected species of herbivorous fish and fish habitat correlations. Mar. Ecol. Prog. Ser., 132:21–30.
Harvey, E. S., D. Fletcher, and M. Shortis.
2000. A comparison of the precision and accuracy of reef-fish lengths determined visually by divers with estimates produced by a stereo-video system. Fish. Bull. 99(1)63–71.
Harvey, E., and M. Shortis.
1996. A system for stereo-video measurement of subtidal organisms. Mar. Tech. Soc. J. 29(4):10–22.
1998. A system for stereo-video measurement of subtidal organisms. Mar. Tech. Soc. J. 32(2): 3–17.
Hayes, J. P.
1987. The positive approach to negative results in toxicology studies. Ecol. Environ. Safety 14:73–77.
Hourigan, T. F., T. C. Tricas, and E. S. Reese.
1988. Coral reef fishes as indicators of environmental stress in coral reefs. *In* Marine organisms as indicators (D. K.Soule and G. S. Keppel, eds.), p. 107–135. Springer, New York, NY.
Jones, R. S., and J. A. Chase.
1975. Community structure and distribution of fishes in an enclosed high island lagoon in Guam. Micronesia 11: 127–148.
Kulbicki, M.
1989. Correlation between catch data from bottom longlines and fish censuses in the SW lagoon of New Caledonia. *In* Proc 6th int coral reef symp, (Townsville Australia) 2:305–312.
Kulbicki, M., G. Mou-Tham, P. Thollot, and L. Wantiez.
1993. Length weight relationships of fish from the lagoon of New Caledonia. Naga (2–3):26–30.
McCormick, M. I., and J. H. Choat.
1987. Estimating total abundance of a large temperate-reef fish using visual strip-transects. Mar. Biol. 96(4): 469–478.
Medley, P., G. Gaudian, and S. M. Wells.
1993. Coral reef fisheries stock assessment. Rev. Fish. Biol. Fisher. 3(Sep):242–285.
Mumby, P. J., A. R. Harborne, P. S. Raines, and J. M. Ridley.
1995. A critical assessment of data derived from Coral Cay Conservation volunteers. Bull. Mar. Sci., 56(3):737–751.
Peterman, R. M.
1990a. Statistical power analysis can improve fisheries research and management. Can. J. Fish. Aquat. Sci., 47: 2–15.
1990b. The importance of reporting statistical power: the forest decline and acidic deposition example. Ecology 71: 2024–2027.
Polunin, N. V. C., and C. M. Roberts.
1993. Greater biomass and value of target coral reef fishes in two small Caribbean marine reserves. Mar. Ecol. Prog. Ser. 100:167–176.
Russ, G.
1985. Effects of protective management on coral reef fishes in the central Philippines. *In* 5th int coral reef symp. 4:219–224.
Russ, G. R., and A. C. Alcala.
1996. Do marine reserves export adult fish biomass? Evidence from Apo Island, central Philippines. Mar. Ecol. Prog. Ser. 132:1–9.
Samoilys, M. A.
1989. Abundance and species richness of the coral reef fish on the Kenyan Coast: the effects of protective management and fishing. *In* Proc 6th int coral reef symp (Townsville Australia), 2:261–266.
Sokal, R. R., and F. J. Rohlf.
1995. Biometry: the principles and practice of statistics in biological research, 3rd ed. Freeman, New York, NY, 887 p.
St John, J., G. R. Russ, and W. Gladstone.
1990. Accuracy and bias of visual estimates of numbers, size structure and biomass of coral reef fish. Mar. Ecol. Prog. Ser. 64:253–262.
Sweatman, H. P. A.
1985. The influence of adults of some coral reef fishes on larval recruitment. Ecol. Mono. 55(4):469–485.

Dynamics of larval fish abundance in Penobscot Bay, Maine

Mark A. Lazzari
Maine Department of Marine Resources
P.O. Box 8
West Boothbay Harbor, Maine 04575
E-mail address: mark.lazzari@state.me.us

Abstract–Biweekly ichthyoplankton surveys were conducted in Penobscot Bay, Maine, during the spring and early summer of 1997 and 1998. Larvae from demersal eggs dominated the catch from late winter through spring, but not in early summer collections. Larval fish assemblages varied with temperature, and to a lesser extent, plankton volume, and salinity, among months. Temporal patterns of larval fish abundance corresponded with seasonality of reproduction. Larvae of taxa that spawn from late winter through early spring, such as sculpins (*Myoxocephalus* spp.), sand lance (*Ammodytes* sp.), and rock gunnel (*Pholis gunnellus*) were dominant in Penobscot Bay in March and April. Larvae of spring to early summer spawners such as winter flounder (*Pleuronectes americanus*) Atlantic seasnail (*Liparis atlanticus*), and radiated shanny (*Ulvaria subbifurcata*) were more abundant in May and June. Penobscot Bay appears to be a nursery for many fishes; therefore any degradation of water quality during the vernal period would have wide reaching effects on the nearshore fish community.

Manuscript accepted 6 July 2000.
Fish. Bull. 99:81–93 (2001).

For most fish, the greatest mortality occurs during early life stages (Hjort, 1914; Cushing, 1975; Leggett and Deblois, 1994). Therefore, it is essential that fish eggs and larvae develop in favorable habitats that maximize the probability of survival. Bigelow (1926) recognized the significance of the coastal shelf for the production of fish larvae within the Gulf of Maine, noting that most larvae were found within the 200-m contour. He also observed that larval drift was generally to the southwest and that abundance increased progressively to the west with the result that few larvae were observed off eastern Maine and in the Bay of Fundy. Other surveys (Fish and Johnson, 1937; Marak, 1960; Marak and Colton, 1961; 1962) further defined the composition of the ichthyoplankton of the Gulf of Maine. Ichthyoplankton of inshore waters of the Gulf of Maine has been documented for the Damariscotta, Sheepscot, and Sullivan Harbor estuarine systems and nearby waters in the central area of the Maine coast (Graham and Boyar, 1965; Graham, 1972; Chenoweth, 1973; Hauser, 1973; Lee, 1975; Laroche, 1980; 1982; Shaw, 1981; Townsend, 1981; 1983; 1984). However, the ichthyoplankton of Penobscot Bay has not been studied despite the fact that it is the largest embayment in the region and that coastal environments, such as bays and estuaries, may constitute favorable habitats for the early life stages of a large number of marine fishes (Frank and Leggett, 1983).

This study describes the results of a two-year, spring survey of larval fishes in Penobscot Bay, Maine. The objectives of the study were 1) to describe the structure of the larval fish community, 2) to determine the temporal and spatial variation in species diversity and abundance, and 3) to relate these variations to differences in location and environmental variables.

Materials and methods

Field methods

Penobscot Bay is a large (80-km) drowned river valley typical of the Maine coast. It has a drainage area of over 21,000 km^2 (Haefner, 1967). The study area is about 40 km long and varies in depth from 15 to 110 m. Sixteen ichthyoplankton stations (Fig. 1) were selected to encompass Penobscot Bay for the larval surveys. Six upper bay stations (R1–R6) were located in the northern estuarine portion of the bay between Isleboro Island and the mainland. Seven midbay stations (B1–B7) were located in the central portion of the bay. Three lower bay stations (O2–O4) were located in the sourthern estuarine portion of the bay adjacent to the islands of North Haven and Vinalhaven.

In 1997, seven, two- or three-day cruises (97I–97VII) were conducted biweekly from 4 April through 25 June 1997 to coincide with spring and summer spawning times for many fishes. Data collection involved towing a 1.0-m, 333-micron mesh plankton net equipped with a General Oceanics flowmeter during daylight hours (Fig. 1). The net was hauled for 20 minutes in stepped oblique fashion at the surface, at 10 m, and at 20 m, or to within 5 m of the bottom. At each station, a vertical profile of salinity and temperature was collected with a Seabird 19 CTD (conductivity, temperature, and depth) probe.

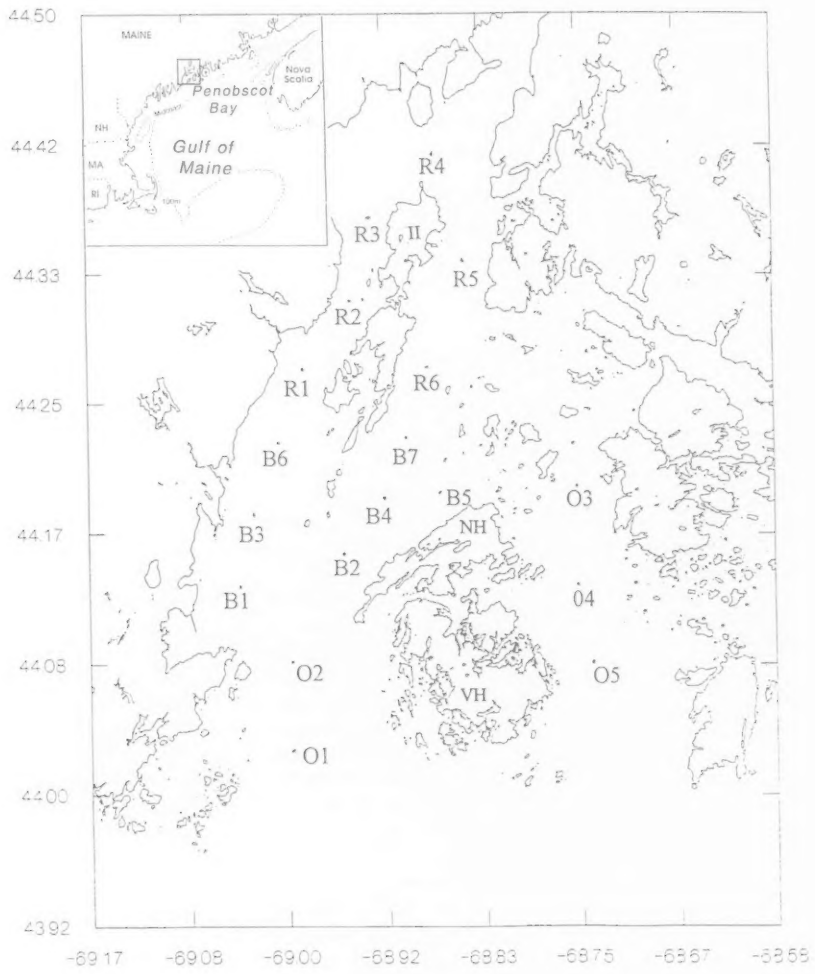

Figure 1

Map of stations sampled biweekly with a 1.0-m plankton net in Penobscot Bay, Maine, from 4 April to 25 June 1997 and from 18 March to 30 April 1998. II = Iselboro Island; NH = North Haven Island; and VH = Vinalhaven Island.

In 1998, four one- or two-day cruises (98I–98IV) were conducted biweekly from 18 March through 30 April 1998 and data collection was the same as in 1997 except that ten ichthyoplankton stations were sampled in the lower bay only. Eight of these stations were sampled in 1997 including five midbay stations (B1–B5) and three lower bay stations (O2–O4). Two additional lower bay stations, O1 and O5, were added in 1998. Larvae from both years were preserved in 5% formalin for later identification to the lowest taxon possible by the Atlantic Reference Center of the Huntsman Marine Biological Laboratory in St. Andrews, New Brunswick, and for quantitative determination of larval fish densities (number of larvae per filtered 100 m^3). Fish larvae were measured for standard length, or in some cases notochord length, to the nearest mm. Plankton volume standardized by volume filtered was determined for each tow by displacement of the unidentified plankton.

Data analysis

Larval fish abundance and environmental data were analyzed by using three multivariate techniques: principal components analysis (PCA), multivariate analysis of variance (MANOVA), and canonical correlation analysis (CCA). PCAs of the variance-covariance matrices derived from both environmental and larval abundance data were performed to reduce intercorrelated variables to a smaller number of uncorrelated variables. This procedure provided a concise description and comparison of complex spatial

and temporal patterns of the larval fish assemblage and environmental data (Gauch, 1982). Varimax rotation was performed on factors from the PCAs in both cases because rotated solutions tend to extract components that correlate highly with a smaller number of variables than unrotated PCAs (Stevens, 1986). This step aided in the interpretation of the factors. Rotated factor scores from the PCA were used as the dependent variables in the MANOVA because they were uncorrelated, thus satisfying the assumption of independence for parametric statistical tests.

Environmental data were log-transformed to satisfy assumptions of univariate normality and then summarized by PCA. The resulting factor scores were grouped by month, and means were compared by MANOVA to assess the null hypothesis that environmental variables did not differ among months. This analysis was followed by a Tukey-Kramer multiple range test to detect which monthly means differed. This test controls for increases in the type-I error rate associated with unequal sample sizes (Day and Quinn, 1989). Temporal changes in environmental variables were interpreted by evaluating product moment correlations of the environmental variables and factor scores from PCA. I considered only variables that were significantly correlated with an individual factor in interpreting that factor (significance levels were adjusted for multiple comparisons, where $p'=1-(1-p)^{1/k}$ and k equals the number of comparisons [Sokal and Rohlf, 1981]). The results of these analyses were used to discriminate among months.

The analysis of larval fish assemblage composition was similar to that performed for environmental data. However, fish taxa not present in 5% of the samples were eliminated to reduce the influence of rare taxa (taxa that were excluded were present in five of 102 samples in 1997 and two of 40 samples in 1998) as potential outliers (Gauch, 1982). A matrix of angularly transformed [arcsine of the square root of a proportion (Sokal and Rohlf, 1981)] relative abundances for the m = 12 taxa in n = 102 samples in 1997, and the m = 13 taxa in n = 40 samples in 1998 were constructed and summarized by PCA. Varimax rotated factor scores generated from PCA of the relative abundance matrix were compared among months by using MANOVA (unbalanced design). The null hypothesis was that mean factor scores (and taxonomic composition) did not change among months. This was followed by a Tukey-Kramer test of significantly affected factors to identify the extent to which monthly means differed.

Factor scores were then grouped by location and served as the dependent variables in MANOVA to test for differences in sample location (upper, mid, or lower bay). The null hypothesis was that mean factor scores (and taxonomic composition) did not change among locations. A Tukey-Kramer test was performed to identify location mean factor scores that differed significantly. Temporal and spatial changes in the taxonomic composition of larval fish assemblages were then interpreted by identifying which factors were affected by month and location treatments and by evaluating product-moment correlations of angularly transformed relative abundance data and significant PCA factor scores (i.e. "loadings" on factors significantly affected by time and location; Pielou, 1984). The relationships of the factor scores from PCA of the relative larval fish abundance matrix and the log-transformed environmental variables were examined by CCA.

Table 1

Mean (± standard error) environmental variables for the entire study period, reported by month for 1997 and 1998. Temperature (°C) and salinity recorded as mean for top 20 m of the water column and volume displacement (Pvol) in mL of unidentified plankton per 100 m^3.

Month	Temperature	Salinity	Depth (m)	Pvol
1997				
April	3.37 (0.13)	30.56 (0.13)	74.0 (9.4)	17.3 (1.7)
May	5.49 (0.12)	30.24 (0.08)	58.0 (11.8)	4.2 (0.5)
June	8.52 (0.22)	30.44 (0.05)	46.8 (8.2)	13.7 (2.1)
1998				
March	2.41 (0.01)	29.90 (0.05)	38.8 (18.8)	34.4 (0.5)
April	4.23 (0.14)	30.14 (0.05)	56.5 (10.7)	25.5 (0.9)

Standard lengths, or notochord lengths, from 1997 and 1998 were compared among cruises (sample dates) for each species by using Kolmogorov-Smirnov two-sample tests. The null hypothesis was that size distribution did not differ significantly between sample dates.

Results

A total of 102 plankton net samples and CTD measurements were collected during biweekly sampling between 4 April and 25 June 1997 in Penobscot Bay. Sixteen stations were sampled on five of the seven sampling trips; however, inclement weather (wind speeds >25 knots) during the first week of April (4–7, 97I) and from late April to early May (29 April–1 May 97III) limited the number of stations that could be sampled during these trips to 10 and 12, respectively. The number of cubic meters of water filtered per 20-minute tow varied from 137.5 to 755.7 m^3 depending on station location and sample date. The total volume of filtered in 1997 was 44,622 m^3.

In 1998, 40 plankton net samples and CTD measurements were collected during approximately biweekly sampling between 18 March and 30 April 1998. Ten stations were sampled on each of the four sampling trips. The number of cubic meters of water filtered during each 20-minute tow varied from 54.2 to 582.5 m^3 depending on station location and sample date. The total volume of water filtered in 1998 was 12,459 m^3.

Environmental data

Station depth ranged from 20 m at mean low water at the upper bay station R4 to 91 m at station O2 (Table 1).

Table 2

Correlations among environmental variables and factor scores from varimax-rotated PCA of the log-transformed environmental data. Underlined values significant at $P = 0.05$, adjusted for multiple comparisons such that $P < 0.01$ for a significant correlation.

	Depth	Pvol	Temp	Salinity	Factor 1	Factor 2
1997						
Depth	1.00				0.08	0.98
Pvol	0.07	1.00			0.84	–0.06
Temperature	–0.13	–0.35	1.00		–0.68	–0.05
Salinity	0.20	0.44	–0.24	1.00	0.71	0.25
1998						
Depth	1.00				0.08	0.83
Pvol	–0.08	1.00			–0.90	0.08
Temperature	0.18	–0.71	1.00		0.90	–0.09
Salinity	–0.16	–0.29	0.21	1.00	0.42	–0.68

Station mean water temperatures for the top 20 m of the water column in 1997 were variable and ranged from 2.3°C on 4 April to 10.8°C on 25 June. Station mean salinity ranged between 27.8 ppt on 30 April and 31.2 ppt on 16 April. Plankton volume ranged from 0.8 to 44.9 mL per 100 m^3 and generally was greatest during early April (97I) with a secondary peak in volume observed in late June (97VII). Greatest plankton volumes occurred at the lower bay stations. In 1998, mean water temperatures ranged from 2.4°C on 18 March to 5.3°C on 30 April. Mean salinity ranged between 29.6 ppt on 18 March and 30.6 ppt on 30 April. Station plankton volume in 1998 ranged from 6.1 to 280 mL per 100 m^3 and was greatest during late April (98IV) at the lower bay stations.

We compared environmental variables among months to aid in the characterization of Penobscot Bay. PCA of log-transformed variables identified two factors that explained 69% of the total variance in 1997 and 76% in 1998 (Table 2). Factor 1 was related to temperature, plankton volume, and salinity in 1997 and in 1998. Factor 2 was related to depth in both years. MANOVA of mean factor scores indicated significant differences by month in 1997 (Wilk's lambda=0.792, $P<0.001$) and 1998 (Wilk's lambda=0.778, $P<0.001$). Temperature was negatively correlated and plankton volume and salinity were positively correlated with PCA factor 1 in 1997 (Table 2). *Post hoc* comparisons of monthly scores for factor 1 indicated that the mean scores for April were different from those for May and June. In 1998, temperature was positively correlated and plankton volume negatively correlated with PCA factor 1 (Table 2) and *post hoc* comparisons indicated that the mean scores for March were different from those for April. Salinity was correlated with both PCA factor 1 (positively) and factor 2 (negatively) in 1998. Depth was positively correlated with factor 2 in both 1997 and 1998. *Post hoc* comparisons of monthly scores for PCA factor 2 indicated that the mean scores for April were different from those for May and June in 1997; the mean score for March was different from that for April in 1998.

Fish larvae

Differences existed between the two years in the kinds of fish larvae found in Penobscot Bay. At least, 26 species (23 individuals [1.5%] not identified to species) belonging to 15 families were identified (Table 3). A total of 23 species (15 families) were found in 1997, and 16 species (9 families) in 1998; 13 species were common to both years. Differences in taxonomic composition were mainly due to the collection of rare specimens during the year, such as inquiline snailfish (*Liparis inquilinus*) in 1997 and pollock (*Pollachius virens*) in 1998. In addition, several species that were present in 1997, including American eel (*Anguilla rostrata*), capelin (*Mallotus villosus*), fourbeard rockling (*Enchelyopus cimbrius*), Atlantic tomcod (*Microgadus tomcod*), cunner (*Tautogolabrus adspersus*), Atlantic mackerel (*Scomber scombrus*), alligatorfish (*Aspidophoroides monopterygius*), windowpane flounder (*Scophthalmus aquosus*), and American plaice (*Hippoglossoides plattessoides*), did not occur in the 1998 collections. In contrast, pollock, snake blenny (*Lumpenus lampraetiformis*) and Arctic shanny (*Stichaeus punctatus*) were collected only in 1998. The assemblage of species was slightly more diversified in 1997 than in 1998 with Shannon-Wiener indices of H′=3.1 and 2.8, respectively. The three most abundant species in 1997 (*U. subbifurcata*, *Ammodytes* sp., *P. americanus*) constituted about 59% of all captures compared with 68% in 1998 (*M. octodecimspinosus*, *P. gunnellus*, *Ammodytes* sp.).

A total of 779 larvae of 23 species of fishes were collected during the seven cruises in 1997 (Table 3). The most commonly occurring larvae (>35% of the samples) were Atlantic seasnail (*Liparis atlanticus*), winter flounder (*Pleuronectes americanus*), radiated shanny (*Ulvaria subbifurcata*), sand lance (*Ammodytes* sp.), and *H. plattessoides*. Rare larvae (<1% of the samples) included Atlantic cod (*Gadus morhua*), Gulf seasnail (*Liparis coheni*), *L. inquilinus*, shorthorn sculpin (*Myoxocephalus scorpius*), and *S. aquosus*. The highest number of species (14) occurred dur-

Table 3

Egg type, total density (number/100 m^3), and percent frequency of occurrence (FO) of larval fishes collected by 1.0 m plankton net from April to June 1997 (102 samples) and March to April 1998 (40 samples) in Penobscot Bay. D = demersal; P = pelagic.

Family / Species	Egg type	1997		1998	
		Density	FO	Density	FO
Anguillidae					
Anguilla rostrata	—	0.004	2		
Clupeidae					
Clupea harengus	D	0.009	4	0.072	15
Osmeridae					
Mallotus villosus	D	0.022	5		
Gadidae					
Enchelyopus cimbrius	P	0.034	11		
Gadus morhua	P	0.002	1	0.022	5
Microgadus tomcod	D	0.007	2		
Pollachius virens	P			0.007	3
Labridae					
Tautogolabrus adspersus	P			0.007	3
Stichaeidae					
Lumpenus lampraetiformis	D			0.086	23
Ulvaria subbifurcata	D	0.462	41	0.014	5
Stichaeus punctatus	D			0.014	3
Pholidae					
Pholis gunnellus	D	0.099	27	1.428	75
Cryptacanthodeidae					
Cryptacanthodes maculatus	D	0.054	12	0.294	33
Ammodytidae					
Ammodytes sp.	D	0.350	35	0.596	35
Scombridae					
Scomber scombrus	P	0.016	4		
Cottidae					
Hemitripterus americanus	D	0.064	21	0.215	43
Myoxocephalus aenaeus	D	0.022	9	0.237	35
M. octodecimspinosus	D	0.034	9	1.550	40
M. scorpius	D	0.004	1	0.366	33
Agonidae					
Aspidophoroides monopterygius	D	0.007	3		
Cyclopteridae					
Liparis atlanticus	D	0.182	51	0.043	13
L. coheni	D	0.002	1	0.187	23
L. inquilinus	D	0.002	1		
Bothidae					
Scopthalmus aquosus	D	0.002	1		
Pleuronectidae					
Hippoglossoides platessoides	P	0.094	30		
Pleuronectes americanus	D	0.229	47	0.029	8

ing mid-April (97II). The most abundant larvae were *U. subbifurcata* (26% of total number), *Ammodytes* sp. (20%), *P. americanus* (13%), and *L. atlanticus* (10%). Total density of all larvae combined ranged from 0.6 larvae per 100 m^3 in mid-May (97IV) to 3.9 larvae per 100 m^3 in late June (97VII). The high larval densities in late June were a result of the large number of *U. subbifurcata* collected at the three lower bay stations.

In 1998, 726 larvae of 16 species of fishes (Table 3) were collected over the four sampling cruises. The most common

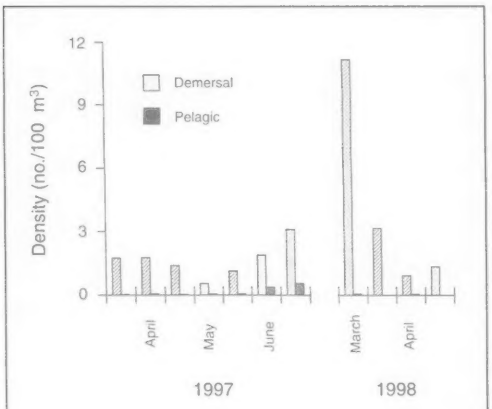

Figure 2

Total density (number/100 m^3) of larval fishes by egg type and sample date in Penobscot Bay, Maine: 4–7, 15–16, and 29–30 April; 12–13, 28–29 May; 9–10 and 24–25 June 1997; and 18 March, 7, 15, 30 April 1998.

larvae (>35% of the samples) were rock gunnel (*Pholis gunnellus*), sea raven (*Hemitripterus americanus*), longhorn sculpin (*Myoxocephalus octodecimspinosus*), grubby (*M. aenaeus*), and *Ammodytes* sp., whereas *P. virens* and *S. punctatus* were the least common (<3%). *Myoxocephalus octodecimspinosus* (30% of total number), *P. gunnellus* (27%), and *Ammodytes* sp. (11%) were the most abundant larvae collected. The greatest number of species (12) were found during mid-March (98I). Densities of all larvae combined declined from 11.4 larvae per 100 m^3 in mid-March (98I) to about one larva per 100 m^3 in mid-April (98III). The high larval densities in mid-March resulted from the high numbers of *M. octodecimspinosus* and *P. gunnellus* larvae collected at that time.

Larvae originating from demersal eggs dominated the catches in both years (Table 3). In terms of abundance, most larvae collected in 1997 came from demersal eggs (70%) that dominated the catch at all stations. Larvae from demersal eggs composed most of the catch (>90%) until mid (79%) and late June (60%) when the number of larvae originating from pelagic eggs increased (Fig. 2). Overall, five of 23 species (22%) of larvae came from pelagic eggs in 1997, but by late June (97VII), four of the eight species (50%) collected hatched from pelagic eggs. Larvae from demersal eggs dominated the catches in 1998 to an even greater extent than in 1997 (Fig. 2). Two of the 16 species (13%) and four larvae (0.04%) collected in 1998 originated from pelagic eggs (three specimens of *G. morhua* and one of *P. virens*). *Ulvaria subbifurcata* were the most abundant larvae in 1997 with densities up to 9.1 per 100 m^3 at the lower bay stations, whereas in 1998, *M. octodecimspinosus* and *P. gunnellus* were the most abundant larvae, with station densities up to 12.9 and 6.1 larvae per 100 m^3, respectively. Densities of sand lance (*Ammodytes* sp.) were highest (4 per 100 m^3) at the upper bay and midbay stations in 1997 and 1998, respectively. *Pleuronectes americanus* were more abundant in 1997 with densities up to 1.7 larvae per 100 m^3 at the midbay stations (B2, B3, B4). Larvae from pelagic eggs were rare in both years.

Several species appeared in plankton samples from most sampling dates in 1997 (Table 4). One species, *H. plattessoides* was taken during all seven cruises but was absent from the 1998 collections. *Ammodytes* sp. occurred from early April (97I) through late May (97V) in 1997 and from mid-March (98I), early April (98II), and late April (98IV) in 1998. *Pleuronectes americanus* and *L. atlanticus* were present from mid-April (97II) to late June (97VII) and *H. americanus* and *P. gunnellus* were found from early April (97I) to mid June (97VI). Four of the five species of fish larvae originating from pelagic eggs were taken during only one cruise. In 1998, three species, *P. gunnellus*, *H. americanus* and *M. aenaeus*, were collected on all four cruises. Atlantic herring (*Clupea harengus*) and wrymouth (*Cryptacanthodes maculatus*) occurred from mid-March (98I) through mid April (98III). *Myoxocephalus octodecimspinosus, M. scorpius, and L. coheni* were taken only during the first two cruises.

Size of the most abundant species changed little over the survey time period (Table 4). For example, winter flounder larvae were 2–4 mm during mid April (97II) and 3–7 mm during late June (97VII) indicating successive spawning events or no observed growth. The length-frequency distributions of most larvae were not significantly different among sample dates (Kolmogorov-Smirnov two sample test, $P>0.05$). However, the proportion of larger larvae increased over time for three taxa collected over a two month period in 1997 (i.e. *Ammodytes* sp., *P. gunnellus*, *H. plattessoides*, Table 4). Few species showed a change in length frequency distribution during the shorter 1998 survey (Kolmogorov-Smirnov two sample test, $P>0.05$).

Temporal changes in the abundance of fish larvae were observed in both years. Two peaks in mean density of larval fish were observed among all locations in 1997, whereas only a single peak was seen during the shorter 1998 survey. In 1997, the mean density was initially about 1.9 larvae per 100 m^3 in early (97I) and mid-April (97II), then declined to 0.6 larvae per 100 m^3 by mid May (97IV). Larval density increased to 1.2 larvae per 100 m^3 by late May (97V) and peaked at 3.9 larvae per 100 m^3 in late June (97VII). Most of the initial reduction in density was due to fewer *Ammodytes*. sp., *C. maculatus*, and *H. americanus* in the collections, whereas the June increase was due to *U. subbiffurcata*, and to a lesser extent to *E. cimbrius* and *P. americanus*. Densities of fish larvae in 1998 declined from a peak of 11.4 larvae per 100 m^3 in mid-March (98I) to about 1 larva per 100 m^3 in mid-April (98III), before increasing to 1.4 larvae per 100 m^3 on late April. Fewer *Ammodytes*. sp., *C. maculatus*, *L. coheni*, the three *Myoxocephalus* sp., and *P. gunnellus* accounted for the initial reduction. The increase during the latter part of the 1998 survey was due to greater numbers of *L. atlanticus*, *P. americanus*, and *U. subbiffurcata* larvae in collections.

Relative abundance patterns of 12 of the most abundant taxa (by the 5% criterion) in 1997 and 13 taxa in 1998

Table 4

Length-frequency distributions of the more abundant larval fishes collected in Penobscot Bay in 1997 and 1998; and results of the Kolmogorov-Smirnov two-sample test ($P<0.05$).

			Notochord or standard length (mm)												
Year and species	Cruise	*n*	1	2	3	4	5	6	7	8	9	10	>10	Mean	KS test
1997															
U. subbifurcata	I	0													
	II	0													
	III	0													
	IV	8						2	6					6.8	VII>VI
	V	21					1	9	11					6.5	
	VI	54					4	31	17	2				6.3	
	VII	119					25	44	28	10	8	3	1	6.5	
P. gunnellus[1]	I	20			2	8	7	2	1					14.6	III>I,II
	II	14			2	1	3	1	2	1	2	2		16.5	
	III	6				1						1	4	20.3	
	IV	1											1	25.0	
	V	1				1								14.0	
	VI	1			1									13.0	
	VII	0													
C. maculatus[1]	I	12								2	1	4	5	20.4	ns
	II	10										3	7	22.1	
	III	0													
	IV	1											1	38.0	
	V	0													
	VI	0													
	VII	0													
Ammodytes sp.	I	7						1		2	2		2	9.0	V>II,III
	II	94				1	4	12	15	11	18	16	17	8.6	
	III	44					1	1	4	8	10	7	13	9.7	
	IV	4						1	1				2	12.0	
	V	2											2	36.5	
	VI	0													
	VII	0													
H. americanus[1]	I	10			2	6	1	1						14.1	IV>I,II
	II	11			1	2	3	2		1	2			15.8	
	III	3			1							1	1	18.3	
	IV	3											3	21.7	
	V	1											1	23.0	
	VI	1				1								14.0	
	VII	0													
L. atlanticus	I	0													
	II	3				1	2							4.7	II>VI
	III	11				7	3	1						4.5	
	IV	10			3	7								3.7	
	V	18			8	8	2							3.7	
	VI	17			10	5	2							3.5	
	VII	21		1	9	8	2		1					3.7	
P. americanus	I	0													
	II	1		1										2.0	VII>IV
	III	18		1	11	6								3.3	
	IV	24		1	9	14								3.5	

continued

Table 4 (continued)

Year and species	Cruise	*n*	Notochord or standard length (mm) 1	2	3	4	5	6	7	8	9	10	>10	Mean	KS test
P. americanus (cont.)	V	16		1	7	5	3							3.6	
	VI	17			6	8	1	2						3.9	
	VII	24			7	7	3	5	2					4.5	
H. platessoides	I	1					1							5.0	VII>VI
	II	4				2	1	1						4.8	
	III	2				1		1						5.0	
	IV	3			1	1			1					4.7	
	V	4				2	1		1					5.0	
	VI	17		1	3	3	9			1				4.5	
	VII	10				2	1	2	4		1			6.2	
1998															
P. gunnellus[1]	I	134	2	16	46	37	18	9	5	1				13.8	ns
	II	47	1	12	14	8	7	1	1	2	1			13.7	
	III	12		3	2	3	1	1	2					14.1	
	IV	3			1	1			1					14.7	
C. maculatus[1]	I	18								3	6	5	4	19.6	ns
	II	12									4	6	2	20.0	
	III	10								1	3	6		19.5	
	IV	0													
Ammodytes sp.	I	72					5	16	22	15	4	4	6	7.7	ns
	II	9						3		1	1	2	2	8.9	
	III	0													
	IV	1										1		10.0	
H. americanus[1]	I	8		1		4	1	1	1					14.5	III>I
	II	15			1		3	3	4	1	2	1		16.7	
	III	5							3	1		1		17.8	
	IV	2											2	23.0	
L. coheni	I	19					4	3	4	1	1	6		7.5	II>I
	II	7								1			6	11.0	
	IV	0													
	V	0													
M. aenaeus	I	22					2	15	5					6.1	ns
	II	9					4	4			1			5.9	
	III	2						1	1					6.5	
	V	2					1	1						5.5	
M. octodecimspinosus	I	200						1	12	46	45	40	56	9.6	II>I
	II	16							2	1	2		11	10.4	
	III	0													
	IV	0													
M. scorpius	I	38						1		1		6	30	11.5	II>I
	II	13											13	14.0	
	VI	0													
	VII	0													

[1] scale + 10 mm.

were examined in detail (Table 5). Relative abundances of fishes changed over the course of the study in both 1997 and 1998 (Fig. 3). Three factors (species assemblages) were retained from the PCA of the relative abundance matrices in each year. In 1997, MANOVA and *post hoc* comparisons of mean factor scores indicated a significant temporal effect on factors 1 and 2 (Wilk's lambda=0.198, $P<0.0001$). Values for taxa that were most abundant in June (*E. cim-*

Table 5

Product-moment correlations between principal component scores and the angularly transformed relative abundances of larval fishes. Underlined values significant at $P < 0.05$, adjusted for multiple comparisons such that $P < 0.004$ for a significant correlation. Rotated factor 1 explained 36% of the total variance, factor 2 explained 20%, and factor 3 explained 15% in 1997, and rotated factor 1 explained 35% of the total variance, factor 2 explained 28%, and factor 3 explained 11% in 1998.

	1997			1998		
Taxon	Factor 1	Factor 2	Factor 3	Factor 1	Factor 2	Factor 3
Clupea harengus				0.05	0.51	–0.04
Mallotus villosus	0.02	–0.16	0.08			
Enchelyopus cimbrius	0.44	–0.14	0.11			
Lumpenus lampraetiformis				–0.07	0.34	0.02
Ulvaria subbifurcata	0.97	–0.22	0.10	–0.11	–0.11	0.05
Pholis gunnellus	–0.22	0.46	–0.41	0.67	0.40	0.58
Cryptacanthodes maculatus	–0.14	0.23	–0.39	0.63	–0.01	0.11
Ammodytes sp.	–0.17	0.98	0.05	0.06	0.92	0.31
Hemitripterus americanus	–0.15	0.37	–0.27	0.13	0.02	0.73
Myoxocephalus aenaeus	–0.12	0.31	–0.13	0.41	0.58	0.35
M. octodecimspinosus	–0.14	0.07	–0.41	0.80	0.58	–0.07
M. scorpius				0.56	0.66	0.17
Liparis atlanticus	0.39	–0.13	0.55	–0.42	0.16	–0.05
L. coheni				0.67	0.10	0.40
Pleuronectes americanus	0.06	–0.23	0.89	–0.20	–0.09	–0.13
Hippoglossoides platessoides	0.48	–0.07	0.27			

brius, H. plattesoides, U. subbifurcata) were uniformly positively correlated with factor 1. Species that were most abundant earlier in the year (*Ammodytes sp., H. americanus, M. aenaeus, P. gunnellus*) were positively correlated with factor 2. Values for several species (*C. maculatus, M. octodecimspinosus,* and *P. americanus*) were not significantly correlated to either factor 1 or 2, but were correlated to factor 3. In 1998, MANOVA and *post hoc* comparisons of mean factor scores indicated a significant temporal effect on factors 1 and 2 (Wilk's lambda=0.341, $P<0.0001$). Values for taxa that were more abundant in March (*Ammodytes sp., C. maculatus, C. harengus, L. coheni, M. aenaeus, M. octodecimspinosus, M. scorpius*) were uniformly positively correlated with factor 1 or factor 2, or with both factors. Values for *H. americanus* were not significantly correlated to either factor 1 or 2, but were highly correlated to factor 3 as their relative abundances increased in April.

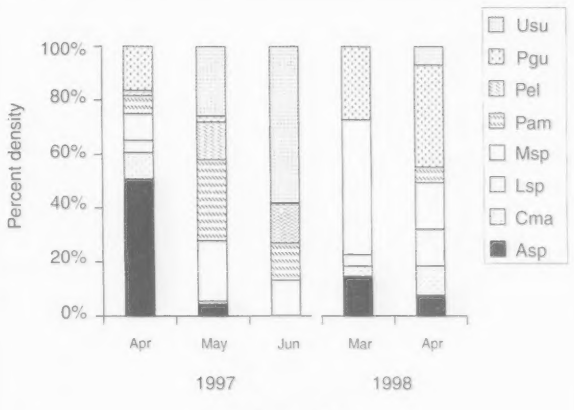

Figure 3

Percent density (number/100 m^3) by month of the dominant larval fishes collected with 1.0-m plankton net in Penobscot Bay, Maine, from April to June 1997 and from March to April, 1998. Asp = *Ammodytes* sp., Cma = *Cryptacanthodes maculatus*, Lsp = *Liparis* spp., Msp = *Myoxocephalus* spp., Pam = *Pleuronectes americanus*, Pel = pelagic spp., Pgu = *Pholis gunnellus*, Usu = *Ulvaria subbiffurcata*.

Assemblage composition was similar among sampling locations as indicated by MANOVA of mean factor scores in 1997 and 1998. In 1997, MANOVA (Wilk's lambda=0.985, $P>0.10$) indicated that means for lower bay, midbay and upper bay sites were not significantly different from each other for any factor. Similarly, MANOVA (Wilk's lambda=0.831, $P>0.08$) indicated that means for lower estuary and bay sites were not significantly different for any factor in 1998.

CCA revealed significant overall association between factor scores from the PCA of the relative fish abundances and environmental variables in 1997 (Wilk's lambda=0.17,

$P<0.0001$) and 1998 (Wilk's lambda=0.21, $P<0.0001$). In 1997, the first canonical correlation (Table 6) indicated that the relative abundance of larval fishes with high positive loading on factor 1 (*E. cimbrius, H. plattesoides,* and *U. subbifurcata*) exhibited a positive association with temperature. These taxa also exhibited a weaker negative association with plankton volume and salinity. Fish taxa that loaded positively on factor 2 were negatively associated with temperature and positively associated with plankton volume and salinity. These species included *Ammodytes sp., H. americanus, M. aenaeus,* and *P. gunnellus.* Fish taxa that loaded positively on factor 3 (*L. atlanticus* and *P. americanus*) were positively associated with temperature and were present in every month sampled. In 1998, the first canonical correlation (Table 6) indicated that the relative abundance of larval fishes with high positive loading on factor 1 (*C. maculatus, L. coheni*, and *P. gunnellus*) and factor 2 (*Ammodytes* sp., *C. harengus*, and *M. aenaeus*) all exhibited a negative association with temperature and a positive association with plankton volume. There was no correlation between factor 3 scores and environmental data for the first canonical correlation (Table 6).

Discussion

Species composition

Ichthyoplankton typical of the Gulf of Maine and the Northwest Atlantic was observed in Penobscot Bay: liparids, sculpins (*Myoxocephalus* spp.), *Ammodytes* sp., *P. gunnellus, U. subbifurcata*, and *P. americanus.* The dominant species are similar to those previously reported for areas of the Maine coast, including the Sheepscot estuary (Graham and Boyar, 1965; Hauser, 1973; Shaw, 1981), the central Maine coast and estuaries (Chenoweth, 1973), the Damariscotta River estuary (Lee, 1975; Laroche, 1980; 1982; Townsend, 1981; 1984), and Sullivan Harbor (Townsend, 1984). Of the twenty-two species collected in the Damariscotta estuary and 21 species collected in Sullivan Harbor (Townsend, 1984), 17 and 18 of these species, respectively, occurred in Penobscot Bay. The dominant species in these two systems was *P. gunnellus* along with the three species of *Myoxocephalus* and a stichaeid, *Lumpenus lampraetiformis* (Townsend, 1984). Twenty-two kinds of boreal larvae with centers of abundance north of the mid-Atlantic coast were found in the Damariscotta and Sheepscot estuaries and along the central coast of Maine (Chenoweth, 1973), and 18 of these taxa were also found in Penobscot Bay. *Pholis gunnellus*, *Liparis* sp., *C. maculatus*, *L. lumpraetiformis*, and Cottidae accounted for 91% of the total catch; the number of larvae declined sharply in spring with the end of the larval stage of these dominant species before reaching a low point in July and August (Chenoweth, 1973). The ichthyoplankton of the St. Lawrence estuary, principally osmerids, gadids, cottids, cyclopterids and pleuronectids, consisted of 25 species (Able, 1978) and 15 of these also occurred in Penobscot Bay.

Significance of demersal eggs

The ichthyoplankton community of Penobscot Bay is dominated by larvae that hatch from demersal eggs within the estuary, whereas larvae that hatched from pelagic eggs are rare. This finding was first noted for the Mystic River estuary (Pearcy and Richards, 1962) and subsequently for the Sheepscot and Damariscotta estuaries (Chenoweth, 1973). Able (1978) observed that the St. Lawrence estuary was almost exclusively inhabited by larvae that hatched from demersal eggs, primarily cottids, stichaeids, *P. americanus*, and *C. harengus* and that the larvae from pelagic eggs were merely strays from more offshore waters. In all of these areas, larvae that hatched from demersal eggs dominated the catch within the estuary, whereas larvae that hatched from pelagic eggs were more common at the mouth of the estuary or adjacent ocean.

Table 6

Canonical correlation coefficients for relative larval fish abundance factor scores and environmental variables in 1997 and 1998. Underlined values significant at $P = 0.05$, adjusted for multiple comparisons such that $P < 0.004$ for a significant correlation.

	1997		1998	
Variables	Standardized coefficients	Correlation with canonical variables	Standardized coefficients	Correlation with canonical variables
Larval fish relative abundance				
Factor 1	0.63	0.66	–0.66	–0.65
Factor 2	–0.58	–0.61	–0.74	–0.74
Factor 3	0.46	0.49	–0.16	–0.09
Environment				
Depth	–0.06	–0.19	0.24	0.36
Plankton	–0.02	–0.37	–0.28	–0.82
Temperature	1.00	1.00	0.66	0.94
Salinity	0.07	–0.21	0.19	0.37

The dominant fishes in Penobscot Bay lay demersal and adhesive eggs (Bigelow and Schroeder, 1953). Fourteen of 16 species (87%) of larvae collected in Penobscot Bay in 1998 and and 17 of 22 (78%) of the larvae collected in 1997 hatched from demersal eggs. Twenty-two species of larvae were taken in the central coastal area of Maine and a comparatively large number of pelagic-egg species (41%) compared with demersal-egg species, as might be expected in an area strongly influenced by coastal water (Chenoweth, 1973). In upper Sheepscot Bay, 42 species of fish larvae were taken (Shaw, 1981), but this relatively high number reflects the long time series (nine years) of this survey and the inclusion of several coastal species that were rare in the total catch. Even so, these catches were dominated by demersal egg-laying species (76%). In the Damariscotta estuary and Sullivan Harbor, only one of 22 species (<5%) taken as larvae came from pelagic eggs (Townsend, 1981; 1984). The ichthyoplankton of the St. Lawrence estuary were almost exclusively forms from demersal eggs (Able, 1978) and only seven of 25 (28%) larval forms collected came from pelagic eggs. However, pelagic eggs did occur in the St. Lawrence estuary, but these were usually nonresident species, such as *S. scombrus* and *G. morhua*, whose larvae were virtually absent from the upper bay. *Gadus morhua* were very rare in Penobscot Bay and the Sheepscot estuary (Chenoweth, 1973; Shaw, 1981) and were absent from the Damariscotta estuary and Sullivan Harbor (Townsend, 1984). Typically, the abundance of larvae from demersal eggs peaked in the winter–spring period whereas larvae from pelagic eggs peaked in the summer (Chenoweth, 1973).

Egg type has major implications on larval fish ecology. Coastal shelf spawners, such as *G. morhua*, *E. cimbrius*, *H. plattesoides*, and *T. adspersus* lay pelagic eggs that may be dispersed over a wide area by the counterclockwise current flow in the Gulf of Maine (Sherman et al., 1984). Nearshore spawners, such as *P. americanus*, *P. gunnellus*, *Myoxocephalus* spp., *U. subbifurcata*, and *C. harengus* lay demersal eggs and depend on protected areas of the coastline for nursery areas. Larvae that hatch from demersal eggs are less likely to be transported out of their nearshore nursery grounds, rather they are entrained in the landward moving bottom layer (Pearcy and Richards, 1962; Norcross and Shaw, 1984).

Variation in distribution and abundance

Larval fish assemblage composition in Penobscot Bay varied considerably over time but not among sampling locations. Interannual and monthly differences in both species composition and abundance of ichthyoplankton in the bay appeared to be associated with differences in environmental conditions, particularly with temperature. Temporal patterns of larval fish abundance corresponded with seasonality of reproduction (Bigelow and Schroeder, 1953). Larvae that hatched from demersal eggs from late winter through early spring, such as *Myoxocephalus* spp., *Ammodytes* sp., and *Pholis gunnellus*, were abundant in Penobscot Bay in March and April and gradually their numbers in plankton samples declined. Such a spawning pattern suggests that adults use the bay and nearshore areas for an extended period of time. Larvae of taxa that hatch later in spring such as *P. americanus*, *L. atlanticus* and *U. subbifurcata*, were abundant in Penobscot Bay in May and June.

These results suggest that temperature is the principal factor controlling the temporal occurrence of fish larvae in Penobscot Bay. Temperature is a primary factor associated with the occurrence and distribution of young stages of fish inhabiting temperate and cold oceans (Obenchain, 1981; Frank and Leggett, 1982; Laprise and Pepin, 1995). This association may be critical in ecosystems characterized by a short growing season (Conover, 1992). However, the influence of temperature on larval occurrence no doubt resulted from species-specific responses of spawning adults. The late winter-early spring species, such as *Myoxocephalus* spp., *Ammodytes* sp., and *Pholis gunnellus*, had a negative association with temperature, whereas late-spring spawners, such as *P. americanus*, *L. atlanticus*, and *U. subbifurcata*, had a positive association. The synchronous emergence of the larvae of several species of fishes in the planktonic environment may be a strategy to further reduce predation (Frank and Leggett, 1983) regardless of temperature. The association observed in this study between salinity and ichthyoplankton may be artifactual. Although the influences of temperature and salinity could not be separated, it seems unlikely that the minute differences in salinity observed between samples would greatly affect marine animals.

Penobscot Bay plays an important role in the early life history of fish inhabiting the central coast of Maine by offering favorable habitat for ichthyoplankton. A hydrographic front off of Penobscot Bay separates the coastline into two different hydrographic regimes (Bigelow, 1927). West of Penobscot Bay, a combination of increased runoff and reduced tidal mixing, favors more rapid development of vertical stratification in spring and summer. East of Penobscot Bay, tidal mixing is enhanced and the development of vertical stratification is much reduced throughout the summer months. Vertical stability of the water column is controlled more by salinity stratification than by temperature, and peaks of stability are the result of influxes of low-salinity surface waters (Townsend, 1984). Therefore, the peak in abundance of both phytoplankton and zooplankton occurs earlier in the western Gulf of Maine and gradually spreads to the east with the onset of vertical stratification during spring and summer (Bigelow, 1927).

Marine fishes may be categorized as those that use the estuaries, such as Penobscot Bay, as primary spawning and nursery areas and those that do not. Winter–early-spring spawning species (*P. gunnellus*, *Ammodytes* sp., *H. americanus*, *Myoxocephalus* spp.) belong to the first group of resident demersal fishes whose larvae hatch from demersal eggs and use the bays and estuaries as nursery areas. Typically, these larvae disappear from collections in April and May. Two species that spawn in late spring, *P. americanus* and *U. subbifurcata*, also use Penobscot Bay as a spawning and nursery habitat and have areas of greatest larval abundance in the midbay and lower bay, respectively. The larvae of *E. cimbrius*, *G. morhua*, *T. adspersus*, *S. scombrus* and *H. plattessoides*, although present,

were not abundant in spring and early summer; therefore Penobscot Bay does not appear to be a primary nursery area for these species. Possibly the numbers of spawning adults of these species are low in the bay or the pelagic eggs that they produce are dispersed before hatching, or both the number of spawning adults are low and the pelagic eggs they produce are dispersed before hatching. Penobscot Bay appears to act as a nursery for many fishes; therefore degradation of water quality during the vernal period would have wide reaching effects on the nearshore fish community.

Acknowledgments

I would like to thank Captain Kevin Lapham for his excellent command of the RV *Nucella* and Lou VanGuelpen of the Atlantic Reference Center at Huntsman Marine Laboratory, New Brunswick. Stan Chenoweth and three anonymous reviewers provided helpful comments to an early draft. This study was supported by a grant from the National Environmental, Data, and Satellite Information Service (NESDIS) through the Island Institute, Rockland, Maine.

Literature cited

Able, K. W.
1978. Ichthyoplankton of the St. Lawrence estuary: composition, distribution and abundance. J. Fish. Res. Board Can. 35:1518–1531.

Bigelow, H. B.
1926. Plankton of the offshore waters of the Gulf of Maine. Bull. U.S.Bur. Fish., vol. XL, 1924, part II, 509 p.
1927. Physical oceanography of the Gulf of Maine. Bull. U.S. Bur. Fish. 40:511–1027.

Bigelow, H. B., and W. C. Schroeder.
1953. Fishes of the Gulf of Maine. U.S. Fish and Wildl. Serv. Fish. Bull. 53(74), 477 p.

Chenoweth, S. B.
1973. Fish larvae of the estuaries and Coast of central Maine. Fish. Bull. 71(1):105–113.

Conover, D. O.
1992. Seasonality and the scheduling of life history at different latitudes. J. Fish Biol. 41 (suppl. B):161–178.

Cushing, D. H.
1975. Marine ecology and fisheries. Cambridge Univ. Press, Cambridge, England, 278 p.

Day, R. W., and G. P. Quinn.
1989. Comparisons of treatments after an analysis of variance in ecology. Ecological Monographs 59:433–463.

Fish, C. J., and M. W. Johnson.
1937. The biology of the zooplankton in the Bay of Fundy and Gulf of Maine with special reference to production and distribution. J. Biol. Board Can. 3:189–322.

Frank, K. T., and W. C. Leggett.
1982. Coastal water mass replacement: its effect on zooplankton dynamics and the predator-prey complex associated with larval capelin (*Mallotus villosus*). Can. J. Fish. Aquat. Sci. 39:991–1003.
1983. Multispecies larval fish associations: accident or adaptation? Can. J. Fish. Aquat. Sci. 40:754–762.

Gauch, H. G.
1982. Multivariate analysis in community ecology. Cambridge Univ. Press, Cambridge, England, 298 p.

Graham, J. J.
1972. Retention of larval herring within the Sheepscot estuary of Maine. Fish. Bull. 70 (2):299–305.

Graham, J. J., and H. C. Boyar.
1965. Ecology of herring larvae in the coastal waters of Maine. Internationa Commission for the Northwest Atlantic Fisheries (ICNAF) Spec. Publ. 6:625–634.

Haefner, P. A.
1967. Hydrography of the Penobscot Bay (Maine) estuary. J. Fish. Res. Board Can. 24:1553–1571.

Hauser, W. J.
1973. Larval fish ecology of the Sheepscot River-Montsweag Bay estuary, Maine. PhD. diss., Univ. Maine, Orono, ME, 79 p.

Hjort, T. J.
1914. Fluctuations in the great fisheries of northern Europe viewed in light of biological research. Rapp. P.-V Cons. Perm. Int. Explor. Mer 20, 228 p.

Laprise, R., and P. Pepin.
1995. Factors influencing the spatio-temporal occurrence of fish eggs and larvae in a northern, physically dynamic coastal environment. Mar. Ecol. Prog. Ser. 122:73–92.

Laroche, J. L.
1980. Larval and juvenile abundance, distribution, and larval food habits of the larvae of five species of sculpins (Family: Cottidae) in the Damariscotta River estuary, Maine. PhD. diss., Univ. Maine, Orono, ME, 169 p.
1982. Trophic patterns among larvae of five species of sculpins (Family: Cottidae) in a Maine estuary. Fish. Bull. 80:827–840.

Lee, W. Y.
1975. Succession and some aspects of population dynamics of copepods in the Damariscotta River estuary, Maine. PhD. diss., Univ., Maine, Orono, ME, 181 p.

Leggett, W. C., and E. Deblois.
1994. Recruitment in marine fishes: Is it regulated by starvation and predation in the egg larval stages? Neth. J. Sea Res. 32:119–134.

Marak, R. R.
1960. Food habits of larval cod, haddock and coalfish in the Gulf of Maine and Georges Bank area. J. Cons. Int. Explor. Mer 25:147–157.

Marak, R. R., and J. B. Colton Jr.
1961. Distribution of fish eggs and larvae, temperature and salinity in the Georges Bank, Gulf of Maine area, 1953. U.S. Fish Wildl. Serv. Spec. Sci. Rep. Fish. 398, 61 p.
1962. Distribution of fish eggs and larvae, temperature and salinity in the Georges Bank, Gulf of Maine area, 1956. U.S. Fish Wild. Serv. Spec. Sci. Rep. Fish. 411, 66 p.

Norcross, B. L., and R. F. Shaw
1984. Oceanic and estuarine transport of fish eggs and larvae: a review. Trans. Am. Fish. Soc. 113(2):153–165.

Obenchain, C. L.
1981. A study of the larval fish community in the New York Bight, July 1974 to June 1976. Rapp. P.-V Reun. Cons. Int. Explor. Mer 178:217–219.

Pearcy, W. G., and S. W. Richards.
1962. Distribution and ecology of fishes of the Mystic River, Connecticut. Ecology 43(2):248–259.

Pielou, E. C.
1984. The interpretation of ecological data. John Wiley and Sons, New York, NY, 286 p.

Shaw, R.
1981. Seasonal species composition, diversity, spatial distributions and tidal retention and transport of ichthyoplankton in the Sheepscot River-Back River-Montsweag Bay estuary system, Maine. PhD. diss., Univ. Maine, Orono ME, 285 p.
Sherman, K.W., W. Smith, W. Morse, and M. Berman.
1984. Spawning strategies of fishes in relation to circulation, phytoplankton production and pulses in zooplankton off the northeast United States. Mar. Ecol. Prog. Ser. 18:1–19.
Sokal, R.R., and F. J. Rohlf.
1981. Biometry. W. H. Freeman and Company, New York, NY, 859 p.
Stevens, J.
1986. Applied multivariate statistics for the social sciences. Lawrence Erlbaum and Associates, Hillsdale, NJ, 341 p.
Townsend, D.W.
1981. Comparative ecology and population dynamics of larval fishes and zooplankton in two hydrographically different areas on the Maine coast. PhD. diss., Univ. Maine, Orono, ME, 282 p.
1983. The relations between larval fishes and zooplankton in two inshore areas of the Gulf of Maine. J. Plankton Res. 5(2):145–173.
1984. Comparison of inshore zooplankton and ichthyoplankton in the Gulf of Maine. Mar. Ecol. Prog. Ser. 15: 79–90.

Population structure of Fraser River chinook salmon (*Oncorhynchus tshawytscha*): an analysis using microsatellite DNA markers

R. John Nelson
Maureen P. Small
Terry D. Beacham
K. Janine Supernault

Pacific Biological Station
Nanaimo, British Columbia
V9R 5K6, Canada
Present address (for R. J. Nelson): SeaStar Biotech Inc.
32056-3749 Shelbourne St.
Victoria, British Columbia
V8P 5S2 Canada
E-mail address (for R. J. Nelson): jnelson@seastarbio.com

Abstract–Microsatellite DNA analysis was applied in a genetic study of 20 chinook salmon populations from four regions within the Fraser River drainage of British Columbia, Canada. Twelve populations were represented by samples collected in different years. A total of 2612 fish were examined at three microsatellite loci. Each locus was highly polymorphic, with 30 alleles at *Ots*101, 28 alleles at *Ots*100, and 35 alleles at *Ots*102. Average observed heterozygosities were 86%, 88%, and 71%, respectively. In a dendrogram analysis of pairwise genetic distances, four geographically based groups were observed consisting of the lower Fraser River, the middle Fraser River, the upper Fraser River, and the Thompson River. An analysis of molecular variance showed that 97.57% of the genetic variance was within populations and 1.80% of the genetic variance was partitioned among populations. We detected significantly different allele frequencies among populations within regional groupings and temporal stability in allele frequencies in populations for which multiple years of samples were analyzed. Regional divergence may reflect colonization patterns following the last ice age, and divergence among populations within regions may reflect local adaptation. The elucidation of population structure of chinook salmon of the Fraser River watershed will be useful information for management designed to conserve genetic biodiversity.

Manuscript accepted 14 July 2000.
Fish. Bull. 99:94–107 (2001).

The Fraser River watershed produces greater numbers of Pacific salmon than any other river system in British Columbia (B.C.). Approximately 65 tributaries of the Fraser River are used as spawning and rearing habitat for chinook salmon (*Oncorhynchus tshawytscha*), and these streams produce up to one third of the commercial catch of chinook salmon from Brirish Columbia (Fraser et al., 1982). Although chinook salmon account for only 1% to 5% of the total escapements of salmon within the watershed (Northcote and Atagi, 1997), these fish are an important cultural, sporting, and food resource. Chinook salmon populations in the Fraser watershed have been negatively impacted by a variety of forces, in some cases reducing (Bradford, 1994) or completely eliminating (Slaney et al., 1996) local populations.

Historical efforts to maintain and enhance salmon runs through transplantation have had mixed results, illustrating that the characteristics of a population influence its ability to thrive in a given environment (Wood, 1995). Also, transplantation of fish and hatchery production practices may alter genetic composition of wild stocks (Waples, 1994). In fisheries, it is important not to over harvest small populations that may contain unique adaptive traits. For the above reasons it is advantageous to understand how population structures evolve in order to protect individual salmon runs and to preserve biodiversity.

Most of the chinook salmon populations of B.C. were founded after the ice of the Wisconsin glaciation retreated approximately 10,000 to 15,000 year ago (McPhail and Lindsey, 1986). If chinook salmon recolonization is similar to that of sockeye and coho salmon (Wood et al., 1994; Small et al., 1998a), reestablishment of the present day B.C. chinook salmon populations may have occurred from at least two different sources, Beringia to the north and Cascadia to the south (Gharrett et al., 1987), and possibly from a refuge in the Queen Charlotte Islands (Warner et al., 1982). The genetic character of the founding fish may be reflected in present day genetic structure, but because Pacific salmon return to their natal streams to spawn (Scheer, 1939; Quinn, 1984), reproductive isolation can lead to divergence of phenotypic and genotypic characters. Neutral genetic markers can be used to measure the degree of reproductive isolation and potential for local adaptation.

Over the years, a variety of methods have been used to examine population structure. Allozyme analysis has long been a mainstay in fish genetics research and has been used to determine population structure in chinook salmon of Alaska (Gharrett et al., 1987), from California to Alaska (Utter et al., 1989), of the Yukon River (Beacham et

al., 1989; Wilmot et al., 1992), of California and Oregon (Bartley et al. 1992), and in British Columbia (Teel et al. 2000). These studies suggest that chinook salmon populations were genetically heterogeneous and that populations could be placed into genetically defined groups corresponding to geographic regions. In some of the earlier studies there was little genetic distinction between geographically separate groups because the allozyme markers showed low polymorphism. However, using 25 polymorphic allozymes, Teel et al. (2000) detected strong population divergence within the Fraser River and among major rivers in British Columbia.

DNA markers can be more polymorphic than allozyme markers and thus may be more sensitive to population structure; with higher levels of polymorphism, there is an increased likelihood for populations to contain unique alleles or to have frequency differences in alleles that are shared among populations. Among the DNA-based markers, mitochondrial DNA has been used to examine genetic structure in chinook salmon populations of the West Coast of North America (Wilson et al., 1987; Cronin et al., 1993). These studies suggest that there is structuring among West Coast chinook salmon populations. However, the low resolution of this method limits its utility. Minisatellite DNA has been used to study Canadian chinook salmon populations. Beacham et al. (1996) found that chinook salmon formed two major regional groups in British Columbia: a southern group consisting of populations of the Fraser River, Vancouver Island, and the southern mainland; and a northern group consisting of populations of the Skeena River, the Yukon River, and the northern mainland. However, owing to technical complexity, the technique is unsuitable for studies involving large numbers of individuals.

Microsatellite DNA loci are highly polymorphic and technically easy to use (Nelson et al., 1998) and provide powerful markers for elucidating population structure. Microsatellite loci have provided information regarding population divergence in chinook salmon (Banks et al., 1996) and other salmonids (Angers et al., 1995; Scribner et al., 1996; Nelson et al., 1998; Small et al., 1998a, 1998b). In our study we exploited the ease of analysis and the highly polymorphic nature of microsatellite DNA loci to study population structure of chinook salmon. We surveyed variation at three microsatellite loci within 20 Fraser River chinook salmon populations and examined temporal stability of microsatellite allele frequencies. We used this information to hypothesize the genetic structure of chinook salmon populations within the Fraser River watershed.

Materials and methods

DNA extraction

Liver or scale samples were analyzed from 2612 individual chinook salmon from 20 populations of the Fraser and Thompson River watersheds (Fig. 1.). Sample sizes ranged from 30 to 347 fish (Table 1). Liver samples were obtained from spawning wild adults. Hatchery adults were sources for the Chehalis-red and Chilliwack-red samples. The nomenclature "-red" refers to the red flesh color of the fish in the population. DNA was extracted from liver and scales archived on scale cards according to the methods of Nelson et al. (1998). Liver samples taken prior to 1994 were subjected to DNA extractions as described in Beacham et al. (1996). Each 25 µL of polymerase chain reaction (PCR) required either 100 ng of genomic DNA, 0.1 to 1 µL of liver extracts, or 5 to 10 µL of scale extract.

PCR amplification

The loci amplified in this work were *Ots*100 (Nelson et al., 1998), *Ots*101 (Small et al., 1998a) and *Ots*102 (Nelson and Beacham, 1999). PCR amplification was carried out in 96-well microtiter plates with a MJ PTC-100 thermal cycler (MJ research, Watertown, MA). 25-µL PCR reactions contained 10 pmol (0.4 µM) of each primer, 80 µM of each nucleotide, 20 mM tris-pH 8.8, 2 mM $MgSO_4$, 10 mM KCl, 0.1% triton ×–100, 10 mM $(NH_4)SO_4$, and 0.1 mg/mL of bovine serum albumin. Primer set *Ots*100 required a 10% final volume of glycerol in the PCR. PCR temperature cycles were preceded by a denaturation incubation of 3 min at 94°C; samples then were held at 80°C while 1 unit of DNA polymerase was added. PCR cycle parameters and primer sequences for each locus are presented in Table 2. Three µLs of 10× loading dye (50 mM EDTA pH 8.0, 30% glycerol, 0.25% bromphenol blue) were added to each reaction and ten µLs of this solution was loaded on each gel lane for electrophoresis.

Gel electrophoresis

Microsatellite alleles were size-fractionated on nondenaturing polyacrylamide gels 17 cm wide by 14.5 cm long. Gels consisted of a 19:1 ratio of acrylamide to bis-acrylamide. Gel contained 2× TAE buffer (Maniatis et al., 1982) as did the gel box reservoirs. Electrophoretic conditions are described in Table 2. Each gel included three 20 base-pair (bp) marker lanes (GenSura Labs Inc., Del Mar, CA) to create a molecular size grid for sizing amplified microsatellites, 24 population samples, and one "standard fish" to estimate the precision of allele sizes (Table 3). Standard deviations were calculated for alleles from two different standard fish for each primer set. Gels were stained with 0.5 µg/mL of ethidium bromide in water and visualized with ultraviolet light (Fig. 2).

Digital images of gels were obtained as described in Nelson et al. (1998). Individual alleles were identified by using the procedure outlined in Small et al. (1998a). A four-bp bin was used for all *Ots*101 alleles. A four-bp bin was used to define smaller alleles of *Ots*100 and five- to eight-bp bins were used for larger alleles. A four-bp bin was used for the smaller alleles of *Ots*102 and five- to six-bp bins were used for larger alleles. These bin sizes (see Table 1 for bin designations) were four or more standard deviations wide according to estimates derived from the standard fish. Bins are referred to as "alleles" throughout the text.

Table 1

Allele frequencies, observed heterozygosity (H_o), and expected heterozygosity (H_e) at loci *Ots*101, *Ots*100, and *Ots*102 for 20 chinook salmon zygosity. The allele number (in basepairs) is the lower limit of the bin. The weighted mean of allele frequencies for regions (L Fr=lower Fraser;

***Ots*101**

Alleles	Harrison 326	Chilliwack White 181	L Fr 507	Quesnel 186	Stuart 294	Nechako 187	Chilko 120	Bridge 56	Cottonwood 51	Mid Fr 893	Tete Jaune 249	Chilliwack Red 29
142	0	0	0	0	0.002	0	0	0	0	0.001	0	0
146	0	0	0	0.008	0.003	0	0.004	0	0	0.003	0	0
150	0	0.003	0.001	0.054	0.02	0.045	0.008	0	0	0.029	0.002	0.017
154	0.003	0.003	0.003	0.056	0.066	0.048	0.042	0.027	0.029	0.053	0.008	0
158	0	0.008	0.003	0.062	0.029	0.059	0.025	0.045	0.127	0.048	0.028	0
162	0.005	0.003	0.004	0.016	0.02	0.064	0.017	0.089	0.078	0.036	0.06	0.052
166	0.035	0.017	0.029	0.046	0.02	0.027	0.017	0.089	0	0.029	0.014	0.034
170	0.014	0.025	0.018	0.054	0.01	0.003	0.017	0.027	0	0.019	0.004	0
174	0.015	0.039	0.024	0.024	0.01	0.019	0.05	0.009	0	0.02	0.036	0
178	0.046	0.028	0.039	0.019	0.015	0.019	0.071	0.071	0.059	0.03	0.042	0.017
182	0.067	0.014	0.048	0.03	0.029	0.037	0.025	0.027	0.049	0.031	0.032	0.034
186	0.069	0.05	0.062	0.054	0.066	0.08	0.038	0.045	0.118	0.064	0.034	0.069
190	0.075	0.11	0.088	0.032	0.097	0.061	0.117	0.089	0.108	0.079	0.112	0.017
194	0.112	0.066	0.096	0.129	0.075	0.04	0.146	0.098	0.118	0.092	0.078	0.121
198	0.126	0.155	0.136	0.097	0.138	0.123	0.117	0.063	0.108	0.117	0.104	0.121
202	0.118	0.08	0.105	0.081	0.109	0.107	0.083	0	0.088	0.091	0.08	0.138
206	0.09	0.072	0.084	0.056	0.068	0.061	0.083	0.045	0.059	0.064	0.058	0.069
210	0.063	0.077	0.068	0.048	0.071	0.04	0.025	0.134	0.049	0.057	0.098	0.034
214	0.044	0.075	0.055	0.038	0.048	0.029	0.004	0.018	0	0.031	0.026	0
218	0.015	0.003	0.011	0.022	0.024	0.053	0.021	0.036	0	0.028	0.042	0.086
222	0.026	0.022	0.025	0.016	0.01	0.021	0.008	0.036	0	0.015	0.06	0.138
226	0.026	0.041	0.032	0.022	0.017	0.011	0.004	0	0	0.013	0.04	0.017
230	0.017	0.03	0.022	0.011	0.015	0.013	0.021	0	0	0.013	0.014	0.017
234	0.014	0.014	0.014	0	0.01	0.011	0.013	0.009	0	0.008	0.012	0
238	0.005	0.008	0.006	0	0.005	0.011	0.021	0.027	0	0.008	0.012	0
242	0.006	0.017	0.01	0.005	0.007	0.008	0.017	0.018	0	0.008	0	0
246	0.003	0.019	0.009	0.008	0.007	0.005	0	0	0.01	0.006	0	0.017
250	0.003	0.011	0.006	0.008	0	0.003	0	0	0	0.002	0	0
254	0.002	0.008	0.004	0.005	0.005	0	0	0	0	0.003	0	0
259	0	0.003	0.001	0	0.002	0	0.008	0	0	0.002	0	0
Hobs	0.844*	0.889	0.86	0.855	0.881	0.877	0.933	0.839	0.686*	0.868	0.863*	0.897
Hexp	0.926	0.934	0.927	0.94	0.932	0.941	0.925	0.929	0.922	0.939	0.936	0.931

***Ots*100**

Alleles	Harrison 347	Chilliwack White 168	L Fr 515	Quesnel 183	Stuart 226	Nechako 174	Chilko 122	Bridge 55	Cottonwood 53	Mid Fr 813	Tete Jaune 254	Chilliwack Red 30
150	0.001	0	0.001	0	0	0	0	0.018	0	0.001	0	0
207	0.01	0	0.007	0	0.011	0.011	0	0.018	0	0.007	0	0
211	0.016	0.009	0.014	0.008	0.018	0.009	0.004	0	0	0.009	0	0
215	0	0	0	0.003	0.004	0.003	0	0.018	0	0.004	0	0
219	0	0	0	0.003	0	0	0	0	0	0.001	0	0
227	0.001	0.009	0.004	0	0	0	0	0	0	0	0	0
231	0.001	0	0.001	0	0	0	0	0	0	0	0	0.017
235	0.004	0	0.003	0.003	0	0.006	0.078	0.009	0	0.014	0	0

Table 1

populations from the Fraser River drainage. Populations out of Hardy-Weinberg equilibrium are indicated by * next to the observed hetero-Mid Fr=middle Fraser; U Fr=upper Fraser) are given. Sample sizes are provided below population names.

Chehalis Red 30	Bowron 55	Holmes 49	Indianpoint 40	Slim 70	U Fr 522	L Shuswap 192	M Shuswap 195	Eagle 33	Coldwater 37	Nicola 233	Thompson 690
0	0	0	0	0	0	0	0	0	0	0	0
0	0	0	0	0	0	0.003	0	0	0	0	0.001
0	0	0	0.013	0	0.003	0.023	0.008	0	0	0.019	0.015
0.033	0.018	0	0.013	0	0.009	0.023	0.023	0	0	0.028	0.022
0.017	0.036	0	0	0	0.018	0.013	0.015	0	0.027	0.004	0.011
0.017	0.036	0.02	0.063	0	0.043	0.029	0.005	0.03	0.027	0.026	0.021
0	0.009	0.02	0.025	0	0.013	0.013	0.021	0.121	0.054	0.028	0.028
0	0	0	0.013	0	0.003	0.003	0.023	0	0.014	0.039	0.021
0	0.027	0.02	0.013	0	0.023	0.005	0.008	0.015	0.014	0.002	0.006
0.05	0.064	0.092	0.013	0.057	0.048	0.008	0.003	0.106	0.054	0.019	0.017
0.017	0.036	0	0.025	0.057	0.032	0.063	0.085	0.106	0.068	0.105	0.086
0.15	0.091	0.051	0.05	0.007	0.048	0.044	0.074	0.091	0.122	0.06	0.064
0.15	0.082	0.153	0.087	0	0.093	0.065	0.095	0.242	0.054	0.026	0.068
0.05	0.091	0.143	0.138	0.007	0.081	0.182	0.215	0.121	0.041	0.099	0.153
0.133	0.136	0.061	0.175	0.164	0.12	0.195	0.208	0.015	0.068	0.09	0.148
0.1	0.036	0.143	0.1	0.029	0.08	0.068	0.044	0.03	0.068	0.058	0.056
0.067	0.091	0.092	0.05	0.1	0.071	0.109	0.054	0.03	0.054	0.071	0.074
0.067	0.091	0.102	0.063	0.121	0.093	0.094	0.046	0.045	0.108	0.073	0.072
0.017	0.018	0	0.025	0.093	0.03	0.042	0.026	0.015	0.095	0.097	0.057
0	0.018	0.01	0.025	0.007	0.031	0.005	0.018	0	0.068	0.06	0.03
0.033	0.027	0.01	0.063	0.136	0.065	0	0.008	0	0.027	0.026	0.012
0.067	0.045	0.031	0.025	0.114	0.049	0	0.021	0	0	0.021	0.013
0.017	0.036	0.041	0.025	0.05	0.025	0	0	0	0.014	0.009	0.004
0.017	0	0	0	0.036	0.011	0	0.003	0.015	0.014	0.013	0.007
0	0.009	0	0	0.014	0.009	0.008	0	0	0.014	0	0.003
0	0	0	0	0.007	0.001	0.003	0	0	0	0.015	0.006
0	0	0.01	0	0	0.002	0	0	0	0	0.011	0.004
0	0	0	0	0	0	0.003	0	0	0	0	0.001
0	0	0	0	0	0	0	0	0.015	0	0.002	0.001
0	0	0	0	0	0	0	0	0	0	0	0
0.867	0.964	0.776	0.975	0.814	0.86	0.865	0.841	0.636*	0.784	0.888	0.851
0.933	0.927	0.898	0.925	0.9	0.933	0.891	0.882	0.879	0.946	0.94	0.92

Chehalis Red 30	Bowron 50	Holmes 46	Indianpoint 39	Slim 70	U Fr 519	L Shuswap 210	M Shuswap 192	Eagle 31	Coldwater 62	Nicola 268	Thompson 713
0	0	0	0	0	0	0	0	0	0	0	0
0	0	0	0	0	0	0	0	0	0	0	0
0	0.01	0	0	0	0.001	0	0	0	0	0	0
0	0	0	0	0	0	0	0	0	0.024	0	0.002
0	0	0	0	0	0	0	0	0	0	0	0
0	0	0	0	0	0	0	0	0	0	0	0
0	0	0	0	0	0.001	0	0	0	0	0	0
0	0.04	0	0.013	0	0.005	0	0	0	0	0.002	0.001

continued

Table 1 (continued)

***Ots*100 (continued)**

Alleles	Harrison 347	Chilliwack White 168	L Fr 515	Quesnel 183	Stuart 226	Nechako 174	Chilko 122	Bridge 55	Cottonwood 53	Mid Fr 813	Tete Jaune 254	Chilliwack Red 30
239	0.001	0.003	0.002	0.098	0.027	0.032	0.115	0.027	0.009	0.056	0.002	0.1
243	0	0.006	0.002	0.049	0.051	0.029	0.078	0.027	0.085	0.05	0.016	0.067
247	0.006	0.006	0.006	0.022	0.02	0.02	0.012	0	0	0.017	0.033	0.033
251	0.006	0.009	0.007	0.005	0.029	0.009	0	0	0	0.011	0.081	0.033
255	0.004	0	0.003	0.044	0.027	0.055	0.012	0.045	0.009	0.034	0.039	0.017
260	0.019	0.03	0.022	0.101	0.093	0.055	0.012	0.018	0.019	0.065	0.063	0.117
266	0.039	0.024	0.034	0.063	0.1	0.069	0.004	0.027	0.028	0.061	0.039	0.05
271	0.058	0.083	0.066	0.022	0.044	0.023	0.045	0.091	0.057	0.039	0.059	0.1
276	0.032	0.068	0.044	0.06	0.024	0.034	0.004	0.027	0.047	0.033	0.065	0.05
281	0.13	0.083	0.115	0.137	0.08	0.083	0.07	0.073	0.198	0.099	0.091	0.067
288	0.101	0.134	0.112	0.145	0.053	0.075	0.078	0.055	0.057	0.082	0.106	0.017
293	0.111	0.089	0.104	0.046	0.058	0.124	0.053	0.118	0.142	0.078	0.128	0.133
299	0.118	0.077	0.105	0.057	0.097	0.055	0.102	0.1	0.094	0.08	0.089	0.067
305	0.086	0.092	0.088	0.06	0.066	0.057	0.07	0.082	0	0.06	0.057	0.067
311	0.13	0.119	0.126	0.038	0.084	0.069	0.131	0.027	0.075	0.073	0.053	0
318	0.084	0.107	0.091	0.025	0.075	0.095	0.119	0.1	0.17	0.082	0.02	0.033
326	0.026	0.045	0.032	0.003	0.035	0.08	0.012	0.091	0.009	0.036	0.033	0.033
334	0.007	0.003	0.006	0.005	0.004	0.003	0	0.027	0	0.005	0.026	0
342	0.006	0	0.004	0.003	0	0.006	0	0	0	0.002	0	0
358	0.003	0.003	0.003	0	0	0	0	0	0	0	0	0
Hobs	0.876	0.869	0.868	0.907	0.947	0.908	0.893	0.8*	0.849	0.905	0.882	0.867
Hexp	0.911	0.917	0.913	0.923	0.938	0.937	0.918	0.927	0.887	0.939	0.929	0.933

***Ots*102**

Alleles	Harrison 302	Chilliwack White 180	L Fr 482	Quesnel 174	Stuart 255	Nechako 129	Chilko 114	Bridge 47	Cottonwood 48	Mid Fr 767	Tete Jaune 262	Chilliwack Red 29
134	0	0	0	0	0	0	0	0	0	0	0	0
163	0	0	0	0	0	0	0	0	0	0	0	0
167	0	0	0	0	0	0.008	0.004	0.011	0	0.003	0	0
171	0.003	0	0.002	0	0.002	0	0	0	0.021	0.002	0	0
175	0	0.008	0.003	0.02	0.045	0.004	0.009	0	0.01	0.022	0	0.086
179	0.015	0.008	0.012	0.052	0.049	0.07	0.031	0.106	0	0.051	0.008	0.138
183	0.065	0.106	0.08	0.178	0.267	0.163	0.364	0.138	0.229	0.233	0.302	0.224
187	0.038	0.017	0.03	0.066	0.055	0.066	0.039	0.053	0	0.053	0.006	0.017
192	0.023	0	0.015	0	0.004	0.027	0.004	0	0.01	0.007	0	0
197	0.003	0.014	0.007	0.006	0.025	0.008	0.035	0.011	0	0.017	0	0
201	0.007	0.003	0.005	0.02	0.004	0.008	0.013	0	0.01	0.01	0	0.017
205	0.008	0.014	0.01	0.011	0.002	0.008	0	0	0	0.005	0	0
209	0.018	0.047	0.029	0.026	0.012	0.023	0.009	0	0.042	0.018	0.013	0.034
213	0.041	0.047	0.044	0.086	0.065	0.07	0.066	0.245	0.115	0.085	0.073	0.034
217	0.142	0.106	0.129	0.075	0.057	0.101	0.083	0.043	0.313	0.087	0.042	0.069
221	0.151	0.122	0.14	0.057	0.043	0.054	0.083	0.043	0.01	0.052	0.055	0.086
226	0.098	0.106	0.101	0.023	0.029	0.07	0.018	0.064	0	0.033	0.029	0.017
231	0.046	0.081	0.059	0.057	0.122	0.089	0.026	0.053	0.021	0.077	0.015	0.017

Table 1 (continued)

Chehalis Red 30	Bowron 50	Holmes 46	Indianpoint 39	Slim 70	U Fr 519	L Shuswap 210	M Shuswap 192	Eagle 31	Coldwater 62	Nicola 268	Thompson 713
0.033	0.08	0.011	0.09	0.057	0.032	0.002	0	0	0	0.007	0.003
0.033	0.08	0.033	0.103	0.057	0.039	0.002	0.01	0	0	0	0.004
0	0	0.011	0	0.007	0.02	0	0.003	0	0	0	0.001
0	0	0.033	0.051	0	0.048	0.007	0.003	0.016	0	0.007	0.006
0.017	0.02	0.022	0.013	0.007	0.027	0.055	0.044	0.016	0.008	0	0.029
0.167	0.12	0.087	0.141	0.164	0.099	0.048	0.036	0.016	0	0	0.025
0.017	0.03	0.065	0.026	0.029	0.038	0.083	0.065	0.065	0.073	0.083	0.076
0.15	0.04	0.054	0.051	0.1	0.069	0.138	0.094	0.065	0.016	0.018	0.076
0.017	0.11	0.098	0.051	0.121	0.075	0.136	0.096	0.258	0.016	0.014	0.083
0.133	0.15	0.185	0.064	0.093	0.104	0.155	0.201	0.081	0.056	0.023	0.115
0	0.03	0.054	0.077	0.007	0.067	0.067	0.07	0.032	0.073	0.087	0.073
0.183	0.09	0.087	0.09	0.136	0.122	0.112	0.188	0.065	0.073	0.14	0.135
0.1	0.1	0.12	0.064	0.114	0.093	0.076	0.063	0.097	0.065	0.08	0.074
0.017	0.06	0.054	0.077	0.05	0.056	0.069	0.065	0.065	0.145	0.158	0.102
0.017	0.02	0.022	0.038	0.036	0.039	0.026	0.052	0.065	0.032	0.08	0.052
0.05	0	0.043	0.026	0.014	0.022	0.01	0.005	0.032	0.242	0.131	0.067
0.05	0.01	0.011	0.026	0.007	0.026	0.005	0.005	0.097	0.153	0.106	0.053
0.017	0.01	0	0	0	0.014	0.007	0	0.032	0.024	0.062	0.025
0	0	0.011	0	0	0.001	0.002	0	0	0	0.002	0.001
0	0	0	0	0	0	0	0	0	0	0	0
0.933	0.86	0.826	0.923	0.814	0.871	0.914	0.88	0.806	0.855	0.907	0.886
0.9	0.92	0.913	0.923	0.9	0.929	0.9	0.885	0.903	0.871	0.918	0.919

Chehalis Red 30	Bowron 50	Holmes 44	Indianpoint 40	Slim 66	U Fr 521	L Shuswap 185	M Shuswap 167	Eagle 37	Coldwater 54	Nicola 231	Thompson 674
0	0	0	0	0	0	0.027	0	0.054	0	0	0.01
0	0	0	0	0	0	0.03	0	0.027	0	0	0.01
0	0	0	0	0	0	0	0	0	0	0	0
0	0	0	0	0	0	0.008	0.012	0	0.009	0.026	0.015
0	0.02	0.023	0.025	0.045	0.016	0	0.012	0.041	0.167	0.134	0.065
0	0.07	0.08	0.063	0.091	0.041	0.024	0.033	0.149	0.102	0.18	0.093
0.05	0.19	0.193	0.138	0.167	0.233	0.116	0.207	0.135	0.046	0.058	0.114
0.017	0.04	0.011	0	0.015	0.012	0.084	0.174	0.108	0.065	0.017	0.083
0	0.01	0	0.013	0.008	0.003	0	0.009	0	0	0.011	0.006
0	0	0	0.025	0.015	0.004	0.003	0	0	0	0	0.001
0.033	0.02	0.045	0.013	0	0.01	0.003	0	0	0	0	0.001
0	0	0.011	0.025	0.015	0.005	0.003	0.006	0	0	0.002	0.003
0.017	0.03	0.057	0.087	0.061	0.032	0.027	0.051	0	0.019	0.019	0.028
0.167	0.24	0.205	0.162	0.152	0.12	0.035	0.057	0.041	0.148	0.115	0.077
0.183	0.14	0.091	0.087	0.121	0.079	0.049	0.036	0.041	0.157	0.195	0.104
0.1	0.06	0.023	0.038	0.015	0.051	0.024	0.009	0.027	0.046	0.009	0.017
0.05	0.04	0.011	0.038	0.03	0.03	0.014	0.021	0	0.009	0.015	0.015
0.017	0.04	0	0.038	0.03	0.02	0.022	0.006	0	0.046	0.022	0.019

continued

Table 1 (continued)

*Ots*102 (continued)

Alleles	Harrison 302	Chilliwack White 180	L Fr 482	Quesnel 174	Stuart 255	Nechako 129	Chilko 114	Bridge 47	Cottonwood 48	Mid Fr 767	Tete Jaune 262	Chilliwack Red 29
236	0.043	0.067	0.052	0.083	0.045	0.085	0.053	0.032	0.021	0.059	0.053	0.034
241	0.065	0.05	0.059	0.055	0.045	0.043	0.022	0.085	0.031	0.045	0.132	0.069
246	0.05	0.047	0.049	0.009	0.024	0.016	0.031	0.053	0	0.02	0.074	0.017
251	0.03	0.042	0.034	0.026	0.022	0.019	0.009	0	0.01	0.018	0.048	0.034
256	0.038	0.022	0.032	0.032	0.012	0.008	0.044	0.011	0.073	0.024	0.122	0.034
261	0.028	0.039	0.032	0.052	0.022	0.023	0.022	0.032	0.063	0.032	0.021	0
267	0.022	0.017	0.02	0	0.029	0.016	0.009	0	0	0.014	0	0.034
273	0.015	0.003	0.01	0.009	0.016	0.008	0.009	0	0	0.01	0	0
279	0.005	0.003	0.004	0.011	0.002	0	0	0	0.021	0.005	0	0
285	0.01	0.014	0.011	0.006	0	0.004	0	0	0	0.002	0	0
291	0.013	0	0.008	0	0	0.004	0.013	0	0	0.003	0	0.034
297	0.01	0.014	0.011	0.009	0	0.004	0	0	0	0.003	0.004	0
303	0.003	0	0.002	0.029	0.004	0.004	0.004	0.021	0	0.01	0.004	0
309	0.002	0.006	0.003	0	0	0	0	0	0	0	0	0
325	0.005	0	0.003	0.003	0	0	0	0	0	0.001	0	0
321	0.002	0	0.001	0	0	0	0	0	0	0	0	0
333	0.002	0	0.001	0	0	0	0	0	0	0	0	0
Hobs	0.714*	0.628*	0.699	0.632*	0.761*	0.713*	0.684*	0.723	0.833	0.714	0.775*	0.862
Hexp	0.927	0.928	0.927	0.931	0.894	0.93	0.842	0.894	0.833	0.906	0.859	0.897

Table 2

Primer sequences, PCR cycle, and gel-running conditions for microsatellite loci *Ots*100, *Ots*101, and *Ots*102.

Locus	Primer sequence	PCR cycle denature	Anneal	Extend	No. of cycles	Gel conditions: % acrylamide	Gel conditions: Voltage (V)	Gel conditions: Time (h)
*Ots*100	F 5′TGAACATGAGCTGTGTGAG-3′ R 5′-ACGGACGTGCCAGTGAG-3′.	94°C/20s	57°C/20s	72°C/20s	30	7	60	18
*Ots*101	F 5′ACGTCTGACTTCAATGATGTTT-3′ R 5′TATTAATTATCCTCCAACCCAG-3′	94°C/30s	53°C/30s	72°C/30s	30	8	70	17
*Ots*102	F 5′AGGATCCAATAAGGAGTGATA-3′ R 5′ACTAGGTATCCCCTTAACCA-3′	94°C/20s	50°C/10s	72°C/20s	30	6	60	17

Data analysis

A pedigree analysis was performed on chinook salmon families to document the inheritance of microsatellite alleles at each locus. Chinook salmon families were obtained from domesticated strains originating in Robertson Creek and Big Qualicum River, B.C. For each locus, we examined inheritance in 6 families (12 offspring per family). Population genetic data were analyzed by using GENEPOP version 3.1 (Raymond and Rousset, 1995a) and ARLEQUIN version 1.1 (Schneider et al., 1997). Allele frequencies and heterozygosities were estimated for each population at each locus and conformation to Hardy-Weinberg equilibrium (HWE) was tested with a simulated Fisher's exact test (Guo and Thompson, 1992). A gametic disequilibrium test was also performed. Differences in allele frequencies among different sample years, populations, and regions (populations grouped into regions) were examined by using pairwise tests in ARLEQUIN which is analogous to Fisher's exact test (described in Raymond and Rousset, 1995b). An analysis of molecular variation (AMOVA) was also performed by using ARLEQUIN to measure the distribution of molecular variance at several levels: among individuals, among samples taken in different years for the same population, among all populations (with year classes combined), and among regions. *F*-statistics (Wright, 1951) and their stan-

Table 1 (continued)

Chehalis Red 30	Bowron 50	Holmes 44	Indianpoint 40	Slim 66	U Fr 521	L Shuswap 185	M Shuswap 167	Eagle 37	Coldwater 54	Nicola 231	Thompson 674
0.033	0.02	0	0.125	0.038	0.047	0.016	0.006	0	0.019	0.006	0.01
0.2	0.01	0.136	0.013	0.053	0.102	0.005	0	0	0	0.009	0.004
0.017	0.01	0.034	0.025	0.008	0.046	0.014	0.003	0	0	0.006	0.007
0.083	0	0.034	0.025	0.03	0.039	0.008	0.009	0	0	0.004	0.006
0.017	0.01	0.023	0.025	0.03	0.073	0.016	0.009	0	0	0	0.007
0	0.03	0.023	0	0.008	0.016	0.016	0.006	0.014	0	0.002	0.007
0	0	0	0	0	0.002	0.019	0.003	0	0	0	0.006
0.017	0	0	0	0	0.001	0.003	0.006	0.014	0	0.004	0.004
0	0	0	0	0	0	0.016	0.015	0	0	0	0.008
0	0	0	0	0	0	0.011	0.021	0.081	0.009	0	0.013
0	0	0	0.025	0.023	0.007	0.103	0.066	0.068	0	0	0.048
0	0.01	0	0.013	0.038	0.009	0.116	0.096	0.095	0	0.011	0.065
0	0	0	0	0.008	0.003	0.057	0.093	0.041	0.111	0.089	0.08
0	0.01	0	0	0	0.001	0.041	0.027	0	0.046	0.065	0.044
0	0	0	0	0	0	0.016	0.003	0.027	0	0	0.007
0	0	0	0	0	0	0.038	0.003	0.041	0	0	0.013
0	0	0	0	0	0	0.038	0.003	0	0	0	0.011
0.9	0.8	0.75	0.875	0.829	0.808	0.535*	0.575*	0.297*	0.796	0.68*	0.602
0.9	0.88	0.886	0.925	0.857	0.896	0.941	0.898	0.92	0.889	0.883	0.933

dard deviations were calculated for each locus and for all loci combined according to Weir and Cockerham (1984) by using FSTAT (Goudet, 1995). FSTAT also provided pairwise F_{st} values for populations and regions. We used the notations F_{st}, F_{is}, and F_{it} for Weir and Cockerham's (1984) θ, f, and F, respectively. In all analyses, probability values were adjusted to correct for the number of simultaneous tests as discussed by Lessios (1992). Thus, the significance level is taken to be 0.05/number of simultaneous comparisons.

Graphical analysis of genetic relationship between populations was performed. A neighbor-joining (NJ) (Saitou and Nei, 1987) dendrogram was constructed by using PHYLIP 3.5c (Felsenstein[1]). The allele frequency matrix was resampled 1000 times in a bootstrap resampling procedure and Cavalli-Sforza and Edwards (1967) chord distances among populations were estimated for each matrix. A consensus NJ dendrogram of chord distances was generated to determine the stability of nodes within the dendrogram. For presentation, a NJ dendrogram with the original branch lengths was constructed and bootstrap values over 50% were plotted onto the nodes of the dendrogram.

In several populations we suspected a null allele at *Ots*102. These populations had moderate heterozygote deficiencies and a large number of individuals whose other two loci amplified but that failed to amplify at *Ots*102, even after PCR stringency was relaxed. We generated an estimate of the frequency of the null allele by recoding, as null allele homozygotes, two out of every three of the individuals failing to amplify at *Ots*102. Corrected allele fre-

Table 3

Observed precision of allele size determination (bp) for repeated analysis of heterozygous fish at loci *Ots*101, *Ots*100, and *Ots*102. "*n*" is the number of times each fish was analyzed. Standard deviation (SD) was calculated and the range of observed measurements is shown.

Locus	*n*	Mean	SD	Range
*Ots*101	44	221.77	1.08	220–224
	103	199.47	0.96	196–201
	44	167.93	0.79	166–169
	103	153.49	0.94	151–155
*Ots*100	18	367.17	1.86	360–367
	103	322.07	1.73	318–325
	18	281.28	1.23	279–283
	103	251.81	1.13	249–254
*Ots*102	74	270.35	1.34	268–273
	70	225.54	1.10	223–228
	70	188.30	1.08	186–190
	74	181.15	0.86	180–183

[1] Felsenstein, J. 1993. PHYLIP (Phylogeny Inference Package), version 3.4. Univ. Washington, Seattle, WA. [Available from author, Department of Genetics, Box 357360, Univ. Washington, Seattle, WA 98195-7360.]

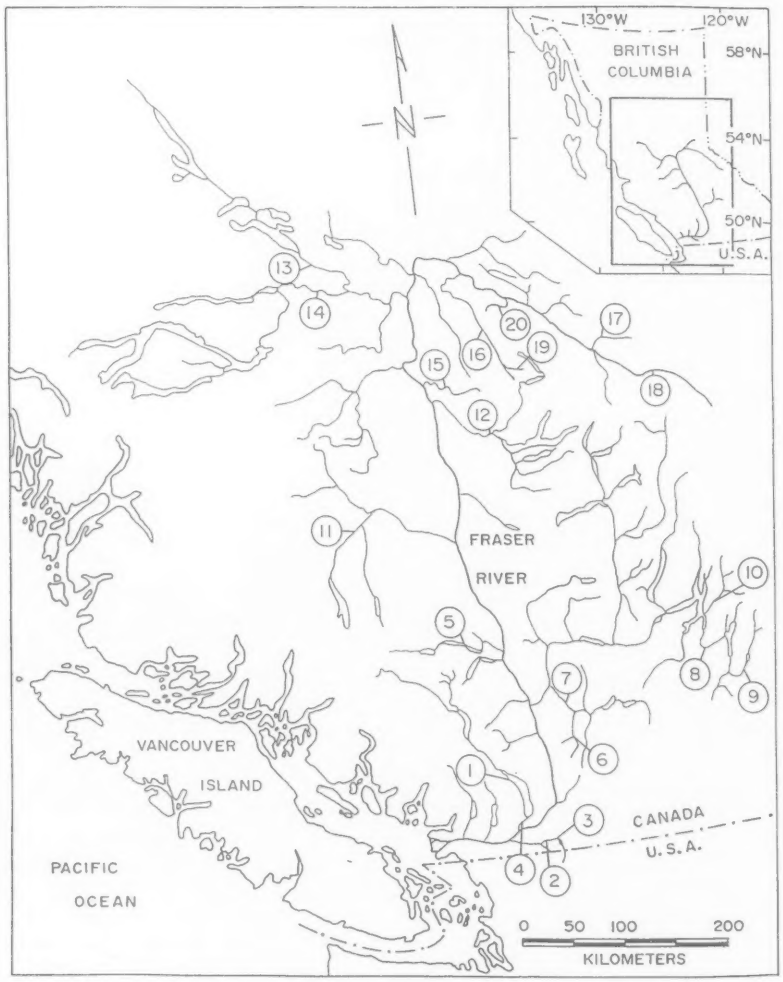

Figure 1

Map of the Fraser River watershed showing locations of chinook salmon populations with inset of the map of British Columbia. Numbers are placed at the collection sites where the populations were obtained: 1 = Harrison, 2 = Chilliwack-white, 3 = Chilliwack-red, 4 = Chehalis-red, 5 = Bridge, 6 = Coldwater, 7 = Nicola, 8 = Lower Shuswap, 9 = Middle Shuswap, 10 = Eagle, 11 = Chilko, 12 = Quesnel, 13 = Stuart, 14 = Nechako, 15 = Cottonwood, 16 = Bowron, 17 = Holmes, 18 = Tete Jaune, 19 = Indianpoint, 20 = Slim.

quencies in the presence of a null allele were generated by using the maximum likelihood method of the utilities option in GENEPOP. The data set with corrected allele frequencies was tested in a NJ dendrogram analysis.

Results

Pedigree analysis and allele assignment

All loci displayed normal Mendelian inheritance; each heterozygous parent (two allele bands) passed each of its two bands to approximately 50% of its offspring, and each homozygous parent (one allele band) passed its single band to 100% of its offspring. Assignment of alleles was based on the empirically determined standard error of band size estimation as reported in Table 3. The size range for each allele was set to allow for 95% confidence of allele assignment.

Heterozygosity and allele frequencies

Heterozygosity was consistently high at *Ots*101 and *Ots*100 (Table 1), ranging from 0.636 to 0.975 at *Ots*101(0.86 average), and from 0.80 to 0.947 (0.88 average) at *Ots*100. Het-

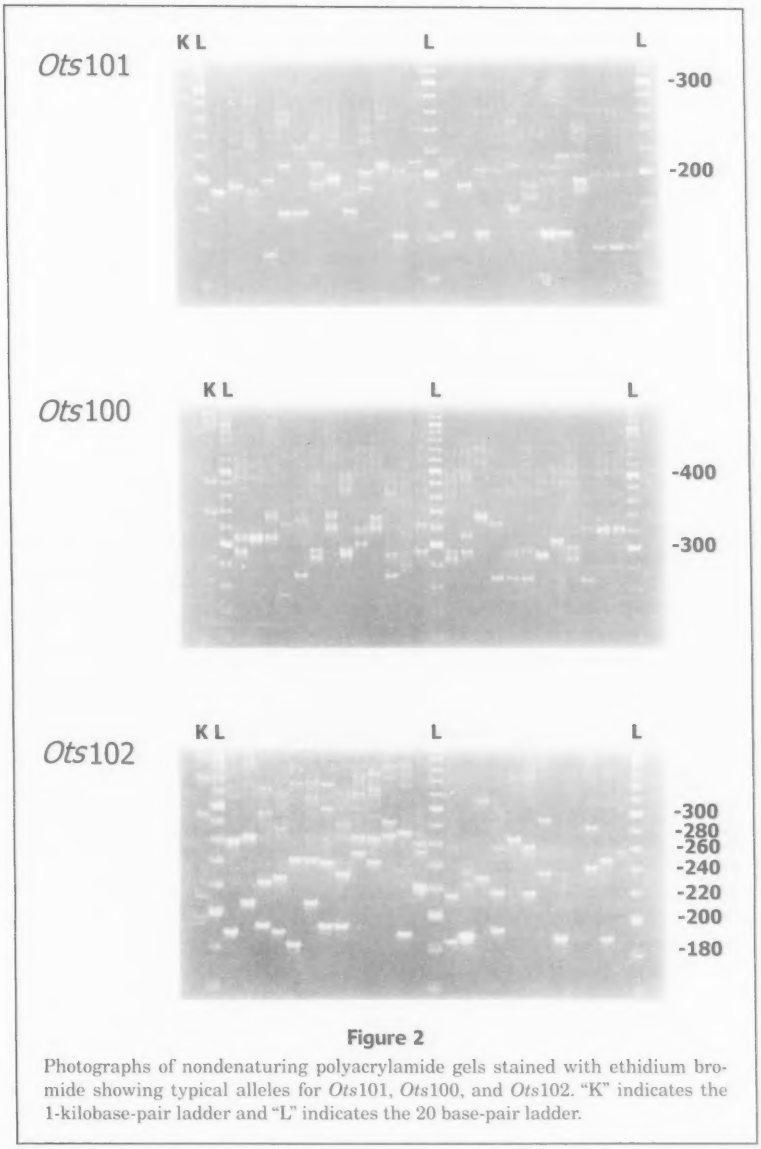

Figure 2

Photographs of nondenaturing polyacrylamide gels stained with ethidium bromide showing typical alleles for *Ots*101, *Ots*100, and *Ots*102. "K" indicates the 1-kilobase-pair ladder and "L" indicates the 20 base-pair ladder.

erozygosity values had a wider range at *Ots*102, ranging from a low of 0.297 in Eagle River to a high of 0.9 in Chehalis-red (average of 0.706). The apparently low heterozygosity found in some populations at *Ots*102 may have been partially due to the presence of a null allele. With the exception of Bridge River, all allele frequencies showed significant variation among the different populations. In pairwise tests, Bridge River was not significantly different (P nondifferentiation=0.00004) from Harrison River, Chilliwack-white, Chilliwack-red, Chehalis-red, Coldwater River, Middle Shuswap River, Eagle River, Stuart River, and Cottonwood River. All other populations were significantly different from each other.

Hardy-Weinberg equilibrium and treatment of the null allele

We tested each of the 20 populations for significant deviations from HWE proportions at each locus. Conformation to HWE was rejected at the 5% level (P<0.05/20) in four populations (Harrison River, Tete Jaune River, Cottonwood River, and Eagle River) at *Ots*101, in one population (Bridge River) at *Ots*100, and in 12 populations at *Ots*102 (see Table 1). All rejections of conformation to HWE were due to a deficiency of heterozygotes. Single locus F_{IS} values for *Ots*101, *Ots*100, and *Ots*102 were 0.079, 0.050, and 0.261, respectively, and 0.127 for

all loci combined. All values were significantly greater than zero ($P<0.005$), indicating that populations tended towards disequilibrium at each locus. Gametic disequilibrium tests indicated that loci were unlinked.

Because of a suspected null allele at *Ots*102, most populations showed a deficiency of heterozygotes at this locus; this locus also had a high and significant F_{is} value. When the dendrogram analysis was redone with the corrected data set, the regional structure was improved, in that all the middle Fraser River populations grouped together and bootstrap values were higher for regional nodes. Thus the major conclusion of this study was unaffected by the suspected null allele. However because the null allele was not observed in the pedigree analysis, its presence remains speculative and we have kept the original data set for the analysis presented here. Observed homozygote excesses are likely not due to our inability to resolve alleles because we observed a large number of individuals that amplified at the other two loci of the study but failed to amplify at *Ots*102, suggesting the presence of a null homozygote. Observed heterozygote deficiency could also be due to a partial disequilibrium; however no single population showed disequilibrium at all three loci.

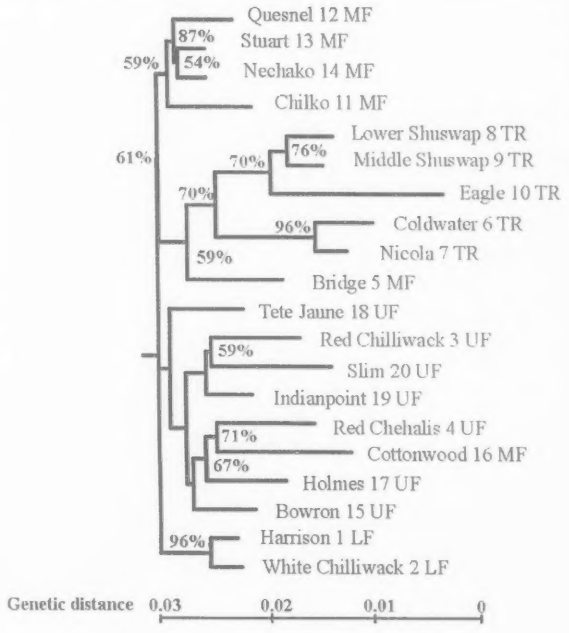

Figure 3

Neighbor-joining dendrogram of 20 chinook salmon populations from the Fraser River watershed. The dendrogram shows branch lengths, and the bootstrap values at the nodes were the percentage of dendrograms in which the populations beyond the node were grouped together out of 1000 dendrograms. The numbers following the place names correspond to map numbers in Figure 1. "MF", "TR, "UF" and "LF" indicate middle Fraser, Thompson River, upper Fraser and lower Fraser River respectively.

Temporal stability of allele frequencies, and population and regional variability

Comparisons of samples from different years for the same population suggested that there is temporal stability in allele frequencies within populations. With the exception of a single comparison within the Harrison River samples (the 1988 samples differed from the 1992 samples [P nondifferentiation=0.0003]), sample sets within populations were indistinguishable. Analysis of molecular variance showed that 97.57% ($P<0.01$, 5719 df) was within populations and that 1.80% ($P<0.01$, 16 df) of the total genetic variance was among populations. A small but significant 0.63%, ($P<0.01$, 3 df) of the genetic variance was apportioned between regions. Because population year classes were not significantly different from each other and variability among populations exceeded variability among year classes, year classes were combined into single populations for the rest of the analysis. All regions were significantly different from each other in pairwise tests ($P<0.008$).

Dendrogram

To determine if there was a pattern to allele frequency differences, we constructed a NJ dendrogram (Fig. 3) of pairwise genetic distances. This analysis suggested that geography at least partially underlies genetic relationships among chinook salmon populations in the Fraser River drainage. The NJ dendrogram consisted of four major branches, and are congruent with regional groupings (Fig. 3). The lower Fraser River branch includes Harrison River and Chilliwack and is supported in 96% of the dendrograms. The Thompson River branch is supported at 70% and includes Bridge River (from the middle Fraser River) in 59% of the dendrograms. The middle Fraser River branch is supported in 59% of the dendrograms. The largest branch, supported in 32% of the dendrograms, includes all the upper Fraser River populations, as well as the Chilliwack-red and Chehalis-red hatchery populations, and Cottonwood River from the middle Fraser River region.

This graphic analysis of genetic relationships shows regional groupings consisting of lower, middle, and upper Fraser River population groups, and a well-defined Thompson River group. These groupings are modestly supported because most of the genetic variance is within populations and only a small amount of the variance is among regions.

Population and regional differences

Wright's F statistics (Wright, 1951) were calculated to determine the degree of structuring between and within the regional population groupings. When all the populations were kept separate, the F_{st} values indicated diver-

gence among populations with single locus values of 0.011 (SD=0.002) for *Ots*101, 0.021(SD=0.004) for *Ots*100 and 0.038 (SD=0.007) for *Ots*102. The multiple locus value was 0.023 (SD=0.008). To determine the patterns of genetic relationship between sample groups within the individual regional groupings, pairwise F_{st} values were calculated for each pair of samples (Table 4). The highest pairwise F_{st} values were observed between populations of different regional groups. In order to estimate the degree of genetic isolation between the regional groupings suggested by dendrogram analysis, populations were combined by geographic region and pairwise F_{st} values were calculated (Table 5). The greatest value observed was between the Thompson River and upper Fraser River regions (0.0161) and the lowest value was between the upper and middle Fraser regions (0.006). F_{st} values were significant at each locus: *Ots*101 0.006 (SD=0.002), *Ots*100 0.008 (SD=0.00)1, and *Ots*102 0.022 (SD=0.008), for combined loci 0.012 (SD=0.005) (all $P<0.005$).

Discussion

Our results show significant genetic diversity within and between chinook salmon populations spawning in the tributaries of the Fraser River. The genetic relationship between the populations from the different tributaries suggest that there are four regional assemblages: upper Fraser River, middle Fraser River, lower Fraser River, and the Thompson River. These regional assemblages are concordant with the interpretation of the population structure seen by Teel et al. (2000) based on allozyme analysis. This concordance was observed with two very different marker sets. We employed three markers with average observed heterozygosities of 86%, 88%, and 71%, whereas out of the 25 polymorphic enzymes used by Teel et al., the highest heterozygosity was 0.441. The concordance of these two marker types with geography suggests that the genetic differences observed are not due simply to genetic drift but

Table 4

Pairwise F_{st} values among populations of the Fraser River watershed. Vertical lines indicate regional groupings. Abbrevations are as follows: Haris. = Harrison, Chil.w = Chilliwack-white, Che.-r = Chehalis-red, Ipoint = Indianpoint, Chil.-r = Chilliwack-red, TJ = Tete Jaune, Coldwt. = Coldwater, L.Shu. = Lower Shuswap, Cotton = Cottonwood, Ques. = Quesnel.

	Haris.	Chil.-w	Che.-r	Holmes	Bowron	Ipoint.	Chil.-r	Slim	TJ	Nicola	Coldwt.	L. Shu.	M. Shu.	Eagle	Cotton	Bridge	Ques.	Stuart	Nechako	Chilko
Haris.																				
Chil.-w	0.003																			
Che.-r	0.016	0.018																		
Holmes	0.019	0.020	0.010																	
Bowron	0.021	0.019	0.013	0.003																
Ipoint.	0.016	0.011	0.014	0.008	0.002															
Chil.-r	0.019	0.019	0.019	0.012	0.011	0.001														
Slim	0.028	0.023	0.018	0.018	0.007	0.009	0.010													
TJ	0.023	0.019	0.025	0.012	0.020	0.015	0.012	0.024												
Nicola	0.026	0.028	0.040	0.036	0.031	0.027	0.026	0.034	0.045											
Coldwt.	0.027	0.025	0.038	0.035	0.032	0.030	0.031	0.039	0.047	0.004										
L. Shu.	0.022	0.023	0.032	0.023	0.021	0.018	0.020	0.027	0.029	0.039	0.043									
M. Shu.	0.029	0.031	0.039	0.027	0.024	0.024	0.024	0.034	0.030	0.044	0.049	0.006								
Eagle	0.034	0.033	0.044	0.023	0.028	0.032	0.029	0.041	0.037	0.038	0.035	0.023	0.027							
Cotton	0.024	0.027	0.023	0.020	0.018	0.025	0.030	0.037	0.029	0.038	0.036	0.037	0.037	0.047						
Bridge	0.021	0.018	0.019	0.010	0.009	0.011	0.017	0.022	0.019	0.023	0.018	0.028	0.024	0.032	0.029					
Ques.	0.017	0.015	0.025	0.013	0.009	0.005	0.008	0.021	0.017	0.032	0.032	0.019	0.022	0.032	0.025	0.017				
Stuart	0.018	0.014	0.026	0.015	0.014	0.009	0.008	0.022	0.013	0.032	0.030	0.024	0.026	0.032	0.025	0.018	0.009			
Nechako	0.011	0.009	0.018	0.017	0.013	0.007	0.007	0.021	0.016	0.022	0.020	0.023	0.026	0.030	0.020	0.011	0.007	0.005		
Chilko	0.026	0.022	0.043	0.023	0.021	0.018	0.017	0.037	0.018	0.045	0.046	0.037	0.034	0.041	0.024	0.026	0.017	0.011	0.018	

Table 5

Table of pairwise F_{st} values among major regions in the Fraser River drainage.

	Lower Fraser	Mid Fraser	Upper Fraser
Lower Fraser	0.0000		
Mid Fraser	0.0115	0.0000	
Upper Fraser	0.0147	0.0062	0.0000
Thompson	0.0146	0.0125	0.0161

rather reflect patterns of historical colonization and present day gene flow (or lack thereof). Concordance of both allozyme and microsatellite data indicates that the simple method used in our study to designate alleles does not greatly bias or skew the results.

During the retreat of the Wisconsin glacial ice sheet, the headwaters of the Fraser and Thompson Rivers were ice free before the lower Fraser River channel was ice free, and therefore drained through the Columbia River. McPhail and Lindsey (1986) suggested that freshwater fish colonized the upper Fraser River and the Thompson River by means of the Columbia River during this time. Allozyme analysis of chinook salmon show that the Thompson River populations are distinct from the population of the other Fraser River tributaries (Utter et al., 1989; Teel et al., 2000). Similarly, coho salmon from the Thompson River are genetically distinct from coho salmon in the lower Fraser River (Small et al., 1998a). In our analysis, the Thompson River populations formed a distinct group, consistent with the hypothesis that the Thompson River watershed may have been colonized by a different founder group than other regions of the Fraser River. In addition, strong genetic substructuring *within* the Thompson River watershed was observed. This structuring, also observed by Teel et al. (2000), suggests that there may be sufficient genetic isolation within the Thompson River watershed to allow for the persistence of locally adapted populations.

If the upper Fraser and Thompson Rivers were both colonized by means of the Columbia River, then tests of the genetic relationship between these groups might show the upper Fraser and Thompson Rivers more closely related to each other than to other regions. However, based upon our study, they are the most distantly related, suggesting that either the upper Fraser was not colonized by the same population that founded the Thompson River populations, or that migration may have obscured the origins of fish inhabiting this region. This hypothesis is currently being tested by analyzing chinook salmon populations from the Skeena and Nass Rivers (possible source populations) and by increasing the resolution of the genetic structure of coho salmon in the Fraser River watershed by analyzing more microsatellite loci.

The high bootstrap support for the lower Fraser group suggests that this region was colonized by a single founder population. This hypothesis seems likely because the river mouths are separated by approximately 15 kilometers. The close genetic association between the Harrison and Chilliwack Rivers (F_{st}=0.003) indicates either that straying occurs routinely between them or that colonization was so recent that the populations have not diverged.

The red-flesh Chehalis and Chilliwack populations were introduced in the 1980s from broodstocks originating in the upper and middle Fraser River. Sources of the brood stocks included the Bowron, Chilko, and Quesnel Rivers and Slim Creek[2] These populations are artificially maintained by selecting red-flesh fish for broodstock. Our analysis places these populations with the upper Fraser River populations, reflecting their origins.

The regional groupings and patterns of genetic relationships within each region provide a starting point for discussion of the events that led to the repopulating of these regions by chinook salmon and the degree of isolation of different populations. Although only in the early stages, this information forms a base upon which to begin assigning management and fishery enhancement priorities such that genetic diversity present in wild populations is preserved. This information, along with life history and ecological data, will also be useful for the determination of whether a regional grouping of populations can be considered an evolutionarily significant unit (Waples, 1991).

Acknowledgments

Samples were collected with the assistance of J. Candy and the staff of the Habitat and Assessment Branch of the Department of Fisheries and Oceans. Funding was provided by the Department of Fisheries and Oceans. C. Wood and R. E. Withler provided helpful discussion. We thank five anonymous reviewers for improvements to the manuscript.

Literature cited

Angers, B., L. Bernatchez, A. Angers, and L. Desgroseillers.
1995. Specific microsatellite loci for brook charr reveal strong population subdivision on a microgeographic scale. J. Fish. Biol. (suppl A) 47:177–185.

Banks, M. A., B. A. Baldwin, and D. Hedgecock.
1996. Research on chinook salmon (*Oncorhynchus tshawytscha*) stock structure using microsatellite DNA. Bull. Natl. Inst. Aquacult. suppl. 2:5–9.

Bartley, D., B. Bentley, J. Brodziak, R. Gomulkiewicz, M. Mangel, and G. A. E. Gall.
1992. Geographic variation in population genetic structure of chinook salmon from California and Oregon. Fish. Bull. 90:77–100.

Beacham, T. D., C. B. Murray, and R. E. Withler.
1989. Age, morphology and biochemical genetic variation of Yukon River chinook salmon. Trans. Am. Fish. Soc. 118: 46–63.

Beacham, T. D., R. E. Withler, and T. A. Stevens.
1996. Stock identification of chinook salmon (*Oncorhynchus tshawytscha*) using minisatellite DNA variation. Can. J. Fish. Aquat. Sci. 53:380–394.

[2] Cross, C. 1998. Personal commun. Department of Fisheries and Oceans, 555 West Hastings St. Vancouver, B.C., V6B 5G3, Canada.

Bradford, M. J.
1994. Trends in the abundance of chinook salmon (*Oncorhynchus tshawytscha*) of the Nechako River, British Columbia. Can. J. Fish. Aquat. Sci. 51:965–973.
Cavalli-Sforza, L. L., and A. W. F. Edwards.
1967. Phylogenetic analysis: models and estimation procedures. Am. J. Hum. Gen. 19:233–257.
Cronin, M. A., W. J. Spearman, R. L. Wilmot, J. C. Patton, and J. W. Bickham.
1993. Mitochondrial DNA variation in chinook (*Oncorhynchus tshawytscha*) and chum salmon (*O. Keta*) detected by restriction enzyme analysis of polymerase chain reaction (PCR) products. Can. J. Fish. Aquat. Sci. 50:708–715.
Fraser, F. J., P. J. Starr, and A. Y. Fedorenko.
1982. A review of the chinook and coho salmon of the Fraser River. Can. Tech. Rep. Fish. Aquat. Sci. 1126, 132 p.
Gharrett, A. J., S. M. Shirley, and G. R. Tromble.
1987. Genetic relationships among populations of Alaskan chinook Salmon (*Oncorhynchus tshawytscha*). Can. J. Fish. Aquat. Sci. 44:765–774.
Goudet, J.
1995. FSTAT, version 1.2: a computer program to calculate *F*-statistics. J. Hered. 86:485–486
Guo, S. W., and E. A. Thompson.
1992. Performing the exact test of Hardy-Weinberg proportions for multiple alleles. Biometrics 48:361–372
Lessios, H. A.
1992. Testing electrophoretic data for agreement with Hardy-Weinberg expectations. Mar. Biol. 112:517–523.
Maniatis, T., E. F. Fritsch, and J. Sambrook.
1982. Molecular cloning: a laboratory manual. Cold Spring Harbor Laboratory, Cold Spring Harbor Laboratory, New York, NY.
McPhail, J. D., and C. C. Lindsey.
1986. Zoogeography of freshwater fishes of Cascadia (the Columbia system and rivers north to the Stikine). *In* Zoogeography of North American freshwater fishes (C. H. Hocutt and E. O. Wiley. eds.), p. 615–637. J. Wiley and Sons, Inc., New York, NY.
Nelson, R. J., and T. D. Beacham.
1999. Isolation and cross species amplification of microsatellite loci useful for study of Pacific salmon. Animal Genetics 30:228–229.
Nelson, R. J., T. D. Beacham, and M. P. Small.
1998. Microsatellite analysis of the population structure of a Vancouver Island sockeye salmon (*Oncorhynchus nerka*) stock complex using nondenaturing gel electrophoresis. Mol. Mar. Biol. Biotech. 7:312–319.
Northcote, T. G., and D. Y. Atagi.
1997. Pacific salmon abundance trends in the Fraser River watershed compared with other British Columbia Systems. *In* Pacific salmon and their ecosystems: status and future options (D. J. Stouder, P. A. Bisson, and R. J. Naimons, eds.), p. 199–219. Chapman and Hall, New York, NY.
Quinn, T. P.
1984. Homing and straying in Pacific Salmon. *In* Mechanisms of migration in fishes (J. D. McCleave, G. P. Arnold, J. J. Dodson, and W. H. Neill, eds.), p. 357–362. Plenum Press, New York, NY.
Raymond, M. and F. Rousset.
1995a. GENEPOP (versions 1.2 and 3.1): population genetics software for exact tests and ecumenism. Heredity 86:248–249.
Raymond, M., and F. Rousset.
1995b. An exact test for population differentiation. Evolution 49:1280–1283.
Saitou, N. and M. Nei.
1987. The neighbor-joining method: a new method for reconstructing phylogenetic trees. Mol. Biol. Evolution 4: 406–425.
Scheer, B. T.
1939. Homing instinct in salmon. Q. Rev. Biol. 14:408–430.
Schneider, S., J. M. Kueffer, D. Roessli, and L. Excoffier.
1997. Arlequin, verison 1.1: a software for population genetic data analysis. Genetics and Biometry Laboratory, Univ. Geneva, Switzerland.
Scribner, K.T., J. R. Gust, and R. L. Fields.
1996. Isolation and characterization of novel salmon microsatellite loci: cross-species amplification and population genetic application. Can. J. Fish. Aquat. Sci. 53:833–841.
Slaney, T. L., K. D. Hyatt, T. G. Northcote, and R. J. Fielden.
1996. Status of anadromous salmon and trout in British Columbia and Yukon. Fisheries 21:20–35.
Small, M.P., T. D. Beacham, R. E. Withler, and R. J. Nelson
1998a. Discriminating coho salmon (*Oncorhynchus kisutch*) populations within the Fraser River, British Columbia. Mol. Ecol. 7:141–155.
Small, M. P., R. E. Withler, and T. D. Beacham.
1988b. Population structure and stock identification of British Columbia coho salmon, *Oncorhynchus kisutch*, based on microsatellite DNA variation. Fish. Bull. 96:843–858.
Teel, D. J., G. B. Milner, G. A. Winans, and W. S. Grant.
2000. Genetic population structure and origin of life-history types in chinook salmon in British Columbia, Canada. Trans. Am. Fish. Soc. 129:194–209.
Utter, F., G. B. Milner, G. Stahl, and D. Teel.
1989. Genetic population structure of chinook salmon, *Oncorhynchus tshawytscha*, in the Pacific Northwest. Fish. Bull. 87:239–264.
Waples, R. S.
1991. Definition of "species" under the Endangered Species Act: application to Pacific salmon. U.S. Dep. Commer., NOAA Tech. Memo., NMFS, F/NWC-194, p. 29.
Waples, R. S.
1994. Genetic considerations in recovery efforts for Pacific Salmon. Cons. Biol. 8:884–886.
Warner, B. G., R. W. Mathewes, and J. J. Clague.
1982. Ice-Free conditions on the Queen Charlotte Islands, British Columbia, at the height of the late Wisconsin glaciation. Science (Washington D.C.) 218:675–677.
Weir, B. S. and C. C. Cockerham.
1984. Estimating *F*-statistics for the analysis of population structure. Evolution 38:1358–1370.
Wilmot, R. L., R. Everett, W. J. Spearman, and R. Baccus.
1992. Genetic stock identification of Yukon River chum and chinook salmon 1987 to 1990. Alaska Fish Wild. Res. Cent. U.S. Fish Wild. Serv. Prog. Rep. 132 p.
Wilson, G. M., W. K. Thomas, and A. T. Beckenbach.
1987. Mitocondrial DNA analysis of Pacific Northwest populations of (*Oncorhynchus tshawytscha*). Can. J. Fish. Aquat. Sci. 44:1301–1305.
Wood, C. C.
1995. Life history variation and population structure in sockeye salmon. Am. Fish. Soc. Symp. 17:195–216.
Wood, C. C., B. E. Riddell, D. T. Rutherford, and R. E. Withler.
1994. Biochemical genetic survey of sockeye salmon (*Oncorhynchus nerka*) in Canada. Can. J. Fish. Aquat. Sci. 51(suppl. 1):113–131.
Wright, S.
1951. The genetical structure of populations. Ann. Eugen. 15:323–354.

Annual and batch fecundities of yellowfin sole, *Limanda aspera*, in the eastern Bering Sea

Daniel G. Nichol

Erika I. Acuna

Resource Assessment and Conservation Engineering Division
Alaska Fisheries Science Center
National Marine Fisheries Service, NOAA
7600 Sand Point Way NE, BIN C15700
Seattle, Washington 98115-0070

E-mail address (for D. G. Nichol): dan.nichol@noaa.gov

Abstract–Annual and batch fecundities of yellowfin sole, *Limanda aspera*, in the eastern Bering Sea were determined. Most individuals had a determinate, group-synchronous mode of oocyte development as evidenced by a distinctly separate distribution of fully yolked oocytes in more advanced ovaries. The spawning of batches by an individual female occurs in uninterrupted succession, as indicated by the presence of oocytes with migratory-stage nuclei in nearly all females undergoing oocyte hydration. Total fecundity ranged from 295,615 to 3,635,108 oocytes per female and is described by $3.3225 \times TL^{3.6312}$, where T = total fish length (cm). The length-fecundity relationship was found to be the same in both southeast and northwest areas of the eastern Bering Sea, despite known growth differences between the two areas. Individual females spawn from 8 to 11 batches. The first batch spawned is generally smaller in number than succeeding batches. After spawning begins, fish remain in the nearshore spawning area (<30 m bottom depth) until spent. The presence of residual chorion tissue from unspawned ova in the ovary lumen of some maturing females indicates that at least some females are capable of spawning more than one series of batches within one reproductive season. The annual fecundity, therefore, for such individuals is consequently considered indeterminate

Manuscript accepted 10 August 2000.
Fish. Bull. 99:108–122 (2001).

Yellowfin sole, *Limanda aspera*,[1] have historically been among the more abundant fishes in the eastern Bering Sea, where biomass estimates have exceeded 2 million metric tons (t) annually since 1980[2] (Wilderbuer et al., 1992; Nichol, 1998). Yellowfin sole has been an important commercial trawl species with annual catches averaging 135,630 t from 1991 to 1998.[2] Yellowfin sole spawn from May through August in nearshore waters of Bristol Bay northward to at least Nunivak Island (Fadeev, 1970; Nichol, 1995) at depths less than 30 m (Nichol, 1995). Yellowfin sole, like many other flatfishes, are batch spawners (Nichol, 1995). They spawn pelagic eggs that have been observed in the plankton with diameters of approximately 0.76–0.85 mm (Waldron, 1981; Matarese et al., 1989). Adult yellowfin sole generally undergo long migrations from wintering grounds near the shelf-slope break to spring-summer grounds at bottom depths less than 50 m (Wakabayashi, 1989; Nichol, 1998).

Annual fecundity has been used as a measure of reproductive output for many species; its use as a parameter in fishery population models makes it relevant to stock assessment. Annual fecundity is defined as the total number of eggs spawned by a female in a single year. Batch fecundity, defined as the number of eggs released at one time, can be estimated for any female from counts of hydrated oocytes as long as the female is not ovulating or spawning. Directly estimating annual fecundity from counts of advance-stage oocytes is feasible only if the number of eggs to be spawned is determinate or fixed prior to spawning (Hunter et al., 1985, Hunter et al., 1992). Females with a determinate fecundity, just prior to spawning, will have a fixed number of advanced-yolked oocytes that are separated from the other less developed oocytes by a distinct gap in size; these can either be spawned in batches or all at once. In contrast, species whose ovaries are characterized by continuous oocyte size distributions may be able to develop unyolked oocytes continually and add them to the stock of advanced-yolked oocytes even after spawning begins. These species will typically develop multiple groups of oocytes with size distributions that overlap. The method to estimate annual fecundity in such species with the least error uses batch fecundity, spawning frequency, and spawning season duration (Yamamoto, 1956; Hunter and Macewicz, 1985a). Prior to estimating annual fecundity, we examined oocyte size distributions to determine which mode of oocyte development yellowfin sole undergoes.

Assuming that yellowfin sole females have a determinate fecundity, two potential problems associated with estimating annual fecundity must be addressed. First, because yellowfin sole spawn eggs in batches, annual fecundity may be underestimated if partially spawned fish are included in estimates.

[1] Scientific name follows Cooper and Chapleau (1998).

[2] Wilderbuer, T. K., and D. Nichol. 1998. Yellowfin sole. Section 3 *in* Stock assessment and fishery evaluation report for the groundfish resources of the Bering Sea/Aleutian Islands regions. North Pacific Fishery Management Council, 605 West 4th Ave, Suite 306, Anchorage, AK 99501.

Identifying partially spawned ovaries can be difficult with unaided macroscopic observation. With microscopic observation, however, identification of postovulatory follicles (POFs) within an ovary verifies that at least one batch has been spawned (Hunter and Macewitz, 1985a; Hunter et al., 1992). Histological analysis of collected ovaries was employed in our study in part to identify POFs. Second, annual fecundity may be overestimated if the eventual loss of oocytes due to atresia (oocyte resorption) is not taken into account. Oocyte atresia can occur in varying degrees throughout the spawning season, depending on the species and environmental conditions (Hunter and Macewicz, 1985b; Macewicz and Hunter, 1994; Walker et al., 1994; McFarlane and Saunders, 1997). This bias can be minimized if ovaries chosen for fecundity estimates are well developed and near spawning condition.

Understanding the spawning characteristics along with other life-history parameters may help determine how fish abundance varies with changing environmental or fishing conditions. Moreover, knowledge of the fecundity and the spawning characteristics can help define how species, such as yellowfin sole, relate to other species from a phylogenetic perspective. In our study, we evaluate the annual and batch fecundities of yellowfin sole with reference to its spawning habits.

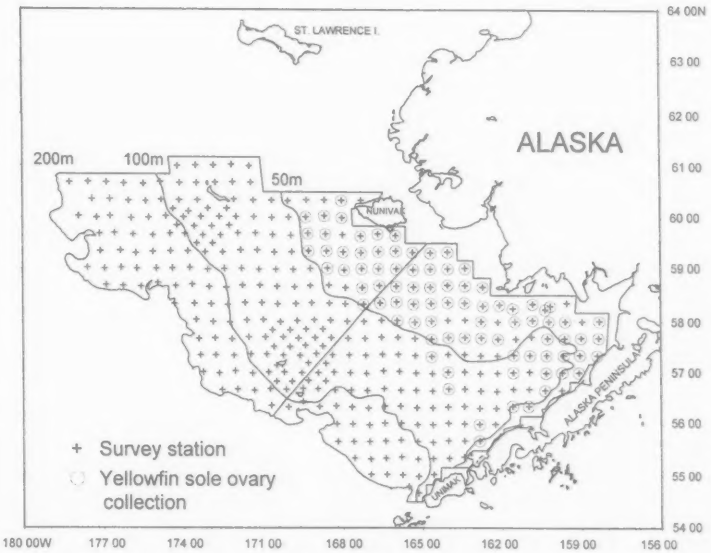

Figure 1

Location of yellowfin sole (*Limanda aspera*) ovary collections within the eastern Bering Sea trawl survey area, 1993. Stations where yellowfin sole ovaries were collected are circled. The diagonal line separates the northwest from the southeast sampling areas.

Materials and methods

Summary of collections

A total of 767 ovary pairs were collected in June and July of 1993 during a groundfish trawl survey in the eastern Bering Sea, conducted by the Alaska Fisheries Science Center (Nichol, 1995). Collections were made at 83 stations at depths shallower than 50 m (Fig. 1). Whole ovaries were extracted from approximately 10 females per station and then preserved in 10% formalin (3.7% formaldehyde) buffered with 19 g/liter sodium acetate-trihydrate. Females were selectively chosen by size: 2 females 25–30 cm total length (TL), 4 females 31–35 cm TL, and 4 females >35 cm TL. All females less than 25 cm TL were immature and therefore were not collected. Each preserved ovary lobe was weighed to the nearest milligram. Ovaries were assigned a maturity code based on a 5-point maturity classification scale for macroscopic examination (Table 1). These assignments were verified with histological evaluation.

Histological evaluation of ovaries

Histological cross sections were prepared from the middle portion of one ovary from each fish. Most sections (93%) were taken from the blind side; however, sections were occasionally taken from the eyed-side if fixation was not complete. Ovary tissues were embedded in paraffin, sectioned at 6 µm, then stained with hematoxylin and eosin.

Each ovary section was examined for the following oocyte stages: early perinuclear, late-perinuclear, partially yolked (PY), advanced-yolk (AY), migratory-nucleus (MN), unovulated hydrated (HY), and ova (ovulated, hydrated) (Howell,1983). We also noted the presence of postovulatory follicles (POF), atretic oocytes, and residual chorion tissue.

The maximum diameter of AY through MN oocytes were measured with an ocular micrometer. Oocyte diameters were measured from five of the largest spherical nonatretic oocytes with a centrally located nucleus. The average maximum oocyte diameters were then computed for each fish.

Examination of oocyte atresia

Occurrence of alpha (α) stage atresia (Hunter and Macewicz, 1985b) among advanced vitellogenic oocytes (AY, MN, and HY) and PY oocytes was recorded for 75 females by using histological ovary cross sections. Samples included 28 maturing (maturity-code 2) females with AY-stage oocytes and no evidence of POFs, 13 fish with AY and HY oocytes and no POFs, 23 fish that had spawned at least one batch (POFs present), and 11 fish with evidence of residual chorion tissue in the ovary lumen and no other evidence of batch spawning (no HY, ova, POFs). A 2 × 2 mm grid was used to count atretic and nonatretic PY oocytes, and AY through HY oocytes. One ovary section

was examined for each female. Grid counts were repeated 4 to 12 times at different locations within each ovary section, until counts totaled approximately 180 oocytes.

Testing for homogeneity within the ovary

Prior to subsampling for total fecundity, we tested (two-way ANOVA; *t*-tests) for differences in oocyte density (number of oocytes per gram of ovary tissue) and mean oocyte diameter between eyed-side and blind-side ovarian lobes and among three ovary positions (anterior, middle, posterior). Twenty ovaries histologically identified with AY oocytes (maturity-code 2) and no evidence of prior batch spawnings (i.e. no POFs) were selected from fish over a broad length range. AY oocytes were defined as those with yolk filling more than half the volume of the oocyte. Tissue samples averaging 10.5 mg (SD=2.9559) and 267 oocytes (SD=90.0) were taken from anterior, middle, and posterior positions along the long axis of each ovarian lobe (six subsamples per fish). All AY through MN stage oocytes from each tissue sample were counted manually with the aid of a dissecting microscope. Fifty of these oocytes per tissue sample were randomly selected for oocyte area measurements. Oocyte areas were measured with a microscopic image analysis system with Optimas 5.0 software (BioScan, Inc., 1992). Black and white images were generated with a video camera attached to a dissecting microscope (transmitted light) and were viewed on a 13-inch (diagonal) color monitor. The resolution was set to 640 × 480 pixels, corresponding to 4.149 µm/pixel at 25× magnification. Oocyte diameter was calculated from oocyte area by

$$Diameter = 2 \cdot \sqrt{\frac{Area}{\pi}}. \quad (1)$$

Oocyte size distributions

Oocyte areas were measured to determine whether there was a hiatus between distributions of AY oocytes and less advanced oocytes. Areas of oocytes in partially yolked (PY), unyolked, and AY stages were measured by using preserved tissue (as above), and calculated diameters were plotted for 75 of the 324 females examined for fecundity. These were the same females used to examine ooctye atresia, thus representing prespawning through partially spawned females, as well as those with residual chorion material present. PY-stage oocytes were considered as those with yolk that filled less than half the volume of the oocyte. Subsamples were taken from the anterior or middle portion of one ovary and weighed to the nearest 0.001 g. All PY and AY oocytes were counted separately. For the purpose of oocyte counts and measurements, MN oocytes were not distinguished from AY oocytes. No attempt was made to count unyolked oocytes or measure unyolked oocytes less than approximately 0.05 mm. Random oocyte area measurements by image analysis (at 25×) included 50 AY oocytes, 50 PY oocytes (if they existed), and 50 unyolked oocytes. The three oocyte diameter distributions were then plotted for each fish as PY and AY oocyte distributions in terms of number of oocytes per gram of ovary tissue and unyolked oocytes in terms of percent frequency of the 50 measured.

Total fecundity and batch fecundity estimation

Because of findings from the testing of homogeneity within ovaries (see "Results" section), two tissue subsamples were taken from the ovaries of each fish: one from the posterior third of either ovary, and one from either the middle or anterior third of either ovary. To estimate total fecundity, defined as the standing stock of AY through HY oocytes, only ovaries with no evidence of prior batch spawnings (no ova, no POFs, nor residual chorion material) were used. To eliminate less developed ovaries that contained many PY oocytes, we also limited fecundity samples to those with maximum oocyte diameters ≥0.35 mm as measured from histological slides. Area measurements of AY through MN stage oocytes with image analysis and counts were conducted in the same manner as the above test for homogeneity.

To determine the proportional mass of each ovary section (WF_p, WF_m, and WF_a), one of the paired ovaries from each of the 20 fish tested for oocyte homogeneity was cut into thirds, mid-way between anterior-middle and mid-way between middle-posterior tissue positions. Each section was weighed to the nearest 0.001 g. The proportional mass (section wt/sum of section wts) of anterior, middle, and posterior sections averaged respectively 0.536 (SE=0.0095), 0.311 (SE=0.0086) and 0.153 (SE=0.0059) of the total ovary mass.

Total fecundity was computed as

$$Total\ fecundity = \left[\frac{no_p}{wt_p}(WF_p) + \frac{no_{am}}{wt_{am}}(WF_{am})\right] POW, \quad (2)$$

where no_p = number of AY-HY oocytes in tissue sample from posterior position of either ovary;

no_{am} = number of AY-HY oocytes in tissue sample from either anterior or middle positions of either ovary;

wt_p = weight of tissue sample from posterior position of either ovary;

wt_{am} = weight of tissue sample (g) from either middle or anterior position of either ovary;

WF_p = weighting factor computed as the average proportional mass of the posterior third of either ovary; 0.153 g (n=20);

WF_{am} = weighting factor computed as the average proportional mass of anterior and middle ovary sections combined; 0.536 g + 0.311 g = 0.837 g (n=20); and

POW = paired ovary weight (g).

Batch fecundity was estimated from those ovaries containing HY oocytes (maturity-code 3). Subsample weights averaged 52 mg. Both HY oocytes (batch oocytes) and AY oocytes (remaining oocytes) were counted. Batch fecundity was computed as above (Eq. 2), substituting no_p and no_{am} with

Table 1

Maturity code criteria for yellowfin sole (*Limanda aspera*) ovaries based on macroscopic examination. Corresponding histological descriptions are included. LP = late perinucleus stage oocyte; PY = partially yolked oocyte; AY = advanced yolked oocyte; MN = oocyte with migratory nucleus; HY = unovulated hydrated oocyte. POFs = postovulatory follicles. PY is defined as an oocyte with yolk globules that filled less than half the volume of the oocyte.

Maturity code	Condition	Macroscopic examination	Histological examination
1	immature	Ovary clear to slightly pink or grey-pink. No distinct oocytes. Ovarian wall thin and taut around ovary interior.	LP is the most advanced oocyte stage. Ovarian wall diameter thin (generally <2 µm).
2	maturing	Ovary usually opaque with distinct vitellogenic oocytes. A network of veins covers the ovary.	PY or AY oocytes present (yolk globules present). MN oocytes may be present. POF may be present.
3	hydrated	As in code 2, but some portion of oocytes are translucent (hydrated-unovulated). Hydrated oocytes are larger than the opaque oocytes and are randomly scattered about the ovary.	HY oocytes (yolk coalesced) present, each surrounded by a follicle. AY oocytes present if prior to last batch. MN oocytes usually present if prior to last batch. POF may be present.
4	spawning	Hydrated (translucent) oocytes in lumen of ovary (ovulated). A continuous band of hydrated oocytes may also be visible from the ovary sides. Eggs may run with slight pressure. If all oocytes are translucent, they represent the last batch of eggs to be spawned in the season.	Ova present. AY oocytes present if prior to last batch. POFs present. MN oocytes usually present if prior to last batch.
5	spent	Deflated ovary, often with blood. Ovary wall thick and often flaccid around ovary interior.	LP to PY oocytes present. Ovarian wall diameter thick (generally >3 µm).

numbers of HY oocytes in the respective subsample. Ovaries were categorized by stages in the batch spawning succession: a first batch was recognized by the presence of HY and AY oocytes, and absence of POFs. A middle batch was recognized by the presence of HY oocytes, AY oocytes, and POFs. A final batch was recognized by the presence of HY oocytes and the absence of remaining AY or MN oocytes.

Fecundity-total length relationships were computed for total and batch fecundity by using Gauss-Newton nonlinear least squares regression (SAS Institute, 1989). The number of batches spawned from a female for a given fish length was then estimated as the estimated total fecundity divided by the estimated batch fecundity.

Results

Histological evaluation

Histological evaluation of 767 ovary pairs, in most cases (93%), verified the general ovary codes that were assigned macroscopically (Table 1). Resulting groupings are shown in Table 2. We note here that maturing (maturity-code 2) ovaries included females that had spawned one or more batches (POF present) but contained no hydrated oocytes (HY) or ova; these ovaries were indistinguishable macroscopically from advancing ovaries that had not yet spawned a batch. Early perinucleus stage oocytes were present in all ovaries examined. Late perinucleus stage oocytes were present in all but one of the mature fish ovaries (n=665; maturity-codes 2–5).

Migratory nucleus stage (MN) oocytes, vitellogenic oocytes that are precursors to hydrated oocytes, were present in 96% of the females undergoing oocyte hydration and 91% of spawning females. The high occurrence of MN oocytes among fish about to spawn a batch suggests that fish do not wait extended periods between batch spawnings.

Postovulatory follicles were observed in 121 of the ovaries examined. POFs were present in 50 of 75 females undergoing hydration, indicating for these fish that at least one batch was previously spawned. For the other 25 females with hydrated ovaries containing no POFs, HY oocytes represented the first batch of a series of batches. We could not distinguish more than one apparent age of POF among the 50 fish that had begun spawning. This indicates that yellowfin sole either resorb POFs before a succeeding batch is ovulated or that POFs of different ages (from different batches) are present but are indistinguishable.

Evidence of more than one series of batch spawnings

A total of 16 females with maturing ovaries (maturity-code 2) contained residual chorion tissue within the ovary lumen (Table 2; Fig. 2). The chorion tissue in these cases was sufficiently large to conclude that they were unspawned ova from a previous spawning. The ovaries ranged from those in early stages of yolk accumulation

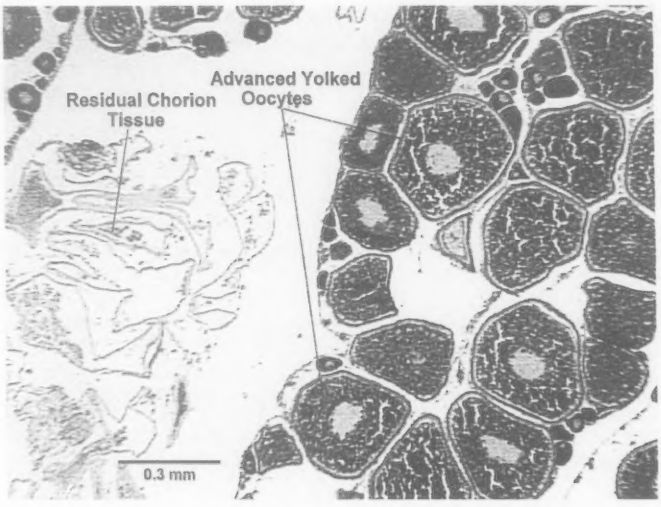

Figure 2

Histological section of a yellowfin sole (*Limanda aspera*) ovary with advancing yolked oocytes and remnants of chorion tissue leftover from previous spawning. The 38-cm-TL female was captured 17 June 1993 at a bottom depth of 27 m. The yolked oocytes averaged 0.31 mm in diameter, well below the mean diameter of yolked oocytes from spawning individuals (>0.44 mm).

Table 2

Occurrence of oocyte stages, postovulatory follicles, and other postspawning remnants within immature, maturing, hydrated, spawning, and spent yellowfin sole (*Limanda aspera*) ovaries. Histological examination of ovary cross sections.

Oocyte stage or intra-ovarian structure	Ovary maturity code					Total fish
	Immature (1)	Maturing (2)	Hydrated (3)	Spawning (4)	Spent (5)	
Early perinucleus	102	415	75	23	152	
Late perinucleus	58	415	75	23	151	
Partially yolked	8	349	17	7	82	
Advanced-yolked	0	409	72	23	0	
Migratory nucleus	0	63	72	21	0	
Hydrated-unovulated (HY)	0	0	75	3	0	
Ova	0	0	0	23	0	
Postovulatory follicles	0	13	50	19	40	
Atretic-HY	0	0	0	0	21	
Atretic ova	0	7	9	1	52	
Residual chorion tissue	0	15	1	0	29	
Number of fish	102	415	75	23	152	767

(mean AY diameters=0.27 mm), to those that contained AY oocytes near maximum size (mean AY diameter=0.43 mm). These ovaries did not contain POFs or MN stage oocytes; therefore ovaries were not advanced enough for there to be recent spawning from the existing AY standing stock.

It is possible that these fish had already spawned at least one series of batches, were spent, and were readying

Table 3

Two-way analysis of variance results comparing differences of oocyte density (top), and mean oocyte diameter (bottom) between blind and eyed-side ovaries and among anterior, middle, and posterior tissue subsampling positions in yellowfin sole, *Limanda aspera*. Paired *t*-tests (H_0=d_{post}–d_{ant}; H_0=d_{post}–d_{mid}) among ovary positions indicate significantly (P<0.05) greater oocyte densities (d) in posterior tissue samples compared with either anterior or middle positions. SS = sum of squares; MSE = mean square error.

Source	df	SS	MSE	*F*	*P*-value
Oocyte density (no. oocytes/g ovary tissue)					
Fish	19	3,391,989,272	178,525,751	62.32	0.0001
Ovary	1	3,466,212	3,466,212	1.21	0.2708
Position	2	25,951,981	12,951,981	4.53	0.0125
Ovary × position	2	9,505,128	4,752,564	1.68	0.1914
Error	95	268,371,656	2,824,965		
Corrected total	119	3,699,284,249			
Mean oocyte diameter					
Fish	19	5.7136	0.3007	183.25	0.0001
Ovary	1	0.0003	0.0003	0.19	0.6655
Position	2	0.0034	0.0017	1.02	0.3600
Ovary × position	2	0.0022	0.0011	0.68	0.5044
Error	5975	9.8053	0.0016		
Corrected total	5999[1]	15.5248			

[1] n = 6000; 2-ovary × 3-ovary positions × 20-fish × 50-oocytes/fish.

another standing stock of oocytes for spawning within the same reproductive season.

Homegeneity of oocytes between and within ovaries

Two-way ANOVA on mean oocyte diameters indicated that the means were not significantly different between ovaries or among the anterior, middle, and posterior ovary positions (Table 3). Additionally, our analysis revealed that oocytes were slightly more concentrated (number of oocytes/g ovary tissue) in posterior tissue samples compared with middle and anterior samples (paired *t*-tests, H_0: d_{post}–d_{ant}=0 and H_0: d_{post}–d_{mid}=0; n=20; P-values <0.05; Table 3). Comparison of oocyte density between middle and anterior tissue samples and between eyed-side and blind-side ovary lobes revealed no significant differences (paired *t*-test; P-value >0.05; Table 3). These results prompted us to take fecundity subsamples from two ovary locations (posterior and middle-anterior position from either ovary lobe) and to incorporate weighting factors (*WF*; Eq. 2) for all calculations of total fecundity.

The evidence for greater posterior-end oocyte densities that was found in 20 test fish prior to fecundity subsampling, was also present after all ovaries were subsampled. Oocyte densities were significantly greater in the posterior ovary end versus the anterior-middle positions among all ovaries sampled for fecundity (paired *t*-test, H_0: d_{post}–$d_{ant/mid}$=0; t=2.59; n=323; P=0.0100). The density of hydrated (HY) oocytes within maturity-code-3 ovaries, used for batch fecundity estimates, was also greater in subsamples taken from the posterior ovary end (paired *t*-test, H_0: d_{post}–$d_{ant/mid}$=0; t=3.40; n=75; P=0.0011). Computation of batch fecundity, therefore, incorporated the same weighting factors described for computation of total fecundity.

Oocyte size distributions

Oocyte diameter plots indicated a hiatus in distribution between AY oocytes and PY oocytes for ovaries with mean AY diameters ≥0.38 mm (Fig. 3). This separation of AY oocytes from other oocyte stages in more advanced ovaries (closer to spawning) is indicative of a determinate mode of oocyte development. In prespawning fish (maturity-code 2, no POFs), oocyte size distributions overlapped for fish with mean AY diameters less than 0.38 mm. PY oocytes, however, were a relatively minor portion in terms of oocyte density of the overall distribution for ovaries with mean AY diameters greater than 0.38 mm (Fig. 3). Oocyte distributions in maturing (maturity-code 2) fish with residual chorion tissue present in the ovary lumen exhibited the same hiatus between PY and AY oocytes where mean AY diameters were ≥0.38 mm (Fig. 3).

The size distribution of AY oocytes for those fish that were either spawning their first batch (maturity-code 4, no POFs; n=13) or had begun spawning (maturity-code 2 or 3, POFs present; n=23) was separated from PY and non-yolked oocyte distributions in 33 of the 36 fish examined. PY oocytes were either absent or were a very small fraction of the number of AY oocytes present. From the histological analysis, we found that 68 of the 86 fish that had begun spawning (maturity-codes 2 and 3 with POFs, and maturity-code 4) did not contain any PY oocytes, further indicating that only one stock of oocytes is advanced prior to the spent ovary condition.

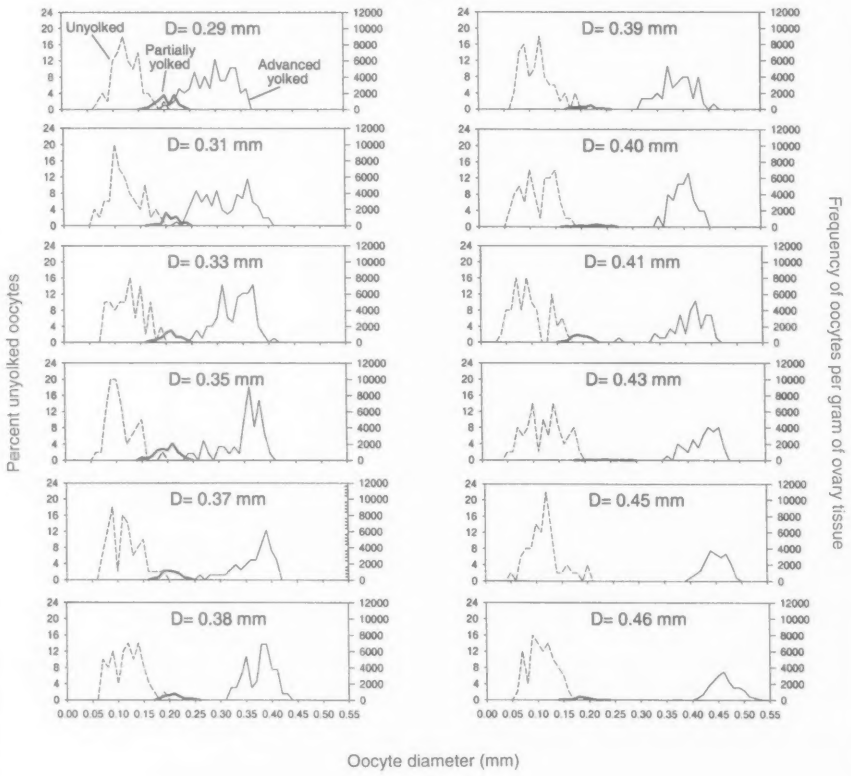

Figure 3

Size distributions for unyolked, partially yolked, and advanced-yolked oocytes for 12 yellowfin sole (*Limanda aspera*) females. Advanced-yolked and partially yolked oocyte diameters are plotted in terms of oocyte density (no. oocytes/g ovary tissue) and unyolked oocytes are plotted in terms of percent frequency. Note that frequencies of unyolked oocytes less than approximately 0.05 mm were not measured. Mean diameters (D) for advanced-yolked oocytes are noted.

Mean oocyte diameters of yolked oocytes (AY through MN) were generally larger among fish that had begun spawning compared with those that had not released a batch (Fig. 4). Ovaries that contained POFs had mean yolked oocyte diameters that on average were greater than 0.44 mm. Yolked oocytes in advancing ovaries with no evidence of recent spawning (no POFs) averaged less than 0.44 mm in diameter. Again, most of the ovaries with residual chorion material were significantly less developed than those with evidence of recent spawning (Fig. 4).

Occurrence of oocyte atresia

Of the 75 females examined histologically for the occurrence of atresia, only 15 (20%) had ovaries containing α-atretic AY, MN, or HY oocytes (Table 4). Within each of these 15 females, the average proportion of α-atretic AY-HY oocytes among all AY-HY oocytes was 0.034. Thus, among all females examined including those with no atresia (n=75), the relative frequency of α-atretic AY-HY oocytes among normal AY-HY oocytes was less than 1%. The occurrence of atretic AY-HY oocytes as well as atretic PY oocytes was higher among females that were either close to spawning or partially spawned compared with those in a prespawning condition (Table 4). As shown with the oocyte distribution plots, normal PY oocytes were more common among females that were in a prespawning condition. Lower frequencies of normal PY oocytes, but higher proportions of atretic PY oocytes among females that were partially spawned or close to spawning, indicated that many PY oocytes do not develop after spawning is initiated. We observed no cases of major atresia (>50% atretic) among advancing oocytes for all ovaries examined histologically. Given the low occurrence of oocyte atresia, we assumed a negligible effect of atresia on estimates of annual fecundity.

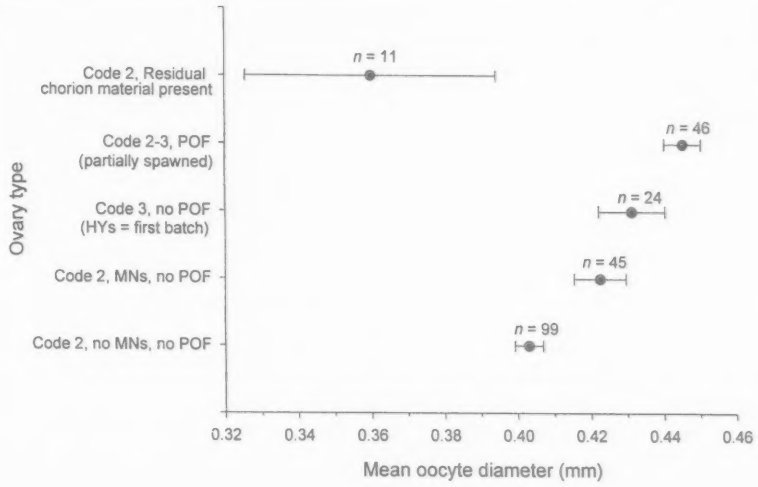

Figure 4

Comparison of mean yolked oocyte diameters among ovaries at different levels of development, from maturing (maturity-code 2) ovaries with no migratory nucleus stage (MN) oocytes (≥0.38 mm) to maturity-code 3 ovaries with postovulatory follicles (POFs) present. Error bars indicate 95% confidence intervals. See Table 1 for description of ovary maturity codes.

Table 4

Occurrence of alpha (α) atretic oocytes among advanced vitellogenic (AY through HY) and partially-yolked (PY) oocytes within yellowfin sole *(Limanda aspera)* ovaries (n=75 females). AY = advanced-yolked; HY = unovulated hydrated.

Maturity code	No. of females sampled	No. of females with α-atretic AY-HY oocytes	Proportion of α-atretic among all AY-HY (min.-max.)	No. of females with PY oocytes	No. of females with α-atretic PY oocytes
Code 2, no POFs (prespawning)	28	2	0.01–0.025	24	3
Code 3, no POFs (first batch)	13	5	0.004–0.058	4	3
Codes 2 and 3, POFs present (partially spawned)	23	6	0.005–0.037	6	3
Code 2, residual chorion tissue present	11	2	0.061–0.134	9	2

Total fecundity

In choosing ovaries to be used to estimate total fecundity, we selected ovaries that were advanced enough that the advancing stock (AY to MN) could be discriminated from less advanced oocytes (PY), yet were not advanced enough for there to have been potential spawning. First, we eliminated ovaries with mean oocyte diameters <0.38 mm due to the overlap in AY and PY distributions. Secondly, we eliminated ovaries with mean oocyte diameters greater than 0.44 mm (n=20) in an attempt to eliminate partially spawned ovaries that could not be identified with histological evaluation; POFs were not found in these ovaries; however, because the level of oocyte advancement (mean AY diameter) was similar to ovaries that did contain POFs (Fig. 4), the occurrence of recent batch spawning was possible.

Inclusion of ovaries with mean AY-oocyte diameters <0.38 mm as well as those >0.44 mm can potentially bias estimates of total fecundity. Estimates of total fecundity, measured from fish where distributions of PY and AY oocytes overlapped (Fig. 3), were higher than estimates from ovaries with more advanced oocytes (Fig. 5; Table 5). We compared yellowfin sole length-fecundity relationships of fish with ovaries that had mean AY-oocyte diameters ≥0.38 mm and ≤0.44 (n=148) to those with mean diameters <0.38 mm (n=80). Linear comparisons of the log(*length*)-log(*fecundity*) relationships between the two data sets indicated similar slopes (F=0.08; P=0.7725; df=1,

Table 5

Yellowfin sole (*Limanda aspera*) length-fecundity coefficients for nonlinear least-squares fit using equation $F = aL^b$, where F = fecundity and L = fish length (cm). MOD = mean oocyte diameter of advanced yolked oocytes. SE = standard error of estimate. Confidence intervals (CI) indicate approximate 95% bounds for predicted values of the mean (SAS Institute, 1989).

	Constants						
	a		*b*				
Fecundity type	Estimate	SE	Estimate	SE	*n*	r^2	Fecundity estimate for 35-cm female (Value ±95% CI)
Total							
MOD ≥ 0.38–0.44 mm[1]	3.322	2.909	3.631	0.243	148	0.60	1,343,807 ±64,406
MOD < 0.38 mm	4.947	5.564	3.550	0.311	80	0.64	1,496,401 ±105,108
All data (MOD ≤0.44 mm)	2.988	2.074	3.672	0.192	248	0.62	1,397,492 ±56,054
Batch	1.648	3.138	3.188	0.528	75	0.32	137,862 ±17,111

[1] Ovaries with mean AY through MN oocyte diameters ≥0.38 mm and ≤0.44 mm were considered the most appropriate for use in estimating total fecundity.

221) but different intercepts (F=6.77; P=0.01; df =1, 222). We also tested whether the inclusion of ovaries with mean oocyte diameters >0.44 mm would have a significant effect on the fish-length–fecundity relationship (Table 6). When ovaries with mean oocyte diameters >0.44 mm were included, estimates of total fecundity at length were significantly reduced. No such effect was apparent when the data were limited to ovaries with mean oocyte diameters ≤0.44 mm (Table 6).

Total fecundity as a function of fish length for yellowfin sole was estimated as

$$F = 3.3225 \times TL^{3.6312},$$

where F = standing stock of AYs; and
TL = total fish length in centimeters (Table 5).

Total fecundity ranged from 295,615 oocytes in a 29-cm-TL fish to 3,635,108 oocytes in a 39-cm-TL fish (Fig. 6).

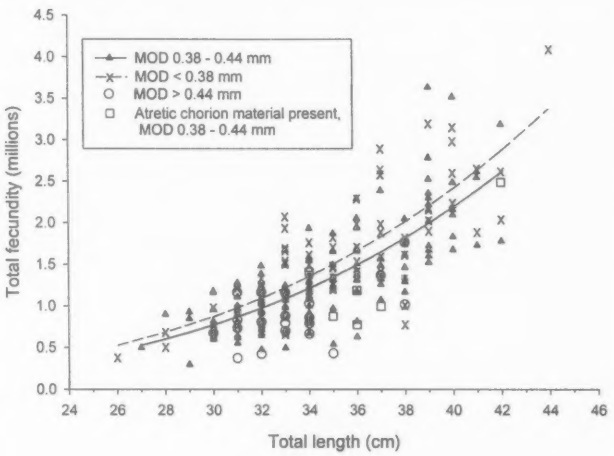

Figure 5

Total fecundity as a function total length (cm). Data for yellowfin sole (*Limanda aspera*) ovaries with mean AY diameters (MOD) 0.38 mm to 0.44 mm (n=148) were compared with ovaries with MOD <0.38 mm (n=80), ovaries with MOD >0.44 mm (n=20), and ovaries with residual chorion material present (n=7). Yellowfin sole ovaries with MOD 0.38 mm to 0.44 mm were considered most appropriate for use in total fecundity. Curves indicate predicated values from nonlinear regression. MOD = mean oocyte diameter of AY through MN oocytes.

Batch fecundity

Batch fecundity was estimated for 75 females and ranged from 2,400 to 408,000 oocytes and larger fish generally had larger batches (Figs. 6 and 7). The number of oocytes in the first batch was in most cases lower than in succeeding batches, although the variability of the first batch for a given fish length was quite high (Fig. 7). Twenty-five of the fish examined contained ovaries with unovulated hydrated (HY) oocytes and no evidence of prior batch spawnings, thus representing the first batch. Three fish contained ovaries with only one hydrated batch remaining (no AYs left), thus representing the last batch. The remaining "middle batch" fish (n=47) possessed ovaries containing unovulated hydrated oocytes and POFs, indicating that at least one batch had been previously spawned.

Batch fecundity, irrespective of batch order, is described in terms of fish length by

$$B = 1.6481 \times TL^{3.1879},$$

Table 6

Linear regression results from the model $\log(F) = \log(a) + b\log(L) + \log(c)$; the log-transformation of model $F = aL^b c$, where F = total fecundity, L = fish length (cm), and a, b, c are coefficients. Coefficient c represents the interaction of mean oocyte diameter on F. A series of regressions were run, first by using all data where the mean yolked oocyte diameter was ≥0.38, then with data sets that excluded ovaries with high mean oocyte diameters (i.e. ovaries with mean oocyte diameters >0.46 mm, >0.45 mm, >0.44 mm).

Mean oocyte diameter range of ovaries used in analysis	Estimate				
	Log(a)	b	Log(c)	P-value of H_0: log(c) = 0	n
≥ 0.38 mm	6.40	3.43	–1.22	0.003	168
0.38–0.46 mm	6.35	3.44	–1.22	0.006	165
0.38–0.45 mm	5.84	3.42	–1.06	0.026	160
0.38–0.44 mm[1]	3.07	3.44	–0.33	0.525	148

[1] This data set, which excluded ovaries with mean oocyte diameters > 0.44 mm, indicated no significant effect of mean oocyte diameter on the estimate of total fecundity.

where B = batch fecundity; and
TL = total fish length in centimeters (Table 5).

Number of batches

The number of batches that a female of a given length spawns was estimated as F/B (above). Yellowfin sole are estimated to spawn an average of 8 to 11 batches prior to the spent ovary condition. The frequency of batches appears to be slightly higher for larger fish.

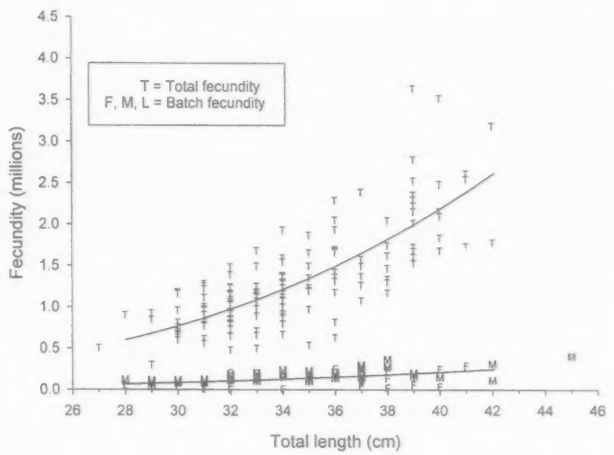

Figure 6

Total and batch fecundity by fish length for yellowfin sole (*Limanda aspera*) in the eastern Bering Sea. Batch fecundity symbols F, M, and L correspond respectively to first, middle, and last batch fecundity estimates.

Discussion

Determinate or indeterminate fecundity?

Fish with determinate fecundity are defined as those with ovaries whose advancing stock of oocytes represent the entire number of eggs to be spawned that year (Hunter et al., 1989; Horwood and Walker, 1990; Hunter et al., 1992). Fish with indeterminate fecundity, in contrast, are defined as those whose ovaries continuously mature yolked oocytes from unyolked oocytes; thus the "standing stock" of advanced oocytes does not represent the total number of eggs to be spawned that year (Hunter et al., 1989). Oocyte size frequencies of various stage oocytes (i.e. advanced-yolked, partially yolked, unyolked) have been used as criteria to determine if a fish has determinate fecundity (Hunter et al., 1989; Hunter et al., 1992; Horwood and Walker, 1990). If a break or "hiatus" has occurred between the advanced-yolked distribution and the less advanced ones, then the advanced-yolked distribution could be considered the determinate stock. This break in oocyte distributions was observed for yellowfin sole, and it is clear that batches are spawned from the advanced-yolked mode. A determinate mode of oocyte development in yellowfin sole is further indicated by the fact that total fecundity was substantially lower in fish that had spawned at least one batch (Fig. 8)—an indication that there is no oocyte recruitment to the advanced oocyte stock once spawning begins. Hence, although yellowfin sole spawns eggs intermittently in batches, they undergo a group synchronous mode of oocyte development.

In contrast to other fish with determinate fecundity, yellowfin sole fecundity estimates were higher among individuals with less-developed ovaries where PY and AY oocyte distributions overlapped (Fig. 5). Hunter et al. (1992) indicated the opposite for Dover sole; they found that fecundity among individuals where the advanced-stock size

distribution was not well separated from less developed oocytes was lower because oocyte recruitment to the advanced stock was not complete. We suggest two reasons for this difference between the two species. First, the discrimination between PY and AY oocytes and the criteria used to separate them were likely different for the two studies. Exact discrimination between oocytes that will not develop and those that are viable cannot occur until the distributions are completely separate. Second, rates of oocyte atresia between the two species may be different. Higher rates of PY and AY atresia may account for a decrease in fecundity as the AY distribution advances. As Hunter et al. (1992) noted, the fate of PY oocytes is uncertain; perhaps some individuals retain them for an additional series of batch spawnings.

Although multiple groups of oocytes are not continuously developed as are those observed for indeterminate fishes, such as the northern anchovy, *Engraulis mordax* (Hunter and Leong, 1981), yellowfin sole appear to have the potential to recover spent ovaries and spawn another series of batches. Remnants of chorions from hydrated oocytes in the lumen of ovaries containing a unimodal stock of advancing yolked oocytes with diameters significantly less than those of spawning fish (Fig. 4) suggest that at least some individuals can produce more than one series of batches in a single year. Annual fecundity for each of these individuals would be significantly greater than the estimated total fecundity. Although yellowfin sole exhibit a determinate group-synchronous mode of oocyte development, some individuals may spawn more than one series of batches; therefore, annual fecundity must be considered indeterminate.

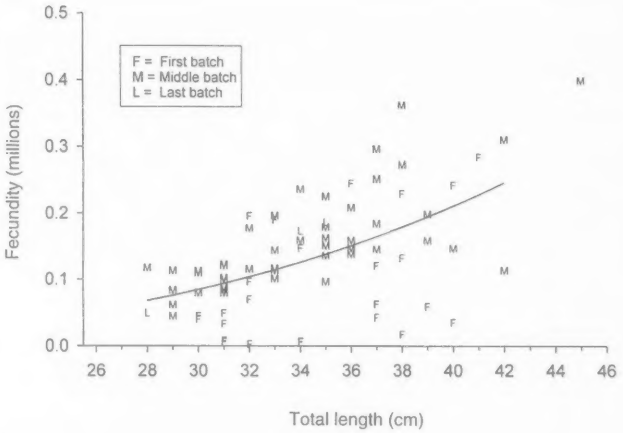

Figure 7

Batch fecundity as a function of fish total length for yellowfin sole (*Limanda aspera*) in the eastern Bering Sea (n=75). First, middle, and last batches are indicated. The curve represents the nonlinear least squares regression for all the batches.

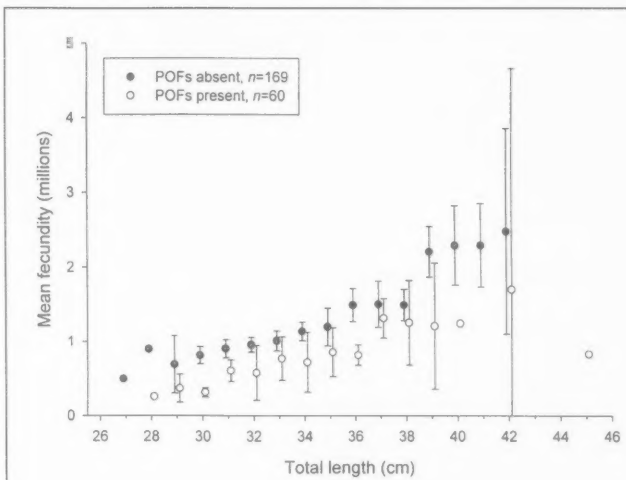

Figure 8

Comparison of mean total fecundity (no POF and mean oocyte diameter ≥0.38 mm) at length and the mean fecundity observed in yellowfin sole (*Limanda aspera*) that had already spawned at least one batch (POFs present).

Comparison of total fecundity between southeast and northwest areas

Total fecundity for yellowfin sole was compared for the northwest and southeast areas of the eastern Bering Sea. Although Nichol (1997) found that yellowfin sole growth and size at maturity were greater in the northeast area of the eastern Bering Sea compared with the southeast area (Fig. 1), we found no differences in fecundity between areas. Neither slopes (ANCOVA: F=0.09; P=0.77; df =1, 144) nor intercepts (ANCOVA: F=0.56; P>0.10; df =1, 145) were different for the log-transformed (linear) length-fecundity relationships.

Comparison of results with those from other authors

With the exception of fecundity data presented by Fadeev (1970), the relationship between yellowfin sole fecundity and fish length appears similar between east and west sides of the Bering Sea and among years (Fig. 9). Ivankov and Ivankova (1974), who reported that yellowfin sole in the northwestern Sea of Japan spawn up to five batches, presented slightly lower values of total fecundity compared with our results. Tikhonov (1977) presented similar length-fecundity relationships for yellowfin sole off

the west coast of Kamchatka for five different years, 1963–69. Because methods (i.e. selection criteria for ovaries) likely varied among studies, critical interpretation of these comparisons is difficult.

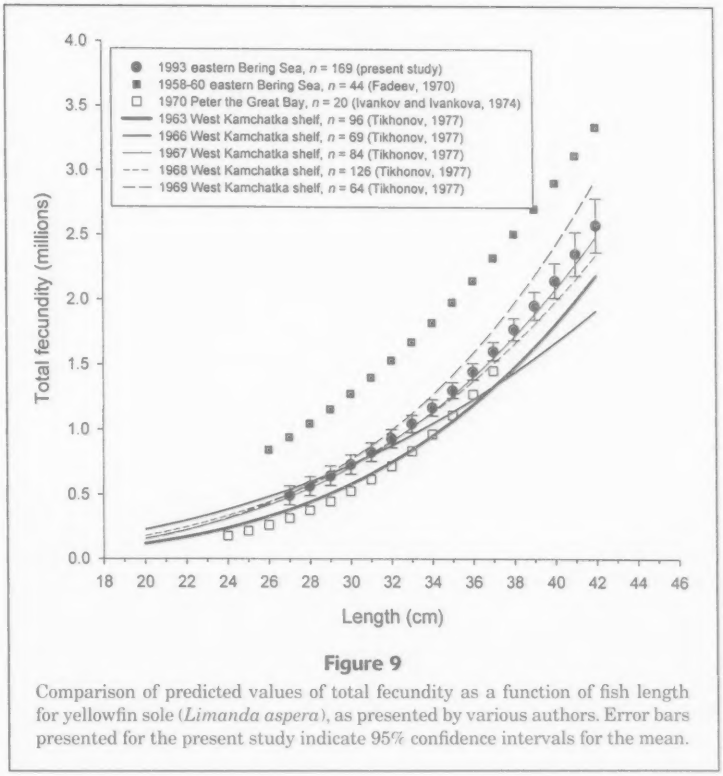

Figure 9

Comparison of predicted values of total fecundity as a function of fish length for yellowfin sole (*Limanda aspera*), as presented by various authors. Error bars presented for the present study indicate 95% confidence intervals for the mean.

Comparison of yellowfin sole with other species

Yellowfin sole is more fecund and spawns smaller eggs than other flatfish species in the eastern Bering Sea (Table 7). Most flatfishes in the eastern Bering Sea, with the exception of northern rock sole (*Lepidopsetta polyxystra,* Orr and Matarese, 2000), spawn pelagic eggs intermittently (in batches). Longhead dabs, also within the genus *Limanda* (*proboscidea*), have similar reproductive characteristics to yellowfin sole in respect to their high fecundity at length, small diameter of eggs, shallow spawning location, and spring-summer spawning season (Table 7).

Yellowfin sole are most closely related to yellowtail flounder, *Limanda ferruginea* (Cooper and Chapleau, 1998), a western Atlantic species ranging from the Gulf of St. Lawrence to Chesapeake Bay (Howell, 1983; Zamarro, 1992). Although only morphological characters were used to determine the phylogenetic relationships of these two species among pleuronectids (Cooper and Chapleau, 1998), yellowfin sole and yellowtail flounder also share very similar life history characteristics. Fecundity ranges, egg diameter, egg type, spawning interval, and spawning seasons are very similar between the two species (Table 7). Like yellowfin sole females, yellowtail flounder females develop oocytes in a group-synchronous manner (Howell, 1983). In addition, they have MN oocytes present in their ovaries that contain hydrated oocytes, indicating that spawning of batches is similarly continuous (Zamarro, 1992). Yellowtail flounder spawn approximately 7 batches compared with 8–11 for yellowfin sole in the eastern Bering Sea. In short, closely related species share more than just morphological similarities; reproductive characteristics also reflect a shared evolutionary history.

Spawning habits

Yellowfin sole in the eastern Bering Sea have been observed from prespawning to spawning conditions from mid-May through August (Fadeev, 1970; Nichol, 1995). Observations of eggs and early-stage larvae in ichthyoplankton surveys conducted in the eastern Bering Sea (Musienko, 1963; Waldron, 1981) indicate that spawning may not completely end until September. Given that the spawning season is protracted and that spawning of a series of batches is fairly rapid, individuals may have the potential to recover spent ovaries and spawn more than one series of batches within a single year. The possibility that residual chorion tissue is left over from the previous year's spawning seems unlikely given that it would have been retained within the ovary for more than 8 months (Sep–May).

Yellowfin sole remain in the spawning area (<30 m bottom depth) until a series of batches have been spawned. The absence of partially spawned fish, those with ovaries containing POFs and AY oocytes, found outside the spawning area (>30 m) indicate that after spawning begins (first batch) fish remain in the spawning area until spent. Again, the presence of MN oocytes in most ovaries undergoing oocyte hydration indicates that there is very little lag period between batch spawnings. This evidence refutes an earlier assertion by Nichol (1995) that yellowfin sole may migrate in and out of the spawning area between batch spawnings. However, some females do migrate out of the spawning area after a series of batches has been completely spawned; both spent and maturing (maturity-code 2) females with evidence of completed batch spawnings (i.e. with residual chorion tissue) were observed in spawning (<30 m) and nonspawning (>30 m) waters.

Acknowledgments

Claire Armistead, Jan Haaga, Mark Conrad, and Gary Walters aided with tissue collections. Frank Morado, Lisa

Table 7

Fecundity and spawning habits of nine species of flatfishes found in the eastern Bering Sea and yellowtail flounder *(Limanda ferruginea)* from the Atlantic coast of North America. Spawning interval refers to whether eggs are spawned intermittently (batch) or all at once (synchronous). Numbers in parentheses are the range of fish lengths used for the respective fecundity estimates. All estimates are for the eastern Bering Sea except where noted.

Species	Fecundity range	Egg diameter in plankton	Egg type	Spawning interval	Spawning location (bottom depth)	Spawning season
Yellowfin sole (*Limanda aspera*)	295,615–3,635,108[1] (27–42 cm)	0.76–0.85 mm[2]	pelagic[2, 3]	batch[4, 5]	< 30 m[4]	May–Sep[4, 6]
Alaska plaice (*Pleuronectes quadrituberculatus*)	56,300–312,600[5] (28–50 cm)	1.67–2.21 mm[2]	pelagic[2, 3]	batch[5]	75–150 m[7]	Apr–Jun[5]
Arrowtooth flounder (*Atheresthes evermanni*)	246,000–2,224,000[8] (48–83 cm)	~ 3 mm[2]	mesopelagic[2]	batch[9]	108–360 m[10]	Dec–Mar[11]
Flathead sole (*Hippoglossoides elassodon*)	51,600–160,100[5] (22–42 cm)	2.75–3.75 mm[2, 7]	pelagic[2, 3, 7]	batch[5]	50–150m[7]	Feb–May[5]
Greenland turbot (*Reinhardtius hippoglossoides*)	15,000–215,000[12] (73–106 cm)	4.00–4.50 mm[2, 7]	bathypelagic[7]	—	> 100 m[2]	Oct.–Dec[11]
Longhead dab (*Limanda proboscidea*)	78,000–841,200[5] (14–26 cm)	0.72–0.87 mm[2]	pelagic[7]	batch[13]	26–35 m[7]	July–Aug[5, 13]
Pacific halibut (*Hippoglossus stenolepis*)	200,000–4,000,000[14] (83–200 cm)	2.90–3.80 mm[2, 7]	pelagic[2, 3]	batch[15]	300–500 m[15]	Nov–Mar[7]
Northern rock sole (*Lepidopsetta polyxystra*)	150,000–400,000[5] (22–42 cm)	0.87–1.00 mm[5]	demersal[2, 16]	synch.	70–140 m[15]	Mar–Jun[16]
Starry flounder (*Platichthys stellatus*)	913,4005–11,000,000[17] (38–56 cm)	0.88–1.28 mm[2]	pelagic[2]	batch[5]	11–75 m[7]	May–Jun[5]
Yellowtail flounder (*Limanda ferruginea*)	333,500–4,215,000[18, 19] (28–54 cm)	0.75–0.90 mm[20]	pelagic[20]	batch[21]	—	May–Sep[22, 23]

[1] Present study.
[2] Matarese et al. (1989).
[3] Waldron (1981).
[4] Nichol (1995).
[5] Fadeev (1965); Fecundity range represents the average fecundity at 2-cm minimum and 2-cm maximum fish lengths.
[6] Musienko (1963).
[7] Musienko (1970).
[8] Zimmermann (1997).
[9] Rickey (1995).
[10] Hirshberger and Smith (1983); from Gulf of Alaska.
[11] Pertseva-Ostroumova (1961).
[12] Lear (1970); Estimated from *Reinhartius hippoglossoides* from the Newfoundland area.
[13] Nichol; personal obs., 1999.
[14] Schmitt and Skud (1978); from Gulf of Alaska.
[15] St. Pierre (1984).
[16] Shubnikov and Lisovenko (1964).
[17] Orcutt (1950); fish was 56.5 cm standard length; from Monterey Bay, California.
[18] Pitt (1971); from Grand Banks, off Newfoundland.
[19] Howell and Kesler (1977); from off southern New England.
[20] Yevseyenko and Nevinskiy (1981); from Northwest Atlantic.
[21] Zamarro (1992); from Grand Banks, off Newfoundland.
[22] Pitt (1970); from Northwest Atlantic, off Newfoundland.
[23] Walsh (1992); from Grand Banks, off Newfoundland.

Mooney, and personnel at East-side Medical Laboratory, Inc. performed most of the histological processing. Beverly Macewicz provided knowledgeable suggestions that improved both the analyses and the text. We also thank Dave Somerton, Jay Orr, Gary Walters, Gary Duker, and James Lee for helpful reviews prior to the submission to this journal. Two anonymous reviewers improved final versions of the manuscript.

Literature cited

BioScan, Inc.
1992. BioScan Optimas user guide, fifth ed. BioScan, Inc., Edmonds, WA

Cooper, J. A., and F. Chapleau.
1998. Monophyly and interrelationships of the family Pleuronectidae (Pleuronectiformes), with a revised classification. Fish. Bull. 96:686–726.

Fadeev, N. S.
1965. Comparative outline of the biology of fishes in the southeastern part of the Bering Sea and condition of their resources. Translated by Isr. Prog. Sci. Transl. 1972. *In* Soviet fisheries investigations in the northeastern Pacific, part 4 (P. A. Moiseev, ed.), p. 112–129. [Available from U.S. Dep. Commer., Natl. Tech. Inf. Serv., Springfield, VA, as TT 67-51206.]
1970. Fisheries and biological characteristics of the eastern Bering Sea yellowfin sole. Translated by Isr. Prog. Sci. Transl., 1972. *In* Soviet fisheries investigations in the northeastern Pacific, part 5 (P. A. Moiseev. ed.), p. 332–396. [Available from U.S. Dep. Commer., Natl. Tech. Inf. Serv., Springfield, VA, as TT 71-50127.]

Hirshberger, W. A., and G. B. Smith.
1983. Spawning of twelve groundfish species in Alaska and Pacific coast regions, 1975–81. U.S. Dep. Commer., NOAA Tech. Memo. NMFS-F/NWC-44, 50 p.

Horwood, J. W., and M. Greer Walker.
1990. Determinacy of fecundity in sole (*Solea solea*) from the Bristol Channel. J. Mar. Biol. Assoc. U.K. 70:803–813.

Howell, W. H.
1983. Seasonal changes in the ovaries of adult yellowtail flounder, *Limanda ferruginea*. Fish. Bull. 81:341–355.

Howell, W. H., and D. H. Kesler.
1977. Fecundity of the southern New England stock of yellowtail flounder, *Limanda ferruginea*. Fish. Bull. 75: 877–880.

Hunter, J. R., and R. Leong.
1981. The spawning energetics of female northern anchovy, *Engraulis mordax*. Fish. Bull. 79:215–230.

Hunter, J. R., N. C. H. Lo, and R. J. H. Leong.
1985. Batch fecundity in multiple spawning fishes. *In* An egg production method for estimating spawning biomass of pelagic fish: application to the northern anchovy, *Engraulis mordax* (R. Lasker, ed.), p. 67–78. U.S. Dep. Commer., NOAA Tech. Rep. NMFS 36.

Hunter, J. R., and B. J. Macewicz.
1985a. Measurement of spawning frequency in multiple spawning fishes. *In* An egg production method for estimating spawning biomass of pelagic fish: application to the northern anchovy, *Engraulis mordax* (R. Lasker, ed.), p. 79–93. U.S. Dep. Commer., NOAA Tech. Rep. NMFS 36.
1985b. Rates of atresia in the ovary of captive and wild northern anchovy, *Engraulis mordax*. Fish. Bull. 83:119–136..

Hunter, J. R., B. J. Macewicz, and C. A. Kimbell.
1989. Fecundity and other aspects of the reproduction of sablefish, *Anoplopoma fimbria*, in central California waters. Calif. Coop. Oceanic Fish. Invest. Rep. 30:61–72.

Hunter, J. R., B. J. Macewicz, N. C. H. Lo, and C. A. Kimbrell.
1992. Fecundity, spawning, and maturity of female Dover sole *Microstomus pacificus*, with an evaluation of assumptions and precision. Fish. Bull. 90:101–128.

Ivankov, V. I., and Z. G. Ivankova.
1974. Fecundity of flounders in the northwestern Sea of Japan. J. Ichthyol. 14:868–876.

Lear, W. H.
1970. Catch statistics, length and age composition of Greenland halibut in the Newfoundland area. Fish. Res. Board Can. Tech. Rep. 179, 27 p.

Macewicz, B. J., and J. R. Hunter.
1994. Fecundity of sablefish, *Anoplopoma fimbria*, from Oregon coastal waters. Calif. Coop. Oceanic Fish. Invest. Rep. 35:160–174.

Matarese, A. C., A. W. Kendall Jr., D. R. Blood, and B. M. Winter.
1989. Laboratory guide to early life history stages of Northeast Pacific fishes. U.S. Dep. Commer., NOAA Tech. Rep. NMFS 80, 652 p.

McFarlane, G. A., and M. W. Saunders.
1997. Fecundity of Pacific hake (*Merluccius productus*) for three stocks off the west coast of North America. Calif. Coop. Oceanic Fish. Invest. Rep. 38:114–119.

Musienko, L. N.
1963. Ichthyoplankton of the Bering Sea. (Data of the Bering Sea expedition of 1958–1959). Translated by Isr. Prog. Sci. Transl., 1968. *In* Soviet fisheries investigations in the northeastern Pacific, part 1 (P.A. Moiseev, ed.), p. 251–286. [Available from U.S. Dep. Commer., Natl. Tech. Inf. Serv., Springfield, VA, as TT 67-51203.]
1970. Reproduction and development of Bering Sea fishes. Translated by Isr. Prog. Sci. Transl., 1972. *In* Soviet fisheries investigations in the northeastern Pacific, part 5 (P.A. Moiseev, ed.), p 161–224. [Available from U.S. Dep. Commer., Natl. Tech. Inf. Serv., Springfield, VA, as TT 71-50127.]

Nichol, D. G.
1995. Spawning and maturation of female yellowfin sole in the eastern Bering Sea. *In* Proceedings of the international flatfish symposium, October 1994, Anchorage, Alaska, p. 35–50. Univ. Alaska, Alaska Sea Grant Rep. 95-04.
1997. Effects of geography and bathymetry on growth and maturity of yellowfin sole, *Pleuronectes asper*, in the eastern Bering Sea. Fish. Bull. 95:494–503.
1998. Annual and between sex variability of yellowfin sole, *Pleuronectes asper*, spring-summer distributions in the eastern Bering Sea. Fish. Bull. 96:547–561.

Orcutt, H. G.
1950. The life history of the starry flounder, *Platichthys stellatus* (Pallus). Calif. Dep. Fish Game, Fish Bull. 78, 64 p.

Orr, J. W., and A. C. Matarese.
2000. Revision of the genus *Lepidopsetta* Gill, 1862 (Teleostei: Pleuronectidae) based on larval and adult morphology, with a description of a new species from the North Pacific Ocean and Bering Sea. Fish. Bull. 98:539–582.

Pertseva-Ostroumova, T. A.
1961. The reproduction and development of far eastern flounders, Izdate'lstvo Akad. Nauk. SSSR, 483 p. [Transl. by Fish Res. Board Can., 1967, Transl. Ser. 856, 1003 p.]

Pitt, T. K.
1970. Distribution, abundance, and spawning of yellowtail flounder, *Limanda ferruginea*, in the Newfoundland area of the northwest Atlantic. J. Fish. Res. Board Canada 27 (12):2261–2271.

1971. Fecundity of the yellowtail flounder (*Limanda ferruginea*) from the Grand Bank, Newfoundland. J. Fish. Res. Board Canada 28(3): 456–457.

Rickey, M. H.
1995. Maturity, spawning, and seasonal movement of arrowtooth flounder, *Atheresthes stomias*, off Washington. Fish. Bull. 93:127–138.

St. Pierre, G.
1984. Spawning locations and season for Pacific halibut. Int Pac. Halibut Comm. Sci. Rep. 70, 46 p.

SAS Institute Inc.
1989. SAS/STAT user's guide, version 6, fourth ed., vol. 2. SAS Institute Inc. Cary NC, 846 p.

Schmitt C. C. and B. E. Skud.
1978. Relation of fecundity to long-term changes in growth, abundance and recruitment. Int. Pac. Halibut Comm. Sci. Rep. 66, 31 p.

Shubnikov, D. A., and L. A. Lisovenko.
1964. Data on the biology of rock sole of the southeastern Bering Sea. Translated by Isr. Prog. Sci. Transl., 1968. *In* Soviet fisheries investigations in the northeastern Pacific, part 2 (P.A. Moiseev, ed.), p. 220–226. [Available from U.S. Dep. Commer., Natl. Tech. Inf. Serv., Springfield, VA, as TT 67-51204.]

Tikhonov, V. I.
1977. Changes in the fecundity and rate of maturation of the yellowfin sole. Sov. J. Mar. Biol. 3(3):214–218. [Engl. transl. of Biol. Morya].

Wakabayashi, K.
1989. Studies on the fishery biology of yellowfin sole in the eastern Bering Sea. [In Jpn., Engl. Summ.] Bull. Far Seas Fish. Res. Lab. 26:21–152.

Waldron, K. D.
1981. Ichthyoplankton. *In* The eastern Bering Sea shelf: oceanography and resources, vol. 1 (Donald W. Hood and John A. Calder, eds.), p. 471–493. U.S. Dep. Commer., Natl. Oceanic Atmos. Admin., Mar. Poll. Assess., U.S. Gov. Print Off., Washington, D.C.

Walker, M. G., P. R. Witthames, and I. Bautista de los Santos.
1994. Is the fecundity of the Atlantic mackerel (*Scomber scombrus*: Scombridae) determinate? Sarsa 79(1):13–26.

Walsh, S. J.
1992. Factors influencing distribution of juvenile yellowtail flounder (*Limanda ferruginea*) on the Grand Bank of Newfoundland. Neth. J. Sea Res. 29:193–203.

Wilderbuer, T. K., G. E. Walters, and R. G. Bakkala.
1992. Yellowfin sole, *Pleuronectes asper*, of the eastern Bering Sea: biological characteristics, history of exploitation, and management. Mar Fish. Rev. 54(4):1–18.

Yamamoto, K.
1956. Studies on the formation of fish eggs. I. Annual cycle in the development of ovarian eggs in the flounder, *Liopsetta obscura*. J. Fac. Sci. Hokkaido Univ. Ser. VI, Zool. 12:362–376.

Yevseyenko, S. A., and M. M. Nevinski.
1981. On the development of the eggs and larvae of the yellow-tailed dab *Limanda ferruginea* Storer and their passive transport in the northwestern Atlantic. J. Ichthyol. 21:65–74.

Zamarro, J.
1992. Batch fecundity and spawning frequency of yellowtail flounder (*Limanda ferruginea*) on the Grand Bank. Northwest Atl. Fish. Org. Sci. Counc. Stud., 15:43–51.

Zimmermann, M.
1997. Maturity and fecundity of arrowtooth flounder, *Atheresthes stomias*, from the Gulf of Alaska. Fish. Bull. 95: 598–611.

Analysis of contemporary genetic structure of even-broodyear populations of Asian and western Alaskan pink salmon, *Oncorhynchus gorbuscha*

Claire Noll[1]
Natalia V. Varnavskaya[2]
Evgeny A. Matzak[3]
Sharon L. Hawkins[1]
Victoria V. Midanaya[2]
Oleg N. Katugin[3]
Charles Russell[1]
Natalya M. Kinas[2]
Charles M. Guthrie III[1]
Hiroshi Mayama[4]
Fumio Yamazaki[5]
Bruce P. Finney[6]
Anthony J. Gharrett[1,7]

E-mail address (for A. J. Gharrett, contact author): ffajg@uaf.edu

Abstract–Even-year pink salmon (*Oncorhynchus gorbuscha*) populations from the Russian Far East and Japan exhibit genetic structure that reflects their geographic relationships. Extension of genetic analysis to include data from Bering Sea and northern Gulf of Alaska populations shows a combined genetic structure with three prominent groupings that correspond to the three North Pacific Ocean basins—the Sea of Okhotsk, the Bering Sea, and the Gulf of Alaska—and that are consistent with geographic, geologic history, and oceanographic features. Analysis of 35 Asian collections at 39 variable allozyme loci (54 total) allowed examination of population structure of even-year pink salmon. Although most (98.5%) of the genetic variation occurred within collections (populations), the 1.5% attributable to among-collection divergence was sufficient to detect population structure and provide a basis for some stock separation. Differences between western Kamchatka populations and eastern Sakhalin Island populations indicate that little gene flow occurs between those regions and argues against an interregional fluctuating stock model.

Manuscript accepted 22 August 2000.
Fish. Bull. 99:123–138 (2001).

Pink salmon (*Oncorhynchus gorbuscha*) are the most abundant Pacific salmon species and spawn along most of the Pacific rim coastline north of 40°N latitude (Heard, 1991). The species is unique among salmonids in having a determinate life cycle. Adults return to their natal streams to spawn at 2 years of age, which has resulted in separate broodlines in even and odd years (Heard, 1991). Most of the range supports spawning runs of both broodlines, although they may differ in numbers. The southern part of the North American Pacific coast has only small even-year runs; and in western Alaska, even-year runs are much more abundant than odd-year runs (Heard, 1991). The pattern of a numerically dominant broodline in many areas has changed since early this century, perhaps in response to changes in fishing intensity (Takagi et al., 1981) or climate cycles (Mantua et al., 1997). Optimum management and conservation of the pink salmon resource requires thorough knowledge of their biology, including population structure, relationships among populations, and the extent of genetic exchange among local populations and between geographically distinct regions. Genetic divergence among groups of salmon also may provide a basis for stock identification by fish managers (Beacham et al., 1985; Pella and Milner, 1987).

Although DNA-based analyses have become available in recent years (e.g. Park and Moran, 1994), allozyme analysis remains a powerful method for pink salmon studies because they exhibit variability at a number of loci. From allozyme data, marked broodline differences have been demonstrated between pink salmon populations from the Russian Pacific coast (Gagalchii, 1986; Glubokovsky et al., 1989; Kartavtsev, 1991; Zhivotovsky et al., 1989; Kartavtsev et al., 1992) and from the North American Pacific coast (Aspinwall, 1974; McGregor, 1983; Beacham et al., 1988). Although based on few allozyme loci, genetic divergence within each broodline also has been observed among pink salmon collections from many regions of Russia (Gagalchii, 1986; Glubokovsky et al., 1989);

[1] National Marine Fisheries Service, Auke Bay Laboratory, 11305 Glacier Hwy., Juneau, Alaska 99801-8626.
[2] Kamchatka Scientific Research Institute of Fisheries and Oceanography, Kamchat-NIRO, Petropavlovsk-Kamchatsky 683602, Kamchatka, Russia.
[3] Pacific Research Fisheries Centre (TINRO-CENTRE), 4 Shevchenko Alley, Vladivostok 690600, Russia.
[4] Hokkaido Salmon Hatchery, Fisheries Agency of Japan, 2-2 Nakanoshima, Toyohira-ku, Sapporo 062, Japan.
[5] Hokkaido University, Laboratory of Genetics and Embryology, Faculty of Fisheries, Hakodate 041, Japan.
[6] Institute of Marine Science, University of Alaska Fairbanks, Fairbanks, Alaska 97735.
[7] Fisheries Division, University of Alaska Fairbanks, 11120 Glacier Hwy., Juneau, Alaska 99801.

more extensive allozyme surveys show divergence within broodlines in several North American regions (Beacham et al., 1985, 1988; Gharrett et al., 1988; Shaklee et al., 1991). Genetic divergence is usually attributed to random genetic drift, adaptation to local environmental conditions, or both, which can occur because salmon home to their natal streams to spawn (for an overview, see Allendorf et al., 1987).

The genetic compositions of populations are also molded by other events in their evolutionary histories. If populations share multiple genetic characteristics, then they may share a common origin (colonization or gene flow) or may be derived from different ancestral lines that have experienced homogenizing selection pressures (similar historical environments). The far North Pacific Ocean, Bering Sea, and Sea of Okhotsk are of special interest in the evolution of salmon population structure because these basins encountered the most extreme environmental conditions during the late Pleistocene Epoch. During the last 100,000 years, the environment ranged from extremely favorable (modern conditions) to extremely harsh, which in some areas undoubtedly led to extirpation of many salmon populations. Comparison of the nature and extent of genetic variation within regions to variation among regions is one means of exploring the recent history of a species. Reports of genetic variation among chum salmon (*O. keta*; Wilmot et al., 1994; Winans et al., 1994; Seeb and Crane, 1999), sockeye salmon (*O. nerka*; Varnavskaya et al., 1994a, 1994b; Wilmot et al, 1994), and pink salmon (Gharrett et al., 1988; Varnavskaya and Beacham, 1992; Shaklee and Varnavskaya 1994) are mostly limited to a single region with few reference populations from other regions, or they skip across intervening regions. In addition for sockeye salmon, there are relatively few informational loci and the variation among populations within a region is often large. Consequently, it is difficult to formulate a coherent picture for any Pacific salmon species. The data available for a broader range of Asian populations (Glubokovsky et al., 1989) are based on too few loci to provide a strong basis for broader comparisons.

One advantage of studying pink salmon is that they are distributed almost continuously throughout the northern region. Tagging studies indicate that pink salmon from streams in large contiguous areas of the coast make similar movements and may occupy the same areas within the high seas during portions of their ocean migrations (Takagi et al., 1981). Although it is not clear to what extent this movement pattern reflects either a shared history or shares physical effects (such as the direction of prevailing currents), populations within a region presumably experience similar marine environments. The few genetic data that address the relatedness of even-year pink salmon from both Pacific coasts are limited by the number of genetic characters examined or by geographic area (Gharrett et al., 1988; Zhivotovsky et al., 1989; Shaklee and Varnavskaya, 1994).

Our study analyzed numerous allozyme loci in populations from the even-year broodline of pink salmon from Asian waters and compared those data with data from western Alaska populations (Gharrett et al., 1988). The study included most of the geographic groups identified by Takagi et al., (1981). We substantially expanded the number of allozyme loci sampled in Asian even-year populations to determine the genetic structure of those populations and to investigate the genetic relatedness within and among large areas of the pink salmon range. The questions we addressed are 1) Is there evidence of genetic structure for even-year pink salmon populations? 2) How does the genetic structure of Asian even-year pink salmon relate to the adjacent western Alaskan and Aleutian island populations? and 3) How does the genetic structure of Western Alaska and Asian pink salmon relate to geographic and oceanographic features and to recent geological history?

Materials and methods

Tissue samples from returning adult spawners were collected 1) from four river systems on southern Sakhalin Island (Dolinka, Lutoga, Monetka, and Ochepukha rivers) between 6 August and 19 September 1990; 2) from two river systems in the Magadan region of Russia (Tauy River on 26 July 1990 and Uglekanka River on 3 September 1990); 3) from seven river systems on the Kamchatka Peninsula (Utka, Pymta, Kol, Bistraya, Vorovskaya, Karaga, and Ossora rivers) between 29 July and 3 September 1990 (Fig. 1); 4) at hatcheries on three streams in Japan (Kushiro, Tokushibetsu, and Yurappu Rivers) between 21 and 29 September 1990; and 5) in five collections taken at different times during the return to a hatchery in Sawmill Bay in Prince William Sound, Alaska, between 27 August and 8 September 1988. There are no natural spawning runs of pink salmon in Japan; consequently, the hatchery samples are all that were available to represent Japan. Also, the samples from Prince William Sound, in the center of the North American range are intended to provide an idea of the extent of difference between Asian and North American pink salmon for the entire suite of allozyme loci examined in the Asian fish. The Znamenka River, a tributary of the Ochepukha River, was sampled repeatedly and considered separately in some analyses.

Pieces of heart, eye, liver, and skeletal muscle were sampled in the field and frozen on wet ice, frozen gel-packs, or dry ice until they were transferred to temporary storage at –20°C or to liquid nitrogen dewars at –196°C. Long-term storage was maintained at –85°C. The samples were analyzed by using horizontal starch-gel electrophoresis (Utter et al., 1974). Eight different gel buffers were used (Table 1). Proteins were revealed by using standard staining recipes (Aebersold et al., 1987). All allozyme data were collected at the NMFS Auke Bay Laboratory. An Excel™ file of allele frequency data can be downloaded by anonymous ftp from *ftp://wwwabl.afsc.noaa.gov* in file *SIDA/pink_salmon/evenasia*.

Variability at isoloci (Allendorf and Thorgaard, 1984) was assigned to one of the loci, and the other was treated as monomorphic, which for low frequencies (P<about 0.15) has little influence on the analysis (Gharrett and Thomason, 1987). The genotypic frequencies observed at each

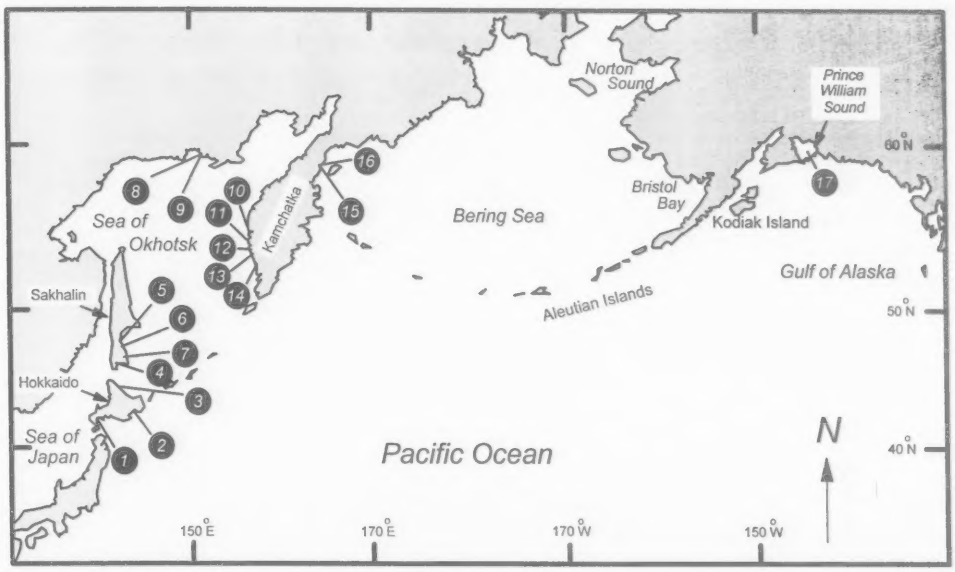

Figure 1

Map of location sites where fish were collected for tissue samples. Unless otherwise indicated, one collection of fish from the lower river was made. Japan: 1 = Yurappu River, Yacumo Hatchery (22 Sep 1990), 2 = Kushiro Hatchery (29 Sep 1990), 3 = Tokushibetsu Hatchery (17 Sep 1990). Sakhalin Island, Russia: 4 = Lutoga River, lower river (13 and 17 Jul 1990) and hatchery (29 Jul 1990 and 8 Nov 1990), 5 = Dolinka River (6 and 16 Aug 1990), 6 = Ochepukha River, lower river (8 and 22 Aug, and 3 Sep 1990) and upper river (6 and 9, and 11 Sep 1990) and Znamenka River, a major tributary of Ochepukha River (13, and 26 Aug 1990, 3, 6, , 9, 11, 13, 17, and 19 Sep 1990), 7 = Monetka River (18 and 19 Jul 1990). Magadan region, Russia: 8 = Tauy River (26 Jul 1990), 9 = Uglekanka River (3 Aug 1990). Western Kamchatka Peninsula, Russia: 10 = Vorovskaya River (31 Jul 1990), 11 = Kol River (30 Jul 1990), 12 = Pymta River (29 Jul 1990), 13 = Utka River (29 Jul 1990), 14 = Bistraya River (3 Aug 1990). Eastern Kamchatka Peninsula, Russia: 15 = Ossora River (28 Jul 1990), 16 = Karaga River (2 Aug 1990). Alaska: 17 = Prince William Sound, Armin F. Koernig Hatchery, Evans Island, Sawmill Bay, five collections in 1990.

locus were tested for departure from expected Hardy-Weinberg equilibrium frequencies by using a Pearson χ^2-goodness-of-fit test. Alleles were pooled to eliminate classes with expected values of less than four. Isoloci could not be tested for Hardy-Weinberg equilibrium because single-locus data were not available.

Homogeneity of allele frequencies was examined by using log-likelihood ratio analysis (G-test, Sokal and Rohlf, 1995); tests were performed among collections within a river, among rivers within a region, and among regions. The regions were Japan (Hokkaido Island), Sakhalin Island, western Kamchatka, eastern Kamchatka, and Alaska (Prince William Sound). Significance of tests that indicated low probability ($P<0.05$) based on χ^2 distributions and that had small expected numbers in rare classes (<4) were confirmed by using a Monte-Carlo procedure analogous to the one described by Roff and Bentzen (1989). Significance of multiple tests was corrected according to Cooper (1968). Heterogeneity within and among regions was compared by using an approximate F-statistic:

$$F_{df\,among,\,df\,within} = (G_{among}/df_{among})/(G_{within}/df_{within}).$$

Neighbor-joining trees (Saitou and Nei, 1987) were constructed by using chord distances (Cavalli-Sforza and Edwards, 1967; Wright, 1978). Genetic variability within and among streams, regions, and continents was partitioned hierarchically by gene diversity analysis (Chakraborty and Leimar, 1987) and analysis of variance (Weir and Cockerham, 1984; Weir, 1996). Average unbiased heterozygosities and their standard errors were calculated according to Nei (1978).

The five collections from Prince William Sound were, in a strict sense, temporal collections from the mixed fishery in the Sound and were not intended to represent collections from discrete drainages. Nevertheless, for convenience of analysis, they were treated as unique collections from a single system in the genetic distance and gene diversity analyses.

Results

A total of 54 genetic loci were scored. The 17 loci with frequencies of the common allele less than 0.95 in at least

Table 1

Loci analyzed in even-year pink salmon broodlines from Japan, Russia, and Alaska, their enzyme numbers and designations (Shaklee et al., 1990), the tissue(s) and buffer(s) in which they were scored, and the level of variability observed.

Enzyme	Enzyme number	Locus	Tissue[1]	Buffer[2]	Level of variability[3]
Aconitate hydratase	4.2.1.3	*sAH**	L	8	2
		*mAH-1**	H	4,5,6	2
		*mAH-2**	H	4,5,6	3
		mAH-3[4,5]*	H,M	4,5,6	2
		mAH-4[4,5]*	H,M	4,5,6	3
Alanine aminotransferase	2.6.1.2	*ALAT*[4]*	M	2	2
Aspartate aminotransferase	2.6.1.1	*sAAT-1,2*[4]*	M,H	4,6	2
		sAAT-3[4,5]*	E	7	3
		*sAAT-4**	L	8	3
		mAAT-1[4]*	M,H	4,6	1
		*mAAT-2**	L	8	1
Creatine kinase	2.7.3.2	*CK-A1*[4,5]*	M	1	2
		CK-A2[4,5]*	M	1	2
		*CK-B**	E	7	2
		*CK-C1**	E	7	3
		*CK-C2**	E	7	2
Formaldehyde dehydrogenase	1.2.1.1	*FDHG*[4]*	H	2	2
Fumarate hydratase	4.2.1.2	*FH**	M	4	3
Glucose-6-phosphate isomerase	5.3.1.9	*GPI-A*[4,5]*	M	1	2
		GPI-B1,2[4,5]*	M	1	2
Glutathione reductase	1.6.4.2	*GR*[4]*	E	4,5	3
Glycerol-3-phosphate dehydrogenase	1.1.1.8	*G3PDH-1*[4,5]*	M	2,3	3
Guanine deaminase	3.5.4.3	*GDA**	L	7,8	3
L-Iditol dehydrogenase	1.1.1.14	*IDDH**	L	7	2
Isocitrate dehydrogenase	1.1.1.42	*mIDHP-1*[4]*	M,H	4	1
		mIDHP-2[4]*	M,H	4	1

continued

one collection were *sAAT-3**, *sAAT-4**, *mAH-2**, *mAH-4**, *CK-C1**, *FH**, *GDA**, *G3PDH-1**, *GR**, *LDH-A1**, *sMDH-A1**, *sMDH-B2**, *mMEP-1**, *PEP-LT**, *PEPB**, *PEPD-2**, and *PGDH**. At 22 other variable loci, the frequency of the common allele was greater than 0.95 in all collections: *sAAT-1,2**, *mAH-1**, *sAH**, *mAH-3**, *ALAT**, *CK-A1**, *CK-A2**, *CK-B**, *CK-C2**, *FDHG**, *GPI-A**, *GPI-B2**, *IDDH**, *mIDHP-1**, *LDH-B1**, *LDH-B2**, *MPI**, *PEPD-1**, *PGM-2**, *TPI-2**, and *TPI-4**. The remaining 15 loci were monomorphic for the same allele in all collections.

The allelic frequencies observed are generally comparable to data for the few loci published by Russian geneticists (Altukhov et al., 1983; Salmenkova and Omelchenko, 1983; Zhivotovsky et al., 1989; Kartavtsev, 1991; Kartavtsev et al., 1992) except that we observed the *PGDH*95* allele in all regions. Detection of that allele requires careful adjustment of the buffer pH, otherwise it migrates with the common allele. The pH at which Gharrett et al. (1988) analyzed *PGDH** did not distinguish that allele from the **100* allele.

Tests of conformance to Hardy-Weinberg expectations for genotypic frequencies were made for 126 locus-collection combinations. Of these, four did not conform ($P<0.05$); this is fewer than would be expected at random. However, the sample size for most tests was small; therefore only large deviations from Hardy-Weinberg expectations would have been detected. Homogeneity within and among drainages, geographic regions, and continents or marine basins was tested by using 28 loci at which more than 5 variant alleles were observed (Table 2). Four rivers on Sakhalin Island were the only drainages from which multiple, temporally stratified collections were sampled during the spawning season. The numerous samples collected within the Ochepukha River system permitted treatment of its Znamenka tributary as a fifth separate system. Only a subset of loci was scored in some collections, but at least one collection from each river was scored for the entire set of loci. No overall heterogeneity ($P>0.05$) was observed for any Sakhalin drainage, and only a few loci suggested heterogeneity (Table 2), which vanishes when corrections

Table 1 (continued)

Enzyme	Enzyme number	Locus	Tissue[1]	Buffer[2]	Level of variability[3]
Lactate dehydrogenase	1.1.1.27	*LDH-A1*[4,5]*	M	1	3
		LDH-A2[4,5]*	M	1	1
		LDH-B1[4]*	H	1	2
		*LDH-B2**	L	1	2
		LDH-C[4,5]*	E	7	1
Malate dehydrogenase	1.1.1.37	*sMDH-A1,2**	L	6	3
		sMDH-B1,2[4,5]*	M	2,3	3
Malic enzyme	1.1.1.40	*mMEP-1*[4,5]*	M	3,4	3
Mannose-6-phosphate isomerase	5.3.1.8	*MPI*[4,5]*	H	2	2
Peptidase:					
Cytosol non-specific dipeptidase (glycyl-leucine)	3.4.–.–	*PEPA*[4]*	M	2	1
Tripeptide aminopeptidase (zinc enzyme) (leucyl-glycyl-glycine)	3.4.–.–	*PEPB*[4]*	M	1	3
Leucyl-tyrosine peptidase	3.4.–.–	*PEP-LT**	M	2,4	3
Phosphoglucomutase	5.4.2.2	*PGM-2*[4,5]*	M	3	2
Phogluconate dehydrogenase	1.1.1.44	*PGDH*[4,5]*	E	3	3
Phosphoglycerate kinase	2.7.2.3	*PGK-1**	L	8	1
		*PGK-2**	L	8	1
X-proline dipeptidase	3.4.13.9	*PEPD-1*[4,5]*	M	2	2
		PEPD-2[4,5]*	M	2	3
Superoxide dismutase	1.15.1.1	*sSOD-1*[4,5]*	L	7	1
		*mSOD**	H	1,2	1
Triose-phosphate isomerase	5.3.1.1	*TPI-1*[4]*	E	7	1
		TPI-2[4]*	E	7	2
		TPI-3[4]*	E	7	1
		TPI-4[4]*	E	7	2

[1] E = eye; H = heart; L = liver; M = muscle; preferred tissue listed first.
[2] 1 = lithium hydroxide (Ridgway et al., 1970);
2 = Tris-EDTA-borate (Boyer et al., 1963);
3 = amine citrate, pH 6.1 (Clayton and Tretiak, 1972);
4 = Tris-citrate, pH 7.0 (Shaw and Prasad, 1970);
5 = Tris-citrate discontinuous (Schaal and Anderson, 1974);
6 = amine-citrate-EDTA, pH 7.2 (modified from Clayton and Tretiak, 1972);
7 = Tris-glycine (Holmes and Masters, 1970);
8 = amine-citrate, pH 6.8 (modified from Clayton and Tretiak, 1972).
[3] 1 = monomorphic;
2 = low (frequency of most prevalent allele >0.95);
3 = high (frequency of most prevalent allele ≤0.95).
[4] Loci included in 36-locus version of neighbor-joining tree and gene diversity analysis.
[5] Loci included in 21-locus version of neighbor-joining tree.

are made for multiple testing. This is especially notable for the series of collections from the Znamenka (9 collections, P=0.43) and Ochepukha (6 collections, P=0.52) rivers. No heterogeneity was detected among Sakhalin drainages (G=131.01, 127 df; P=0.39).

The three Japanese (Hokkaido) collection sites were the Tokushibetsu River on the Sea of Okhotsk coast, the Kushiro River facing the northwestern Pacific Ocean, and the Yurappu River southwest of the Kushiro River on Hokkaido's eastern coast. The synthetic Yurappu stock is derived in large part from Okhotsk coast stocks, including the Tokushibetsu stock. The genetic profile of the Yurappu stock resembles that of the Tokushibetsu stock except at *sAAT-3** (P=0.018, analysis not shown), which suggests a founder effect or subsequent divergence. The Yurappu sample was not used in subsequent analyses. Overall heterogeneity was observed between the Kushiro and Tokushibetsu Rivers (G=48.87, 33 df; P=0.037) (Table 2), although tests at the four loci suggest heterogeneity was not significant after correction for multiple testing.

Table 2

Hierarchical homogeneity tests. Levels are among collections within streams, among streams within drainages, among drainages within a region, among Asian regions, and between Asia and Prince William Sound, Alaska. Degrees of freedom of tests at lower levels of hierarchy may differ from (be lower than) those necessary for the overall hierarchical analysis. — indicates that no test was possible because there were data for only one collection. The hierarchical nature of the analysis precludes multiple testing corrections in the table because several different hypotheses are possible.

	*sAAT-4**		*sAH**		*GDA**		*FDHG**		*sAAT-3**		*CK-C1**		*PGDH**		*TPI-2**	
Collection site	*G*	df	*G*	df	*G*	df	*G*	df	*G*	df	*G*	df	*G*	df	*G*	df
Asia																
Hokkaido	0.96	1	1.46	1	0.66	4	1.8	2	0.48	1	1.36	1	8.79[a]	3	0	1
Sakhalin																
Dolinka	—		—		—		—		—		—		0.71	3	—	
Lutoga	—		1.81	1	3.55	4	0.82	2	0.03	1	—		7.49	9	0	1
Monetka	—		1.64	1	5.45	4	0.01	2	0.01	1	0.02	1	6.89[a]	3	0	1
Ochepukha																
Other	—		—		—		—		—		—		7.01	15	—	
Znamenka	—		0	1	3.14	4	0.09	2	0.002	1	—		25.31	24	0	1
Within Ochepukha	—		0	1	3.14	4	0.09	2	0.002	1	—		32.32	39	0	1
Between Ochepukha	—		4.67[a]	1	1.01	4	4.74[a]	2	0.001	1	0.70	1	4.42	3	0	1
Total Ochepukha	—		4.67	2	4.15	8	4.82	4	0.003	2	0.70	1	36.74	42	0	2
Within Sakhalin	—		8.12	4	13.15	16	5.65	8	0.03	4	0.72	2	51.83	57	0	4
Among Sakhalin	—		1.21	3	10.84	12	7.33	6	0.96	3	7.53	3	6.40	9	0	3
Total Sakhalin	—		9.34	7	23.99	28	12.98	14	1	7	8.25	5	58.22	66	0	7
Northern Sea of Okhotsk	—		—		—		0.20	2	—		—		3.29	3	0	1
Western Kamchatka	—		0	2	10.07	8	8.03	8	10.61[a]	4	1.08	2	11.67	12	0	4
Eastern Kamchatka	—		0	1	6.28	4	0.02	2	1.31	1	0.14	1	3.19	3	0	1
Within Asia	0.96	1	10.80	11	41.00	44	23.04	28	13.40	13	10.84	9	85.16	87	0	14
Among Asia	6.64[b]	1	3.04	3	39.75[d]	12	19.89[a]	8	56.59[d]	3	3.00	3	65.95[d]	12	0	4
Total Asia	7.60[a]	2	13.84	14	80.75[a]	56	42.93	36	69.99[d]	16	13.84	12	151.11[d]	99	0	18
North America																
Prince William Sound	7.8	4	2.45	4	10.02	16	3.20	8	3.96	4	4.90	4	18.58[a]	12	3.38	4
Total within	15.40[a]	6	16.29	18	90.77	72	46.13	44	73.95[d]	20	18.74	16	169.69[d]	111	3.38	22
Between Alaska and Asia	0.95	1	0	1	107.53[d]	4	23.51[d]	2	269.38[d]	1	8.83[b]	1	43.12[d]	3	39.30[d]	1
Total for collections	16.34[a]	7	16.29	19	198.30[d]	76	69.64[a]	46	343.33[d]	21	27.57	17	212.81[d]	114	42.68[b]	23

	*TPI-4**		*mAH-4**		*G3PDH-1**		*GPI-B2**		*GPI-A**		*LDH-A1**		*LDH-B1**	
Collection site	*G*	df	*G*	df	*G*	df	*G*	df	*G*	df	*G*	df	*G*	df
Asia														
Hokkaido	5.30[a]	1	0	2	0.14	3	1.33	3	2.9	2	0	3	1.45	2
Sakhalin														
Dolinka	—		—		0.02	3	—		—		—		—	
Lutoga	0.07	1	2.76	2	1.69	9	0	3	1.01	2	1.05	3	1.05	2
Monetka	1.39	1	1.73	2	0.47	3	1.45	3	0	2	0	3	0	2
Ochepukha														
Other	—		—		3.16	15	—		—		—		—	
Znamenka	1.39	1	0.76	2	12.71	24	0	3	1.39	2	1.43	3	0	2
Within Ochepukha	1.39	1	0.76	2	15.88	39	0	3	1.39	2	1.43	3	0	2
Between Ochepukha	0.81	1	0.20	2	0.01	3	0	3	0.83	2	0.22	3	2.20	2
Total Ochepukha	2.20	2	0.97	4	15.89	42	0	6	2.22	4	1.65	6	2.20	4
Within Sakhalin	3.66	4	5.45	8	18.06	57	1.45	12	3.23	8	2.70	12	3.25	8
Among Sakhalin	1.41	3	5.41	6	4.54	9	3.93	9	2.22	6	6.76	9	2.14	6
Total Sakhalin	5.06	7	10.86	14	22.60	66	5.38	21	5.45	14	9.47	21	5.39	14
Northern Sea of Okhotsk	0.19	1	0.64	2	0.33	3	0.19	3	0.19	2	—		0	2

continued

Table 2 (continued)

Collection site	*TPI-4**		*mAH-4**		*G3PDH-1**		*GPI-B2**		*GPI-A**		*LDH-A1**		*LDH-B1**	
	G	df	*G*	df	*G*	df	*G*	df	*G*	df	*G*	df	*G*	df
Western Kamchatka	8.87	4	7.85	8	14.91	12	13.24	12	6.60	8	2.99	12	2.07	8
Eastern Kamchatka	1.67	1	2.53	2	0.003	3	1.58	3	0	2	2.47	3	0	2
Within Asia	21.10	14	21.88	28	37.98	87	21.72	42	15.14	28	14.92	39	8.91	28
Among Asia	17.06[b]	4	14.21	8	10.69	12	13.85	12	9.58	8	7.59	12	1.60	8
Total Asia	38.16[b]	18	36.08	36	48.66	99	35.56	54	24.72	36	22.51	51	10.5	36
North America														
Prince William Sound	0	4	2.98	8	7.32	12	3.17	12	6.55	8	13.31[b]	12	6.78	8
Total within	38.16[a]	22	39.06	44	55.98	111	38.73	66	31.27	44	35.82	63	17.28	44
Between Alaska and Asia	7.36[b]	1	28.86[d]	2	42.64[d]	3	28.71[d]	3	6.12[a]	2	23.20[d]	3	4.09	2
Total for collections	45.52[b]	23	67.93[a]	46	98.62	114	67.44	69	37.39	46	59.02	66	21.37	46

Collection site	*LDH-B2**		*PEPLT**		*PGM-2**		*PEPD-1**		*PEPD-2**		*FH**		*GR**	
	G	df	*G*	df	*G*	df	*G*	df	*G*	df	*G*	df	*G*	df
Asia														
Hokkaido	0	3	0.88	2	1.37	2	0	1	2.56	4	0	2	2.90	2
Sakhalin														
Dolinka	—		—		—		—		—		—		—	
Lutoga	1.05	3	—		1.05	2	0	1	1.52	8	0	2	0.35	2
Monetka	0	3	—		1.41	2	2.04	1	6.28[a]	4	2.78	2	2.95	2
Ochepukha														
Other	—		—		—		—		7.46	20	—		—	
Znamenka	1.39	3	—		1.39	2	4.25	3	11.10	28	5.25	2	0.08	2
Within Ochepukha	1.39	3	—		1.39	2	4.25	3	18.56	48	5.25	2	0.08	2
Between Ochepukha	3.01	3	—		0.81	2	1.10	1	5.81	4	2.44	2	0.03	2
Total Ochepukha	4.40	6	—		2.20	4	5.35	4	24.37	52	7.68	4	0.11	4
Within Sakhalin	5.45	12	—		4.66	8	7.39	6	32.16	64	10.46	8	3.41	8
Among Sakhalin	8.11	9	—		0.62	6	2.24	3	13.24[a]	12	6.49	6	3.67	6
Total Sakhalin	13.56	21	—		5.28	14	9.63	9	45.41	76	16.95	14	7.08	14
Northern Sea of Okhotsk	—		—		0	2	0	1	0.57	4	—		—	
Western Kamchatka	3.00	9	7.00	6	0	8	8.34	4	16.05	16	6.34	6	10.05	8
Eastern Kamchatka	0	3	1.30	2	0	2	0.27	1	0.81	4	0.72	2	0.18	2
Within Asia	16.56	36	9.17	10	6.65	28	18.24	16	65.40	104	24.00	24	20.21	26
Among Asia	5.23	12	9.78	6	10.08	8	6.45	4	74.59[d]	16	79.18[d]	8	76.78[d]	8
Total Asia	21.79	48	18.95	16	16.73	36	24.69	20	139.99	120	103.18[d]	32	96.98[d]	34
North America														
Prince William Sound	3.20	12	5.60	8	8.16	8	2.37	4	3.09	16	11.02	8	3.26	8
Total within	24.99	60	24.55	24	24.89	44	27.06	24	143.09	136	114.20[d]	40	100.24[d]	42
Between Alaska and Asia	12.25[b]	3	6.27[a]	2	2.94	2	0.32	1	18.69[c]	4	6.72[a]	2	33.91[d]	2
Total for collections	37.24	63	30.82	26	27.82	46	27.38	25	161.78	140	120.92[d]	42	134.15[d]	44

Collection site	*sMDH-A1,2**		*sMDH-B1,2**		*mMEP-1**		*MPI**		*PEPB**		*mAH-2**		Total for loci	
	G	df	*G*	df	*G*	df	*G*	df	*G*	df	*G*	df	*G*	df
Asia														
Hokkaido	0.09	4	2.74	6	0.77	2	0.001	2	6.64[a]	2	4.30[a]	1	48.87[a]	62
Sakhalin														
Dolinka	—		1.95	6	5.95[a]	2	—		—		—		8.63	14
Lutoga	0.77	4	4.47	18	3.67	6	0.21	2	0.05	2	—		34.47	89

continued

Table 2 (continued)

Collection site	*sMDH-A1,2**		*sMDH-B1,2**		*mMEP-1**		*MPI**		*PEPB**		*mAH-2**		Total for loci	
	G	df	*G*	df	*G*	df	*G*	df	*G*	df	*G*	df	*G*	df
Monetka	1.75	4	1.20	6	0.01	2	0.34	2	1.33	2	2.07	1	41.20	59
Ochepukha														
Other	—		25.79	30	3.28	10	—		—		—		46.70	90
Znamenka	0.11	4	37.29	48	4.14	16	1.35	2	8.47	6	0	1	121.04	186
Within Ochepukha	0.11	4	63.08	78	7.43	26	1.35	2	8.47	6	0	1	167.74	276
Between Ochepukha	0.03	4	6.60	6	1.25	2	1.87	2	3.16	2	—		45.91	58
Total Ochepukha	0.15	8	69.68	84	8.67	28	3.22	4	11.62	8	0	1	213.66	334
Within Sakhalin	2.67	16	77.30	114	18.30	38	3.77	8	13.01	12	2.07	2	297.94	496
Among Sakhalin	8.52	12	16.07	18	1.10	6	2.28	6	3.54	6	4.44	3	131.01	177
Total Sakhalin	11.19	28	93.37	132	19.40	44	6.05	14	16.55	18	6.51	5	428.95	673
Northern Sea of Okhotsk	0.60	4	0	6	0.66	2	0	2	9.55[b]	2	—		16.41	41
Western Kamchatka	0.16	12	18.47	24	4.87	8	5.21	8	6.08	8	6.55	3	190.11	220
Eastern Kamchatka	4.08	4	4.02	6	3.38	2	1.57	2	2.14	2	1.42	1	39.07	61
Within Asia	16.11	52	118.60	174	29.07	58	12.82	28	40.96	32	18.78	10	723.41	1057
Among Asia	74.76[d]	16	45.82[b]	24	8.14	8	15.98[a]	8	76.91[d]	8	15.69[b]	4	768.81[d]	236
Total Asia	90.87[a]	68	164.42	198	37.21	66	28.81	36	117.87[d]	40	34.47[b]	14	1492.22[d]	1293
North America														
Prince William Sound	5.67	16	13.22	24	4.12	8	6.27	8	11.49	8	8.31[a]	3	176.78[a]	247
Total within	96.53	84	177.64	222	41.33	74	35.08	44	129.36[d]	48	42.78	17	1669.01[d]	1540
Between Alaska and Asia	9.40	4	12.09	6	4.06	2	1.73	2	12.88[b]	2	2.33	1	717.87[d]	62
Total for collections	105.93	88	189.73	228	45.39	76	36.81	46	142.24[d]	50	45.11[c]	18	2386.85[d]	1602

[a]$P < 0.05$, [b]$P < 0.01$, [c]$P < 0.001$, [d]$P < 0.0001$.

No overall heterogeneity was observed in tests among collections within each of the remaining geographic regions: northern Okhotsk coast, eastern Kamchatka, and western Kamchatka (Table 2). The northern Okhotsk and western Kamchatka collections each had a single locus that indicated heterogeneity, but neither test was significant after correction for multiple testing.

The Alaska (Prince William Sound) collections exhibited low heterogeneity over all loci (G=176.78, 147 df; P=0.047) (Table 2); tests at three loci suggested that heterogeneity was not significant after correction for multiple testing. Although not the focus of this paper, the overall heterogeneity suggests local genetic structure in even-year pink salmon within Prince William Sound.

The collections of even-year pink salmon within the Asian geographic regions were relatively homogeneous, but we found strong heterogeneity among regions (G=1492.22, 1257 df; $P<10^{-4}$) (Table 2). Of the nine loci that individually suggest heterogeneity, eight (*GDA**, *sAAT-3**, *PGDH**, *PEPD-2**, *FH**, *GR**, *sMDH-A1**, and *PEPB**) showed significant heterogeneity (P<0.05) after correction for multiple testing. The ratios of heterogeneities among regions to heterogeneity within regions (approximate F's) for each locus (not shown) were significant (P<0.05) for 13 of 28 loci, and comparisons of *GDA**, *sAAT-3**, *PGDH**, *PEPD-2**, *FH**, *GR**, *sMDH-A1**, *sMDH-B2**, and *PEPB** were highly significant (P<0.001).

At the next level of hierarchy, between continents, Asian samples (in aggregate) differed overall from the Alaska samples with which they were compared (G=717.87, 62 df; $P<<10^{-6}$) (Table 2); many of the loci examined contribute to the difference. After correction for multiple tests, *GDA**, *FDHG**, *sAAT-3**, *PGDH**, *TPI-2**, *mAH-4**, *G3PDH-1**, *GPI-B2**, *LDH-A1**, and *GR** were strongly significant (P<0.001). Of these loci, *GDA**, *sAAT-3**, *PGDH**, *mAH-4**, *G3PDH-1**, *LDH-A1**, and *GR** had appreciable variation (common allele <0.95) in at least some populations. These results suggest that at least seven allozyme loci may prove useful for distinguishing among even-year pink salmon stocks from different regions of the northern Pacific Ocean (Hawkins et al., 1998).

Data from 36 loci common to all regions were used to estimate pairwise chord distances (Cavalli-Sforza and Edwards, 1967) with which we constructed an unrooted neighbor-joining tree (Fig. 2). The tree supports a geographic basis for the variability observed among collections and suggests a geographic relationship among regions. Four clusters are evident along the tree axis: in linear order, they consisted of the collections from southern Okhotsk (Hokkaido Island and Sakhalin Island), western Kamchatka, eastern Kamchatka, and Alaska. The greatest distance was between the Alaska cluster and all the other collections. When the Magadan samples were included in a similar tree with data from 34 loci, they

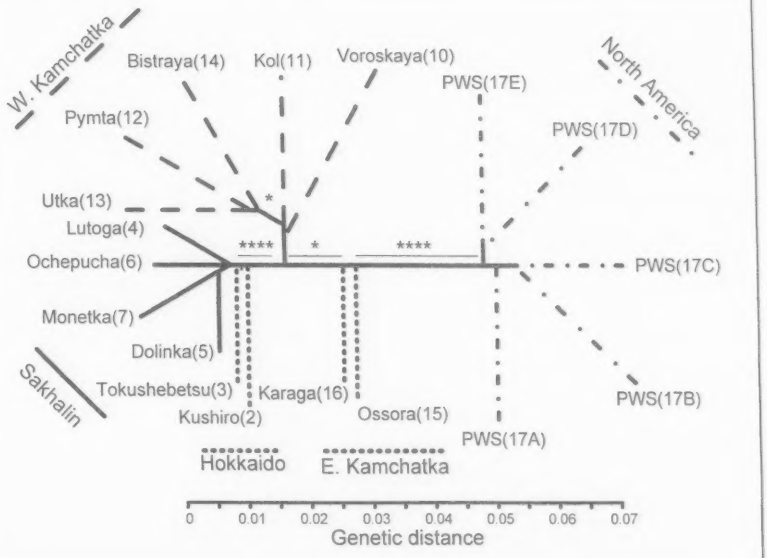

Figure 2

Neighbor-joining tree of even-year pink salmon broodlines from Japan, Russia, and Prince William Sound based on Cavalli-Sforza and Edwards (1967) chord distances from allele frequencies at 36 loci. Significance between nodes or for collections joined at nodes were tested within regions by using log-likelihood ratios (*G*-tests; Sokal and Rohlf, 1995) of the 36 loci to test homogeneity of branches joined at a node, and between basins by tests of homogeneity among the populations of the two adjacent regions. The numbers following the population names correspond to their locations in Figure 1. PWS = Prince William Sound.

clustered with the eastern and western Kamchatka collections (not shown). The arrangement of the other clusters remained as in Figure 2.

The variation at 36 loci common to all collections was partitioned by using gene diversity analysis (G_{ST}'s; Chakraborty and Leimar, 1987) and analysis of variance (θ_{ST}'s; Weir and Cockerham, 1984; Weir, 1996) (Table 3). Analysis of variance accounts for bias inherent in analyses that use finite samples from and small numbers of populations. Differences between the G_{ST}'s and θ_{ST}'s are most apparent at upper levels of the hierarchy where fewer groups are compared. Although biased, the G_{ST}'s have been widely used, so we summarize results of partitioning variation with G_{ST}'s but included θ_{ST}'s parenthetically. On average, variation within streams accounted for 97.2% (95.57%) of the total, with 0.63% (0.05%) attributable to differences among streams within regions, 0.65% (1.29%) to differences among regions within continents, and 1.52% (3.09%) to differences between continents.

We combined our data with available data (Altukhov et al., 1983; Salmenkova and Omelchenko, 1983; Zhivitovsky et al., 1989; Kartavtsev, 1991; Kartavtsev et al., 1992) to conduct a log-likelihood ratio analysis to test for homogeneity within and among Asian regions. The primary (variable) loci for which data were available were *PGDH** (omitting collections missing the **95* allele), *G3PDH-1**, and *MDH-B1,2**. These data included collections from Primorie, western Sakhalin Island, and the Kuril Islands in addition to the regions we reported (Table 4). There was no overall heterogeneity within regions and only a single test suggested heterogeneity. However, *PGDH** and *MDH-B1,2** exhibited strong heterogeneity ($P<10^{-4}$) among regions.

Data from an earlier study of genetic diversity in Alaska pink salmon (Gharrett et al., 1988) were included to produce an unrooted neighbor-joining tree based on 21 loci common (Appendix 1) to that study and the present one (Fig. 3). Data from all collections were condensed by region, except for Japan, where the collections were heterogeneous. Some regions were represented by a single collection; data for the Aleutian Islands collections were pooled because they exhibited no heterogeneity, but as a group differed from other Western Alaska regions (Gharrett et al., 1988). The Magadan collections were omitted from our analysis because data from several of the 21 loci were unavailable. As in the previous analysis, the tree showed a clear geographic basis for genetic variation. A cluster containing the Japan and Sakhalin Island collections adjoined the western Kamchatka group. A longer span joined the latter with a cluster consisting of the eastern Kamchat-

Table 3

Gene diversity analysis of even-year pink salmon broodlines. Relative gene diversities are estimated from the variable loci in the 36-locus set that these collections had in common. Estimates and standard deviations are jackknife estimates over loci and based on the total expected heterozygosity at each level of hierarchy (G's; Chakraborty and Leimar, 1987) or analysis of variance (θ's; Weir, 1996) in parentheses.

Source	Number of collections	G_{ST} (θ_{SS})	G_{SL} (θ_S-θ_S)	G_{LR} (θ_S-θ_P)	G_{RT} (θ_P)
Asia	13	0.0150 ±0.0007 (0.0144 ±0.0011)	0.0051 ±0.0001 (0.0003 ±0.0001)	0.0099 ±0.0007 (0.0140 ±0.0012)	
Southern Sea of Okhotsk	6	0.0024 ±0.0001 (0.0000 ±0.0002)	0.0016 ±0.0001 (–0.0003 ±0.0001)	0.0007 ±0.0001 (0.0003 ±0.0001)	
Hokkaido	2	0.0022 ±0.0002 (–0.0008 ±0.0004)			
Southern Sakhalin	4	0.0014 ±0.0001 (–0.0002 ±0.0001)			
Western Kamchatka	5	0.0085 ±0.0003 (0.0019 ±0.0003)			
Eastern Kamchatka	2	0.0053 ±0.0005 (0.0030 ±0.0010)			
Alaska (Prince William Sound)	5	0.0089 ±0.0004 (0.0005 ±0.0005)			
Total	18	0.0280 ±0.0021 (0.0443 ±0.0055)	0.0063 ±0.0002 (0.0005 ±0.0001)	0.0065 ±0.0005 (0.0129 ±0.0011)	0.0152 ±0.0019 (0.0309 ±0.0055)

Table 4

Log-likelihood ratio analysis of allozyme data available for Asian even-year pink salmon broodlines (Altukhov et al., 1983; Salmenkova and Omelchenko, 1983; Zhivotovsky et al., 1989; Kartavtsev, 1991; Kartavtsev et al., 1992; our paper). Data include three alleles or allele pools (*100, *95, and *90) at *PGDH** for 4587 individuals from 42 collections, two alleles or allele pools (*100 and all others) at *G3PDH** for 6398 fish from 53 collections, and three alleles or allele pools (*100, fast alleles, and slow alleles at *sMDH-B1,2** for 6336 individuals from 53 collections.

Region	*PGDH** G (df)	*G3PDH** G (df)	*MDHB-1,2** G (df)
Hokkaido	5.84 (2)	0.52 (1)	0.80 (2)
Primoriya	6.08 (6)	8.10 (4)	16.66* (8)
Western Sakhalin Island	0.71 (2)	1.04 (3)	6.03 (6)
Eastern Sakhalin Island	19.67 (16)	14.99 (12)	34.94 (24)
Kuril Islands	33.36 (26)	11.83 (13)	16.67 (26)
Northern Sea of Okhotsk	4.37 (4)	2.02 (5)	15.88 (10)
Western Kamchatka	7.50 (10)	8.53 (5)	9.42 (10)
Eastern Kamchatka	3.04 (2)	0.03 (2)	6.59 (4)
Total within region	80.58 (68)	47.07 (45)	107.00 (90)
Among regions	110.05*** (14)	13.92 (7)	50.21*** (14)
Total	190.61*** (82)	60.99 (52)	157.21** (104)

* = $P < 0.05$; ** = $P < 0.001$; *** = $P < 0.0001$.

ka, Aleutian Islands, Norton Sound, and Bristol Bay collections. A cluster consisting of Kodiak Island and Prince William Sound collections was separated from the other groups by the longest distance in this tree. The neighbor-joining tree suggested three large geographic aggregations of pink salmon populations which correspond to marine basins: the Sea of Okhotsk, the Bering Sea, and the Gulf of Alaska. Using those basins as the basis for gene diversity hierarchy, we partitioned the variation. We estimated the proportion of the total variation attributable to differ-

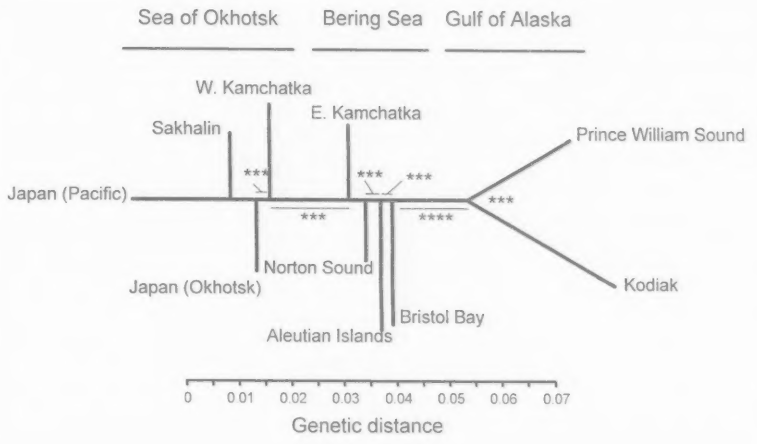

Figure 3

Neighbor-joining tree based on allele frequencies at 21 loci, showing Cavalli-Sforza and Edwards (1967) chord distances among pink salmon from Japan, Russia, and Alaska. Significance between nodes or of collections joined at nodes were tested within basins by using log-likelihood ratios (G-tests; Sokal and Rohlf, 1995) of the 21 loci to test homogeneity of branches joined at a node, and between basins by tests of homogeneity of the two adjacent branches. Jack-knifing populations to test the stability of the tree produced two local rearrangements that involved only the Aleutian Islands and Bristol Bay collections. The eastern Pacific Ocean and Bering Sea collections had the following sample sizes: Bristol Bay, n = 146; Aleutian Islands, n = 642; Norton Sound, n = 201; and Kodiak Island, n = 66 (Gharrett et al., 1988).

Table 5

Gene diversity analysis of even-year pink salmon broodlines. Relative gene diversities are estimated from the 21-locus set common to collections of this study and that of Gharrett et al. (1988). Estimates and standard deviations are jackknife estimates based on the total expected heterozygosity at each level of hierarchy.

Source	Number of regions	G_{ST}	G_{SG}	G_{GT}
Sea of Okhotsk	3	0.0031 ±0.0006		
Bering Sea	4	0.0079 ±0.0003		
Gulf of Alaska	2	0.0043 ±0.0006		
Total	9	0.0230 ±0.0025	0.0055 ±0.0002	0.0175 ±0.0025

ences among regions (G_{ST}) as well as to the average variation among regions within a basin (G_{SG}) and among basins (G_{GT}) (Table 5). The diversity within areas was low, ranging from 0.31 to 0.79%, and averaging 0.55%. The diversity among areas was 1.75%, and the average within each stream was 98.25%.

We also analyzed genetic variability by comparing average expected heterozygosities (Nei, 1978). Eastern Pacific pink salmon populations appeared to have higher heterozygosities than western populations. With the 36-locus data set, the average heterozygosity of the five Alaska collections was 0.074 ±0.004 (mean ±SE) compared with 0.056 ±0.004 for 13 Asian collections. Using the 21 loci common to the three geographic regions shown by Figure 3, we estimated heterozygosities of 0.061 ±0.002 for three regions within the Sea of Okhotsk, 0.073 ±0.004 for four regions in the Bering Sea, and 0.099 ±0.003 for the two regions in the Gulf of Alaska. Heterozygosities for these samples of allozyme loci increased from west to east.

Discussion

Heterogeneity among even-year pink salmon populations in Asian regions contrasted strongly with the relative homogeneity we observed within regions. For example,

western Kamchatka and eastern Sakhalin Island face each other across the Sea of Okhotsk but have different allele frequencies at *PEPD-2*100* [0.71 ±0.02 (SE) for western Kamchatka versus 0.61 ±0.01 for eastern Sakhalin), *GR*100* (0.90 ±0.01 versus 0.97 ±0.005), *PEPB*100* (0.91 ±0.01 versus 0.79 ±0.01), and *PGDH*100* (0.76 0.02 versus 0.82 ±0.01). Therefore, it is unlikely that there is substantial gene flow between these regions. If large movements of spawning pink salmon occur (fluctuating stock hypothesis; e.g. Zhivotovsky and Glubokovsky, 1989; Shuntov et al. 1994), our results suggest that they are restricted to within-region movements for even-year pink salmon. Moreover, the relative homogeneity observed within regions does not necessarily indicate large numbers of strays. Relatively small exchanges between drainages (say 10 fish or so per generation) can arrest genetic divergence (e.g. Gharrett, 1994). This level of straying does not, however, provide demographic insurance against overfishing or environmental catastrophes in the short run (Hop and Gharrett, 1989).

The contemporary genetic structure of even-year pink salmon has practical implications for fishery scientists. Genetic differences among populations can be used as markers for stock identification. It is often necessary to manage a species that has as many small populations as pink salmon as a regional assemblage. The regional basis for genetic structure observed in Asian pink salmon lends itself to stock separation analyses (Hawkins et al., 1998).

Most of the genetic variability observed in even-year pink salmon is attributable to within-population variability (e.g. Gharrett et al., 1988; Beacham et al., 1988). However, low levels of divergence among populations do not preclude hierarchical population structure. In our study we saw little or no temporal structure among Sakhalin Island populations. This finding does not necessarily conflict with observations of temporal structure observed by Altukhov et al. (1983) who used much larger numbers of fish (but fewer alleles), by McGregor et al. (1998) who used multiple years of data and numerous loci, and by Brykov et al. (1999) who used highly variable mitochondrial DNA haplotypes, because their tests had much greater statistical power. In addition, allozymes may not be appropriate for detecting some kinds of population structure because a very low level of gene flow can "homogenize" frequencies of neutral or nearly neutral loci. Note, for example, the genetic component observed for time of return within a spawning season (Smoker et al., 1998) and the persistence of a genetic marker for time of spawning (Lane et al., 1990).

The strong regional structure we observed in Asian even-year pink salmon populations is a stark contrast to the nearly complete absence of structure reported for odd-year Kamchatka pink salmon (Varnavskaya and Beacham, 1992; Shaklee and Varnavskaya, 1994). However, the latter surveys covered smaller geographic ranges and included neither Sakhalin Island nor Japanese pink salmon populations. These combined studies involving numerous allozyme loci confirm the work of Zhivotovsky et al. (1989) who, using four allozyme loci, also recognized the brood-year differences; and who estimated that 1.6% (we estimated 1.75%) and 0.6% of the total genetic variability were attributable to interregional divergence for even- and odd-year broods, respectively.

The differences observed between Asian and North American even-year pink salmon are not surprising; they have been reported previously for both even-year (Zhivotovsky et al., 1989) and odd-year broodlines (Varnavskaya and Beacham, 1992; Shaklee and Varnavskaya, 1994). However, the strong coherence of populations within each of the major North Pacific basins (Sea of Okhotsk, Bering Sea, and Gulf of Alaska) is striking. Each basin includes a range of habitats and climates that suggests that the genetic similarity among populations within a geographic region does not result from convergent or homogeneous selection. The differences among populations of different basins are also reflected by the different average heterozygosities. The apparent directional change in heterozygosities could be interpreted in terms of differences in effective population size, age of the populations, or the extent of environmental variation. However, speculation is probably not warranted because three different variables can be arranged in a monotonic pattern in two of six different possible orders.

A more evocative explanation of the genetic structure combines geographic and oceanographic influences, as well as recent geologic history. Populations in the contemporary Sea of Okhotsk, Bering Sea, and Gulf of Alaska are separated geographically by land masses and oceanographically by the different currents that flow into or between the oceanic basins and that influence migration routes of the fish (Royce et al., 1968). The geographic separation was greatly exacerbated by the limits and effects of late Pleistocene glaciation. In their northern range, pink salmon populations experienced increased isolation between the marine basins as a result of lower sea level, loss of freshwater habitat to increased ice cover, and more extensive sea ice. Just as recent fluctuations in salmon productivity have resulted from relatively minor climate changes (Mantua et al., 1997), less favorable freshwater and marine environmental conditions undoubtedly decreased the sizes and numbers of populations dramatically, further isolating the remaining populations in this region.

During the past several 100,000 years, there have been periodic changes in climate, sea level, glacial extent, and oceanographic conditions. It is important to realize that our modern, interglacial conditions are an extreme (Sancetta and Silvestri, 1986) and that the oceanic record of global ice volumes (from the $\delta^{18}O$ record in marine sediments) and geologic evidence (Mann and Hamilton, 1995) from the north Pacific realm during that period indicate that lower sea levels, more extensive glaciation, colder sea surface temperatures, and more extensive and southerly sea ice were typical (Bartlein et al., 1991; Rohling et al., 1998). The relative proportion of the ^{18}O isotope ($\delta^{18}O$) in a stratum of a core is related to the portion of the earth's water tied up in ice at the time corresponding to the stratum, and consequently the sea level in relation to the modern sea level.

At the last glacial maximum (LGM: ca. 14,000–20,000 years before the present [BP]), the paleogeography of the

North Pacific coast line was severely altered, reducing the sizes of the enclosed basins as well as the circulation among them. $\delta^{18}O$ records (e.g. Bartlein et al., 1991; Rohling, 1998), and limited data from Beringia (Hopkins, 1982) suggest that during most of the mid-Wisconsin glaciation, sea level was 50 m lower than at present and that at the LGM, the level was 120 to 130 m lower in areas not affected by ice loading or tectonic activity (Fairbanks, 1989). Sakhalin Island was connected to the mainland and Hokkaido Island, blocking the northern outflow of the Sea of Japan; and the connection of a smaller Sea of Okhotsk with the Pacific Ocean through the Kurile islands was restricted. In the Bering Sea, the extensive continental shelf was exposed, blocking circulation through the Bering Strait. To the south, the Aleutian Islands and the Alaska Peninsula were joined to about 170°W, and many of the islands to the west were also connected, thus limiting the connections between the Gulf of Alaska and the Bering Sea. In Cook Inlet, glaciers may have remained advanced throughout the middle Wisconsin glaciation (Reger and Updike, 1983).

Pink salmon spawning habitat along the Gulf of Alaska was nearly completely eliminated at the LGM and much of the Beringian coastline was probably ice bound much of the year, minimizing available freshwater habitat. Coastal areas of the Gulf of Alaska, including most of the continental shelf, were extensively glaciated during the Quaternary Period, although a few isolated areas of the outer coast may have been ice free (Hamilton, 1986); and the ice cover of the eastern Aleutians coalesced with the Alaska Peninsula and ice caps covered all the major islands (Thorson and Hamilton, 1986). In these areas there may have been ephemeral streams from melted snow or ice at the southern margin, near the present shelf break. Although the rivers draining the Yukon-Kuskokwim region flowed over the exposed shelf and probably served as a refugium, the Bering Sea appears to have had sea ice cover much of the year (Sancetta, 1983; Sancetta and Robinson, 1983); and seasonal sea ice may have persisted as far south as 54°N for 6–8 months a year during the LGM (de Vernal and Pedersen, 1997). On the Asian side, glaciation was much less extensive and included some alpine glaciation; but few glaciers extended to tidewater, except possibly on the southeast side of the Kamchatka Peninsula (Bespalyy, 1984; Velichko, 1984; Anderson, 1981). Freshwater habitat was probably not reduced to the extent of the Gulf of Alaska coast. Nevertheless, the Sea of Okhotsk, like the Bering Sea, probably had sea ice cover much of the year (Sancetta, 1983; Sancetta and Robinson, 1983).

Harsh conditions greatly reduced marine surface water productivity over the entire region (Morley et al., 1991; Keigwin et al., 1992; deVernal and Pederson, 1997). Microfossils indicate that the subarctic Pacific Ocean was similar to the present day Sea of Okhotsk, with cold fresh surface water and a highly stratified water column. Sea surface temperatures estimated by CLIMAP were 2° to 4°C colder than present throughout the year over most of the area (Moore et al., 1980). Off Japan, temperatures were even colder (>6°C) at the LGM, indicating that the cold Oyashio Current penetrated farther south than it does at present (Moore et al., 1980).

Most of the description above considered the LGM, but $\delta^{18}O$ records indicate that periodically other major glacial advances occurred at about 135,000 BP (^{18}O stage 6), about 225,000 BP (^{18}O stage 8), and so forth (Bartlein et al., 1991). Another less extensive advance may have occurred in the North Pacific region about 75 ka BP (Hopkins, 1982). It is likely that those events also influenced the distribution and demographics of salmon species including pink salmon.

Many of the streams populated by pink salmon are short coastal streams that are transient. Consequently, in maximizing productivity opportunities, pink salmon may exhibit a higher level of gene flow (straying) than other Pacific salmon (Quinn, 1984). Geologic evidence suggests that the LGM did not affect Asian streams as broadly or severely as Alaskan streams. However, the freshwater environments were less favorable than at present, and it would be expected that the harsh marine environment severely reduced productivity, probably creating a situation in which many local populations repeatedly went extinct. The ability to exploit spawning habitat rapidly would have been an advantage during the LGM and many local extinctions were probably followed by recolonization. As a consequence, it is likely that a few systems provided the source for stock colonization following deglaciation. In the eastern range where habitat was ice-covered, re-establishment of pink salmon probably depended on colonization from the Bering or more southerly refugia, or possibly from the "off-year" broodline, if the rigid two year life cycle relaxes in marginal environments, such as appears to have happened in the Laurentian Great Lakes (e.g., Kwain and Chappel, 1978).

Overall, the geological events should have accentuated geographic boundaries and increased the importance of random drift. Divergence between Asian and North American populations suggests colonization from different refugia, and significant, but lesser, regional divergence supports homing in pink salmon, at least regionally. However, the low overall divergence observed among both Asian and North American populations (G_{ST}=0.023) suggests that the populations studied are either recently diverged and derived from a single population or from genetically similar ancestral populations, or that there is sufficient gene flow to arrest divergence. One of the advantages of studying pink salmon is that there are two broodlines occupying much of the same range. It will be interesting to examine the genetic structure of odd-broodline pink salmon in the same range, which will represent a second natural experiment with which to examine the influences of geography, oceanography, and geologic history on the genetic structure of pink salmon populations.

Acknowledgments

We are indebted to many individuals who assisted in providing samples and grateful to Hanhvan Thi Nguyen and Bichhang Thi Nguyen for their valuable assistance in the laboratory. R. Wilmot provided helpful comments and help with federal bureaucratic processes. Two anonymous reviewers provided constructive criticism.

Literature cited

Aebersold, P. B., G. A. Winans, D. J. Teel, G. B. Milner, and F. M. Utter.
1987. Manual for starch gel electrophoresis: a method for the detection of genetic variation. U.S. Dep. Commer., NOAA Tech. Rep. NMFS 61.

Allendorf, F., N. Ryman, and F. Utter.
1987. Genetics and fishery management: past, present, and future. *In* Population genetics and fishery management (N. Ryman and F. Utter, eds.), p. 1–20. Univ. Washington Press, Seattle, WA.

Allendorf, F., and G. A Thorgaard.
1984. Tetraploidy and the evolution of salmonid fishes. *In* Evolutionary genetics of fishes (B. J. Turner, ed.), p. 1–53. Plenum, New York, NY.

Altukhov, Yu. P., E. A. Salmenkova, V. T. Omelchenko, and V. N. Efanov.
1983. Genetic differentiation and population structure of pink salmon of the Sakhalin-Kuril region. [English transl.] Biologiya Morya 2:46–51.

Anderson, B. G.
1981. Late Weichselian ice sheets in Eurasia and Greenland. *In* The last great ice sheets (J. H. Denton and T. J. Hughes, eds.), p. 3–65. John Wiley & Sons, New York, NY.

Aspinwall, N.
1974. Genetic examination of North American populations of the pink salmon, *Oncorhynchus gorbuscha*, possible evidence for the neutral mutation-random drift hypothesis. Evolution 28:295–305.

Bartlein, P. J., P. M. Anderson, M. E. Edwards, and P. F. McDowell.
1991. A framework for interpreting paleoclimatic variations in eastern Beringia. Quatern. Internat. 10–12:1991.

Beacham, T. D., R. E. Withler, and A. P. Gould.
1985. Biochemical genetic stock identification of pink salmon (*Oncorhynchus gorbuscha*) in Southern British Columbia and Puget Sound. Can. J. Fish. Aquat. Sci. 42:1474–1483.

Beacham, T. D., R. E. Withler, C. B. Murray, and L. W. Barner.
1988. Variation in body size, morphology, egg size, and biochemical genetics of pink salmon in British Columbia. Trans. Am. Fish. Soc. 117:109–126.

Bespalyy, V. G.
1984. Late Pleistocene mountain glaciation in Northeastern USSR. *In* Late Quaternary environments of the Soviet Union (A. A. Velichko, H. E. Wright Jr., and C. W. Barnosky, eds.), p. 31–33. Univ. Minnesota Press, Minneapolis, MN.

Boyer, S. H., D. C. Fainer, M. A. Naughton.
1963. Myoglobin: Inherited structural variation in man. Science (Washington D.C.)140:1228–1231.

Brykov, V. A., N. Polyakova, L.A. Skurikhina, A.D. Kukhlevsky, O.N. Kirillova, D. Churikov, A.I. Pudovkin, and A. J. Gharrett.
1999. Analysis of mtDNA indicates weak temporal genetic heterogeneity in pink salmon spawning runs in two rivers on Sakhalin Island. J. Fish Biol. 55:617–635.

Cavalli-Sforza, L. L., and A. W. F. Edwards.
1967. Phylogenetic analysis: models and estimation procedures. Evolution 21:550–570.

Chakraborty, R., and O. Leimar.
1987. Genetic variation within a subdivided population. *In* Population genetics and fishery management (N. Ryman and F. Utter, eds.), p. 89–120. Univ. Washington Press, Seattle, WA.

Clayton, J. W., and D. N. Tretiak.
1972. Amino citrate buffer for pH control of starch gel electrophoresis. J. Fish. Res. Board Can. 29:1169–1172.

Cooper, D. W.
1968. The significance level in multiple tests made simultaneously. Heredity 23:614–617.

de Vernal, A., and T. F. Pedersen.
1997. Micropaleontology and palynology of core PAR87A-10: A 23,000 year record of paleoenvironmental changes in the Gulf of Alaska, northeast North Pacific. Paleoceanography 12:821–830.

Fairbanks, R. G.
1989. A 17,000-year glacio-eustatic sea level record: influence of glacial melting rates on the Younger Dryas event and deep ocean circulation. Nature 342:637–642.

Gagalchii, N. G.
1986. Population genetic analysis of the Kamchatka pink salmon *Oncorhynchus gorbuscha* (Walb.). Cand. Sci. diss., Leningrad State Univ., Leningrad.

Gharrett, A. J.
1994. Genetic dynamics of a small population system: a model applicable to interaction between hatchery and wild fish. Aquacult. Fish. Manage. 25(suppl. 2):79–97.

Gharrett, A. J., C. Smoot, A. J. McGregor, and P. B. Holmes.
1988. Genetic relationships of even-year northwestern Alaskan pink salmon. Trans. Am. Fish. Soc. 117:536–545.

Gharrett, A. J., and M. A. Thomason.
1987. Genetic changes in pink salmon (*Oncorhynchus gorbuscha*) following their introduction into the Great Lakes. Can. J. Fish. Aquat. Sci. 44:787–792.

Glubokovsky, M. K., L. A. Zhivotovsky, R. M. Victorovsky, A. M. Bronevsky, K. I. Afanas'ev, V. V. Efremov, L. N. Ermolenko, B. A. Kalabushkin, V. G. Kovalev, A. N. Makoedov, T. V. Malinina, S. P. Pustovoit, and G. A. Rubtsova.
1989. Population organization of the pink salmon. [English transl.] Genetika 25:1275–1285.

Hamilton, T. D.
1986. Late Cenozoic glaciation in the central Brooks Range. *In* Glaciation in Alaska: the geologic record (T. D. Hamilton, K. M. Reed, and R. M. Thorson, eds.), p. 9–49. Alaska Geological Society, Anchorage, AK.

Hawkins, S., N. Varnavskaya, J. Pohl, and R. Wilmot.
1998. Simulations of the even-year Asian pink salmon (*Oncorhynchus gorbuscha*) genetic baseline to determine accuracy and precision of stock composition estimates. N. Pac. Anadr. Fish Comm. Bull. 1:213–219.

Heard, W. R.
1991. Life history of pink salmon (*Oncorhynchus gorbuscha*). *In* Pacific salmon life histories (C. Groot and L. Margolis, eds.), p. 119–230. UBC Press, Vancouver, Canada.

Holmes, R. S., and C. J. Masters.
1970. Epigenetic interconversion of the multiple forms of mouse liver catalase. FEBS Letters 11:45–48.

Hop, H., and A. J. Gharrett.
1989. Genetic relatedness of Arctic grayling in the Koyukuk and Tanana rivers, Alaska. Trans. Am. Fish. Soc. 118:290–295.

Hopkins, D. M.
1982. Aspects of the paleogeography of Beringia during the late Pleistocene. *In* Paleoecology of Beringia (D. M. Hopkins, J. V. Matthews, C. E. Schweger, and S. B. Young, eds.), p. 3–28. Academic Press, New York, NY.

Kartavtsev, Yu. F.
1991. Temporal and spatial variability in allelic frequencies in populations of pink salmon, *Oncorhynchus gorbuscha*. [English transl.] J. Ichthyol. 31(2):87–98.

Kartavtsev, Yu. F., V. V. Efremov, M. V. Smirnov, E. V. Ivankova, and N. E. Polyakova.
1992. Analysis of genotype distributions at allozyme loci

in populations of pink salmon, *Oncorhynchus gorbuscha*. [English transl.] J. Ichthyol. 32(4):102–115.

Keigwin, L. D., G. A. Jones, and P. N. Froelich.
1992. A 15,000 year paleoenvironmental record from Meiji Seamount, far northwestern Pacific. Earth Planet. Sci. Lett. 111:425–440.

Kwain, W., and J. A. Chappel.
1978. First evidence for even-year spawning pink salmon, *Oncorhynchus gorbuscha*, in Lake Superior. J. Fish. Res. Board Can. 35:1373–1376.

Lane, S., A. J. McGregor, S. G. Taylor, and A. J. Gharrett.
1990. Genetic marking of an Alaskan pink salmon population, with an evaluation of the mark and marking process. Am. Fish. Soc. Symp. 7:395–406.

Mann, D. H., and T. D. Hamilton.
1995. Late Pleistocene and Holocene paleoenvironments of the North Pacific coast. Quartern. Rev. 14:449–471.

Mantua, N. J., S. R. Hare, Y. Zhang, J. W. Wallace, and R. C. Francis.
1997. A Pacific interdecadal climate oscillation with impacts on salmon production. Bull. Am. Meteorol. Soc. 78:1069–1079.

McGregor, A. J.
1983. A biochemical genetic analysis of northern Southeast Alaskan pink salmon (*Oncorhynchus gorbuscha*). M.S. thesis, Univ. Alaska, Juneau, AK, 94 p.

McGregor, A. J., S. Lane, M. A. Thomason, L. A. Zhivotovsky, W. W. Smoker, and A. J. Gharrett.
1998. Migration timing, a life history trait important in the genetic structure of pink salmon. N. Pac. Anadr. Fish Comm. Bull. 1:262–273.

Moore, T. C., Jr., L. H. Burckle, K. Geitzenauer, B. Luz, A. Molina-Cruz, J. H. Robertson, H. Sachs, C. Sancetta., J. Thiede, P. Thompson, and C. Wenkam.
1980. The reconstruction of sea surface temperatures in the Pacific ocean of 18,000 B.P. Marine Micropaleontology 5:215–247.

Morley, J. J., L. E. Heusser, and N. J. Shackleton.
1991. Late Pleistocene/Holocene radiolarian and pollen records from sediments in the sea of Okhotsk. Paleoceanography 6:121–131.

Nei, M.
1978. Estimation of heterozygosity and genetic distance from a small number of individuals. Genetics 89:583–590.

Park, L. K., and P. Moran.
1994. Developments in molecular genetic techniques in fisheries. Reviews in fish biology and fisheries 4:272–299.

Pella, J. J., and G. B. Milner.
1987. Use of genetic marks in stock composition analysis. *In* Population genetics and fishery management (N. Ryman and F. Utter, eds.), p. 247–276. Univ. Washington Press, Seattle, WA.

Quinn, T. P.
1984. Homing and straying in Pacific salmon. *In* Mechanisms of migration in fishes (J. D. McCleave, G. P. Arnold, J. J. Dodson, and W. H. Neill, eds.), p. 357–362. Plenum Press, New York, NY.

Reger, R. D., and R. G. Updike.
1983. A working model for late Pleistocene glaciation of the Anchorage Lowland, upper Cook Inlet, Alaska. *In* Glaciation in Alaska—extended abstracts from a workshop (R. M. Thorson and T. D. Hamilton, eds.), p. 71–74. Univ. Alaska Museum Occasional Paper 2, Fairbanks, AK.

Ridgway, G. J., S. W. Sherburne, and R. D. Lewis.
1970. Polymorphisms in the serum esterases of Atlantic herring. Trans. Am. Fish. Soc. 99:147–151.

Roff, D. A., and P. Bentzen.
1989. The statistical analysis of mitochondrial polymorphisms: chi-square and the problem of small samples. Mol. Bio. Evol. 6:539–545.

Rohling, E.J., M. Fenton, F.J. Jorissen, P. Bertrand, G. Ganssen, and J. P. Caulet.
1998. Magnitudes of sea-level lowstands of the past 500,000 years. Nature 396:162–165.

Royce, W. F., L. S. Lenwood, and A. C. Hartt.
1968. Model as of oceanic migrations of Pacific salmon and comments on guidance mechanisms. U.S. Fish Wildlf. Serv. Fish. Bull. 66:441–462.

Saitou, N., and M. Nei.
1987. The neighbor-joining method: a new method for constructing phylogenetic trees. Mol. Biol. Evol. 4:406–425.

Salmenkova, E. A., and V. T. Omelchenko.
1983. Polymorphism of NADP-dependent isocitrate dehydrogenase and malate dehydrogenase in populations of chum and pink salmon. [In Russian, English abstract.] Biologiya Morya 3:24–28.

Sancetta, C.
1983. Effect of Pleistocene glaciation upon oceanographic characteristics of the North Pacific Ocean and Bering Sea. Deep Sea Res. 30:851–869.

Sancetta, C., and S. W. Robinson.
1983. Diatom evidence on Wisconsin and Holocene events in the Bering Sea. Quaternary Res. 20:232–245.

Sancetta, C., and S.-M. Silvestri.
1986. Pliocene-Pleistocene evolution of the North Pacific Ocean-atmosphere system, interpreted from fossil diatoms. Paleoceanography 1:163–180.

Schaal, B. A., and W. W. Anderson.
1974. An outline of techniques for starch gel electrophoresis of enzymes from the American oyster *Crassostrea virginica* Gmelin. Georgia Marine Science Center Tech. Rep. 74-3.

Seeb, L. W., and P. A. Crane.
1999. High heterogeneity in chum salmon in Western Alaska, the contact zone between northern and southern lineages. Trans. Am. Fish. Soc. 128:58–87.

Shaklee, J. B., F. W. Allendorf, D. C. Morizot, and G. S. Whitt.
1990. Gene nomenclature for protein-coding loci in fish. Trans. Am. Fish. Soc. 119:2–15.

Shaklee, J. B., D. C. Klaybor, S. Young, and B. A. White.
1991. Genetic stock structure of odd-year pink salmon, *Oncorhynchus gorbuscha*, Walbaum, from Washington and British Columbia and potential mixed-stock fisheries applications. J. Fish Biol. 29(suppl. A):21–34.

Shaklee, J. B., and N. N. Varnavskaya.
1994. Electrophoretic characterization of odd-year pink salmon (*Oncorhynchus gorbuscha*) populations from the Pacific coast of Russia and comparison with selected North American populations. Can. J. Fish. Aquat. Sci. 51(suppl. 1):158–171.

Shaw, C. R., and R. Prasad.
1970. Starch gel electrophoresis of enzymes—a compilation of recipes. Biochem. Genet. 4:297–320.

Shuntov, V. P., V. V. Lapko, A. A. Balanov, and A. V. Startsev.
1994. Interannual changes in anadromous migrations of salmons in waters of the Sakhalin-Kuril Region. (NPAFC [North Pacific Andadramous Fisheries Comm.] Doc. 107) Laboratory of Applied Biocenology, Pacific Research Institute of Fishery and Oceanography (TINRO) 1994. Vladivostok, Russia, 20 p.

Smoker, W. W., A. J. Gharrett, and M. S. Stekoll.
1998. Genetic variation of return date in a population of pink salmon: A consequence of fluctuating environment

and dispersive selection? Alaska Fishery Res. Bulletin 5:46–54.

Sokal, R. R., and F. J. Rohlf.
1995. Biometry, third ed. W.H. Freeman and Co., New York, NY, 887 p.

Takagi, K., K. V. Aro, A. C. Hartt, and M. B. Dell.
1981. Distribution and origin of pink salmon (*Oncorhynchus gorbuscha*) in offshore waters of the North Pacific Ocean. Committee on Biology and Research. Int. North Pac. Fish. Comm. Document 2178, Bulletin 40, International North Pacific Fisheries Commission, Vancouver, Canada.

Thorson, R. M., and T. D. Hamilton.
1986. Glacial geology of the Aleutian Islands. *In* Glaciation in Alaska: the geologic record (T. D. Hamilton, K. M. Reed, and R. M. Thorson, eds.), p. 171–191. Alaska Geological Society, Anchorage, AK.

Utter, F. M., H. O. Hodgins, and F. W. Allendorf.
1974. Biochemical genetic studies in fishes: potentialities and limitations. *In* Biochemical and biophysical perspectives in marine biology, vol. 1 (D. C. Malins and J. R. Sargent, eds.), p. 213–238. Academic Press, San Francisco, CA.

Varnavskaya, N. V., and T. D. Beacham.
1992. Biochemical genetic variation in odd-year pink salmon (*Oncorhynchus gorbuscha*) from Kamchatka. Can. J. Zool. 70:2115–2120.

Varnavskaya, N. V., C. C. Wood, and R. J. Everett.
1994a. Genetic variation in sockeye salmon (*Oncorhynchus nerka*) populations of Asia and North America. Can. J. Fish. Aquat. Sci. 51:132–146.

Varnavskaya, N. V., C. C. Wood, R. J. Everett R. L. Wilmot, V. S. Varnavsky, V. V. Midanaya, and T. P. Quinn.
1994b. Genetic differentiation of subpopulations of sockeye salmon (*Oncorhynchus nerka*) within lakes of Alaska, British Columbia, and Kamchatka, Russia. Can. J. Fish. Aquat. Sci. 51:147–157.

Velichko, A. A.
1984. Late Pleistocene spatial paleoclimatic reconstructions. *In* Late quaternary environments of the Soviet Union (A. A. Velichko, H. E. Wright Jr., and C. W. Barnosky, eds.), p. 261–285. Univ. Minnesota Press, Minneapolis, MN.

Weir, B. S.
1996. Genetic data analysis II. Sinauer Assoc. Inc., Sunderland, MA.

Weir, B. S., and C. C. Cockerham.
1984. Estimates of *F*-statistics for the analysis of population structure. Evolution 38:1358–1370.

Wilmot, R. L., R. J. Everett, W. J. Spearman, R. Baccus, V. V. Varnavskaya, and S. V. Putivkin.
1994. Genetic stock structure of western Alaska chum salmon and a comparison with Russian Far East stocks. Can. J. Fish. Aquat. Sci. 51:84–94.

Winans, G. A., P. B. Aebersold, S. Urawa, and N. V. Varnavskaya.
1994. Determining continent of origin of chum salmon (*Oncorhynchus keta*) using genetic stock identification techniques: status of allozyme baseline in Asia. Can. J. Fish. Aquat. Sci. 51:95–113.

Wright, S.
1978. Evolution and the genetics of populations, vol. 4: Variability within and among natural populations. Univ. Chicago Press, Chicago, IL.

Zhivotovsky, L. A., and M. K. Glubokovsky.
1989. Role of migration and selection in genetic differentiation of pink salmon (*Oncorhynchus gorbuscha*). [English transl.] Doklady Akademii Nauk SSSR 308:1235–1240.

Zhivotovsky, L. A., M. K. Glubokovsky, R. M. Victorovsky, A. M. Bronevsky, K. I. Afanasev, V. V. Efremov, L. N. Ermolenko, B. A. Kalabushkin, V. G. Kovalev, A. N. Makoedov, T. V. Malinina, S. P. Pustovoit, and G. A. Rubstova.
1989. Genetic differentiation of pink salmon. Genetika 25: 1261–1274. [English transl.].

Validation of age estimation and back-calculation of fish length based on otolith microstructures in tilapias (Pisces, Cichlidae)

Jacques Panfili
Institut de Recherche pour le Développement, LASAA
B.P. 70
29280 Plouzané, France
E-mail address: panfili@ird.fr

Javier Tomás
Port Erin Marine Laboratory
Port Erin
Isle of Man IM9 6JA, United Kingdom

Abstract–Two tilapia species, *Sarotherodon melanotheron* (brackishwater fish) and *Oreochromis niloticus* (freshwater fish), were marked with tetracycline and reared in Côte d'Ivoire (West Africa) in intensive (fish fed) and extensive (fish unfed) conditions. Juvenile and adult otoliths of the two species were examined. They were cut into transverse thin sections (10 to 40 µm), and otolith microincrements were counted on the sulcus along the ventral axis. Results for both species showed that microincrements are laid down daily. The number of days of growth reflects the number of microincrements (regression with slope not different from 1 and intercept not different from 0; $P>0.05$). This technique has a tendency to underestimate age ($P<0.05$): for *S. melanotheron*, the mean bias error is 4.4 d for juveniles (48 to 169 d of growth) and 8.1 d for adults (34 to 185 d of growth); for *O. niloticus*, the mean bias error is 0.9 d for juveniles (31 to 62 d of growth) and 5.1 d for adults (36 to 65 d of growth). Back-calculation of individual length at marking is very sensitive to an uncoupling between otolith and fish-specific growth rates. With the present data, back-calculated lengths overestimated actual size. When otolith and fish growth were coupled, length was back-calculated accurately.

Manuscript accepted 9 August 2000.
Fish. Bull. 99:139–150 (2001).

"Tilapia" is the common name for three genera of endemic cichlids from Africa, *Oreochromis*, *Sarotherodon*, and *Tilapia*. Species belonging to these three genera are widely distributed in tropical areas and have colonized all kinds of continental waters as natural or introduced species. Their adaptative capabilities have also been used in developing an aquaculture for these species worldwide (Lowe-McConnell, 1982; Wootton, 1984; Pullin et al., 1988). Both the reproduction and growth strategies in tilapias, however, differ among populations depending on environmental conditions (Kolding, 1993). Therefore, correct estimates of age is of great importance in assessing different growth strategies, as well as in characterizing different populations, by means of parameters such as size at first maturity. Despite the need for accurate age estimates, age at first maturity has not been the subject of many studies in tilapias and the question remains whether the observed differences in size at maturity are due to growth or to age differences (Eyeson, 1983; Legendre and Ecoutin, 1989; Duponchelle and Panfili, 1998). Moreover, tilapias can be sexually active a few months after hatching as shown in studies on tilapia reared in aquaculture (Eyeson, 1983).

Since Pannella's (1971) work, otolith microincrements have been widely used to estimate the age of fish in days, useful for studies on larvae and juvenile fish (Jones, 1992). Several authors have studied microincrements in tilapia otoliths, but their results have not been applied to field research. One possible reason is that there is not a standard and simple method available for choosing and preparing the otolith. Previous works have used different otoliths and preparation techniques: sagitta cut transversally and acid etched for *Tilapia guineensis* (Fagade, 1980), sagitta cut transversally and observed with scanning electron microscope for *Oreochromis niloticus* (Tanaka et al., 1981), lapillus observed whole in photonic microscopy for *Tilapia mariae* (Rosa and Ré, 1985), sagitta cut sagittally and observed in scanning electron microscopy for *Oreochromis aureus* (Karakiri and Hammer, 1989), and sagitta cut transversally, etched and stained for *Oreochromis niloticus* (Zhang and Runham, 1992). Each of these authors, except Fagade (1980), has validated the daily deposition of microincrements. Nevertheless, all fish used for validation were juveniles and were reared under controlled conditions in aquaria, far from their natural environment. To date, no attempt has been made to estimate growth for tilapia in natural waters nor age at maturity by using microincrements.

The first aim of our study was to assess whether examination of microincrements in otoliths yields valuable estimates of age (in days) for both juveniles and adults of *Sarotherodon melanotheron* (brackishwater species) and *Oreochromis niloticus* (freshwater species). To obtain results that could be applied to field studies, fish were reared

in an environment as similar as possible to natural conditions. The second aim was to develop a standard method for otolith preparation and examination to be used for both species. Both objectives are particularly useful in the case of *S. melanotheron* for which no validation has previously been published. We chose to carry out experiments in two aquaculture stations in Côte d'Ivoire (Africa), where the fish and the otoliths were simultaneously marked with external tags and tetracycline, respectively, to follow fish and otolith growth. Tetracycline labels have been used widely to mark calcified structures since the first assays (Weber and Rigway, 1967; Meunier, 1974), and we improved this universal marker for marking tilapia otoliths. During the validation process, special attention was paid to the accuracy of the age estimations (Campana and Jones, 1992). Geffen (1992) reported in her review on validation that there is a lack of analysis of the variation in increment number at a given age and we focused on that particular point. Our data on individual fish and otolith tagging were useful to test a growth back-calculation model commonly used for fishes (Francis, 1990, for review; Campana and Jones, 1992; Smedstad and Holm, 1996) and particularly to test the problem of uncoupling between somatic and otolith growth reported in previous studies (Mosegaard et al., 1988; Reznick et al., 1989; Secor and Dean, 1989). The final aim of our study was to obtain an accurate, precise, and simple tool for age estimation for future life history studies on tilapias.

Materials and methods

Rearing experiments

Fish were reared in two aquaculture stations in Côte d'Ivoire (West Africa), a country that experiences a transitional equatorial climate with two dry and two rainy seasons (Durand and Skubich, 1982; Durand and Guiral, 1994). Juveniles and adults of *Sarotherodon melanotheron* and *Oreochromis niloticus* were used in the experiments. Juvenile fish were obtained from synchronous layings, whereas adults, males and females, were caught in the natural environment. *Sarotherodon melanotheron* was reared at the Layo station (Centre de Recherches Océanologiques) located on the Ebrié lagoon. One-hundred and ninety-eight adults of *S. melanotheron* ranging between 90 and 130 mm FL (fork length) were marked and randomly assigned to three 4-m^3 cages (C1, C2, C3) immersed in the lagoon. Another forty four adults between 170 and 210 mm FL were marked and kept in a 25-m^3 cage (C4). After hatching, juveniles were transferred to a 3-m^3 concrete tank supplied with a constant flow of water from the lagoon. Fish were fed daily with formulated pellets. *Oreochromis niloticus* was reared at the Bouaké station (Institut des Savanes). One-hundred and fifty-two adults of *O. niloticus* were marked and released in two 400-m^2 ponds (A1 and A2) that had been previously enriched with organic matter (density of 0.2 fish/m^2). Juveniles were kept in two 50-m^2 ponds (J1 and J2) after hatching. No food was supplied; fish were sustained by natural resources.

Marking and sampling

Juveniles were not marked, therefore the "date of marking" actually refers to the date of birth. Adults caught in the field were marked by injecting tetracycline into the peritoneal cavity (50 mg/kg of live weight) and tagged with plastic T-bar anchor tags. Fish were measured (standard length at marking (SL_m, millimeters), weighed (grams), and sex was determined at the date of marking (Table 1). All *O. niloticus* adults and only *S. melanotheron* adults kept in cage C4 were tagged. After marking, both species were sampled in cages and ponds at monthly intervals. After capture, all individuals were measured (standard length at capture (SL_c, millimeters), weighed (grams), sexed and their otoliths (sagittae) removed. Randomly selected otoliths were prepared for analysis. Table 1 shows the dates of marking and sampling, otolith subsamples, and the number of days between marking and recapture for the two species.

Otolith preparation

Only the right otolith was prepared according to the technique described by Secor et al. (1992). After testing all possible planes of the section (i.e. sagittal, transverse, frontal), we chose the transverse section plane. Each otolith was then embedded in polyester resin before being sectioned transversally (with an Isomet saw) to avoid extra polishing and taking care to leave material on both sides of the core's plane. The resulting section was attached to a glass slide with thermoplastic glue (CrystalBond), ground with wet sand paper (grit ranging from 400 to 1200 per paper), and polished (polishing cloth with alumina paste ranging from 3 to 1/3 µm) on one side until reaching the primordium. The block was then turned over, affixed again to a slide with the polished face down, and ground and polished to remove extra material until the core area was reached. The thickness of the resulting sections ranged between 10 and 40 µm. Microincrement readability was improved by polishing the surfaces with 1/3 µm alumina paste. Otoliths with over-ground surfaces or with damage in the reading axis were discarded.

Otolith interpretation and variables measured

Terminology used in our study refers to that of Kalish et al. (1995). Microincrements were interpreted and counted as number of D-zones (reading) along the sulcus, chosen as the standard axis for reading (Fig. 1). Otoliths of adults were read under an epifluorescent microscope (Leica, 50W HBO lamp, 355–420 nm D filter) because the tetracycline deposit emits a yellow-green fluorescence under UVB at 390 nm. Microincrements were counted between the tetracycline mark and the otolith edge on a monitor coupled with a video with 1250× magnification. In juvenile otoliths, microincrements were counted from the primordium to the outer edge of the otolith under 400× and 1000× magnifications on the monitor coupled with video.

Each otolith was read twice by the same reader, first from the primordium to the edge and then back from the

Table 1

Number of otoliths for each sampling date and number of days between marking and sampling (in brackets) for *Sarotherodon melanotheron* and *Oreochromis niloticus* marked in Layo and Bouaké. [1] = adults tagged with anchor tags.

Species	Date of marking or birthdate	Date of sampling					
Sarotherodon melanotheron							
Adults		22 Nov 93	22 Dec 93	20 Jan 94	25 Feb 94	31 Mar 94	22 Apr 94
Cage C1	19 Nov 93	1 (34 d)	1 (64 d)	1 (93 d)	1 (129 d)	1 (163 d)	1 (185 d)
Cage C2	19 Nov 93	1 (34 d)	1 (64 d)	1 (93 d)	1 (129 d)	1 (163 d)	1 (185 d)
Cage C3	19 Nov 93	1 (34 d)	1 (64 d)	1 (93 d)	1 (129 d)	1 (163 d)	1 (185 d)
Cage C4[1]	19 Nov 93	4 (34 d)	4 (64 d)	4 (93 d)	4 (129 d)	4 (163 d)	4 (185 d)
Juveniles			22 Dec 93	20 Jan /94	26 Feb 94	31 Mar 94	22 Apr 94
Tank	4 Nov 93		5 (48 d)	5 (77 d)	5 (114 d)	5 (147 d)	5 (169 d)
Oreochromis niloticus							
Adults						3 Mar 94	1 Apr 94
Pond A1[1]	26 Jan 94					15 (36 d)	15 (65 d)
Pond A2[1]	26 Jan 94					15 (36 d)	15 (65 d)
Juveniles							
Pond J1	2 Feb 94					7 Mar 94	5 Apr 94
						15 (33 d)	16 (62 d)
Pond J2	14 Feb 94					17 Mar 94	15 Apr 94
						15 (31 d)	16 (60 d)

edge to the primordium following the same growth axis (Campana, 1992). If no significant difference was found between these two readings for the whole sample after a paired *t*-test, the mean was used to estimate the age (Campana and Jones, 1992). To maintain unbiased readings, physical data (size, date of capture) were not given to the reader.

Three variables were measured on each otolith: 1) the otolith diameter at capture (OD_c) which corresponds to the maximum length on the anteroposterior axis of the otolith before sectioning; 2) the otolith radius at capture (R_c) which corresponds to the distance between the primordium and the edge along the sulcus axis; and 3) the otolith radius at marking (R_m) which corresponds to the distance between the primordium and the tetracycline mark along the sulcus axis for the adults marked (Fig. 1). Variables were measured with TNPC image processing software (Visilog software platform, Noesis, France).

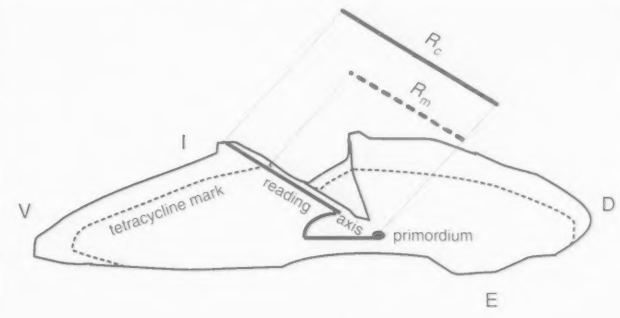

Figure 1

Diagram of the variables measured and of the reading axis used in reading thin otolith sections of tilapias. R_c = otolith radius at capture, R_m = otolith radius at marking (tetracycline mark), D = dorsal face, E = external face, I = internal face, V = ventral face.

Validation of the time of deposition of microincrements

The term validation refers here to the accuracy of the age estimation in tilapias by counting the number of microincrements in the otoliths (N_{inc}). The number of days involved in the validation experiment (D in days) refers to the microincrements deposited between hatching and the date of capture for juveniles and between the date of tetracycline labeling and the date of capture for adults. Pannella's hypothesis (1971) of a daily deposition rate for microincrements was tested for the two development stages of both species.

The accuracy of the method was tested by establishing the relation between the number of microincrements counted and the number of days involved in the experiment. A Student test on the linear regression was used to establish if the microincrements were deposited daily (slope equal to 1) and if the deposition started on the

first day (intercept equal to 0). The difference between the number of microincrements and the number of days of growth was plotted against time.

Validation of back-calculation for *Oreochromis niloticus*

Using tagged individuals, we assessed the validity of back-calculating fish length at marking. Several back-calculation models are described in the literature and each one assumes a different relationship between fish growth and otolith growth (Francis, 1990). Francis (1990) recommends Whitney and Carlander's model where a constant proportionality between fish growth and otolith growth throughout the life of the fish is assumed. Moreover, Francis (1990) recommends the regression of fish length against otolith length. Two approaches were considered in this study.

If the relationship between fish length and otolith length was linear,

$$SL_c = a + b \times R_c \tag{1}$$

with a body proportional hypothesis (BPH), then the back-calculation formula would be

$$SL_{mb} = \left(\frac{a + b \times R_m}{a + b \times R_c} \right) \times SL_c . \tag{2}$$

If the relationship between fish length and otolith length was nonlinear and for example multiplicative,

$$Log(SL_c) = c + d \times Log(R_c) \tag{3}$$

with a body proportional hypothesis (BPH), then the back-calculation formula would be

$$Log(SL_{mb}) = d \times Log\left(\frac{R_m}{R_c} \right) + Log(SL_c), \tag{4}$$

where SL_c = standard length at capture;
SL_{mb} = back-calculated standard length at marking;
R_c = otolith radius at capture;
R_m = otolith radius at marking (tetracycline mark); and
a, b, c, d = constants.

The validation of the back-calculation model was carried out on otoliths of adult *O. niloticus* labeled with tetracycline. For each individual, fish length measured at marking (SL_m, millimeters) was compared with the individual fish length back-calculated at marking from the otolith (SL_{mb}, millimeters). The mean of the differences between measured and back-calculated fish lengths was compared by means of a Student test with a theoretical mean equal to 0.

The specific growth rates of the fish length (G_{SL} in %/d) or of the otolith radius length (G_{OL} in %/d) were calculated following Ricker's formula (1975):

$$G_{SL}(\%/d) = \frac{\log(SL_c) - \log(SL_m)}{D} \times 100 \tag{5}$$

$$G_{OL}(\%/d) = \frac{\log(R_c) - \log(R_m)}{D} \times 100 \tag{6}$$

where SL_c = standard length at capture;
SL_m = standard length observed at marking;
R_c = otolith radius at capture;
R_m = otolith radius at marking; and
D = number of days of growth.

The relationships between these specific growth rates and the differences between observed and back-calculated lengths at marking were established.

Results

Microincrement identification and tetracycline labeling

Preparing tilapia otoliths for examination is time-consuming; it takes sixty to ninety minutes to prepare one otolith. A final polishing with 1/3 µm alumina powder is an important improvement for microstructure reading when dealing with thin sections ranging between 10 and 40 µm of thickness. The central core of the otolith of both species seems to correspond to the fusion of several primordia (up to six) even though it remains a small structure easily recognizable during the grinding process. Two accessory growth centers are visible on any transverse section of juvenile otoliths between the 13th and the 28th microincrements. They are located on both sides of the core on the dorsal and ventral halves of the otolith, where they appear to control the growth of the otolith on the dorsoventral axis. Microstructures are more clearly identified along the sulcus or along the dorsoventral axis as typically alternated L-zones and D-zones. Cross-checking and narrower microstructures are more common on the dorsoventral axis than in the sulcus region. As a result, we chose to interpret the microincrements along the sulcus axis (Fig. 1). Microincrements were counted from the hatching check which was clearly identifiable in the core area. For at least the first 30 microincrements the otolith grows predominantly along the dorsoventral axis and towards the external face. To avoid underestimating the number of microstructures during this first growth stage, the first 15 to 20 microincrements were counted along the core-ventral axis. Other microstructures along the ventral axis, interpreted as subdaily increments, rapidly increased in number and made the reading difficult. The shift to the sulcus axis was completed by following any conspicuous microincrement along the core-ventral axis to the sulcus region where the reading was finished (Fig. 1), provided accessory growth centers had not been encountered in this area.

The tetracycline mark was present in all otoliths examined, except one otolith of *S. melanotheron* sampled in April 1994. The mark was more intense on *O. niloticus*

Table 2

Results of microincrement readings for adults and juveniles *Sarotherodon melanotheron*. D = number of days between marking (adults) or birth (juveniles) and capture; SD = standard deviation; CI (95%) = confidence interval for mean at 95%; CV = coefficient of variation.

		Number of microincrements				
	D (d)	*n*	Mean	SD	CV (%)	CI (95%)
Adults	34	6	28.3	2.8	10.4	25.4–31.3
	64	6	56.1	8.9	16.6	46.7–65.5
	93	3	88.5	10.0	12.2	63.7–113.3
	129	7	119.4	7.7	6.7	112.3–126.2
	163	4	150.7	23.5	16.5	113.4–188.1
	185	3	176.7	11.0	6.7	149.4–203.9
Juveniles	48	4	48.6	2.3	5.0	45.0–52.3
	77	4	76.9	2.2	3.0	73.3–80.4
	114	5	109.9	2.1	2.0	107.3–112.5
	147	4	132.9	17.1	13.7	105.6–160.1
	169	5	164.5	6.1	3.9	156.9–172.1

Table 3

Linear regressions between the number of microincrements (N_{inc}) and the number of days between marking or birth and capture (D), $D = a + b \times N_{inc}$, and Student tests for slope (b=1) and intercept (a=0) for *Sarotherodon melanotheron*. F = result of model ANOVA; ns = no significant difference (P>0.05); r^2 = coefficient of determination.

				Intercept			Slope		
Group	*n*	*F*	r^2 (%)	*a*	*t*	a = 0	*b*	*t*	*b* = 1
Juveniles	22	524.7	96.3	4.348	0.88	ns	0.923	–1.91	ns
Adults	29	658.4	96.1	–4.844	–1.11	ns	0.968	–0.85	ns
Juveniles and adults	51	1176.3	96.0	–1.899	–0.57	ns	0.957	–1.54	ns

otoliths than *S. melanotheron* even though the quantities injected in both species were identical (50 mg per kg of live weight). In all cases the tetracycline deposit coincided with a check in the otolith structure, confirming that the marking is synonymous with stress to the fish. Other checks present along the sulcal axis interrupted the microstructure deposition pattern without any regularity. The growth of the otoliths in the region between the tetracycline deposit and the edge (i.e. between marking and capture) was always smaller for *S. melanotheron* than for *O. niloticus* for comparable sizes regardless of the date of capture.

Validation of microincrement deposition in otoliths of *Sarotherodon melanotheron*

Microincrement interpretation on adult *S. melanotheron* otoliths is difficult and requires a minimum magnification of 1000× for the microincrements between the tetracycline mark and the outer edge. Results of otolith reading for adults and juveniles are summarized in Table 2. The mean of the two readings was used as the value of the microincrement count of each otolith because the difference between the two readings was not significant in the whole sample (paired t-test, t=0.02, P>0.05). Results showed a tendency to underestimate true age, even though this underestimation was less pronounced in juvenile fish than in adults (Table 2). The mean underestimation was 8.1 d for adults and 4.4 d for juveniles; both means were significantly different from 0 (respectively t=4.19 and t=2.36, P<0.05). The number of increments were plotted against the days of growth. An ANOVA conducted with the resulting linear models (Table 3) with adults or juveniles, or both, showed a coefficient of determination (r^2) significantly different from 0 (P<0.001). The slopes were not different from 1 and the intercepts were not different from 0 (Table 3). Thus the microincrements counted on the transverse section of *S. melanotheron* otoliths can be considered structures that are deposited daily. The technique appears to accurately estimate the age of *S. melanotheron* in days.

The dispersal of residuals in Figure 2 was more important in large individuals. Underestimation slightly in-

Table 4

Results of microincrement readings for adults and juveniles *Oreochromis niloticus*. D = number of days between marking (adults) or birth (juveniles) and capture; SD = standard deviation; CI (95%) = confidence interval for mean at 95%; CV = coefficient of variation.

		Number of microincrements				
	D (d)	*n*	Mean	SD	CV (%)	CI (95%)
Adults	36	25	31.1	2.5	8.2	30.0–32.1
	65	27	59.7	2.6	4.4	58.7–60.8
Juveniles	31	12	31.9	2.5	8.2	30.2–32.1
	33	9	30.5	1.3	4.5	29.5–31.5
	60	9	59.4	3.7	6.4	56.6–62.3
	62	13	60.4	2.3	3.9	59.0–61.8

creased with the duration of the experiment although the coefficient of variation did not increase with time (Table 2). Variability in precision was nevertheless higher for adults than for juveniles. Figure 2 also shows that the difference between the number of increments and the number of growth days was equal to zero for only a few individuals.

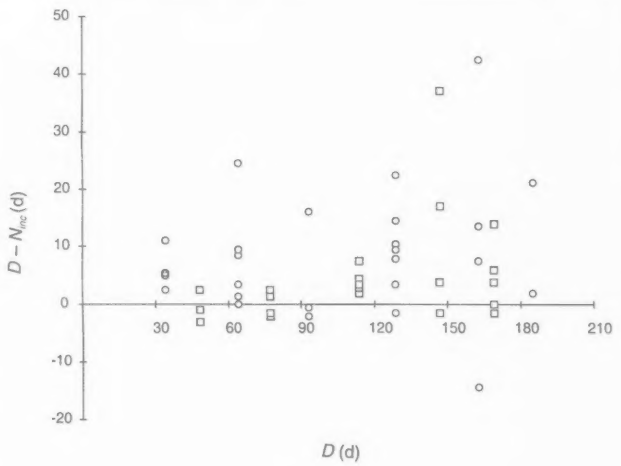

Figure 2

Individual differences between the number of days of growth (D) and the number of microincrements counted on transverse otolith section (N_{inc}) for adults (○) and juveniles (□) *Sarotherodon melanotheron*.

Validation of microincrement deposition in otoliths of *Oreochromis niloticus*

The distinction of microincrements was much greater in *O. niloticus* than in *S. melanotheron* otoliths resulting in an easier interpretation of microincrement deposition in *O. niloticus*. Results of microincrement counts for adults and juveniles of *O. niloticus* are summarized in Table 4. As for *S. melanotheron*, the two readings of each otolith were not significantly different across the whole sample; thus the mean of the two counts was used as the otolith microincrement value (paired t-test, t=0.85, P>0.05). Microincrement values in otoliths of adults after 36 and 65 d underestimated the true age of the fish by 4.9 and 5.2 d, respectively. Both values significantly differed from 0 (respectively t=9.78 and t=10.44, P<0.05) but were not significantly different from each other (P>0.05). Therefore the deviation between the true age and the estimated age was similar between 36 and 65 d and approximately equal to five days.

In otoliths of juveniles, the mean of the differences between the number of days and microincrements counted did not differ significantly from 0 in ponds J1 (0.9 d) and J2 (0.6 d) (t=1.18 and t=0.45 [P>0.05], respectively). For juveniles reared in pond J1, age was underestimated after 33 and 62 d of growth (Table 4), whereas ages of juveniles in pond J2 (31 and 60 d of growth) were accurately estimated (Table 4). A one-level nested ANOVA was carried out to check whether the pond or the age, or both, had had an effect in the difference between the true age and the estimated age. Results showed a significant effect of the pond ($F_{(1,39)}$=7.57, P<0.05) but not of age ($F_{(2,39)}$=1.13, P>0.05). Furthermore, a multiple rank test showed that no significant differences existed between the means at 31, 60, and 62 d and between the means at 33, 60, and 62 d (P>0.05), but that a significant difference existed between 31 and 33 d (P<0.05). Thus an effect of the pond on otolith deposition could not be confirmed.

The relation between the number of microincrements and the number of days before capture was established to test the accuracy of the age estimation (Table 5). The resulting r^2 was significantly different from 0 for adults or juveniles, or for both (P<0.001). The slopes of the model were not different from 1 (Table 5, P>0.05), which shows that the deposition rate of microincrements is daily. The num-

Table 5

Linear regressions between the number of microincrements (N_{inc}) and the number of days between marking or birth and capture (D), $D = a + b \times N_{inc}$ and Student tests for slope (b=1) and intercept (a=0) for *Oreochromis niloticus*. F = result of model ANOVA; ns = no significant difference (P>0.05); r^2 = coefficient of determination; s = significant difference (P<0.05).

				Intercept			Slope		
Group	n	F	r^2 (%)	a	t	$a = 0$	b	t	$b = 1$
Juveniles	43	1122.6	96.5	0.293	0.21	ns	0.975	–0.85	ns
Adults	52	1264.9	97.0	–4.522	–3.47	s	0.989	–0.45	ns
Juveniles and adults	95	1696.5	94.8	–1.347	–1.12	ns	0.963	–1.59	ns

ber of days of growth explains the number of microincrements counted. Nevertheless, the intercept differed from 0 for adults (P<0.05). It therefore seems that the deposition of new increments did not start on the first day after marking and that this difference (5 d) remained constant for one to two months of growth (Tables 4 and 5), suggesting that the increment technique is accurate for estimating the age of *O. niloticus* in days.

Residual dispersal was similar for adults and juveniles and seems constant through time (coefficient of variation in Table 4 and Fig. 3). Age was especially overestimated in juvenile fish (Fig. 3). As for *S. melanotheron*, a difference between the number of increments and the number of growth days equal to zero was very rare with *O. niloticus* otoliths. The trend in the deviation of the age estimation was the same over time for a given pond (Fig. 3).

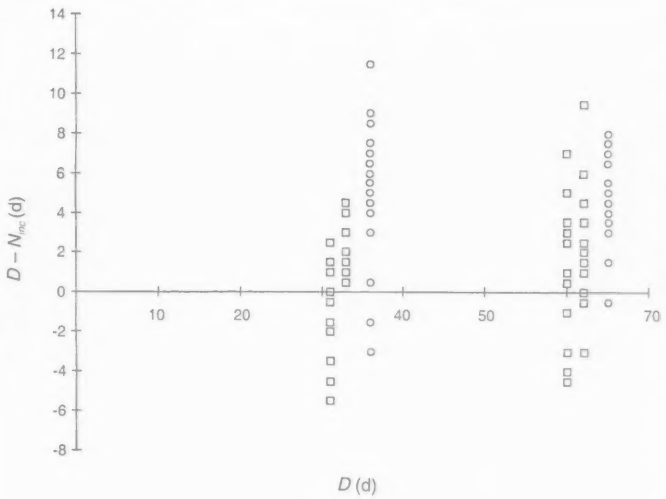

Figure 3

Individual differences between the number of days of growth (D) and the number of microincrements counted on transverse otolith section (N_{inc}) for adults (○) and juveniles (□) *Oreochromis niloticus*.

Validation of back-calculation of length in *Oreochromis niloticus*

The relation between fish length and otolith length was determined by establishing the regression of fish standard length at capture on the otolith radius at capture (Table 6). Both the linear and the multiplicative models were tested by an ANOVA (F calculated, Table 6) and had highly significant relationships (P<0.001). A comparison of the variances suggested that the coefficient of determination in the multiplicative model was significantly higher than that in the linear model (P<0.05). As a result, the regression used for the back-calculation of fish length was the multiplicative form. The observed dispersion of residuals reinforced this choice.

The observed low value of r^2 for the linear regression was due to the importance of the dispersion of points around the model for adults (Fig. 4). Nevertheless, this dispersion was also observed in the relation between fish length and otolith diameter at capture (Fig. 4), prior to any otolith preparation. In this case the linear regression had a higher coefficient of determination (Table 6). The dispersion can be explained by the natural growth variation which appears with age, and which is strong for this species.

The back-calculated formula used to compare the observed length at marking and the back-calculated length with otolith transverse sections was therefore

$$Log(SL_{mb}) = 0.899278 \times Log\left(\frac{R_m}{R_c}\right) + Log(SL_c). \quad (7)$$

Back-calculated lengths at marking were overestimated in the whole sample and this tendency did not depend on fish size at marking (Fig. 5). The mean of the differences

(mean=8.5 mm, standard deviation=8.7 mm) was significantly different from 0 (t=6.94, P<0.05). As a result, back-calculation of fish length overestimated the length of fish that had grown for one or two months.

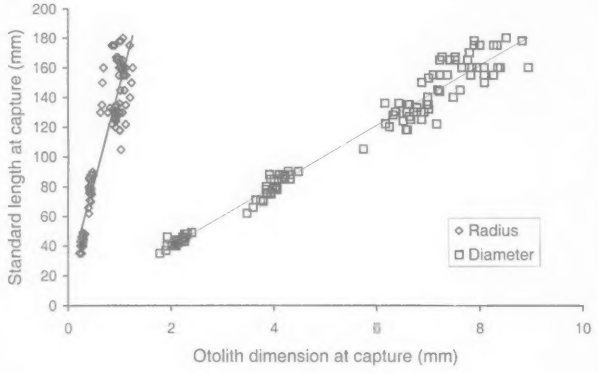

Figure 4

Relationship between standard length and otolith dimension (radius or diameter) observed at capture for *Oreochromis niloticus*. The lines show the linear regression models.

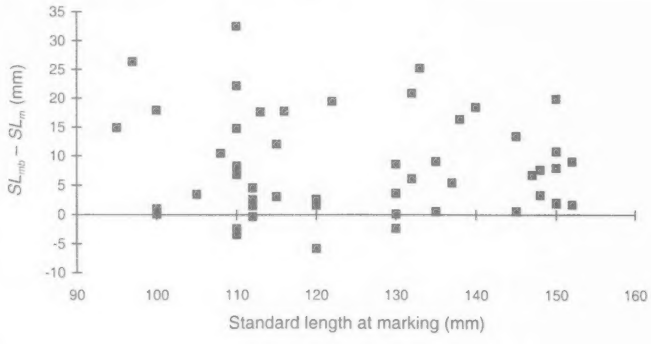

Figure 5

Differences between standard length back-calculated at marking (SL_{mb}) and standard length observed at marking (SL_m) for each *Oreochromis niloticus* (36 and 65 days after marking).

The relation between the specific growth rate of the fish (G_{SL}) and the difference between back-calculated and observed length at marking was positive because overestimation increases with the specific growth rate, regardless of the duration of the experiment (Fig. 6). The actual under- or overestimation of back-calculated length seems to depend on the coupling between the specific growth rates of the otolith and the fish (Fig. 7). An uncoupling between somatic and otolith growth rates would explain the deviation of the back-calculated length from the measured value (Fig. 7). That is to say, if the specific growth rates of the fish and the otolith are identical, the back-calculation gives a very good approximation of the length at marking (i.e. the difference is almost equal to zero), whereas if the otolith growth rate is higher than the fish growth rate, then the back-calculation underestimates the length at marking. Inversely if the somatic growth rate is higher than the otolith growth rate, the back-calculation will overestimate the length at marking. Moreover, when the uncoupling between otolith and somatic growth rates rises, the overestimation of the back-calculation increases (Fig. 7).

Discussion

Otolith preparation and interpretation of microincrements in tilapias

Transversal sections (in contrast to sagittal or frontal sections) of otoliths are the clearest and most reliable way to interpret microincrements in tilapia otoliths. Although some authors have worked on sagittal sections (Fagade, 1980; Karakiri and Hammer, 1989) the concavoconvex shape of the otoliths in adults makes it very difficult to obtain a plane that would include both the core area and the otolith edge. Zhang and Runham (1992), who prepared transverse sections of adult *O. niloticus* otoliths with their histological technique (Zhang et al., 1991), obtained sections with clear microincrements. Rosa and Ré (1985) reported that sagittae in

Table 6

Relations between SL_c (standard length at capture) and R_c (otolith radius at capture) or OD_c (otolith diameter at capture) for *Oreochromis niloticus*. F is calculated from the ANOVA for testing the model. r^2 = coefficient of determination.

Model	n	Regression	F	r^2 (%)
Linear	108	$SL_c = 17.13 + 130.31 \times R_c$	612.5	85.1
Multiplicative	108	$Log(SL_c) = 5.02 + 0.899 \times Log(R_c)$	1117.3	91.3
Linear	119	$SL_c = -0.609 + 20.33 \times OD_c$	4163.8	97.2

juvenile *Tilapia mariae* were too thick to allow observation of the microstructures without previous preparation and decided to work on lapilli. Despite the long and time-consuming process (about 1 h for preparing each transverse section of a sagitta), it appears to be the best way to observe otolith microincrements for both juvenile and adult tilapia. To avoid parallax when observing microstructures on thick preparations (Campana, 1992; Neilson, 1992), a thickness of 10 to 40 µm and a fine polishing of the sections are necessary.

Zhang and Runham (1992) observed microincrements of juvenile *O. niloticus* otoliths under a maximum magnification 400× with light microscopy, whereas Rosa and Ré (1985) used magnifications ranging from 600× to 1250× while working on *Tilapia mariae* lapilli. Our results show that microincrement observation and interpretation require a minimum magnification of 1000× for adult tilapias. These high magnifications with compound microscopes are required to observe microincrements in the sulcus area where they are found to have such a compressed arrangement that no space is left for subdaily increments (Zhang and Runham, 1992). Therefore, to interpret microincrements in tilapia otoliths accurately, we strongly recommend preparing thin transverse sections (10–40 µm), polishing them finely (1/3 mm), and observing them under high magnifications (minimum of 1000×).

In interpreting microstructures in tilapia otoliths, four types of problems were encountered: 1) difficulty in interpreting microstructures in the otolith region that correspond to first-growth stages; 2) difficulty in having to switch the reading axis (starting in the dorsoventral area and finishing along the sulcus area); 3) difficulty in reading some zones; and 4) difficulty in identifying microstructures near the outer edge of the otolith. Microincrements around the hatching check are very faint and narrow and require high magnifications to be identified. Narrow increments were also reported on *Tilapia mariae* lapilli by Rosa and Ré (1985). The presence of accessory growth centers on both sides of the core area in the dorsoventral plane of the otolith were also observed by Karakiri and Hammer (1989) and Zhang and Runham (1992) on *O. niloticus* otoliths. These authors estimated the date of formation of these accessory growth centers to be between 21 and 30 days and between 16 and 28 days after hatching, respectively. Secondary growth centers in Ivorian tilapia otoliths were located between the 13th and the 28th microincrements; therefore our results agree with observations made by these authors. It is likely that the presence of accessory growth centers represents a shift in the growth of the otolith, meaning that growth along the dorsoventral axis is favored at this stage.

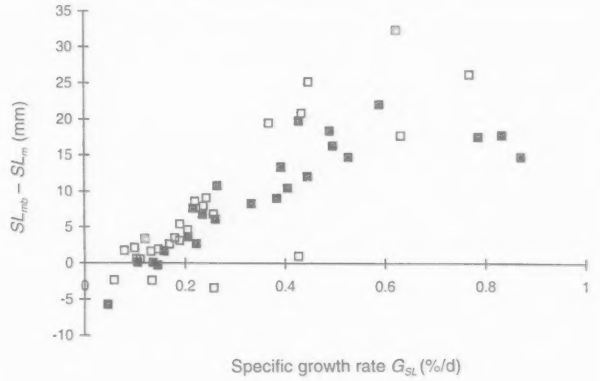

Figure 6

Relation between the difference of standard length back-calculated at marking (SL_{mb}) and standard length observed at marking (SL_m) versus the specific growth rate of standard length (G_{SL}) for *Oreochromis niloticus*, 36 days (■) and 65 days (□) after marking.

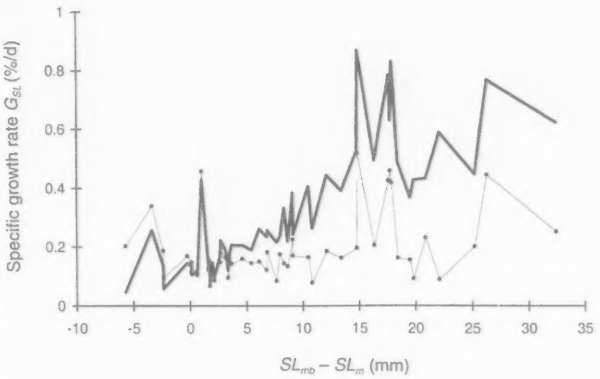

Figure 7

Relations between the specific growth rate (otolith length [thin curve] or standard length [bold curve]) and the individual difference of the standard length back-calculated at marking (SL_{mb}) and the standard length observed at marking (SL_m) for *Oreochromis niloticus*.

The use of the dorsoventral axis to read microincrements may induce reader error. Ambiguities arise because of the numerous subdaily structures deposited during the fast growing period (Zhang and Runham, 1992); thus reading along the sulcus region is recommended. However, as the growth of the otolith along the sulcus is relatively indistinct during the first 15 to 20 microincrements, proper information can only be gathered along the core-ventral axis. Certain regions in otoliths, especially near the edge, have been difficult to read for numerous other species (Campana, 1992). Tilapia otoliths also exhibit unreadable

parts as reported and observed by Zhang and Runham (1992). Otoliths of both species are difficult to interpret and attention should be paid to the need for trained readers capable of properly interpreting microincrements in tilapia otoliths.

Validation of microincrement deposition in tilapias

Tetracycline remains a universal marker for otoliths (Beamish and McFarlane, 1987; Brothers, 1990; Geffen, 1992). In our study only one *S. melanotheron* did not reveal any tetracycline deposit on its otolith. Because the fish is necessarily handled, injecting tetracycline induces a strong calciotraumatic effect on the otolith (Meunier and Boivin, 1978; Pannella, 1980; Campana and Neilson, 1985; Panfili and Ximénès, 1992). As a result, the mark is easily recognizable in the otolith and corresponds to a check in the otolith structure. This check probably reflects a cessation in the growth of the otolith that could last several days. In our study, underestimation of age was constant (equal to 5 days) for adult *O. niloticus* which indicates that the growth of the otolith was stopped with the tetracycline injection and resumed five days later. When using microincrement counts, the effect of marking should be considered, but it is difficult to estimate the time elapsed between injection and resumed growth of the otolith.

We estimated the age of juvenile and adult *O. niloticus* and *S. melanotheron* accurately using the same microincrement examination and interpretation on thin otolith transverse preparations. Tanaka et al. (1981) and Zhang and Runham (1992) had similar results on transverse sections of juvenile *O. niloticus* otoliths. The former observed otoliths with scanning electron microscopy and the latter observed stained otoliths. Karakiri and Hammer (1989) also reported daily increment deposition on sagittal sections of *Oreochromis aureus* otoliths observed with scanning electron microscopy. Our technique of preparation is the only one that has been validated for two different species and for several developmental stages.

Precision in age estimation with otolith microincrements was calculated for both species and showed that the error ranges between 4.4 d in juveniles and 8.1 d in adults for *S. melanotheron*, and between 0.9 d in juveniles and 5.1 d in adults for *O. niloticus*.

Validation of back-calculation and influence of individual growth rates

We validated the back-calculation model with a body proportional hypothesis (BPH) developed by Whitney and Carlander (1956, in Francis, 1990) and commonly recommended and used in the literature (Francis, 1990; Smedstad and Holm, 1996; Horppila and Nyberg, 1999). Back-calculation models rely on the assumption that otolith size and fish size are related and that a relation between them can be established. It is assumed that 1) the frequency of formation of each structure is constant and 2) the width of each increment is proportional to the growth of the fish (Campana and Jones, 1992). Caution should be taken when calculating the relationship because, as stated by Francis (1990) and Campana and Jones (1992), if the aim is to backcalculate a mean fish length from any otolith dimension, the resulting regression must have fish length as a dependent variable and otolith dimensions as independent variables. It is therefore very important to set up the most suitable relationship relating fish length and otolith length. Some works have shown that many factors influence this relationship. Wright et al. (1990) reported that the relation of fish length to otolith length was linear for smolts belonging to the high mode (fast growth) and curvilinear for smolts belonging to the low mode (slow growth). The relationship is also affected by food supply (Rice et al., 1985) or seasonal changes (Thomas, 1983). Furthermore, Reznick et al. (1989) showed that slow growing guppies (*Poecilia reticulata*) have larger otoliths than fast growing guppies of similar lengths, even though both groups of fish shared the same genetic background, had the same feeding schedule, and were reared under the same conditions. In this context, the use of the model of Whitney and Carlander is particularly suitable because it assumes that if a fish is 10% smaller than the mean length of the population for a given otolith size, this deviation will be constant throughout the life of the fish. We chose the curvilinear model for the relationship between fish length and otolith length because it fitted the existing data better. Bradford and Geen (1987) also found no significant difference between the curvilinear model and the linear model and therefore used the former because it adjusted total data better. Smedstad and Holm (1996) compared several back-calculation formulae for cod otoliths and concluded that the nonlinear one was better. These relationships seem to depend on the axis of the otolith chosen for back-calculation. Back-calculation results could have been less variable if the diameter of the whole otolith had been used in the relationship with fish length instead of the radius on the transverse otolith section (Fig. 4; Table 6). Unfortunately, because it was impossible to interpret the microincrements along the anteroposterior axis (diameter), that axis was discarded for back-calculation. A prerequisite of back-calculation is the assumption that the frequency of formation of microincrements is constant along the axis of analysis (Campana and Jones, 1992) and that assumption could not be made in the anteroposterior axis otoliths of our study.

Our study shows that back-calculated fish lengths are greater than measured fish lengths at marking among fish that have grown between one and two months. These results agree with those obtained by Rijnsdorp and Visser[1] on plaice (*Pleuronectes platessa*) grown for 19 months, although the back-calculation model used by these authors was the Dahl-Lea model (1920, in Francis, 1990). Two main points can be related to the observed overestimation. First, it is related to fish growth: the larger the fish growth, the larger the overestimation, although previous authors found an inverse relationship. This overestima-

[1] Rijnsdorp, A. D., and T. A. M. Visser. 1987. Tetracycline labelling of otoliths in plaice. ICES, C.M. 1987/G:33, 12 p.

tion may be result of back-calculation model being different or the marking-recapture interval being longer. Second, rather than fish growth rates alone, it appears that the coupling between fish growth and otolith growth plays a major role in explaining the observed overestimation of fish length. As shown in our study, underestimation of back-calculated fish length corresponds more to otolith growth rates compared with fish growth rates, and vice versa. These aspects must be discussed in light of the relationship between fish size and otolith size, the influence of fish growth on the overestimation of fish length, and the evidence of uncoupling between fish and otolith growth rates (Mosegaard, et al., 1988; Reznick, et al., 1989; Secor and Dean, 1989). Figure 6 shows that the higher the fish growth rates, the higher the deviation of the back-calculated fish length, implying that the faster a fish grows the further the fish is from the model. Secor and Dean (1989) considered that the ratio of otolith size to fish size increases in starved fish, as well as in fish with slow growth rates. Thomas (1983) considered this relationship to correct the underestimation resulting from using the Lee back-calculation model. Because fish growth rates have an influence on the observed estimations, they raise the question of what was the influence of fish growth rates on otolith growth rates along the sulcus axis in our study? Geffen (1992) proposed establishing the relationship between fish and otolith growth rates prior to back-calculation. Unfortunately this method is difficult to achieve in the field because it would mean marking fish from any studied populations, which unfortunately rarely happens.

Finally, Bradford and Geen (1987) advised caution when back-calculating fish length because otolith growth seems to be more conservative than fish growth. In our study, this assumption takes force because tilapias used in the experiments were starved before the beginning of the rearing experiments and experienced high growth rates after placement in ponds. Otolith growth rates followed fish growth rates within a certain range. When fish growth decreased below a certain limit, the otolith continued to grow. When fish growth increased, otolith growth also increased to a certain extent. This finding confirmed that the rate of growth in otoliths is conservative compared with the rate of somatic growth. Furthermore, the otolith represents an essential part of the equilibrium and sensory system of fish and thus cannot follow only fish growth rates. As a result, high growth rates in fish will imply a bigger dispersion of the data, or heterocedasticity around the relation of fish length to otolith length, which is observed here for larger individuals. The uncoupling of fish and otolith growth thus explains the difference between back-calculated and measured fish lengths at marking. Therefore caution should be taken when establishing the relationship of fish length to otolith length by using a representative sample of the individuals in their natural environment. In conclusion, the model developed by Whitney and Carlander represents a valid model for studies in the field because it considers individual variability in the relationship of fish length to otolith length but further work is needed to validate the use of other back-calculation models.

Acknowledgments

We specially thank Saurin Hem (IRD, Montpellier, France) and Philippe Cecchi (IRD, Bouaké, Côte d'Ivoire) for their valuable help in marking and rearing experiments. We acknowledge the CRO (Centre de Recherches Océanologiques, Abidjan, Côte d'Ivoire) and the IDESSA (Institut des Savanes, Bouaké, Côte d'Ivoire) for their logistic support during the rearing experiments. Thanks are also due to Jacques Baron (Université de Bretagne Occidentale, Brest, France) for his assistance and guidance in the statistical treatments. Marcus Belchier helped with the English text. We thank him especially. We also appreciate the comments of one anonymous reviewer which improved the manuscript.

Literature cited

Beamish, R. J., and G. A. McFarlane.
1987. Current trends in age determination methodology. *In* The age and growth of fish (R. C. Summerfelt and G. E. Hall, eds.), p. 15–42. Iowa State Univ. Press, Ames, IA.

Bradford, M. J., and G. H. Geen.
1987. Size and growth of juvenile chinook salmon back-calculated from otolith growth increments. *In* The age and growth of fish (R. C. Summerfelt, and G. E. Hall, eds.), p. 453–461. Iowa State Univ. Press, Ames, IA.

Brothers, E. B.
1990. Otolith marking. Am. Fish. Soc. Symp. 7:183–202.

Campana, S. E.
1992. Measurement and interpretation of the microstructure of fish otoliths. *In* Otolith microstructure examination and analysis (D. K. Stevenson and S. E. Campana, eds.), p. 59–71. Can. Spec. Publ. Fish. Aquat. Sci. 117.

Campana, S. E., and C. M. Jones.
1992. Analysis of otolith microstructure data. *In* Otolith microstructure examination and analysis (D. K. Stevenson, and S. E. Campana, eds.), p. 73–100. Can. Spec. Publ. Fish. Aquat. Sci. 117.

Campana, S. E., and J. D. Neilson.
1985. Microstructure of fish otoliths. Can. J. Fish. Aquat. Sci. 42:1014–1032.

Duponchelle, F., and J. Panfili.
1998. Variations in age and size at maturity of female Nile tilapia, *Oreochromis niloticus*, populations from man-made lakes of Cote d'Ivoire. Environ. Biol. Fishes 52:453–465.

Durand, J. R., and D. Guiral.
1994. Hydroclimat et hydrochimie. *In* Environnement et ressources aquatiques de Côte d'Ivoire: les milieux lagunaires (J. R. Durand, P. Dufour, D. Guiral, and S. G. F. Zabi, eds.), p. 59–90. ORSTOM (Office de la Recherche Scientifique et Technique d'Outre-Mer)Editions, Paris.

Durand, J. R., and M. Skubich.
1982. Les lagunes ivoiriennes. Aquaculture 27:211–250.

Eyeson, K. N.
1983. Stunting and reproduction in pond-reared *Sarotherodon melanotheron*. Aquaculture 31:257–267.

Fagade, S. O.
1980. The structure of the otoliths of *Tilapia guineensis* (Dumeril) and their use in age determination. Hydrobiologia 69:169–173.

Francis, R. I. C .C.
1990. Back-calculation of fish length: a critical review. J. Fish Biol. 36:883–902.

Geffen, A. J.
1992. Validation of otolith increment deposition rate. *In* Otolith microstructure examination and analysis (D. K. Stevenson and S. E. Campana, eds.), p. 101–113. Can. Spec. Publ. Fish. Aquatic Sci. 117.
Horppila, J., and K. Nyberg.
1999. The validity of different methods in the backcalculation of the lengths of roach—a comparison between scales and cleithra. J. Fish Biol. 54:489–498.
Jones, C. M.
1992. Development and application of the otolith increment technique. *In* Otolith microstructure examination and analysis (D. K. Stevenson, and S. E. Campana, eds.), p. 1–11. Canadian Special Publication of Fisheries and Aquatic Sciences 117.
Kalish, J. M., R .J. Beamish, E. B. Brothers, J. M. Casselman, C. Francis, H. Mosegaard, J. Panfili, E. D. Prince, R. E. Thresher, C. A. Wilson, and P. J. Wright.
1995. Glossary. *In* Recent developments in fish otolith research (D. H. Secor, J. M. Dean, and S.E. Campana, eds.), p. 723–729. Belle W. Baruch Library in Marine Science, vol. 19, Univ. South Carolina Press, Columbia, SC.
Karakiri, M., and C. Hammer.
1989. Preliminary notes on the formation of daily increments in otoliths of *Oreochromis aureus*. J. Appl. Ichthyol. 5:53–60.
Kolding, J.
1993. Population dynamics and life-history styles of Nile tilapia, *Oreochromis niloticus*, in Ferguson's Gulf, lake Turkana, Kenya. Environ. Biol. Fishes 37:25–46.
Legendre, M., and J. M. Ecoutin.
1989. Suitability of brackish water tilapia species from the Ivory Coast for lagoon aquaculture. I—Reproduction. Aquat. Liv. Res. 2:71–79.
Lowe-McConnell, R. H.
1982. Tilapias in fish communities. *In* The biology and culture of tilapias, (R. S. V. Pullin and R. H. Lowe-McConnell, eds.), p. 83–113. ICLARM (International Center for Living Aquatic Resources Management) Conference Proceedings, vol. 7, Manila.
Meunier, F.
1974. La technique de marquage vital des tissus squelettiques des poissons. Bull. Fra. Pisc. 255:51–57.
Meunier, F. J., and G. Boivin.
1978. Action de la fluorescéine, de l'alizarine, du bleu de calcéine et de diverses doses de tétracycline sur la croissance de la truite et de la carpe. Ann. Biol. Anim. Bioch. Biophys. 18:1293–1308.
Mosegaard, H., H. Svedäng, and K. Taberman.
1988. Uncoupling of somatic and otolith growth rates in arctic char (*Salvelinus alpinus*) as an effect of differences in temperature response. Can. J. Fish. Aquat. Sci. 45:1514–1524.
Neilson, J. D.
1992. Sources of error in otolith microstructure examination. *In* Otolith microstructure examination and analysis (D. K. Stevenson and S. E. Campana, eds.), p. 115–126. Can. Spec. Publ. Fish. Aquat. Sci. 117.
Panfili, J., and M. C. Ximénès.
1992. Measurements on ground or sectioned otoliths: possibilities of bias. J. Fish Biol. 41:201–207.
Pannella, G.
1971. Fish otoliths: daily growth layers and periodical patterns. Science (Washington D.C.) 173:1124–1127.
1980. Growth pattern in fish sagittae. *In* Skeletal growth of aquatic organisms: biological records of environmental change (D. C. Rhoads and R. A. Lutz, eds.), p. 519–560. Plenum Press, New-York and London.
Pullin, R .S. V., T. Bhukaswan, K. Tonguthai, and J. L. MacLean.
1988. The second international symposium on tilapia in aquaculture. ICLARM Conference Proceedings 15, Bangkok and Manila, 623 p.
Reznick, D., E. Lindbeck, and H. Bryga.
1989. Slower growth results in larger otoliths: an experimental test with guppies (*Poecilia reticulata*). Can. J. Fish. Aquat. Sci. 46:108–112.
Rice, J. A., L. B. Crowder, and F. P. Binkowski.
1985. Evaluating otolith analysis for bloater *Coregonus hoyi*: do otoliths ring true? Trans. Am. Fish. Soc. 114:532–539.
Ricker, W. E.
1975. Computation and interpretation of biological statistics of fish populations. Fish. Res. Board Can. Bull. 191, 409 p.
Rosa, H. C., and P. Ré.
1985. Influence of exogenous factors on the formation of daily microgrowth increments in otoliths of *Tilapia mariae* (Boulenger, 1899) juveniles. Cybium 9:341–357.
Secor, D. H., and J. M. Dean.
1989. Somatic growth effects on the otolith-fish size relationship in young pond-reared striped bass, *Morone saxatilis*. Can. J. Fish. Aquat. Sci. 46:113–121.
Secor, D. H., J. M. Dean, and E. H. Laban.
1992. Otolith removal and preparation for microstructural examination. *In* Otolith microstructure examination and analysis (D. K. Stevenson and S. E. Campana, eds.), p. 19–57. Can. Spec. Publ. Fish. Aquat. Sci. 117.
Smedstad, O. M., and J. C. Holm.
1996. Validation of back-calculation formulae for cod otoliths. J. Fish Biol. 49:973–985.
Tanaka, K., Y. Mugiya, and J. Yamada.
1981. Effects of photoperiod and feeding on daily growth patterns in otoliths of juvenile *Tilapia nilotica*. Fish. Bull. 79:459–466.
Thomas, R. M.
1983. Seasonal variation in the relationship between otolith radius and fish length in the pilchard off south west Africa. S.-Afr. J. Mar. Sci. 1:133–138.
Weber, D., and G. J. Rigway.
1967. Marking Pacific salmon with tetracycline antibiotics. J. Fish. Res. Board Can. 24:849–865.
Wootton, R. J.
1984. Introduction: strategies and tactics in fish reproduction. *In* Fish reproduction: strategies and tactics (G. W. Potts and R. J. Wootton, eds.), p. 1–12. Academic Press, London.
Wright, P. J., N. B. Metcalfe, and J. E. Thorpe.
1990. Otolith and somatic growth rates in Atlantic salmon parr, *Salmo salar* L.: evidence against coupling. J. Fish Biol. 36:241–249.
Zhang, Z., and N. W. Runham.
1992. Otolith microstructure pattern in *Oreochromis niloticus* (L.). J. Fish Biol. 40:325–332.
Zhang, Z., N. W. Runham, and T. J. Pitcher.
1991. A new technique for preparing fish otoliths for examination of daily growth increments. J. Fish Biol. 38:313–315.

Bayesian methods for analysis of stock mixtures from genetic characters

Jerome Pella
Auke Bay Laboratory
Alaska Fisheries Science Center
National Marine Fisheries Service, NOAA
11305 Glacier Hwy.
Juneau, Alaska 99801-8626
E-mail address: Jerry.Pella@noaa.gov

Michele Masuda
Auke Bay Laboratory
Alaska Fisheries Science Center
National Marine Fisheries Service, NOAA
11305 Glacier Hwy.
Juneau, Alaska 99801-8626

Abstract—An implementation of Bayesian methods to assess general stock mixtures is described. An informative prior for genetic characters of the separate stocks in a mixture is derived from baseline samples. A neutral, low-information prior is used for the stock proportions in the mixture. A Gibbs sampler—the data augmentation algorithm—is used to alternately generate samples from the posterior distribution for the genetic parameters of the separate stocks and for the stock proportions in the mixture. The posterior distribution incorporates the information about genetic characters in the baseline samples, including relatedness of stocks, with that in the stock-mixture sample to better estimate genotypic composition of the separate stocks. Advantages over usual likelihood methods include greater realism in model assumptions, better flexibility in applications, especially those with missing data, and consequent improved estimation of stock-mixture proportions from the contributing stocks. Two challenging applications illustrate the technique and its advantages.

Manuscript accepted 13 September 2000.
Fish. Bull. 99:151–167 (2001).

Fisheries that exploit mixed stocks are very common, and their management oftentimes requires assessment of composition of the mixed catches (Begg et al., 1999). Multilocus genotypes of fish are a natural tag by which to infer their origins. The unknown proportions from stocks comprising a stock mixture, or its stock composition, can be estimated from genotype counts in a random sample of the stock-mixture individuals if relative frequencies (RFs) of the genotypes vary among the contributing stocks. Larger differences in genotypic RFs among stocks result in more accurate and precise stock composition estimates. The conditional maximum likelihood (CML) method (Fournier et al., 1984; Millar, 1987; Pella and Milner, 1987) has most commonly been used for stock-mixture analysis. Baseline samples drawn from the separate contributors are used in estimating the RFs of the observed stock-mixture genotypes in each stock. The CML stock composition estimate maximizes a likelihood function of the stock-mixture genotypes as if their RFs in the baseline stocks were known without error. The baseline multilocus genotype RFs determine the outcome of a stock-mixture analysis. Larger errors in these estimated RFs result in larger stock composition errors. Usually the variation in CML stock composition estimates from baseline and stock-mixture sampling is evaluated by the bootstrap method.

The estimation of the baseline multilocus genotype RFs depends on the mode of inheritance of the observed markers. Among molecular markers developed for fish, allozymes, mitochondrial DNA (mtDNA), minisatellite DNA, and microsatellite DNA are widely known for their utility in stock-mixture analysis. For mtDNA, the entire haplotype passes as a unit from female to offspring and the baseline multilocus haplotype RFs are estimated directly by their observed RFs in the baseline samples. For allozymes, minisatellite DNA, and microsatellite DNA, the multilocus genotypes pass from parents to offspring under the usual rules of diploid inheritance. The expected multilocus genotype RFs for diploids equal the products of the genotypic RFs at the individual loci (or subsets of them) that pass independently from parents to offspring. In the special case when Hardy-Weinberg equilibrium holds at a locus, its expected genotypic RFs are determined by its allele RFs: the homozygote RFs equal the squares of their allele RFs and the heterozygote RFs equal twice the product of their allele RFs. To compute the estimated baseline multilocus genotype RFs for diploids, observed RFs of alleles or genotypes in the baseline samples replace corresponding unknown RFs. The few-

er the number of unknown RFs that need to be estimated from the available baseline samples, the more reliable the estimated baseline multilocus genotype RFs become (Altham, 1984). Therefore, under Altham's principle, allele RFs are to be estimated if Hardy-Weinberg equilibrium holds, and genotype RFs at the locus otherwise. If alleles among a linked subset of loci are not inherited independently, the multilocus genotype RFs for the subset have to be estimated directly from their observed RFs in the baseline samples.

The search for genetic variation by which to distinguish among populations of fish and other marine organisms has provided an embarrassment of riches. The numbers of mtDNA haplotypes (Epifanio et al., 1995; Bowen et al., 1996; Rosel et al., 1999) and alleles at minisatellite and microsatellite loci (O'Connell and Wright, 1997) can often be so large that reliable estimation of their RFs in stocks is a concern. Baseline sample sizes are usually limited, and the relative precision of estimated RFs for the numerous haplotypes, alleles, or genotypes (HAGs) declines with the magnitude of their RFs. Resulting stock composition estimates for the stock mixture may suffer. Grouping or binning of HAGs may help to control variation in estimation of their baseline RFs (O'Connell and Wright, 1997). However, for stock-mixture analysis, the practical details of grouping so as to balance the loss of information about the mixture against the gain in precision of the baseline RFs are unresolved. Bayesian methods developed for estimating allele RFs at a locus (sec. 3.7 of Lange, 1997) and for estimating cell probabilities in contingency tables (Bishop et al., 1975; Sutherland et al., 1975; Leonard, 1977) offer another attack on the problem. The Bayesian methods are applied later in estimating the RFs by using genetic similarities of stocks.

Conditional maximum likelihood does not use the information in the stock-mixture sample to improve the estimates of baseline multilocus genotype RFs, and the omission becomes ever more meaningful with the accumulation of mixture individuals from a series of analyses performed on stock mixtures of the same baseline populations. The unconditional maximum likelihood (UML) (Pella and Milner, 1987) or unconditional least squares (ULS) (Xu et al., 1994) methods have been suggested to remedy this shortcoming for analysis of a single mixture. For either approach, estimates are provided both for the stock proportions and baseline genotypic RFs by optimizing a criterion of fit to counts in both the baseline and stock-mixture samples. However, the fitting criteria may have local optima (Smouse et al., 1990), and effective search for the global optimum and corresponding estimates from both methods is unresolved. A practical compromise for either method is to find a particular local optimum by starting the search from the CML estimate of stock proportions and stock genotypic RFs, the latter evaluated from the baseline samples alone.

None of the past approaches—CML, UML, or ULS—makes use of the genetic similarities among stocks to estimate the relative frequencies of haplotypes, alleles, or genotypes more accurately in the separate stocks. Common HAGs are shared universally among stocks; HAGs with moderate RFs are shared at least regionally, and rare HAGs occur only sporadically. Instead, the similarities in HAG RFs are viewed solely as limiting success in distinguishing the origins of the stock-mixture individuals. Improved estimates of HAG RFs, to replace simple observed values, would generally benefit accuracy and precision of stock composition estimation, especially as the number of rare or uncommon HAGs increases (e.g. Xu et al., 1994). Estimation of RFs for rare HAGs in separate stocks from baseline samples is especially problematic. Even when present in a population, they may well be absent from the baseline sample. The Bayesian proposal for stock-mixture analysis will shrink the observed baseline HAG RFs of individual stocks toward better-established grand, regional, or group means in order to control HAG RF estimation error.

All past approaches—CML, UML, or ULS—produce estimates of stock proportions that become increasingly biased as the true stock-mixture proportions become more uneven (Pella and Milner, 1987; Xu et al., 1994). Contributions from abundant stocks are underestimated and those from less common or even absent stocks are overestimated. No effective general solution for this bias has been proposed. The Bayesian proposal results in a probability distribution for the stock composition estimates, the location of which can be characterized by various measures, such as the mean, median, and mode, which differ in their bias when viewed as potential point estimators.

Finally, the previous estimation methods appear limited in capacity to attack practical problems that fail to fit the standard mold of a sampled stock mixture and complete baseline. In particular, missing information for entire stocks from the baseline is very difficult to accommodate (Smouse et al., 1990). Despite their availability for a decade or more, nothing has been accomplished using these methods to incorporate genetic similarities of baseline stocks to deal more realistically with missing data. The Bayesian proposal will initially fill in missing baseline HAG RFs with appropriate grand, regional, or group means, proxies that are revised later during analysis of the stock-mixture sample.

Bayes methods have the potential to correct for these shortcomings better than the likelihood or least squares methods. In our study we describe the rationale for this new approach to stock-mixture analysis, develop the statistical models, and outline the numerical algorithms by which to quantify uncertainty in stock proportions of the mixture as well as in the baseline HAG RFs in the separate contributing stocks. Software developed for performing the computations and summarizing results is available at our anonymous ftp site, with address *ftp://wwwabl.afsc.noaa.gov/sida/mixture-analysis/bayes*. Two applications with special difficulties are used as illustrations. First, a winter stock mixture thought to be composed of four Northwest Atlantic harbor porpoise (*Phocoena phocoena*) populations is assessed. These porpoise populations are characterized by mtDNA haplotypes, the number of which exceeds baseline and stock-mixture sample sizes. Second, a Southeast Alaska steelhead trout (*Oncorhynchus mykiss*) stock mixture is resolved to two populations, only one of which could be sampled separately. Allozymes, mi-

crosatellites, and mtDNA were available for independent and confirming assessments of stock-mixture proportions from the two populations.

Methods

The premise of the Bayes method for estimating an unknown quantity, θ, is that some information about θ is available before sampling begins. This information is in the form of a prior probability density, $\pi(\theta)$. After sampling, the new data obtained, $\boldsymbol{Y}$, are used to revise the prior to the posterior probability density for the unknown, $\pi(\theta|\boldsymbol{Y})$. The posterior is obtained by application of Bayes's theorem, which states that the posterior is proportional to the product of the prior and the likelihood of the sample, $\pi(\boldsymbol{Y}|\theta)$, viz.

$$\pi(\boldsymbol{\theta}|\boldsymbol{Y}) = k^{-1}\pi(\boldsymbol{\theta})\pi(\boldsymbol{Y}|\boldsymbol{\theta}), \quad (1)$$

where $k = \int_{\theta} \pi(\boldsymbol{\theta})\pi(\boldsymbol{Y}|\boldsymbol{\theta})d\boldsymbol{\theta}$.

Once the posterior for θ is known, a variety of point estimates—mode, median, or mean—as well as the Bayesian posterior probability interval (the apparent counterpart of frequentist confidence intervals, but which actually is a direct probability statement about the unknown) for θ can be derived from it. In stock-mixture analysis, the unknowns separate into two evident blocks [$\theta = (\boldsymbol{p},\boldsymbol{Q})$]: 1) the stock proportions of the mixture, $\boldsymbol{p}$; and 2) the parameters, $\boldsymbol{Q}$, needed to determine the genetic composition—stock-mixture haplotype or multilocus genotype RFs—of the baseline stocks. For haploids, $\boldsymbol{Q}$ represents the baseline haplotype RFs. For diploids, $\boldsymbol{Q}$ represents the array of baseline allele and genotype RFs that are needed under Altham's principle to compute the stock-mixture genotype RFs in the baseline stocks. The new information comes from the baseline and stock-mixture samples for which the likelihood functions are unchanged from earlier likelihood methods. The stock-mixture sample provides counts of haplotypes or multilocus genotypes, and the baseline samples provide counts from the separate stocks of the haplotypes or alleles and genotypes at the loci comprising the mixture multilocus genotypes.

The standard stock-mixture analysis for complete baseline and stock-mixture samples by Bayes methods will be outlined here, with details given in following sections. Extension to nonstandard applications will be indicated by example. First, a prior for $\theta = (\boldsymbol{p},\boldsymbol{Q})$ is developed, which is a product of block priors for its components, $\boldsymbol{p}$ and $\boldsymbol{Q}$. The prior proposed for $\boldsymbol{p}$, which will be called "uninformative," allows any substantive stock-mixture sample information regarding $\boldsymbol{p}$ to overwhelm that from the prior. The prior for $\boldsymbol{Q}$, used to analyze the stock-mixture sample, is informative and will be derived from the baseline samples to quantify uncertainty in the genotypic composition of the contributing stocks. Second, the standard likelihood function for the haplotype or multilocus genotype counts seen in the stock-mixture sample is described. Third, and last, the data augmentation algorithm, a Gibbs sampler, is used to alternately generate a sequence of samples from the posterior distributions for $\boldsymbol{p}$ and $\boldsymbol{Q}$. The stock identities of the mixture-sample individuals are reassigned at each sampling cycle by using a chance mechanism that reflects their uncertainty. The stock identities simplify greatly the revision of the prior distributions for $\boldsymbol{p}$ and $\boldsymbol{Q}$ to account for the stock-mixture sample information; just as with the baseline samples, counts of mixture individuals and their HAGs by stock are available at each cycle. Assignment of individuals to stock origin contrasts with their fractional allocation by the CML method (Pella and Milner, 1987). These samples from the posterior distributions are used to quantify the final uncertainty in $\boldsymbol{p}$ and $\boldsymbol{Q}$ after observing the stock-mixture sample.

Prior for stock-mixture proportions, $\pi(\boldsymbol{p})$

The prior for $\boldsymbol{p}$ can incorporate information about the stock-mixture composition other than that in the stock-mixture sample if such is available. More commonly, however, such information is either unavailable or else the researcher prefers to let that of the stock-mixture sample dominate, just as it does with the earlier likelihood or least squares methods. Therefore, the prior proposed will be restricted, providing no useful information about the stock-mixture composition. Such an uninformative prior for the stock proportions of a c-stock mixture must be defined over the stock composition simplex,

$$S(\mathbf{p}) = \left\{\mathbf{p}: 0 < p_i < 1, \sum_{i=1}^{c} p_i = 1\right\},$$

and have negligible effect on the posterior distribution. The Dirichlet probability density can accommodate these requirements, and it is natural to use it as a prior with compositional count data both for computational convenience and for its interpretation as additional data. Prior draws of $\boldsymbol{p}$ from the Dirichlet probability density,

$$\pi(\mathbf{p}) = D(\mathbf{p}|\alpha_1,\alpha_2,\ldots,\alpha_c) = \frac{\Gamma\left(\sum_{i=1}^{c}\alpha_i\right)}{\prod_{i=1}^{c}\Gamma(\alpha_i)}\prod_{i=1}^{c} p_i^{\alpha_i - 1}, \quad (2)$$

$$\alpha_i > 0, i = 1,\ldots,c,$$

have means, variances, and covariances given by

$$E(p_i) = \alpha_i / \alpha_0,\ \mathrm{var}(p_i) = \alpha_i(\alpha_0 - \alpha_i)/\left(\alpha_0^2(\alpha_0 + 1)\right),$$

$$\mathrm{cov}(p_i, p_k) = -\alpha_i\alpha_k / \left(\alpha_0^2(\alpha_0 + 1)\right), i,k = 1,2,\ldots,c, \text{ and} \quad (3)$$

$$\alpha_0 = \sum_{i=1}^{c}\alpha_i.$$

If a prior draw of $\boldsymbol{p} \sim D(\alpha_1,\alpha_2, \ldots, \alpha_c)$ (the notation "$x \sim f$" means "x is distributed as the probability density or probability function f") was obtained for the stock proportions of a stock mixture, and then a stock-mixture sample of size M was drawn such that the individuals could be correctly identified to stock origin, their counts, $\mathbf{Z}=(z_1,z_2, \ldots, z_c)$, would have a conditional multinomial distribution,

$$\pi(\mathbf{Z} \mid \mathbf{p}, M) = \frac{M!}{z_1! z_2! \cdots z_c!} p_1^{z_1} p_2^{z_2} \cdots p_c^{z_c},$$

or $\mathbf{Z} \mid \boldsymbol{p} \sim Mult(M, \boldsymbol{p})$. The posterior for $\boldsymbol{p}$, given $\boldsymbol{Z}$, would be the Dirichlet (computational convenience), $\mathbf{p} \mid \mathbf{Z} \sim D(z_1 + \alpha_1, \ldots, z_c + \alpha_c)$. Notice that the prior parameters enter the posterior density in parallel with the sample counts and therefore could be viewed as counts obtained before the stock mixture was sampled (additional data) (sec. 3.5, Gelman et al., 1995). In fact, the mixture individuals are identified to stock origin (with unavoidable random error) during each cycle of the data augmentation algorithm later when samples are generated from the posterior. With the stock origins identified at a cycle, the uncertainty in $\boldsymbol{p}$ is described by the Dirichlet posterior with parameters equal to the sums of stock counts and prior parameters $(z_i+\alpha_i)$.

With equal values summing to 1 assigned to its parameters or "prior counts," $\alpha_1 = \alpha_2 = \ldots = \alpha_c = c^{-1}$, the Dirichlet prior meets our initial requirements. Specifically, the density is defined over the stock composition simplex, and the additional data, which is neutral in the sense of favoring equal stock proportions (mean stock proportions are c^{-1}), would be equivalent to adding just a single individual to the stock-mixture sample. Means, variances, and covariances (substitute $z_i + c^{-1}$ for α_i in Eq. 3) of the resulting posterior distribution of $\mathbf{p} \mid \mathbf{Z}$, $D(z_1 + c^{-1}, \ldots, z_c + c^{-1})$, approximate closely with increase of stock-mixture sample size, the observed stock proportions, their estimated variances, and their estimated covariances, respectively, from standard frequentist analysis of the multinomial sample, $\boldsymbol{Z}$. Therefore, given the stock assignments of the mixture individuals, the posterior distribution for $\boldsymbol{p}$ will be a reasonable description of its uncertainty for both Bayesian and frequentist statisticians.

Prior for genetic parameters given baseline samples, $\pi(Q|Y)$

The genetic compositions—haplotype or multilocus genotype RFs—of the separate stocks are determined by their RFs of haplotypes, alleles, or genotypes, $\boldsymbol{Q}$. An estimate of $\boldsymbol{Q}$ from the baseline samples must be used in place of the unknown $\boldsymbol{Q}$ to estimate the stock genetic compositions. When baseline samples are large, the observed and unbiased value of $\boldsymbol{Q}$, together with measures of precision, may be sufficient to anchor the stock-mixture analysis. Commonly, baseline sample sizes are more limited and some tradeoff between bias and precision (sec 1.4.2 of Carlin and Louis, 1996; Bishop et al., 1975) in estimation of $\boldsymbol{Q}$ may well be advisable. The essential idea is to shrink the observed RFs of HAGs for individual stocks toward central values that are more reliably determined and are consistent with the genetic similarity of the stocks. An informative Bayes prior distribution for these unknown genetic parameters underlying the stock-mixture sample can be derived from the baseline samples and would provide for such shrinkage. The statistical modeling begins with the allele RFs at a single locus but applies equally to haplotypes, alleles, or genotypes. Later, the modeling is extended to cover multiple loci.

The Bayesian scenario begins with an imaginary experiment in which the RFs of the T distinct alleles for a single locus are drawn for each of the c baseline stocks (sec. 3.7 of Lange, 1997). Denote the resulting unobserved RFs for the ith stock by $\boldsymbol{q}_i=(q_{i1}, q_{i2},\ldots, q_{iT})$. The draws from the stocks are independent and from a common Dirichlet probability density, which is the Bayes prior for baseline sampling, $\pi(\boldsymbol{q}_i) = D(\beta_1,\beta_2, \ldots, \beta_T)$. The justification for the Dirichlet prior for baseline sampling parallels that for the earlier stock-mixture composition prior, $\pi(\boldsymbol{p})$, that is, computational convenience and its simple interpretation as additional data. Next, baseline samples of $n_1,n_2,\ldots,n_c$ alleles of the locus are available from the c stocks. The counts of the different alleles—$\boldsymbol{y}_i=(y_{i1},y_{i2}, \ldots, y_{iT})$ for the ith stock—have the multinomial distribution, $Mult(n_i, \boldsymbol{q}_i)$, and therefore the baseline posterior for the unknown allele RFs in each stock is also a Dirichlet distribution, $\boldsymbol{q}_i \mid \boldsymbol{y}_i \sim D(\beta_1+y_{i1},\beta_2+y_{i2}, \ldots, \beta_T+y_{iT})$. The posterior mean of $\boldsymbol{q}_i \mid \boldsymbol{y}_i$ can be written as a weighted average of the observed and prior mean RFs (Bishop et al., 1975; Sutherland et al., 1975),

$$E(q_{it} \mid \beta, \boldsymbol{y}_i) = (y_{it} + \beta_t)/(n_i + \beta_\cdot) = \frac{n_i}{n_i + \beta_\cdot}\left(\frac{y_{it}}{n_i}\right) + \frac{\beta_\cdot}{n_i + \beta_\cdot}\left(\frac{\beta_t}{\beta_\cdot}\right), \qquad t = 1,2,\ldots,T, \qquad (4)$$

where the observed RF is y_{it}/n_i, its prior mean is $\beta_t/\beta_\cdot$, and $\beta_\cdot = \sum \beta_t$. If the baseline sample is missing ($n_i=0$), the posterior mean equals the prior mean. Otherwise, the posterior mean ranges between the observed and prior mean RFs (as a function of $\beta_\cdot \geq 0$). Shrinkage from the usual estimator of $\boldsymbol{q}_i$, the observed allele RFs, toward the prior mean increases with the prior "sample size," $\beta_\cdot$, but so does bias in estimates of the allele RFs. Therefore, the magnitude of the prior parameters should be no larger than necessary to satisfactorily control estimation error.

Although the choice of a Dirichlet baseline prior was partly for convenience, the resulting posterior density has good properties. The posterior mean is a reliable estimator for the unknown allele RFs: it is strongly consistent, becomes unbiased for large baseline sample size, and moderates the extremes of the usual estimates—the observed RFs—among baseline stocks. All posterior means for the allele RFs are positive, so that absence of an allele from a stock's baseline sample implies it is only rare and was missed in sampling rather than it is nonexistent.

The values for the baseline prior parameters, $\beta_1,\beta_2, \ldots, \beta_T$, have been arbitrary. To complete the specification of the baseline posterior, which will serve as the stock-mixture

prior for the allele RFs, their values must be assigned. Two approaches—empirical Bayes and pseudo-Bayes—are considered in which the prior parameters are functions of allele counts in the baseline samples. The empirical Bayes method was previously developed for geneticists to estimate allele RFs (Lange, 1997). In this method, the values assigned to the βs are those which maximize the Bayes prior predictive distribution (Gelman et al., 1995) for the allele counts in the baseline samples. This distribution is the marginal distribution of the allele counts, which results from averaging their multinomial distribution, $Mult(n_i, \boldsymbol{q}_i)$, weighted by the prior probability of $\boldsymbol{q}_i$, $D(\beta_1, \beta_2, \ldots, \beta_T)$. The prior predictive distribution is parameterized by the βs alone, and the optimizing values can be computed from the allele counts (Appndx. 1). Limited experience during this study indicates that, with large baseline samples of a few baseline stocks, or lesser baseline samples for large numbers of baseline stocks, the empirical Bayes method can provide values for the prior parameters, which result in sensible weighting of the observed sample and prior means. Commonly, baseline sampling is more limited, and pragmatism requires a less-demanding alternative method.

The pseudo-Bayes method is based on several practical considerations to determine values for the baseline prior parameters. First, the baseline prior parameters, $\beta_1, \beta_2, \ldots, \beta_T$, have no intrinsic value, other than as tuning parameters by which to perform stock-mixture analysis. Nonetheless, a sound rationale and simple computational formulas for their values are desirable. Second, the prior mean should reflect the similarity of the allele RFs among the baseline stocks. Third, the weights assigned to the prior and observed allele RFs should allow a realistic evaluation of the uncertainty in the genetic composition of the stock, yet not cause misleading bias in the estimated stock composition. Loci with large variation among stocks have more effect on estimated stock composition than those with small variation. Therefore, shrinkage from observed allele RFs toward prior means for loci with large variation should be less than for loci with small variation. If the prior parameter sum, $\beta_\cdot$, is substantially smaller than the baseline sample sizes, the bias will be limited. However, with $\beta_\cdot = 0$, all weight goes to the observed RFs. Then, when a baseline sample misses an allele that is present, sampling error will be underestimated (as it is with bootstrapping under the CML method). Fourth, and last, the weight assigned to the observed RFs for a stock should be positively related to its baseline sample size.

The pseudo-Bayes method of this proposal is original to estimating allele RFs and appears in practice to satisfy the aforementioned criteria. The prior mean will be centered within the observed allele RFs for the stocks of the baseline samples with

$$\beta_t = \tilde{\beta}_\cdot \cdot \bar{y}_t, \quad t = 1,2,\ldots,T,$$

where $\tilde{\beta}_\cdot$ = is an estimate (Appndx. 2) of the value for $\beta_\cdot$ that minimizes the baseline risk, or expected squared-errors between the posterior means at Equation 4 and the unknown allele RFs of all baseline stocks, and

$\bar{y} = \frac{1}{c}\sum_{i=1}^{c}\frac{y_{it}}{n_i}$ = is the baseline center, or unweighted arithmetic mean, of the observed RFs for the t-th allele among stocks.

With this definition for the βs, the prior mean equals the baseline center. The posterior mean for any stock is the weighted average of its observed allele RFs and the baseline center as at Equation 4. Although the central allele RFs for the entire set of baseline stocks anchors the estimation of $\boldsymbol{Q}$ in this description, extensions to accommodate regional or other groupings of stocks could be accomplished as simply by anchoring on regional or group centers.

Complete analysis of the baseline requires repeated and separate application of the empirical Bayes or pseudo-Bayes methods to each locus. Suppose a total of H loci compose the stock-mixture multilocus genotypes. Let the hth locus have J_h alleles with prior parameters $\boldsymbol{\beta_h} = (\beta_{h1}, \beta_{h2}, \ldots, \beta_{hJ_h})$ and allele RFs in the ith stock of $\boldsymbol{q_{ih}} = (q_{ih1}, q_{ih2}, \ldots, q_{ihJ_h})$. If $\boldsymbol{Q_i}$ denotes the ith stock's combined arrays, $\boldsymbol{q_{i1}}, \boldsymbol{q_{i2}}, \ldots, \boldsymbol{q_{iH}}$, then the prior for the allele RFs of the complete baseline, $\boldsymbol{Q}=(\boldsymbol{Q}_1, \boldsymbol{Q}_2, \ldots, \boldsymbol{Q}_c)$, will be

$$\pi(\mathbf{Q}) = \prod_{i=1}^{c}\pi(\mathbf{Q}_i) = \prod_{i=1}^{c}\prod_{h=1}^{H}\pi(\mathbf{q}_{ih}) = \left(\prod_{h=1}^{H} D(\beta_{h1}, \beta_{h2}, \ldots, \beta_{hJ_h})\right)^{c},$$

that is, prior draws for allele RFs are independent among stocks and loci.

The baseline samples are drawn independently from the stocks. Denote by $\boldsymbol{Y_i} = (\boldsymbol{y_{i1}}, \boldsymbol{y_{i2}}, \ldots, \boldsymbol{y_{iH}})$ the H arrays of allele counts in the baseline sample for the ith stock, and by $\boldsymbol{Y}$, the entire baseline collection of $\boldsymbol{Y_1}, \boldsymbol{Y_2}, \ldots, \boldsymbol{Y_c}$. Then the Bayesian posterior density for the allele RFs of the entire baseline is the product of Dirichlet densities,

$$\pi(\boldsymbol{Q} \mid \boldsymbol{Y}) = \prod_{i=1}^{c}\pi(\boldsymbol{Q}_i \mid \boldsymbol{Y}_i) = \prod_{i=1}^{c}\prod_{h=1}^{H}\pi(\boldsymbol{q}_{ih} \mid \boldsymbol{y}_{ih}) = \prod_{i=1}^{c}\prod_{h=1}^{H} D(\beta_{h1} + y_{ih1}, \ldots, \beta_{hJ_h} + y_{ihJ_h}), \quad (5)$$

and each density in the product has a mean vector, for the stock and locus, equal to a weighted average of the observed allele RFs and corresponding prior means (as at Eq. 4). Although the statistical modeling of the baseline samples has been described with alleles and loci, it applies equally to any combination of independent components: alleles at loci, haplotypes at mtDNA, and genotypes at loci in Hardy-Weinberg disequilibrium.

Stock-mixture sample likelihood function for unknowns, $g(\boldsymbol{X}|\boldsymbol{\theta})$

The stock-mixture sample likelihood function is proportional to the probability of drawing the observed stock-mixture genotypes as a function of the unknowns, $\boldsymbol{p}$ and

$\boldsymbol{Q}$. Denote the count of the jth allele of the hth locus for the mth mixture individual by x_{mhj}. Let the collection of such counts, $\boldsymbol{X}_m$, denote the multilocus genotype of the mth individual, and let the array $\boldsymbol{X}$ denote the collection of such arrays for the M individuals composing the stock-mixture sample. Further, let the RF of individuals with the genotype $\boldsymbol{X}_m$ in the ith stock, which depends on that stock's allele RFs, $\boldsymbol{Q}_i$, be denoted as $f(\boldsymbol{X}_m \mid \boldsymbol{Q}_i)$. The RF of the genotype in the stock mixture is the weighted sum, $\sum p_i f(\boldsymbol{X}_m \mid \boldsymbol{Q}_i)$, and so the likelihood function for the stock-mixture sample is

$$g(\boldsymbol{X} \mid \mathbf{p}, \mathbf{Q}) = \prod_{m=1}^{M} \left(\sum_{i=1}^{c} p_i f(\mathbf{X}_m \mid \mathbf{Q}_i) \right). \quad (6)$$

In the Bayesian view, $\boldsymbol{X}$ is fixed and $g(\boldsymbol{X} \mid \boldsymbol{p}, \boldsymbol{Q})$ is a random function of the unknowns, $\boldsymbol{p}$ and $\boldsymbol{Q}$. Again, although the likelihood function for the stock-mixture genotypes has been described with alleles and loci, it applies equally to stock-mixture genotypes of any combination of independent components: alleles at loci, haplotypes at mtDNA, and genotypes at loci in Hardy-Weinberg disequilibrium.

Posterior distribution of the unknowns, $\pi(\theta \mid \boldsymbol{X}, \boldsymbol{Y})$

The Bayesian assessment of the unknown stock proportions in the stock mixture and of the baseline RFs of haplotypes, alleles, or genotypes is provided by their joint posterior distribution. This posterior distribution is proportional to the product of the prior density for the unknowns and the likelihood function of the stock-mixture sample, given the unknowns. The prior density for the stock-mixture proportions is the uninformative Dirichlet of Equation 2. The baseline posterior at Equation 5 becomes the stock-mixture prior for the HAG RFs. Prior information on stock-mixture composition and the HAG RFs is reasonably considered independent, so the joint prior for the unknowns is the product (Eqs. 2 and 5),

$$\pi(\mathbf{p}, \mathbf{Q}) = \pi(\mathbf{p}) \pi(\mathbf{Q} \mid \mathbf{Y}). \quad (7)$$

The posterior distribution for $\boldsymbol{p}$ and $\boldsymbol{Q}$ with the stock-mixture sample observed, $\pi(\boldsymbol{p}, \boldsymbol{Q} \mid \boldsymbol{X}, \boldsymbol{Y})$, is proportional to the product of their likelihood at Equation 6 and their prior at Equation 7. Analytic evaluation of the posterior distribution is impractical because of the prodigious computation required, caused by the combinatorial explosion of terms in the likelihood function with increase in stock-mixture sample size (Bernardo and Girón, 1988). Instead, a sufficient number of samples are drawn sequentially from the posterior distribution to accurately describe it. The data augmentation algorithm (Tanner and Wong, 1987; Diebolt and Robert, 1994) can be used to draw the sequence of samples. The idea underlying the algorithm is that the estimation problem would be much simplified if the stock identities of the mixture individuals were known. Given the stock identities, the posterior distribution for the stock proportions and HAG RFs in the baseline stocks simply requires updating of the Dirichlet priors with multinomial counts from the stock mixture.

The stock identities of the mixture individuals are determined by chance in the data augmentation algorithm. Let $\boldsymbol{z}_m = (z_{m1}, z_{m2}, \ldots, z_{mc})$ indicate the stock origin of the mth mixture individual by a single "1" at the coordinate of the contributing stock, and $c-1$ "0"s at the remaining coordinates. For later reference, let $\boldsymbol{Z} = (\boldsymbol{z}_1, \boldsymbol{z}_2, \ldots, \boldsymbol{z}_M)$ denote the stock origins of all the mixture individuals. If $\boldsymbol{p}$ and $\boldsymbol{Q}$ were known, the proportion of mixture individuals with genotype $\boldsymbol{X}_m$ that came from the ith stock could be calculated as

$$w_{mi} = p_i f(\boldsymbol{X}_m \mid \boldsymbol{Q}_i) / \sum_{k=1}^{c} p_k f(\boldsymbol{X}_m \mid \boldsymbol{Q}_k), \qquad i = 1,2,\ldots c. \quad (8)$$

Equivalently, the probability that a randomly drawn mixture individual with genotype $\boldsymbol{X}_m$ came from the ith stock is w_{mi} of Equation 8. The data augmentation algorithm draws the missing stock identity, $\boldsymbol{z}_m$, for each mixture individual from the multinomial distribution, $\boldsymbol{z}_m \sim Mult(1, \boldsymbol{w}_m)$, where the probabilities for the stocks listed by $\boldsymbol{w}_m = (w_{m1}, w_{m2}, \ldots, w_{mc})$ are computed from the current samples of $\boldsymbol{p}$ and $\boldsymbol{Q}$. Colloquially, the stock identity of each stock-mixture individual is randomly assigned with the probability for any stock equal to the stock-mixture fraction of the genotype contributed by the stock.

In broad outline, the data augmentation algorithm used to draw posterior samples is straightforward. After the initial sample is obtained (as described later), a sequence of samples is drawn with each sample dependent only on the preceding sample, that is, the algorithm is a Markov chain Monte Carlo (MCMC) method. At the kth sample, two steps are performed:

1 Draw stock identities of the mixture individuals, $\boldsymbol{z}_m^{(k)} \sim \text{Mult}(1, \boldsymbol{w}_m^{(k)})$, using Equation 8 for genotype $\boldsymbol{X}_m$ and the current values $\boldsymbol{p} = \boldsymbol{p}^{(k)}$ and $\boldsymbol{Q} = \boldsymbol{Q}^{(k)}$, $m = 1,2, \ldots, M$.
2 Draw $\boldsymbol{p}^{(k+1)}$ and $\boldsymbol{Q}^{(k+1)}$ from their respective posterior densities, $\pi(\boldsymbol{p} \mid \boldsymbol{X}, \boldsymbol{Y}, \boldsymbol{Z}^{(k)})$, and $\pi(\boldsymbol{Q} \mid \boldsymbol{X}, \boldsymbol{Y}, \boldsymbol{Z}^{(k)})$.

The stock identities, $\boldsymbol{Z}^{(k)}$, of the stock-mixture sample are sufficient statistics for $\boldsymbol{p}$ (Pella et al., 1996). With them available, the genetic data of the stock-mixture sample is of no value to estimation of $\boldsymbol{p}$. Therefore, the posterior for $\boldsymbol{p}$ is obtained by updating the Dirichlet prior for $\boldsymbol{p}$ with the counts of stock identities for the mixture individuals,

$$\pi(\boldsymbol{p} \mid \boldsymbol{X}, \boldsymbol{Y}, \boldsymbol{Z}^{(k)}) = \pi(\boldsymbol{p} \mid \boldsymbol{Z}^{(k)}) = D\left(\frac{1}{c} + \sum_{m=1}^{M} z_{m1}^{(k)}, \frac{1}{c} + \sum_{m=1}^{M} z_{m2}^{(k)}, \ldots, \frac{1}{c} + \sum_{m=1}^{M} z_{mc}^{(k)} \right). \quad (9)$$

The posterior density for HAG RFs of the genetic components, $\pi(\boldsymbol{Q} \mid \boldsymbol{X}, \boldsymbol{Y}, \boldsymbol{Z}^{(k)})$, updates the stock-mixture prior, or baseline posterior, $\pi(\boldsymbol{Q} \mid \boldsymbol{Y})$, at Equation 5 for the HAG counts from the identified mixture individuals as

$$\pi(\mathbf{Q}_i \mid \mathbf{X}, \mathbf{Y}, \mathbf{Z}^{(k)}) = \prod_{h=1}^{H} \pi(\mathbf{q}_{ih} \mid \mathbf{X}, \mathbf{y}_{ih}, \mathbf{Z}^{(k)}) = \quad (10)$$

$$\prod_{h=1}^{H} D\left(\begin{array}{c}\beta_{h1}+y_{ih1}+\sum_{m=1}^{M}(z_{mi}^{(k)}x_{mh1}),\ldots,\beta_{hJ_h}+y_{ihJ_h}+\\ \sum_{m=1}^{M}(z_{mi}^{(k)}x_{mhJ_h})\end{array}\right), \quad (10)\ \text{(cont.)}$$

$$i=1,2,\ldots,c.$$

Notice that each of the updated Dirichlet parameters for the HAG RF in the ith stock equals the sum of the prior parameter, the HAG count in the baseline sample, and the HAG count for the mixture individuals identified to the stock.

The data augmentation algorithm cycles the two steps and eventually outputs a sequence, or chain, of samples of stock proportions and baseline genetic parameters from the posterior Bayes distribution. However, the early samples of a chain are influenced by the starting values of $\boldsymbol{p}$ and $\boldsymbol{Q}$. To make valid inferences, early burn-in samples must be discarded and a sufficient number of subsequent samples must be generated to accurately describe the posterior. Statistics to determine the number of samples to generate per chain—the Raftery and Lewis (1996) convergence diagnostic—or to monitor convergence of multiple chains to the desired posterior density—the Gelman and Rubin (1992) shrink factor—are widely used in practice and are comparatively inexpensive to compute. Although these two statistics are used in the applications that follow, MCMC research is currently very active (e.g. Brooks and Roberts, 1999), and alternatives may prove to be superior for these purposes. Main interest is usually in the stock composition of a stock mixture and so in the later applications the statistics have been applied only to samples of $\boldsymbol{p}$ even though they can be applied to samples of $\boldsymbol{Q}$ as well. However, convergence of samples for $\boldsymbol{p}$ without corresponding convergence for $\boldsymbol{Q}$ is not thought to be possible.

The diagnostic outlined by Raftery and Lewis (1996) determines the number of samples required for estimating quantiles (q) of posterior distributions with a specified accuracy (r) and probability (s). The FORTRAN implementation of the diagnostic, called GIBBSIT,[1] is applied in later examples (with q=0.975, r=0.02, and s=0.95) to each of several chains of stock proportions generated from different starting values. The diagnostic first requires that an initial pilot sample be generated for each chain, which is used to compute its recommended number of samples. An additional number of samples are generated to satisfy the maximum recommended. The combined samples—original pilot samples and the additional samples—are used with GIBBSIT as pilot samples to compute recommended sample sizes again. Further samples are generated if the maximum recommended sample size for any stock exceeds the number so far generated. This iterative scheme is applied to the first chain, beginning with a pilot sample size of 235 (the initial number recommended from the chosen values of q, r, and s). The other chains are run the length of the first chain and then analyzed separately by GIBBSIT. If GIBBSIT suggests that any of the chains should be longer than the first chain, then all the chains are run for the largest number of samples recommended for all stocks and all chains.

Gelman and Rubin (1992) recommended running a small number of independent chains with dispersed starting points to reduce the possibility that a chain is accepted as representative of the posterior distribution before convergence has occurred. To monitor convergence of the chains to the posterior density, a univariate statistic, called the shrink factor (Gelman and Rubin, 1992), is computed[2] for each of the stock proportions. One chain per stock is started, with most of the stock mixture initially contributed by that stock. Once chains of samples are generated and length determined from the Raftery and Lewis diagnostic, shrink factors for all stocks are computed to verify that the chains have converged. The shrink factor is computed from the second halves of the chains and compares the variation within a single chain for a given parameter to the total variation among the chains. Estimates of shrink factors close to one indicate convergence, and acceptable values are less than 1.2 (see Kass et al., 1998). Because the shrink factor is computed from the second halves of chains, the first halves of chains are discarded as burn-in samples. The purpose of discarding initial burn-in samples is to remove dependence on the starting values. Samples subsequent to the burn-in samples may be thought of as coming from the desired posterior distribution. Once convergence of chains has been verified, the MCMC samples (after burn-in discard) of stock composition estimates are combined and summarized with various statistics (equivalent to parameters because of the large samples): means, standard deviations, and empirical percentiles (2.5, 50, and 97.5). Baseline haplotype, allele, or genotype RFs can be summarized similarly.

Checking the fit of the stock-mixture model

Current stock-mixture modeling presumes that a stock mixture composed of random genotypes from the contributing stocks occurs and that a simple random sample of the mixture individuals has been drawn. Further, it is assumed that simple random samples of HAGs from all contributing stocks are available by which to estimate, with an appropriate and known genetic model, the stock-mixture genotype RFs in each of the separate stocks. Samples are considered small in relation to the populations sampled, so that the multinomial distribution can be used to describe sampling variation in counts. These assumptions may be plausible in many applications, but violations can also occur. For example, baseline samples of juvenile salmon, drawn before their families have mixed, would have extra-multinomial variation (Waples

[1] FORTRAN program GIBBSIT (version 2.0) can be obtained without cost from the general archive at *http://lib.stat.cmu.edu/*.

[2] Our current FORTRAN program for the diagnostic is a translation of Gelman's S function itsim (free from the Statlib S archive at *http://lib.stat.cmu.edu/*), and its modification (version 0.4) in CODA (Best et al., 1995) (free from the MRC Biostatistics Unit, University of Cambridge, at *http://www.mrc-bsu.cam.ac.uk/bugs/*).

and Teel, 1990), as would stock-mixture samples if the populations segregated (McKinnell et al., 1997). The Bayes method opens the way for checking that the models fit. Lack of fit is indicated if the observed samples are unusual realizations of the Bayes posterior predictive distribution (Gelman et al., 1995). Test statistics should be designed to detect suspected problems in stock-mixture analysis: unrepresentative samples, unsatisfactory priors, presence of extra stocks, etc. In particular, the haplotype, allele, or genotype counts in the actual baseline samples should not be outliers of their corresponding predictive distribution. When violations to the assumptions are detected, the posterior distribution of stock proportions and baseline genetic parameters would be misleading. New samples drawn by improved design, or alternate sampling models, could be needed to make the stock-mixture analysis trustworthy.

Samples are easily drawn from the posterior predictive distribution. The kth predictive baseline sample for the HAG counts in a stock is simply a multinomial sample with size equal to that of the actual sample and with probabilities equal to the HAG RFs in the kth posterior sample. The kth predictive stock-mixture sample is obtained in two steps. First, a multinomial sample of M individuals identified to stock is drawn, with probabilities equal to the stock proportions in the kth posterior sample. Second, the stock-mixture genotype of each individual is generated by sequentially drawing the HAGs of the multiple characters by using the HAG RFs for its stock from the kth posterior sample.

Applications

Two applications are considered next to illustrate use of the Bayesian method. In the first application, large numbers of mtDNA haplotypes are present in the baseline and stock-mixture samples and pose special difficulty in analysis. The fairly common availability of mtDNA data makes this application of general interest. In the second application, only one of two populations in a stock mixture could be sampled separately. The Bayesian solution for the missing baseline samples from the second population should be of special interest to biologists concerned with assessing stock mixtures of anadromous and resident populations in streams (Busby et al., 1996; Michael, 1983), and of general interest for extensions to the standard stock-mixture analysis.

Example 1: mtDNA samples from harbor porpoise (*Phocoena phocoena*) of the northwest Atlantic Ocean (Rosel et al., 1999) Rosel et al. (1999) obtained mtDNA sequence data for samples from four summer breeding populations—Gulf of Maine-Bay of Fundy, Gulf of St. Lawrence, Newfoundland, and West Greenland—of harbor porpoises in the northwest Atlantic and from a wintering group along the mid-Atlantic states. The authors were reasonably certain that the wintering group comprised one or more of the summer populations. Because of special conservation concerns for the Gulf of Maine-Bay of Fundy population, the authors wished to determine if it alone could have been the wintering group. Contingency table analysis of the mtDNA haplotype frequencies indicated only that the Gulf of Maine-Bay of Fundy population was almost surely not alone ($P<0.06$), if at all present. Rosel et al. (1999) used a stock-mixture analysis by the CML method to attempt to delimit the population contributions better with the mtDNA data. Here the Bayesian method is applied to the same data for comparison. Summer sample sizes for each of the populations were between 40 and 80 individuals, and the winter sample size was 41. A total of 67 distinct haplotypes was observed in the summer samples, and the winter sample of 41 individuals included an additional 8 singleton haplotypes previously unseen. Among the total of 253 individuals of all samples, the five most numerous haplotypes were represented by 45 (18%), 42 (17%), 15 (6%), 9 (4%), and 7 (3%) individuals. Most haplotypes were sporadic in samples; the most common counts in the summer and winter samples being 0 and 1. The occurrence of a few fairly common and many scarce haplotypes is characteristic of mtDNA data (Xu et al., 1994) and poses special difficulty in estimation. For example, under the CML method, stock-mixture haplotypes contributed by a particular stock have another apparent source if absent from its baseline sample.

Four chains of samples were generated by data augmentation with both the empirical Bayes and pseudo-Bayes methods for specifying the baseline prior "count" parameters. The total prior "sample size," $\beta_\cdot = \sum_t \beta_t$, computed by the methods was 22 (pseudo-Bayes) and nearly 2000 (empirical Bayes). An initial pilot chain of 235 samples was analyzed by using the FORTRAN implementation of GIBBSIT, which indicated that chains of 2012 samples should be run (given q=0.975, r=0.02, and s=0.95). The four chains were begun with diverse values for population proportions: one chain was begun for each population, with it composing 0.95 of the stock mixture and the other three populations composed equal parts (thirds) of the remainder (0.05). The four chains had mixed sufficiently, or converged, by their second halves so that the Gelman-Rubin shrink factors were less than 1.03 for any one population. The samples from the second halves were pooled to represent 4024 draws from the posterior distribution. Predictive baseline samples were generated from the posterior samples for haplotype RFs, and indicated lack of fit only for the empirical Bayes method (Fig. 1). Therefore, only the posterior distribution from the pseudo-Bayes method will be described further. Parameters for population proportions computed from the posterior sample (Fig. 2) include the mean, mode, median, standard deviations, and equal-tail bounds of posterior intervals (Table 1). Conditional maximum likelihood estimates for the winter sample were computed for comparison, along with bootstrap evaluation of their precision from 1000 resamplings. Corresponding statistics of the bootstrap sample for the CML method are the means, standard errors, and 95% confidence bounds (Table 2). This CML analysis differs from that of Rosel et al. (1999) by using 1) the counts of all individual haplotypes instead of pooling to form subsets with larger counts, and 2) an alternate method for constructing confidence bounds. Rosel et al. (1999) used the

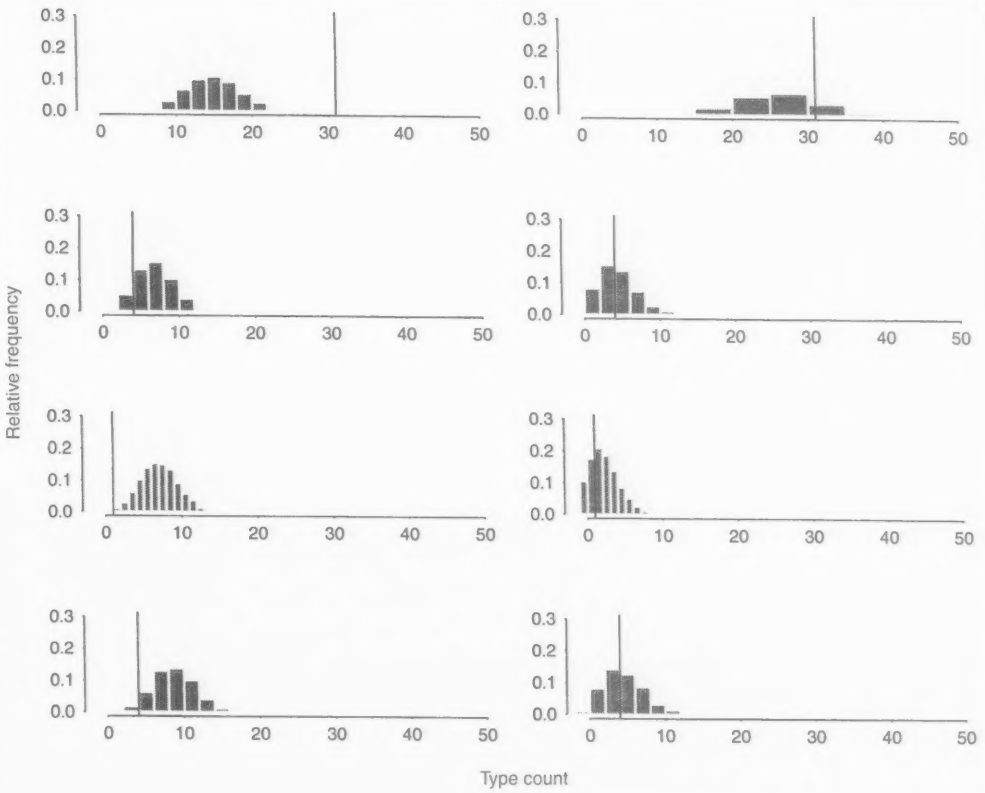

Figure 1

Histograms of predictive baseline population (Gulf of Maine-Bay of Fundy, top; Gulf of St. Lawrence, second; Newfoundland, third; and West Greenland, bottom) sample counts for the most common haplotype in the pooled summer and winter samples, by empirical Bayes (left) and pseudo-Bayes (right) methods. The actual count of the haplotype in each baseline sample is shown as a spike.

Table 1

Parameters of the posterior density for harbor porpoise population proportions composing the winter stock mixture. Reported proportions do not necessarily sum to 1.0 because they are rounded.

				Posterior quantiles		
Population	Mean	Mode[1]	SD	2.5%	Median	97.5%
Gulf of Maine-Bay of Fundy	0.12	0.02	0.13	0.00	0.08	0.46
Gulf of St. Lawrence	0.48	0.69	0.19	0.14	0.48	0.84
Newfoundland	0.15	0.02	0.16	0.00	0.10	0.52
West Greenland	0.24	0.26	0.18	0.00	0.22	0.66

[1] The mode is computed by 4-dimensional binning of the Markov chain Monte Carlo samples for stock proportions, each bin with sides of 0.05, and then normalizing the bin center having maximum count.

percentile interval (Efron and Tibshirani, 1993) for confidence bounds. The alternate method, called the nonsymmetric percentile bootstrap (Lunneborg, 2000), is expected to have superior coverage properties to the standard percentile method for the usual skew distributions of stock-mixture composition estimates. The confidence

Table 2

The conditional maximum likelihood point estimate for harbor porpoise population proportions composing the winter stock mixture, and its bootstrap standard error and 95% confidence bounds (nonsymmetric percentile method). Reported proportions do not necessarily sum to 1.0 because they are rounded.

Population	Point estimate	SE[1]	95% Confidence bounds	
			Lower	Upper
Gulf of Maine-Bay of Fundy	0.19	0.14	0.00	0.37
Gulf of St. Lawrence	0.40	0.16	0.13	0.77
Newfoundland	0.18	0.15	0.00	0.35
West Greenland	0.24	0.15	0.00	0.48

[1] These standard errors are reduced by 30% to 50% from those reported by Rosel et al. (1999). At our earlier recommendation, the authors pooled subsets of haplotypes without a well-grounded basis in order to avoid the small counts of individual haplotypes used here. The point estimate is unchanged, but the confidence intervals differ mainly because a new method was used in their computation.

bounds were computed with an update of the program, SPAM 3.2 (Debevec et al., in press), available on the internet at *http://www.cf.adfg.state.ak.us/geninfo/research/genetics/Software/SpamPage.htm*.

Both the pseudo-Bayes and conditional maximum likelihood methods are in agreement on the population composition of the winter sample in five respects (Tables 1 and 2). First, any of the populations could be involved in the stock mixture and comprise much (upper posterior bounds range from 0.46 to 0.84, and upper confidence bounds, from 0.35 to 0.77) of it. Second, the contributions by any of the populations are very imprecisely determined from the mtDNA counts (widths of all interval estimates exceed 0.35, and standard deviations or standard errors range from 0.13 to 0.19). Third, more than one population seems to be present, given that none of the interval estimates includes 1.0. Fourth, the most frequent estimates, or modes, of the Bayes posterior imply that the mix is almost entirely composed of the Gulf of St. Lawrence and West Greenland populations (Fig. 2). Fifth, and last, the Gulf of St. Lawrence population was almost certainly present (lower 95% posterior bound for the proportion, 0.14; corresponding lower 95% confidence bound, 0.13).

The claim that the Gulf of St. Lawrence population was wintering along the mid-Atlantic coast is important to the conservation issue. Is its presence conspicuous to a direct examination of the genetic samples? The answer is yes if one knows where to look. The Bayes method actually identifies the stock origins of the stock-mixture individuals during generation of each sample from the posterior distribution, and so the posterior identity distribution—the relative frequency of assignment to each population—for each stock-mixture individual is available. The identity distributions of mixture individuals showed 4 of the 33 (12%) winter porpoise were more likely than not (posterior probabilities=0.60, 0.64, 0.67, 0.72) to be from the Gulf of St. Lawrence, and 4 more were more certainly (posterior probabilities=0.87, 0.88, 0.88, and 0.89) from that population. Corresponding probabilities (Eq. 5, Pella and Milner, 1987) from the CML method for the first (0.62, 0.69, 0.70, 0.81) and second groups (1, 1, 1, 1) agreed reasonably. The summer samples contained the following numbers of the same 8 haplotypes: Gulf of Maine-Bay of Fundy, 2 of 80 (3%); Gulf of St. Lawrence, 14 of 40 (35%); Newfoundland, 4 of 42 (10%); and West Greenland, 6 of 50 (12%). Except for the Gulf of St. Lawrence population, in which these haplotypes were fairly common, their observed RFs in the other populations were half or less of that (24%) in the winter sample. With the observed haplotype RFs assumed to be accurate, the probability is less than 0.05 that 8 of 33 individuals with the haplotypes came from any population other than Gulf of St. Lawrence. The conjunction of necessary sampling errors—higher frequencies of the 8 haplotypes in the other populations or lower frequency in the stock mixture—without the presence of Gulf of St. Lawrence is deemed highly improbable from the Bayes computations. Without the posterior probabilities of stock identities, a search for direct evidence of the presence of particular populations in the winter sample would have been futile.

A total of 25 sets of simulated baseline and stock-mixture samples of harbor porpoise mtDNA haplotypes was generated for each of four experiments. Sizes of the simulated samples equaled those of the actual data. The experimental conditions that were controlled include the proportions from the four populations in the stock mixtures and their haplotype RFs. In three of the experiments, the Gulf of St. Lawrence population comprised 0.95 of the stock mixture, and the other stocks comprised equal thirds of the remaining 0.05. In the fourth experiment, the four populations contributed equal parts (0.25) to the stock mixture. The haplotypes of the samples were drawn with replacement from either the original baseline samples (0% addition) or augmented baseline samples for which half (50% addition) or all (100% addition) of the missing haplotypes were replaced by singletons. The conditional maximum likelihood method was applied to each set of simulated samples just as it had to the actual samples. The Bayes method was similarly applied, but with a single exception—a long fixed sequence of 5000 samples (first 2500 discarded as burn-in) was generated for all sets to reduce processing labor. Average point estimates among the 25

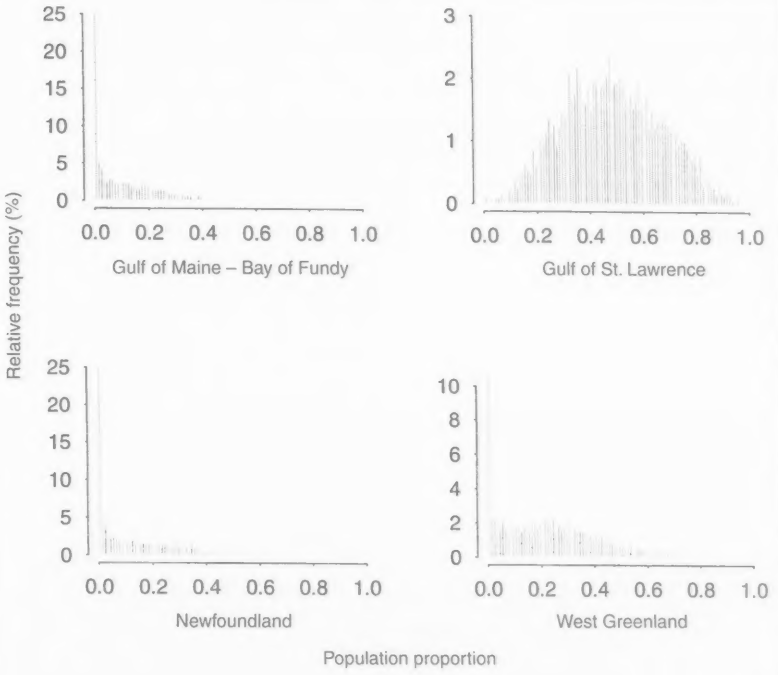

Figure 2

Histograms of samples from the posterior distribution of unknown proportions of summer populations of harbor porpoise (Gulf of Maine-Bay of Fundy, Gulf of St. Lawrence, Newfoundland, and West Greenland) in the wintering group.

sets of samples for each experiment—Bayes mode, Bayes mean, and conditional maximum likelihood (CML) estimate—and their standard errors were computed (Table 3).

The main lesson of these simulations is that the Bayes method, as configured, performs reasonably well in the frequency sense, that is, under repeated sampling. The Bayes posterior mode seems to be a practical point estimator for population proportions in stock mixtures: it was less biased than the Bayes posterior mean and the conditional maximum likelihood estimate when the experimental conditions caused bias. As is characteristic of stock-mixture composition bias, uneven population contributions combined with large variation in estimated contributions were aggravating. When the populations contributed equally (stock mixture 4), bias was negligible for any estimator, given the large variation of estimated population proportions, but with unequal contributions (stock mixtures 1–3), the bias became increasingly severe because the haplotypes were added to the populations and increased the variation in estimated contributions. Lower bias of the Bayes mode was not without cost because its variation among sets of samples was generally larger than that of the Bayes mean or conditional maximum likelihood estimate for the more-difficult third and fourth stock mixtures.

Example 2: Sashin Creek steelhead (*Oncorhynchus mykiss*) stock mixture Sashin Creek on Baranof Island in Southeast Alaska contains a population of anadromous rainbow trout, or steelhead, in its lower portion. In addition, a self-sustaining population above a barrier waterfall was created in 1926 by a transplant from the lower to the upper portion (which includes two lakes). Although the falls was a barrier to upstream migration, migrating juveniles from the upper portion apparently survived the plunge to the lower river. Samples of mature adults returning from the ocean, obtained from the lower portion, were compared with similar samples from the upper population for allozymes (21 loci with 2–6 alleles per locus), microsatellites (10 loci with 3–26 alleles per locus), and mtDNA (5 haplotypes). An excess of homozygotes at loci (Wahlund effect) provided evidence that the samples came from a mixture of both populations. In particular, the allozyme, PGK2, appeared to be fixed (100%) in the upper population, yet the fixed allele represented less than 50% of the PGK2 alleles in the stock-mixture sample from the lower portion. Biologists[3] were able to infer that roughly 25% of the stock mixture probably originated from the upper popula-

[3] Thrower, F. 2000. NMFS, Auke Bay Laboratory, Juneau, AK 99801-8626.

Table 3

Average point estimates—Bayes mode, Bayes mean, and conditional maximum likelihood (CML) estimate—and their standard errors (in parentheses) for 25 simulated samplings of four stock mixtures composed of harbor porpoises from the Gulf of Maine-Bay of Fundy, Gulf of St. Lawrence, Newfoundland, and West Greenland. The haplotypes of stock mixtures were drawn from the original baseline samples (0%) or augmented baseline samples for which half (50%) or all (100%) of the missing haplotypes were replaced by singletons. Baseline and stock-mixture sample sizes were those reported by Rosel et al. (1999) and analyzed earlier in this section. Reported proportions do not necessarily sum to 1.0 because they are rounded.

Stock mixture and estimator	Gulf of Maine-Bay of Fundy	Gulf of St. Lawrence	Newfoundland	West Greenland
Stock mixture 1: 0%	0.95	0.01666	0.01666	0.01666
Bayes mode	0.91 (0.07)	0.03 (0.02)	0.02 (0.00)	0.04 (0.07)
Bayes mean	0.76 (0.17)	0.07 (0.11)	0.09 (0.12)	0.08 (0.12)
CML mean	0.82 (0.09)	0.04 (0.06)	0.07 (0.08)	0.06 (0.08)
Stock mixture 2: 50%	0.95	0.01666	0.01666	0.01666
Bayes mode	0.85 (0.15)	0.04 (0.07)	0.07 (0.11)	0.04 (0.07)
Bayes mean	0.71 (0.20)	0.09 (0.13)	0.11 (0.13)	0.09 (0.13)
CML mean	0.68 (0.13)	0.09 (0.10)	0.14 (0.09)	0.10 (0.09)
Stock mixture 3: 100%	0.95	0.01666	0.01666	0.01666
Bayes mode	0.72 (0.30)	0.08 (0.19)	0.04 (0.06)	0.16 (0.27)
Bayes mean	0.59 (0.24)	0.12 (0.17)	0.12 (0.16)	0.17 (0.20)
CML mean	0.56 (0.13)	0.12 (0.13)	0.13 (0.11)	0.19 (0.14)
Stock mixture 4: 0%	0.25	0.25	0.25	0.25
Bayes mode	0.25 (0.26)	0.18 (0.29)	0.21 (0.22)	0.36 (0.34)
Bayes mean	0.27 (0.22)	0.23 (0.22)	0.24 (0.21)	0.26 (0.23)
CML mean	0.30 (0.14)	0.21 (0.14)	0.24 (0.13)	0.25 (0.15)

tion. Their method depended on the fixed condition of the locus in the upriver population: removal of about 25% of such mixture individuals resulted in the remainder meeting Hardy-Weinberg equilibrium. This approach was difficult to generalize to the other loci, most of which were highly variable. Further, the approach could not provide a complete description of the genetic composition of the lower-river population. To use the information better, all loci available for each type of genetic data were analyzed to provide a Bayes posterior distribution of the population proportions and their allele (allozymes and microsatellites) or haplotype RFs (mtDNA). Each type of genetic data was treated separately in order to examine the consistency of population composition estimates from independent data.

The stock-mixture prior distributions for the baseline characters required some change to accommodate the single-population baseline. As is routine, loci were assumed to have been inherited independently, and their alleles were in Hardy-Weinberg equilibrium for either population. However, the baseline prior parameters (βs) for each genetic character of the upstream population were uninformative: their sum, the baseline prior "sample size," equaled just 1, and each equaled the inverse of the number (J_h) of HAGs. (empirical Bayes or pseudo-Bayes methods for computing the prior parameters were not applicable with a single baseline population.) With the baseline sample counts for locus h denoted as $\mathbf{y_h} = (y_{h1}, \ldots, y_{hJh})'$, the stock-mixture prior (or baseline posterior) of HAG RFs for the upstream population was

$$\pi(\mathbf{Q}_{up} \mid \mathbf{Y}_{up}) = \prod_{h=1}^{H} D(y_{h1} + J_h^{-1}, \ldots, y_{hJ_h} + J_h^{-1}).$$

Notice that the stock-mixture prior "sample size" was the unit-augmented actual sample size, n_h+1, where $n_h=\sum y_{hj}$.

The corresponding downstream population stock-mixture prior reflected the even greater uncertainty in that population's characteristics by a downstream stock-mixture prior "sample size" equal to only 1, yet with average HAG RFs closely approximating those from the counts, $\mathbf{x_h} = (x_{h1}, \ldots, x_{hJh})'$, seen in the stock-mixture sample, viz.

$$\pi(\mathbf{Q}_{down} \mid \mathbf{X}) = \prod_{h=1}^{H} D\left(\frac{x_{h1} + J_h^{-1}}{\sum_j x_{hj} + 1}, \ldots, \frac{x_{hJ_h} + J_h^{-1}}{\sum_j x_{hj} + 1}\right).$$

The prior for population proportions, $\pi(\boldsymbol{p})$, was the standard Dirichlet, $D(0.5,0.5)$. Three chains were generated, beginning from diverse upriver population proportions of 0.95, 0.50, and 0.05 (Fig. 3). The chain lengths for allozymes and microsatellites were 10,000 samples with the first 5000 discarded as burn-in. The posterior sample comprised the 15,000 samples from their second halves. The chain lengths for mtDNA were 100,000 samples and the posterior sample comprised the 150,000 samples from their second halves.

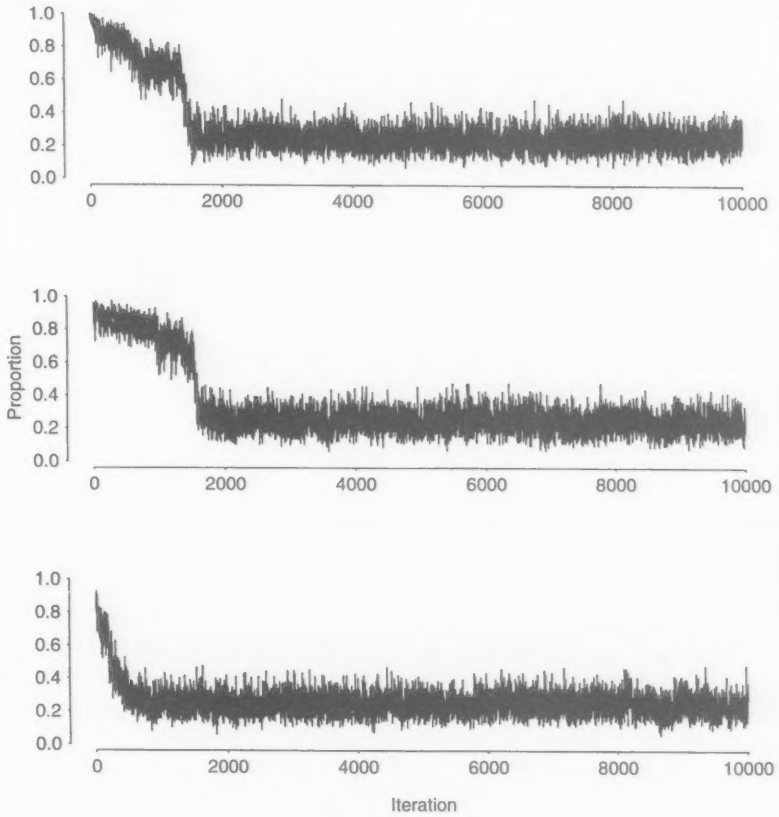

Figure 3

The three chains of posterior samples for the unknown proportion from the upper Sashin Creek steelhead population present in the lower Sashin Creek stock mixture, based on microsatellite data. Each chain was initiated with a different value for the unknown upper proportion, 0.95, 0.50, and 0.05. All chains tracked to high proportions during the early phase and later stabilized at the equilibrium posterior distribution.

Table 4

Parameters of the marginal posterior density for the upriver steelhead proportion in the lower-river stock mixture.

				Posterior quantiles		
Data	Mean	Mode	SD	2.5%	Median	97.5%
Allozymes	0.25	0.22	0.07	0.12	0.24	0.40
Microsatellites	0.24	0.22	0.06	0.13	0.24	0.37
MtDNA	0.41	0.00	0.19	0.01	0.46	0.70

The posterior marginal distributions of the upriver proportion from allozymes and microsatellites were nearly identical and their modes (0.22) or means (0.24, 0.25) were supportive of the earlier approximate assessment of 0.25 (Table 4). Either data set points with high probability (0.95) to an upriver population presence between 0.1 and 0.4 of the lower-river stock mixture. The mtDNA was not nearly as informative in regard to population composition, judging from the

resulting posterior marginal distribution. Its standard deviation roughly equaled threefold, and its posterior interval length, twofold, that from allozymes or microsatellites.

Discussion

Analysts, accustomed to using likelihood or least squares methods for stock-mixture problems, should not be deterred by the novelty of the proposed Bayes method. Instead, the Bayesian implementation should be seen as eminently practical and sensible. The data augmentation algorithm recognizes each mixture individual as an entity and labels it with a stock origin. Given the stock assignments, the observed stock proportions are obvious estimates of the stock composition. In concurrence, the means, variances, and covariances of the Bayes posterior distribution for stock proportions approximate closely the observed stock proportions, their estimated variances, and their estimated covariances, respectively, from frequentist methods. Given the current stock proportions and genetic parameters of an MCMC chain, the random labeling accurately reflects the uncertainty in stock origins. Each mixture individual is assigned to one of the baseline stocks, by using probabilities of stocks proportional to each stock's contribution of its genotype to the mixture. Stock proportions and genetic parameters of the MCMC chain gravitate toward their true values because draws from the posterior, which integrates the baseline and stock-mixture information, are more probable nearby.

One goal in developing a Bayesian method of stock-mixture analysis was to replace the conditional maximum likelihood assumption of ignorable baseline sampling error by modeling that acknowledged the uncertainty in genetic composition of the baseline stocks. Ignorable baseline sampling error is especially unrealistic in applications for which uncommon genotypes are present. Stock-mixture individuals, particularly those with uncommon genotypes, may be contributed by stocks whose baseline samples imply their absence. Current bootstrap resampling of the baseline samples does not accommodate reasonably this mismatch between stock-mixture presence and apparent absence of a genotype in a baseline stock. The individual is presumed to come from a stock different from that of the contributor. Such mismatches become frequent when many rare and uncommon genotypes occur, such as in mtDNA data. The simulations for harbor porpoise showed that as greater numbers of rare haplotypes occurred in the populations, the bias of the CML estimator became severe. When none of the baseline samples can explain presence of a stock-mixture genotype, the CML assumption leaves only an outside source. Data sets generated during bootstrap resampling can require an apparent outside source even when the original samples did not. Pooling of uncommon types to circumvent their effects on estimation should be preceded by careful study to assure information useful to stock-mixture composition is not lost.

Some potential to improve stock-mixture assessment by Bayesian methods arises from the prior for $\theta=(\boldsymbol{p},\mathbf{Q})$, which has no counterpart in the likelihood approach. The Bayes proposal for stock-mixture analysis emulates the objectivity of likelihood methods by letting stock-mixture sample information dominate that of the neutral low-information prior for stock proportions. If information about $\boldsymbol{p}$ is truly unavailable, or the researcher prefers to withhold it and let the "data do the talking," the neutral low-information prior will be adequate. However, the resulting composition estimates may be so imprecise as to be of limited practical value. If additional information is available, either customizing the prior to include it, or updating the posterior (it becomes the prior) with the additional information may improve precision. As an example of updating, the three independent data sets for Sashin Creek steelhead trout could be integrated sequentially into a single posterior for population proportions.

In attempting to maintain objectivity for description of the uncertainty in genotypic composition of the separate stocks, the empirical Bayes method for specifying the baseline prior parameters was examined. The empirical Bayes method for choosing prior parameters for the haplotype, allele, or genotype RFs provided excessive weight to the prior mean for harbor porpoise, with the prior "sample size" parameter, $\beta_\cdot$, for harbor porpoise of nearly 2000, many-fold the total of actual sample sizes. In addition, the empirical Bayes method consistently weighted prior means heavily on several applications examined and not reported. Information in these typical baseline samples is evidently inadequate for estimation of the prior parameters. A full Bayesian analysis, which views them as random variables (sec. 5.3 of Gelman et al., 1995), would require an informative prior for them. Because such an informative prior was not evident, the pseudo-Bayes approach (Bishop et al., 1975) was adopted.

Under the pseudo-Bayes approach, the posterior mean for HAG RFs of stocks interpolates between observed values for individual stocks and a baseline central value for all stocks, with the shrinkage, or weighting, determined by the values of the baseline prior parameters. The best choice for values of the prior parameters remains an open question. Possibly, the prior parameter values could be chosen for their performance in experiments of simulated stock-mixture analyses. However, the computations involved would be extensive and without guarantee beforehand of a clear solution. This proposal included an objective criterion—minimum squared-error risk of baseline allele RFs—by which to determine weighting between the prior and observed HAG RFs from the baseline samples alone. Researchers who find choice of weighting a deterrent to application of the Bayes method can set the baseline prior parameters to zero with the qualification that variation of stock proportions may be understated as with the CML method. In return, the Bayes algorithm easily includes the information in the stock-mixture and baseline samples in assessing stock proportions. The simulations for harbor porpoise showed that the weighting from the pseudo-Bayes method resulted in good frequency performance.

In many practical applications, fisheries managers require a point estimate of stock composition. The well-known bias of the conditional maximum likelihood estimate has been troublesome for this reason. Any corrections for its bias have referred estimated stock proportions to simple one-dimensional graphical relationships between simulation averages and known stock proportions. The

simulations for harbor porpoise showed that the Bayesian posterior mode had considerably less bias in situations for which the CML estimate was severely biased. The mode has intuitive appeal as the most frequent estimate from the posterior. Its promise for situations requiring point estimates needs to be explored by simulation in further applications. In addition, computation of the multidimensional mode requires some smoothing of the posterior samples, such as the binning used here (see footnote, Table 1). Stock grouping, followed by summing of individual stock proportions for group totals, may also be necessary because finding posterior modes becomes more problematic with large numbers of stocks.

The Dirichlet distribution was the basis for probability modeling because it is a natural choice. First, it is defined for random compositions (i.e. arrays with nonnegative elements that sum to one). Second, the posterior for multinomial data can be written in closed form and is also Dirichlet. Third, the prior parameters can be interpreted as additional data. Fourth, and last, it is easy to sample by computer. However, compositional data are also nicely modeled with the logistic normal density (Aitchison, 1986; Billheimer et al., 1998), whose flexibility and relation to normal theory may have advantages in stock-mixture analysis. Use of geographical structure for the stock proportions in complex stock mixtures comprising many stocks is an area for exploration with the logistic normal and Bayesian hierarchical methods.

Acknowledgments

We much appreciated the opportunity to examine the genetic samples of harbor porpoises and steelhead trout. The harbor porpoise samples were made available by Patricia E. Rosel of the National Ocean Service, NOAA, 219 Fort Johnson Road, Charleston, SC 29412, and the steelhead trout samples were made available by Frank Thrower, National Marine Fisheries Service, Auke Bay Laboratory, Juneau, AK 99801-8626. The manuscript was revised after many insightful comments received from colleagues. Our special thanks for their reviews and ideas go to Eric Anderson of the University of Washington, Joel Reynolds of the Alaska Department of Fish and Game, Peter Smouse of Rutgers University, Jim Murphy and Richard Wilmot of the Auke Bay Laboratory, and three anonymous reviewers of the *Fishery Bulletin*.

Literature cited

Aitchison, J.
1986. The statistical analysis of compositional data. Chapman & Hall, New York, NY, 416 p.

Altham, P. M. E.
1984. Improving the precision of estimation by fitting a model. J. Roy. Statist. Soc. B 46:118–119.

Begg, G. A., K. D. Friedland, and J. B. Pearce.
1999. Stock identification-its role in stock assessment and fisheries management: a selection of papers presented at a symposium of the 128th annual meeting of the American Fisheries Society in Hartford, Connecticut, USA, 23–27 August 1998. Fish. Res. 43/1–3, 249 p.

Bernardo, J. M., and F. J. Girón.
1988. A Bayesian analysis of simple mixture problems. *In* Bayesian statistics 3 (J. M. Bernardo, M. H. DeGroot, D. V. Lindley, and A. F. M. Smith, eds.), p. 67–78. Oxford Univ. Press, Oxford.

Best, N. G., M. K. Cowles, and S. K. Vines.
1995. CODA: convergence diagnosis and output analysis software for Gibbs sampling output, version 0.3. MRC Biostatistics Unit, Cambridge, UK, 41 p. + addendum.

Billheimer, D., P. Guttorp, and W. F. Fagan
1998. Statistical analysis and interpretation of discrete compositional data. NRCSE Tech. Rep. 11, Univ. Washington, Seattle, WA, 29 p. + appendix.

Bishop, Y. M. M., S. E. Fienberg, and P. W. Holland.
1975. Discrete multivariate analysis: theory and practice. MIT Press, Cambridge, MA, 557 p.

Bowen, B. W., A. L. Bass, A. Garcia-Rodriguez, C. E. Diez, R. van Dam, A. Bolten, K. A. Bjorndal, M. M. Miyamoto, and R. J. Ferl.
1996. Origin of hawksbill turtles in a Caribbean feeding area as indicated by genetic markers. Ecol. Applications 6:566–572.

Brooks, S. P., and G. Roberts.
1999. On quantile estimation and Markov chain Monte Carlo convergence. Biometrika 86:710–722.

Busby, P. J., T. C. Wainwright, G. J. Bryant, L. J. Lierheimer, R. S. Waples, F. W. Waknitz, and I. V. Lagomarsino.
1996. Status review of west coast steelhead from Washington, Idaho, Oregon, and California. U.S. Dep. Commer., NOAA Tech. Memo. NMFS-NWFSC-27, 261 p.

Carlin, B. P., and T. A. Louis.
1996. Bayes and empirical Bayes methods for data analysis. Chapman & Hall, New York, NY, 399 p.

Debevec, E. M., R. B. Gates, M. Masuda, J. Pella, J. Reynolds, and L. W. Seeb.
In press. SPAM (version 3.2): statistics program for analyzing stock mixtures. J. Heredity.

Diebolt, J., and C. P. Robert.
1994. Estimation of finite stock-mixture distributions through Bayesian sampling. J. Roy. Statist. Soc. B 56:363–375.

Efron, B., and R. J. Tibshirani.
1993. An introduction to the bootstrap. Chapman & Hall, New York, NY, 436 p.

Epifanio, J. M., P. E. Smouse, C. J. Kobak, and B. L. Brown.
1995. Mitochondrial DNA divergence among populations of American shad (*Alosa sapidissima*): how much variation is enough for mixed-stock analysis? Can. J. Fish. Aquat. Sci. 52:1688–1702.

Fournier, D. A., T. D. Beacham, B. E. Riddell, and C. A. Busack.
1984. Estimating stock composition in mixed stock fisheries using morphometric, meristic, and electrophoretic characteristics. Can. J. Fish. Aquat. Sci. 41:400–408.

Gelman, A., and D. B. Rubin.
1992. Inference from iterative simulation using multiple sequences. Stat. Sci. 7:457–511.

Gelman, A., J. Carlin, H. S. Stern, and D. B. Rubin.
1995. Bayesian data analysis. Chapman & Hall, New York, NY, 526 p.

Kass, R.E. (Moderator), B. P. Carlin, A. Gelman, and R. M. Neal (Panelists).
1998. Markov chain Monte Carlo in practice: a roundtable discussion. Am. Statist. 52:93–100.

Lange, K.
1997. Mathematical and statistical methods for genetic analysis. Springer, New York, NY, 265 p.
Leonard, T.
1977. Bayesian simultaneous estimation for several multinomial distributions. Commun. Statist.-Theor. Meth. A6: 619–630.
Lunneborg, C. E.
2000. Data analysis by resampling: concepts and applications. Duxbury Press, Pacific Grove, CA, 568 p. + xvii.
McKinnell, S., J. J. Pella, and M. L. Dahlberg.
1997. Population-specific aggregations of steelhead trout (*Oncorhynchus mykiss*) in the North Pacific Ocean. Can. J. Fish. Aquat. Sci. 54:2368–2376.
Michael, J. H., Jr.
1983. Contribution of cutthroat trout in headwater streams to the sea-run population. Calif. Fish Game 69(2):68–76.
Millar, R. B.
1987. Maximum likelihood estimation of mixed stock fishery composition. Can. J. Fish. Aquat. Sci. 44:583–590.
O'Connell, M., and J. M. Wright.
1997. Microsatellite DNA in fishes. Rev. Fish Biol. Fish. 7:331–363.
Pella, J. J., and G. B. Milner.
1987. Use of genetic marks in stock composition analysis. *In* Population genetics and fisheries management (N. Ryman and F. Utter, eds.), p. 247–276. Univ. Washington Press, Seattle, WA.
Pella, J., M. Masuda, and S. Nelson.
1996. Search algorithms for computing stock composition of a stock-mixture from traits of individuals by maximum likelihood. U.S. Dep. Commer., NOAA Tech. Memo. NMFS-AFSC-61, 68 p.
Raftery, A. E., and S. M. Lewis.
1996. Implementing MCMC. *In* Markov chain Monte Carlo in practice (W. R. Gilks, S. Richardson, and D. J. Spiegelhalter, eds.), p. 115–130. Chapman & Hall, London.
Rosel, P. E., S. C. France, J. Y. Wang, and T. D. Kocher.
1999. Genetic structure of harbor porpoise *Phocoena phocoena* populations in the Northwest Atlantic based on mitochondrial and nuclear markers. Mol. Ecol. 8:S41–S54.
Smouse, P. E., R. S. Waples, and J. A. Tworek.
1990. A genetic stock-mixture analysis for use with incomplete source population data. Can. J. Fish. Aquat. Sci. 47:620–634.
Sutherland, M., P. W. Holland, and S. E. Fienberg.
1975. Combining Bayes and frequency approaches to estimate a multinomial parameter. *In* Studies in Bayesian econometrics and statistics in honor of Leonard J. Savage (S. Fienberg and A. Zellner, eds.), p. 585–617. North-Holland Publishing Company, New York, NY.
Tanner, M. A., and W. Wong.
1987. The calculation of posterior distributions by data augmentation (with discussion). J. Am. Statist. Assoc. 82: 528–550.
Waples, R. S., and D. J. Teel.
1990. Conservation genetics of Pacific salmon. I. Temporal changes in allele frequency. Conserv. Biol. 4:144–156.
Xu, S., C. J. Kobak, and P. E. Smouse.
1994. Constrained least squares estimation of mixed population stock composition from mtDNA haplotype frequency data. Can. J. Fish. Aquat. Sci. 51:417–425.

Appendix 1—The empirical Bayes method for maximum likelihood estimation of the Dirichlet prior parameters from the prior predictive distribution (adapted from Lange, 1997).

If the allele RFs at a locus for the ith stock, $\mathbf{q}_i=(q_{i1}, \ldots, q_{iT})'$, are distributed as the Dirichlet density, $D(\boldsymbol{q}_i \mid \beta_1,\beta_2, \ldots, \beta_T)$, and the allele counts, $\mathbf{y}_i=(y_{i1},\ldots,y_{iT})'$, in a random sample of n_i alleles have the multinomial distribution, $Mult(n_i,\boldsymbol{q}_i)$, then the prior predictive distribution (Gelman et al., 1995) for the allele counts, obtained by integrating the product of the probability distributions, $Mult(n_i,\boldsymbol{q}_i)$ and $D(\boldsymbol{q}_i \mid \beta_1,\beta_2, \ldots,\beta_T)$, over the simplex, $S(\boldsymbol{q}_i)$, is

$$\int_{S(\mathbf{q}_i)} \frac{n_i!}{y_{i1}!\ldots y_{iT}!}\prod_{t=1}^{T} q_{it}^{y_{it}} \frac{\Gamma(\beta_\bullet)}{\prod_{t=1}^{T}\Gamma(\beta_t)} q_{it}^{\beta_t-1} = \frac{n_i!}{y_{i1}!\ldots y_{iT}!}\frac{\Gamma(\beta_\bullet)}{\Gamma(n_i+\beta_\bullet)}\prod_{t=1}^{T}\frac{\Gamma(y_{it}+\beta_t)}{\Gamma(\beta_t)}, \quad (1)$$

where $S(\mathbf{q}_i)=\left\{\mathbf{q}_i: 0<q_{it}<1, \sum_{t=1}^{T} q_{it}=1\right\}$ (Lange, 1997).

Estimation of the β's begins with the logarithm of Equation 1, which can be viewed as the ith component of the loglikelihood or support function for the unknown β's,

$$LogL_i(\beta_1,\ldots,\beta_T) = \log\left(\frac{n_i!}{y_{i1}!\ldots y_{iT}!}\right)+\log\Gamma(\beta_\bullet)-\log\Gamma(n_i+\beta_\bullet)+\sum_{t=1}^{T}\left(\log\Gamma(y_{it}+\beta_t)-\log\Gamma(\beta_t)\right). \quad (2)$$

The total support function for all baseline samples is the sum of the individual support functions at Equation 2,

$$LogL(\beta_1,\ldots,\beta_T)=\sum_{i=1}^{i} LogL_i(\beta_1,\ldots,\beta_T).$$

The score function for β_t, s_t, is the first derivative of the total support function,

$$s_t=\frac{\partial LogL}{\partial\beta_t}=\sum_{i=1}^{i}\frac{\partial LogL_i}{\partial\beta_t} = c\psi(\beta_\bullet)-\sum_{i=1}^{i}\psi(n_i+\beta_\bullet)+\sum_{i=1}^{i}\left(\psi(y_{it}+\beta_t)-\psi(\beta_t)\right), \quad (3)$$

where $\psi(w) = \frac{d}{dw}\log\Gamma(w)$ is the digamma function.

The elements of the information matrix are

$$-\frac{\partial^2 LogL}{\partial\beta_t\partial\beta_u} = -c\psi'(\beta_\bullet) + \sum_{i=1}^{c}\psi'(n_i+\beta_\bullet) - \delta_{tu}\sum_{i=1}^{c}\left(\psi'(y_{it}+\beta_t) - \psi'(\beta_t)\right), \quad (4)$$

where the Kronecker delta is defined as $\delta_{tu}=0$ if $t\neq u$, $\delta_{tu}=1$ if $t=u$, and

$$\psi'(w) = \frac{\delta^2}{\delta^2 w}\log\Gamma(w)$$

is the trigamma function. The observed information matrix, or negative Hessian of the total support function, can be written as

$$\left(-\frac{\partial^2 LogL}{\partial\beta_t\partial\beta_u}\right)_{T\times T} = \mathbf{D} - b\mathbf{1}\mathbf{1}', \quad (5)$$

where $\mathbf{D}$ is a diagonal matrix with main diagonal elements

$$d_{tt} = \sum_{i=1}^{c}\left(\psi'(\beta_t) - \psi'(y_{it}+\beta_t)\right), \qquad t = 1,2,\ldots,T, \quad (6)$$

$\mathbf{1}$ is the unit column vector of T "1"s, and

$$b = c\psi'(\beta_\bullet) - \sum_{i=1}^{c}\psi'(n_i+\beta_\bullet) \text{ is a scalar.} \quad (7)$$

A quasi-Newton search for the maximum likelihood estimate of $\boldsymbol{\beta}=(\beta_1, \beta_2, \ldots\beta_T)'$ is performed. At the kth step

$$\boldsymbol{\beta}^{(k+1)} = \boldsymbol{\beta}^{(k)} + [\mathbf{D}^{(k)} - \tilde{b}^{(k)}\mathbf{1}\mathbf{1}']^{-1}\mathbf{S}^{(k)}, \quad (8)$$

where $\boldsymbol{\beta}^{(k)}$ = the approximation of the maximum likelihood estimate at the kth step,
$\mathbf{D}^{(k)}$ = denotes the matrix $\mathbf{D}$ at Equation 6 when evaluated at $\boldsymbol{\beta}^{(k)}$,
$\tilde{b}^{(k)}$ = denotes the minimum of either the scalar, b, at Equation 7 when evaluated at $\boldsymbol{\beta}^{(k)}$ or the ratio, $(1-\varepsilon)/[\mathbf{1}'(\mathbf{D}^{(k)})^{-1}\mathbf{1}]$ with ε being an arbitrary constant in (0,1), and
$\mathbf{S}^{(k)}$ = the vector of scores at Equation 3 evaluated at $\boldsymbol{\beta}^{(k)}$.

An arbitrary choice for $\boldsymbol{\beta}^{(1)}$ such as the unit column, $\mathbf{1}$, can be used to start the search.

Appendix 2—Minimum squared-error risk estimate of $\beta_\bullet$ with the prior mean fixed (an extension of sec. 12.2.3 of Bishop et al., 1975).

Let the baseline risk criterion be the expected value of the squared distance of any matrix estimator of baseline RFs from the true values,

$$R(\hat{\mathbf{Q}},\mathbf{Q}) = \sum_{i=1}^{c}\sum_{t=1}^{T} n_i E(\hat{q}_{it} - q_{it})^2.$$

Denote the random version of the posterior mean of $\mathbf{q_i}\,|\,\mathbf{y_i}$ by

$$\hat{\mathbf{q}}_\mathbf{i} = \hat{\mathbf{q}}_\mathbf{i}(\beta_\bullet,\lambda) = \frac{n_i}{n_i+\beta_\bullet}\left(\frac{\mathbf{y_i}}{n_i}\right) + \frac{\beta_\bullet}{n_i+\beta_\bullet}\lambda,$$

where $\mathbf{y_i} = (y_{i1}, y_{i2}, \cdots, y_{iT})'$ = the array of sample allele counts from the ith stock,
λ = the baseline center, $\bar{\mathbf{y}}=(\bar{y}_1, \bar{y}_2, \cdots \bar{y}_T)'$,
$\hat{\mathbf{q}}_\mathbf{i} = (\hat{q}_{i1}, \hat{q}_{i2}, \cdots, \hat{q}_{iT})'$ and

$\bar{y}_t = \frac{1}{c}\sum_{i=1}^{c} y_{it}/n_i, t = 1,2,\ldots,T,$ = the arithmetic average of the observed RFs of the tth allele among stocks.

With $\beta_\bullet$ and λ viewed as fixed, the baseline risk is

$$R(\hat{\mathbf{Q}},\mathbf{Q}) = \sum_{i=1}^{c}\left(\frac{n_i}{n_i+\beta_\bullet}\right)^2\left(1-\sum_{t=1}^{T}q_{it}^2\right) + \sum_{i=1}^{c}\left(\frac{\beta_\bullet}{n_i+\beta_\bullet}\right)^2 n_i\sum_{t=1}^{T}(q_{it}-\lambda_t)^2.$$

The value of $\beta_\bullet$ that minimizes the risk is found by setting the derivative of the risk function (with respect to $\beta_\bullet$) equal to zero and solving. The minimizing value of $\beta_\bullet$ must satisfy the following equation:

$$\beta_\bullet = \sum_{i=1}^{c} n_i^2\frac{\left(1-\sum_{t=1}^{T}q_{it}^2\right)}{(n_i+\beta_\bullet)^3}\Bigg/\sum_{i=1}^{c} n_i^2\frac{\sum_{t=1}^{T}(q_{it}-\lambda_t)^2}{(n_i+\beta_\bullet)^3}.$$

The equation includes the unknown RFs, $\boldsymbol{q_i}$, and the observed RFs are substituted for their unknown values for estimation. The equation can be iterated to solve for the optimal $\beta_\bullet$. Beginning with an arbitrary value, $\beta_\bullet=1$, on the right-hand side, the first revised value for optimal $\beta_\bullet$ results on the left-hand side. This new approximation for optimal $\beta_\bullet$ is used on the right-hand side to compute the next revision, and so on to convergence. If the resulting solution for optimal $\beta_\bullet$ is less than 1, setting $\beta_\bullet$ equal to 1 seems to be a practical remedy when numerical problems occur in sampling of HAG RFs from their Dirichlet posterior during MCMC computations.

The potential role of marine reserves in the management of shortraker rockfish (*Sebastes borealis*) and rougheye rockfish (*S. aleutianus*) in the Gulf of Alaska

SungKwon Soh
School of Fisheries, mail stop 357980
University of Washington
Seattle, Washington 98195
Present address: Ministry of Maritime Affairs and Fisheries
139 Chungjong-No 3
Seodaemun-Gu
Seoul, 120-715, Republic of Korea
E-mail address: sksoh@hotmail.com

Donald R. Gunderson
School of Fisheries, mail stop 357980
University of Washington
Seattle, Washington 98195

Daniel H. Ito
Alaska Fisheries Science Center
National Marine Fisheries Service, NOAA
7600 Sand Point Way NE
Seattle, Washington 98115-0070

Abstract–Shortraker and rougheye rockfish (*Sebastes borealis* and *S. aleutianus*) have been an independent management subgroup of the Gulf of Alaska slope rockfish assemblage since 1991. Special concerns are proposed for the management of these species because they are very slow growing, long-lived, and commercially important.

Marine reserves (harvest refugia) have often been proposed as a valuable management tool for mitigating overfishing and maintaining species and habitat diversity. Their effectiveness in fisheries management, however, is poorly understood and concepts regarding their use are largely untested. Our study investigated the potential role of harvest refugia in the management of these two species by using a Geographic Information System (GIS) application to design harvest refugia networks of varying spatial extent. Twenty-year projections employing a population dynamics model were used to compare ending biomass and fishing mortality under the current management system with biomass and fishing mortality under refuge management systems. The results indicate that harvest refugia can be used to greatly reduce discards and serial overfishing of substocks without reducing current catch levels.

Manuscript accepted 24 July 2000.
Fish. Bull. 99:168–179 (2001).

Over 70 species of rockfish (genus *Sebastes*) inhabit the geographic region between the Gulf of California and the Bering Sea, and many of these species are important components in the groundfish fisheries in this region. Rockfish are viviparous, and several species mature slowly (>5–10 years), have long life spans (50–140 years), and are particularly vulnerable to overfishing. Several species off the Pacific coast currently subsist at dangerously low levels (Murray et al., 1999), and it is anticipated that rebuilding these stocks will require long periods of time (several decades in some cases). Many ecologists and fishery managers see marine reserve (or no-take refuge) networks as an attractive supplement to current management systems in the conservation and management of rockfish stocks (Murray et al., 1999). Our study explores the potential use of harvest refugia in the specific case of shortraker (*S. borealis*) and rougheye (*S. aleutianus*) rockfish in the Gulf of Alaska.

We review the current management system for shortraker and rougheye rockfish in the Gulf of Alaska, describe problems confronted under this system, and suggest refuge management as a supplement to the current management regime. The comparison of future biomass and fishing mortality between the current system and the refuge system will be discussed on the bassis of twenty-year projections from a population dynamics model. The potential impacts of harvest refugia on other Gulf of Alaska fisheries will also be discussed.

Current management system

Groundfish in the Gulf of Alaska are currently managed by the North Pacific Fishery Management Council (NPFMC). Scientists on the Gulf of Alaska groundfish plan team compile a Stock Assessment and Fishery Evaluation report every year. This report includes recommended acceptable biological catch (ABC) levels for each stock and stock complex (including the shortraker-rougheye complex) under the Fishery Management Plan. The NPFMC then

Table 1

Gulf-wide discard rates (%) for the four slope rockfish management subgroups in the commercial fishery during 1991–97. Data are from weekly production and observer reports.

Management subgroup	1991	1992	1993	1994	1995	1996	1997
Pacific ocean perch	15.7	21.5	79.2	60.3	19.8	17.2	14.3
Shortraker and rougheye rockfiish	42.0	10.4	26.8	44.8	30.7	22.2	22.0
Northern rockfish	—	—	26.5	17.7	12.7	16.5	27.8
Other slope rockfish	20.0	29.7	48.9	65.6	72.5	75.6	52.1

considers ABC recommendations, social and economic factors, and determines total allowable catches (TACs). Shortraker and rougheye rockfish are considered as a management unit in the setting of TACs.

In fishery management, fishing seasons are imposed to regulate fishing effort based on three catch levels: total allowable catch (TAC), acceptable biological catch (ABC), and overfishing level (OFL). There is an open, directed fishery (with allowances for bycatch) until the catches reach the TAC level. The TAC level is often lower than the ABC but frequently they have been the same for the shortraker-rougheye rockfish subgroup. Once the ABC is reached, these species are prohibited to be caught and must be returned to the sea. Finally, the fishery is closed when it reaches the overfishing level. A directed fishery for shortraker-rougheye rockfish occurred only in 1991 and 1992; the fishery has since been designated as a bycatch-only fishery.

A constant exploitation-rate strategy has been used for the shortraker and rougheye rockfish subgroup. Fishing mortality for determining ABC was set equal to natural mortality (F=M rule), which, like $F_{0.1}$, was generally considered to be conservative (Deriso, 1987). This has been used to determine ABC since 1991, when these stocks were established as an independent management subgroup of the slope rockfish assemblage. The main reason for using this simple management procedure compared with the more sophisticated one used for Pacific ocean perch and other species is a lack of historical catch data and biological information. In 1997, revised definitions of ABC and OFL replaced the Plan Team's previous procedures (NMFS, 1996): ABC is a preliminary description of the acceptable harvest (or range of harvests) for a given stock or stock complex and overfishing is defined as any amount of fishing in excess of a prescribed maximum allowable rate. For rougheye rockfish, fishing mortality rates for OFL and ABC are determined by

$$F_{OFL} = F_{30\%} \text{ and } F_{ABC} \leq F_{40\%},$$

where "$F_{X\%}$" refers to the fishing mortality rate associated with an equilibrium level of spawning per recruit equal to $X\%$ of the equilibrium level of spawning per recruit in the absence of any fishing (Clark, 1991; 1993).

For shortraker rockfish, the equations are $F_{OFL} = M$ and $F_{ABC} \leq 0.75 \times M$ because there is less information for this species.

Fish discards are a serious problem under the current management system because fish are discarded when the catch of a management category attains ABC. Discard rates for the four slope rockfish subgroups in the Gulf of Alaska were estimated as shown in Table 1 (Heifetz et al., 1997). There are two situations which result in discards at sea. One case happens under "bycatch only" status, where theoretically, only a fixed percentage of the haul-by-haul catch can be retained and the rest must be discarded to protect the stocks from a directed fishery. This "retained" catch should be available only when the bycatch status is still open. The other case occurs under prohibited status. If the total harvest exceeds ABC levels, all catch must be discarded.

Shortraker and rougheye rockfish are a slow-growing, long-lived species. Maximum age for rougheye rockfish, for example, is about 140 years (Chilton and Beamish, 1982) and the von Bertalanffy growth parameter, K, for this species is about 0.05. Both shortraker and rougheye rockfish are very large fish; $L_\infty \cong 55$ cm for rougheye rockfish and $L_\infty \cong 72$ cm for shortraker rockfish. McDermott (1994) estimated natural mortality of rougheye and shortraker as 0.030–0.039 and 0.027–0.042, respectively, using the gonadosomatic index method (Gunderson, 1997a). Maturity analysis showed that about 50 percent are mature at 43.87 cm FL (about 20 years) for rougheye rockfish, whereas about 50 percent are mature at 44.90 cm FL for shortraker rockfish (McDermott, 1994).

Rougheye rockfish undertake only limited migrations once they have recruited to the fishing ground (Gunderson, 1997b) and this is generally considered to be true for shortraker rockfish as well. Historical catch locations show specific habitat preferences and a patchy distribution for shortraker and rougheye rockfish in the Gulf of Alaska. Shortraker and rougheye rockfish present in "hot spots" can be readily overexploited by the fishing industry by targeting these spots and harvesting the fish through specialized harvesting skills.

Refuge management

Harvest refugia are areas protected from some or all fishing activities. The general objectives of creating harvest refugia can be discussed with respect to the fish community, fishery practices, and ecological aspects of fish habitat

(Lindeboom, 1995; Bohnsack and Ault, 1996; Allison et al., 1998; Lauck et al., 1998; Yoklavich (ed.), 1998). Conservation of ecological and demographic characteristics, protection of fish habitat, and ensuring recruitment supply under environmental uncertainty and management shortcomings are among the general benefits of harvest refugia. Harvest refugia may also serve as control communities for comparison with nonrefuge areas, allowing us to determine the effects of exploitation on the ecological community and to disentangle the effects of fishing and environmental change.

However, we still lack detailed and scientifically defensible knowledge regarding the effects of harvest refugia. Because of a lack of information on spatial processes for fish populations, there are only a few quantitative assessments of the effects of refugia on current yields and on future abundance of populations (Polacheck, 1990; Roberts and Polunin, 1991; DeMartini, 1993; Holland and Brazee, 1996). The primary information needed for effective design of harvest refugia includes spatial structure of the population, population dynamics, larval drift trajectories, movements of benthic life stages, descriptions of fish habitats, and a distribution of fishing effort. Limited amounts of such information are available for shortraker and rougheye rockfish. Therefore, the establishment of harvest refugia in our study aims to improve the efficacy of the current harvest-rate strategy by providing a safer management scheme by which to conserve shortraker and rougheye spawning populations from possible depletion. This scheme can be used in combination with the current management strategy as an additional control on harvesting and as an attempt to solve problems that characterize the current management policy.

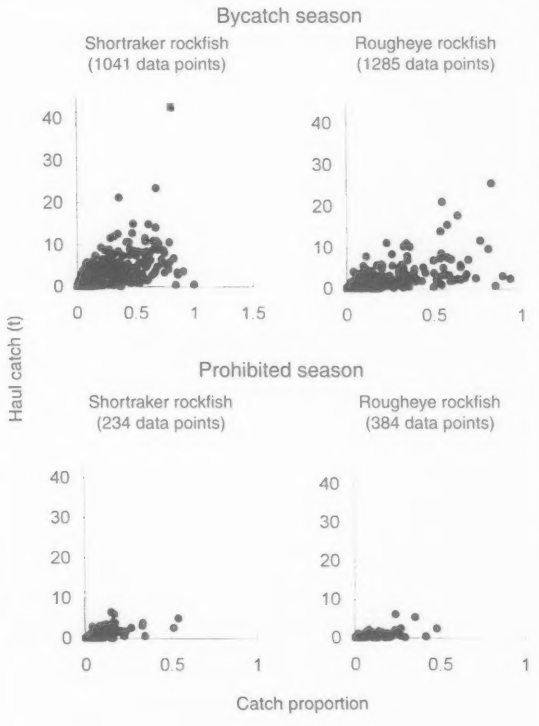

Figure 1

Haul catch of shortraker and rougheye rockfish and the proportion of the total catch made up by these species during the bycatch and prohibited season during 1991–96.

Methods

Documentation of fishery targeting practices

Current management allows vessels to "top-off" their catch during the bycatch season. The purpose of the "bycatch season" is to protect the population from a directed fishery and to allow for "natural" bycatch in other directed fisheries. In theory, targeting of a species can be avoided by allowing retention of only a certain fraction of that species, haul by haul. Such bycatch management measures have failed in instances where fishing deliberately targets bycatch species when their natural bycatch levels are lower than the specified limit. For example, if Pacific ocean perch (POP) is the target species, then vessels can retain bycatch species such as shortraker and rougheye rockfish up to a certain percentage of the total POP catch during the vessel trip. If they prefer, however, they could first fill their bins with POP and then target shortraker and rougheye rockfish. Through "topping-off," the fishery, in essence, becomes a directed fishery for the bycatch species.

To examine the targeting practice for these bycatch species, historical fishing seasons were divided into an allowable bycatch season and a prohibited season, and catch information for each fishing season was compared. During the prohibited season, neither high catches nor high proportions of shortraker and rougheye rockfish occurred (Fig. 1). During the bycatch season, however, both high catches and high proportions were observed. This comparison supports the hypothesis that vessels do target high-value species and that their fishing practices are focused on specific "hot spot" areas. Higher catch-per-unit-of-effort (CPUE) points in regions of short-tow duration (Fig. 2) provide further evidence of the practice of targeting these species. As a result, serial targeting in productive areas would induce early attainment of the ABC and result in discarding afterwards.

Design of harvest refugia

Basic design components of marine refugia are location, size, shape, and number. These components depend on the purpose of the harvest refugia.

In our application, the main goal of establishing harvest refugia for shortraker and rougheye rockfish is to protect adult fish from serial overfishing in areas of high short-

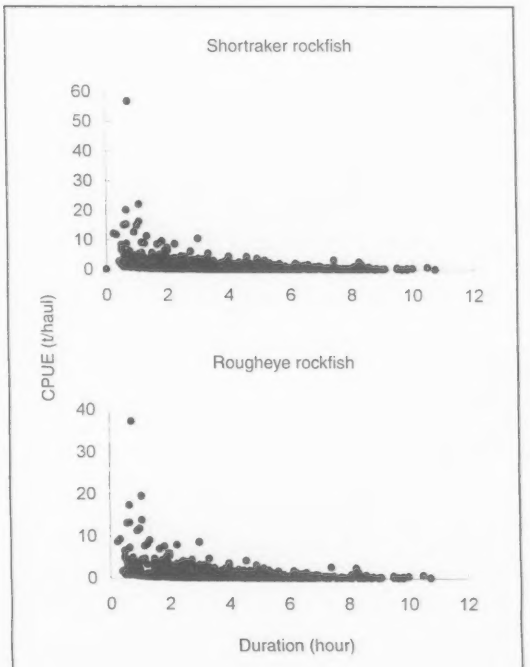

Figure 2

Distribution of haul CPUE (t/haul) versus tow duration for shortraker and rougheye rockfish in the Gulf of Alaska (domestic observer data for trawlers during 1987–96).

raker and rougheye production. Precautions are needed because these stocks are very slow growing, long-lived, and patchy in their distribution. Once "hot spot" stocks are depleted, several decades may be required for them to recover (Francis, 1986). Because this study aimed to develop a method for an objective design of refuge networks and to evaluate the feasibility of alternative management scenarios, no specific area was suggested for practical usage.

Size of refugia was determined by using quantiles from cumulated catch data. The selection of the size for harvest refugia depends on the goals of refuge management in general. Here, three sizes were arbitrarily selected and the effects of refuge size on the fish community and fishery practices were then evaluated. These refuge sizes are referred to as SSR (small-size refugia) MSR (middle-size refugia), and LSR (large-size refugia) and include all 1987–96 catches that exceeded the cutoff points for the 99.8%, 99.5%, and 99.0% quantiles, respectively (Fig. 3). The SSR, MSR, and LSR refugia defined in this manner represented 2.4, 5.4, and 9.5% of the total habitat occupied by shortraker or rougheye rockfish, or by both species.

Because the fishery data only provided net retrieval locations, the exact catch locations of each tow were unknown. This lack of starting-tow locations led us to postulate a circular area around the retrieval point to represent the occurrence of the catch. Although the average tow distance was about 18 km, the width of the continental slope region containing high catches for both species was usually less than 15 km, and trawling was generally conducted along depth contours. Therefore, the basic cell of the harvest refugium was arbitrarily chosen as a 20-km diameter circle, a group of which comprised the refugia for each species. Two species-specific harvest refugia were constructed by using GIS. Because shortraker and rougheye rockfish are currently managed together, the two independent reserves were united in the final design of the harvest refugia. Once a GIS database was established, it became possible to visualize the impact of different design criteria on the spatial distribution of the refuge network almost instantaneously.

Modeling population behavior under refuge management

There were two main goals for the assessment and projection of shortraker and rougheye rockfish stock conditions. The first was to examine the current stock status, to project future biomass, and to evaluate uncertainties in the key parameters under the current management system. The other was to examine the effectiveness of harvest refugia in the management of these species and compare it with the current management system. We employed a population dynamics model to address these goals (Soh, 1998). The model was coded by using AD Model Builder (Fournier, 1994). Determination of parameter uncertainties was based on the Markov Chain Monte Carlo method implemented as part of the AD Model Builder software libraries. Two separate time schedules were used in the modeling process: an assessment section (1961–1996) and a projection section (1997–2016). Inputs to the model included reconstructed catch histories (1961–1996), priors of the parameters, survey biomass estimates, and fixed fishing mortality rates.

Two conditions of fishing mortality were selected for future projection because fishing mortalities in establishing ABC and actual fishing mortalities at sea were not equal. Fishing mortalities used to calculate recommended ABC level were F=0.023 for shortraker and F=0.025 for rougheye rockfish (which were natural mortalities determined by NMFS and referred to as "F for ABC") during 1991–96. These ABC levels were not attained, however, and actual average fishing mortalities estimated by the model were F=0.063 for shortraker and F=0.015 for rougheye rockfish (referred to as "actual F") during 1991–96. If no alternative actions were applied to the current management policy, then projection results under the "actual F" scenario would be more realistic than those under "F for ABC".

In a refuge management system, no fishing was allowed in the refuge areas, and a fixed exploitation rate was applied to the harvestable areas. A major difference between projections of the current management and those of refuge management systems is that refuge management incorporates an adjustment for a discard rate of 29.5% (Table 1) into the system on the assumption that no discards will be necessary under refuge management. As a result,

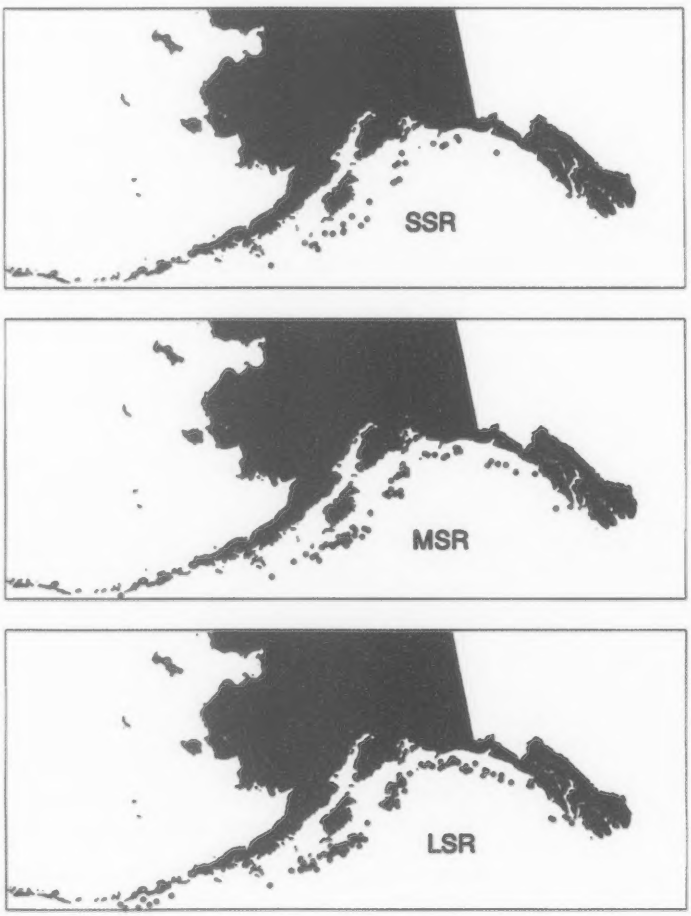

Figure 3

Three sizes of marine refugia are designed and the radius of the basic circle is 10 km. SSR = small-size refugia; MSR = middle-size refugia, and LSR = large-size refugia.

the current actual level of ABC (which includes discards), reduced by average discards, will be applied to future recommended ABC under refuge management. That is, recommended ABC in the harvestable areas will be the recommended ABC under current management multiplied by (1.0 – discard rate), assuming that this average discard rate is constant throughout the future projection years. This reduced ABC does not affect the fishing industry's actual harvest level if they can keep all the catch until ABC is attained.

Considering that they are a very large and valuable species, discards of shortraker and rougheye rockfish are assumed to result primarily from season limits, rather than size limits. Skippers consistently develop their area-specific skills to maximize total income, and high catch rates can result in a short fishing season (Hilborn, 1985). Because harvest refugia in our study were established in high catch-rate zones, or preference zones for shortraker and rougheye rockfish, the harvesting period was assumed to be sufficiently prolonged where shortraker and rougheye rockfish were less dense and regulatory-induced discards would be virtually eliminated as a result.

Model description

A stock reduction analysis model (Kimura et al., 1984) with one-parameter–based Beverton and Holt stock-recruitment relationship (Kimura, 1988) was applied for the stock assessment and future projections. Both analyses were combined to estimate the following relevant parameters:

i = years for the assessment period from 1961 to 1996;
j = years for the future projection period from 1997 to 2016;
λ = weighting factor between survey and fishery information for the combined catch history (= 1.0 when using survey data alone, 0.0 when using fishery data alone);
Q = survey gear efficiency;
d = average annual discard rate;
α = proportion of total biomass in refugia, estimated by cumulated catch data;
M = natural mortality rate;
A = recruitment strength in the Beverton and Holt model;
F_{ABC} = fixed exploitation rate for determining ABC;
ρ = Brody coefficient;
ω = annual growth rate of a fish in weight, $\left(=\frac{W_{k-1}}{W_k}\right)$;
k = age at recruitment;
s = survival rate ($s_i = e^{-(Fi+M)}$);
C^{obs} = observed catches for i and predetermined predicted catches for j;
C^{pred} = predicted catches based on catch equation;
${}^{S}C$ or ${}^{F}C$ = reconstructed catches based on survey (S) or fishery (F) information;
B^{obs} = biomass index from surveys;
B = Gulf-wide total predicted biomass;
B^{ref} = predicted biomass in refugia;
B^{nonref} = predicted biomass in nonrefugia;
R = Gulf-wide total recruits;
R^{ref} = predicted recruits in refugia;
R^{nonref} = predicted recruits in nonrefugia.

Stock assessment

Catch histories, based on survey and fishery information, were reconstructed for both shortraker and rougheye rockfish (Soh, 1998). Because survey data were available from 1961 and fishery data from 1977, survey information was used in the construction of catch history for the years 1961–76, whereas an information weighting factor (λ) was applied to combine the two catch histories for the years of 1977–90. Since 1991, independent catch data for the shortraker-rougheye rockfish subgroup have been available. As a result, the combined catch history, which was used as observed catches ($\mathbf{C}^{obs}$) in the model, can be described as follows:

$$\mathbf{C}^{obs} = \begin{bmatrix} C^{obs}_{1961} \\ \cdot \\ C^{obs}_{1976} \\ C^{obs}_{1977} \\ \cdot \\ C^{obs}_{1990} \\ C^{obs}_{1991} \\ \cdot \\ C^{obs}_{1996} \end{bmatrix} = \begin{bmatrix} {}^{S}C_{1991} \\ \cdot \\ {}^{S}C_{1976} \\ \lambda^{S}C_{1977} + (1-\lambda)^{F}C_{1977} \\ \cdot \\ \lambda^{S}C_{1990} + (1-\lambda)^{F}C_{1990} \\ {}^{F}C_{1991} \\ \cdot \\ {}^{F}C_{1996} \end{bmatrix}.$$

B^1 is defined as an initial biomass at the beginning of 1961 and R_1 is the recruitment in 1961. The pristine biomass level was assumed to be in an equilibrium state. As a result, initial biomass and the annual recruitment biomass to the unexploited stock can be shown as follows:

$$B_1 = B_0 = B_{1961}$$

$$R_1 = R_{1961} = B_0 \frac{1 - s_0 + \rho(s_0^2 - s_0)}{1 - \rho\omega s_0},$$

where survival rate $s_0 = e^{-M}$.

However, biomass in the second year, B_2, can be defined from the SRA model as

$$B_2 = B_{1962} = (1+\rho)s_1B_1 - \rho s_1 s_0 B_0 + R_2 - \rho\omega s_1 R_1,$$

where $B_1 = B_0$ and survival rate $s_i = e^{-(Fi+M)}$.

R_i is the recruitment biomass at the stock size B_i and is modeled by using a stochastic Beverton and Holt stock-recruitment relationship:

$$R_i = R_1 e^{\varepsilon_i}, \varepsilon_i \sim N(0, \sigma_r^2) \text{ for } 2 \le i \le k, \text{ and}$$

$$R_i = R_1 \frac{\frac{B_{i-k}}{B_0}}{1 - A\left(1 - \frac{B_{i-k}}{B_0}\right)} e^{\varepsilon_i}, \varepsilon_i \sim N(0, \sigma_r^2) \text{ for } i > k,$$

where k = the recruitment age (assumed k=30).

Since 1963, biomass has been able to be estimated by using the SRA model based on the Deriso's delay-difference equation (1980):

$$B_i = (1+\rho)s_{i-1}B_{i-1} - \rho s_{i-1}s_{i-2}B_{i-2} + R_i - \rho w s_{i-1}R_{i-1} \text{ for } i \ge 3.$$

Future projection of biomass and recruitment

The following biomass and recruitment models were applied throughout the projection period under the current management system:

$$B_j = (1+\rho)s_{j-1}B_{j-1} - \rho s_{j-1}s_{j-2}B_{j-2} + R_j - \rho\omega s_{j-1}R_{j-1}$$

$$R_j = R_1 \frac{\frac{B_{j-k}}{B_0}}{1 - A\left(1 - \frac{B_{j-k}}{B_0}\right)} e^{\varepsilon_j}, \varepsilon_j \sim N(0, \sigma_r^2).$$

Under the current management system, F_{ABC} was fixed during the projection period. Predetermined predicted catches ("target catches" or "observed catches") could then be calculated from

$$C_j^{obs} = F_{ABC} B_j.$$

The model stock was divided into two subcomponents under the refuge management system: one for refugia and the other for harvestable areas. Stock within refugia was based on the proportion of Gulf-wide biomass in refugia, α, using the spatial distribution of the historical catches to represent the spatial distribution of the actual exploitable biomass.

Under the refuge management system, target or observed catches were fixed to the level of ABC under the current management system minus the average annual discards:

$$C_j^{obs} = (1-d) F_{ABC} B_j,$$

where d = the average annual discard rate for shortraker and rougheye rockfish.

Gulf-wide recruitment was allocated into refugia and non-refugia areas by using

$$R_j^{ref} = \alpha R_j \text{ and } R_j^{nonref} = (1-\alpha) R_j.$$

Initial biomass for the projection years in refugia and non-refugia, where $j = 1$, can also be separated at the beginning of 1997 as

$$B_{j=1}^{ref} = \alpha B_{j=1}$$
$$B_{j=1}^{nonref} = (1-\alpha) B_{j=1}.$$

For, $j = 2$,

$$B_j^{ref} = (1+\rho) s_0 B_{j-1}^{ref} - \rho s_0 s_{j-2} \alpha B_{j-2} + R_j^{ref} - \rho \omega s_0 R_{j-1}^{ref}$$
$$B_j^{nonref} = (1+\rho) s_{j-1} B_{j-1}^{nonref} - \rho s_{j-1} s_{j-2} (1-\alpha) B_{j-2} + R_j^{nonref} - \rho \omega s_{j-1} R_{j-1}^{nonref},$$

where $F_t = 0$ in refuge.

And for $j \geq 3$,

$$B_j^{ref} = (1+\rho) s_0 B_{j-1}^{ref} - \rho s_0^2 B_{j-2}^{ref} + R_j^{ref} - \rho \omega s_0 R_{j-1}^{ref}$$
$$B_j^{nonref} = (1+\rho) s_{j-1} B_{j-1}^{nonref} - \rho s_{j-1} s_{j-2} B_{j-2}^{nonref} + R_j^{nonref} - \rho \omega s_{j-1} R_{j-1}^{nonref}.$$

All fishing mortalities were estimated by using the Newton-Raphson method (Taylor and Mann, 1983).

According to Bayes theorem, posterior log-likelihood is the sum of prior and experimental log-likelihood, $\log L(\theta \mid X) = \log L(\theta) + \log L(X \mid \theta)$. Therefore, posterior values of the other parameters were evaluated by minimizing the total negative log-likelihood:

$$Total(-\log L) = \frac{1}{2\sigma^2} \sum_i \left\{ \log\left(\frac{QB_i}{B_i^{obs}} \right) \right\}^2 + \frac{1}{2\sigma_\varepsilon^2} \left\{ \sum_i \varepsilon_i^2 + \sum_j \varepsilon_j^2 \right\} +$$

$$\frac{1}{2\sigma_{Q_{prior}}^2} \left\{ \log\left(\frac{Q}{Q_{prior}} \right) \right\}^2 + \frac{1}{2\sigma_{M_{prior}}^2} \left\{ \log\left(\frac{M}{M_{prior}} \right) \right\}^2 +$$

$$\frac{1}{2\sigma_{A_{prior}}^2} \left\{ \log\left(\frac{A}{A_{prior}} \right) \right\}^2 + (\lambda - \lambda_{prior})^2.$$

Priors are listed as follows:

Survey catchability coefficient, Q	$Q \sim N(1, 0.6^2)$
Natural mortality, M	$M \sim N(0.03, 0.2^2)$ for shortraker rockfish
	$M \sim N(0.025, 0.2^2)$ for rougheye rockfish
S-R shape parameter, A	$A \sim N(0.889, 0.2^2)$
Catch information weighting factor, λ	$\lambda \sim Uni(0.001, 0.999)$

Impacts of harvest refugia on other fisheries

Establishing no-take zones obviously affects other fisheries in the zones. Main species in the harvest refugia include Pacific ocean perch (*Sebastes alutus*), shortspine thornyhead (*Sebastolobus alascanus*), northern rockfish (*Sebastes polyspinis*), dusky rockfish (*Sebastes ciliatus*), sablefish (*Anoplopoma fimbria*), and rex sole (*Glyptocephalus zachirus*), as well as shortraker and rougheye rockfish. To examine the impacts of harvest refugia on other fisheries, the effects of depth constraints on refuge areas were considered. The reduction rates of "hot spot" catches by using different depth constraints were compared for each species.

Results

Fixed exploitation-rate strategy

Under an "F for ABC" fishing mortality (F=0.023), the ending biomass of shortraker rockfish would increase by about 800 metric tons (t) in twenty years, but the stock would decrease by over 7000 t if current fishing intensity (actual F=0.063) were continued (Table 2). Rougheye rockfish declined under both "F for ABC" and "actual F" fishing scenarios (either F=0.025 or F=0.015) by about 5000–12,000 t. Although the actual fishing mortality was much lower than the fishing intensity for the recommended ABC, rougheye stocks still declined.

Annual recruits of shortraker and rougheye rockfish ranged from about 1% to 3% of annual biomass based on the recruitment scenario, with a Beverton and Holt shape parameter A=0.889. For both scenarios of "F for ABC" and "actual F" fishing conditions, similar recruitment trends occurred in both species. Because the age at recruitment was assumed to be 30 (Nelson, 1986), future recruitment was not affected by the future fishing mortality schedule during the projection years. Recruitment strength varied

relatively little (Fig. 4) and was greatest during the early 1990s.

The estimates of posterior parameter values are shown in Table 3. The mean value of the posterior Q at maximum likelihood was about 0.78 for both species. This value of Q implies underestimation of the actual biomass by the surveys and is consistent with submersible observations by Krieger and Ito (1999), who concluded that the above-bottom distribution of shortraker and rougheye rockfish, together with their preference for steep-slope boulder habitats, would result in a value of Q that was less than 1.0. Natural mortality was estimated to be closer to prior expectations as was the shape parameter (A) in the Beverton and Holt recruitment curve (Beverton and Holt, 1957). Presumably the closeness of prior values and posterior estimates reflects the lack of information about the mortality and stock-recruitment relationship.

The lower posterior value of λ for shortraker rockfish represents more emphasis on fishery information and the increased value of λ for rougheye rockfish represents more emphasis on survey information in the combination of the two catch histories during 1977–90. Survey catch data show that shortraker rockfish are found primarily along the continental slope, whereas rougheye rockfish are distributed more broadly on the continental shelf. Generally, survey coverage in the slope region is relatively sparse, and data are consequently acknowledged to be insufficient. In this regard, more emphasis on fishery information for shortraker rockfish is desirable. The 1996 biomass represented decreases to about 46% and 69% of pristine level (B_{1961}) for shortraker and rougheye rockfish, respectively.

Refugia management strategy

The effects of refuge size on ending biomass, and differences in fishing intensity between current management and refuge management were considered in the projection model of refuge management. Ending biomass in twenty-year future projections and average twenty-year fishing mortality rates were compared for two levels of F ("F for ABC" and "actual F") and three refuge sizes.

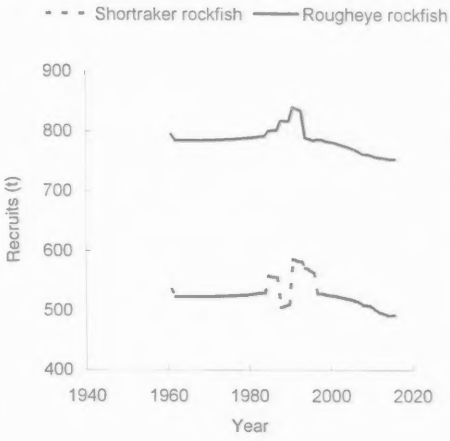

Figure 4

Predicted recruitment trajectories for shortraker and rougheye rockfish using the Beverton and Holt model with shape parameter A = 0.889.

Table 2

Starting and ending biomasses (t) of shortraker and rougheye rockfish under the current management regime, based on a 20-year future simulation (1997–2016). "F for ABC" is the fishing mortality currently used to calculate recommended ABC, and actual average fishing mortality during 1991–96, estimated by stock reduction analysis, is denoted as "actual F".

	Shortraker rockfish		Rougheye rockfish	
Year	F for ABC (F=0.023)	Actual F (F=0.063)	F for ABC (F=0.025)	Actual F (F=0.015)
1997	20,061	20,061	55,896	55,896
2016	20,847	12,623	43,351	50,443

Table 3

Estimates of posterior parameter values and their standard errors. Values in parentheses are standard errors. (B_{1996}=biomass in 1996, M=natural mortality, Q=survey catchability coefficient, A=shape parameter of Beverton and Holt recruitment curve, λ=weighting parameter for survey information in the reconstruction of catch history, and depletion level (B_{1996}/B_{1961})).

	Shortraker rockfish		Rougheye rockfish	
Parameter	Prior	Posterior	Prior	Posterior
B_{1996} (t)	—	20,667 (10,260)	—	56,040 (30,982)
M	0.030 (0.2)	0.031 (0.006)	0.025 (0.2)	0.025 (0.005)
Q	1 (0.6)	0.776 (0.325)	1 (0.6)	0.785 (0.407)
A	0.889 (0.2)	0.889 (0.178)	0.889 (0.2)	0.889 (0.178)
λ	0.5	0.266 (0.565)	0.5	0.554 (0.707)
B_{1996}/B_{1961}	—	0.464 (0.123)	—	0.685 (0.120)

Table 4

Summary of simulations showing ending biomasses (t) and average fishing mortalities from 20-year future projections. Three refuge sizes and two fishing intensity schedules are compared under current and refuge management systems. F values under refuge management pertain only to areas outside of refugia. (SSR=small-size refugia; MSR=middle-size refugia; LSR=large-size refugia)

	Ending biomass (year=2016)				Average F (during 1997–2016)			
	F for ABC (F=0.023)		Actual F (F=0.063)		F for ABC (F=0.023)		Actual F (F=0.063)	
Species	Current	Refuge	Current	Refuge	Current	Refuge	Current	Refuge
Shortraker rockfish								
SSR		23,442		18,270		0.018		0.043
MSR	20,847	23,437	12,623	18,236	0.023	0.022	0.063	0.055
LSR		23,425		18,153		0.030		0.090
Rougheye rockfish								
SSR		50,187		54,764		0.019		0.012
MSR	43,351	50,176	50,444	54,760	0.025	0.023	0.015	0.014
LSR		50,160		54,753		0.030		0.018

Table 5

Percentage of Gulf-wide catches in middle-size refugia (MSR), by species and depth, from domestic observer data (1987–1996). POP = Pacific Ocean perch.

Depth (m)	Shortraker rockfish	Rougheye rockfish	POP	Thornyhead	Northern rockfish	Dusky rockfish	Sablefish	Rex sole
100–713	28	29	15	12	12	17	6	12
200–713	27	28	12	12	1	1	5	6
300–713	23	25	2	9	0	0	3	1

Incorporation of harvest refugia into current management for shortraker and rougheye rockfish resulted in increased ending biomass for both levels of F (Table 4). Under the "F for ABC" scenario, ending biomass increased about 12% for shortraker rockfish and about 16% for rougheye rockfish with refuge management. Under the "actual F" scenario, ending biomass increased about 44% for shortraker and about 8% for rougheye rockfish when refugia were employed. Figure 5 shows the future biomass trajectories for the two management systems. For both fishing intensities, higher Gulf-wide biomass levels were projected in refuge management for both species.

Size differences for harvest refugia had relatively little impact on the ending biomass estimates. Table 4 shows similar ending biomass in refuge management irrespective of refuge sizes for both "F for ABC" and "actual F" scenarios. This is because the same catch removal was applied, irrespective of refuge size.

Impacts of harvest refugia on other target fisheries

Table 5 summarizes the proportion of catches within refugia compared with those from the whole Gulf for major species in the slope region. About 30% of the Gulf-wide catches of shortraker and rougheye rockfish occurred at depths greater than 100 m in MSR. Out of this, over 80% still remained in MSR in depths greater than 300 m. Dusky rockfish had the next highest proportion in MSR but their distribution was primarily confined to the 100–200 m depth interval. Shortspine thornyhead remained at 9% of the Gulf-wide catch in refugia deeper than 300 m. The catch proportions of other major fishes in refugia deeper than 300 m declined to 3% or less. Clearly, if harvest refugia can be established with depth limits greater than 300 m, then the impacts of no-take zones for shortraker and rougheye rockfish on other fisheries seem minor.

Discussion

Understanding the changes in fishing effort under refuge management is important for its practical application. In refuge management, fishing is allowed only in harvestable areas where fish density is assumed to be less than in refuge areas. However, high levels of fishing intensity outside of refugia are to be avoided because high fishing effort

could deplete stocks in nonrefuge areas if adults are sedentary.

The three sizes of refugia resulted in different levels of fishing mortality outside of refugia (Table 4). In the case of middle-size refugia (MSR), fishing mortalities outside of refugia differed little from current Gulf-wide levels. No increased fishing intensity outside of refugia is required under the MSR-based refuge management system, even though harvestable areas are reduced and density is lowered in these areas. It should be remembered, however, that in the projection of refuge management, annual quotas were set to the current annual quotas for shortraker and rougheye rockfish minus discards, and fishermen were assumed to keep all bycatch until quotas were attained. In larger-size refugia (LSR), increased fishing mortality was required in harvestable areas to attain the same amount of quota. Theoretically, this may be acceptable because harvestable areas were reduced and fish density in these areas was less than that outside MSR. In the case of small-size refugia (SSR), fishing mortalities were reduced compared with those under the current management system. Reduced fishing intensity in harvestable areas seem counter-intuitive compared with fishing efforts under the current management system, but this results from applying a reduced annual quota in the refuge management system. However, reduced annual quotas do not mean reductions in landings for the fishing industry because it will probably be possible to keep all catches rather than discard some of them. In this example, lower fishing effort outside of refugia, attainment of the same level of landings for the industry, reduced discards, and increased ending biomass were achieved in refuge management by establishing medium-size or small-size harvest refugia.

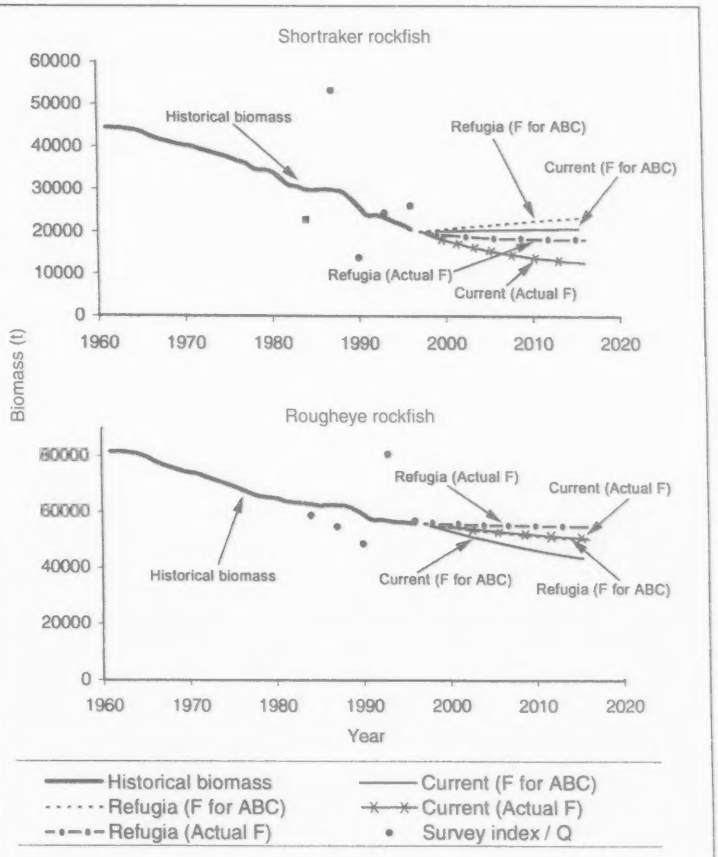

Figure 5

Future Gulf-wide biomass projections for shortraker and roughete rockfish under current management and under refuge management. "*F* for ABC" is $F = 0.023$ for shortraker and $F = 0.025$ for rougheye rockfish; and "actual *F*" is $F = 0.063$ for shortraker and rougheye rockfish. Q is a survey catchability coefficient.

Several additional benefits of refuge management for shortraker and rougheye rockfish can be suggested. Harvest refugia can eliminate serial overfishing of the substocks in areas of high densities, i.e. "hot spot" areas. Larger shortraker and rougheye rockfish have been intensively removed during the past two decades. Length-frequency distributions for shortraker and rougheye rockfish show a reduction of larger fish between foreign (1975–1985) and domestic (1987–1996) observer harvesting periods (Soh, 1998). As shown in Figure 5, shortraker rockfish are being overexploited if the goal is to maintain current stock levels. This overexploitation occurs because shortraker and rougheye rockfish are managed together as one subgroup with one combined quota, but shortraker rockfish are generally larger and commercially more valuable than rougheye rockfish.

Discards are an important problem and should be reduced. However, under the current management system, it may be difficult to reduce discards at sea because skippers search for areas with higher catch rates in order to maximize their fishing success. Although the shortraker-rougheye rockfish fishery has been "bycatch only" since 1993, targeting and retaining fish under "topping-off" strategies have continued during the bycatch season (Fig. 1). This type of targeting practice by fisheries allows earlier attainment of ABC and a prolonged discarding period.

Hot spots, or high density zones, for shortraker and rougheye rockfish can be considered as control areas for monitoring and sustaining the surrounding fish stocks. Because we had no information regarding the life stages of these two species prior to recruitment to their fishing grounds, we were at least interested in maintaining ad-

equate spawner biomass in the hot spots. Adult shortraker and rougheye rockfish are reported to live on habitats containing steep slopes (>20°) and numerous boulders (Krieger and Ito, 1999). If these habitats are degraded by fishing activity and if stocks in these areas become reduced, then Gulf-wide stock stability might be at risk. By establishing harvest refugia, essential fish habitat for adult shortraker and rougheye rockfish can be conserved.

Harvest refugia can also be used to ensure an appropriate proportion of shortraker and rougheye rockfish in catches. Because these two species are managed as one subgroup of the slope rockfish assemblage, the fishing season is subject to the attainment of the combined level of two TACs. This management strategy has led to a discrepancy between the intended ABCs and the actual catches of the two species. Trawl survey estimates of exploitable biomass and recommended ABC show species proportions (shortraker to rougheye rockfish) of 3:7 and 4:6, respectively; whereas, commercial catches show a 6:4 ratio. Obviously, this reversed proportion of exploitation between the two species will incur a faster decrease of the shortraker stock than is expected.

Separate management of these two species may be appropriate but because of their overlapping habitat, there could still be excessive waste through discards. Out of all the trawl hauls with either shortraker or rougheye rockfish sampled by domestic observers during 1987–97, about 50% of the total hauls contained both species. By weight, such hauls containing both species accounted for about 72% of the total catch of shortraker and 78% of the total catch of rougheye rockfish. This finding suggests considerable habitat overlap, even though survey data indicate that individual species have somewhat different bathymetric and habitat preferences (Soh, 1998; Ito, 1999). Nevertheless, refuge networks can probably be designed to take advantage of differences in the habitat preference of shortraker and rougheye rockfish to achieve the desired proportions of these species in commercial catches.

In summary, refuge management can potentially be used to solve a number of management problems. By selecting a moderate size, number, and spatial distribution for harvest refugia, the apparent short-term costs or risks can be reduced as much as possible. A solution to the problems of bycatch waste, protection from stock depletion, preservation of essential fish habitat, preservation of the existing spatial distribution of substocks, and prevention of serial depletion of substocks can potentially be achieved through refuge management.

Uncertainties in the results of our study resulted from the fact that populations may behave and adapt differently under different environments with different fishing pressures. Furthermore, there is an uncertainty regarding the sustainability of recruitment owing to a lack of knowledge of larval and juvenile stages and the impact of annual or interdecadal variability in oceanic conditions.

For practical application of a refuge system, additional research is still needed. Optimum shape, location, and size of refugia can best be achieved through adaptive management, by using monitoring and observations from existing refugia to redesign the network. Potential costs or risks, or both, are also expected. The fishing industry needs to be involved in gaining a full understanding of any loss incurred by the displacement of fishing effort from specified areas. Harvest refugia may prove to be unsuccessful if illegal fishing cannot be controlled. Investigation as to how to prevent such illegal behavior and to promote a practical and effective monitoring system still needs to be undertaken.

Acknowledgments

This paper is based on a dissertation by S. K. Soh, in partial fulfillment of the requirements of a Ph.D. at the University of Washington. The research was supported by grants from Washington Sea Grant and the Joint Institute for the Study of the Atmosphere and Ocean (JISAO) under NOAA cooperative agreement no. NA67RJ0155, contribution no. 668.

Literature cited

Allison, G. W., J. Lubchenco, and M. H. Carr.
1998. Marine reserves are necessary but not sufficient for marine conservation. Ecol. Appl. 8 (suppl. 1):S79–S92.

Beverton, R. J. H., and S. J. Holt.
1957. On the dynamics of exploited fish populations. Fisheries Investment Series 2, vol. 19. U.K. Ministry of Agriculture and Fisheries, London.

Bohnsack, J. A. and J. S. Ault.
1996. Management strategies to conserve marine biodiversity. Oceanography 9:73–82.

Chilton, D. E. and R. J. Beamish.
1982. Age determination methods for fishes studied by the groundfish program at the Pacific Biological Station. Can. Spec. Pub. Fish. Aquat. Sci. 60, 102 p.

Clark, W. G.
1991. Groundfish exploitation rates based on life history parameters. Can. J. Fish. Aquat. Sci. 48:734–750.
1993. The effects of recruitment variability on the choice of a target level of spawning biomass per recruit. *In* Proceedings of the international symposium on management strategies for exploited populations (G. Kruse, D. M. Eggers, R. J. Marasco, C. Pautzke, and T. J. Quinn II, eds.), p. 233–246. Alaska Sea Grant College Program Report 93-02.

DeMartini, E. E.
1993. Modeling the potential of fishery reserves for managing coral reef fishes. Fish. Bull. 91:414–427.

Deriso, R. B.
1980. Harvesting strategies and parameter estimation for an age-structured model. Can. J. Fish. Aquat. Sci. 37:268–282.
1987. Optimal $F_{0.1}$ criteria and their relationship to maximum sustainable yield. Can J. Fish. Aquat. Sci. 44(suppl. 2):339–348.

Fournier, D. A.
1994. AUTODIF, A C^{++} array language extension with automatic differentiation for use in nonlinear modeling and statistics. Otter Research Ltd. P.O.BOX 2040, Sidney, British Columbia V8L 3S3, Canada.

Francis, R. C.
1986. Two fisheries biology problems in West Coast groundfish management. N. Am. J. Fish. Manage. 6:453–462.

Gunderson, D. R.
1997a. Trade-off between reproductive effort and adult survival in oviparous and viviparous fishes. Can J. Fish. Aquat. Sci. 54:990–998.
1997b. Spatial patterns in the dynamics of slope rockfish stocks and their implications for management. Fish. Bull. 95:219–230.

Heifetz, J., J. N. Ianelli, and D. M. Clausen.
1997. Slope rockfish. *In* Stock assessment and fishery evaluation report for the groundfish resources of the Gulf of Alaska, p. 247–288. [Available from North Pacific Fishery Management Council, 605 W 4th Ave, Suite 306, Anchorage, AK 99501.]

Hilborn, R.
1985. Fleet dynamics and individual variation: why some people catch more fish than others. Can. J. Fish. Aquat. Sci. 42:2–13.

Holland, D. S., and R. J. Brazee.
1996. Marine reserves for fisheries management. Marine Resource Economics. 11:157–171.

Ito, D.
1999. Assessing shortraker and rougheye rockfishes in the Gulf of Alaska: addressing a problem of habitat specificity and sampling capability. Ph.D. diss., Univ. Washington, Seattle, WA, 205 p.

Kimura, D. K.
1988. Stock-recruitment curves as used in the stock-reduction analysis model. J. Cons. Int. Explor. Mer 44:253–258.

Kimura, D. K., J. W. Balsiger, and D. H. Ito.
1984. Generalized stock reduction analysis. Can. J. Fish. Aquat. Sci. 41:1325–1333.

Krieger, K. and D. Ito
1999. Distribution and abundance of shortraker rockfish, *Sebastes borealis*, and rougheye rockfish, *S. aleutinus*, determined from a manned submersible. Fish. Bull. 97:264–272.

Lauck, T., C. W. Clark, M. Mangel, and G. R. Munro.
1998. Implementing the precautionary principle in fisheries management through marine reserves. Ecological Applications 8(1):S72–S78.

Lindeboom, H. J.
1995. Protected areas in the North Sea: an absolute need for future marine research. Helgolander Meeresunters 49:591–602.

McDermott, S. F.
1994. Reproductive biology of rougheye and shortraker rockfish, *Sebastes aleutianus* and *Sebastes borealis*. M.S. thesis, Univ. Washington, Seattle, WA, 76 p.

Murray S. N., R. F. Ambrose, J. A. Bohnsack, L. W. Botsford, M. H. Carr, G. E. Davis, P. K. Dayton, D. Gotshall, D. R. Gunderson, M. A. Hixon, J. Lubchenco, M. Mangel, A. MacCall, D. A. McArdle, J. C. Ogden, J. Roughgardon, R. M. Starr, M. J. Tegner, and M. M. Yoklavich.
1999. No-take reserve networks: sustaining fishery populations and marine ecosystems. Fisheries 24 (11):11–25.

NMFS (National Marine Fisheries Service).
1996. Environmental assessment/regulatory impact review for Amendment 44 to the Fishery Management Plan for the groundfish fishery of the Bering Sea and Aleutian Island area and Amendment 44 to the Fishery Management Plan for the groundfish fishery of the Gulf of Alaska to redefine acceptable biological catch and overfishing, Appendix B. Alaska Fisheries Science Center, NMFS, 7600 Sand Point Way NE., Seattle, WA 98115-0070, 24 p.

Nelson, B. D.
1986. Population parameters of rougheye rockfish (*Sebastes aleutianus*). M.S. thesis, Univ. Alaska, Juneau, AK, 103 p.

Polacheck, T.
1990. Year around closed areas as a management tool. Natural Resource Modeling 4(3):327–354.

Roberts, C. and N. Polunin.
1993. Marine reserves: simple solutions to managing complex fisheries. Ambio 22(6):363–368.

Soh, S. K.
1998. The use of harvest refugia in the management of shortraker and rougheye rockfish (*Sebastes borealis*/*Sebastes aleutianus*) in the Gulf of Alaska. Ph.D. diss., Univ. Washington, Seattle, WA, 194 p.

Taylor, A. E., and W. R. Mann.
1983. Advanced calculus. John Wiley and Sons, New York, NY.

Yoklavich, M., editor.
1998. Marine harvest refugia for west coast rockfish: a workshop. U.S. Dep. Commer, NOAA Tech. Memo. NMFS-SWFSC-255, 159 p.

The diet of the large coral reef serranid *Plectropomus leopardus* in two fishing zones on the Great Barrier Reef, Australia

Jill St John

Garry R. Russ

Department of Marine Biology
James Cook University
Townsville, Queensland 4811 Australia
Present address (for J. St John): Western Australian Marine Research Laboratories
PO Box 20
North Beach, Western Australia 6020, Australia
E-mail address (for J. StJohn): jstjohn@fish.wa.gov.au

Ian W. Brown

Southern Fisheries Centre
P.O. Box
Deception Bay, Queensland 4508 Australia

Lyle C. Squire

27 Barrett St.
Bungalow, Queensland 4870 Australia

Abstract—The diet of *Plectropomus leopardus* (Serranidae, Lacepede 1802) was examined on two pairs of reefs in the Cairns Section of the Great Barrier Reef Marine Park, Australia. For both pairs, one reef was open to fishing and the other had been closed to fishing for eight years; however zoning appeared to be ineffective as there was no difference in the size structure of leopard coralgrouper populations on either open or closed reefs. Two fishing methods were used to sample reefs concurrently, and the size structure and diet of *P. leopardus* that were speared randomly (n=587) were compared to samples caught by line (n=85). Adult *P. leopardus* were highly piscivorous (96% of prey was fish by number), and two families of fishes, Pomacentridae and Labridae, composed approximately half of their diet (index of relative importance=48.4%). Numerical composition of fish in the diet varied significantly among reefs, but there were no patterns related to reef closures when fish prey were classified by taxa or by their habitat. Fishes categorized as living in the demersal reef habitat were the dominant prey consumed, followed by midwater fishes. When the data from reefs were pooled, the abundance of families in the diet differed between locations (north and south) but not between fishing zones. Dietary overlap was high between the different fishing zones and was very high in relation to naturally occurring spatial and temporal variability in the diet of *P. leopardus* found in other studies. With line fishing larger and hungry fish are caught, and the few data on natural prey suggest tentatively that line catches are biased toward *P. leopardus* feeding on pelagic fishes. The coral reefs and surrounding waters provide the major food source of *P. leopardus*, whereas sandy areas are much less important. Our data suggest that the coral trout fishery is resilient to changes in abundances of particular prey species because the diet of *P. leopardus* is broad and because the two major prey families are diverse and abundant on coral reefs.

Manuscript accepted 25 April 2000.
Fish. Bull. 99:180–192 (2001).

Groupers (Serranidae) are an important fishery resource throughout the tropics (Ralston, 1987; Heemstra and Randall, 1993; Polunin and Roberts, 1996) and are a favored target species of fishermen (Bohnsack, 1982; Randall, 1987; Koslow et al., 1988; Russ and Alcala, 1996). Like many other large piscine predators, the life history characteristics of groupers (Bohnsack, 1982; Russ, 1991) make them vulnerable to overfishing (Sluka and Sullivan, 1998).

Unlike most other multispecies tropical habitats, the Great Barrier Reef (GBR) supports a line fishery that targets relatively few genera (Russ, 1991). The groupers of the genus *Plectropomus* support the most valuable commercial fin-fishery in Queensland (Trainor, 1991), with an annual value of $A10 million. Groupers bring a consistently high price (about $20/kilogram retail for fillet) on the Australian market and are highly valued in the "live export" market to Asia (Miles[1]) Also, groupers are targeted by recreational line (Blamey and Hundloe[2]) and spear fishermen (Steven[3]), and recreational fishing is expanding with the rapid growth of the tourist industry on the GBR. *Plectropomus leopardus*[4] is the dominant component of the three main coral trout species caught on the GBR by all fishermen (Williams and Russ, 1994; Steven[3]), and by Australian standards, this species is subjected to considerable fishing pressure.

Intense fishing pressure has been implicated in the drastic declines of grouper populations off Florida and the Caribbean (Sadovy, 1994; Bohnsack et al., 1994). In Australia, fishery managers have already detected a decline in abun-

[1] Miles, A. 1997. Research, not rumors, needed for live fishing industry. Exploring Reef Science. May newsl. [Available from CRC Reef Research Centre, James Cook University, Townsville 4811, Australia.]

[2] Blamey, R. K., and T. J. Hundloe. 1991. Characteristics of recreational boat fishing in the Great Barrier Reef region. Unpubl. report to the Great Barrier Reef Marine Park Authority (GBRMPA) PO Box 1379, Townsville, Queensland 4810, Australia.

[3] Steven, A. 1988. An analysis of fishing activities on possible predators of the crown of thorns starfish (*Acanthaster planci*) on the Great Barrier Reef. Unpubl. report to GBRMPA, PO Box 1379, Townsville, Queensland 4810, Australia. 131 p.

[4] The official common name of *Plectropomus leopardus* is leopard coralgrouper, formerly known as bluedotted coraltrout (Heemstra and Randall, 1993).

dance of *P. leopardus* in some parts of the GBR, particularly close to centers of human population (Craik, 1981). Furthermore, fishing pressure is expected to intensify owing to increases in both commercial and recreational demand for this species. Maintaining grouper stocks on coral reefs depends on careful management of these fisheries.

Strategies of coral reef management include closing reefs to all forms of exploitation. This strategy is designed to protect reef-fish stocks and habitats (Williams and Russ, 1994), which enables populations of reef fishes to regain or maintain natural levels of abundance (see review by Roberts and Polunin, 1991). Since the establishment of the Great Barrier Reef Marine Park (GBRMP) in 1981, the major management strategy has involved partitioning of reefs into six main zones that permit different levels and types of fishing.[5] Actual fishing pressure on reefs in these zones, however, has not been measured in many areas of the marine park (Williams and Russ, 1994).

Most concerns about the impact of fishing have focused on the reduction of stock abundance (Russ, 1991). Both direct and indirect trophic effects on the structure of coral reef-fish communities by the removal of piscivores remain poorly understood (Hixon, 1991; Russ, 1991; Steneck, 1998). Some authors have argued that the removal of large piscivorous fishes leads to compensatory increases in overall abundance or changes in relative abundance of prey often termed "prey release" (Beddington and May, 1982; Goeden, 1982; Beddington, 1984; Grigg et al., 1984; Koslow et al., 1988). Russ (1991) and Jennings and Lock (1996), however, argued that the evidence for "prey release" on coral reefs is limited and equivocal. In 1978 Goeden suggested that depleting the abundance of *P. leopardus* may irreversibly alter the structure of the community of coral-reef fishes on the GBR, and yet, 20 years later, nothing is known about the trophic impacts of this fishery.

Coral reefs with different fishing histories represent valuable large scale manipulations of predator densities (Jennings and Polunin, 1997). In contrast to results of smaller-scale predator-removal experiments on site-attached coral reef fishes (Caley, 1993; Hixon and Beets, 1993; Carr and Hixon, 1995), large-scale "experiments" of predator removal by fishing have not demonstrated that predators play an important role in structuring fish communities. Several studies have compared prey populations on fished and unfished reefs but have found no evidence for corresponding changes in diversity or biomass of potential prey species (Bohnsack, 1982; Russ, 1985; Jennings and Polunin, 1997; Russ and Alcala, 1998a, 1988b). These studies, however, were hampered by a lack of dietary information necessary to determine exactly which prey fishes are important in the diet of the fished species. For coral reef piscivores, commercially important or otherwise, quantitative studies on food consumption, feeding strategies, and comprehensive lists of prey species are rare (but see Norris, 1985; Norris and Parrish, 1988; Sweatman, 1984; St John, 1999). Studies of predator-prey relationships on coral reefs cannot progress further without knowledge of the prey consumed (Jennings and Polunin, 1997).

Information on the trophic biology of groupers is important for protecting the stocks and ensuring a healthy fishery for the future. Knowledge of the breadth of the diet and the specific habitat of important prey will indicate the resilience of stocks to changes in prey abundance or habitat destruction. Furthermore, baseline information on the diet of unfished populations is needed as a comparison for diets of fished populations. Such information should include some measure of spatial variation in regard to the diet. Fishing activities may alter the trophic ecology of the species targeted by altering the structure or the behavior of the wild population or both. For example, removing larger individuals of *P. leopardus* may alter the diet of the population because larger predators eat larger prey. St John (1999) found that the composition of the fish diet of *P. leopardus* on the GBR varied with size until predators attained 35 cm (TL). If this result applies to other geographic areas, fishing could affect the trophic impact of *P. leopardus* populations where legal minimum size limits are less than 35 cm (TL) or do not exist (e.g. Okinawa, Japan). On the GBR, however, such effects would be minimal because the legal minimum length is 38 cm (TL).

Fishing may also affect the behavior of piscivores. Line fishermen use baited hooks and throw bait into the water (termed burleying) to attract leopard coralgroupers to their fishing sites on the GBR. The use of bait to catch these fish could affect feeding behavior or feeding-related patterns of movement of *P. leopardus* in fished reefs and may have short- or long-term effects on the feeding ecology of *P. leopardus*.

Compared with commercially important fishes in many other ecosystems, relatively little is known about the diet of adult *P. leopardus* on the GBR, despite the huge numbers of *P. leopardus* fished from the reefs on the GBR annually (but see Choat, 1968; Goeden, 1978; Kingsford, 1992; St John, 1995, 1999). In all the existing studies, most samples were collected by spear, presumably to avoid possible dietary biases caused by line fishing methods. Thus, nothing is known about the trophic impacts associated with line fishing, which uses baited hooks at local fishing sites and which is by far the most common method used to catch *P. leopardus*. A comparison of stomach contents between *P. leopardus* caught by spear and those caught by hook and line at the same reefs will provide information on the selectivity of line fishing and trophic impact of this species.

Our study is the first to examine the diet of a large commercial species of coral reef fish at reefs in open and closed fishing zones. The feeding ecology of *P. leopardus*, a major coral reef piscivore, was examined at reefs zoned open and closed to fishing for eight years in the Cairns section of the GBRMP. Although the primary aim of this study was to describe and compare the diet of *P. leopardus* on reefs in two fishing zones, we pooled reefs and compared the diet by location to assess the natural spatial variability in the diet of *P. leopardus* in this region. Also, we assessed the size structure and diet of *P. leopardus* caught by two fishing methods: nonselective spear fishing (described in the "Materials

[5] 1987. Central Zoning Information Pamphlet. GBRMPA, PO Box 1379, Townsville, Queensland 4810, Australia. Fold-out pamhlet with no pagination.

and methods" section) and baited line fishing. Fishing pressure was assessed by comparing differences in the size structure of populations of *P. leopardus* between fished and unfished reefs using size information from the catch at each reef as well as fishery independent estimates from visual surveys done just prior to sampling (Ayling and Ayling[6]; Brown et al.[7]).

Materials and methods

Study sites and sampling design

Two pairs of mid-continental shelf reefs at the southern end of the Cairns section of the GBR Marine Park were sampled in January and February 1992 (Table 1). Each pair comprised one reef that had been closed to fishing for eight years (Marine National Park (MNP) 'B') and another open to commercial and recreational fishing activities (General Use (GU) 'B'). These reefs will subsequently be referred to as "closed" and "open" zones. The northern pair, Wardle Reef (closed) and Nathan Reef (open), and the southern pair, Noreaster Reef (closed) and Potter Reef (open), were approximately 30 km apart, and the reefs within pairs were 5 and 10 km minimum distance from each other respectively (Fig. 1).

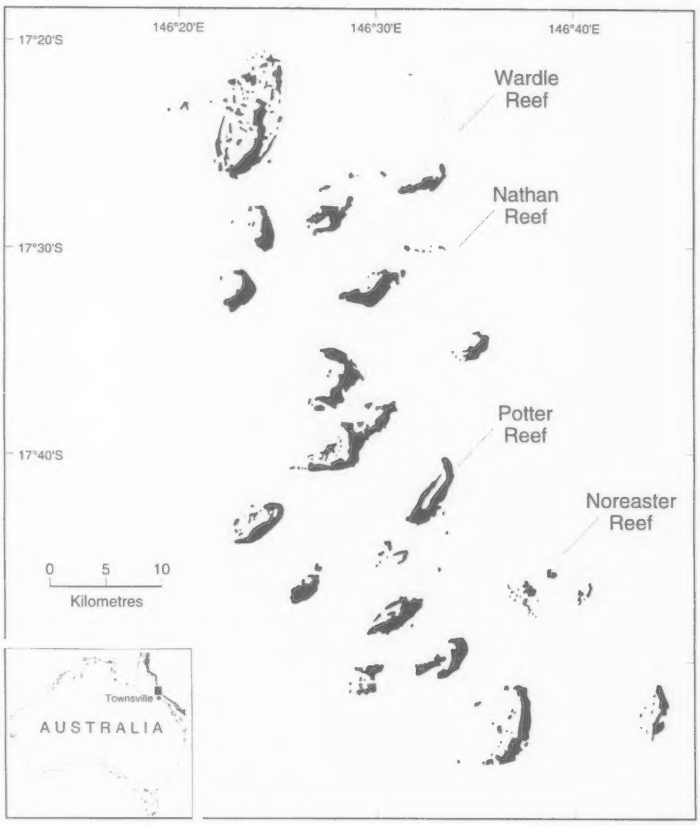

Figure 1

The southern part of the Cairns section of the Great Barrier Reef Marine Park showing Nathan and Potter Reefs (zoned GU 'B', all fishing allowed) and Wardle and Noreaster Reefs (zoned MNP 'B', closed to all fishing).

Collection of *P. leopardus*

Each reef was fished by line and spear simultaneously. Two teams of experienced fishermen collected fish by spear and line during daylight hours (0600–1800 h). Line fishermen worked in pairs from two small boats and used single hook rigs with pilchards (*Sardinops neopilchardus*) as bait. Spear fishermen worked in two pairs and hunted each fish as soon as it was seen in an attempt to obtain a sample representative of the size distribution of the actual population of coral trout. If two or more grouper were spotted simultaneously, the choice of the target was not based on size, and spear fishermen were deliberately not size selective. Spear fishing, however, has some inherent biases. Larger fish will be sighted first by spear fishermen because they will approach a diver more readily than smaller fish and are more conspicuous at distances (Kulbicki, 1998). These biases, however, should be similar at all reefs. Furthermore, the detection of camouflaged species, such as *P. leopardus*, increases with disturbance of the habitat when divers flush out these fish earlier at disturbed or fished reefs (Kulbicki, 1998), and this disturbance may increase the speared catch. Amount of catch, however, was not the focus of this study.

Samples were stored on ice in the small boats and frozen on board the mother ship (up to several hours later). Fork length (FL) of captured coral trout was measured to the nearest 0.5 cm.

Stomach contents

Only stomach contents were used in dietary analysis of *P. leopardus* (St John, 1995). The mouth and gills of each specimen were examined for regurgitated prey (Parrish, 1987). The stomach was opened and any contents were removed. Stomach contents were fixed in 10%

[6] Ayling, A. M. and A. L. Ayling. 1992. Effects of fishing pilot study: visual surveys on Cairns section closed reefs that will be opened under the new zoning plan. Unpubl. report to GBRMPA, PO Box 1379, Townsville, Queensland 4810, Australia, 48 p.

[7] Brown, I. W., L. C. Squire, C. Baltus, and M. Sellum. 1996. Effect of zoning changes on the fish populations of unexploited reefs—stage 2: post-opening assessment. Unpubl. report to GBRMPA, PO Box 1379, Townsville, Queensland 4810, Australia, 40 p.

formal calcium acetate (FCA), a buffered formalin solution (approximately 10 mL of FCA for every gram of stomach content) for a minimum of seven days and then stored in 70% ethanol.

Stomach contents were classified broadly into natural prey or bait. All bait in our study were pilchards (*Sardinops neopilchardus*), which does not occur naturally in the area. Every natural prey item was identified under low magnification to the lowest taxonomic group possible (St John, 1995). Fish were identified following Randall et al. (1990) by using several keys (Allen, 1975; Masuda et al., 1984; Smith and Heemstra, 1986; Myers, 1991).

Families of prey fishes were classified by the area where they were most commonly found (Randall et al., 1990; senior author, personal obs.). Prey fishes from the "demersal reef substrata" habitat swam around and above coral, but used it for shelter (e.g. Pomacentridae and Scaridae). Fishes categorized as using the "benthic reef substrata" habitat were benthic dwellers that remained very close to the substrata (e.g. Blenniidae). Fishes categorized as in the "adjacent sands" habitat dwelled over, on, or within the sandy areas adjacent to reefs (e.g. Mullidae). Pelagic fishes in the "midwater" habitat were found from the water surface to a depth of approximately 1 m over the reef (e.g. Clupeidae and Caesionidae).

Wet weights of the stomach contents were measured after preservation in 70% ethanol. Before weighing, the stomach contents were emptied into a sieve (St John, 1995) and shaken or sponged, or both shaken and sponged, to remove excess surface liquid (Parker, 1963). Wet weights of stomach contents were excluded from weight analyses when there was evidence of regurgitation of food from the stomach, (e.g. digested prey in the mouth or gills or an empty stomach that was stretched or everted), but this condition was rare.

Generally, weights of digested prey reflected prey size and therefore were a useful measure of the diet (St John, 1995). Less than 14% of the prey was highly digested, and such fish could not be separated for weighing. In these cases, individual prey weights were estimated from total weights of the stomach sample, taking into account the digestion stage and the size (when known) of all individuals in the sample.

The contents of the stomach were assumed to represent daily feeding in *P. leopardus* because prey items were mostly digested after 24 hours (St John, 1995).

Data analyses

Kolmogorov-Smirnov (K-S) (Sokal and Rohlf, 1981) tests were used to compare size structures of leopard coral-grouper populations on reefs on both closed and open zones to fishing.

Fisher's exact tests were used to compare the frequency of prey items in the diet because the categories (fishing zones, reefs, habitats, fishing methods and families of prey) were all nominal (Mehta and Patel, 1992). Because Fisher's exact tests do not compare nested data sets, comparisons within zones or locations used pooled data. Data from reefs were pooled when they did not differ significantly (i.e. $P>0.05$). Because the differences in number of prey per family in the diet was statistically marginal in reefs in the open zone ($P=0.056$), we used the $P=0.01$ level of significance to compare open and closed zones when reefs were pooled. Also, the $P=0.01$ level of significance was used when sample sizes were small (e.g. in the comparison between the natural diet of line-caught and speared fish).

An independent t-test was used to compare the mean number of families consumed in each fishing zone. Prior to analysis, the variances were tested for homogeneity by using Cochran's test, which was not significant (Cochran's test statistic=0.84, $P>0.05$). Because the null hypothesis was not rejected, the power of the test to detect specified differences was calculated following Cohen (1988). In the calculations of power, the sample means were assumed to be representative of the parametric means for each treatment group. A nonsignificant result was considered to be inconclusive unless the power of the test ($1-\beta$) was >0.80.

The index of relative importance (IRI) determined for the diet of *P. leopardus* was

$$IRI = 0.5 \times (\%\ \text{prey number} + \%\ \text{prey weight}).$$

This measure was used in Schoener's a index of dietary overlap (Schoener, 1970) for pair-wise comparisons of the diet of *P. leopardus* between reefs within each of the two fishing zones. Dietary overlaps were classified by using Langton's (1982) scale: low 0–0.29, medium 0.30–0.59, and high ≥0.60.

Results

Size structure of *P. leopardus*

In total, 672 *P. leopardus*, ranging in size from 13 to 58.5 cm FL, were collected by line and spear from the four reefs (Fig. 2) and fewer *P. leopardus* were caught by line ($n=85$) than by spear ($n=587$) (Table 1).

The speared catch was considered to represent populations of *P. leopardus* on reefs because spear fishermen were deliberately not size selective in this study. The size-structure of the line catch was significantly larger than that of the speared catch (Dmax=0.243, K-S $P<0.01$) when samples from the four reefs were pooled (Fig. 2). Thus, line caught *P. leopardus* were excluded from further analyses of population size structure.

When reef pairs within locations were compared, the size structure of the speared catch on the open reefs differed significantly from the closed reefs (north: Dmax=0.20, K-S, $n=143$, $P<0.01$; south: Dmax=0.13, K-S, $n=131$ $P<0.05$; Fig. 2), but these zonal patterns differed between locations. The size structure of the speared catch differed significantly between the two open reefs (Dmax=0.19, K-S, $n=155$, $P<0.01$, Fig. 2); the proportion of larger fish (>35 cm FL) was 45% at Nathan Reef and 64% at Potter Reef compared with 57% at each of the closed reefs. The results of our study did not demonstrate an effect of fishing on size structure between open and closed reefs.

Stomach contents of fish caught by the two methods

Although the proportion of *P. leopardus* with empty stomachs did not differ between the line-caught and speared catch (Fisher's exact test$_{[1]}$=0.12, P=0.81), the proportion of the catch with natural prey in their stomachs was significantly higher in speared fish (Fisher's exact test$_{[1]}$=7.8, P=0.01) (Table 2). As expected, a much higher proportion of line-caught fish had consumed the bait *S. neopilchardus* (Table 2); however, five *P. leopardus* that were speared at sites where line fishing had not occurred, also had consumed bait.

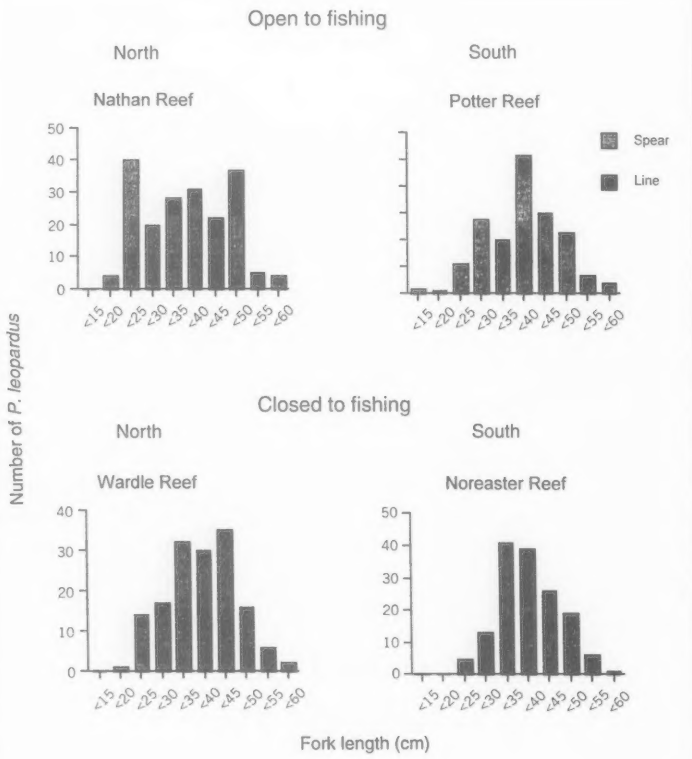

Figure 2

The length-frequency distributions of *P. leopardus* collected by line and spear from the four reefs, Nathan (n=191) , Wardle (n=153), Potter (n=178), and Noreaster (n=150) Reefs.

Assessment of natural diet

Type of prey *Plectropomus leopardus* on the four reefs fed mostly upon fish, some crustaceans, and a few cephalopods (Table 3). Six pieces of hard coral that were found in the stomachs of *P. leopardus* at three reefs were considered to have been ingested incidentally with prey and were excluded from the analysis. The proportions of fish, crustaceans, and cephalopods in the diet of *P. leopardus* did not vary significantly among the four reefs (Fisher's exact test$_{[6]}$=4.84, P=0.56, Table 3). *Plectropomus leopardus* were highly piscivorous. Fish accounted for 95.7% of their diet.

General fish diet Of the 468 prey fish in the diet of *P. leopardus*, 40% were identified to 22 families (Table 4). The abundance of fish prey in a family ranged from one (nine families, Table 4) to 47 individuals (Pomacentridae, Table 4), and total digested prey weights ranged from 0.12 g to 730 g per family (Table 5). The average weight of an individual prey item was 13.7 g.

Two families, Pomacentridae and Labridae, dominated the diet by number (Table 4) and by weight (Table 5) and were the most important prey of *P. leopardus* (*IRI*=27.8% and *IRI*=20.6% respectively, Table 6). Three families, Scaridae, Clupeidae, and Caesionidae, were the next most important prey, each representing about 10% of the diet by IRI and at least

Table 1

Summary of 672 *P. leopardus* collected from the Cairns section of the Great Barrier Reef Marine Park by line and spear fishing, including location of the reef pairs, names of reefs, their fishing status, and date of sampling.

				Sample size (n)		
Location of reef pair	Reef pair	Fishing zone	Date in 1992	Line	Spear	Total
North	Nathan	open	20–22 Jan	33	158	191
	Wardle	closed	23–25 Jan	10	143	153
South	Potter	open	24–26 Feb	23	155	178
	Noreaster	closed	27–29 Feb	19	131	150

Table 2

Stomach contents of *P. leopardus* caught by the two fishing methods. *Plectropomus leopardus* are classified into four groups by the contents of their stomachs: natural prey only, natural prey and bait, bait only, and no contents (empty). Number of *P. leopardus* and the percentage of the total catch are recorded for each group.

	Fishing method			
	Line		Spear	
Stomach contents	Number	%	Number	%
Natural prey only	36	42.4	342	58.2
Natural prey and bait	2	2.3		
Bait only	14	16.5	5	0.8
Empty	33	38.8	240	40.9
Total	85		587	

Table 3

Number of prey fish, crustaceans, and cephalopods found in *P. leopardus* collected from Nathan, Wardle, Potter, and Noreaster Reefs. Numbers of predators with natural prey in their stomachs and empty stomachs in each sample are included.

	Reefs				
Prey groups	Nathan	Potter	Wardle	Noreaster	Total
Fish	121	126	118	103	468
Crustaceans	2	2	6	3	13
Cephalopods		3	2	3	8
Unidentified	2	1	2	1	6
Total prey	125	132	128	110	495
Empty stomachs	85	76	53	59	273
P. leopardus with prey	92	102	100	86	380

Table 4

Number of prey per family identified in the fish diet of *P. leopardus* collected from Nathan, Wardle, Potter, and Noreaster Reefs. Total numbers of prey in families are included and expressed as percentages of the total diet. Total numbers of identified fish, unidentified fish, families of prey, and predator individuals are included. Small-size schooling fishes are underlined.

	Reefs open to fishing		Reefs closed to fishing		Total	
Prey families	North (Nathan)	South (Potter)	North (Wardle)	South (Noreaster)	Number	%
Pomacentridae	12	9	9	17	47	25.3
Labridae	9	8	9	11	37	19.9
Clupeidae	11	9	6	5	31	16.6
Caesionidae		9	1	2	12	6.4
Synodontidae	4	3	1	2	10	5.4
Scaridae	4	2		2	8	4.3
Blenniidae	1	1	5		7	3.8
Acanthuridae	2	3	1		6	3.2
Apogonidae	1	5			6	3.2
Serranidae	3	1		1	5	2.1
Engraulidae	2		1		3	1.6
Fistulariidae	1	1	1		3	1.6
Gobiidae	2				2	1.1
Balistidae			1		1	0.5
Creedidae			1		1	0.5
Lutjanidae		1			1	0.5
Monacanthidae	1				1	0.5
Nemipteridae	1				1	0.5
Platycephalidae			1		1	0.5
Plesiopidae			1		1	0.5
Scorpaenidae	1				1	0.5
Siganidae			1		1	0.5
Identified fish	55	52	39	40	186	
Unidentified fish	66	74	79	63	282	
Number of families	15	12	14	7	22	
No. of *P. leopardus* with prey	92	102	100	86	380	

Table 5

Summed digested weights (in g) of prey in each family in the diet of *P. leopardus* collected from Nathan, Wardle, Potter, and Noreaster Reefs. Total weights of prey in families are included and expressed as percentages of the total diet. Total weight of prey at each reef and number of predator individuals with prey are included. Small-size schooling fishes are underlined.

	Reefs open to fishing		Reefs closed to fishing		Total	
Prey families	North (Nathan)	South (Potter)	North (Wardle)	South (Noreaster)	Number	%
Pomacentridae	235.1	85.3	195.0	215.1	730.4	28.7
Labridae	159.7	58.6	140.5	148.5	507.3	19.9
Scaridae	230.0	127.8		79.7	437.5	17.2
Caesionidae		124.6	1.0	133.3	258.9	10.2
Scorpaenidae	116.5				116.5	4.6
Synodontidae	23.4	58.3	5.6	12.0	99.4	3.9
Blenniidae	0.6	4.3	82.4		87.3	3.4
Acanthuridae	38.7	29.9	16.5		85.1	3.3
Nemipteridae	82.5				82.5	3.2
Serranidae	37.4	10.8		9.8	58.0	2.3
Clupeidae	12.1	10.4	5.9	10.3	38.7	1.5
Plesiopidae			13.2		13.2	.5
Fistulariidae	2.6	1.5	2.8		6.8	.3
Apogonidae	1.0	5.7			6.7	.3
Engraulidae	1.4		4.8		6.2	.2
Balistidae			2.3		2.3	<.1
Gobiidae	2.2				2.2	<.1
Creedidae			1.0		1.0	<.1
Platycephalidae			0.68		0.7	<.1
Siganidae			0.33		0.3	<.1
Lutjanidae		0.2			0.2	<.1
Monacanthidae	0.1				0.1	<.1
Total weight	943.5	517.4	472.0	608.8	2541.7	
No. of *P. leopardus* with prey	92	102	100	86	380	

10% by one of the other dietary measures (Tables 4–6). The body sizes of these prey families were very different, e.g. 31 Clupeidae weighed 39 g, whereas eight Scaridae weighed 438 g (Tables 4 and 5). The remaining 17 families of prey accounted for approximately one quarter of the diet (summed IRI=24.0%, Table 6). Only four families, Pomacentridae, Labridae, Clupeidae, and Synodontidae, were eaten by *P. leopardus* at every reef.

Comparisons between line-caught and speared samples In the diet of the smaller sample caught by line, 21 fish were identified into eight families that were a subset of the 22 prey families found in the speared sample (Table 7). The dietary composition of line-caught *P. leopardus* did not differ significantly from the speared catch (at P=0.01 level of significance, Table 8, see "Materials and methods" section for explanation). When classified by their characteristic habitat (Table 9), however, the number of prey differed significantly between fishing methods (Fisher's exact test$_{[3]}$=18.7, P=0.0003). The proportion of midwater, pelagic prey in the diet was higher in the line catch (67%) than in the speared catch (21%), which was dominated by prey living in the demersal habitat (66% of the diet).

Because all prey families found in the line-caught *P. leopardus* also occurred in speared specimens, prey fishes obtained by the two types of gear identified from each reef were pooled for further analyses to increase the sample size.

Comparisons among reefs and zones The number of families in the diet of *P. leopardus* varied among reefs and ranged from seven families at Noreaster Reef to 15 at Nathan Reef (Table 4). There was no detectable difference in the number of families in the diet of *P. leopardus* between fishing zones ($t_{[2]}$= 1.380, P>0.20, 1–β < 0.33).

Dietary overlap was high between reefs within fishing zones (open reefs: Schoener a=0.68; closed reefs: Schoener a=0.68) and between fishing zones (Schoener a=0.65) when reefs were pooled. IRI values were higher in Pomacentridae and Labridae at the closed reefs than at the open reefs, whereas the opposite pattern occurred for Scaridae and Synodontidae (Table 6).

The number of prey per family in the diet of *P. leopardus* varied significantly among the four reefs (Table 8). This variation, however, could not be related to the zoning of reefs because the diet of *P. leopardus* did not differ

Table 6

The index of relative importance (IRI) calculated for each fish family of prey and expressed as a percentage of the total for all identified fish families in the diet of *P. leopardus*, grouped by reef, fishing zone, and total. Small-size schooling fishes are underlined.

	Reefs open to fishing			Reefs closed to fishing			
Prey families	North (Nathan)	South (Potter)	Both	North (Wardle)	South (Noreaster)	Both	Total
Pomacentridae	23.4	16.9	20.8	32.2	38.9	35.4	27.8
Labridae	16.6	13.3	15.4	26.4	25.9	26.0	20.6
Scaridae	15.8	14.3	15.0		9.0	4.9	9.8
Clupeidae	10.6	9.7	10.1	8.3	7.1	7.7	8.9
Caesionidae		20.7	8.5	1.4	13.4	8.1	8.9
Synodontidae	4.9	8.5	6.1	1.9	3.5	2.7	4.7
Blenniidae	0.9	1.4	1.1	15.1		7.0	4.4
Acanthuridae	3.9	5.8	4.7	3.0		1.4	3.2
Serranidae	4.7	2.0	3.5		2.0	1.1	2.2
Scorpaenidae	7.1		4.4				1.8
Apogonidae	1.0	5.4	3.0				1.6
Nemipteridae	5.3		3.3				1.3
Fistulariidae	1.0	1.1	1.1	1.6		0.8	0.9
Engraulidae	1.9		1.0	1.8		0.8	0.9
Plesiopidae				2.7		1.2	0.7
Gobiidae	1.9		1.0				0.5
Balistidae				1.5		0.7	0.4
Creedidae				1.4		0.7	0.3
Platycephalidae				1.3		0.7	0.3
Siganidae				1.3		0.6	0.3
Lutjanidae		1.0	0.5				0.2
Monacanthidae	0.9		0.5				0.2
No. of *P. leopardus* with prey	92	102	194	100	86	186	380

significantly between fishing zones (at P=0.01 level of significance, Table 8, see "Materials and methods" section for explanation). Furthermore, when pooled by location, the numerical composition of the diet of *P. leopardus* on southern and northern reefs differed significantly (Table 8).

When categorized by their characteristic habitat (Table 9), the number of prey did not differ significantly among reefs (Fisher's exact $test_{[9]}$=14.7, P=0.10) nor between fishing zones (Fisher's exact $test_{[3]}$=3.3, P=0.35, Table 10). Fishes in the majority of prey families (n=11) lived in the demersal reef habitat (Table 9), which was the most important source of prey for *P. leopardus* (61% by number, IRI=67%, Table 10). Prey in three or four families lived in each of the benthic reef, midwater, and adjacent sandy habitats (Table 9). The large number of midwater prey at Potter Reef (Table 10) reflected the relatively large number of Caesionidae consumed at this reef (Table 4).

Discussion

Overall, the diets of *P. leopardus* from reefs in the two fishing zones were not dissimilar. Dietary overlap was high between *P. leopardus* from the reefs with open zones and reefs with closed zones for eight years. When compared to natural variation in diet among *P. leopardus* on the GBR, these values of overlap were very high because there was less similarity in the diet among regional populations of *P. leopardus* (Schoener a value of dietary overlap ranged from 0.26 to 0.42, St John, 1995) and at one reef sampled over time (Schoener a value of dietary overlap ranged from 0.44 to 0.84, St John, 1995). Generally, feeding behavior of *P. leopardus* was similar between fishing zones.

The lack of dietary differences between *P. leopardus* on open and closed reefs is consistent with the lack of meaningful trends in comparing the size and age structures of these populations. Using the catch of both fishing methods, Brown et al.[7] found a slightly higher abundance of legal-size (>38 cm TL) leopard coralgrouper on the closed reefs, as well as a greater proportion of older fish (4+ year class). But, fishing affected the size and age structure of populations on the two open reefs very differently; Nathan Reef showed a large recruitment of the one year class (Brown et al.[7]) and differed from all other reefs. In visual surveys of *P. leopardus* at the four reefs, Brown et al.[7] detected a greater density of larger *P. leopardus* on closed reefs. In contrast, Ayling and Ayling[6] found no differences between fishing zones in the density, average length, and recruitment of *P. leopardus* when surveying the same reefs

just prior to Brown et al.[7] Because decreases in abundance and size of populations are widely recognized as evidence of fishing pressure (Russ, 1991; Jennings and Lock, 1996), fishing pressure between the two zones in this study did not appear to vary.

Eight years of effective protection from substantial fishing pressure should have produced detectable differences in the structure of populations of *P. leopardus* on these closed and open reefs. Generally, studies on the GBR have shown an increase in average size of *P. leopardus* popula-

Table 7

Abundance (in number and percentage) of prey belonging to families in the diet of *P. leopardus* caught by the two fishing methods. Families of fishes living in the midwaters are underlined.

	Line		Spear		
Prey families	Number	%	Number	%	Total
Pomacentridae	2	9.5	45	27.3	47
Labridae	1	4.8	36	21.8	37
Clupeidae	11	52.5	20	12.1	31
Caesionidae	1	4.8	11	6.6	12
Synodontidae	2	9.5	8	4.8	10
Scaridae			8	4.8	8
Blenniidae			7	4.2	7
Acanthuridae	1	4.8	5	3.0	6
Apogonidae			6	3.6	6
Serranidae	1	4.8	4	2.4	5
Engraulidae			3	1.8	3
Fistulariidae	2	9.5	1	0.6	3
Gobiidae			2	1.2	2
Balistidae			1	0.6	1
Creedidae			1	0.6	1
Lutjanidae			1	0.6	1
Monacanthidae			1	0.6	1
Nemipteridae			1	0.6	1
Platycephalidae			1	0.6	1
Plesiopidae			1	0.6	1
Scorpaenidae			1	0.6	1
Siganidae			1	0.6	1
Total	21		165		186
No. of *P. leopardus* with prey	38		342		380

Table 8

Results of Fisher exact tests for the number of prey per family. Information in brackets is Fisher's exact test statistic, degrees of freedom (df), and exact probability levels (*P*). Significance of tests is denoted by ** for $P<0.01$ and * for $P<0.05$, and ns is nonsignificant. Comparisons between fishing zones and fishing methods are tested at $P = 0.01$ level of significance (see "Materials and methods" section for explanation).

Dietary differences among *P. leopardus*				
Fishing zones		Locations		Fishing methods
Open vs. closed (reefs pooled)		North vs. south (reefs pooled)		Speared vs. line caught (reefs pooled)
ns		*		ns
(28.3, df= 21, P=0.046)		(29.0, df=21, P=0.040)		(34.2, df=21, P=0.034)
Open reefs	Closed reefs	North reefs	South reefs	Among 4 reefs
*	ns	ns	ns	**
(22.5, df=16, P=0.056)	(18.5, df=15, P=0.908)	(23.2, df=20, P=0.135)	(19.8, df=11, P=0.155)	(75.2, df=63, P=0.007)

tions on reefs after closure (summarized in Williams and Russ, 1994). Also, population density of *P. leopardus* has differed in other closed-versus-open fishing zones in the Marine Park (Ayling et al., 1991). In contrast, the size structure of populations of *P. leopardus* on four reefs in the GBR showed no effect of protection from fishing after 3–4 years of reef closure (Ferreira and Russ, 1995). Possible reasons for an absence of the effects of fishing include migration by *P. leopardus* among reefs and small differences in the actual fishing pressure between open and closed zones. Other studies on movement of *P. leopardus* indicate that migration of 5–10 km between reefs would be highly unlikely (Davies, 1995; Zeller, 1997). Of a tagged population of 4627 *P. leopardus* on five reefs on the GBR, only 1% moved between reefs in a period of 22 months and only 2% travelled distances of 5–7.5 km (Davies, 1995). Fishing pressure was not measured on any of our four reefs during the eight years of protection, so it is possible that fishing pressure was low on the open reefs; however it seems more likely that the "closed" reefs were fished illegally. Such violations are thought to be relatively common on the GBR, and illegal fishing of these prized food fishes is probably widespread throughout tropical waters. Another documented example of violations of a fishing regulation for a large grouper is found in the Florida Keys, where bans on harvesting Nassau grouper (*Epinephelus striatus*) appeared to be ineffective (Sluka and Sullivan, 1998).

The diet of *P. leopardus* in our study did not differ between fishing zones when families of prey were assessed by either their relative importance in the diet (dietary overlap) or their number of prey. Patterns between fishing zones occurred in four of the 22 families but were considered weak because they were not detected statistically. Pomacentridae and Labridae, which ranked first and second respectively at all four reefs, were more important in the diet in the closed reefs, whereas Scaridae and Synodontidae were more important in the diet on open reefs. Information on prey availability on each reef may explain these results. Lastly, proportions of prey consumed from each of the four habitats were similar among reefs, suggesting that feeding behavior of *P. leopardus* did not differ among these reefs

Two aspects of the diet of *P. leopardus* differed between the locations of the reef pairs. Rare prey families, which occurred only once in the diet in the entire study, were more common at the two northern reefs (eight families) than at the southern pair (one family). Also, *P. leopardus* from the two southern reefs consumed more of the large schooling Caesionidae. However, location of the reefs alone may not explain these patterns because reef location is confounded with time of sampling in our study. The southern pair of reefs was sampled one month after the northern pair.

Similar to other dietary studies of adult *P. leopardus* on the GBR (Choat, 1968; Goeden, 1978; Kingsford, 1992; St John 1995, 1999), our study confirmed that leopard coralgroupers are highly

Table 9

The 22 families of prey classified into four broad habitats on the reef: demersal reef (associated with substrata), benthic reef (strongly associated with reef substrata), midwater and adjacent sands.

Demersal	Benthic	Midwater	Adjacent sands
Acanthuridae	Blenniidae	Caesionidae	Creedidae
Apogonidae	Gobiidae	Clupeidae	Nemipteridae
Balistidae	Scorpaenidae	Engraulidae	Platycephalidae
Labridae		Fistulariidae	Synodontidae
Lutjanidae			
Monacanthidae			
Pomacentridae			
Plesiopidae			
Scaridae			
Serranidae			
Siganidae			

Table 10

Number of prey in the diet of *P. leopardus* on the four reefs in each of the four habitats (demersal reef, benthic reef, midwater, and adjacent sands). Total number and percentage of prey as well as importance of prey in the diet (IRI, index of relative importance) in each habitat are included.

	Open		Closed		Total		
Habitat	North (Nathan)	South (Potter)	North (Wardle)	South (Noreaster)	Number	%	IRI %
Demersal reef	32	29	22	31	114	61.3	67.0
Benthic reef	4	1	5	0	10	5.4	6.6
Midwater	14	19	9	7	49	26.3	19.7
Adjacent sands	5	3	3	2	13	7.0	6.7
Total	55	52	39	40	186		100

piscivorous. Thus, unlike other less piscivorous coral reef serranids (Hobson, 1965; Randall, 1965; Harmelin-Vivien and Bouchon, 1976; Shpigel and Fishelson, 1989), adult *P. leopardus* rely almost entirely on one general type of food (but juveniles consume crustaceans, St John, 1999). Also, nearly half of their diet (IRI=48.4%) comprised just two families of fishes, Pomacentridae and Labridae, but this finding does not suggest that the food supply of *P. leopardus* was limited. *Plectropomus leopardus* have been reported to consume more than 20 species in each of these two families (St John, 1995), which are highly diverse and abundant on coral reefs. On the GBR, Pomacentridae, with some 120 species, is the most numerically abundant family, and Labridae represents the second most speciose family (Randall et al., 1990). Therefore, the diet of *P. leopardus* was not dependent on a few species.

The variety of prey fishes in the diet of *P. leopardus* reflects the groupers large home range (Samoilys, 1997; Zeller, 1997) that includes several habitats (Goeden, 1978; Kingsford, 1992; Samoilys, 1997). *Plectropomus leopardus* consumed fishes in families that lived in all four broad habitats on coral reefs: adjacent sands, midwater, benthic reef substrata, and demersal reef substrata. Yet, prey from the demersal reef environment and the midwaters were six times more important than prey in the other two habitats. The diverse and abundant families of fishes that live on or over adjacent sands, or dwell among the benthic reef substrata (e.g. Gobiidae and Blenniidae) were not important food for adult *P. leopardus*. Similarly, piscivores reported from coral reefs elsewhere have usually focused on prey in reef habitats. In the Caribbean, tethered prey consistently disappeared from sites close to areas of natural reef rather than from areas of adjacent sediment (Shulman, 1985), and rates of encounter with predators for surgeonfishes in bottles were highest at reef edges compared with other sediment habitats (Sweatman and Robertson, 1994).

Lastly, the results of our study suggest several differences in the catch and diet of *P. leopardus* caught by the two fishing methods. Such information is useful for managers when considering the impacts of different types of fishing methods on the fish population. Line fishing catches larger fish than nonselective spear fishing; however nonselective spear fishing probably never occurs in the real fishery. Based on the comparison of line catch and spear catch, baited lines appear to attract a higher proportion of hungry *P. leopardus* to common fishing sites, but predators may leave the site after they have eaten bait. Therefore, line fishing can affect the trophic ecology of *P. leopardus* reef-wide, even when it is concentrated at just a few sites on reefs. Also, line fishing may alter patterns of movement of *P. leopardus* temporarily, and such opportunistic behavior will be difficult to detect in movement studies on this species (e.g. Samoilys, 1997; Zeller, 1997). Thus, when reefs are partitioned into different fishing zones, line fishing could facilitate the movement of *P. leopardus* across reserve boundaries from protected areas. In one study on the GBR, *P. leopardus* had low flux rates across reserve boundaries (Zeller and Russ, 1998). Another, more tentative, result of our study is that line-caught fish appear to eat more midwater pelagic fishes, which suggests that line fishermen or the methods used in line fishing target *P. leopardus* hunting this prey. Whether line fishermen chose sites where pelagic schooling fishes congregate (e.g. near the reef edge) or whether pelagic prey are attracted to a fishing site after fishermen burley the waters, is uncertain.

In conclusion, eight years after reefs have been closed to fishing, no differences that could be linked to zoning were detected in size structure of populations and diets of *P. leopardus*. Results of this dietary study, however, can offer some insights for the management of the *P. leopardus* fishery. Even though fish are the dominant food of this predator, and the main fish prey are associated with the coral reef substrata, *P. leopardus* are not dependent on a narrow range of species for food. A diverse mixture of Pomacentridae and Labridae species represents nearly half of their diet, and overall, the diet of *P. leopardus* is sufficiently broad to be resilient to the depletion of several species of prey.

Acknowledgments

We acknowledge and thank two anonymous referees for pertinent comments about the manuscript, Tony Ayling for providing his visual census data, the Squire family for accommodating J. St John, and the staff of the Northern Fisheries Center for the use of their facilities. This research was supported by the Great Barrier Reef Marine Park Authority, a Freda Bage Fellowship (Australian Federation of University Women, Queensland) to J. St John, and Australian Research Council funds to G. R. Russ.

Literature cited

Allen, G. R.
1975. Damselfishes of the South Seas. TFH Publications, Neptune City, NJ, 271 p.

Ayling, A. M., A. L. Ayling, and B. D. Mapstone.
1991. Possible effects from protection by fishing pressure on recruitment rates of the coral trout (*Plectropomus leopardus*: Serranidae). *In* Recruitment processes (D. A. Hancock, ed.), p. 210–215. Australian Society for Fish Biology Workshop, Hobart, August 1991.

Beddington, J. R.
1984. The responses of multispecies systems to perturbations. *In* Exploitation of marine communities (R. M. May, ed.), p. 209–225. Springer-Verlag, Berlin.

Beddington, J. R., and R. M. May.
1982. The harvesting of interacting species in a natural ecosystem. Sci. Am. 247:42–49.

Bohnsack, J. A.
1982. Effects of piscivorous predator removal on coral reef fish community structure. *In* Gutshop '81: fish food habit studies (G. M. Caillet and C. A. Simenstad, eds.), p. 258–267. Wash. Sea Grant Publ., Seattle, WA.

Bohnsack, J. A., D. E. Harper and D. B. McClellan.
1994. Fisheries trends from Monroe County, Florida. Bull. Mar. Sci. 54:982–1018.

Caley, M. J.
1993. Predation, recruitment and the dynamics of communities of coral-reef fishes. Mar. Biol. 117:33–43.

Carr, M. H. and M. A. Hixon.
1995. Predation effects on early post-settlement survivorship of coral reef fishes. Mar. Ecol. Prog. Ser. 124:31–42.
Choat, J. H.
1968. Feeding habits of and distribution of *Plectropomus maculatus* Serranidae at Heron Island. Proc. R. Soc. Qd. 80(2):13–18.
Cohen, J.
1988. Statistical power analysis for the behavioral sciences (2nd ed.). Lawrence Erlbaum Associates, Hillsdale, NJ, 567 p
Craik, G. J. S.
1981. Underwater survey of coral trout *Plectropomus leopardus* Serranidae populations in the Capricornia Section of the Great Barrier Reef Marine Park. Proc. 2nd Int. Cor. Reef Symp. 1:54–58.
Davies, C.
1995. Patterns of movement of three species of coral reef fish on the Great Barrier Reef. Unpubl. Ph. D. diss., Dept. of Marine Biology, James Cook University of North Queensland, Australia, 170 p.
Ferreira, B. P., and G. R. Russ.
1995. Population structure of the leopard coralgrouper, *Plectropomus leopardus*, on fished and unfished reefs off Townsville, Central Great Barrier Reef, Australia. Fish. Bull. 93:629–642
Goeden, G. B.
1978. A monograph of the coral trout *Plectropomus leopardus*. Res. Bull. Qld. Fish. Ser. 1:1–42.
1982. Intensive fishing and a 'keystone' predator species: ingredients for community instability. Biol. Conserv. 22: 273–281.
Grigg, R. W., J. J. Polovina, and M. J. Atkinson.
1984. Model of a coral reef ecosystem. III: Resource limitation, community regulation, fisheries yield and resource management. Coral Reefs 3:23–27.
Harmelin-Vivien, M. L., and C. Bouchon.
1976. Feeding behavior of some carnivorous fishes (Serranidae and Scorpaenidae) from Tulear (Madagascar). Mar Biol 37:329–340.
Heemstra, P., and J. Randall.
1993. FAO species catalogue. Vol 16: Groupers of the world family Serranidae, subfamily Epinephelinae: an annotated and illustrated catalogue of grouper, rockcod, hind, coral grouper and lyretail species known to date. FAO Fisheries Synopsis, FAO, Rome, 383 p.
Hixon, M. A.
1991. Predation as a process structuring coral-reef fish communities. *In* The ecology of fishes on coral reefs (P. F. Sale, ed.), p. 475–508. Academic Press, San Diego, CA.
Hixon, M. A. and J. P. Beets.
1993. Predation, prey refuges, and the structure of coral-reef fish assemblages. Ecol. Monogr. 63(1):77–101.
Hobson, E. S.
1965. Diurnal-nocturnal activity of some inshore fishes in the Gulf of California. Copeia 1965:291–302.
Jennings, S., and J. M. Lock.
1996. Population and ecosystem effects of reef fishing. *In* Reef fisheries (N. V. C. Polunin and C. M. Roberts, eds.), p. 193–218 Fish and fisheries series. Chapman and Hall, London.
Jennings, S., and N. V. C. Polunin.
1997. Impacts of predator depletion by fishing on the biomass and diversity of non-target reef fish communities. Coral Reefs 16:71–82.
Kingsford, M. J.
1992. Spatial and temporal variation in predation on reef fishes by coral trout (*Plectropomus leopardus*, Serranidae). Coral Reefs 11:193–198.
Koslow, J. A., F. Hanley, and R. Wicklund.
1988. Effects of fishing on reef fish communities at Pedro Bank and Port Royal Cays, Jamaica. Mar. Ecol. Progr. Ser. 43:210–212.
Kulbicki, M.
1998. How the acquired behaviour of commercial reef fishes may influence the results obtained from visual censuses. J. Exp. Mar. Biol. Ecol. 222:11–30.
Langton, R. W.
1982. Diet overlap between Atlantic Cod, *Gadus morhua*, silver hake, *Merluccius bilinearis*, and fifteen other northwest Atlantic finfish. Fish. Bull. 804:745–759.
Masuda, H., K. Amaoka, C. Araga, T. Uyeno, and T. Yoshino.
1984. The fishes of the Japanese archipelago. Tokai Univ. Press, Tokyo, 374 p.
Mehta, C., and N. Patel.
1992. StatXact. CYTEL Software Corporation, Cambridge, 442 p.
Myers, R. F.
1991. Micronesian reef fishes: a practical guide to the identification of the inshore marine fishes of the tropical and central Pacific, 2nd ed. Coral Graphics, Barrigada, Guam.
Norris, J. E.
1985. Trophic relationships of piscivorous coral reef fishes from the Northwestern Hawaian Islands. M.S. thesis, Univ. Hawaii, Honolulu, HI, 71 p.
Norris, J. E. and J. D. Parrish
1988. Predator-prey relationships among fishes in pristine coral reef communities. Proc. 6th Intl. Coral Reef Symp. 2:107–113.
Parker, R. R.
1963. Effects of formalin on length and weight of fishes. J. Fish. Res. Board Canada 20(6):1441–1455.
Parrish, J. D.
1987. The trophic biology of snappers and groupers. *In* Tropical snappers and groupers: biology and fisheries management (J. J. Polovina and S. Ralston, eds.), p. 405–463. Westview Press Inc., Boulder, CO.
Polunin, N. V. C. and C. M. Roberts.
1996. Reef fisheries. *In* Fish and fisheries series, p. 193–218. Chapman and Hall, London.
Ralston, S.
1987. Mortality rates of snappers and groupers. *In* Tropical snappers and groupers: biology and fisheries management (J. J. Polovina and S. Ralston, eds.), p. 375–404. Westview Press Inc., Boulder, CO.
Randall, J. E.
1965. Food habits of the Nassau grouper (*Epinephelus striatus*) 6th meeting. Assoc Island Mar Labs Caribb. 6:13–16.
1987. A preliminary synopsis of the groupers (Perciformes: Serranidae: Epinephelinae) of the Indo-Pacific region. *In* Tropical snappers and groupers: biology and fisheries management (J. J. Polovina and S. Ralston, eds.), p. 89–187. Westview Press Inc., Boulder, CO.
Randall, J. E., G. R. Allen, and R. C. Steene.
1990. Complete diver's and fisherman's guide to fishes of the Great Barrier Reef and Coral Sea. Crawford House Press, Bathurst, 507 p.
Roberts, C. M., and N. V. C. Polunin.
1991. Are marine reserves effective in management of reef fisheries? Rev. Fish Biol. Fisheries 1:65–91.
Russ, G. R.
1985. Effects of protective management on coral reef fishes

in the central Philippines. Proc. 5th Int. Coral Reef Congr. 4:219–224.

1991. Coral reef fisheries: effects and yield. *In* The ecology of fishes on coral reefs (P. F. Sale, ed.), p. 601–636. Academic Press, San Diego, CA.

Russ, G. R. and A. C. Alcala.

1996. Marine reserves: rates and patterns of recovery and decline of large predatory fish. Ecol. Applic. 6:947–961.

1998a. Natural fishing experiments in marine reserves 1983–1993: community and trophic responses. Coral Reefs 17:383–397.

1988b. Natural fishing experiments in marine reserves 1983–1993: roles of life history and fishing intensity in family responses. Coral Reefs 17:399–416.

Sadovy, Y.

1994. Grouper stocks of the Western Central Atlantic: the need for management and management needs. Proc. Gulf Caribb. Fish. Inst. 43:43–64.

Samoilys, M. A.

1997. Movement in a large predatory fish: coral trout, *Plectropomus leopardus* (Pisces: Serranidae) on Heron Reef, Australia. Coral Reefs 16:151–158.

Schoener, T. W.

1970. Nonsynchronous spatial overlap of lizards in patchy habitats. Ecology 513:408–418.

Shpigel, M., and L. Fishelson.

1989. Habitat partitioning between species of the genus Cephalopholis (Pisces Serranidae) across the fringing reef of the Gulf of Aqaba (Red Sea). Mar. Ecol. Prog. Ser. 58:17–22.

Shulman, M. J.

1985. Recruitment of coral reef fishes: effects of distribution of predators and shelter. Ecology 66(3):1056–1066.

Sluka, R., and K. Sullivan.

1998. The influence of spear fishing on species composition and size of groupers on patch reefs in the upper Florida Keys. Fish. Bull. 96:388–392.

Smith, M. M., and P. C. Heemstra.

1986. Smith's sea fishes. Springer-Verlag, Berlin, 1047 p.

Sokal, R. R., and F. J. Rohlf.

1981. Biometry, 2nd ed. W.H. Freeman, San Francisco, CA, 859 p.

Steneck, R. S.

1998. Human influences on coastal ecosystems: Does overfishing create trophic cascades? Tree 13(11):429–430.

St John, J.

1995. Feeding ecology of the coral trout, *Plectropomus leopardus* Serranidae on the Great Barrier Reef, Australia. Ph.D. diss., James Cook University of North Queensland, Townsville, Australia, 277 p.

1999. Ontogenetic changes in the diet of a large coral reef grouper *Plectropomus leopardus* (Serranidae): patterns in taxa, size and habitat of prey. Mar. Ecol. Prog. Ser. 233–246.

Sweatman, H. P. A.

1984. A field study of the predatory behaviour and feeding rate of a piscivorous coral reef fish, the lizardfish *Synodus englemani*. Copeia 84:187–193.

Sweatman, H. P. A., and D. R. Robertson.

1994. Grazing halos and predation on juvenile Caribbean surgeonfishes. Mar. Ecol. Prog. Ser. 111:1–6.

Trainor, N.

1991. Commercial line fishing. The Queensland Fisherman, March 9(3):17–24.

Williams, D. M., and G. R. Russ.

1994. Review of data on fishes of commercial and recreational fishing interest on the Great Barrier Reef. Vol. I: Research publication 33. Great Barrier Reef Marine Park Authority, Townsville, Australia, 103 p.

Zeller, D. C.

1997. Home range and activity patterns of the coral trout *Plectropomus leopardus* (Serranidae). Mar. Ecol. Prog. Ser. 154:65–77.

Zeller, D. C., and G. R. Russ.

1998. Marine reserves: patterns of adult movement of the coral trout (*Plectropomus leopardus* (Serranidae)). Can. J. Fish Aquat. Sci. 55:917–924.

Estimating tag-shedding rates for skipjack tuna, *Katsuwonus pelamis*, off the Maldives

M. Shiham Adam

Renewable Resources Assessment Group
T. H. Huxley School of Environment, Earth Sciences and Engineering
Imperial College of Science Technology and Medicine, RSM Building
Prince Consort Road
London SW7 2BP, United Kingdom
Present address: Pelagic Fisheries Research Program
Joint Institute of Marine and Atmospheric Research
University of Hawaii at Manoa
Honolulu, Hawaii 96822
E-mail address: msadam@soest.hawaii.edu

Geoffrey P. Kirkwood

Renewable Resources Assessment Group
T. H. Huxley School of Environment, Earth Sciences and Engineering
Imperial College of Science, Technology and Medicine
RSM Building, Prince Consort Road
London SW7 2BP, United Kingdom

One source of uncertainty in fishery assessments based on tag release and recapture data arises from tag shedding—the loss of tags from fish from the time of tagging until tag recovery. Independent estimation of tag-shedding rates from double tagging experiments is an integral part of well-designed tagging experiments. Failure to allow for tag shedding can result in biases in estimates of important parameters derived from tag-recapture data, such as fishery-induced and natural mortality, and migration rates. A wide variety of methods have been proposed for estimating shedding rates using data from double tagging experiments, the variety in part resulting from the nature of the data available from the experiments. The earlier literature has been well integrated and reviewed by Wetherall (1982). More recently, Xiao (1996) has developed a general model that unifies the estimation of tag-shedding rates from double tagging experiments with exact and pooled times at liberty. Some recent examples of application of these methods include Xiao et al. (1999) for school gummy shark and Fabrizio et al. (1999) for lake trout.

Tag shedding is of two types (Wetherall, 1982). Type-I shedding is a one-time event and occurs immediately after tagging, usually as a result of suboptimal placement of tags in the fish. Effectively, it reduces the number of tags initially put out to sea. Type-II shedding is the loss of a tag or both tags over a period of time after the fish has been tagged and released back into the sea. For long-lived species, it may not occur at a constant rate because some tags are likely to have been applied more effectively than others, and some may become firmly embedded (with growth of muscle tissues), such that they are very unlikely to be detached from the fish (Kirkwood, 1981).

The Ministry of Fisheries and Agriculture, Maldives, carried out two tagging experiments: one in 1990–91 (Yesaki and Waheed, 1992) and the other between 1993 and 1995 (Anderson et al., 1996). The latter tagging experiment included a double tagging experiment in which 504 skipjack tuna, *Katsuwonus pelamis*, were double tagged, by using the same type of tags and techniques of tagging as used in the single tagging experiment (Anderson et al., 1996). As of end 1996, a total of 53 of these fish had been recovered. These data are considered to be of immediate importance for designing large-scale experiments in the Indian Ocean, strategic tagging simulation studies (e.g. Bertignac, 1996), and for comparing the estimated rates with those obtained from similar tuna double tagging experiments conducted elsewhere. Our note reports estimates of tag-shedding rates carried out in the Maldives.

Materials and methods

Tagging methods

Tagging was conducted on board local vessels fishing for skipjack tuna with pole-and-line gear using livebait. Plastic dart tags (100 mm × 1.5 mm diameter), manufactured by Hallprint™, Australia, were used throughout the experiment. The captured fish were gently placed on deck, quickly slipped onto a wet wooden measuring board, and held in place by biologists wearing cotton gloves. The first tag was inserted dorsally on the left-hand side, at an acute angle adjacent to the second dorsal fin so that the barb was caught under the fin-ray extension or the neural spine. The second tag was inserted about 1–2 cm posterior to the first on the right-hand side in the same manner. Consecutively numbered pairs of tags were used; even numbers were inserted on the left-hand side and odd numbers on the right. Where possible, fish were returned to the water, facing the vessel's bow, in a slightly head-down fashion. Tagging times (from hooking to release into the sea) ranged from 14 to 18 seconds. More details of the tagging program can be found in Yesaki and Waheed (1992) and Anderson et al. (1996).

Parameter estimation

The method of parameter estimation used here is the maximum likelihood approach introduced by Kirkwood and Walker (1984) and later extended by Hampton and Kirkwood (1990) and Hampton (1997). This method was developed for use with sets of data where recaptured fish are few, and with few fish that have shed a tag, provided that

Manuscript accepted 21 July 2000.
Fish. Bull. 99:193–196 (2001).

exact dates of recovery are known, as was the case with the data from the Maldives.

Following Kirkwood and Walker (1984), consider an originally single tagged fish. Assuming that α is the type-I retention probability (1−type-I shedding probability) and λ is the type-II shedding rate, assumed to be constant for short-lived species such as the skipjack tuna, then for an originally single tagged fish, the probability of a tag being retained at time t is given by

$$Q(t) = \alpha \exp(-\lambda t). \quad (1)$$

Suppose that fish are double tagged with identical tags and released at time $t = 0$, and let $p_i(t)$ be the probability that the fish is alive and at liberty retaining i (i=0, 1, 2) tags at time t. Then, under the assumption that both tags are retained after immediate shedding and have independent and identical probabilities,

$$\begin{aligned} p_0(t) &= [1 - Q(t)]^2 \\ p_1(t) &= 2Q(t)[1 - Q(t)] \quad (2) \\ p_2(t) &= Q(t)^2. \end{aligned}$$

In practice, identifiable recaptures will consist only of fish retaining either one tag or two tags. If $P'_i(t)$ is the probability that an originally double-tagged fish, recaptured at time t_i, is reported to have retained i tags (i=1, 2), then conditional on the retention of at least one tag, the probability of capturing a fish retaining two tags at time t is

$$P'_2(t) = \frac{p_2(t)}{1 - p_0(t)} \quad (3)$$

and the probability of capturing a fish retaining only one tag at time t is

$$P'_1(t) = \frac{p_1(t)}{1 - p_0(t)}. \quad (4)$$

Suppose n fish were recaptured in the experiment and reported to have retained at least one tag on recapture, and that the ith fish was recaptured at time t_i. Define indicator variables $N_i^{(2)} = 1, N_i^{(1)} = 0$ if two tags were reported upon recapture, and $N_i^{(2)} = 0, N_i^{(1)} = 1$ if only one tag was reported upon recapture.

It follows from Equations 3 and 4 that if all fish suffer the same risks of mortality, the log likelihood (ψ) of the data conditional on recapture times $\{t_i, i=1, 2, \ldots, n\}$ is given by

$$\psi(\alpha, \lambda) = \sum_{i=1}^{n} N_i^{(2)} \ln\left[P'_2(t_i)\right] + N_i^{(1)} \ln\left[P'_1(t_i)\right]. \quad (5)$$

Maximum likelihood estimates of the parameters (α,λ) and their asymptotic standard errors were found by maximizing ψ with respect to them, by using the nonlinear minimization routines in AD Model Builder (Otter Research Ltd., 1996).

Results

The numbers of recoveries of originally double tagged fish reported as retaining one (indicating left- or the right-side tag) or two tags on recapture are shown in Table 1, with their times at liberty.

The maximum likelihood estimate of λ was 0.22/yr (SE=0.13) and that of α was 0.97 (SE=0.03). If α = 1, the maximum likelihood estimate of λ was 0.30/yr (SE=0.065/yr). A likelihood ratio test (Cox and Hinkley, 1974) shows that the full model does not provide a significantly better fit to the data (at 5% level) than its special case (α=1) (P=0.146).

Discussion

One of the most important assumptions in double-tagging experiments and in the model used in our analysis is that shedding rates of the first and second tags is the same (Hearn et al., 1991). A simple way to investigate possible differences in the shedding rates of the first and second tags is to examine the number of returns of fish that have retained either the first or the second tag and their temporal distribution. There were seven recoveries of fish reported to have retained a single tag, of which four fish retained the left tag and three retained the right tag (Table 1). Although few, the similar numbers of recaptured fish with tags on the left side as those on the right side and the temporal distribution of these fish (Table 1) show clearly that there is no evidence of differences in their shedding rates.

Another important assumption, but one that might easily be violated, and that is difficult to test, relates to the way in which double-tagged recoveries were reported. The common assumption (as made here) is that recoveries of fish retaining double tags were always reported as a pair, and never as a "single" tag recovery. It is also assumed that the probability of reporting fish recovered with single or double tags is the same. Hampton (1997) showed that under this assumption, the reporting probability has no influence on the maximum likelihood estimates of α and λ. Given the publicity and incentives to return all the recaptured tags (Anderson et al., 1996), and the procedures adopted in tagging, it is highly unlikely that these reporting-rate assumptions were violated in the Maldives tagging program.

In their original paper describing the method of analysis and application to small data sets, Kirkwood and Walker (1984) noted that potential bias arises because the resulting estimates are conditional on the times of recapture; a different time sequence of recapture times would result in different parameter estimates. Clearly, this potential bias arose in our experiment. Ideally, for robust estimation of the parameters, one would need a data set with large numbers of fish that have shed a tag. This point needs to be borne in mind when designing future tagging experiments for skipjack tuna in the Indian Ocean.

The type-II shedding rate estimate obtained from our experiment is similar to those obtained by Hampton and Kirkwood (1990) for southern bluefin tuna tagged and released during the 1960s and 1970s. However, recent estimates of type-II shedding rates obtained for skipjack tuna from the tropical western Pacific were much lower than those estimated in our study, as were estimates for southern bluefin tuna tagged in 1984 (Table 2). These differences in shedding estimates may be due to differences in the tagging method used and the use of measuring boards instead of cradles. Estimates of λ obtained for fish tagged on measuring boards ranged from 0.17 to 0.22/yr. For fish tagged in cradles, the corresponding range of estimates of λ was 0.05–0.09/yr (Table 2).

In the South Pacific Commission (SPC) double tagging experiments of 1989–92 (Hampton, 1997) and in the CSIRO experiment of 1984 (Hampton and Kirkwood, 1990), specially designed vinyl cradles were used to position the fish dorsal side up, making it easier to insert the tags. It is also likely that such cradles may have helped to keep fish calm, perhaps because the eyes of the fish were covered. In the Maldives experiment, the CSIRO experiments of 1963–77 and the Western Australian Department of Fisheries' experiment of 1970–78 (Hampton and Kirkwood, 1990), measuring boards were used. In many instances in the Maldivian experiment, the fish, particularly large individuals, struggled quite a lot while being tagged. This may have caused additional trauma to the fish and at the same time may have increased the likelihood of the tag being placed suboptimally, thereby increasing the apparent tag-shedding rate. Some fish handlers of the Maldivian tagging program observed that fish struggled less if they were gently laid on the board and the eye was quickly covered with one hand. This technique, however, was not applied universally.

Hampton and Kirkwood (1990) suggested that differences in shedding rates observed in the southern bluefin tuna experiments might also be due to differences in the quality of the tags used. Tags used in the earlier experiments (1960s and 1970s) were inferior, because the streamers were prone to detach. Tags used in later experiments had their heads heat-fused to the shafts and thus were almost impossible to detach under normal conditions (Hampton, 1997). The tags

Table 1

Numbers of recoveries of originally double tagged fish retaining one (indicating which tag, left or right) or two tags on recapture, and times at liberty.

Days at liberty	1 tag	2 tags	Days at liberty	1 tag	2 tags
6		1	61		1
7		1	63		1
8		1	66		1
9		1	71		1
10		2	73		1
11	1 (L)	1	78		1
13		1	90		1
14		3	91		2
15		1	98		1
16		2	142	1 (R)	
17		1	146		1
18	1 (L)		154		1
19		1	191		1
20		2	210		1
21		1	230		1
23		1	240		1
36		1	258	1(L)	
50		1	279	1(R)	
52		1	335		1
59		2	341		1
60	1 (R)		433	1(L)	

Table 2

Comparison of tag shedding rates estimated by using the maximum likelihood method from different double tagging experiments, with data on exact dates of recovery for skipjack (SKJ) and southern bluefin tuna (SBT). CSIRO = Commonwealth Scientific and Industrial Research Organization, Tasmania, Australia; WA Dept. Fish. = Western Australia Department of Fisheries; SPC = South Pacific Commission. P/L = pole and line.

	Parameter estimates ±SE				
Species	α	λ (per yr)	Reference	Experiment	Tagging method
SKJ	0.97 ±0.03	0.22 ±0.13	Our study	Maldives 1993–95	P/L board
SBT	0.93 ±0.02	0.29 ±0.05	Hampton and Kirkwood, 1990	CSIRO 1963–70	P/L board
SBT	0.97 ±0.006	0.17 ±0.01	Hampton and Kirkwood, 1990	CSIRO 1963–70	P/L board
SBT	0.96 ±.0.01	0.17 ±0.04	Hampton and Kirkwood, 1990	CSIRO 1977	P/L board
SBT	0.90 ±0.02	0.19 ±0.05	Hampton and Kirkwood, 1990	WA Dept. Fish. 1970–78	P/L board
SKJ	0.97 ± —	0.09 ± —	Hampton, 1997[1]	SPC 1989–92	P/L cradle
SBT	0.97 ±.007	0.05 ±0.008	Hampton and Kirkwood, 1990	CSIRO 1984	P/L cradle

[1] Estimates obtained by using pooled data.

used in the Maldivian experiment were recently manufactured and therefore this source of bias was unlikely. The higher tag shedding rate observed in the Maldivian data appears most likely to be due to the tagging method employed.

Ideally, experiment-specific double tagging experiments should be carried out to estimate independent experiment-specific tag-shedding rates. The above comparisons suggest that, in cases where independent estimates are not available, care must be exercised when applying estimates of tag-shedding rates obtained from other tagging experiments, especially where different tagging techniques have been used.

Acknowledgments

The authors would like to thank Charles Anderson, Graham Pilling, and Robert Wakeford for their comments on the manuscript. In addition to providing the data, the staff of Marine Research Center, particularly Zaha Waheed and Ahmed Haifz, helped on numerous queries regarding the data. We thank the Hon. Hassan Sobir, former Minster of Fisheries and Agriculture, Maizan Hassan Maniku, Director General Marine Research Center, for their support in this study. The manuscript was improved by comments from two anonymous reviewers. The study was part of the Ph.D. research of the senior author at Imperial College, London, primarily funded by the Islamic Development Bank's Merit Scholarship Program.

Literature cited

Anderson, R. C., M. S. Adam, and A. Waheed.
1996. Tuna tagging activities in the Maldives. *In* Proceedings of the expert consultations on Indian Ocean tunas, 6th session, Colombo, Sri Lanka, 25–29 September 1995 (A. A. Anganuzzi, K. A. Stobberup, and N. J. Webb, eds.), p. 333–347. [Reprinted with minor revisions in Mald. Mar. Res. Bull. 2:83–116.]

Bertignac, M.
1996. A simulation model of tagging experiments for yellowfin tuna in the western Indian Ocean. *In* Status of interactions of Pacific tuna fisheries in 1995 (R. S. Shomura, J. Majkowski, and R. F. Harman, eds.), p. 162–177. FAO Fish. Tech. Paper 365.

Cox, D. R., and D. V. Hinkley.
1974. Theoretical statistics. Chapman and Hall, London, 511 p.

Fabrizio, M.C., J. D. Nicholas, J. E. Hines, B. L. Swanson, and S. T. Schram.
1999. Modelling data from double-tagging experiments to estimate heterogeneous rates of tag shedding in lake trout (*Salvelinus mamaycush*). Can. J. Aquat. Fish. Sci. 56(8):1409–1419.

Hampton, J.
1997. Estimation of tag reporting and tag-shedding rates in a large-scale tuna tagging experiment in the western tropical Pacific Ocean. Fish. Bull. 95:68–79.

Hampton, J., and G. P. Kirkwood.
1990. Tag shedding by southern bluefin tuna *Thunnus maccoyii*. Fish. Bull. 88:313–321.

Hearn, W. S., G. M. Leigh, and R. J. Beverton.
1991. An examination of a tag-shedding assumption, with application to southern bluefin tuna. ICES J. Mar. Sci. 48:41–51.

Kirkwood, G. P.
1981. Generalised models for the estimation of rates of tag shedding by southern bluefin tuna *Thunnus maccoyii*. J. Cons. Int. Explor. Mer 39:256–260.

Kirkwood, G. P., and M. H. Walker.
1984. A new method for estimating tag shedding rates, with application to data for Australian salmon, *Arripis trutta esper* Whitely. Aust. J. Mar. Freshwater Res. 35:601–606.

Otter Research Ltd.
1996. An introduction to AD Model Builder for use in non-linear modeling and statistics. Otter Research Ltd., Nanaimo, B.C., Canada, 68 p.

Wetherall, J. A.
1982. Analysis of double tagging experiments. Fish. Bull. 80(4):687–701.

Xiao, Y.
1996. A general model for estimating tag-specific shedding rates and tag interactions from exact or pooled times at liberty for a double tagging experiment. Can. J. Fish. Aquat. Sci. 53(8):1852–1861.

Xiao, Y., L. P. Brown, T. I. Walker, and A. E. Punt.
1999. Estimation of instantaneous rates of tag shedding for school shark, *Galeorhinus galeus* and gummy shark, *Mustelus antarcticus*, by conditional likelihood. Fish. Bull. 97(1):170–184.

Yesaki, M., and A. Waheed.
1992. Results of the tagging program conducted in the Maldives during 1990. IPTP (Indo Pacific Tuna Development and Management Program), 23 p.

The effect of sea state on estimates of abundance for beluga whales (*Delphinapterus leucas*) in Norton Sound, Alaska

Douglas P. DeMaster
National Marine Mammal Laboratory
National Marine Fisheries Service, NOAA
7600 Sand Point Way, NE
Seattle, Washington 98115
E-mail address: douglas.demaster@noaa.gov

Lloyd F. Lowry

Kathryn J. Frost
Alaska Department of Fish and Game
1300 College Road
Fairbanks, Alaska 99701

Rebecca A. Bengtson
National Marine Mammal Laboratory
National Marine Fisheries Service, NOAA
7600 Sand Point Way, NE
Seattle, Washington 98115

Beluga whales (*Delphinapterus leucas*) are relatively small odontocete cetaceans; standard lengths of newborn calves are about 160 cm and adults range from 300 to 450 cm (Doidge, 1990). At birth, calves are dark slate gray, and the color gradually lightens until they become pure white as adults (Brodie, 1989). When actively swimming or diving, their bodies break the surface only for brief periods. Frost et al. (1985) reported that the average length of surfacing intervals for two radio-tagged beluga whales were 0.9–2.2 seconds.

Aerial surveys are the most common method for estimating the abundance of beluga whales (e.g. Frost and Lowry, 1990; Richard et al., 1990; and Harwood et al., 1996). Beluga whales are readily seen from aircraft in calm, clear waters but become increasingly difficult to detect when the water is murky or when whitecaps are present. Although a reduction in detectability in higher sea states is expected, there have been no published reports to quantify this effect on beluga whale counts. Rather, researchers have usually restricted survey effort to conditions where whitecaps are uncommon (see Harwood et al., 1996). Under those conditions, it has been assumed that the probability of detecting a beluga, given it is at or near the surface, is independent of sea state.

Beluga whales are one of the more important species of marine mammals used by native subsistence hunters in Alaska, Canada, Greenland, and Russia (Lowry et al., 1989; Reeves, 1990; Harwood et al., 1996). To facilitate the sustained use of beluga whales by subsistence-based communities throughout the Arctic, it is necessary to determine safe levels for annual removals. One piece of information required for developing guidelines for these removals is a realistic estimate of the minimum population size (Wade, 1998). In the past, counts of beluga whales have been converted to estimates of abundance by using correction factors based on the following probabilities: 1) the probability that an animal is unavailable to be observed because of being submerged (Frost and Lowry[1]); 2) the probability that an adult-size animal at the surface was missed (Hobbs[2]); and 3) the probability a calf or yearling at the surface was missed (Brodie, 1971). We report the results of an analysis designed to determine whether sea state, as measured by the Beaufort (BF) scale, affects beluga whale density estimates. If such an effect is significant within the range of sea states that are routinely surveyed, failure to consider sea state effects would produce negatively biased estimates of beluga whale abundance.

Methods

Beluga whale aerial surveys were flown in the vicinity of Norton Sound, Alaska (Fig. 1), in June 1993, 1994, and 1995. Two primary observers were used during the line-transect surveys, one looking out each side of the aircraft. Within any particular year, the same observers flew the entire survey period and did not rotate positions. Surveys were flown between the hours of 0900 and 1800 local time. The survey was done in a passing mode, where whales were counted, while the survey aircraft remained on the trackline.

The survey aircraft was a twin-engine, high-wing Aero Commander. Mean air speed was 220 km/h during surveys, and the target survey altitude was 330 m. However, when cloud cover precluded survey effort at 330 m, the survey altitude was reduced to 264 m. Each of the viewing ports contained a flat window, which was marked with a grease pencil to establish five consecutive "bins" for recording sightings (Lowry and DeMaster[3]). An inclinome-

[1] Frost, K. J., and L. F. Lowry. 1995. Radio-tag based correction factors for use in beluga whale population estimation. Working paper for the Alaska Beluga Whale Committee, Scientific Workshop, 5–7 April 1995. [Available from ADF&G, 1300 College Road, Fairbanks, AK 99701.]

[2] Hobbs, R. 1998. Personal commun. National Marine Mammal Laboratory, 7600 Sand Point Way, NE., Seattle, WA 98115.

[3] Lowry, L. F., and D. P. DeMaster. 1996. Beluga whale surveys in Norton Sound, Alaska: June 1995. Alaska Beluga Whale Committee Report 96-2, 6 p. [Available from ADF&G, 1300 College Road, Fairbanks, AK 99701.]

Manuscript accepted 11 August 2000.
Fish. Bull. 99:197–201 (2001).

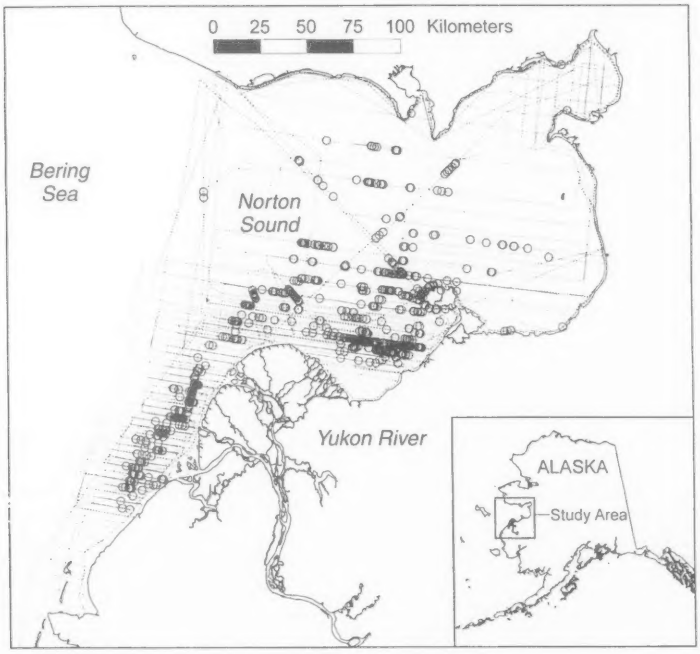

Figure 1

Map of the Norton Sound and Yukon River delta region showing beluga whale aerial survey transects flown in June 1993–95 (dashed lines). Circles reflect sightings of beluga whales, where all three years of data are combined.

ter was used to measure sighting angles for the bins. The inner edge of the first sighting bin was offset 330 m from the center of the track line, and the outer edge of the outer bin was 2100 m from the center of the track line. Position data were collected by means of an onboard global positioning system that sent data directly to a laptop computer. All sightings were reported by the observers to a third person who entered the data into the onboard laptop computer. A continuous record of sea state was maintained by the recorder, according to the BF scale (Table 1).

Within the study area, surveys were conducted along the coast and on offshore transects. Very few beluga whales were seen on the coastal flights and they were always on the shoreward side of the aircraft, very near shore. To minimize the effect of very low densities of beluga whales seen in a wide range of BF sea states in the coastal band (defined as survey effort conducted while the aircraft was centered approximately 1.1 km offshore), only survey data from the offshore transects were used in our analysis. The number of on-effort track miles surveyed during offshore transects was 10,362 km.

Survey data were analyzed with the computer program DISTANCE (Laake et al., 1994). Each sighting of beluga whales was considered to be a grouped cluster within a single sighting bin. Animals were sighted in juxtaposed bins only a few times. In those situations, the bin that included a majority of animals in the group was used to designate the sighting bin for that sighting. However, it should be noted that in this area at this time of year, we did not observe coherent schooling behavior of beluga whales. Rather, beluga whales were observed in highly dispersed linear aggregations. Therefore, analysis of group size by sea state was not undertaken because group size was predominantly a function of whether the transect was crossing or flying parallel to a "line" of beluga whales.

Table 1

Summary of the relationship between Beaufort (BF) sea state number, wind speed, and sea surface condition.

BF sea state	Wind speed (km/h)	Sea surface conditions
0	0	no ripples
1	1–5	ripples, no foam on crests
2	6–11	small wavelets, crests glassy
3	12–19	large wavelets, scattered whitecaps
4	20–28	small waves, numerous whitecaps
5	29–38	moderate waves, many whitecaps, some spray

Table 2

Summary of beluga whale densities (animals seen/km^2) from Norton Sound, Alaska, by Beaufort (BF) sea state number. Numbers in parentheses represent 95% confidence intervals.

BF sea state	1993	1994	1995
1	0.217 (0.115–0.409)	0.107 (0.048–0.243)	0.294 (0.122–0.710)
2	0.111 (0.060–0.207)	0.052 (0.032–0.087)	0.046 (0.015–0.142)
3	0.039 (0.022–0.069)	0.138 (0.075–0.256)	0.111 (0.043–0.288)
4	0.009 (0.003–0.031)	0.075 (0.015–0.367)	insufficient survey effort

Table 3

Summary of sighting statistics for beluga whales in Norton Sound, Alaska, by Beaufort (BF) sea state, for 1993–95 data combined. Densities were estimated as weighted average, where weights were proportional to survey effort.

BF sea state	No. of observations	Survey effort (km)	Average density (SE) (animals seen/km^2)
1	653	2343	0.206 (0.051)
2	416	3916	0.071 (0.014)
3	397	3618	0.069 (0.013)
4	19	490	0.053 (0.026)

The line-transect analysis was stratified by BF sea state. Using Eberhardt's (1968) multiple comparison test, we did not reject the null hypothesis that sea state specific density was independent of survey year; therefore, sighting data by BF sea state were pooled across years, where average density for each sea state was calculated as a weighted average proportional to distance searched. Differences in average density by BF sea state pooled across years and in the effective strip width by BF sea state in a given year were also tested using Eberhard's multiple comparison test, whereas differences in the average encounter rate by BF sea state were tested by using a goodness-of-fit test based on the number of sightings and survey effort for each BF sea state. All statistical tests were performed with the type-I error set at 0.05. The variance of the ratio of the estimated average density in BF sea state 1 to the weighted average density in BF sea states 2, 3, and 4 was estimated with the delta method (Seber, 1973). Search effort in BF sea state 0 and BF sea state 5 was conducted only in 1995 and was relatively small (e.g. 264 km of effort in BF sea state 0 and 50 km of effort in BF sea state 5); therefore, sightings data for these sea states were not used in our analysis.

Density estimates reported in our note have not been corrected for either the period of time that animals were underwater (and therefore not observable), or the number of animals at the surface that were missed. Further, it was necessary to assume that the actual density of beluga whales was independent of sea state and was relatively constant between years. Given the distribution of sightings observed during the three years of survey effort, this assumption seemed reasonable, except for the northern portion of Norton Sound, where beluga whales were not observed (Fig. 1). The proportion of total survey effort conducted in this area was relatively small (8%); whereas the percent of survey effort conducted in BF sea-state-1 conditions in this area was approximately three times the percent of survey effort in the overall survey (i.e. 63% vs. 23%). The effect of this heterogeneity in the distribution of sightings in relation to BF sea state was assumed to be negligible, although it was recognized that the bias associated with this factor would produce negatively biased density estimates in BF sea state 1 in contrast to other sea states.

Results and discussion

The yearly density estimates for beluga whales in June of 1993, 1994, and 1995 by sea-state category are presented in Table 2. In two of the three years, the highest annual density estimate always occurred in BF sea state 1. For the pooled data for all three years (Table 3), the encounter rate (i.e. number of sightings per km of survey effort) was not random with respect to sea state (chi square=403, $P<0.001$); the largest chi square value was associated with the number of sightings in BF sea state 1. In addition, the estimated density for BF sea state 1 was significantly greater than the estimated density for BF sea states 2, 3, or 4. There were no significant differences between estimated density for BF sea states 2, 3, and 4, although the estimated density for BF sea state 4 was approximately 50% of the estimated density in BF sea states 2 and 3. These data are consistent with the hypothesis that the probability of sighting beluga whales in BF sea state 1 is significantly greater than that for sighting beluga whales

in BF sea states 2, 3, and 4. The average density in BF sea state 1 (0.206 whales/km^2) was more than three times greater than the average density in BF sea states 2, 3, and 4 (0.068 whales/km^2, SE=0.009). Further, the average density in BF sea state 1 was greater than the average density observed in any individual year by a factor of two or more. That is, the average density estimates (whales sighted/km^2) for beluga whales derived from our surveys in 1993, 1994, and 1995 were 0.074 (SE=0.023), 0.083 (SE=0.027), and 0.097 (SE=0.035), respectively (Lowry and DeMaster[3]) compared with an average density of 0.206 whales/km^2 for BF sea state 1.

A preliminary estimate for a correction factor that would account for sea state, based on the ratio of the estimated average density for BF sea state 1 in relation to the weighted average density in BF sea states 2, 3, and 4, is 3.023 (CV=0.285). Given our inability to discriminate among density estimates for BF sea states 2, 3, and 4, it is not possible at this time to develop a BF-specific correction factor for Norton Sound beluga whale surveys.

As noted earlier, we did not observe coherent groups of beluga whales during the survey, although they were aggregated in their general distribution. Therefore, we have not reported on the effect of sea state on estimates of group size. Further, because surveys were conducted at survey altitudes of either 264 m or 330 m in some years, interpreting the effect of sea state on average effective strip width (ESW) was not possible. However, the available data for a given year at a constant altitude (i.e. 330 m) indicated that there was not a significant relationship between sea state and ESW. For example, in 1994 the ESWs for BF sea states 1, 2, 3, and 4, were 0.35, 0.58, 0.54, 0.20 km, respectively, where there were no significant differences in ESW for a given sea state. The effect of sea state on encounter rate (i.e. number of sightings per km of survey effort), as noted earlier, was significant (Table 3). Not surprisingly, the same pattern reported for estimated density versus sea state was observed for encounter rate. That is, the encounter rate for BF sea state 1 (0.28 sightings/km) was significantly greater than the encounter rates for BF sea states 2, 3, or 4 (0.11, 0.11, and 0.04 sightings/km, respectively).

Beluga whale aerial surveys are flown in a variety of conditions and with methods adapted to regional circumstances. The results and conclusions presented in this note relate specifically to line-transect surveys in the Norton Sound region flown in an airplane similarly configured to the Aero Commander used in our study. Norton Sound is a large, exposed area and has frequent windy conditions. Some of the transects that we flew were very long, and sea state sometimes varied considerably along a transect. Nonetheless, because of the strong effect of sea state on density that we were able to detect, possible sea state effects should be considered in all beluga whale surveys. However, the authors recognize other factors not controlled for in our study may have influenced the results (e.g. behavioral responses of beluga whales to sea state). Clearly, additional studies are warranted.

Several approaches that should be considered in designing aerial surveys for the purpose of estimating beluga whale abundance are 1) restrict survey effort to conditions of BF sea state 1 or less; 2) continue to survey in sea states higher than BF sea state 1 and incorporate sea state effects in data analysis, 3) estimate the probability of sighting through the use of a third (independent) observer, or 4) increase the probability of sighting animals on the track line through the use of a belly window and third observer. The first approach is not feasible in the Norton Sound region and might prove difficult to implement in other localities. The latter approaches provide more flexibility in the field. Correction factors can then be used to adjust for reduced sightings in higher sea states, or analytical models can be developed that incorporate sea state as a covariate, as was done for harbor porpoise (*Phocoena phocoena*) by Forney et al. (1991).

Acknowledgments

Surveys were expertly flown by Tom Blaesing. Observers and data recorders in addition to DeMaster, Lowry, and Frost, included Robert Nelson, Debbie Blaesing, and Dieter Betz. Funding for this study was provided by the Alaska Beluga Whale Committee, the National Marine Fisheries Service, and the Alaska Department of Fish and Game. Early versions of the manuscript were improved by comments from John Bengtson, Rod Hobbs, Pierre Richard, and Janice Waite, two anonymous reviewers, and the scientific editor.

Literature cited

Brodie, P. F.
1971. A reconsideration of aspects of growth, reproduction, and behavior of the white whale with reference to the Cumberland Sound, Baffin Island, population. J. Fish. Res. Can. 28:1309–1318.
1989. The white whale *Delphinapterus leucas* (Pallas, 1776). *In* Handbook of marine mammals, vol. 4 (S. H. Ridgway and R. Harrison, eds.), p. 119–144. Academic Press, London.

Doidge, D. W.
1990. Age-length and length-weight comparisons in the beluga, *Delphinapterus leucas*. *In* Advances in research on the beluga whale, *Delphinapterus leucas* (T. G. Smith, D. J. St. Aubin, and J. R. Geraci, eds.), p. 59–68. Can. Bull. Fish. Aquat. Sci. 224,

Eberhardt, L. L.
1968. An approximation to a multiple-comparison test. Copeia 2:314–319.

Forney, K. A., D. A. Hanan, and J. Barlow.
1991. Detecting trends in harbor porpoise abundance from aerial surveys using analysis of covariance. Fish. Bull. 89:367–377.

Frost, K. J., and L. F. Lowry.
1990. Distribution, abundance, and movements of beluga whales, *Delphinapterus leucas*, in coastal waters of western Alaska. *In* Advances in research on the beluga whale, *Delphinapterus leucas* (T. G. Smith, D. J. St. Aubin, and J. R. Geraci, eds.), p. 39–71. Can. Bull. Fish. Aquat. Sci. 224.

Frost, K. J., L. F. Lowry, and R. R. Nelson.
1985. Radiotagging studies of belukha whales in Bristol Bay, Alaska. Mar. Mamm. Sci. 1:191–202.

Harwood, L. A., S. Innes, P. Norton, and M. C. S. Kingsley.
1996. Distribution and abundance of beluga whales in the Mackenzie estuary, southeast Beaufort Sea, and west Amundsen Gulf during late July 1992. Can. J. Fish. Aquat. Sci. 53:2262–2273.

Laake, J. L., S. T. Buckland, D. R. Anderson, and K. P. Burnham.
1994. Distance user's guide. Colorado Cooperative Fish and Wildlife Research Unit, Colorado State Univ., Ft. Collins, CO, 84 p.

Lowry, L. F., J. J. Burns, and K. J. Frost.
1989. Recent harvests of beluga whales, *Delphinapterus leucas*, in western and northern Alaska and their potential impact on provisional management stocks. Rep. Int. Whal. Comm. 39:335–339.

Reeves, R. R.
1990. An overview of the distribution, exploitation and conservation status of belugas, worldwide. *In* For the future of the beluga: proceedings of the international forum for the future of the beluga, (J. Prescott and M. Gauquelin, eds.), p. 47–58. Univ. Quebec Press, Quebec, Canada.

Richard, P. R., J. R. Orr, and D. G. Barber.
1990. The distribution and abundance of belugas, *Delphinapterus leucas*, in eastern Canadian subarctic waters: a review and update. *In* Advances in research on the beluga whale, *Delphinapterus leucas* (T. G. Smith, D. J. St. Aubin, and J. R. Geraci, eds.), p. 23–38. Can. Bull. Fish. Aquat. Sci. 224.

Seber, G. A. F.
1973. The estimation of animal abundance. Hafner Press, New York, NY, 506 p.

Wade, P. R.
1998. Calculating limits to the allowable human-caused mortality of cetaceans and pinnipeds. Mar. Mammal Sci. 14:1–37.

Age and growth of the scaled herring, *Harengula jaguana*, from Florida waters, as indicated by microstructure of the sagittae

Daryl J. Pierce

Behzad Mahmoudi

Florida Fish and Wildlife Conservation Commission
Florida Marine Research Institute
100 Eighth Avenue S. E.
St. Petersburg, Florida 33701-5095
Present address (for D. J. Pierce): RR1 71 Hack Road
Dalton, Pennsylvania 18414
E-mail address (for D. J. Pierce): darylip@aol.com

Raymond R. Wilson Jr.

College of Marine Science
University of South Florida
140 7th Avenue South
St. Petersburg, Florida 33071-5095

Scaled herrings, *Harengula jaguana* (Clupeidae), inhabit nearshore (40-m isobath, rarely 500-m) warm temperate and tropical waters of the western Atlantic Ocean from coastal New Jersey to off southern Brazil, including the waters of Bermuda, the Gulf of Mexico, and the Caribbean Sea (Whitehead, 1985). They are an important link in the nearshore neritic food web as predators of zooplankton and as common prey for many species of piscivorous fishes, sea birds, and marine mammals (Odum and Heald, 1972; Carr and Adams, 1973; Reintjes[1]). Although *H. jaguana* is popular live bait for anglers throughout Florida, it has relatively minor commercial importance as bycatch in regional purse-seine fisheries. However, Houde (1977) estimated a potential yield of 41–92 million kg per year for this species from a survey of *H. jaguana* eggs and larvae in the eastern Gulf of Mexico.

Limited age and growth information exists for *H. jaguana*. Martinez and Houde (1975) reported ages of up to three years determined from scale circuli of fish collected from Biscayne Bay, Florida. Hubold and Mazzetti (1982) identified three age groups of *H. jaguana* from Guanabara Bay, Brazil, with length-frequency analysis. However, daily growth increments of otoliths provide a better means of aging short-lived species (Pannella, 1974; Brothers et al., 1976) and are typically better for age determination than are scales (Jones, 1992). The objective of our study was therefore to determine ages from validated periodicities of otolith (sagitta) daily rings and to use the ages and lengths to compare growth rates of *H. jaguana* from the Atlantic coast with those from the Gulf coast of Florida.

Materials and methods

Adult *H. jaguana* were sampled monthly from commercial purse-seine catches from nearshore waters adjacent to West Palm Beach and Tampa Bay, Florida, between February 1992 and December 1993. By using cast nets, juvenile and adult fish were collected monthly in Tampa Bay and in alternate months near West Palm Beach. From each sample (purse-seine and cast net) the sex of approximately 100 fish was determined, and these fish were measured to the nearest 1.0 mm (standard, fork, and total lengths) and weighed to 0.1 g. Length-length and sex-specific weight-length relationships were computed for each coast. Weight-length regressions from $\log_{10}$-transformed data were described by least-squares linear regression and tested for differences between sexes within each coast and between coasts by analysis of covariance (ANCOVA). A total of 4210 (30 to 174 mm FL) *H. jaguana* were collected from off West Palm Beach and 29,994 (30 to 179 mm FL) fish were collected from Tampa Bay.

Each month, sagittae were removed from four fish randomly selected from within each 10-mm-FL (fork length) size class, sex, and coast. Otoliths were cleaned and stored dry in labeled containers. Sagittae were then processed, sectioned (transverse), and aged as in Secor et al. (1991) using an Olympus BH-2 compound microscope with transmitted light at 500×. Sagittae were read three separate times by the same reader in random sequence with a two-week interval between counts. Increment counting began at the first identifiable increment around the core (presumed to be day one) and continued along the medial plane of the sulcal ventral lip. Age was taken as the arithmetic mean of the three counts of the daily rings and accepted for analysis if the range of the three did not vary more than 10% from the mean. All rejected sagittae were counted a fourth time to replace the most extreme count, but were removed from further analysis if rejected a second time. The sex-specific relationship of otolith radius (core to medial edge of the sagitta) to fish length (FL) was linearly regressed for aged fish from each coast to examine the relationship between otolith growth and somatic fish growth.

During fall 1995, *H. jaguana* (50–80 mm FL) were marked with tetracycline and held in indoor tanks (568-L Nalgene tanks with a subgravel filtration system) to validate daily increment formation. Aquariums were kept at water

[1] Reintjes, J. W. 1979. Coastal herrings and associated species: a profile of species or groups of species, their biology, ecology, current exploitation with economic and social information. Submitted to the Gulf of Mexico Fish. Manage. Council SEFC/NMFS NOAA, Beaufort, NC 28516, 170 p.

Manuscript accepted 13 September 2000.
Fish. Bull. 99:202–209 (2001).

Table 1

Length-length, weight-length, and otolith radius-fish length least-squares linear regressions of *H. jaguana* from off West Palm Beach and Tampa Bay, Florida. Two standard errors of the parameters are in parentheses. The length-length and pooled weight-length data include immature-size fish. TL = total length (mm); FL = fork length (mm); SL = standard length (mm); Log_{10}(WT) = transformed total fish weight (g); Log_{10}(FL) = transformed fork length (mm); OR = median otolith radius (mm) from the core to the ventral edge of the sulcus; Range = range of fork lengths (TL was used for TL vs. SL) included in regression relationships.

				$Y=a+bX$		
Y	X	n	Range	a	b	r^2
West Palm Beach						
SL	FL	682	34–166	−1.412 (0.1294)	0.964 (0.0013)	0.9987
FL	SL	682	34–166	1.581 (0.1321)	1.035 (0.0014)	0.9987
TL	FL	822	34–172	−2.116 (0.2521)	1.191 (0.0024)	0.9964
FL	TL	822	34–172	2.108 (0.2073)	0.836 (0.0017)	0.9964
TL	SL	676	30–172	−0.002 (0.3288)	1.231 (0.0035)	0.9944
SL	TL	676	30–172	0.489 (0.2656)	0.807 (0.0023)	0.9944
Log_{10}(WT) (females)	Log_{10}(FL)	195	91–166	−5.104 (0.202)	3.172 (0.095)	0.9578
Log_{10}(WT) (males)	Log_{10}(FL)	169	84–161	−4.956 (0.194)	3.105 (0.091)	0.9647
Log_{10}(WT) (pooled)	Log_{10}(FL)	987	45–166	−5.138 (0.024)	3.187 (0.012)	0.9961
OR (females)	FL	22	91–166	−0.116 (0.098)	0.004 (0.0007)	0.8666
OR (males)	FL	22	98–161	−0.218 (0.113)	0.005 (0.0008)	0.8792
Tampa Bay						
SL	FL	1482	30–151	−1.140 (0.1136)	0.960 (0.0011)	0.9979
FL	SL	1482	30–151	1.382 (0.1166)	1.038 (0.0012)	0.9979
TL	FL	1475	30–151	−2.357 (0.1399)	1.281 (0.0014)	0.9980
FL	TL	1475	30–151	2.152 (0.1141)	0.831 (0.0009)	0.9980
TL	SL	1473	34–178	0.881 (0.1382)	0.799 (0.0011)	0.9968
SL	TL	1473	34–178	−0.742 (0.1739)	1.247 (0.0018)	0.9968
Log_{10}(WT) (females)	Log_{10}(FL)	1742	74–151	−5.048 (0.056)	3.144 (0.027)	0.9678
Log_{10}(WT) (males)	Log_{10}(FL)	1300	77–145	−4.983 (0.062)	3.114 (0.015)	0.9693
Log_{10}(WT) (pooled)	Log_{10}(FL)	10,219	28–151	−5.088(0.011)	3.163 (0.006)	0.9905
OR (females)	FL	84	76–146	−0.106 (0.055)	0.004 (0.0005)	0.8418
OR (males)	FL	73	77–145	−0.101 (0.064)	0.004 (0.0005)	0.8133

temperatures of 26–28°C and a salinity of 30–31‰ with an average photoperiod of 10 h/day. Fish were fed twice daily a combination of Tetramin® flake food and frozen brine shrimp. Fish were injected in the dorsal musculature with 0.05 mL of 0.06-mg oxytetracycline (OTC) solution/g body weight on 30 October, 14 November, and 6 December. Fish were sacrificed 7 days following the second (n=50) and third (n=30) injections. Otoliths were prepared and polished as previously described, examined with a combination of transmitted and incident ultraviolet light to fluoresce the OTC marks, and number of increments between all OTC marks were counted.

Forty transverse sections aged with the light microscope were also examined with a scanning electron microscope (SEM). Sagittae of unknown ages were selected by fish-size category and the quality of the section (i.e. core was on the surface of the section and there were no apparent large cracks) from those prepared for age analysis. The sections were etched with 0.12 N HCl for 1–5 seconds. Micrographs were read by using the same procedures and acceptance criteria described above. A paired sample t-test (Zar, 1996) was used to determine if the difference ($d_j=X_{1j}-X_{2j}$) between the light and SEM counts was significantly different from zero.

Harengula jaguana growth rates were estimated from the aged sagittae and compared with modal analysis of length frequencies. For each coast, sex-specific growth rates were estimated by using the least-squares linear regression of age on FL. Analysis of covariance was used to compare growth rates between sexes. The data were pooled if there were no significant differences, and pooled growth rates were compared for Florida's coasts by analysis of covariance. Cohort modal groups were assigned an approximate spawning month based upon estimated ages from the sagittae samples representative of the mode. The difference of the mean lengths between the largest and smallest modes from the same spawning month divided by the number of days between the two modes was defined as the modal growth. All statistical analyses were made with SAS software (SAS Institute Inc., 1989).

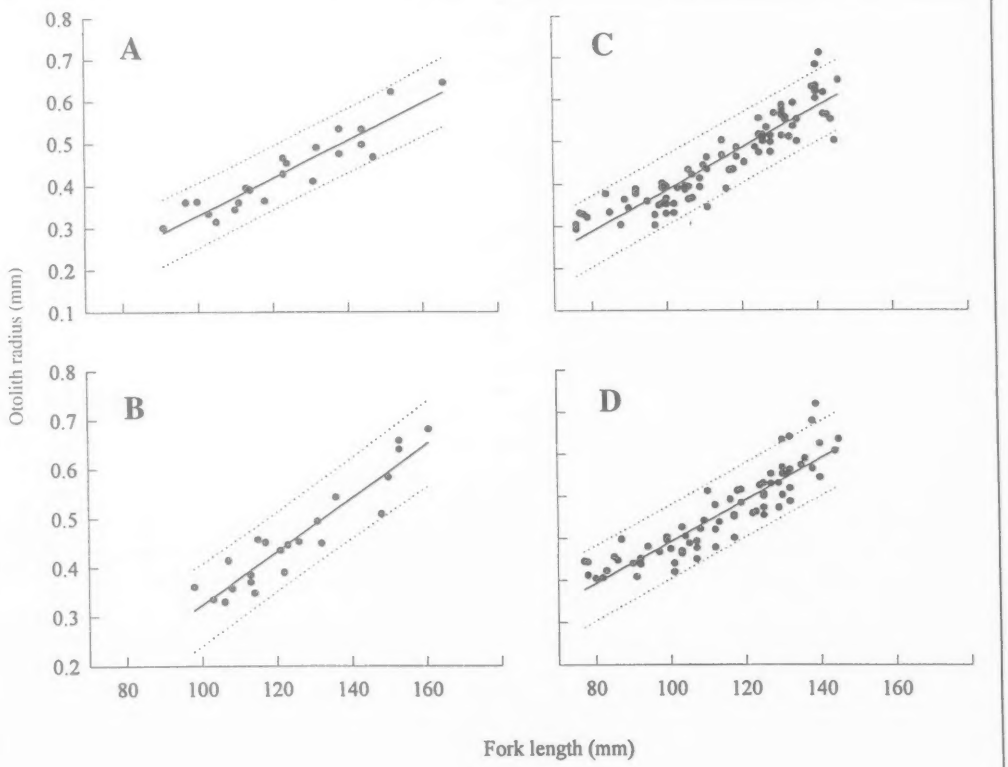

Figure 1

Medial otolith radius (mm) versus fork length (mm), and predicted medial otolith radius (mm) for *H. jaguana* off West Palm Beach and in Tampa Bay, Florida. (**A**) West Palm Beach females; (**B**) West Palm Beach males; (**C**) Tampa Bay females; and (**D**) Tampa Bay males. The dashed lines are upper and lower 95% confidence levels.

Table 2

Modeled least-squares regression growth rates of *H. jaguana* from off West Palm Beach and Tampa Bay, Florida. Numbers in parentheses are two standard errors of the estimated parameter. *AGE* = mean incremental counts (days); FL = fork length (mm); Range = range of age (days) included in the regression.

Capture site and sex of fish	n	Range	$FL = a + (b \times AGE)$		r^2
			a	b	
West Palm Beach					
females	18	175–269	32.337 (44.979)	0.4142 (0.2020)	0.5124
males	16	154–325	38.646 (24.444)	0.3569 (0.0963)	0.7968
pooled[1]	75	100–325	2.143 (10.263)	0.5050 (0.0519)	0.8381
Tampa Bay					
females	65	149–335	33.605 (13.642)	0.3542 (0.0592)	0.6944
males	57	141–370	50.034 (16.285)	0.2728 (0.0690)	0.5317
pooled[1]	178	78–370	13.902 (7.568)	0.4247 (0.0355)	0.7648

[1] Data include both immature and adult fishes.

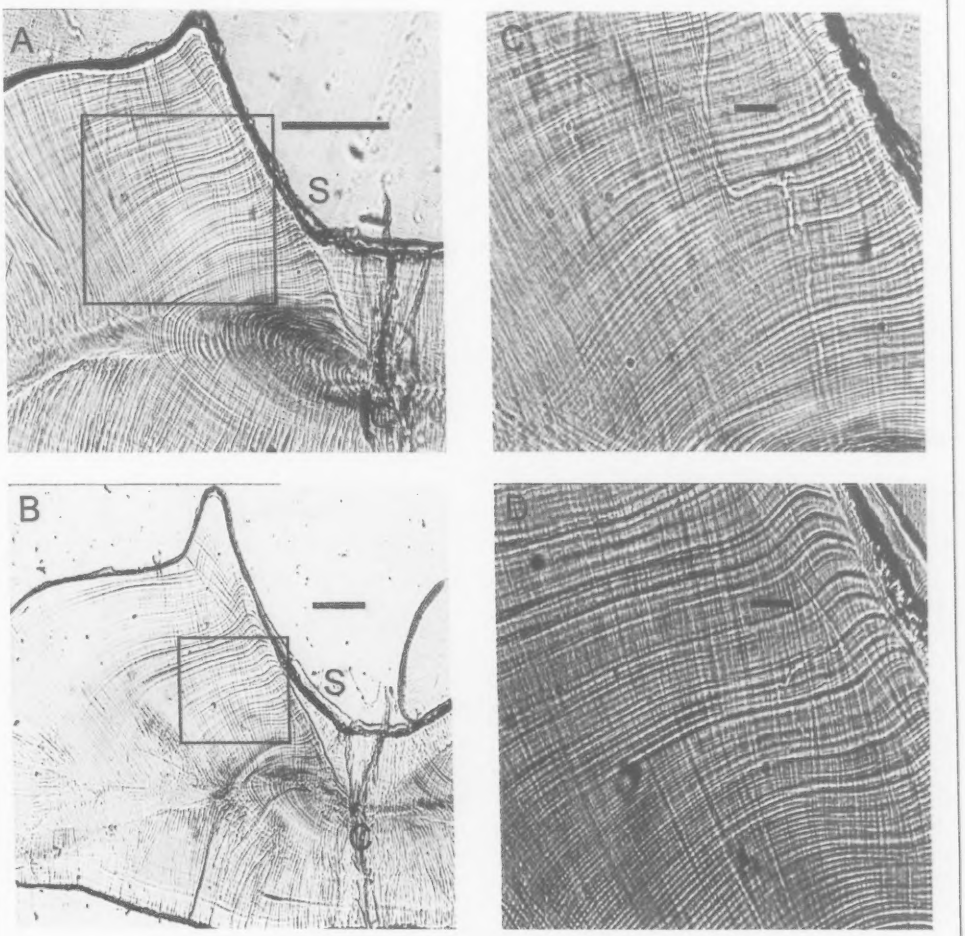

Figure 2

Transverse section of sagittal otoliths of (**A**) a young Tampa Bay juvenile *H. jaguana* (71 mm FL, 174 days old) and (**B**) an older Tampa Bay male (131 mm FL, 280 days old; scale bar=0.1 mm), and (**C** and **D**) the medial reading plane within the larger box shown on the transverse section of A and B, respectively (scale bar=0.02 mm). c = core; s = sulcus.

Results

Relationships between standard, fork, and total lengths, as well as weight-length regressions were calculated for fish off West Palm Beach and Tampa Bay (Table 1). The weight-length regressions between sexes for each coast showed no significant differences between slopes (ANCOVA, F=1.04, df=1, 360, P=0.309 for West Palm Beach; F=2.22, df=1, 3038, P=0.136 for Tampa Bay) or intercepts (ANCOVA, F=1.46, df=1, 361, P=0.227 for West Palm Beach; F=3.82, df=1, 3039, P=0.0508 for Tampa Bay). The pooled weight-length regressions for east and west coasts of Florida showed a significant difference between slopes (ANCOVA, F=5.50, df=1, 11,205, P=0.019) but not between intercepts (ANCOVA, F=3.37, df=1, 11,205, P=0.066). Thus, fish from off West Palm Beach were heavier at length than fish from Tampa Bay. The relationship of sagittal medial axis (OR) to fish length (FL) was linear (Table 1; Fig. 1, A–D).

Harengula jaguana otoliths from field collections were difficult to interpret (Fig. 2, A–D). Fifty-five percent of the counted sagittae had to be examined a fourth time and overall 84 (25%) of the sagittae were rejected. Yet, increment formation appeared to be daily for the laboratory-reared fish. Forty-five otoliths produced an average of 14.5 increments (SE=0.20) between the first and second OTC marks in an elapsed time of 15 days. Eleven otoliths averaged 21.0 increments (SE=0.25) between the second and third OTC marks in 22 days. The mean age of the OTC-

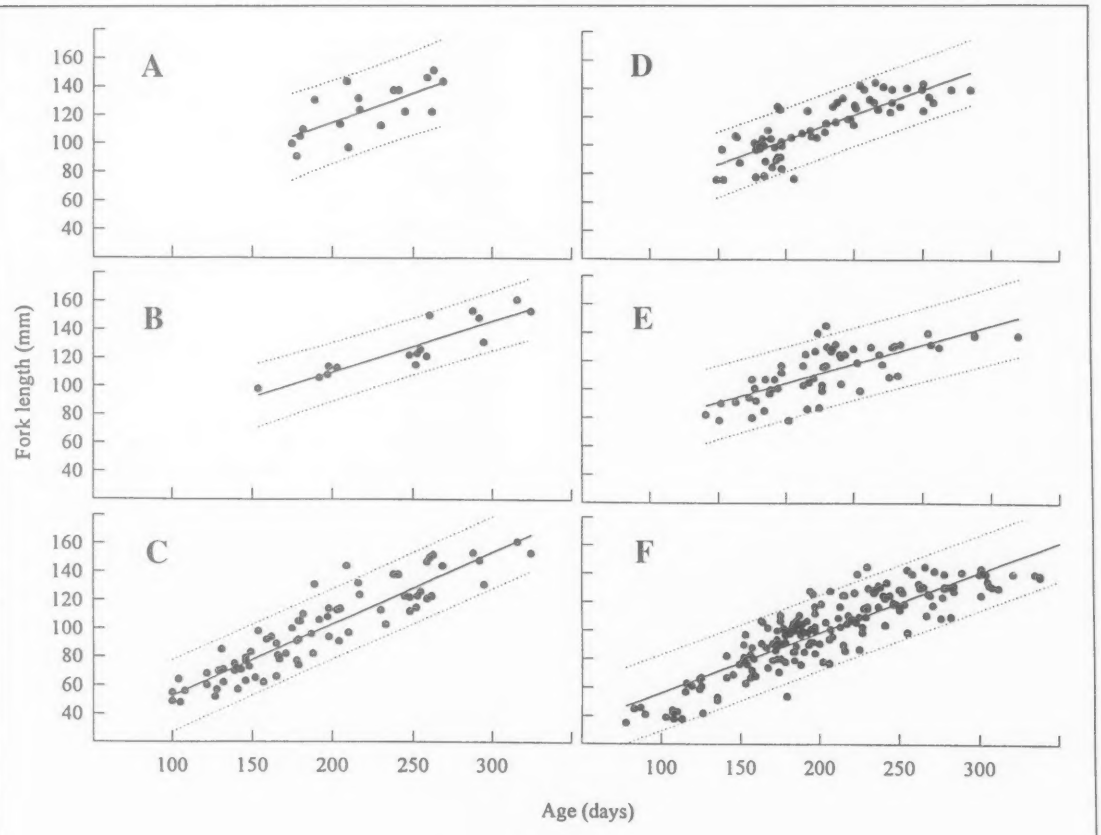

Figure 3

Observed ages (days) versus fork length (mm), and predicted fork length (mm) for *H. jaguana* off West Palm Beach and in Tampa Bay, Florida. (**A**) West Palm Beach females; (**B**) West Palm Beach males; (**C**) West Palm Beach pooled sex; (**D**) Tampa Bay females; (**E**) Tampa Bay males; and (**F**) Tampa Bay pooled sex. The extended size range in the pooled samples was due to the inclusion of immature juveniles specimens of indeterminable sex. The dashed lines are upper and lower 95% confidence levels.

injected fish was 141 days and ages varied from 125 to 165 days and lengths varied from 56 to 78 mm FL. Age estimated from 17 sagittae (41 to 131 mm FL) by using a SEM compared with transmitted light was not significantly different from zero (paired t=0.397, P>0.05).

Harengula jaguana grow rapidly and live little more than a year (Table 2; Fig. 3, A–F). Observed ages varied from 141 to 370 days for males and from 149 to 335 days for females. Growth rates (slope) were not significantly different for males and females in either West Palm Beach (ANCOVA, F=0.29, df=1, 30, P=0.595) or in Tampa Bay (ANCOVA, F=3.24, df=1, 118, P=0.074). Intercepts were also not significantly different in either West Palm Beach (ANCOVA, F=2.71, df=1, 31, P=0.109) or in Tampa Bay (ANCOVA, F=0.98, df=1, 119, P=0.325); therefore the data were pooled for each coast. Pooled growth rates (immature and adult) for Tampa Bay were significantly different from West Palm Beach (ANCOVA, F=6.09, df=1, 249, P=0.014).

Combined commercial purse-seine and cast-net length-frequency databases showed multiple juvenile recruitment peaks between June and November 1993 in Tampa Bay and between June and August 1992 from West Palm Beach (Fig. 4, A–B). Growth rates estimated from cohort length frequencies in Tampa Bay from February 1993 to May 1993 (spawned in September 1992) showed growth from 85 mm to 135 mm FL over 90 days, an average growth rate of 0.55 mm/day. A similar rate was obtained for fish at 45-mm mode in July 1993 (spawned in April 1993) that grew 125 mm FL by December 1993, a period of 150 days producing an average growth rate of 0.53 mm/day.

Discussion

Polished transverse sections of *H. jaguana* otoliths allowed enumeration of age in days. Houde et al. (1974) reported

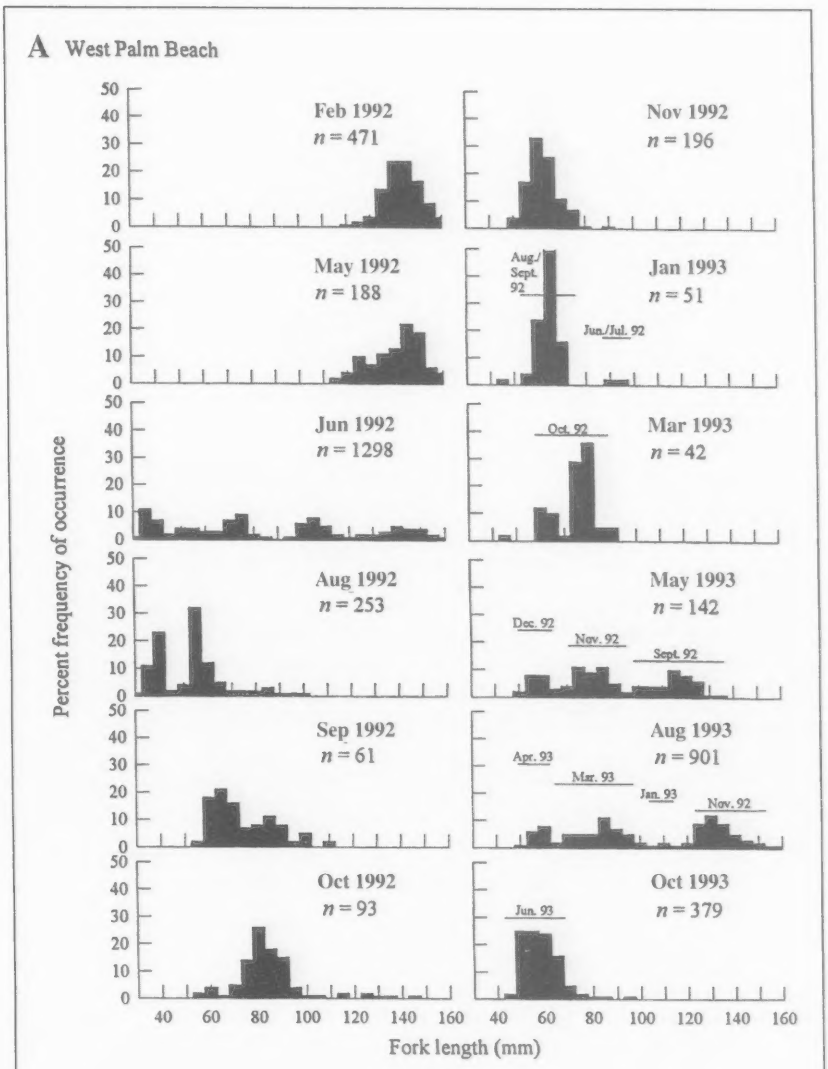

Figure 4

Observed monthly fork length frequencies of *H. jaguana* collected from off West Palm Beach and in Tampa Bay, Florida. Cohort age was determined from the sagittal microstructure and labeled with the estimated spawn date. (**A**) West Palm Beach 1992–93; (**B**) Tampa Bay 1993.

that *H. jaguana* larvae <8.9-mm TL did not show any ossification and that maxillaries and dentaries in the head region were first to ossify at 14.0 mm TL; but these authors did not describe the formation of the otoliths (sagittae, lapilli, or asterisci) for laboratory hatched and reared larvae collected from south Florida. Therefore, the first identifiable increment about the core could form as early as 4–5 days (yolksac absorption) to 14 days (first ossification in the head region) after hatching but no later than transformation into juvenile (25 days after hatching). Thus, growth from the daily counts could be underestimated by 4–25 days.

Hubold and Mazzetti (1982) calculated a von Bertalanffy growth curve for *H. jaguana* in Guanabara Bay, Brazil, based upon three values of length-at-age assigned from length-frequency analyses of fish caught in July 1979. They identified only two modal length-at-age groups—105 mm (age 2) and 140 mm FL (age 3)—estimating the mean length at age 1 to be 40 mm FL. Applying either Houde and Palko's (1970) (0.7 mm TL/day growth rate for labora-

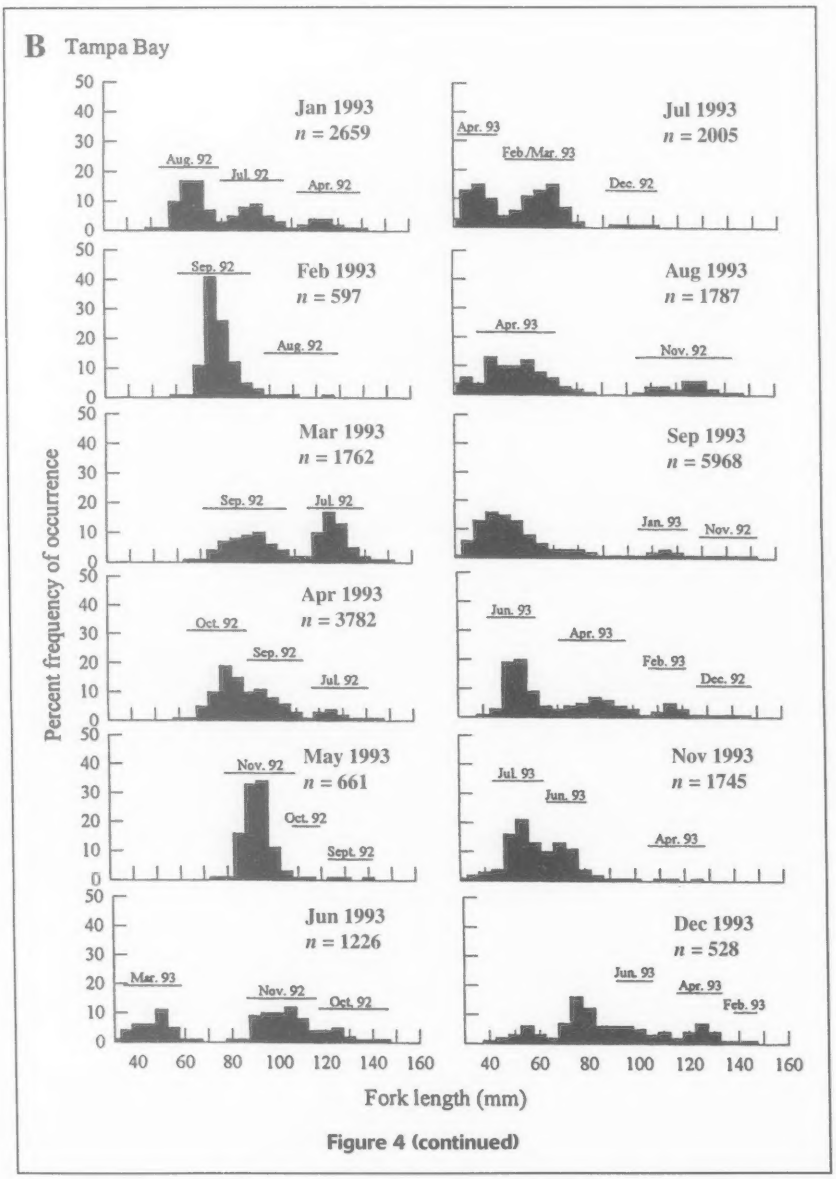

Figure 4 (continued)

tory-reared juveniles) or our measured growth rates (0.5 mm FL/day) to Hubold and Mazzetti's (1982) length for age-1 fish (40 mm) suggests that the fish were not one year old, but probably only 30 to 40 days old. Using scales from *H. jaguana* collected in Biscayne Bay, Florida, Martinez and Houde (1975) cited fish lengths of age class one (106 mm SL), age class two (136.6 mm SL), and age class three (142 mm SL). The majority of the fish growth occurred in the first year; there was little increase in size between the second and third years.

Length-frequency modes (Fig. 4) corroborate the growth rates for *H. jaguana* derived from sagittal microstructure and are consistent with estimates of 11–13 mm TL per month reported by Christmas and Waller (1973) for Mississippi waters, and 12.5 mm TL per month by Gunter (1945) for Texas. Low (1973) reported growth rates from 9 to10 mm TL per month for young-of-the-year fish in Biscayne Bay, Florida, which are close to those reported in our study. Identifying individual age cohorts is subjective, especially for older fish where modal groups tend to overlap.

Multiple recruitment periods are consistent with the serial spawning behavior of *H. jaguana* reported by Martinez and Houde (1975), who found fish maturing at 78–85 mm SL and continuous ripening of oocytes during a protracted

spawning season from February to August. Other authors (Gunter, 1945; Springer and Woodburn, 1960; Low, 1973; Modde and Ross, 1981) have noted one to two peak spawning events in April or September, or in both months. Observed length frequencies from our collections, specifically in Tampa Bay, suggest nearly continuous spawning year round. Fish spawned early could conceivably reach maturity and become a spawner in the fall of the same year.

In summary, *H. jaguana* are evidently fast-growing, short-lived fish. In coastal waters off West Palm Beach they appear to attain heavier weights and larger sizes at age than do fish inhabiting Tampa Bay. Although these differences might be genetically influenced, local environmental conditions seem the more likely cause of the observed significant variation in *H. jaguana* growth rates between coasts of Florida.

Acknowledgments

We would like to thank Peter Hood, Mike Murphy, Jim Quinn, Judy Leiby, Llyn French, and three anonymous reviewers for comments that improved the manuscript. We would also like to thank Renee Bishop for extensive help in producing the SEM micrographs. This manuscript was used in partial fulfillment of a Master of Science degree for Daryl Pierce from the University of South Florida, College of Marine Science, St. Petersburg. The research was funded in part by the Florida Saltwater Fishing License revenues.

Literature cited

Brothers, E. B., C. P. Mathews, and R. Lasker.
1976. Daily growth increments in otoliths from larval and adult fishes. Fish. Bull. 74:1–8.

Carr, W. E. S., and C. A. Adams.
1973. Food habits of juvenile marine fishes occupying seagrass beds in the estuarine zone near Crystal River, Florida. Trans. Am. Fish. Soc. 102(3):511–540.

Christmas, J. Y., and R. S. Waller.
1973. Estuarine vertebrates, Mississippi. *In* Cooperative Gulf of Mexico estuarine inventory and study, Mississippi (J. Y. Christmas, ed.), p. 320–406. Gulf Coast Res. Lab., Ocean Springs, MS.

Gunter, G.
1945. Studies on marine fishes of Texas. Publ. Inst. Mar. Sci. Univ. Tex. 1:1–90.

Houde, E. D.
1977. Abundance and potential yield of the scaled sardine, *Harengula jaguana*, and aspects of its early life history in the eastern Gulf of Mexico. Fish. Bull. 75:613–628.

Houde, E. D., and B. J. Palko.
1970. Laboratory rearing of the clupeid fish *Harengula pensacolae* from fertilized eggs. Mar. Biol. 5:354–358.

Houde, E. D., W. J. Richards, and V. P. Saksena.
1974. Description of eggs and larvae of scaled sardine, *Harengula jaguana*. Fish. Bull. 72:1106–1122.

Hubold, G., and M. V. Mazzetti.
1982. Growth, morphometry, and aspects of life history of the scaled sardine *Harengula jaguana* Poey, 1865 in the Guanabara Bay (Brazil). Meeresforschung 29:80–88.

Jones, C. M.
1992. Development and application of the otolith increment technique. *In* Otolith microstructure examination and analysis (D. K. Stevenson and S. E. Campana, eds.), p. 1–11. Can. Spec. Publ. Fish. Aquat. Sci. 117.

Low, R. A., Jr.
1973. Shoreline grassbed fishes in Biscayne Bay, Florida, with notes on the availability of clupeid fishes. M.S. thesis, Univ. Miami, Coral Gables, FL, 145 p.

Martinez, S., and E. D. Houde.
1975. Fecundity, sexual maturation, and spawning of scaled sardine (*Harengula jaguana* Poey). Bull. Mar. Sci. 25:35–45.

Modde, T., and S. T. Ross.
1981. Seasonality of fishes occupying a surf zone habitat in the northern Gulf of Mexico. Fish. Bull. 78:911–922.

Odum, W. E., and E. J. Heald.
1972. Trophic analysis of an estuarine mangrove community. Bull. Mar. Sci. 22(3):671–738.

Pannella, G.
1974. Otolith growth patterns: an aid in age determination in temperate and tropical fishes. *In* The ageing of fish (T. B. Bagenal, ed.), p. 28–39. Unwin. London.

SAS Institute Inc.
1989. SAS/STAT user's guide, version 6, 4th ed. SAS Institute Inc., Cary, NC, 846 p.

Secor, D. H., J. M. Dean, and E. H. Laban.
1991. Manual for otolith removal and preparation for microstructure examination. Baruch Inst. Tech. Rep. 91-1, Univ. South Carolina, Columbia, SC, 85 p.

Springer, V. G., and K. D. Woodburn.
1960. An ecological study of the fishes of the Tampa Bay area. Fl. Dep. Nat. Resour., Fla. State Board Conserv. Mar. Lab. Prof. Pap. Ser. 1, 104 p.

Whitehead, P. J. P.
1985. FAO species catalogue. Vol 7: Clupeoid fishes of the world: an annotated and illustrated catalogue of the herrings, herrings, pilchards, sprats, anchovies and wolf-herrings. Part 1: Chirocentridae, Clupeidae and Pristgasteridae. FAO Fish. Synopsis 125, FAO, Rome.

Zar, J. H.
1996. Biostatistical analysis, 3rd ed. Prentice Hall, Upper Saddle River, NJ, 662 p.

A comparison of catches of swordfish, *Xiphias gladius,* and other pelagic species from Canadian longline gear configured with alternating monofilament and multifilament nylon gangions

Heath H. Stone

Biological Station
Fisheries and Oceans Canada
531 Brandy Cove Road
St. Andrews, New Brunswick, E5B 2L9 Canada
E-mail address: stoneh@mar.dfo-mpo.gc.ca

Langille K. Dixon

P.O. Box 144
Woods Harbour
Nova Scotia B0W 2E0, Canada

The Canadian large pelagic longline fishery extends from Georges Bank south of Nova Scotia to the Flemish Cap, east of Newfoundland, and operates from May through November, when swordfish (*Xiphias gladius*), the main species targeted, migrate into and adjacent to the Canadian EEZ. Fishing effort progresses from west to east and back again and from offshore to inshore along the edge of the continental shelf (Stone and Porter, 1999) following swordfish movements associated with seasonal warming trends of surface water temperature, and a northward movement of the edge of the Gulf Stream (Beckett, 1974). In winter, swordfish are confined to warmer waters associated with the Gulf Stream outside the Canadian EEZ and are not easily accessed by the Canadian fleet. In recent years, national swordfish quotas for the Canadian fishery (established by the International Commission for the Conservation of Atlantic Tunas) have been reached by early fall.

Pelagic longlining was first introduced as a method for fishing swordfish in Canadian Atlantic waters in 1962, having been stimulated by reports of incidental swordfish catches by foreign longliners targeting tuna or laminid sharks (Beckett[1]). Prior to 1962, harpooning was the principal method used to capture swordfish on the continental shelf, where large females (mean round weight ~120 kg) were targeted as they swam or "basked" in surface waters during the day. This fishery occurred primarily during July and August, and required calm, clear weather to visually detect individual fish (Beckett[1]). During the early to mid 1960s, the Canadian fleet rapidly converted to surface longline gear which proved to be far more efficient than harpooning. Not only were daily catches much higher, but vessels could operate during inclement weather (unsuitable for harpooning) and fish farther offshore as waters cooled over the continental shelf. As a result, the fishing season extended, the fishing area expanded, catch rates increased, and the average weight of fish declined because both male and female swordfish were captured (Caddy, 1976; Hurley and Iles, 1981; Beckett[1]).

Pelagic longline gear adopted for use by Canadian fishermen is similar to that used in the New England fishery (Berkeley et al., 1981) and consists of a continuous backline up to 64 km long, supported in the water column by styrofoam floats with up to 2000 baited hooks suspended on gangions spaced at regular intervals (Fig. 1). Although the general design of pelagic longline gear is relatively simple, operating characteristics (including area, month and time of set, surface temperature, fishing depth, number of hooks between floats, bait) can significantly affect the catch rates and species composition of the catches. With swordfish fishing, usually three to five hooks are attached between floats and lightsticks are attached intermittently to some of the gangions above the bait to attract swordfish or their potential prey species. The gear is set during the early evening, allowed to soak overnight for 6–12 hours and retrieved at daybreak. The length of the float lines determines the depth of the backline, and along with the length of the gangions, distance between buoys and speed at which the backline is set (i.e. the gear tends to sink more at slower setting speeds) determine the actual depth the baits will fish. In the Canadian swordfish fishery, baits are often fished at depths of 12 m or less in the upper water column to take advantage of the diurnal feeding migrations of swordfish and their movement into near surface waters at night (Carey and Robison, 1981).

In the early 1960s, the first floating longlines used modified halibut bottom longline gear buoyed by a variety of objects (Beckett[1]). Both the backline and gangions were made of tarred multifilament nylon and the gangions were spliced directly to the backline. Monofilament nylon was first used by Canadian fishermen in the late 1960s, when a short (~38 cm) mono leader was attached between the tarred multifilament nylon segment of the gangion and the hook. In the late 1970s (following an eight year closure of the Canadian fishery when it was illegal to land swordfish in Canadian ports owing to perceived high levels of mercury in swordfish meat), gangions consisted of an upper tarred multifilament section with a clip for attaching it to the

[1] Beckett, J. S. 1971. Canadian swordfish longline fishery. Int. Comm. Conserv. Atl. Tunas. SCRS Report 80/71/36, 14 p. International Commission for the Conservation of Atlantic Tunas, 8 Corazon de Maria, 28002 Madrid, Spain.

Manuscript accepted 22 August 2000.
Fish. Bull. 99:210–216 (2001).

backline and a lower monofilament leader to which the hook was attached. The monofilament leader made up one half (~1.8 m) of the overall length of the gangion (~3.6 m) and was considered to yield better catch rates because it was assumed to be less visible to swordfish and other pelagic species. This innovation also effectively reduced shark damage to the gear because only the monofilament leader had to be replaced if it was bitten off. In the late 1980s, fishermen began to use monofilament nylon for both sections of the gangion and for the backline on the assumption that this would further improve catch rates by decreasing overall visibility of the gear.

Canadian pelagic longline fishermen have been using monofilament gangions for over a decade now and generally agree over its ability to outperform the older tarred multifilament nylon gangions in terms of swordfish catchability, although this theory has never been tested scientifically. In this note, the results of a collaborative science and industry study involving the Canadian Department of Fisheries and Oceans and the Nova Scotia Swordfishermen's Association are presented. Our study was designed to compare the catchability of swordfish and other pelagic species on commercial longline gear configured with alternate monofilament and tarred multifilament nylon gangions. It was based on the premise that some species can avoid capture on the tarred multifilament gangions which are thicker, darker, and possibly more "visible" than the monofilament nylon gangions.

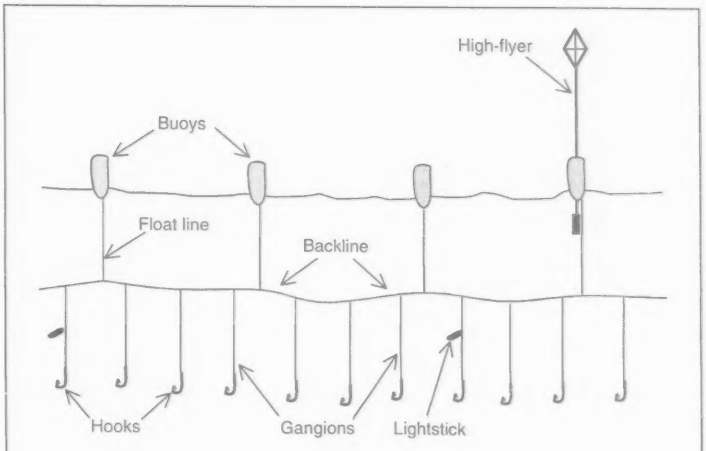

Figure 1

Schematic diagram illustrating typical Canadian pelagic longline gear configuration. (Note: this configuration differs slightly from the one used in our experiment.)

Materials and methods

The study was conducted aboard the 19-m fishing vessel *Nova Blue* from 22 July to 2 August 1999, along the edge of Georges Bank (depth to bottom: 360–1400 m) from Corsair Canyon to the Northeast Peak (Fig. 2). This area is closed annually to commercial longlining operations from 1 January to 1 August to reduce bycatches of bluefin tuna and small swordfish. Therefore, no other vessels were fishing in this closed area at the time this experiment was conducted. The gear was deployed each evening between 1800–2300 h in surface waters following the 20–22°C isotherm from south to north, allowed to soak overnight, and hauled back from north to south beginning at daybreak (~0600 h) the following morning. Haulback operations generally required 10 hours—occasionally exceeding 12 hours when the gear parted off or became entangled.

Ten surface longline sets were completed with standard commercial longline gear configured with alternately spaced monofilament and tarred multifilament nylon gangions. It was assumed that this approach would minimize the variability in catches between gangion types resulting from the different depth and temperature regimes over the length of the set (i.e. up to 64 km). Generally, 20 sections of gear were deployed for most sets (one section=72 hooks and 23 buoys), yielding a total of 1440 hooks per set (for sets 4–10), although there was some variation in hook number for the first three sets (set 1: 1008 hooks; sets 2–3: 1656 hooks). Although the 1:1 ratio of gangion types was not maintained in some gear sections owing to gear damage and subsequent replacement, the overall ratio for the entire set remained at 1:1.

Monofilament gangions consisted of two 3.6-m sections of 400-lb test, 2-mm diameter monofilament nylon attached together with stainless steel crimps, with the lower section or leader attached to a no. 9 Mustad J-hook (Fig. 3). Multifilament gangions had a 3.6-m upper section of tarred braided nylon (400 lb test, 5-mm diameter), and a lower 3.6-m monofilament leader (400-lb test, 2-mm diameter) to which a no. 9 Mustad J-hook was attached. Therefore, the lower section (leader) of both gangion types was monofilament nylon and the upper section varied between multifilament and monofilament nylon material. With this configuration, only the leader section had to be replaced if damaged by sharks. Each leader also had three luminous green beads and one in 20 had a green lightstick attached 1 m above the hook (Fig. 3). When the gear were set, gangions were clipped onto a monofilament backline (730 lb test) at intervals of 36 m after baiting the hooks with whole Atlantic mackerel (*Scomber scombrus*). Styrofoam buoys with 2–4 m droplines were clipped to the backline after every third hook, and a highflyer attached to the backline at the end of each section. Fishing depth during each set was estimated to vary between 9 and 11 m from the surface.

The catch (in numbers) of all pelagic species was recorded by gangion type for each section of gear within a set. The curved lower jaw fork length (LJFL, cm) was obtained for

all commercial-size swordfish (i.e. ≥119 cm LJFL) by using a metal tape measure. No measurements were obtained for live or dead under-size swordfish (i.e. <119 cm LJFL based on visual estimation); however, their catch was recorded. Under-size swordfish were not brought aboard the vessel but were released in the water by cutting the gangion as close to the hook as possible. Other species were not measured because most of these were also released alive after capture.

Chi-square (χ^2) was used to determine if the observed frequency of catches by gangion type for each species differed significantly (α<0.05) from an expected 1:1 ratio for individual and combined sets. Catches of commercial-size and under-size swordfish were combined for this analysis because the method for size determination of under-size fish was considered too subjective for a separate analysis by size category. Only cases where 10 or more observations were available for each species were used for within-set comparisons. Because very few captures of any species occurred on gangions with lightsticks attached, the influence of lightsticks on catch rates in this experiment were assumed to be negligible, even though they are often used by fishermen (at much higher deployment rates) to improve catches of swordfish. A two-way ANOVA was used to examine differences in the mean lengths (LJFL) of commercial-size swordfish ≥119 cm LJFL) by set and gangion type after testing for homogeneity of variances.

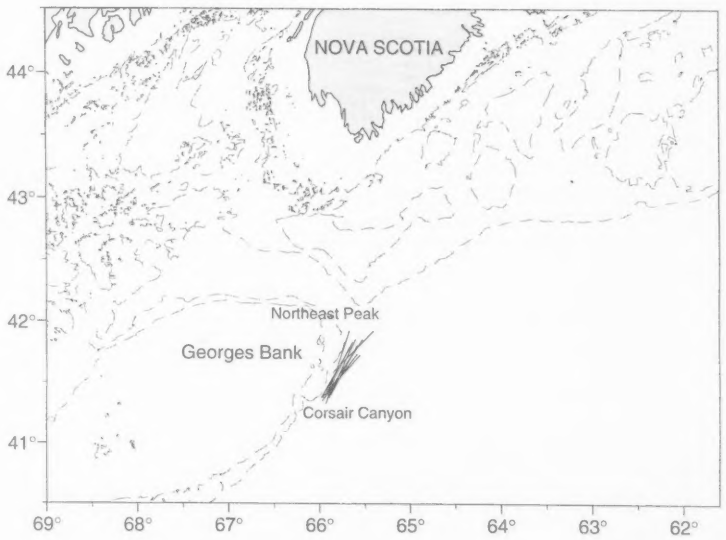

Figure 2

Geographic location of ten pelagic longline sets conducted off Georges Bank between 22 July and 2 August 1999, to examine the catches of pelagic species on monofilament and tarred multifilament nylon gangions.

Results

The primary species captured included swordfish (*Xiphias gladius*), blue shark (*Prionace glauca*), shortfin mako shark (*Isurus oxyrinchus*), pelagic stingray (*Dasyatis violacea*), loggerhead turtle (*Caretta caretta*), white marlin (*Tetrapturus albidus*), common dolphinfish (*Coryphaena hippurus*) and yellowfin tuna (*Thunnus albacares*). A total of 1093 captures (all eight species combined) occurred from 10 pelagic longline sets, with 66.7% of captures occurring on monofilament and 33.3% on multifilament gangions. Catches of swordfish averaged 38.8 fish per set (based on 334 kept plus 54 released as under-size), followed by blue shark (34.1/set), shortfin mako shark (9.7/set), pelagic stingray (9.4/set), loggerhead turtle (6.6/set), white marlin (6.0/set), common dolphinfish (3.7/set), and yellowfin tuna (1.0/set).

Commercial-size swordfish ranged from 120 to 242 cm LJFL (mean=154.4 ±21.14, n=334). Swordfish captured on monofilament nylon and multifilament nylon gangions were very similar in mean length (154.7 ±21.66 and 153.8 ±20.18 cm LJFL, respectively) and overall size composition (Fig. 4). There was no significant difference between mean lengths of commercial-size swordfish by set or gangion type, nor was there evidence of an interaction between these factors (F=0.736, P=0.690, df=333, 19), indicating that there were no size-related preferences for one gangion type over the other for swordfish ≥119 cm LJFL.

Observed swordfish captures by gangion type differed significantly from an expected 1:1 ratio in all but two of the 10 sets, with higher catches on monofilament gangions compared with the multifilament (Table 1). Similarly, observed captures of blue sharks differed significantly from expected in 3 of 10 sets, with higher catches on the monofilament gangions. For all other species, fewer than 10 sets were available for χ^2 comparisons because less than 10 individuals were captured for some sets. In the case of mako shark, only 5 of 10 sets had sample sizes ≥10, but no significant difference occurred between the observed and expected catch frequency by gangion type, although more captures occurred on monofilament gangions for most sets. For white marlin and loggerhead turtle, only 2 of 10 sets had sample sizes ≥10 and showed no significant differences in catch by gangion type, although most occurred on monofilament. However, for pelagic stingrays, 3 out of 4 sets available for comparison showed significant differences between observed and expected catches by gangion type, with higher catches on the monofilament gangions. The catch per set of yellowfin tuna and common dolphinfish was too low for statistical comparisons. Captures of all species combined were significantly higher on monofilament gangions for 9 out of 10 sets (Table 1).

For all species, 60% or more of catches from combined sets occurred on monofilament gangions (Table 2). When the catches by species for all 10 sets were pooled, the

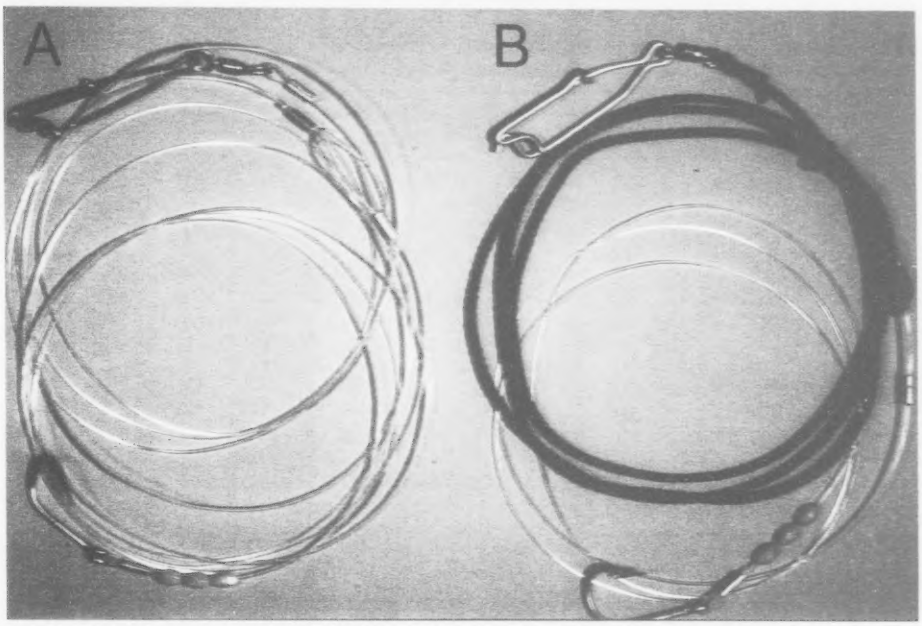

Figure 3

Monofilament nylon (**A**) and tarred multifilament nylon (**B**) gangions used for ten pelagic longline sets conducted off Georges Bank from 22 July to 2 August 1999.

observed captures by gangion type differed significantly from an expected 1:1, with the monofilament nylon outperforming the tarred multifilament nylon gangions for 6 of 8 species (Table 2). The catch ratio by gangion type (i.e. monofilament versus multifilament) for all species combined was 2:1 and was highest for yellowfin tuna (9:1) and lowest for mako shark (1.5:1).

Discussion

The purpose of our analysis was to examine differences in pelagic longline catch by species for two different types of gangion and was based on the premise that monofilament nylon gangions currently used by Canadian pelagic longline fishermen yield higher catches than the tarred multifilament nylon gangions used in the past. Although only a small data set from a limited geographic area was available for this analysis, it was apparent in the case of swordfish and blue shark that catches were significantly higher on monofilament gangions, which yielded double the catch of the multifilament gangions for

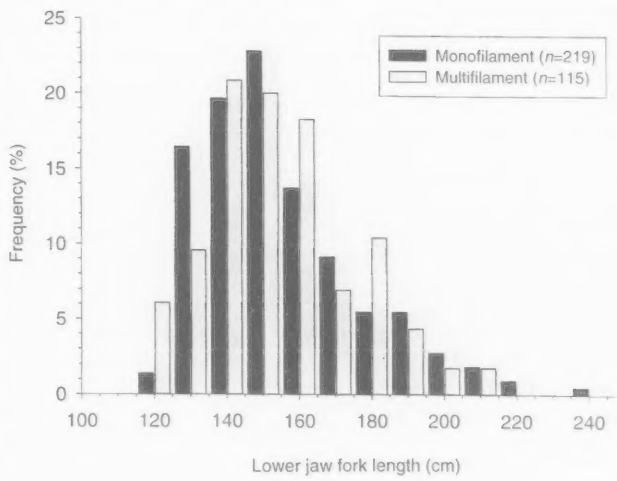

Figure 4

Size distributions of commercial-size swordfish ≥119 cm LJFL) captured on monofilament and tarred multifilament nylon gangions during a pelagic longline study conducted off Georges Bank from 22 July to 2 August 1999.

Table 1

Summary of pelagic longline catch by species and gangion type for sets 1 through 10. Chi-square statistics (χ^2) and corresponding *P*-values are presented for comparisons of catch by gangion type for species where total catch exceeded 10 individual per set. M = monofilament gangion; B = multifilament gangion.

	Set 1				Set 2				Set 3				Set 4				Set 5			
Species caught	M	B	χ^2	*P*	M	B	χ^2	*P*	M	B	χ^2	*P*	M	B	χ^2	*P*	M	B	χ^2	*P*
Swordfish	22	6	9.14	0.003	31	26	0.44	0.508	23	9	6.13	0.013	27	14	4.122	0.042	44	23	6.58	0.010
Yellowfin tuna	0	0	—	—	0	0	—	—	1	0	—	—	0	0	—	—	2	0	—	—
Mako shark	5	1	—	—	7	7	0.00	1.000	11	6	1.47	0.225	5	5	0.000	1.000	11	5	2.25	0.134
Blue shark	9	3	3.00	0.083	10	7	0.53	0.467	39	19	6.90	0.009	12	5	2.882	0.090	9	6	0.60	0.439
White marlin	4	1	—	—	8	1	—	—	4	0	—	—	7	3	1.600	0.206	5	2	—	—
Dolphinfish	2	0	—	—	4	3	—	—	2	0	—	—	6	1	—	—	1	2	—	—
Stingray	13	4	4.77	0.029	7	9	0.25	0.617	3	3	—	—	7	1	—	—	4	1	—	—
Loggerhead turtle	3	4	—	—	4	0	—	—	6	4	0.40	0.527	3	1	—	—	4	0	—	—
Total	58	19	39.00	0.000	71	53	18.00	0.106	89	41	48.00	0.000	68	30	38.0	0.000	80	39	41.00	0.000

	Set 6				Set 7				Set 8				Set 9				Set 10			
Species caught	M	B	χ^2	*P*	M	B	χ^2	*P*	M	B	χ^2	*P*	M	B	χ^2	*P*	M	B	χ^2	*P*
Swordfish	31	12	8.40	0.004	19	8	4.48	0.034	11	4	3.27	0.071	27	14	4.122	0.042	25	12	4.57	0.033
Yellowfin tuna	0	0	—	—	1	1	—	—	1	0	—	—	2	0	—	—	2	0	—	—
Mako shark	3	3	—	—	6	2	—	—	7	4	0.82	0.366	1	4	—	—	2	2	—	—
Blue shark	30	20	2.00	0.157	51	26	8.12	0.004	47	19	11.88	0.001	13	5	3.556	0.059	5	6	0.09	0.763
White marlin	1	1	—	—	5	0	—	—	1	0	—	—	7	3	1.600	0.206	5	2	—	—
Dolphinfish	2	1	—	—	2	0	—	—	0	0	—	—	3	2	—	—	5	1	—	—
Stingray	11	1	8.33	0.004	12	4	4.00	0.046	1	0	—	—	1	4	—	—	4	4	—	—
Loggerhead Turtle	4	4	—	—	5	2	—	—	2	2	—	—	5	6	0.091	0.763	4	3	—	—
Total	83	42	41.00	0.000	101	43	58.00	0.000	70	29	41.00	0.000	59	38	21.00	0.033	52	30	22.00	0.015

some sets. Although only the upper half of the multifilament gangion was made from braided nylon material (based on a configuration used by fishermen in the past), the differences in catches for these two species between this gangion and one constructed entirely of monofilament nylon were striking. A similar trend for the other pelagic species was not as evident on a set-by-set basis owing to lower catches; however, for combined sets, more captures occurred on the monofilament gear overall. Although these results clearly indicate differences in catches between gangion types, the influence of oceanographic conditions off Georges Bank, such as water temperature and thermocline depth, likely influence the availability and catchability of all species. Therefore, it is important to point out that results could differ among geographic areas with different oceanographic regimes.

Reports of higher catches on monofilament gear have also been made for other species. Monofilament snoods (gangions) give higher catch rates for cod and haddock compared with multifilament snoods, and thinner snoods tend to give better catch rates than thicker ones (Bjordal and Lokkeborg, 1996). Under good light conditions, monofilament lines were observed to catch as much as three times more cod than multifilament lines (Bjordal and Lokkeborg, 1996). Over the past decade, Canadian bluefin tuna fishermen have gradually shifted to finer gauges of monofilament nylon line (i.e. from 400 lb to 120 lb test) for use on rod and reel gear because it is their perception that bluefin tuna have learned to recognize and avoid the heavier monofilament nylon line. The lower visibility of monofilament gangions used on longline gear is commonly used to explain why they give better catches than gangions made of multifilament nylon; however, the reason for the difference in catching power is unclear. Some pelagic fish species may be able to detect multifilament nylon gangions more readily because of their thicker diameter (5 mm versus 2 mm for monofilament) and darker color, and can make this distinction even during periods of darkness (i.e. when the pelagic longline gear is fishing). The higher visibility of multifilament lines may cause a restrained response towards attacking the baited hooks.

Whether multifilament nylon gangions are more easily detected by some species, likely depends on the role that vision plays as the dominant sensory mechanism. Some pelagic species have large eyes (i.e. yellowfin tuna, swordfish, white marlin, mako and blue shark) and are efficient visual predators even in dim light. Becuase visual acuity or resolution of detail improves with the size of the eye (Blaxter, 1980), some pelagic species may be better at detecting and avoiding the multifilament nylon gangions

Table 2

Summary of pelagic longline catches by species and gangion type for all sets combined. Chi-square statistics (χ^2) and corresponding *P*-values are presented for all species. M = monofilament gangion; B = multifilament gangion.

Species	Gangion	*n*	% by gangion type	Ratio (M:B)	χ^2	*P*	% of total catch
Swordfish	M	260	67.0	2.03:1.00	44.90	0.000	35.7
	B	128	33.0				35.2
Yellowfin tuna	M	9	90.0	9.00:1.00	6.40	0.011	1.2
	B	1	10.0				0.3
Mako shark	M	58	59.8	1.49:1.00	3.72	0.054	7.8
	B	39	40.2				10.7
Blue shark	M	225	66.0	1.94:1.00	34.84	0.000	30.9
	B	116	34.0				31.9
White marlin	M	47	78.3	3.62:1.00	19.27	0.000	6.5
	B	13	21.7				3.6
Dolphinfish	M	27	73.0	2.70:1.00	7.81	0.005	3.7
	B	10					2.8
Stingray	M	63	67.0	2.03:1.00	10.89	0.001	8.6
	B	31	33.0				8.5
Loggerhead turtle	M	40	60.6	1.54:1.00	2.97	0.085	5.5
	B	26	39.4				7.1
Total	M	729	66.7	2.00:1.00	123.00	0.000	100.0
	B	364	33.3				100.0

than others, as evidenced by the range of catch ratios between monofilament and multifilament gangions for the various species encountered during our study (Table 2).

Although no differences in the size of swordfish ≥119 cm LJFL occurred between gangion types, more swordfish were captured on monofilament gangions, along with other bycatch species. Although catches of all species were higher on the monofilament gear, the percentage of total catch represented by each species for each gear type was very similar (Table 2, last column). Therefore, by fishing an extra one or two sets with the multifilament gear, fishermen would get the same amount of catch as they would have if monofilament gear were used, but at greater cost because more sets and days at sea would be required to yield the same catch. Furthermore, the absence of any species-specific trends between gangion types indicates that the use of monofilament gangions does not reduce the bycatch of other pelagic species.

Catch-per-unit-of-effort (CPUE) indices based on commercial fishery statistics are often used in analytical models to investigate trends in resource abundance, particularly in the stock assessments for swordfish and bluefin tuna conducted by the International Commission for the Conservation of Atlantic Tunas. Catch rates are generally standardized for the effects of gear, area, month, and other factors by using general linear models (e.g. Hoey et al. 1997). The importance of gear changes and their effect on commercial catch rates is clearly evident in this study and underscores the need to detect and account for changes in gear technology in the development of any commercial catch rate series used in analytical stock assessments.

Acknowledgments

The expertise and assistance of the crew of the *Nova Blue* are greatly appreciated, for without their help this study would not have been possible. We also thank R. Halliday, J. Neilson, J. Hoey, and J. Porter for their many useful comments on an earlier draft of this manuscript. We also thank the Canadian Department of Fisheries and Oceans for permitting the experiment to be conducted in a closed area.

Literature cited

Beckett, J. S.
1974. Biology of swordfish, *Xiphias gladius* L., in the northwest Atlantic Ocean. *In* Proceedings of the international billfish symposium, Kailua-Kona, Hawaii, 9–12 August 1972. Part 2: Review and contributed papers (R. S. Shomura and F. Williams, eds.), p. 103–106. U.S. Dep. Commer., NOAA Technical Report NMFS SSRF-675.

Berkeley. S. A., E. W. Irby, and J. W. Jolly.
1981. Florida's commercial swordfish fishery: longline gear and methods. Florida Cooperative Extension Service, Univ. Miami, Miami, FL, Florida Sea Grant Marine Advisory Bull. MAP-14, 23 p.

Bjordal, A., and S. Lokkeborg.
1996. Longlining. Fishing News Books, Oxford, England, 156 p.

Blaxter, J.H.S.
1980. Vision and the feeding of fishes. *In* Fish behaviour and its use in the capture and culture of fishes (J. E. Bardach, J. J. Magnuson, R. C. May, and J .M. Reinhart, eds.), p. 32–56. ICLARM. Manilla, Philippines.

Caddy, J. F.
1976. A review of some factors relevant to management of swordfish fisheries in the northwest Atlantic. Canada. Dep. of Environment. Fish. Mar. Serv. Res. Dev. Tech. Rep. 633, 36 p.

Carey, F. G, and B. H. Robison.
1981. Daily patterns in the activities of swordfish, *Xiphias gladius*, observed by acoustic telemetry. Fish. Bull. 79(2): 277–292.

Hoey, J. J., J. M. Mejuto J. M., Porter H. H. Stone, and Y. Uozumi.
1997. An updated biomass index of abundance for North Atlantic swordfish, 1963–1995. Int. Comm. Conserv. Atl. Tunas Col. Vol. Sci. Pap. 46 (3):354–361.

Hurley, P. C. F., and T. D. Iles.
1981. A review of the Canadian swordfish fishery. Int. Comm. Conserv. Atl. Tunas Col. Vol. Sci. Pap. 15 (1):348–360.

Stone, H. H., and J. M. Porter.
1999. Updated age-specific CPUE for Canadian swordfish longline (1988–1997), with information on nominal CPUE for yellowfin, bigeye and albacore tuna bycatch. Int. Comm. Conserv. Atl. Tunas Col. Vol. Sci. Pap. 49 (1):407–422.

Superintendent of Documents **Publications** Order Form

*5178

☐ YES, please send me the following publications:

____ Subscriptions to *Fishery Bulletin*
for $55.00 per year ($68.75 foreign)

The total cost of my order is $ _____ . Prices include regular domestic postage and handling and are subject to change.

_____
(Company or Personal Name) (Please type or print)

_____
(Additional address/attention line)

_____
(Street address)

_____
(City, State, ZIP Code)

_____
(Daytime phone including area code)

_____
(Purchase Order No.)

Charge your order. IT'S EASY!

VISA

MasterCard

Please Choose Method of Payment:

☐ Check Payable to the Superintendent of Documents

☐ GPO Deposit Account ☐☐☐☐☐☐☐–☐

☐ VISA or MasterCard Account

☐☐☐☐☐☐☐☐☐☐☐☐☐☐☐☐

☐☐☐☐ (Credit card expiration date)

To fax your orders (202) 512-2250

_____
(Authorizing Signature)

Mail To: Superintendent of Documents
P.O. Box 371954, Pittsburgh, PA 15250-7954

Thank you for your order!

Fishery Bulletin

Guide for Contributors

Content

Articles published in *Fishery Bulletin* describe original research in fishery marine science, engineering and economics, and the environmental and ecological sciences, including modeling. Articles may range from relatively short to extensive.

Notes are reports of 5 to 10 pages without an abstract and describing methods or results not supported by a large body of data.

Although all contributions are subject to peer review, responsibility for the contents of papers rests upon the authors and not upon the editor or the publisher. It is therefore important that the contents of the manuscript are carefully considered by the authors.

Submission of an article is understood to imply that the article is original and is not being considered for publication elsewhere. Manuscripts should be written in English. Authors whose native language is not English are strongly advised to have their manuscripts checked by English-speaking colleagues prior to submission.

Preparation

Title page should include authors' full names and mailing addresses, the corresponding author's telephone, FAX number, and e-mail address, and a list of key words to describe the contents of the manuscript.

Abstract should not exceed one double-spaced typed page. It should state the main scope of the research but emphasize its conclusions and relevant findings. Because abstracts are circulated by abstracting agencies, it is important that they represent the research clearly and concisely.

Text must be typed double-spaced throughout. A brief introduction should portray the broad significance of the paper; the remainder of the paper should be divided into the following sections: Materials and methods, Results, Discussion (or Conclusions), and Acknowledgments. Headings within each section must be short, reflect a logical sequence, and follow the rules of multiple subdivision (i.e. there can be no subdivision without at least two items). The entire text should be intelligible to interdisciplinary readers; therefore, all acronyms, abbreviations, and technical terms should be spelled out the first time they are mentioned. The scientific names of species must be written out the first time they are mentioned; subsequent mention of scientific names may be abbreviated. Follow Scientific Style and Format: the CBE Manual for Authors, Editors, and Publishers (6th ed.), for editorial style, and the most current issue of the American Fisheries Society's Common and Scientific Names of Fishes from the United States and Canada, for fish nomenclature. Dates should be written as follows: 11 November 1991. Measurements should be expressed in metric units, e.g. metric tons as t; if other units of measurement are used, please make this fact explicit to the reader. The numeral one (1) should be typed as a one, not as a lower-case el (l). Use of appendices is discouraged.

Text footnotes should be numbered with Arabic numerals and inserted at the bottom of text. Footnote all personal communications, unpublished data, and unpublished manuscripts with full address of the communicator or author, or, as in the case of unpublished data, where the data are on file. Authors are advised to avoid references to nonstandard (gray) literature, such as internal, project, processed, or administrative reports. Where these references are used, please include whether they are available from NTIS (National Technical Information Service) or from some other public depository.

Literature cited comprises published works and those accepted for publication in peer reviewed literature (in press). Follow the name and year system for citation format. In the text, cite as follows: Smith and Jones (1977) or (Smith and Jones, 1977). If there is a sequence of citations, list alphabetically by author(s): Smith, 1987; Smith and Jones, 1985; Smith and Peterson, 1986. Abbreviations of serials should conform to abbreviations given in Serial Sources for the BIOSIS Previews Database. Authors are responsible for the accuracy and completeness of all citations.

Tables should not be excessive in size and must be cited in numerical order in the text. Headings within tables should be short but ample enough to allow the table to be intelligible on its own. All unusual symbols must be explained in the table legend. Other incidental comments may be footnoted with italic numerals. Use the asterisk only to indicate probability in statistical data. Zeros should precede all decimal points for values less than one.

Figures must be cited in numerical order in the text. The senior author's last name and the figure number should be written on the back of each one. Hand-drawn illustrations should be submitted as originals and not as photocopies. Submit photographs as glossy prints or slides with good contrast, otherwise we cannot guarantee a good final printed copy. Graphs should be submitted as laser-printed copies, not as photocopies. Label all figures with Helvetica typeface and capitalize the first letter of the first word in axis labels. Italicize species name and variables in equations. Use zeros before all decimal points. Use uppercase Times Roman bold typeface to label the parts of a figure, e.g. A, B, C, etc. Each figure legend should explain all symbols and abbreviations in the figure and should be double-spaced and placed at the end of the manuscript.

Copyright law Government publications are not copyrighted; they fall within the public domain. If an author reproduces any part of a government publication in his work, reference to source is appreciated.

Submission

Send printed copies (original and three copies without staples) to the Scientific Editor:

Dr. John V. Merriner
Southeast Fisheries Science Center
National Marine Fisheries Service
101 Pivers Island Road
Beaufort, NC 28516

Once the manuscript has been accepted for publication, you will be asked to submit an electronic copy of your manuscript to the Managing Editor. The electronic copy should be submitted in WordPerfect or Microsoft Word text format and placed on a 3.5-inch disk that is double-sided, double or high density, and that is compatible with either DOS or Macintosh systems.

A copy of page proofs will be sent to the author for final approval prior to publication.
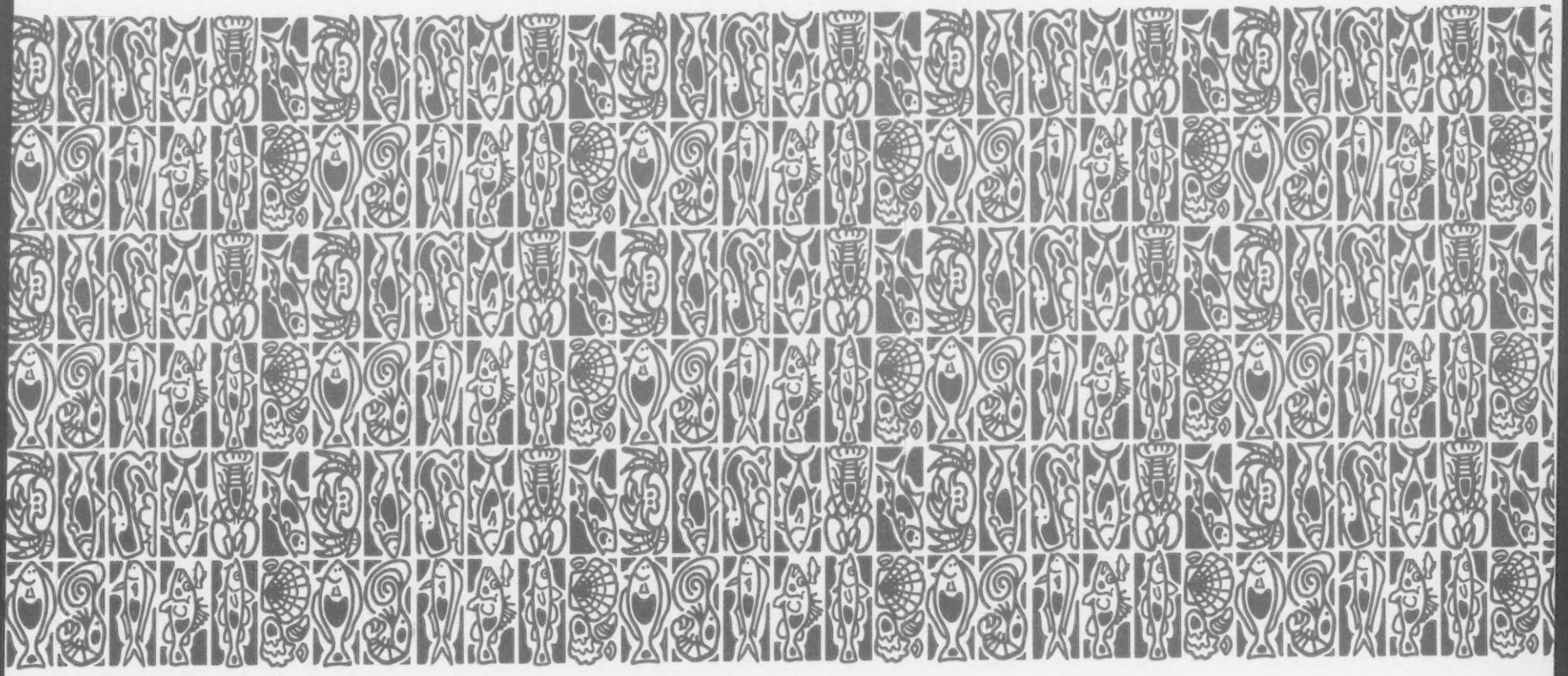
Reprints (copies of published articles and notes) are available free of charge to the senior author (50 copies) and to his or her laboratory (50 copies). Additional copies may be purchased in lots of 100 when the author receives page proofs.